Sedimentology, Sequence stratigraphy and Spatial-temporal Patterns of the late Paleocene Succession, western Sirt Basin, Libya

IBRAHIM ELTAIB DAW ELKANOUNI

Sedimentology, Sequence stratigraphy and Spatial-temporal Patterns of the late Paleocene Succession, western Sirt Basin, Libya

Ibrahim Eltaib Elkanouni

Thesis submitted for the qualification of Doctorate of

Philosophy (PhD) in geology

Department of Earth Sciences

Durham University

2013

Supervised by

Dr. Stuart Jones & Prof. Maurice Tucker

Abstract

In the western Sirt Basin, sedimentation during the Late Paleocene was characterized broadly by shallow-marine carbonates, local build-ups and deeper-water shales and marls on the Dahra Platform and in the Dor al Abid/Zallah Troughs. Seven lithofacies and eleven associated microfacies have been recognised within the Selandian/Thanetian carbonate succession in the study area, and these range from mud-supported carbonates to grain-dominated facies. The Dahra Formation on the Dahra Platform was deposited on a homoclinal carbonate ramp with inner, mid and probably outer ramp facies, each with distinctive sub-facies and microfacies. The similarity of facies and associated microfacies throughout the Dahra Formation suggest deposition under similar conditions throughout the east and west Dahra Fields on the Dahra Platform, and these persisted during deposition of the Zelten and Harash Formations. The Mabruk Member, which consists mainly of mainly shallow-water carbonates bounded above and below by deeper-marine shale and marl, accumulated in lagoonal and reefal environments, probably in a rimmed-shelf setting. Different types of diagenetic alteration occurred at various stages in the Paleocene sediment's history including dissolution, cementation and compaction. Primary and secondary types of porosity were developed within the studied rocks, particularly in the Dahra Formation, where the depositional facies, diagenesis and the pattern of carbonate cycles played an important role in porosity creation and preservation.

The Selandian/Thanetian succession is dominated by a regressive trend, especially on the Dahra Platform, which resulted in the development of shallowing-up cycles. Numerous key surfaces have been documented with characteristic funnel-shaped and bell-shaped log patterns, based on which a number of depositional sequences have been recognized. These sequences comprise both transgressive systems tract and highstand systems tract and are commonly defined by transgressive surfaces, particularly on the Dahra Platform. The possible lack of reef-building organisms along with tectonic subsidence and/or significant sea-level rise resulted in the development of a drowning unconformity on the top of the Mabruk Member.

The thickness of the entire Paleocene succession is generally thicker in the trough areas and thinner over the platform. The latter is dominated by uniform and monotonous strata with a significant thickness of shallow-marine carbonates, suggesting relative stability in tectonics, sea-level and climate. The high temperature recorded from the aqueous inclusions in the Thanetian section is possibly due to the passage of hydrothermal fluids from deeper parts of the area; the high thermal conductivity of carbonates, along with the Mid-Late Tertiary uplift and erosion may also have been involved. The overall similarity of the Paleocene palaeotopography suggests that differential subsidence and sea-level fluctuation were the dominant process that controlled the spatial and temporal variation of the Paleocene facies.

Table of contents

List of Figures

List of Tables

Dedication

I would like to dedicate this work to the spirit of my beloved father, who was encouraging, supporting and sponsoring me throughout his life. I would like to dedicate this piece of work to my cherished mother, who always keeps asking Allah to save me and give me all success, to my wife, children, brothers and sisters.

Declaration

The material contained in the thesis has not previously been submitted for a degree in this or any other institution. The work described in this thesis is entirely that of the author, except where reference is made to previous published or unpublished work.

Ibrahim Eltaib Elkanouni
November 2013

Acknowledgements

First and foremost, thanks and praise to the LORD God (ALLAH) for creating me and making me with an inquiring mind and the ability to write a thesis of sorts.

I would like to gratefully acknowledge the teaching and support of my supervisors: Dr. Stuart Jones and Prof. Maurice Tucker. Thank you Stuart for your administration and academic provision, and for your constructive comments, advices and moral support. Thank you very much Maurice for all your corrections, suggestions and valuable supervision. Your wide-ranging experience, and clear explanations, discussions and corrections were essential in shaping and developing the ideas at all stages of this study. In actual fact, I cannot find sufficient words to express my sincere thanks and gratitude to prof. Tucker for his scientific support.

My thanks and gratitude extend to Dave Stevenson, Gary Wilkinson and Mathew for their technical support. I must also thank all my postgrad and postdoc friends of the Earth Sciences Department that have make my time here easier, particularly Juan Carlos, Dr. Shann, Dr. Mohammed Abdulwahab, Amelie and Abdulmonem Alborki.

I must thank gratefully the Libyan Petroleum Institute for its sponsorship and fund of this study. Special thanks to Waha Oil Company and CPTL for enable me to access the core samples from the Dahra and Mabruk Fields.

My research study benefitted significantly from conversations with local experts in carbonate sedimentology and general geology of the study area, particularly Prof. Ali Sbeta, Dr. Ibrahim Mohan and Dr Mohammed Mresah.

My deepest gratitude and thanks to my parents, who without them I would not reach to this stage of education. I would like to record my gratitude and love to my mother, my children (Raghd, Aisha, Abdulmohimen and Asma), brothers, and sisters. Last, but by no means least, my most sincere thanks and love go to my wife for her encouragement, patience and moral support not only during the period of this study but also throughout our lives.

CHAPTER ONE: INTRODUCTION

1.1. General Introduction

Geological studies in Libya started in the early 20th century by Italian geologists and continued through the mid-century by French, and U.S. geologists. By the end of 1960' s several papers on the geology of Libyan oil fields had been published and highlighted the importance of Libya as a major hydrocarbon producing country.

The northern part of the country is situated on a tectonically active subsident margin, which includes the Cyrenaica Platform, Benghazi Basin, Sirt Basin and the offshore Sabratah Basin. The southern part of the country lies within a stable cratonic area and includes the Al Kufra Basin, Murzuq Basin and Ghadamis Basin (Gumati, et al., 1991). The Sirt Basin developed through inter- and intra-plate movements resulting from the relative motion of the American, African and Eurasian plates during the opening of the Atlantic Ocean and the development of the Mediterranean on the foreland of the African Plate (Anketell, 1996). The sedimentary succession in the Sirt Basin, which is typical of those developed in a failed rift system, ranges in age from Cambro-Ordovician to Recent. The Sirt basin is the most important sedimentary basin in Libya as it is a site of most oil and gas production of the country. The Paleocene strata, however, are economically important in that about one-quarter of Libyan production of hydrocarbon is contained in them.

The Paleocene rocks in the Sirt basin have been the subject of many regional studies that have dealt mainly with structure and tectonics, stratigraphy and broad sedimentology, especially in the central and eastern part of the basin. Gumati and Kanes (1985) produced a subsidence curve that exhibits a sudden flattening corresponding to the Maastrichtian, and this possibly indicates a suspension of subsidence during Maastrichtian time. The same authors stated that the advent of the Danian was accompanied by widespread rising sea level, possibly in response to a regional phase of subsidence. This resulted in the deposition of thick open-marine mud-rocks in the subsiding areas. The stable platforms, on the other hand, were largely dominated by carbonate deposits.

Sinha and Mriheel (1996) studied the evolution of the Paleocene succession in the south-central Sirt Basin and recognised several transgressive-regressive marine cycles. In the western part of the basin the tectonic movements in the Dahra Platform were more downward through vertical isostatic subsidence until late Eocene time. During the late Eocene-Oligocene the platform underwent a major regional tilting

towards the axis of the Ajdabiya Trough (Roohi, 1996). Abadi (2002) studied the tectonics of the Sirt Basin and the interfaces between tectonic subsidence analysis, stress inversion and gravity modelling, and concluded that Sirt Basin evolution is marked by a large number of rifting pulses from Late Jurassic/Early Cretaceous to early Eocene, with three major rifting phases. The third phase (Paleocene to early Eocene) is characterised by differential subsidence and fault reactivation.

There are few published studies, however, on the sedimentology and stratigraphy of the late Paleocene. Detailed petrographic, sedimentological and sequence stratigraphic studies of the Late Paleocene succession in the western part of the basin have not been conducted. This research study aims to provide new information to the geology of Paleocene time in the western part of the Sirt Basin, through study of the Paleocene succession and discusses its spatial and temporal variations, palaeoenvironments, cyclicity, facies, sequence stratigraphy and post-depositional processes resulting from regional, local and lab work.

The literature reviews of the Paleocene Epoch showed that the Paleocene was a time of renewed vertical movements, which produced a strong differentiation between the sedimentation patterns on the horsts and in the grabens. Limestone, dolomitic limestone/dolomite, argillaceous limestone/marl, and shale are all present in the studied Paleocene strata, which were deposited on a homoclinal carbonate ramp and carbonate shelf. Analysis of post-depositional changes of the studied Paleocene rocks shows different types of alteration that occurred at different stages of the sediment history; among them dissolution, cementation and compaction are the most common processes. Primary and secondary types of porosity have been documented in the studied rocks, particularly in the Dahra Formation, where the depositional facies and diagenesis played an important role in their creation and preservation.

The overall pattern of shale and carbonate strata reflects alternating transgressive-regressive cycles in the Paleocene succession. Spatially, carbonates are confined to the structurally higher platform areas, whereas shales occupy the troughs. In the study area, particularly on the Dahra Platform, the late Paleocene succession is dominated by a regressive trend, which resulted in the development of shallowing-up cycles. A number of key surfaces have been recognised within the succession with characteristic funnel-shaped and bell-shaped well-log patterns. The thickness of the Paleocene succession in the study area is commonly close to the underlying structure;

thicker in the trough areas and thinner over the platforms; this was probably the response to subsidence and widespread sea-level fluctuations.

This study gives added value to the petroleum geology of the western part of the basin and contributes new data based on an integrated approach utilizing data from different subdisciplines of upstream geosciences such as seismic, wire-line logs and core samples. The practical work examined more than 50 wire-line logs, several seismic sections, and morethan 1500 feet (~457metres) of core samples representing the Dahra Formation, and its equivalent, the Zelten and Harash Formations in the Dahra Platform and adjacent Dor al Abid Trough. More than 320 thin-sections have been examined petrographically and around two hundreds of samples have also been investigated using scanning electron microscopy, cathodoluminescence microscopy, X-ray diffraction, stable isotope analysis and Fluid inclusion petrography.

1.2. Aims and Objectives

According to the literature, no detailed sedimentology and sequence stratigraphic studies for the Late Paleocene succession have been published so far. This study is the first to deal with the detailed sedimentology and petrography of the Dahra, Mabruk, Zelten and Harash Formations in the western Sirt Basin. It is also the first to interpret the sequence stratigraphic framework of the Selandian/Thanetian succession in the study area.

Inspired by the need to document these carbonates and the necessity to explore and understand the role of tectonics, eustasy, climate and sediment production on the spatial and temporal variations of the Paleocene successionin the western sirt basin, in this research I have focused on the thickness discrepancies, lithological variations, palaeoenvironments, cyclicity and facies association of the studied Paleocene succession. The overall aim of this project is to address the implication of the above mentioned processes on the syn-depositional carbonates in the western Sirt Basin. Specifically this study will address four inter-dependant principle aims:

1- To identify the distribution and thickness variations of the carbonate depositional facies and its associated microfacies in the western Sirt Basin.

2- To investigate and fully constrain the burial carbonate diagenesis and resulting reservoir quality for the Late Paleocene succession of the western Sirt

Basin.

3- To apply sequence stratigraphy to the Paleocene carbonate successions and determine the key factors that controlled the spatial and temporal distribution of the facies.

4- To identify the role tectonic subsidence has played during the Late Paleocene rifting in the western Sirt Basin and how carbonate facies variations and detailed petrography can be used as supporting evidence.

1.3. Location and geographic setting of the study area

The study area, which is located between the coordinates 28°44′50.02′′& 30° 12′ 6.74′′ N and 16° 53′ 10.77′′& 18° 00′ 44.06′′E), covers the most prominent northwest-southeast trending tectonic features in the western Sirt Basin. It includes the Dahra Platform and Dor al Abid Trough. Broadly, the area is bounded by the Maradah Trough on the east and northeast, by the Zallah Trough on the southwest and by the Waddan Uplift on the west (Fig.1.1).

The Dahra Platform is bounded on the west and southwest by the Dor al Abid and Zallah Troughs, respectively, and on the south and southeast by the Al Kotlah Graben, whereas the Al Hagfah (Maradah) Trough represents the east – north-eastern border of the Dahra Platform (Fig. 1.1). The northern boundary of the platform is not clearly defined, although it might extend to the offshore area. The Dor al Abid Trough is bordered on the southwest by the northernmost part of the Al Hulayq High. Here the trough swings abruptly SSW into the Abu Tumayam Trough which is bordered on the west by the SSW arm of the Al Hulayq High and on the east by the Southern Platform (Anketell, 1996).

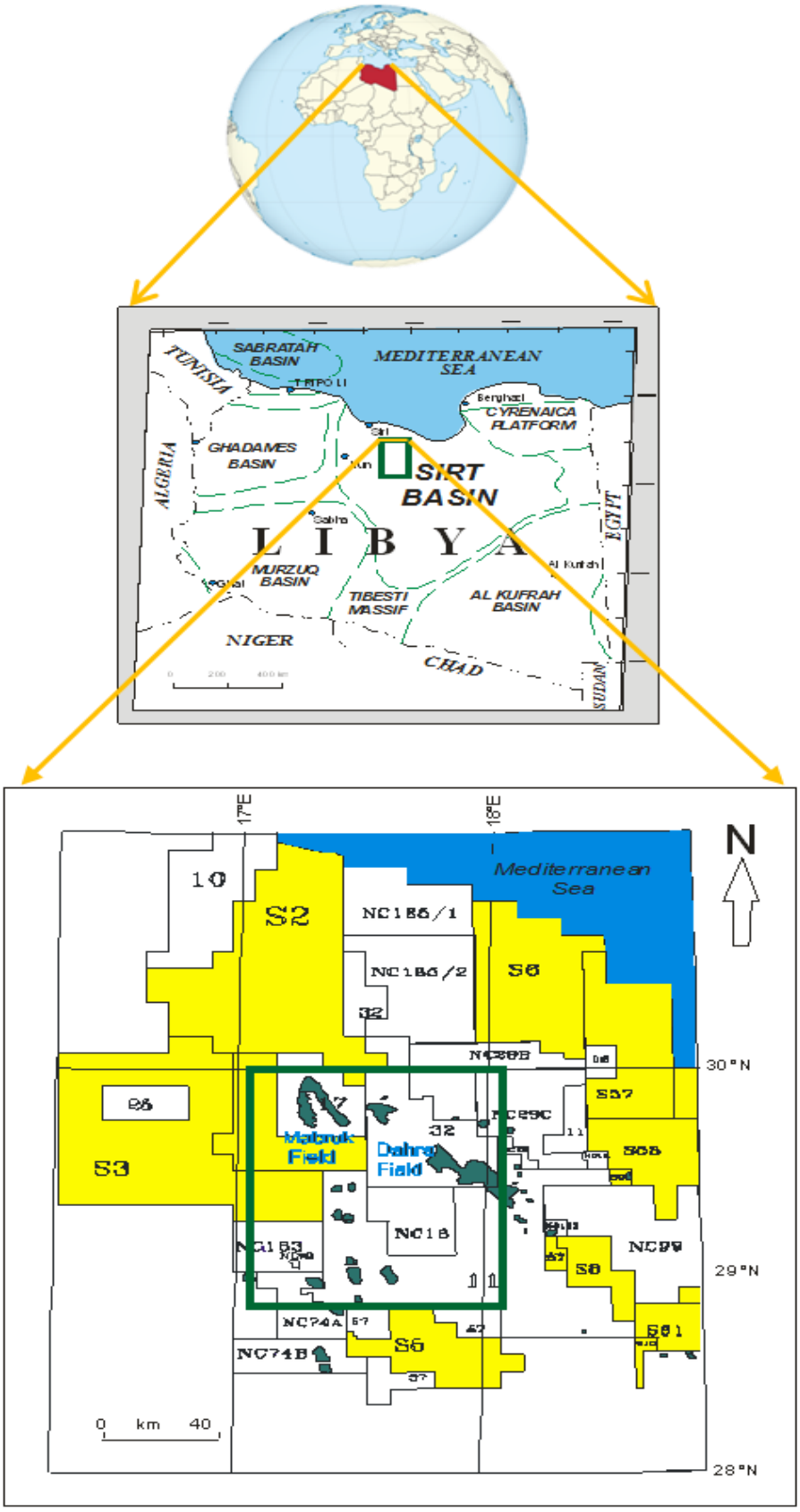

Figure 1.1 Location map of the study area.

1. 4. Data Base

This study has been carried out based on the following materials:

1. More than 1500 feet of slabbed core sample retrieved from six wells located on the Dahra Platform and Dor al Abid Trough in the western Sirt Basin.
2. Three hundred and twenty thin-sections, among them about two hundred sections were uncovered, polished, impregnated and stained and/or half stained.
3. Around 50 electrical well logs (spontaneous potential, neutron, gamma ray, sonic, resistivity and density) with mainly 1:500 scale
4. Spectral gamma ray charts for a few wells (surface) at 1:200 scale
5. Several seismic sections across the Dahra Platform and Dur al Abid Trough
6. Conventional core analysis results
7. Tectonic and concession maps of the Sirt Basin

1.5. Methods of study

To achieve the overall aims and specific objectives of this study, based on the above noted data-base, the following tools and techniques have been applied:

1.5.1. Core logging

Detailed core logging was undertaken on the 1:100 scale to reveal the various geological character and to document the subtle sedimentological features. It involved noting lithology, sedimentary structure, texture, degree of bioturbation, cycles, thickness, dolomitized intervals and fossil content. Sample location, sedimentary cycles and sequence stratigraphic approach were involved as well. The carbonate facies were classified according to Dunham's textural classification (1962) and Embry and Klovan (1971). Brief descriptions and remarks have been added were necessary. The logs were drawn using CorelDraw X5 and the final core logs of the studied wells are presented in Appendix one.

1.5.2. Wire-line Logs

Although many of the available wire-line logs are somewhat old, especially the gamma ray, they have been utilized were possible to get the most possible accurate results. These electrical logs involve spontaneous potential, resistivity, sonic, gamma-ray, neutron, density and conductivity. They have been used to delineate and correlate different sedimentary facies within the same structural setting (platform/trough).

1.5.3. Seismic Sections

A few regional seismic lines located on the Dahra Platform, in Dor al Abid Trough and across these two adjacent structural elements have been used. Most of these lines are already interpreted by either the operating company or other organizations. The author has introduced his own explanation of these lines in order to interpret the Paleocene succession in the context of tectonics and other geological processes and its outcome on the facies distribution in the study area.

1.5.4. Computer based-mapping and cross-sections

A number of thickness, topography and structure maps have been produced using Surfer software. These maps represent the whole Paleocene Succession, Danian, Selandian, Thanetian ages, and each Paleocene rock unit (8 Formations), along with the topographic and structure map of the uppermost Cretaceous (Maastrichtian) Kalash Formation.

In addition to the sedimentological logs, CorelDraw X5 has also been used to conduct several stratigraphic and structural cross-sections on the Dahra Platform and across the Dahra Platform and Dor al Abid Trough. The regional cross-sections have either been constructed using available data, or modified from published reviews.

1.5.5. Petrography and analytical techniques

A variety of petrographic and analytical procedures have been employed in this study; they include: polarized microscopy (thin-sections), SEM, CL, XRD, stable isotopes, and fluid inclusions.

1.5.5.1. Thin-sections

A polarised microscope was used in describing around 320 thin-sections representing the core samples recovered from the Dahra (and Mabruk), Zelten and Harash Formations in the western part of the Sirt Basin. Since the studied rocks are composed of limestone and dolomite a large number of the thin-sections were stained or half stained, using the method described by Adams et al. (1984) adapted from Dickson (1965). The thin-sections were classified according to Dunham (1962) and Embry and Klovan (1971).

Each thin-section description involves type and percentage of carbonate grains (skeletal /non-skeletal), cement, matrix, porosity, diagenetic minerals and diagenetic processes. Environment of deposition and depositional texture (classification) are also included.

1.5.5.2. Scanning Electron Microscopy

The high magnification attainable and extreme depths of field make SEM an excellent tool for examining the details of mineral morphology, grain-cement relationships, and porosity, especially microporosity (Emery and Robinson, 1993).

A total of 40 samples have been analysed using secondary electron mode and back-scattered mode of the SEM. Some of the samples were examined in the Department of Physics, Durham University. The coating process used a Cressington Coating System 308R. The rest of samples were analysed in the SEM Lab at the Libyan Petroleum Institute Laboratories in Tripoli, Libya.

1.5.5.3. Cathodoluminescence Microscopy (CL)

CL is a surface phenomenon and luminescence can be obtained from any highly polished surface, whether it is a rock chip or a thin section. In this study a number of un-polished, double-polished, un-covered, and un-stained thin-sections were used to distinguish original depositional material from altered depositional carbonate and cement, and to address the mineral paragenesis.

The most important ions affecting luminescence intensity in carbonates are Mn^{2+} and Fe^{2+}, with the manganese activating luminescence and the iron quenching it. Hence variations in luminescence intensity usually reflect a variation in the ratio of Mn^{2+} to Fe^{2+} in a crystal (Adams and Mackenzie, 1998).

The CL colours produced in calcite and dolomite by Mn^{2+} range from yellow to dark reds and pinks. Broadly, low Mg calcites give a yellow CL, high Mg calcites are orange to red, and dolomite is characteristically a brick-red colour.

1.5.5.4. X-Ray diffraction analysis

XRD is a fast and reliable method of determining the bulk mineralogy of carbonate rocks (aragonite, calcite, dolomite, siderite, etc.). Part of the study was to examine the samples to determine the mineralogical composition of the whole rock; this was achieved via running a total of 43 samples in the X-ray diffraction apparatus at the XRD Lab in the Libyan Petroleum Institute Laboratories in Tripoli, Libya.

1.5.5.5. Stable Isotope Analyses

Oxygen isotope data are used to determine past water composition and temperature. Carbon isotope records are used to constrain ocean nutrient and water circulation patterns, and the concentration of atmospheric carbon dioxide. Both stable isotopes can be used for stratigraphic studies.

A total of 189 samples from five wells were chosen to be analysed for $\delta^{13}C$ and $\delta^{18}O$ signature (matrix-whole rock). Some of the samples was analysed in the *Stable-Isotope and Luminescence Laboratory* at the University of Birmingham, whereas the rest of the samples were analysed in the Stable Isotope Laboratory at the Earth Sciences Department, Durham University. The analytical procedures were the same but at Durham they were carried out using an Isotope Ratio Mass Spectrometer Thermo Finnigan Gasbench II connected to a Thermo Finnigan MAT 253. The procedure was as follows:

100 -140 μg of powdered carbonate were placed into 4 ml glass vials then sealed by a lid and pierceable septum. The vials were placed in a heated sample rack (90°C) where the vial head space was replaced by pure helium via an automated needle system as part of a GV Instruments Multiflow preparation system. Samples were then manually injected with approximately 200μl of phosphoric acid and left to react for 1 hour before the headspace gas was sampled by needle and introduced into a continuous-flow GV Isoprime mass-spectrometer. Samples were calibrated using IAEA standards NBS-18 and NBS-19 and reported as ‰ on the VPDB scale.

1.5.5.6. Fluid Inclusions

Fluid inclusions are the only direct records of palaeo-fluids existing in the subsurface, and as such, have the potential to record conditions accompanying geological processes. Fluid inclusion petrography was undertaken by Fluid Inclusion Technologies, Inc. in Tulsa, Oklahoma, U.S.A.

Thin-sections were prepared from two wells located on the Dahra Platform, and at depths warranting further examination following the preliminary assessment of the Fluid Inclusion Stratigraphy (FIS) results. The sections were then examined under a petrographic microscope using a variety of fluid inclusion techniques (e.g. UV-fluorescence, microthermometry, etc.) in order to verify the presence of petroleum-bearing inclusions in the rock samples. Petrographic examination was also necessary to verify that petroleum bearing fluid inclusions present in the samples and responsible for

the observed mass spectra are not relict features (i.e., that they were not already present in the mineral grains prior to deposition). In this study the fluid inclusion results were used to estimate the time and temperature of carbonate cementations and utilized to determine the burial history of the study area.

1. 6. Thesis outline

The present research study is organised in seven chapters. Chapter 1 starts with a short literature review and outline the main scientific problems the thesis will address. It also includes the main aims and specific objectives, location of the study area, data-base and the methodology. In Chapter 2 a review of regional geology of Libya as a whole with a brief outline on its sedimentary basins is presented. It focuses on the Sirt Basin, its structural and stratigraphic evolution with emphasies on the western part of the basin. In the same chapter the stratigraphy of the Paleocene succession and its various rock units in the study area are also introduced.

Chapter 3 represents comprehensive sedimentological and petrographic investigations of core samples retrieved from the late Paleocene rocks in the study area. The sedimentological description has been performed according to Dunham, 1962; Embry and Klovan, 1971, and Choquette and Pray, 1970. Thorough petrographic examination and facies analysis along with the facies sequence and environmental interpretation of the whole succession are presented in this chapter.

Detailed investigation and documentation for the diagenetic processes and products of the studied rocks along with the impact of these processes and events on the reservoir characteristics of these rocks are addressed in Chapter 4.

Chapter 5 provides a review of the classical stratigraphy of the area along with the results of a sequence stratigraphic application. This chapter shows how sequence stratigraphy combines lithology, fossils and facies analysis and recognizes packages of strata each of which was deposited during a cycle of relative sea-level change and/or changing sediment supply.

Investigations of the possible effects of tectonic, eustatic sea-level and climatic processes on the distribution of different sedimentary facies during the Paleocene Epoch in the study area are treated in Chapter 6. Comprehensive conclusions of the entire thesis along with recommendations for further work are available together in Chapter 7. The appendices show the data used and produced in this research are present at the end.

CHAPTER TWO: REGIONAL GEOLOGY OF LIBYA

2.1. Introduction

In view of the country almost being in the Sahara, except for the northern parts, difficulties of travel have, in the past, caused the country to remain unmapped, and geological information has been acquired slowly (Conant and Goudarzi, 1967).

The geological studies in Libya started in 1911 with surveys by many Italian geologists, including Gregory (1911), Marinelli (1920) and Ahlmann (1928). Desio and his co-workers published reports on their studies in the country from 1911 to 1943. French geologists studied the former Fezzan province of south-western Libya and published their work in many geological reports from 1943 to 1955. Geologists from the U.S. Geological Survey made hydrological and geological surveys from 1952 to 1964, which resulted in many short reports, including 1: 2,000,000 topographic and geological maps.

The intensive search for oil began in Libya in 1953, and the geological studies then become more focused on the subsurface of the oil fields. By the end of 1960s several papers on the geology of Libyan oil fields had been published. These include the Zelten field (Fraser, 1967), Augila field (Williams, 1968), Intisar A field (Terry and Williams, 1969), and the Sarir field (Sanford, 1970). The first symposium on the geology of Libya was held in 1969, which provided important geologic information on Libya, and since then a series of symposia on the geology and petroleum geology of Libya has been hold regularly. In addition, there have been a number of significant publications since 1960 dealing with surface exposures, although some of these have extended into the subsurface. These include Jordi and Lonfat (1963) and Gobrbandt (1966b) on the western flank of the Sirt Basin (Hun Graben); Desio et al (1963), Burollet (1963) and Magnier (1963) on the Jabal Nefusa (western Libya); and Pietersz (1968), and Barr and Hammuda (1971) on northern Cyrenaica. Important summaries of plate tectonics in relation to Libya have been made by Anketel (1996), Guiraud (1998) and Morgan et al. (1998).

Libya can be divided into two geological provinces, each of which includes a number of sedimentary basins. The northern part of the country is situated on a tectonically active and subsiding margin (unstable shelf) and includes from west to east the Pelagian Shelf (Tripolitania Basin), Jeffara Trough, Sirt Basin and Cyrenaica Platform. The southern part of Libya, which lies within a stable, cratonic area, includes the Ghadamis, Murzuq and Kufra Basins. Major hydrocarbon discoveries have been

made in the Palaeozoic reservoirs in the Ghadamis and Murzuq Basins, and in Mesozoic and Cenozoic reservoirs in the Sirt and Pelagian Basins (Gumati et al, 1996).

The Phanerozoic sedimentary column in the country varies in thickness from zero at basement outcrops in the south, to more than 7000 m encountered in the offshore Sirt Basin to the north. The age of these sediments ranges from Cambrian to Recent. A number of transgressive and regressive cycles occurred during the Phanerozoic. Marine incursions during the Ordovician, Silurian, Devonian, Carboniferous, Late Cretaceous and Tertiary reached far south into Libya (Conant and Goudarzi, 1967). Thus the sedimentary section is dominated by marine shales, carbonates and evaporites in the northern parts of the country; it becomes increasingly clastic southwards, with an increasing frequency of stratigraphic hiatuses (Gumati et al, 1996).

The volcanic events in Libya are believed to have been concurrent with movements along deep-seated fractures, perhaps associated with the great orogenic pulse of the Alpine cycle. Precambrian crystalline rocks occur in south and south-eastern Libya in the area of the Tibesti Mountains, Jabal Archenu, and Jabal Auenat. These rocks are metamorphic, composed of para- and ortho- gneiss, quartzite and marble, all intruded by granitic rocks (Goudarzi, 1959).

According to Energy Intelligence Research, in 2003 Libya was the 11th largest exporter of petroleum in the world and reached the peak of 3.3 million barrels a day in 1970; it currently produces about 1.7 million barrels of crude a day. According to the National Oil Corporation (NOC), only around 30 per cent of Libya has been explored for hydrocarbons. There are about 320 producing fields with a total reserve exceeding 50 billion barrels of oil and 40 trillion cubic feet of gas.

2.2. Geographic setting

Libya is situated on the Mediterranean coast of North Africa, between latitudes 20^{o} and 33^{o} N and longitudes 10^{o} and 25^{o} E, and has an area of about 1,760,000 square kilometres. It extends about 1900 kilometres east to west, along the southern fringe of the Mediterranean Sea, and about 1450 kilometres north to south. The country is bordered by Egypt to the east, Sudan to southeast, Chad and Niger to the south, and Tunisia and Algeria to the west, whereas the Mediterranean Sea represents its northern boundary (Fig. 2.1).

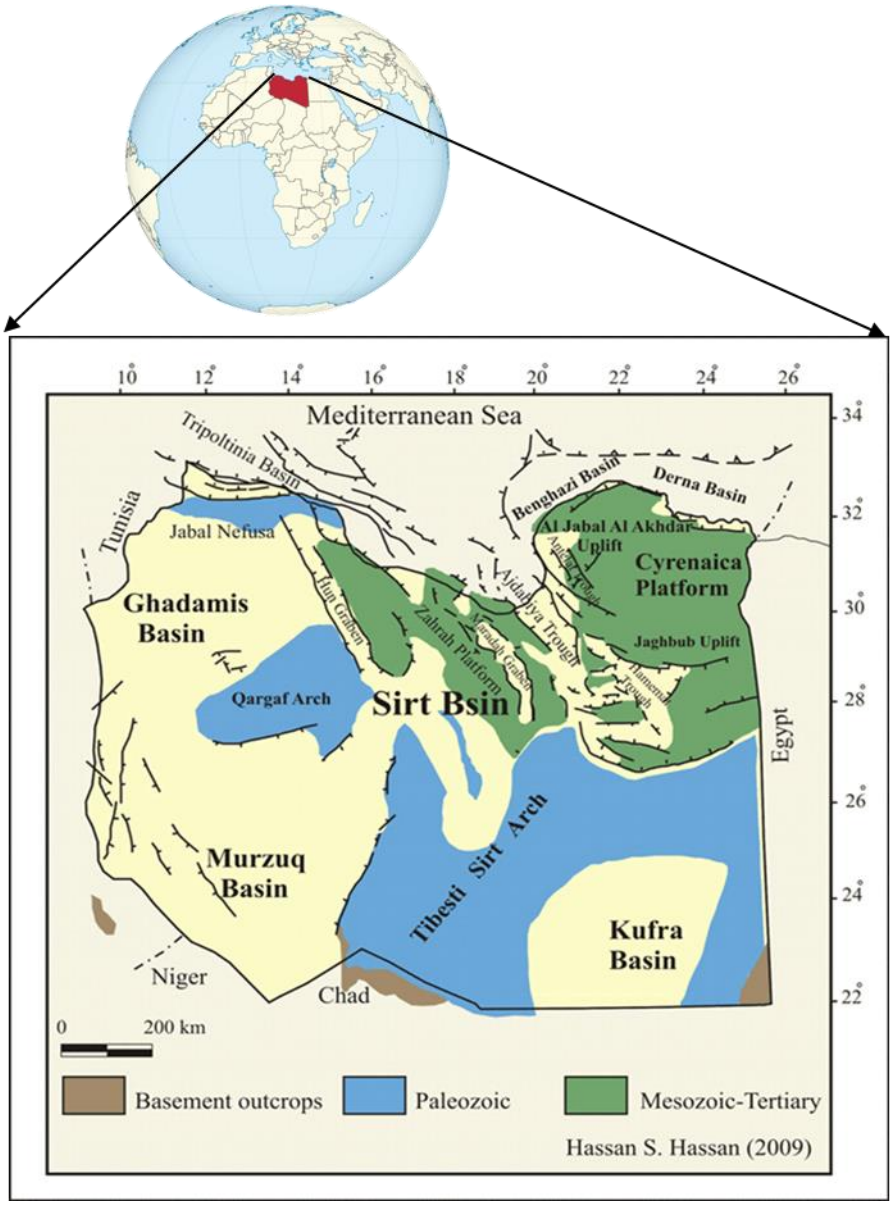

Figure 2.1 Major structural features and sedimentasry basins in Libya (after Rusk, 2002 and Hassan,2009).

2.3. Geological setting

The African Plate, as a part of the southern Gondwana continent, collided with northern Laurasia to form the super continental landmass (Pangaea) at the end of Palaeozoic (Guan et al., 2005).The collision involved a significant strike-slip component, and a major dextral shear-zone developed along the line of contact. The later break-up of Pangaea in the early Mesozoic involved the establishment of a spreading axis throughout the Mediterranean region (Hallett, 2002).

Rifting occurred along the northern margin of the African plate as a result of dextral shearing between the African and European plates, developing a complex horst

and graben system (Selley, 1996). Cloetingh (1988), Ziegler (1988) and Janssen (1996) have shown that tectonic processes taking place at plate boundaries influence the state of stress in large parts of the adjoining plates and affect the evolution of the sedimentary basins located on these plates.

Libya as a whole is a cratonic basin on the northern fringes of the African shield (Goudarzi, 1970). Its northern part is situated on a tectonically active subsiding margin, whereas the southern part of the country lies within the stable cratonic area (Gumati, et al., 1991) (Fig.2.2). Structurally Libya is part of the Mediterranean foreland formed by the North African shield, and as a result of its position at the leading edge of the African Plate, the country was affected by successive phases of continental collision and plate divergence (Pickford, 1992).

Several periods of major tectonic development in Libya have affected its structural and stratigraphic history, and include: folding and consolidation in the Precambrian; the formation of a NW-SE trending fault system during the Cambrian; and the development of regional highs and lows during the Silurian and Devonian time. The modification of pre-existing structural trends into WNW-ESE directions occurred during the Late Palaeozoic and Early Mesozoic (Thomas, 1995).

The structure of southern Libya was influenced by the Pan African event; the central part was affected by the Variscan tectonic events, whereas the structures of the northern portion are attributed to the Tethyan extension and alpine tectonic movements (Goudarzi, 1980).Marine strata, however, of Palaeozoic, Mesozoic, and Cenozoic ages abound in the northern part of Libya, whereas Palaeozoic and Mesozoic continental rocks of predominate in the south.

According to Selley (1996) compressional folds are almost absent, but block faulting, tilting, subsidence and uplift occurred, with angular and parallel unconformities common between formations. Caledonian and Hercynian, as well as movements during Late Cretaceous and Oligocene through Miocene times and possibly Holocene too, developed the major features that form the present-day structural elements of Libya.

The Precambrian basement is exposed in the Al Awaynat region in southeast Libya, the Tibesti region along the southern border of the country, the Thamboka region in the southwest, and the nearby Qarqaf Arch (the border between Ghadamis and Murzuq Basins) (Fig. 2.1).

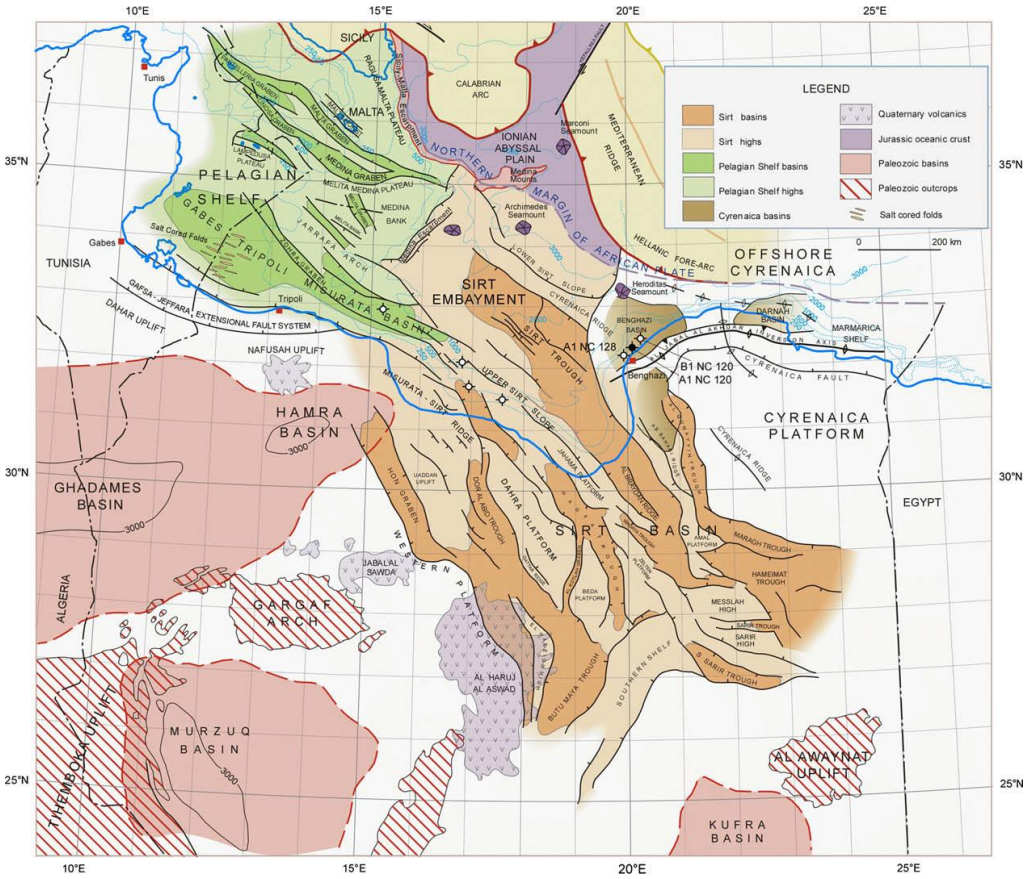

Figure 2.2 Tectonics and structural elements map for Libya and surrounding offshore areas (Fiduk, 2009 modified from Gibbs, 2004).

The basement is generally overlain unconformably by Cambrian rocks, though this contact is often onlapped by younger rock units ranging from Ordovician to Paleogene in age. The first sediments to be deposited after the Pan-African Orogeny were Infracambrian continental sandstones. Such rocks are found around the Tibesti Massif at the Libyan-Chad border and in the Cyrenaica area in the eastern part of Libya (Hallett, 2002).The same author stated that the Ordovician tectonic events- in Libya- produced a series of broad, northwest-southeast to north-south troughs and swells which include the Tihemboka High, the Murzuq-Jadu Trough and the Tripoli-Tibesti Uplift which controlled deposition during the Early Palaeozoic. Deposition of mostly continental siliciclastics during the Cambrian and marginally marine to marine siliciclastics during the Ordovician and Silurian continued essentially without interruption from Morocco to the Middle East (Rusk, 2002).

Tectonic events during the Late Silurian Caledonian orogeny initially defined the limits of the Paleozoic basins of Libya. The east-west-trending Qarqaf Arch separated the Ghadamis and Murzuq Basins; the north-south-trending Sirt-Tibesti Arch separated the Murzuq and Kufrah Basins and, generally, the Ghadamis Basin from the eastern Cyrenaica–Western Desert Basin (Klitzsch, 1971; Bellini and Massa, 1980) (Fig. 2.2)

From the Early Devonian, Caledonian structural movements were significant. An initial collision of the Laurasian landmass with Gondwana was followed by collision with the African Plate. In this compressional regime external cratonic sag basins suffered stresses from a north to east direction. In view of the differential uplift and subsidence of these basins, strata were folded and subjected to erosion. The Devonian in Libya is dominated by widespread deltaic complex, which is interrupted by uplift and erosion in the mid-Devonian. The Devonian deformation was reactivated during the Variscan movements in the Carboniferous and Permian. Variscan movements influenced the entire African Plate, quite intensely in many areas, causing deep erosion of early formed strata and a widely distributed strong unconformity across North Africa (Sun.et al., 2010). Besides, the older Palaeozoic strata being folded uplifted and eroded (Aliev et al., 1971; Burollet et al., 1978; Boote et al., 1998). In the Late Carboniferous and Permian, several rift basins and grabens formed along the northern margin of the African plate by extension as a result of the initial breakup of Gondwana and the opening of the Tethyan seaway (Guiraud, 1998).

The Carboniferous Period is characterized by fluvial, deltaic and littoral deposits along the North African territory. In Libya a flooding event in the mid-Carboniferous produced carbonate deposits, after which much of the north African margin was uplifted and deformed as a result of the Variscan orogeny. During the Late Carboniferous, extensive erosion took place, a series of swells and sags were established across North Africa. In Libya the Sirt and Qarqaf Arches, Nafusah and Ennedi-Al Awaynat Uplifts and their associated troughs were formed (Hallett, 2002).

Widespread uplift and severe erosion during the Variscan orogeny, particularly along the Sirt-Tibesti Arch, Qarqaf Arch, and Jefara uplift, further accentuated the Palaeozoic basin margins (Rusk, 2002).Permian basalts and granites have been recorded in the Pelagian Basin and Sirt Basin, respectively. Marine sediments of Permian age have also been encountered offshore Libya, and they thin southwards towards the

Nafusah Uplift. This may represent the southern margin of the Tethyan Basin at this time.

The Mesozoic-Tertiary tectonic evolution of the African Plate is directly linked to the opening history of the Atlantic Ocean and the dynamics of Africa-Eurasia convergence (Guiraud et al., 1992). The North African continental margin was characterized by extension and crustal thining during the Triassic. Extensional faults of Triassic age along with several unconformities were developed in Libya. The continental and marine deposition during the Mesozoic in the Murzuk and Ghadames Basins continued offshore in the Tripolitania Basin, where the thickness of post-Permian to Upper Cretaceous marine siliciclastics and carbonates may exceed 12,000 ft. Tectonic activity in the Tripolitania Basin and surrounding offshore areas during the Mesozoic was dominated by east-west-oriented dextral transtension related to movement of the African Plate relative to the Eurasian Plate (Van Houten, 1980; Anketell, 1996).

Evidence of continental Jurassic is rare, but the incipient rifts of the Triassic probably continued to develop. Jurassic rocks in the Jabal Nafush, which pass into continental equivalents to the south, have a more marine aspect than in the Triassic.
Morgan et al., (1998) demonstrated that the African plate began to drift northwards during the early Late Cretaceous, and this movement has continued to the present-day (Fig. 2.3). This drift has been calculated to be about 2.5cm/year. There is evidence of subsidence and pull-apart in the eastern part of the Sirt Basin in the Lower Cretaceous, where continental sandstones covered almost the entire area.

The rift phase ended with marine incursion from the Tethys Ocean in the Early Cretaceous. Central Libya apparently remained a positive area (the Sirt Arch) until the Early Cretaceous when the arch collapsed (Fig. 2.4). Graben structures were filled with predominantly continental sandstones of the Nubian Formation (Tawdros et al., 1999a), and remained subaerially exposed until the Cenomanian, when a major flooding event took place.

The uppermost Cretaceous-Early Tertiary tectonics in the Mediterranean region were compressional associated with the middle Alpine (Laramide) Orogeny. This compressional regime led to dextral movements in the area and the northward subduction of Tethyans oceanic crust, and eventually to the closing of the Mediterranean (Biju-Duval et al., 1974) (Fig. 2.5). The Cretaceous-Tertiary boundary

in Libya, in general, is not marked by any apparent disruption, and no evidence has been found of the iridium layer which marks the boundary in many parts of the world.Tertiary volcanics occur in the Jabal Oweinat-Arknu complex, Jabal Hassawna, Jabal As Sawda, and Jabal Alharuj Al Asswad in Libya.

In the northern sector of the Ghadamis Basin, only a thin succession of Tertiary shallow-marine sediments is present, and it thickens considerably northward towards the Tripolitania Basin and eastward towards the Sirt Basin. In the east on the Cyrenaican platform, deposition of thick, dominantly carbonate strata occurred (Rusk, 2002). Nevertheless gentle tectonic forces during Paleocene times resulted in the gradual tilting of north-western Libya towards the east. In the eastern part of Libya several ridges were uplifted and appeared as islands, both along the southern Stable Shelf (Strougo, 1986) and the northern Unstable Shelf from northern Cyrenaica (Guiraud, et al., 1999). The Ghadamis Basin became emergent by the end of Paleocene whereas subsidence continued in the Sirt Basin. This regional tilting became one of the most persistent features of Cainozoic deposition in Libya (Hallett, 2002).

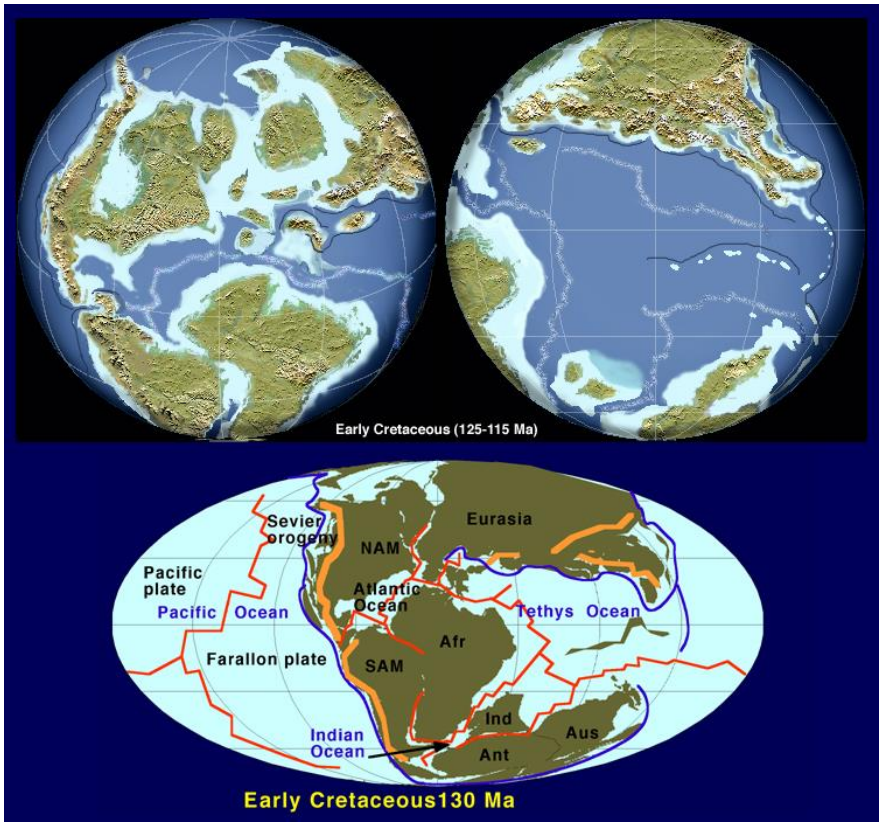

Figure 2.3 Plate reconstructions showing the early opening of the Atlantic and the northward drift of the African plate during the Early Cretaceous (from Northern Arizona University Web)

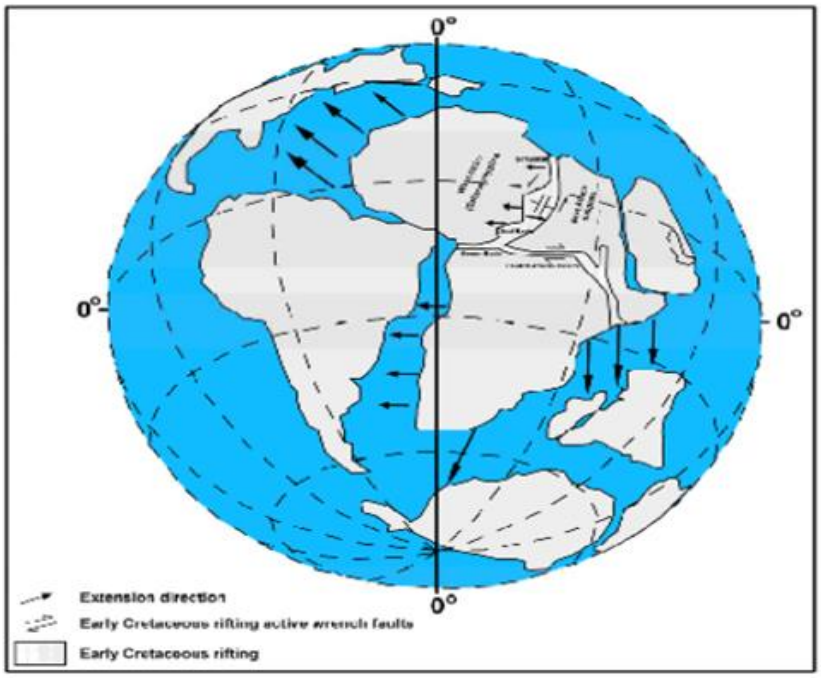

Figure 2.4 Plate reconstruction showing the early opening phase of the South Atlantic and the geometry of the early Cretaceous rift systems in Africa (after Fairhead and Green 1989; Fairhead and Binks 1990; Guiraud and Maurin, 1991, and Anketell,1996).

Cenozoic rocks in Libya show predominantly shallow marine facies that contain major oil and gas accumulations, including reefs, bioherms and near-shore sands particularly in the Sirt Basin. They contain excellent shale and evaporite seals.

The Paleocene succession in Libya is dominated for the most part by shallow-water carbonates deposited in restricted shallow-shelf to open-marine environments. The carbonate platforms usually have a clearly definable ramp margin with more argillaceous sediments occurring in the deeper-water area, basin- ward of the platform margin.

During the Eocene, several carbonate ramps and platforms were established in the Pelagian, Sirt and Cyrenaica Basins. The early Eocene was characterised by uplift of the Cyrenaica area in eastern Libya and the subsequent erosion produced a regional unconformity separating the Cretaceous from the Tertiary (Rolich, 1980; Barr & Berggren, 1980), and it was followed by deposition of Ypresian to Middle Miocene sediments. In the late Eocene, the motion of Africa relative to Europe changed from compressional to right lateral, then into a NW-SE compressional regime in the Early Miocene (Van der Meer et al., 1993). During the Late Eocene to Recent, magmatic activity became widespread on a regional scale and there was extensive basaltic volcanism in North Africa (Wilson & Guiraud, 1998).

During the Oligocene, sediments accumulated in a pull-apart basin formed as a result of strike-slip fault movement. During the Miocene, the most distinct tectonic event of the Alpine collision during the late Cretaceous ended. This was succeeded by a reactivation of the Sabratah-Cyrenaica wrench zone and significant rifting that affected sedimentation in the Pelagian Basin (Hallett 2002), with rapid subsidence in central parts of the basin. Tertiary marine sedimentary rocks of Eocene, Oligocene and Miocene ages occur in Cyrenaica, where they include the greater part of the rocks exposed there, and in the Sirt Basin, and on the Pelagian Shelf. Orogenic movements-beginning in Oligocene time continued into the late Miocene resulting in some crustal warping. The Quaternary rocks in the northern part of Libya are principally continental deposits, but there was one large marine incursion during the Tyirrenhian stage (Goudarzi, 1959). The chief regional structures in Libya are the Jefara Basin, Ghadames basin, Gargaf Arch, Murzuq Basin, Tibesti-Haruj Uplift, Kufra Basin, Cyrenaica Uplift, and Sirt Basin. (Figs. 2.1 and 2.2).

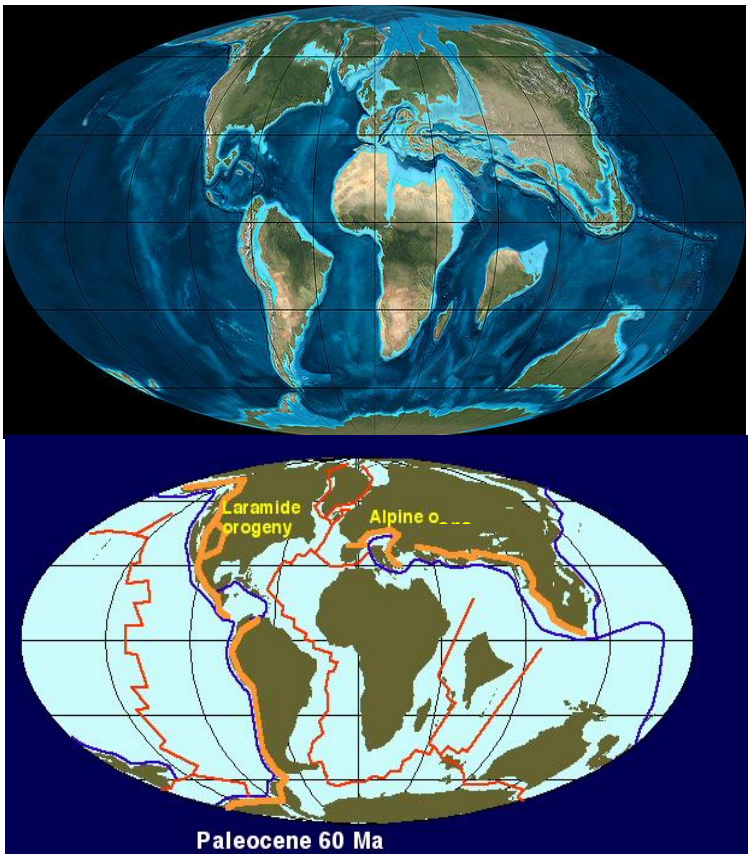

Figure 2.5 During the Paleocene Africa was heading north towards Europe, slowly closing the Tethys Ocean. (Wiki web).

2. 4. SEDIMENTARY BASINS IN LIBYA

As shown in Figure1, Libya consists of four major onshore basins; the Ghadamis Basin in the western part of the country, the Murzuk Basin in the south west, the Kufra Basin in the south east, and the Sirt Basin in the north central part. The Gabes-Tripoli Basin (Sabratah Basin/Pelagian basin) represents the only Libyan offshore basin. In this section a very brief review of the geology of each basin is presented, with the exception of the Sirt basin, whose structural and stratigraphic history is markedly different from the onshore Libyan basins, and the study area is located in it. It is thus dealt with in more detail in a separate section below.

The Ghadamis Basin covers the north-western part of Libya and extends into Tunisia and Algeria. It spreads over an area of 200,000 square kilometres. The western limit of Ghadamis Basin is generally taken along the Messaoud high; the northern limit is marked by the NafusaUplift and the southern limit by the Qarqaf Arch, where the basement rocks are exposed at the core of Jabal Alhasawnah (V.D. Mamgain, 1979) (Fig. 2.1).

The Ghadamis Basin is considered an intracratonic basin and formed during Early Palaeozoic time. The geodynamic history of the Ghadamis Basin was mostly influenced by the Variscan and Alpine unconformities (e.g. Boote et al., 1998; Underdown et al., 2007). Major structural elements in the Ghadamis Basin trend ENE-WSW. The sedimentary section in the Ghadamis Basin is punctuated by several regional unconformities. These include the unconformities between the basement and the Cambro-Ordovician, the Silurian and the Devonian, the Upper Palaeozoic and the Lower Mesozoic, and the Lower and Upper Cretaceous (Hammuda, 1980) (Fig. 2.6). The section becomes thicker and more complete in the central part where the sedimentary thickness exceeds 5000 metres (Goudarzi and Smith, 1978).Most of the Palaeozoic sectionis dominated by continental and marine clastics. These are overlain unconformably by thin continental to marine sediments of Permo-Triassic age.

The Ghadamis Basin has good-to-excellent reservoir and source- rock potential (Hamyouni, 1984). The Silurian shales constitute good source rocks, whereas Paleozoic and Mesozoic clastics, particularly Silurian and Lower Devonian sandstones, provide good reservoirs (Bracaccia et al., 1991; Shah et al., 1993) (Fig. 2.6).

The Murzuq Basin covers the south-western part of Libya, extending into Chad, where it is known of the Djado Basin (Fig. 2.6). It was initiated during the Early Palaeozoic and forms a large intracratonic basin. The sedimentary section in the basin is

punctuated by a number of unconformities which result from epeirogenic movements, particularly during the Palaeozoic. These movements caused pronounced irregularities in the thickness of sedimentary beds in the basin (Conant and Goudarzi, 1967) (Fig. 2.6). The basin is filled with Palaeozoic and Mesozoic sediments of mostly siliciclastics, among which the Mesozoic section is dominated by continental siliciclastics. Cambro-Ordovician and Silurian-Devonian siliciclastics are well developed in the southern part of the basin, while in the northern part the Devonian Tadrart sandstone unconformably overlies the Cambro-Ordovician sandstones (Pallas, 1980).

The Murzuq Basin is filled with sediment ranging in age from the Cambrian to Quaternary and has a maximum total thickness of more than 5,760 metres (mainly siliciclastics) in the deepest parts (Hamyouni, 1984). Palaeozoic siliciclastics form good reservoirs and are sourced by the Silurian shales (Meister *et al.*, 1991). The Silurian strata (main source rock), together with the Devonian and Carboniferous intervals are mature over most of the basin (Hamyouni, 1984).

The Kufra Basin is one of the least accessible and least known of all Libyan basins. It covers about 400,000 square kilometres area in the southeastern part of Libya (Fig. 2.1).The overall geological setting of this basin is similar to that of the Murzuq Basin; both basins overlie basement rocks, are intracratonic, and composed dominantly of siliciclastic sediments (Fig. 2.6). Its Palaeozoic sedimentary section is composed largely of marine sediments that were deposited in the sedimentary basins and sub-basins of North Africa. It unconformably overlies the Precambrian basement, and is considerably thinner than in the Ghadamis and Murzuq Basins (Gumati *et al*., 1996).It is a relatively shallow Palaeozoic basin with the maximum thickness of around 3,500 metres of siliciclastic sediments (Bellini, 1991).

The central part of the basin is filled with continental Mesozoic siliciclastics (Van Houten, 1980, and Klitzsch and Squyres, 1990) that are broadly comparable in facies to those of the Murzuq Basin. The more continental aspect of the facies in the Kufra Basin compared with those of the western basins suggest that it lay farther from the shores of the Tethyan Ocean (Selley, 1997). So far the hydrocarbon potential of the Kufra Basin appears to be poor, possibly due to the absence of structures, and the thermal maturity of the source rocks.

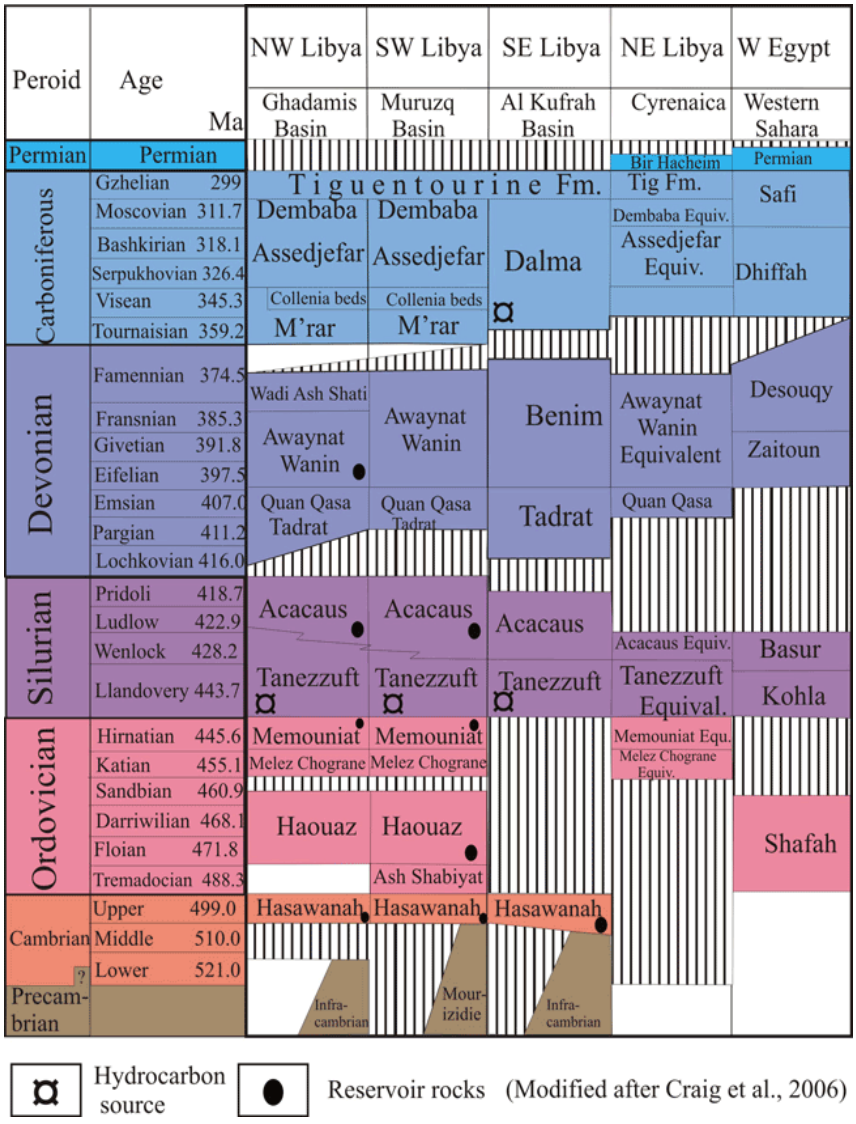

Figure 2.6 Palaeozoic stratigraphic section of southern and eastern basins of Libya.

The Gabes–Tripoli Basin is a Mesozoic–Cenozoic basin which developed over a broad strain zone between the African and European plates during the late Triassic–Middle Jurassic, and is filled with a 10 km-thick succession of Triassic to Recent sediments (Guiraud,1998; Anketell and Mriheel, 2000). Deposition throughout the Gabes–Tripoli Basin was strongly influenced by emergent areas such as the Kasserine and Jaffara Islands, and also by active faulting (related to Cretaceous–Eocene compression of earlier extensional structures) and salt movement (Bishop, 1988; Bernasconi et al., 1991; Zaïer et al., 1998; Anketell and Mriheel, 2000;Reali et al., 2003). Faults associated with the opening of the Tethys Ocean and rifting between the European and African plates controlled sedimentation from the Middle Jurassic to the

present (Morgan and others, 1998). Clastic alluvial sediments from the Saharan Platform were deposited in the southern portion of the basin whereas open marine clastic and carbonate sediments were deposited in the northern portion (Burollet and others, 1978).

The Lower Eocene rocks (Ypressian), which consist of dark-brown marl and mudstone, is considered as the primary source rock in the area, whereas the main reservoir rocks are Lower Eocene and Oligocene to Miocene in age (Klett, 2001) (Fig. 2.7).

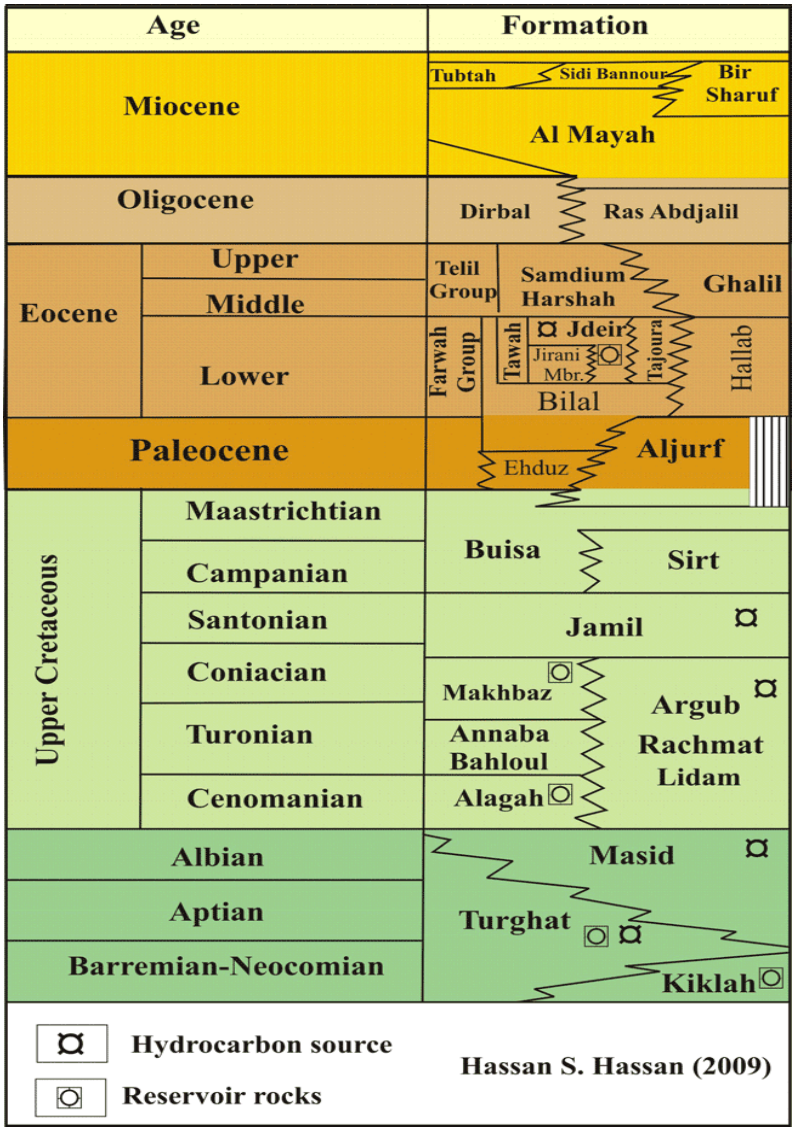

Figure 2.7 Stratigraphic succession of Offshore, NW Libya. Sources: Hammuda (1991), Sbeta (1990), El-Ghoul (1991) and Rusk (2001).

2. 5. Sirt Basin

2. 5. 1. Introduction

The Sirt Basin is one of the youngest sedimentary basins on the African craton. It is located in the north central part of Libya and covers an area of approximately 600,000 square kilometres. It is bounded to the south by the Tibesti Massif and to the west by Nafusah and Qarqaf uplifts; to the northwest the Sirt fault arrays swing westwards into the Gabes-Tripoli Basin; to the east it is bordered by the Cyrenaica platform (Figs. 2.1 & 2.2). The thickness of sediments in the basin increases from about 1km near the Tibesti Uplift in the south to as much as 7 km encountered in the deepest part of the basin (Agedabia Trough) without reaching the basement.

The Sirt Basin is the most important sedimentary basin in Libya as it is the location of most oil and gas production. It ranks 13th among the world's petroleum provinces, having known reserves of 36.7 billion barrels of oil, 0.1 billion barrels of natural gas liquids. More than 23 large oil fields and 16 giant oil fields occur in the province. About 90 percent of the mean total of undiscovered oil (3,545 MMBO), 85 percent of the mean total of undiscovered gas (32,451 BCFC), and 89 percent of the mean total of undiscovered natural gas liquids (1,298 MMBNGL) are estimated to be in the Sirt Basin Province (USGS, 2010).

2.5.2. Tectonic and structural setting of the Sirt Basin

The Sirt Basin province is considered to be a holotype of a continental rift (extensional) area and is referred to as part of the Tethyan rift system (Futyan and Jawzi, 1996; Guiraud and Bos-worth, 1997). It displays an asymmetric half-graben style with gentle ENE dipping platforms and steep WSW facing footwalls (Abadi. 2002). The Sirt Basin developed through inter- and intra-plate movements resulting from the relative motion of the American, African and Eurasian plates during the opening of the Atlantic Ocean and the development of the Mediterranean on the foreland of the African Plate (Anketell, 1996).

The increased volume associated with subcrustal erosion and the heat generation from magma resulted in the doming and expansion of the crust. This process could have produced a crustal uplift of approximately 1-2 km (Arthyushkov et al., 1991) and the formation of the Sirt Arch. This uplift was accompanied by cracking of the rigid crust in response to the rotation of Africa relative to the European block. Strike-slip movement along the Jifarah-Cyrenaica shear zone associated with the opening of the

Mediterranean Sea resulted in the collapse of the Sirt Arch and the formation of the Sirt Basin (Tawadros, 2001). The collapse of the Sirt Arch probably took place in different steps. The initial collapse started in the Triassic in the eastern Sirt Basin and led to the initiation of the Sarir and Hameimat Troughs, followed by the collapse of the main arch during the lower Cretaceous (Tawadros et al., 1991a).

The subsidence of the basin was initiated during the Cambro-Ordovician, and it is thought to have continued subsiding during the Tertiary, reaching a maximum rate of subsidence during the Paleocene – Eocene, corresponding to a period of major crustal extension and reactivation of faults (Berggren, 1974; Gumati and Kanes, 1985; Gumati and Nairn, 1991).The basin, a Mesozoic- Cenozoic intracratonic basin, has evolved as a rifted Tethyan embayment on the northern margin of the African plate. It was developed following a succession of global tectonic events, which led to the breakup of the supercontinent Pangea. The break-up history of the Gondwanan part of Pangaea commenced with the Late Carboniferous and Permian development of the so- called Neo-Tethys and the development of rift system in Gondwana (Ziegler et al., 2001).

These events were marked by opening of the Neo-Tethys in the central and eastern Mediterranean domain during Permian-Triassic time and rifting along the present north-western margin of Africa from middle Triassic onwards (Stampfli, 2000; Ziegler et al., 2001). Gras & Thusu (1998) previously proposed a Triassic age for this and Hallett (2002) pointed out that the evidence for incipient rifting in the Triassic is firmly established.

Presence of Triassic sediments in shallow grabens in the southeast Sirt Basin could provide an indication that the rifting phase in the basin was initiated in the Triassic. However, at least one author has proposed that basin evolution across North Africa and the Middle East is related to lithospheric folding under compression (Wood, 2003). The widespread extension that developed over a broad zone of strain between the two African sub-plates led to the collapse of the Sirt arch during the Early Cretaceous and hence resulted in the formation of the horsts and grabens in the basin (Burk and Dewey, 1974). This event, as explained by Van Houten (1983), resulted from the drift of the African plate, which moved north-central Libya over a fixed mantle hotspot during the Early Cretaceous (Figs. 2.3 & 2.4).

Accepting a rifted origin, some uncertainty exists regarding the timing of initial rifting, probably mainly due to the poor age-dating of the deep stratigraphic succession. Rifting commenced in the Early Cretaceous, peaked in the Late Cretaceous, and

terminated in early Tertiary time, resulting in the triple junction (Sirt, Tibesti, and Sarir arms) within the basin (Harding, 1984; Gras and Thusu, 1998; Ambrose, 2000) (Fig. 2.8). Onset of rifting in the Jurassic was proposed by Abadi (2002) and re-iterated recently by Abadi et al. (2008).

It is widely accepted that the basin was formed by large- scale subsidence and block faulting that started during latest Jurassic/Early Cretaceous time and was reactivated in the Late Cretaceous (Van Houten, 1983) and Paleocene and continued in to the early Eocene (Gumati and Kanes, 1985; Van der Meer and Cloetingh, 1993a, 1993b). The basin has an elongated form and associated major northwest-southeast-trending structural features (horsts and grabens) distinguish it from the adjacent intracratonic basins of Libya (Gumati and Kanes, 1985) (Fig. 2.10). These structural features began forming in the Late Jurassic-Early Cretaceous, and continued to develop until, probably, the Holocene (Selley, 1968). They extend from onshore areas northwards into a complex offshore terrane that includes the Ionian Abyssal Plain to the northeast.

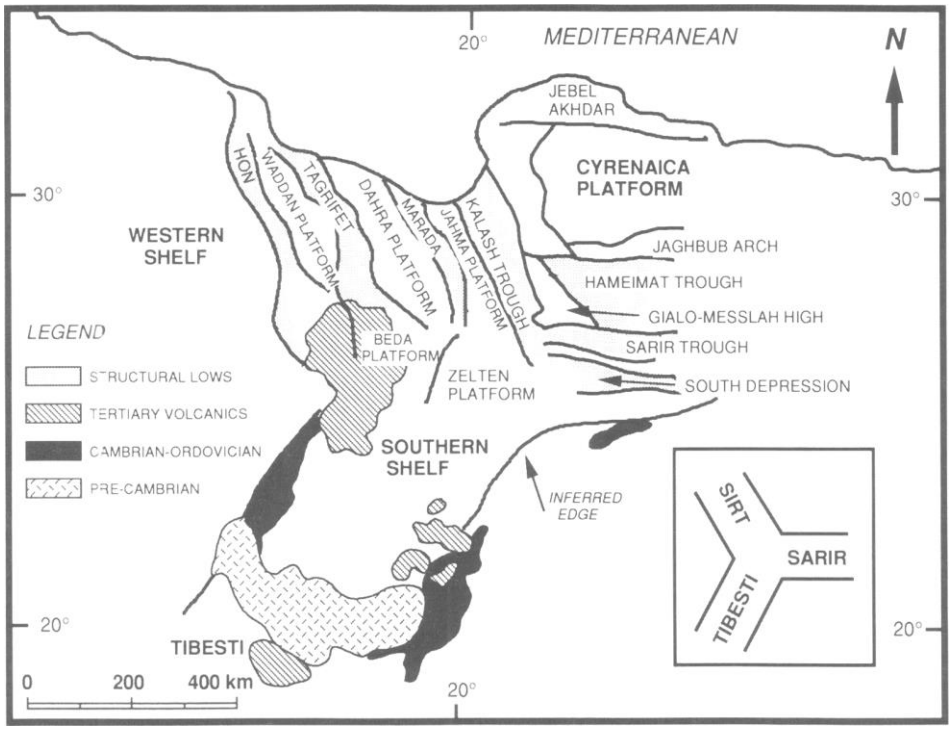

Figure 2. 8 Tectonic elements of the Sirt Basin, showing triple point junction model. Modified after Saenz de Santa Maria (1993).

Based on the Palaeozoic structural trends in Libya the Sirt Arch possibly had an ENE-WSW orientation, and during a long period of emergence in the early palaeozoic, underwent a strong phase of erosion and thick succession of shallow marine to non-marine clastics was deposited during the late Paleozoic to early Mesozoic. Late in early Cretaceous time, the subcrustal magmatic support of the Sirt Arch was removed, and the area collapsed into a series of alternating, NW-SE trending horsts and grabens bounded by deep-seated normal faults (Roohi, 1996) (Fig. 2.10).

Three phases in the evolution of Sirt Basin have been recognized by Harding (1984): a pre-graben sedimentary phase, syn-rift graben development, and post-rift basin fill (Fig. 2.9). The initial pre-graben stage has a regional character to its tectonic, structural and stratigraphic development. The intermediate stage is characterized by normal faulting which resulted in the formation of horsts and grabens and stratigraphic successions. The final stage is characterized by basin- centric subsidence with greater sediment thickness in the central parts of the basin than at its margins.

Paleocene time opened with a new phase of crustal extension beneath the Sirt basin. The renewal vertical movements during the Paleocene produced a strong differentiation between the sedimentation patterns on the horsts and in the grabens in the Sirt Basin. A strikingly greater subsidence rate characterizes the Paleocene and Eocene, and rapid sedimentation was contemporaneous with the basin subsidence. These events were followed by a moderate rate of subsidence that characterizes the major part of the basin (Gumati, 1982). Roohi (1996) has suggested that the block movements in the Sirt Basin were generally downward and nearly vertical with different rates of subsidence until Late Eocene time. During Late Eocene to Oligocene time, a significant down warping movement took place rather abruptly and the present asymmetrical configuration of the Sirt Basin was developed.

The major structure elements of the Sirt Basin, in addition to numerous small horsts and grabens, are; the Hun Graben, Waddan Uplift,Zallah Trough, Dahra Platform, Al Hagfah Trough, Zaltan Platform, and Ajdabiya Trough (Fig. 2.10).

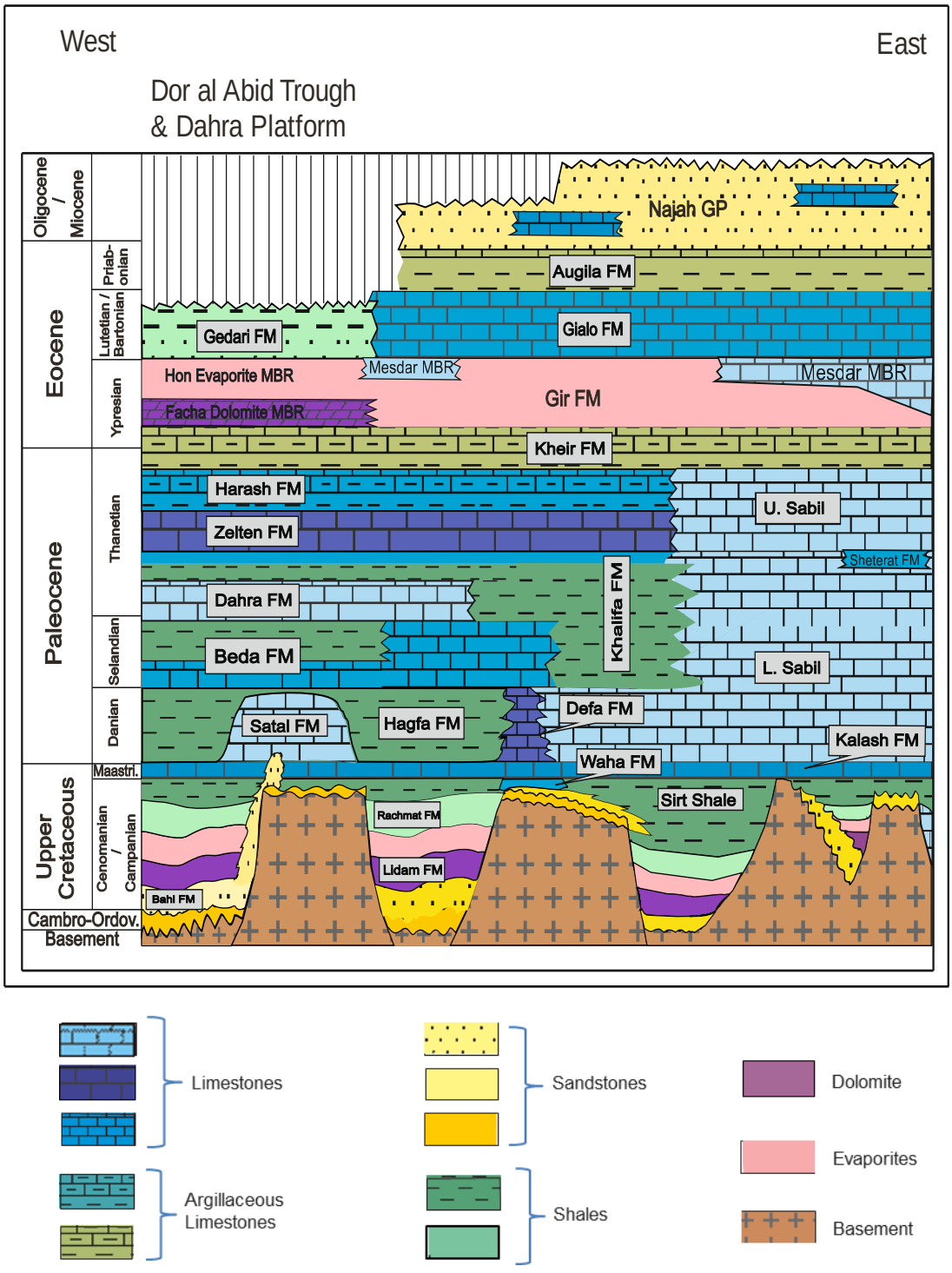

Figure 2.9 Generalized stratigraphic and lithologic chart of the northern Sirt Basin. Compiled and modified by the author, 2012 (nomenclature after Barr and Weegar, 1972).

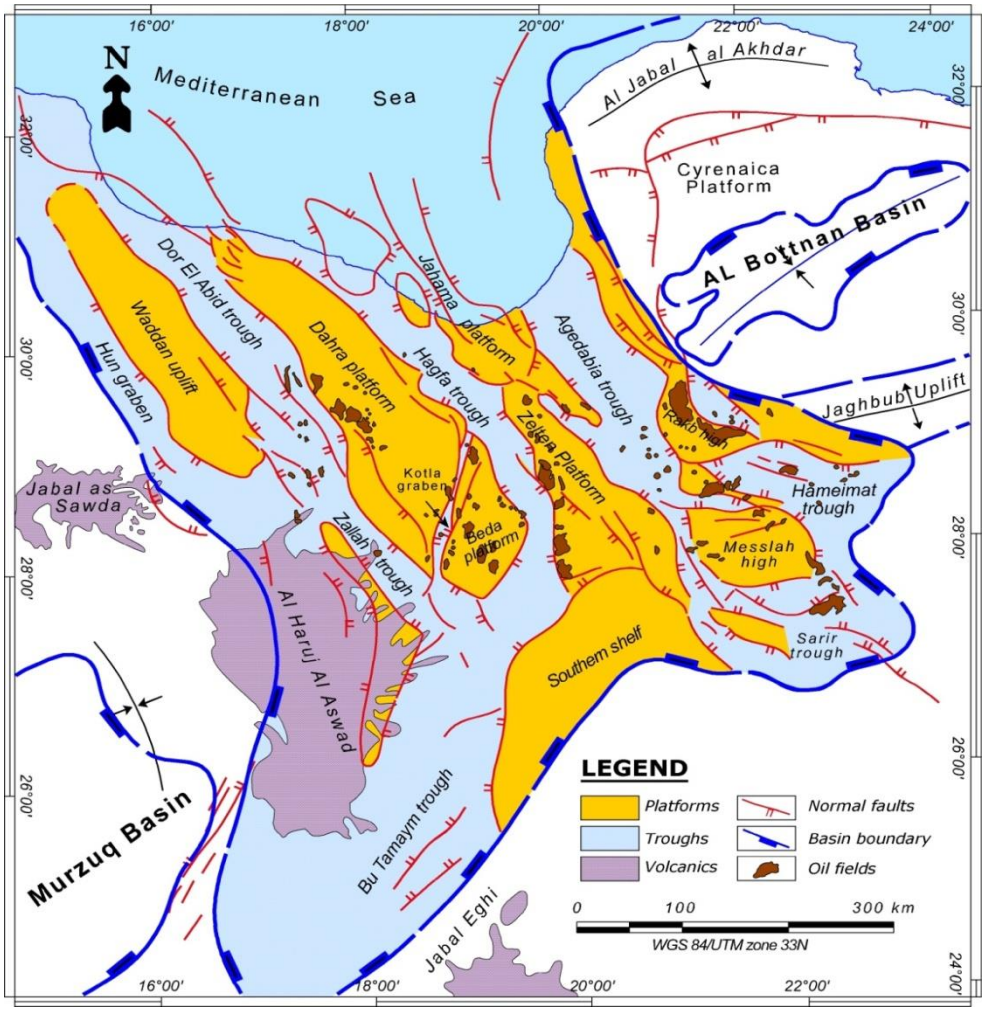

Figure 2.10 Major tectonic elements of Sirt Basin (Abadi, 2002).

2.5.3. Stratigraphic evolution and depositional history of the Sirt Basin

The final stage of the pre-rift phase in Sirt Basin evolution, as recognized by Harding (1984), is characterized by basinal centric subsidence and sediment thickness, and represented by the Upper Jurassic- Lower Cretaceous succession (Nubian Formation). During the syn-rift phase, the basin was subjected to its first major transgression, which resulted in the deposition of marine sediment during Cenomanian time (Bahi, Lidam, and Maragh Formations). The post-rift depositional phase of the basin was on a much gentler scale.

Precambrian rocks have been recorded on several basement highs in the basin, where they predominantly comprise low-grade meta-sediments, volcaniclastics and granitoid intrusives. The radiometric dating of these rocks suggests a Late Precambrian to Early Cambrian age (Koscec et al., 1996).

Generally, the sedimentary succession in the Sirt Basin is typical of those developed in a failed rift system. It ranges in age from Cambro-Ordovician to Recent; It has been assumed that the basement is unconformably overlain by Cambro-Ordovician strata, which are widely spread through-out the basin, but with different names; Gargaf Group, Hofra Formation and Amal Formation. Many authors used the term Pre-Cretaceous or Pre-Upper Cretaceous for these rocks (Figs. 2.9 & 2.11).

Silurian-Devonian strata are known from a few localities in the western part of the basin; Carboniferous and Permian sediments have not been recorded in the Sirt Basin. Sandstones and shales of Triassic age are recorded and well preserved in central and eastern portions of the basin, although non-deposition/erosion occurred on the Waddan Platform and in the Zellah Trough (Corelab report, 2008).

The Late Jurassic- Early Cretaceous succession is well documented and comprises mainly non-marine paralic sandstones and variegated shales (Nubian) (Sinha, 1992 a) with different names as well (Nubian, Sarir, Basal Sandstone). The Variscan Unconformity separates the Nubian formation from the underlying granitic, metamorphic and Cambro-Ordovician basement (Figs. 2.9 & 2.12). During early Alpine time, the Austrian orogenic event resulted in a complex early Cretaceous structural/stratigraphic relationship, which caused widespread emergence and the deposition of a major regressive section during Early Cenomanian time in the northern Sirt Basin. Then a mid-Cenomanian uplift and erosion was followed by a major marine transgression from the north during the late Cenomanian (Wennekers,et al., 1996). This marine transgression covered the basement and non-marine pre-Upper Cretaceous clastics (Nubian sandstone) (Fig. 2.9).

The sandy transgressive sediments, which began to be deposited in the Cenomanian and continued possibly into the basal Paleocene, form a single stratigraphic unit named the Bahi Formation. It consists mainly of sandstones with intercalations of siltstones and shales, and unconformably overlies the Nubian Formation, Amal Formation, or basement volcanics and granites. This is succeeded by shallow-water marine dolomitic limestone and dolomite, and siliciclastics of the Lidam and Maragh Formations, respectively (Fig. 2.9).

Continuing tectonic activity led to the formation of a number of shallow basins during the Turonian in which dolomite, anhydrite and shale were developed (Argub and Etel Formations). The Santonian-Coniacian time was characterized by more open-marine conditions, which led to the deposition of shale, limestone and dolomite of the

Rachmat Formation and shallow-water limestone of the Tagrift Formation in the eastern part of the basin (Fig. 2.9). Deep-marine conditions, especially in the troughs, become established during the Campanian, this resulted in deposition of organic-rich shale (Sirte Shale) which is the main source rock for most of the hydrocarbons in the Sirt Basin.

The uppermost Cretaceous (Maastrichtian) represents the time at which the maximum extent of the marine transgression occurred. Most of the basin was submerged and only the Al Jahamah Platform, few areas of the Az Zahrah Platform and the crest of the Cyrenaican ridge remained as islands during the Maastrichtian (Roohi, 1996). The dominant lithology is the argillaceous, chalky lithofacies of the Kalash Formation. This formation, which occurs over most of the Sirt Basin, is laterally equivalent to the Waha Limestone on the western Zelten Platform (Fig. 2.9).

Sedimentation during late Lower Tertiary was nearly similar to that for the Late Cretaceous, with shallow-marine carbonates and local reefs on the structural highs and deeper-water shales (Hagfa Formation) and carbonates in the structural lows (Fig. 2.12). The Paleocene was a time of renewed vertical movements, which produced a strong differentiation between the sedimentation patterns on the horsts and in the grabens. Transgressive Paleocene seas covered the entire basin (Barr and Berggren, 1981). As a result, a thick succession of marine sediments was deposited in the newly subsident troughs (e.g., Marada Trough). Shales were generally confined to low-energy zones in the trough and blanketed much of the area during the transgressive cycle. Carbonates were deposited on the shelf margins with their facies controlled by water depth, topography, and currents (Gumati, 1982).The basin was dominated, during Paleocene times, by the Az Zahrah-Al Hufrah Carbonate Platform (Satal Bank) in the west, and the As Sabil Platform in the east, in addition to some smaller carbonate platforms in the central parts (Figs. 2.9 & 2.11).

During the Eocene a variety of environments were represented in the basin. These range from deep- water shales through to shallow-water carbonates and evaporites which reach a maximum thickness of over 1800 m in the trough areas (Fig. 2.12). By the end of Eocene time, most the troughs had been filled, and the main trough of the Sirt Basin, the Ajdabiya Trough, contains the thickest sedimentary section in the basin (7000 metres) (Fig. 2.12). It reaches a depth of more than 6000 metres at the coast and may continue to the NW into the eastern Sirt Gulf (Anketell, 1996).

Lithostratigraphically the Oligocene rocks consist predominantly of sandstones, which are locally glauconitic, argillaceous and/or calcareous. The major marine/non-

marine shoreline complex originated in the Oligocene and it persisted through the early Miocene, with fluvial/continental deposition in the southwest and shallow marine to the northeast. In post-Miocene times, the most distinctive event is the major drop in sea level during the Messinian which led to the incision of the As Sahabi channels. Re-establishment of sea -level to its earlier position in Pliocene time filled the vast canyons of the As Sahabi channel and its tributaries (De Heinzelin *et al*., 1980).

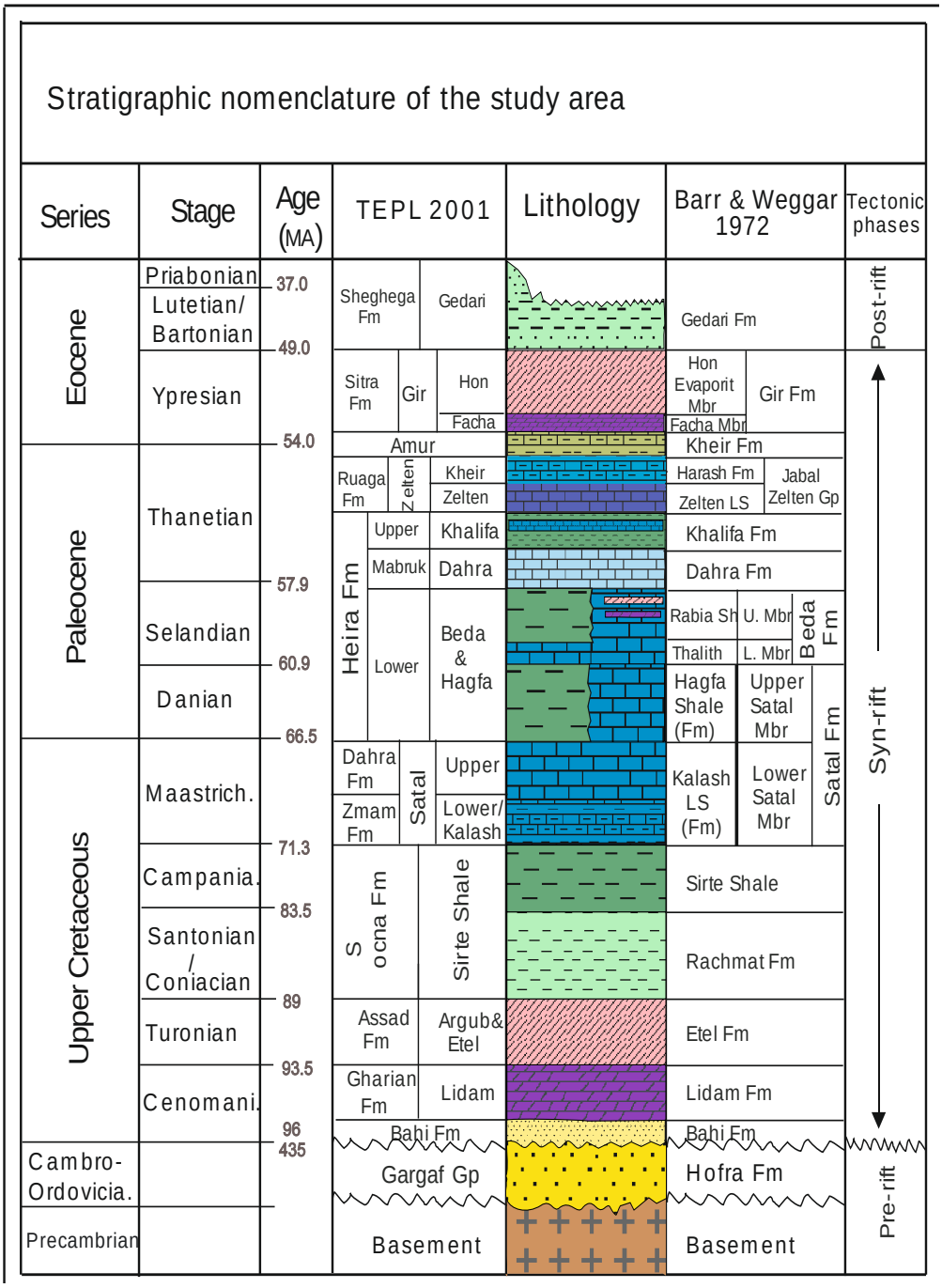

Figure 2 11 Stratigraphic nomenclature of the western Sirt Basin, according to Barr and Weggar, 1972; and TEPL, 2001 (Compiled by the author, 2012).

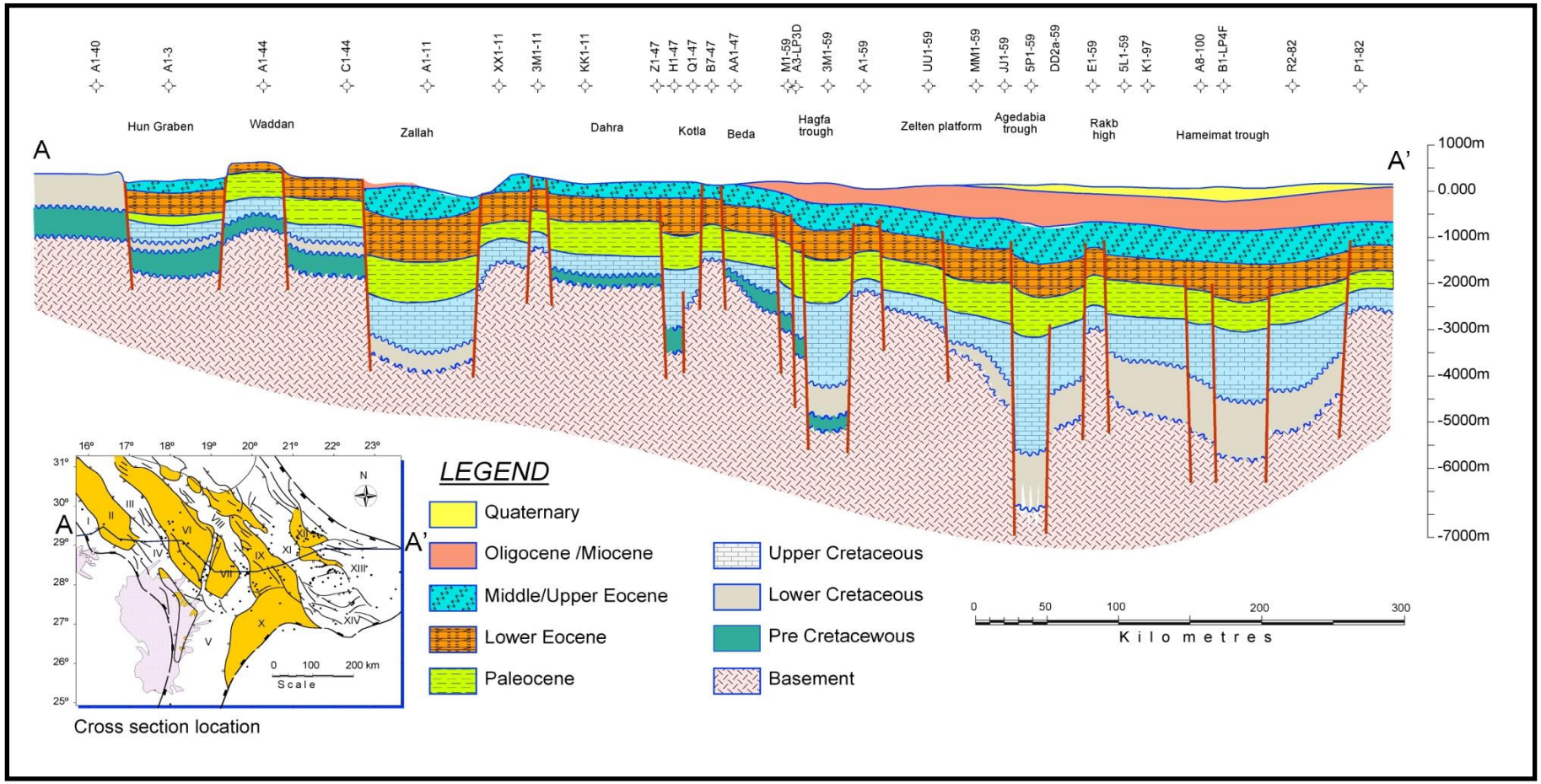

Figure 2.12 Regional structural cross section across the Sirt Basin. Datum is present day sea-level (Abadi, 2002, modified from Roohi, 1996).

2.5.4. Research Area: Dahra Platform, and the Dor al Abid and Zallah Troughs

2.5.4.1. Introduction

The general northwest-southeast arm of the Sirt Basin comprises four major NW-SE grabens with intervening horsts; Hun Graben, Waddan Platform, Dor al Abid Trough, Dahra Platform, Hagfa Trough, Zelten-Jahamah Platform and Ajdabiya Trough. The area of interest, which is located on the western side of the Sirt basin, is comprised mainly of the Dahra Platform, Dor al Abid Trough and Zallah Trough (Fig. 1. 1).

The Dahra Platform, which located between the Dor al Abid Trough and Maradah Trough, is tilted gently to the northeast and occupies an area of about 40,000 km^2. Its southern boundary is represented by the Al Kotlah Graben; the northern boundary is not clearly defined and probably extends to the offshore area (Fig. 2.10). The most prominent structural features on the Dahra Platform are the NW-SE Dahra-Hofrah High and Qattar Ridge on the west; the NW-SE trending Manzila Ridge on the east; and an ENE-WSW trending high connecting the Dahra-Hofrah High and Manzila Ridge.

The Dor al Abid Trough, which is located between the Waddan Uplift and the Dahra Platform, is a NW-SE trending graben with the greatest displacement on the eastern side. It is bordered on the southwest by the northernmost part of the Al Hulayq High, where it swings abruptly SSW into the Abu Tumayam Trough. The Dor al Abid Trough is deepest to the east of the bend in theAl Hulayq horst and shallows steadily to the SSW (Anketell, 1996). The trough is about 50 km wide in the Mabruk area and widen towards the south. The youngest rocks preserved in the trough are of the early Miocene.

The Zallah Trough is an irregular faulted graben that narrows northwards and becomes shallower to form the Dur al Abid Trough. It is bordered to the south by the Abu Tumaym Trough and to the west by the Al Hulayq Ridge and Ma amin Graben, whereas the Waddan and Dahra Platforms formed its northwestern and eastern boundaries, respectively. The Zallah Trough is considered one of the most complex areas in terms of structural relationships in the Sirt Basin. Its stratigraphic section, on the other hand, is represented by rocks as old as Cambro-Ordovician, up to the Miocene.

The Paleocene succession in the study area consists mainly of alternating shallow- marine carbonates and open- marine calcareous shales, with rapid lateral facies changes, which most likely are controlled by the palaeotopography and the differential

subsidence. In addition to academic interest the succession under examination is economically important in that about one-third of Libyan production of hydrocarbons is contained in it. Palaeocene reservoirs, however, contain about 30% of the oil reserves of the Sirt Basin, and oil has been found in structural and stratigraphic traps or a combination of both. The Danian- Thanetian carbonates are the most important producing reservoirs in the giant Dahra and Bahi Fields on the Dahra Platform in the western Sirt Basin, and in the giant Ad Daffah, Al Waha and Zaltan-Nasser Fields, as well as in a number of small fields and the Al Hateibah giant gas- field on the Zaltan Platform in the central Sirt Basin (Futyan and Jawzi, 1996).

2.5.4.2. Geological Setting of the study area

The asymmetry of several of the grabens in the western Sirt Basin has led to the suggestion that the bounding faults are listric faults which sole-out beneath the Mesozoic, with the master-fault and associated synthetic faults on the eastern basin margins, and the antithetic faults forming the western margins. Three systems of faults in the Dahra Platform have been identified by Roohi (1996); these are: NNE-SSW trending faults of Pre-Cretaceous age; NW-SE trending syn-sedimentary faults of Cretaceous age; and NNW-SSE or NW-SE striking faults developed during the Late Tertiary regional tilting. The structural positions of these tectonic features are reflected in the depositional patterns of the Upper Cretaceous-Palaeocene rocks over the Pre-Cretaceous unconformity. Anketell and Kumati (1991b) described the western platform boundary fault inthe Al Hufrah region. They demonstrated a complex series of en-echelon faults, indicating a sinistral strike-slip movement, with associated Riedel shears forming small-scale horst and graben structures. The fault lies close to the assumed junction between the basement of the western and eastern African plates, which were active during the Cretaceous. The platform-margin faults were reactivated as sinistral wrench faults in the Eocene in response to the more rapid movement of the east African Plate in relation to the West African Plate.

The Manzilah Ridge is about 2000 feet structurally lower than the Dahra field which demonstrates that considerable ENE tilt has been imposed on the Dahra Platform since Danian times. It is evident that most of this tilt was imposed during the late Eocene-Oligocene tectonic disturbance, and was accompanied by extensive faulting and fracturing (Halett, 2002). Fault displacement on the platform is usually less than 200 feet, but the platform boundary faults have displacements of 2600 to 3300 feet.

The Dor al Abid Trough is faulted by several normal faults with an almost NNW-SSE trend with displacement of around 800 feet at the base of Upper Cretaceous. Continued subsidence during the Cenozoic has resulted in the formation of structural sag over the Cretaceous graben. During the Late Eocene to Oligocene time, the trough was subjected to deformation and tilting. In the Mabruk area, the depth to the base of the Tertiary is around 5000 feet. The mabruk, Facha and Tagrifet Fields, however, are located updip of the main depocentre of the basin, and are basically faulted anticlines with a northwesterly trend.

The Zallah Trough, as stated above, is considered one of the most complex areas in terms of structural relationships in the Sirt Basin. A very complex system of drag folds and wrench faults within the Paleocene and Eocene has produced flower structures, which in turn, formed oil-traps in that area (Knytle et al., 1996). Subsidence within the Zallah Trough has continued to the present-day and the eastern boundary fault reaches the surface close to well H1-11 (Hallett, 2002). To the west of the Zallah Trough the depth of basement is at only about 5,000 feet, and depth to basement adjacent to the west of Dor al Abid Trough is around 10,000 feet. In the central Zallah Trough, the depth to the base Tertiary is about 8,000 feet.

The sedimentary section in the area starts with sandstone of the Hofra Formation of possible Cambro-Ordovician age. This sandstone is overlain unconformably by Upper Cretaceous marine sediments which, in turn, are overlain by Tertiary marine sediments without any significance interruption. The oldest marine Cretaceous in the Dor al Abid Trough is represented by the Cenomanian Lidam Formation, although the northern part of the Mabruk field was a positive area during pre-Upper Cretaceous up to the Turonian. The youngest rocks preserved in the trough are early Miocene in age (Fig. 2.9). (Hallet, 2002).

The irregular bottom topography that was created, in part, by block faulting during the Early Cretaceous in the Sirt Basin and adjacent area, persisted throughout the remainder of the Cretaceous. This bottom topography was possibly affected by faulting during the Uppermost Cretaceous as indicated by the facies changes from marl through limestone to dolomite during Maastrichtian time throughout the basin.

On the eastern margin of the Zallah Trough a few hundred feet of pre-Cretaceous non-marine sandstone overlies the metamorphic rocks, which in turn, overlie the granitic basement. Lower Cretaceous Nubian Sandstone, along with lacustrine shales of marine and non-marine characteristics, has also been recorded in the

Zallah Trough with upto 2,000 feet thick. The initial incursion of the early Cretaceous sea was followed by a major flooding event in the Cenomanian which extended marine conditions over most of the Sirt Basin, except for the major platform areas which remained as large islands. This marine transgression that continued through the Upper Cretaceous has resulted in the inundation of the low regions and thus a sequence of interbedded shales, carbonates, and some evaporites were deposited.

At the end of Campanian time the uppermost parts of the Dahra Platform structural features became emergent. As shallow-marine deposition progressed, the major highs were gradually submerged by the end of Maastrachtian time except the Manzila Ridge, which was still emergent as an elongated island along the eastern edge of the Dahra Platform (Roohi, 1996). The subsidence curve of Gumati and Kanes (1985) exhibits a sudden flattening corresponds to the Maastrichtian and possibly indicates suspended subsidence during Maastrichtian time. The shallowing of the Maastrichtian Sea was accompanied by deposition of argillaceous limestone of the Kalash Formation over much of the basin and shallower-marine carbonates of the Satal Formation on the Dahra Platform and Dor al Abid Trough (Fig. 2.9). Deposition continued through the lower Tertiary and thick successions of shallow-marine carbonates, shales, and locally, evaporites were deposited in the area.

The start of the Danian was accompanied by widespread rising of the sea level, possibly in response to a regional phase of subsidence. This resulted in the deposition of thick open-marine shales in the subsiding areas (Hagfa Shale). The stable platforms, on the other hand, were largely dominated by carbonate deposits. Thus, distinctive regional Danian carbonate banks were established. The regional, isolated, ellipsoidal-shaped carbonate platform of Maastrichtian to Danian age (Satal Bank) covers the Dahra Platform, crosses the Doral-Abid Trough and extended to the Manzilah Ridge and Al Bayda Platform in the central Sirt Basin (Figs.2.13 and 2.14). The passage from limestone to shale commonly occurs within a distance of a few kilometres and appears to present a ramp configuration rather than an abrupt platform margin (Hallet, 2002).

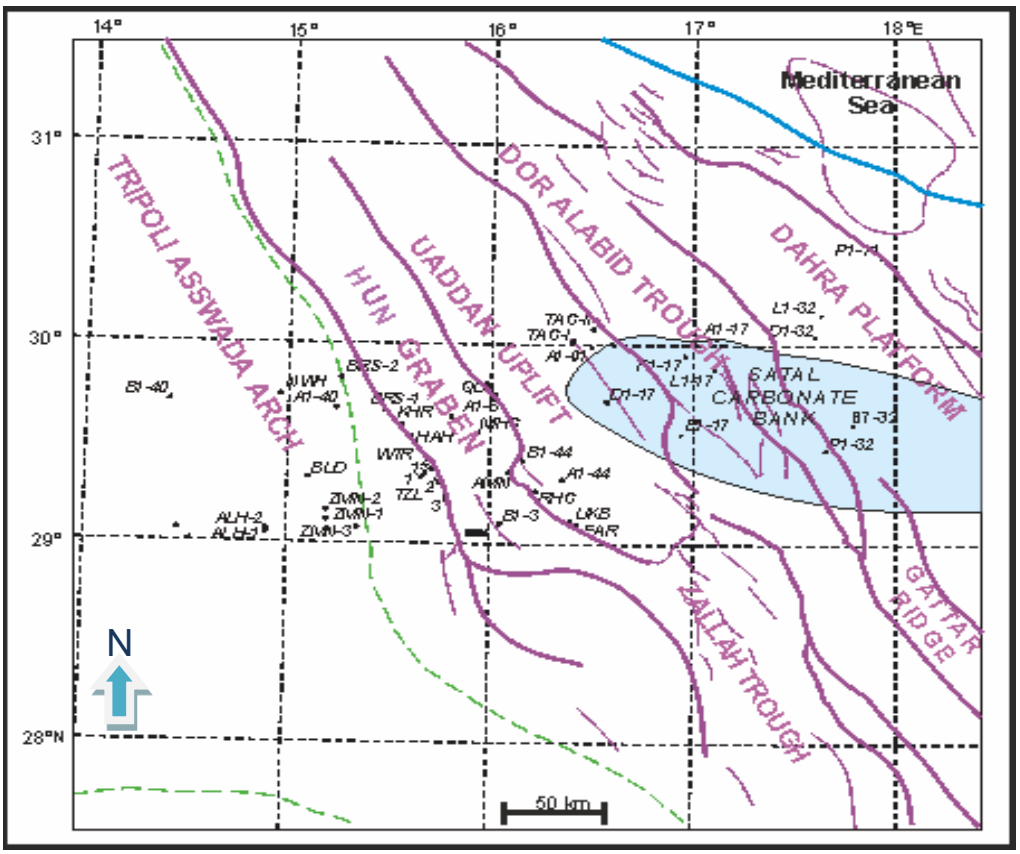

Figure 2.13 Danian carbonate bank (Satal bank) in the western sirt basin (PRC&TPS, 2001).

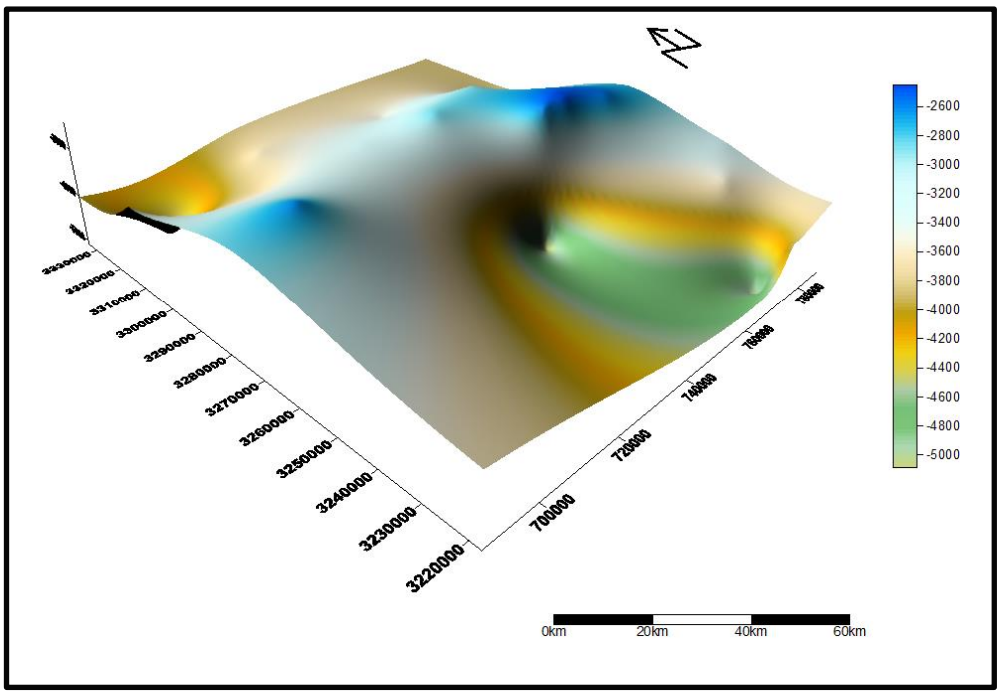

Figure 2.14 3D structure map on top of Satal Formation in the study area.

The Danian Hagfa shale gradually thins as it onlaps the carbonate Satal Bank.

Almost all the pre-Danian palaeotopographic highs were sites of shoal carbonate and reefal growth except the Al Jahamah Platform in the north-central Sirt Basin (Bezan, 1996). The same author pointed out that deposition of the Selandian Beda sediments started with tectonic quiescence along the western shelf of the Sirt Basin. Subsidence temporarily ceased and the carbonate environment dominated both the platforms and troughs, whereas the formation thickens in the Zallah Trough and decreases gradually on the platform areas (Chapter 6).

As a result of a gradual shallowing of the sea carbonate deposition recommenced over the larger part of the study area and the Dahra Formation was deposited. This carbonate deposition was ended by the subsequent transgression over almost the entire area during the late Selandian/Thanetian time, when it was replaced by the open-marine shales of the Khalifa Formation (Fig. 2.11). The interval between the top of the Maastrichtian Kalash Formation and the top of the Khalifa Shale has been traditionally regarded as a Lower Palaeocene depositional sequence by Bezan (1996). This interval, which represents the period between two major transgressive events during the Palaeocene, comprises the Hagfa, the Upper Satal, the Beda, the Dahra and the Khalifa Formations. The Upper Palaeocene depositional sequence, on the other hand, is composed of shelf- margin carbonates at the base and grades upward to marl and limestone of a deep-water environment. It includes the Zelten Limestone, the Harash Formation and the Kheir Formation. Within the latter the Palaeocene/Eocene boundary lies (Fig.2.9).

The thickness of the Palaeocene succession in the study area as a whole approximates close to the underlying structure with thickening in the troughs, where it reaches 3,500 feet, and thinning on the Platforms with less than 1,500 feet (Fig. 2.15). This could indicate that faulting along the edges of the trough was probably syn-sedimentary.

Possibly as a result of the mid-Eocene tectonic activity, many traps on the Dahra Platform are low relief anticlines with a north-western orientation. Alternatively, the complex geometry of the Palaeocene carbonates provides scope for stratigraphic traps. The Dahra field is partly attributed to stratigraphic trapping caused by the rapid shale-out of the Dahra Formation to the west. The Bahi field may be partly fault dependent on its northern margin (Hallett, 2002).

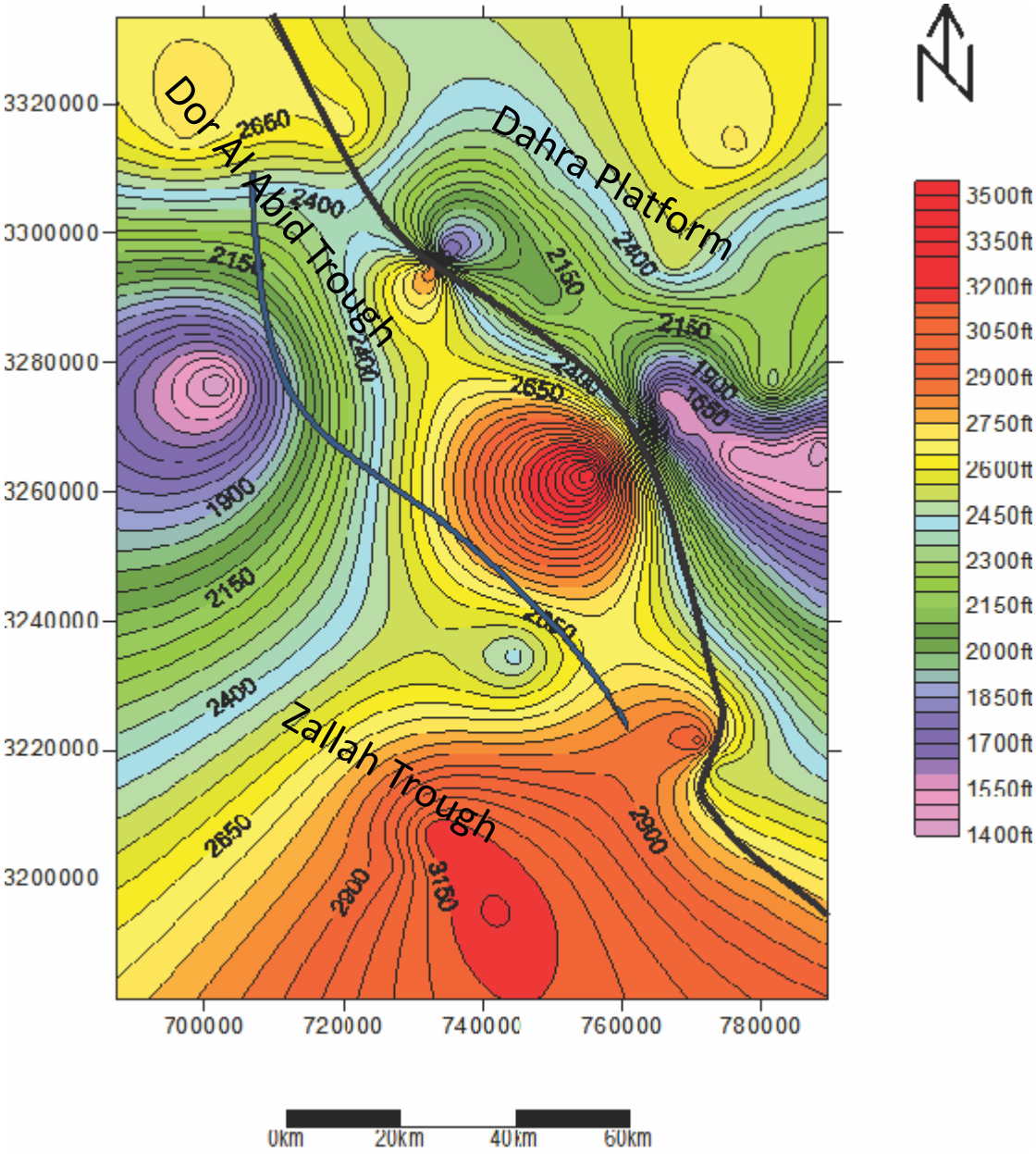

Figure 2.15 Thickness of the total Palaeocene succession in the study area.

2.5.4.3. Palaeocene stratigraphy in the study area

The lithology, stratigraphic position, depositional environment, and petroleum significance of each rock unit within the Palaeocene succession in the study area are briefly reviewed in this section.

2.5.4.3.1. Satal Formation **Age:** Maastrichtian-Danian

The Satal Formation is subdivided by Barr and Weegar (1972) into a lower member of Upper Cretaceous age (Maastrichtian) and an upper member of Lower Palaeocene age (Danian).The contact between these two members is placed at the

stratigraphic position where the underlying unit suddenly becomes more chalky and less dolomitic. This contact coincides with the Maastrichtian-Danian boundary.

The lower member consists of a massive grey to white, moderate to well indurated argillaceous limestone that grades to chalky limestone near the top of the unit. The basal part of Lower Satal was deposited in a relatively deep-marine setting as indicated by the abundance of planktonic microfossils. The thickness of the lower member ranges from 400 to 900 feet in the area. The lower boundary of this member is conformable with the Sirte Shale (Campanian-Maastrichtian) or is unconformable with the Cambrian-Ordovician? Quartzite of the Hofra Formation (Fig.2.9).The upper boundary is marked by a thin (5 -15 feet) diagnostic zone of dense, grey, bivalve limestone (Barr and Weegar, 1972).

The thickness of the upper member of the Satal Formation in the study area ranges from few hundred feet up to 1,500 feet (See Chapter 6). It composed mainly of massive dolomite with traces of anhydrite and fine-grained limestone. Benthic forams, algae and molluscs are common, and a shallow-marine carbonate shelf setting is likely. In the eastern part of the study area it shows a transition from marginal to lagoonal and tidal-flat facies. The upper boundary of the upper member of the Satal Formation is sharp and apparently conformable with the Thalith Member of the Selandian Beda Formation (Barr and Weegar, 1972). The author believes that the Satal Bank was probably drowned as it was terminated by thin beds of Hagfa Shale in the study area (Fig. 2.9).

The Satal carbonate bank extends over an area of 12,000 km^2 from the Waddan Uplift on the west to the Manzilah Ridge on the east and passes laterally and rapidly into the Hagfah Shales (Bezan, 1996) (Fig.2.13). The Upper Satal Member forms the principal reservoir in several fields including the Dahra - Hufrah, Ali, Almas and Arbab fields in the Sirt Basin.

2.5.4.3.2. Hagfa Shale **Age:** Danian

The Hagfa Shale was formally proposed by Barr and Weegar (1972) for a subsurface rock unit in the Sirt Basin lying between the Kalash Formation and the Beda Formation in a conformable relationship with both. The Formation consists mainly of shale with local thin limestone beds, particularly in the upper part. The shale is dominantly grey, soft to medium hard, fissile, splintery and slightly silty, fossiliferous

and calcareous. The limestone is grey, tan and brown, very fine grained, hard, dense, fossiliferous and rarely glauconitic.

The Hagfa Formation is widely distributed in the Sirt Basin, controlled by the palaeogeography of the early Palaeocene time. It is characteristic of the shallower basins, since it present throughout the central Sirt Basin as a deeper-water equivalent of the shelfal carbonates. In the study area, the Hagfa Shale becomes increasingly calcareous and changes abruptly to the Satal Carbonate. It is conformably overlain by the Selandian Beda Formation and overlies the Kalash Limestone of Maastrichtian age (Fig.2.9). The thickness of the formation in the study area varies from zero or very thin on the platform to more than 800 feet in the trough areas (Chapter 6). The abundance of planktonic foraminifers, especially in the lower part of the formation, including *Globoconasa daubjergensis, Globorotalia compressa,*and *Globigerina pseudobulloides* suggest deposition in a fairly deep, open-marine environment.

2.5.4.3.3. Beda Formation **Age:** Selandian

The Beda Formation is widespread over the western part of the Sirt Basin. It is composed predominantly of various interbedded limestones with subordinate calcareous shales and dolomite, which commonly shows a fenestral fabric. The carbonate grains in limestones include ooids, dasycladacean algae, benthic forams, molluscs and echinoids. In the large part of the study area the formation becomes more shaley and is subdivided by Barr and Weegar (1972) into two members: a lower carbonate unit named the Thalith Member, and an upper shale unit named the Rabia Member (Fig.2.9). The Thalith Member is composed of interbeds of argillaceous limestone, calcareous shale and chalky marl. The Rabia Member comprises calcareous shale and mudstone with thin argillaceous limestone interbeds. It is limited in extent to the area around the Dahra - Hufrah fields.

Over much of the study area the Beda Formation overlies either the Danian Hagfa Shale or the upper member of the Satal Formation in a conformable relationship. The Dahra Formation or Khalifa Formation conformably overlies the Beda Formation (Fig. 2.9). The thickness of the Beda Formation in the study area varies widely from few hundred feet in the trough areas up to 1,600 feet on the Dahra Platform (Chapter 6).

The fossiliferous assemblages of the Beda Formation represent a variety of shallow-marine environments of deposition (Barr and Weegar, 1972). The Beda rocks form reservoirs in the Ora, Zaggut and Wadi fields.

2.5.4.3.4. Dahra (Mabruk) Formation **Age:** Selandian-Thanetian

The Dahra Formation was also introduced by Barr and Weegar for a carbonate rock unit restricted to the western part of the Sirt Basin. Its type section was defined in the Fl-32 well, the discovery well of the Dahra East field. Lithologically the formation is composed of argillaceous limestone with subordinate dolomite interbedded with thin shale, particularly at the middle interval. The Dahra Formation consists of, according to Bezan (1996), argillaceous calcilutite limestone interbedded with thick shale intervals at the upper part, and grading downward to skeletal micrite and calcarenitic limestone, frequently dolomitized.

On the Dahra Platform the limestone is broadly light to yellowish grey and ranges from wackestone to grainstone in texture. The main carbonate constituents are benthic forams, echinoderms, molluscs, ooids and green algae. The formation becomes more shaley in the eastern Zallah Trough and passes beneath the Al Haruj al Aswad volcanics as far south as the Abu Tumayam Basin (Bezan, 1996). It is not present to the east and south east of the Dahra Platform, where it is represented by Khalifah Shales.
The Dahra Formation conformably overlies the Beda Formation and underlies the Khalifah Shales (Fig.2.9). The thickness of the Dahra Formation varies from a maximum of 450 feet along the platform/trough margin through around 320 feet in the Zallah and Dor al Abid Troughs to less than 200 feet in the northeastern part of the study area (Chapter 6). According to the fossil assemblages of the Dahra Formation it was deposited in an inner to middle carbonate ramp with local development of reef facies. The Dahra Formation forms the main reservoirs in the Dahra, Hofra and Mabruk oil-fields.

The carbonate unit of the Dahra Formation referred to in some oil company reports as the Mabruk Limestone since it forms the principal reservoir in the Mabruk field, is located in the Dor al Abid Trough. It forms the carbonate member of the shale Heira Formation, where its average thickness is about 150 feet. This carbonate consists of mud to grain-dominated limestone with local occurrence of dolomite in the upper part, and marl with intervals of mud-supported limestone in the lower part. The limestone is largely light yellowish grey to yellowish brown, with wackestone to grainstone and boundstone carbonates. The component grains are dominated by benthic forams, peloids, red algae, corals and calcareous algae. According to the faunal content it was probably deposited on rimmed shelf setting, despite the fact that an isolated platform within a deeper basin model has also been proposed (internal report).

2.5.4.3.5. Khalifa Formation **Age:** Selandian-Thanetian

The Khalifa Formation is mainly a shale unit that separating the underlying Dahra Formation from the overlying Zelten Formation. Its type section was defined by Barr and Weegar, 1972 in concession 59 on the Beda Platform. The formation consists of an upper argillaceous limestone unit and a lower shale interval. The limestone is dark grey, moderately indurated and argillaceous with minor calcareous shale. The lower shale unit is dark grey to black, fissile and slightly pyritic with local thin calcareous intervals (Barr and Weegar, 1972). On the platform crestal areas the lower unit passes into a shallow-water carbonate facies of the Dahra Formation. In the areas where the carbonates of the Dahra and Beda formations are absent or thin, the Khalifa Shale thickens to incorporate the shale intervals equivalent to both formations. The separation of the Khalifa Shale Member from the remaining shales of Selandian and even the Danian time is almost impossible (Bezan, 1996). Accordingly, Esso Standard of Libya designated this compiled shale into the Heira Formation and ranked the shale enveloped carbonate units as formation members.

The Khalifa Formation conformably overlies the Dahra Formation, Beda Formation or Hagfa Shale and is overlain by the Zelten Formation (Fig. 2.9). The formation ranges in thickness from 150 feet on the Dahra Platform through 200 feet in Dor al Abid to more than 400 feet in Zallah Trough (Chapter 6). The fossil assemblage of the shale unit of the Khalifa Formation, which contains planktic forams suggests an open-marine environment of deposition, whereas the common benthic forams, particularly miliolids in the argillaceous limestone unit strongly suggests a shallow-marine setting. On the Dahra Platform and in Dor al Abid Trough the Khalifa Shale is well developed, forming a seal for the underlying Dahra (Mabruk) carbonate reservoir.

2.5.4.3.6. Zelten Formation **Age:** Thanetian

The Zelten Formation is widespread across the western and eastern parts of the Sirt Basin.In the central and south-central parts of the Sirt Basin, the Zelten Formation consists mainly of grey-coloured limestone, slightly argillaceous and chalky interbedded locally with thin, greenish grey, pyritic shale and becomes locally biohermal. It contains common fragments of bryozoan, corals, algae and echinoderms. In the study area, on the Dahra Platform, the formation consists predominantly of light grey to light yellowish grey limestone, slightly argillaceous and locally dolomitic. The limestone is mainly grain-supported packstone and consists primarily of benthic forams,

molluscan shells and echinoderm fragments. Nummulites and bryozoans are locally developed. Mud-supported carbonates, which are frequently dolomitized, are sporadically present.

In the study area, the Zelten Formation conformably overlies the Khalifa Formation and underlies the Harash Formation. Towards the east, the formation is formally referred to as Upper Sabil Member and in the south-central part of the basin the Zelten Formation cannot be differentiated easily from the overlying Harash Formation and thus a Jabal Zelten Group is used instead (Fig. 2.11). The thickness of the Zelten Formation in the study area ranges from less than 200 feet on some platform areas to more than 400 feet in certain trough areas (Chapter 6). The fossil contents and the characteristic sediments of the Zelten Formation indicate an inner to mid platform setting of shallow marine environment. It forms the main reservoir of the Zelten Field in the central part of the Sirt Basin.

2.5.4.3.7. Harash Formation **Age:**Thanetian

This formation was introduced by Barr and Weegar (1972) for widespread rocks in the western and central Sirt Basin. It is composed broadly of white to brown argillaceous limestone with thin interbeds of grey to green, calcareous shale. On the Dahra Platform of the study area, it consists chiefly of light to yellowish grey limestone, locally dolomitic with thin interbeds of greenish grey, fissile and calcareous shale. The limestone is largely grain-supported packstone with local occurrence of wackestones. The component grains are dominated by nummulites, small benthic forams, bryozoan and bivalves. Planktic forams, echinoderms and green algae also occur.

In the study area, the Harash Formation conformably overlies the Zelten Limestone and is overlain by the Kheir Formation. In the south-central part of the basin the Harash Formation cannot be differentiated easily from the underlying Zelten Limestone and thus a Jabal Zelten Group is used instead (Fig. 2.11). In the central Sirt Basin the thickness of the Harash Formation reaches 290 feet, on the Dahra Platfortm it is less than 150 feet, whereas it reaches 360 feet in central part of the Zallah Trough. According to the fossil content and sediment characteristics of the Harash Formation, an inner to mid platform with a shallow-marine environment is strongly suggested.

2.5.4.3.8. Kheir Formation **Age:** Thanetian – Yepressian

The Kheir Formation is widely distributed throughout much of the Sirt Basin. In its type section in the central part of the basin, the formation composed predominantly of alternating beds of shale, marl and limestone. The shale is grey to dark grey, fissile and calcareous. The marl is grey and soft, whereas the limestone is grey, fossiliferous and slightly pyritic.

In the central Sirt Basin the Kheir Formation conformably overlies the Upper Sabil carbonates, and is overlain by the Lower Eocene Gir Formation. It therefore spans the upper Palaeocene/lower Eocene boundary according to recorded foraminifera (Wennekers et al., 1996). Over a large part of the study area, however, the Kheir Formation conformably overlies the Harash Formation and overlain by the Facha Dolomite Member of the Lower Eocene Gir Formation (Fig. 2.9). The thickness of the Kheir Formation in the central Sirt Basin is around 270 feet, whereas in the study area it varies from less than 200 feet in the Dor al Abid Trough to about 400 feet in the Zalah Trough (Chapter 6). The formation contains common microfossils, including *Operculina* and smaller benthic and planktic forams. Thus the open marine environment characteristic of this formation is correlated over long distances across the Sirt Basin, implying stable conditions of sedimentation during the late Palaeocene to early Eocene time (Belazi, 1989).

In the east central part of the Sirt Basin the shale interval of the Kheir Formation provides an impermeable top seal in the Harash and Naser oil-fields.

2.5.5. Summary

Libya is a cratonic basin on the northern fringes of the African shield; its northern part is situated on a tectonically active subsiding margin, whereas the southern part of the country lies within the stable cratonic area (Gumati, et al., 1991).The structure of southern Libya was influenced by the Pan African event; the central part was affected by the Variscan tectonic events, whereas the structures of the northern portion are attributed to the Tethyan extension and alpine tectonic movements (Goudarzi, 1980).Caledonian and Hercynian, as well as movements during Late Cretaceous and Oligocene through Miocene times and possibly Holocene too, developed the major features that form the present-day structural elements of Libya.

The country consists of four major onshore basins: the Ghadamis Basin, the Murzuk Basin, the Kufra Basinand the Sirt Basin. The last, which is the youngest of the Libyan basins, is developed through inter- and intra-plate movements resulting from the relative motion of the American, African and Eurasian plates during the opening of the Atlantic Ocean and the development of the Mediterranean on the foreland of the African Plate (Anketell, 1996). Rifting in the Sirt Basin commenced in the Early Cretaceous, peaked in the Late Cretaceous, and terminated in early Tertiary time, resulting in a triple junction (Sirt, Tibesti, and Sarir arms) within the basin (Harding, 1984; Gras and Thusu, 1998; Ambrose, 2000). Onset of rifting in the Jurassic was proposed recently by Abadi et al. (2008). The basin has an elongate form and associated major northwest-southeast-trending structural features (horsts and grabens) distinguish it from the adjacent intracratonic basins of Libya (Gumati and Kanes, 1985).

The sedimentary succession in the Sirt Basin is typical of those developed in a failed rift system and ranges in age from Cambro-Ordovician to Recent. Sedimentation during the late Lower Tertiary was characterized by shallow-marine carbonates and local reefs on the structural highs and deeper-water shales and carbonates in the structural lows. The Paleocene was a time of renewed vertical movements, which produced a strong differentiation between the sedimentation patterns on the horsts and in the grabens.

The area of interest, which is located on the western side of the Sirt basin, is comprised mainly of the Dahra Platform, Dor al Abid Trough and Zallah Trough. The Paleocene succession in the study area consists mainly of alternating shallow-marine carbonates and open-marine calcareous shales, with rapid lateral facies changes, which most likely are controlled by the palaeotopography and the differential subsidence. The

sedimentary section in the study area starts with sandstone of the Hofra Formation of possible Cambro-Ordovician age. This sandstone is overlain unconformably by Upper Cretaceous marine sediments which, in turn, are overlain by Tertiary marine sediments without any significant interruption

The interval between the top of the Maastrichtian Kalash Formation and the top of the Khalifa Shale has been traditionally regarded as a Lower Paleocene depositional sequence by Bezan (1996). This interval, which represents the period between two major transgressive events during the Paleocene, comprises the Hagfa, the Upper Satal, the Beda, the Dahra and the Khalifa Formations. The Upper Palaeocene depositional sequence, on the other hand, is composed of shelf-margin carbonates at the base and grades upward to marl and limestone of a deep-water environment. It includes the Zelten Limestone, the Harash Formation and the Kheir Formation.

The thickness of the Palaeocene succession in the study area as a whole approximates close to the underlying structure with thickening in the troughs and thinning on the platforms. This could indicate that faulting along the edges of the trough was probably synsedimentary.

The Palaeocene Satal, Beda and Dahra carbonates form reservoirs in many oil-fields in the study area, whereas the shale of Hagfa, Khalifa and Beda (Rabia) represent impermeable top seals for the underlying reservoirs.

CHAPTER THREE: SEDIMENTOLOGY OFTHE DAHRA PLATFORM AND DOR ALABID TROUGH

3.1. Introduction

The Paleocene succession in Libya is dominated largely by shallow-water carbonates deposited in restricted shallow-shelf to open-marine environments. In Sirt Basin, particularly in central and western parts, the succession is characterized by rapid lateral facies changes and vertical alternation of carbonates and shales. The carbonates were deposited on shallow to moderate depth platforms developed upon structural highs, separated by deeper water mudrock facies in basinal depressions.

The study area, which comprises the Dahra Field on the Dahra Platform and Mabruk Field in Dor al Abid Trough, is composed generally of limestone, dolomitic limestone, argillaceous limestone/marl and shale. Carbonates of the Lower Paleocene form a major hydrocarbon reservoir in several fields in the west central Sirte Basin. All those fields are aligned along a WNW-ESE trend, which is interpreted as a reef and shoal belt facies zone tracking a seaward carbonate platform margin, which can be followed across the Dahra-Hofra Platform (Pawellek, 2009).

The grain composition of carbonate sediments and rocks often directly reflects their environment of deposition because of the general lack of transport in carbonate regimens and the direct tie to the biological components of the environment (Moore, 1989). Carbonate sands under the influence of directed currents will exhibit appropriate bedforms and cross-stratification as a function of current characteristics (Ball, 1967). Carbonate muds will be winnowed if enough wave or current energy is present in the environment.

Irrespective from general geology, common lithology and broad environmental setting, almost nothing have been published on sedimentology and petrography of the Dahra, Mabruk, Zelten and Harash Formations in the study area. Hence the results presented here provide new information to the geology of Paleocene Succession in the western part of the Sirt Basin.

Description, discussion and interpretation of the Selandian/Thanetian Carbonates deposited on the Dahra Platform and/or in Dor al Abid Through along with identification of general lithofacies, macrofacies and its associated microfacies are dealt with in detail throughout this chapter. Vertical and lateral variations of these carbonates

both on platform and in trough along with the identification of palaeo-environments and proposition of depositional geological setting are also incorporated.

3.2. Facies analysis

The studied intervals of the Paleocene succession on the Dahra Platform are comprised of the Dahra, Zelten and Harash Formations, whereas in the Dor al Abid Trough only the Dahra Formation equivalent, i.e. the Mabruk Member of the Heira Formation is involved. Complete detailed logs of the cored interval of these carbonate units at 1:100 scale can be found at the Appendix 1.

3.2.1. General Lithofacies

Careful examination of the studied intervals, which is mainly based on macroscopic and microscopic analysis, has resulted in the recognition of four main collective lithofacies; limestone, dolomitic limestone/dolomite, argillaceous limestone/marl, and shale lithofacies. The latter two facies are described below, while macrofacies and its associated microfacies of the carbonates are discussed, in detail in the next section (3.2.2.; Tables 3.1and 3.2).

3.2.1.1. Marl/ argillaceous limestone and shale

In the Dor al Abid Trough the marl is widely distributed and covers large part of the Paleocene succession (Heira Formation), where it locally grades to very calcareous shale (Fig.2.11). It represents the dominant lithofacies within the lower part of Mabruk Member and interbeds with bioclastic and slightly dolomitic limestone. Within the upper part of Mabruk the marl is much less common and occurs as thin layers interbedded with limestone and dolomitic limestone. Itis commonly light grey to greenish grey, locally light olive grey, soft to firm, sub-fissile to sub-blocky, with scattered fragments of coral, red algae, bivalve shells and benthic forams. It is locally burrowed and compacted with the development of pyrite at particular intervals (Fig. 3.1 &Appendix 1). The shale is commonly grey to dark grey, sub-fissile to fissile, brittle and calcareous.

Within the studied interval on the Dahra Platform the term shale is widely used and comprises commonly marl and/or very argillaceous limestone facies. It occurs as medium to thin beds that are intercalated with wackestone/packstone facies in the Dahra

and Harash Formations. It is usually medium grey to greenish grey, fissile, dolomitic, slightly pyritic with scattered small un-identifiable fragments (Fig.3.1&Appendix 1).

3.2.1.2. Limestone, dolomitic limestone/dolomite

Carbonate dominated intervals are widely distributed on the Dahra Platform, where they intercalate with the shale units not only in the Selandian/Thanetian section but also throughout the Paleocene succession. On the other hand, these carbonates are developed at certain intervals in the Dor al Abid Trough, particularly within the Selandian/Thanetian succession. The sedimentological and petrographical characteristics these carbonates are discussed below.

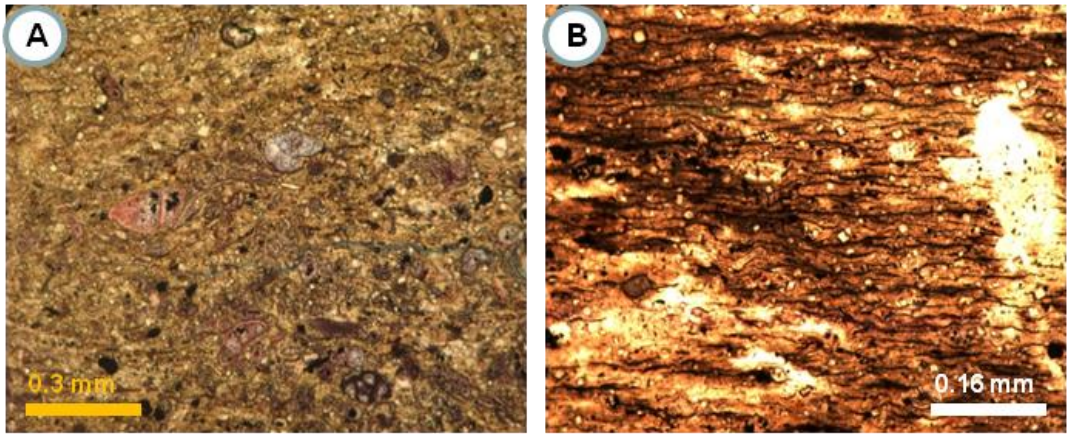

Figure 3.1 Thin-section photomicrographs of: A) Marl lithofacies with scattered benthic forams, pyrite and intragranular Fe-rich calcite. Dahra Fm (3315 ft), well no.7; B) Fissile, dolomitic, compacted and slightly pyritic shale. Dahra Fm (3267 ft), well no. 9.

3.2.2. Macrofacies and associated microfacies

During the course of the petrographic study, the percentages of constituent grains, matrix, cement and porosity were estimated visually using the comparison charts of Baccelle and Bosellini (1965). The carbonate samples were classified according to Dunham (1962), Embry and Klovan (1971), and Wright (1992). To make the name more qualified and to give information on mineral and grain composition, the most abundant grain types in a given sample have been added to the rock name. A semi-quantitative composition of the studied section has been determined using whole rock XRD analysis for selected samples. Burrow density was determined using semi-

quantitative bioturbation index (BI) of Taylor and Goldring (1993) which is composed of six grades.

Macroscopic and microscopic investigations of the studied samples, which include details of grains, cements, microfabrics, micro-sedimentary structures and diagenetic features, has resulted in the recognition of seven main macrofacies and eleven associated microfacies within the Selandian/Thanetian carbonate succession. A brief description of these macrofacies is summarized in Table 3.1, while the occurrence, description and interpretation of the associated microfacies are discussed below:

3.2.2.1. Bioclastic foraminiferal P-P/G

3.2.2.1.1. Bioclastic foraminiferal packstone/grainstone (PMF1)

The bioclastic foraminiferal packstone/grainstone microfaciesis widely distributed, occurring within the Dahra, Zelten and Harash Formations on both the Dahra Platform and Dor al Abid Trough (Table.3.1).

Within the Dahra Formation on the Dahra Platform it is composed predominantly of rotaliids, miliolids, bivalve shells and echinoderm fragments. Bryozoa, intraclasts, coated grains and green algae are less common with scattered planktic forams, crinoids and extraclasts (Fig.3.2A&B). These components are commonly present in a matrix of micrite and cemented patchily by equant calcite. Pyrite, hematite and less commonly glauconite are associated throughout (Fig.3.2 A&C, and Table.3.2). Local development of dolomite crystals as an intragranular cement is present in well No.10 (Fig. 4.3.F–next chapter). The bioclastic foraminiferal packstone microfacies on the Dahra Platform is ascribed to a shallow- marine lagoonal environment with semi-open circulation. It would correspond to SMF 10 of Flügel (2004).

Within the Mabruk Memeber in the Dor al Abid Trough it is comprised mainly of rotaliids, echinoderms and bryozoa. Miliolids, peloids, bivalve shells, green algae and calcareous algae are also present with scattered planktic forams, brachiopods, coral fragments and ostracods (Fig.3.2 C&D). Pressure dissolution seams with scattered stylolites are developed locally, particularly in well No.105, whereas partly cemented fractures were noticed in well No. 66. Pyrite, glauconite, phosphate and rarely limonite are developed locally, particularly at depths 3248-3250 feet in well No. 66, along with bored bioclasts and coarse dolomite crystals (Figs.3.2C& 4.1- next chapter). Extensive

dissolution mainly of bioclastic grains is recorded at 3726 ft. in well No.105 and at 3303.5-3305 ft. in well No. 66; within the latter Fe-minerals are concentrated.
According to the faunal content and based on its stratigraphic position this microfacies represents deposition on an inner-shelf, shallow-marine environment that was separated from the open shelf by a carbonate build-up or reef. It may correspond to SMF 18 of Flügel (2004).

Within the Zelten and Harash Formations on the Dahra Platform it is comprised chiefly of echinoderm fragments, rotaliids, and bryozoa. Bivalves, echinoid spines, miliolids, planktic forams and nummulites are scattered throughout with rare green algae, gastropods, *Alveolina*, *Assilina* and red algae (Tables. 3.1& 3.2). Mechanical and chemical compaction has resulted in the development of fracturing, pressure dissolution seams and stylolites. Some precipitation of pyrite, glauconite and phosphate took place. Extensive dissolution intervals within this microfacies have been recorded in wells No. 9 and No.10, in spite of the fact that most of those intervals contain later coarse calcite and dolomite cements. This microfacies is ascribed to an inner ramp (lagoon or back bank) with a regime of moderate to slightly high energy. It could correspond to SMF 10 of Flügel (2004).

3.2.2.1.2 Dolomitic bioturbated bioclastic packstone (PMF2)

Within the Dahra Formatiion on the Dahra Platform it is composed principally of rotaliida, miliolids, echinoderm and small unidentifiable fragments. Bivalves, gastropods, intraclasts and bryozoans are also present with scattered green algae, peloids, red algae and extraclasts. These component grains are present in a matrix of partially dolomitized and bioturbated micrite (Fig.3.2G) and are locally cemented by syntaxial rim, ferroan calcite and ferroan dolomite cements. Dolomite is widely distributed in this microfacies where it not only replaces large parts of the micrite matrix and some bioclasts but also occurs as void-filling cement (Fig. 4.3- next chapter). The burrowing is usually horizontal, with some occurrence of sub-vertical or sub-horizontal ones. Bioturbation index commonly ranges from 2-4 (Fig. 3.3&Appendix.1). Porosity is almost negligible except where unstable grains, particularly bivalves, are dissolved out. Burrows and bioturbation provide information on conditions of life in sediments and thus about the depositional environment (Curran, 1991). This microfacies, however may

represent deposition in a shallow-marine lagoonal environment and could correspond to SMF 9 or 10 of Flügel (2004).

The dolomitic bioturbated bioclastic packstone microfacies, which is not widely distributed in the Mabruk Member in the Dor al Abid Trough, is composed mainly of rotaliida, echinoderm fragments and bryozoans. Other less common fossil debris includes that of red algae, small forams, corals and ostracods (Fig.3.2 E, F and H). It grades locally to rudstone where a significant percentage of the bioclasts are coarser than 2 mm, particularly in well no.66. The average size of the dolomite crystals that replaced the micrite substrate is around 80 µm, whereas the void-filling dolomites are about 200µm. Burrowing is commonly horizontal with a bioturbation index of almost 3-4 (Fig. 3.3 & Appendix.1).Fe- minerals, particularly pyrite occur locally. Apart from some intragranular voids and microfractures, the overall porosity is negligible. The dolomitic bioturbated bioclastic packstone microfacies in this particular setting is ascribed to an inner-shelf, shallow-marine environment that was possibly separated from the open shelf by a carbonate build-up or reef. It would correspond to SMF 18 of Flügel (2004).

Within the Zelten and Harash Formations on the Dahra Platform it is similar in composition to that in the Dahra Formation, but with the occurrence of echinoid spines and nummulite fragments. Planktic forams, and ostracods are scattered throughout (Tables.3.1& 3.2). These grains are cemented locally with equant sparry calcite cement that is locally iron-rich. A large part of the micrite matrix and bioclasts along with many burrows has been subjected to dolomitization. Burrowing is slightly less extensive than that of the Dahra and Mabruk, as the average of bioturbation index is around 2 (Fig.3.3 & Appendix.1). The average size of dolomite crystals is 20-30µm, whereas much larger crystals of dolomite are recognised as void-filling cement (Figs.4.3F and 4.6- next chapter). Pyrite and rarely glauconite, phosphate and limonite are developed in almost all the studied wells on the Dahra Platform (Table 3.2). Porosity is broadly negligible to poor; although certain intervalshave good to very good dissolution porosity. This microfacies is probably ascribed to a shallow-marine back-bank setting. It may correspond to SMF 9 or 10 of Flügel (2004).

Table 3.1 Facies and associated microfacies of the Dahra Formation on the Dahra Platform

Facies No.	Facies Name	Description	Microfacies	Micro-facies code	Thin-section photos	Depositional setting	Remarks
1.	Bioclastic foraminiferal packstone-packstone/grainstone	Light yellowish grey to v. pale orange, locally mottled, m. sorted with abundant benthic forams and shell fragments of different bioclasts. Levels of echinoderm fragments and/or molluscan shells in wells 7&8. Locally dolomitic and bioturbated. Slightly argillaceous with sporadic development of stylolites and PDS. Local concentration of iron minerals, particularly in wells 10 & 8. Overall porosity is fair to good.	Bioclastic foraminiferal packstone	PMF 1	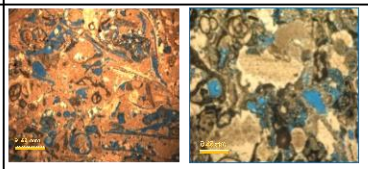 W10-D, 3129 ft. W7-D, 3297 ft	Inner ramp (lagoon)	Similar to SMF 10 of Flügel (2004)
			Dolomitic bioturbated bioclastic packstone	PMF 2	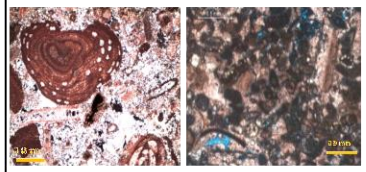 W8-D, 3221ft W9-D, 3195 ft.		Similar to RMF 7 (SMF 10) of Flügel (2004)
2	Foraminiferal bioclastic wackestone-wackestone/packstone	Mainly light grey, locally light yellowish brown or mottled, m. sorted with relatively common rotaliids, miliolids, echinoderm fragments and peloids. Planktic forams, red algae, ostracoda and peloids scattered throughout. Locally dolomitic, bioturbated and slightly rgillaceous. Compaction features locally developed, particularly in wells 10 & 8. Iron minerals developed at few intervals in wells 9 & 8. General porosity is p to fair.	Bioclastic wackestone/ packstone	PMF 3	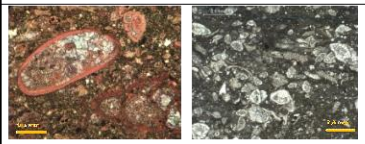 W7-D, 3321 ft. W9-D, 3172 ft.	Inner ramp (lagoon)	Crresponds to RMF 20 or SMF 10 of Flügel (2004)
			Planktic foraminferal Wackestone	PMF 4	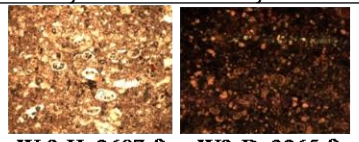 W 9-H, 2687 ft W9-D, 3265 ft.	Mid ramp	Corresponds to RMF 5or SMF 3 of Flügel (2004)
			Dolomitic bioturbated wackestone/pac kstone	PMF 5	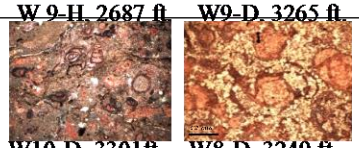 W10-D, 3301ft. W8-D, 3249 ft.	Inner ramp (lagoon)	Similar to SMF 10 of Flügel (2004)

Table 3.1 (Cont). Facies and associated microfacies of the Dahra Formation on the Dahra Platform

Facies no.	Facies Name	Description	Microfacies	Micro-facies code	Thin-section photos	Depositional setting	Remarks
3	Bioclastic mudstone	It is 0nly described in well no.8 and comprises mainly of doilomitic limestone, light yellowish grey to mottled, m.od-well sorted with very scattered benthic forams, peloids and gastropod molds. Bored and/or bioturbnated. Locally chalky and/or argilaceous. Porosity is fair to good.	Dolo lime-mudstone	PMF 6	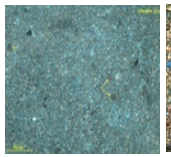 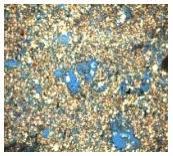 W8-D, 3079 ft .W8-D, 3079 ft.	Inner ramp (lagoon)	Similar to RMF 19 of Flügel (2004)
4	Bioclastic grainstone	Light grey, light yellowish brown to v. pale orange, m. sorted. Benthic forams, green algae and echinoderms common with scattered peloids, molluscan shells, intraclasts and bryozoans. Locally dolomitic, bioturbated, and slightly argillaceous. PDS and stylolites. Brecciated interval at well 9. Fe-minerals and syn-sedimentary compaction features in well 10. Porosity is good to very good.	Bioclastic foraminiferal grainstone	PMF 7	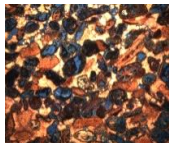 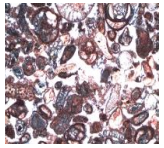 W10-D, 3158 ft. W8-D, 3155 ft.	Inner tomid ramp (possibly carbonate shoal/ or lagoon with an opencirculation (back bank)	Corresponds to SMF 10 or 11of Flugel (2004)

PDS= Pressure dissolution seams PMF= Paleocene microfacies W= Well no. D = Dahra Fm Z= Zelten Fm H= Harash Fm

Negligible Ø= 0-5 % Poor Ø= 5-10% Fair Ø= 10-15% Good Ø= 15-20% V.good Ø=20-25%

All photomicrographs are in PPL, unless otherwise stated

Table 3.1 (Cont). Facies and associated microfacies of the Mabruk Member in the Dor al Abid Trough.

Facies no.	Facies name	Description	Microfacies	Microfacies code	Thin-section photos	Depositional setting	Remarks
1	Bioclastic foraminiferal packstone	Light yellowish grey to pale yellowish brown, m. hard, fine to coarse-grained, poorly to mod. sorted. Abundant to common benthic forams, green algae and echinoderm fragments. Small forams, bryozoa, red algae, coral fragments and molluscan shells dispersed throughout. Locally dolomitic and bioturbated, stylolitic, PDS and stylo-nodular structure. Levels of iron minerals concentration, particularly in well 66. Overall observed porosity ranges from fair in well 66 to good in well 105.	Bioclastic foraminiferal packstone	PMF 1	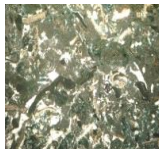 W66, 4277 ft. 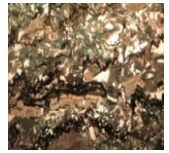 W66, 4305 ft.	Inner shelf (back-reef)	Corresponds to SMF18 of Flugel (2004)
			Dolomitic bioturbated bioclastic packstone	PMF 2	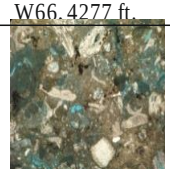 W66, 4348 ft 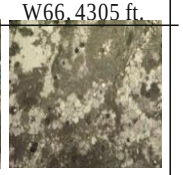 W105, 3642 ft		
2	Foraminiferal bioclastic wackestone-wackestone/ packstone	This facies is present almost exclusively in well 105, where it consists of light grey to light brown, hard, fine to medium-grained, m. sorted. Relatively common small benthic forams, peloids and planktic forams. Bryozoa, echinoid spines and fragments are scattered throughout. Slightly argillaceous, locally bioturbated and dolomitic. Common PDS, stylolites and deformation features with local concentrations of iron erals. Porosity is negligible to poor	Bioclastic wackestone/ packstone	PMF 3	 W105, 3761 ft 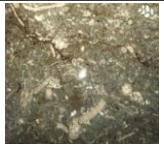 W105, 3762 ft	Inner shelf (lagoon)	Corresponds to RMF 20 or SMF 10 of Flugel (2004)
			Planktic foraminferal wackestone	PMF 4	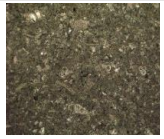 W 105, 3752 ft. 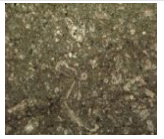 W 105, 3752 ft	Inner to middle shelf	Corresponds to RMF 5 or SMF 3 of Flugel (2004)
			Dolomitic bioturbated wackestone/ packstone	PMF 5	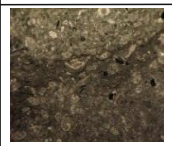 W105, 3712 ft 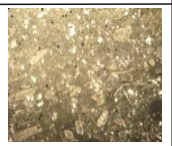 W 105, 3774 ft	Inner shelf	It similar to SMF 10 of Flugel (2004)

Table 3.1 (Cont). Facies and associated microfacies of the Mabruk Member in the Dor al Abid Trough.

Facies no.	Facies name	Description	Microfacies	Microfacies code	Thin-section photos	Depositional setting	Remarks
4	Bioclastic grainstone	Recorded at one interval in wells 66 & 105. It consists mainly of yellowish brown to very pale orange, m. hard, m - well sorted. Common miliolida, small benthic forams, red algae, lithoclasts, green algae and bivalves. Gastropods, echinoderm fragments and peloids are scattered throughout. Rarely argillaceous or dolomitic. PDS and stylo-nodular structures are present along with pyrite, anhydrite and coarse dolomite. Porosity is good to very good.	Bioclastic grainstone	PMF 7	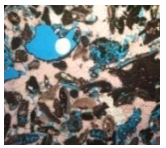 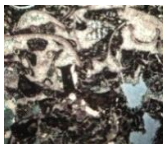 W 66, 4275 ft. W 105, 3736 ft.	Inner to middle shelf carbonate shoal/or lagoon with open circulation - back bank	Corresponds to SMF10 of Flugel (2004)
6	Algal packstone	Light yellowish grey to very pale orange (mottled), fine to coarse-grained, poorly to mod. sorted. Red algae, calcareous algae and coral fragments are common. Benthic forams, bryozoan, molluscan shells, echinoid spines and planktic forams are scattered throughout. Locally burrowed and slightly dolomitic and argillaceous. PDS and stylolites developed locally. Levels of pyrite, glauconite and dark grey iron minerals, particularly in well 103. No observed porosity.	Algal packstone	PMF 9	 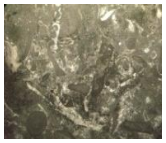 W66, 4253 ft W103, 3607 ft.	Probably middle shelf (bioclastic shoal) or back reef	Corresponds to SMF 18 of Flugel (2004)
7	Bioclastic boundstone	Broadly light grey to light olive grey, locally mottled, fine to coarse-grained, poorly to mod. sorted. Abundant to common coral and calcareous algae with less common red algae and bryozoans. Planktic forams, echinoid spines, miliolids and rotaliids dispersed throughout. Slightly burrowed and intermittently bored. Compaction features developed locally along with pyrite, glauconite and anhydrite. Overall porosity is negligible to poor.	Coral algal boundstone	PMF 10	 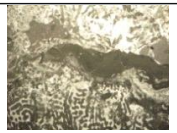 W 66, 4293 ft W 103, 3587 ft	Middle shelfg-probably reef crest	Corresponds to RMF 12 or SMF 1 of Flugel (2004)
			Algal bioclastic boundstone	PMF 11	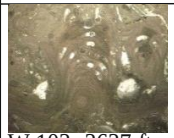 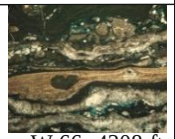 W 103, 3637 ft W 66, 4308 ft	Possibly reef crest or back-reef	Corresponds to SMF 18 of Flugel (2004)

Table 3.1 (Cont). Facies and associated microfacies of the Zelten and Harash Formations on the Dahra Platform.

Facies no.	Facies name	Description	Microfacies	Microfacies code	Thin-section photos	Depositional setting	Remarks
1	Bioclastic foraminiferal packstone-packstone/ grainstone	Light yellowish grey, m. hard, fine to coarse-grained, m. sorted with common benthic forams (particularly rotaliids), bryozoa and bivalve shells. Nummulites, gastropods, planktic forams, echinoderm and green algae are scattered throughout. Slightly argilaceous, dolomitic and bioturbated, with local development of stylolites, PDS and stylonodular structure. Pyrite, glauconite and phosphate also occur locally. Overall porosity ranges from fair to good.	Bioclastic foraminiferal packstone	PMF 1	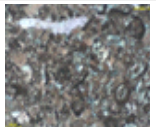 W8-Z, 2747 ft.  W10-Z,2753 ft.	Inner ramp (lagoon)	Corresponds to SMF10 of Flugel (2004)
			Dolomitic bioturbated bioclastic packstone	PMF 2	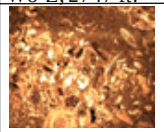 W9-H, 2699 ft  W7-Z, 2790 ft.		
2	Foraminiferal bioclastic wackestone-wackestone/ packstone	Light grey- yellowish grey, m. hard, fine to coarse-grained, m. sorted. Relatively common benthic and planktic forams and echinoderm fragments. Other bioclasts include bryozoa, nummulite, echinoid spines and green algae. Slightly argilaceous and locally bioturbated, dolomitic and/or chalky. PDS and stylolites in well 7, whereas pyrite, phosphate and limonite in well 9. Pporosity is negligible to fair.	Bioclastic wackestone/ packstone	PMF 3	 W 7-Z,2845 ft 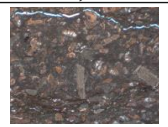 W8-Z, 2726 ft	Inner ramp (lagoon)	Corresponds to SMF 21of Flugel (2004)
			Planktonic foraminiferal wackestone	PMF 4	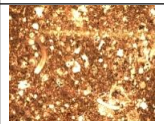 W9-H, 2663 ft 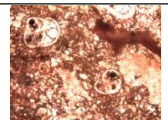 W9-H, 2686 ft	Mid ramp	Corresponds to RMF 5 or SMF 3 of Flugel (2004)
			Dolomitic bioturbated wackestone/ packstone	PMF 5	 W7-H, 2731 ft 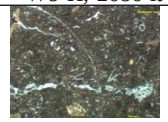 W 8-Z, 2788 f	Inner ramp (lagoon)	Corresponds to SMF 10 of Flugel (2004)
5	Nummulitic packstone	Light yellowish-light olive grey, hard, poorly-moderately sorted, with common nummulites and common to scattered Assilina, bryozoa, echinoderms, molluscan shells and red algae. Slightly argilaceous and bioturbated. Porosity generally good to very good.	Foraminiferal nummulitic packstone	PMF 8	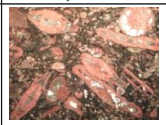 W7-Z, 2779 ft  W9-H, 2659 ft	Middle ramp (probably nummulitic bank)	Similar to SMF 1 of Flugel (2004)

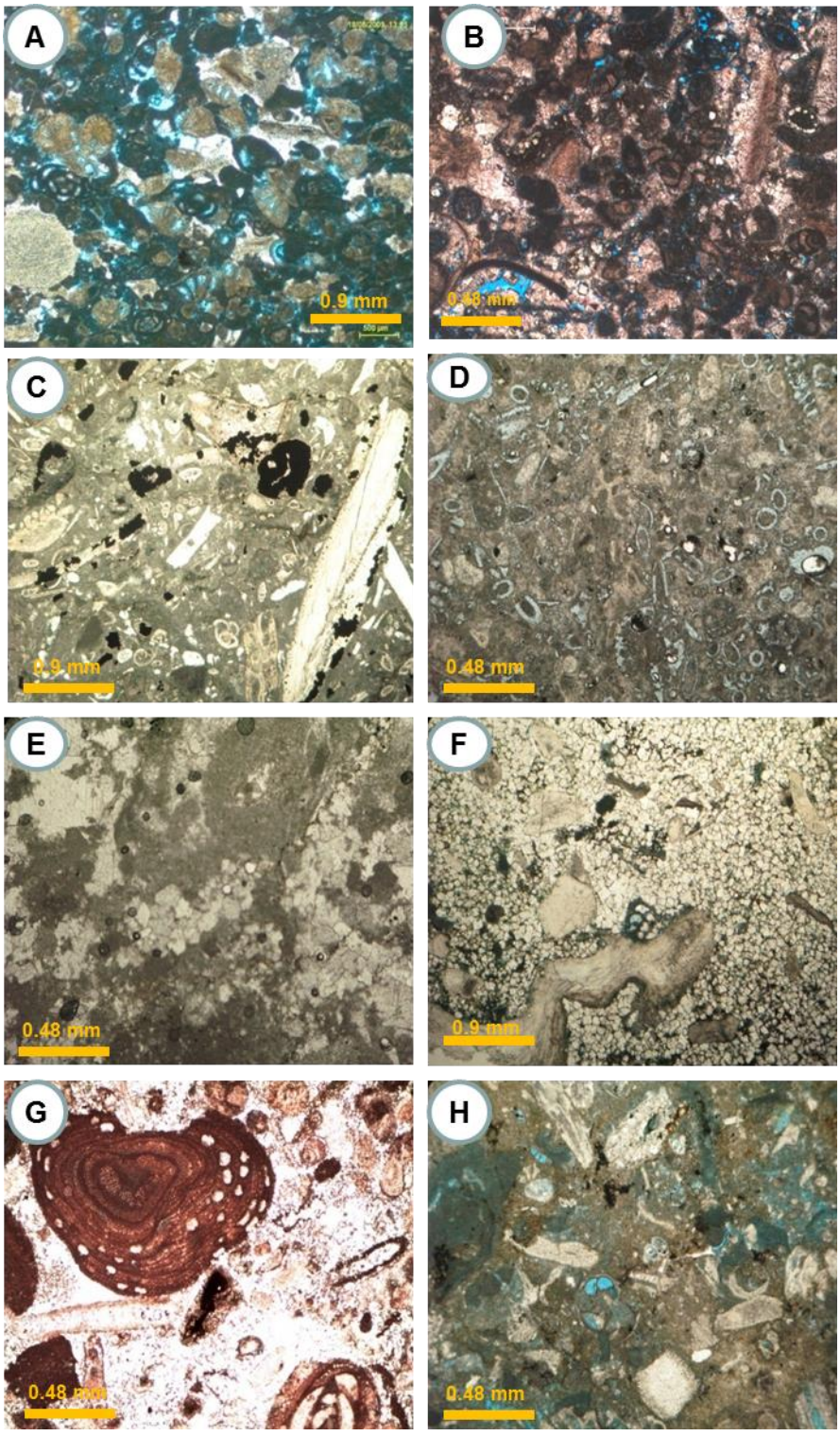

Figure 3.2 Bioclastic foraminiferal packstone/grainstone microfacies with common A: benthic forams, and echinoderms (DahraFm in well no.8), B: Coated grains and miliolids (DahraFm in well no.9),C: bivalves and pyrite (Mabruk Mbr in well no. 66), and D: green algae (Mabruk Mbr in well no. 105). Photos E-H show the general composition and texture of the dolomitic bioturbated bioclastic packstone microfacies, E: Mabruk Mbr in well no.103, F & H:MabrukMbr in well no.66, and G:DahraFm in well no.8).

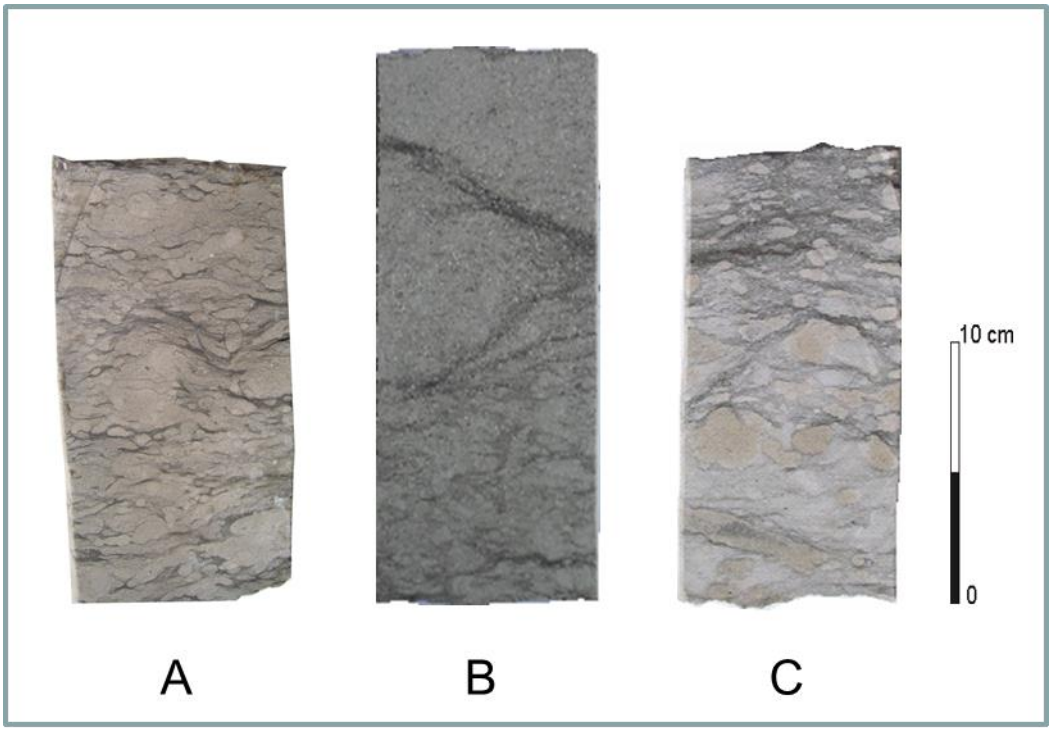

Figure 3.3 Dolomitic bioturbated bioclastic packstone microfacies showing different bioturbation intensity; A) BI= 4, Dahra Formation (3308 ft), well no. 7, Dahra Platform; B) BI= 3-4, Mabruk Member (3704 ft), well no. 105, Dur al Abid Trough; C) BI= 2, Zelten Formation (2745 ft), well no. 10, Dahra Platform.

3.2.2.2. Foraminiferal bioclastic W- W/P

3.2.2.2.1. Bioclastic wackestone/packstone (PMF 3)

The bioclastic wackestone/packstone microfacies is not widely distributed within the Dahra Formation on the Dahra Platform as it occurs mainly in well no.8 and at only one interval in well no.7. It consists principally of rotaliids, small forams and echinoderm fragments. Echinoid spines, miliolids, bryozoan, red algae, bivalve shells and ostracods are scattered throughout (Fig. 3.4). These grains are contained within a matrix of slightly and locally dolomitic micrite. Some of the intergranular voids and many of intragranular pores are filled with syntaxial overgrowths and coarse calcite and dolomite, locally iron-rich cements. At well no. 8 some bioclasts are bored and the micritic substrate is locally burrowed along with the occurrence of pyrite, phosphate and possibly limonite (Table.3.2). According to the fossil assemblages and the relatively

high content of lime mud this microfacies may represents deposition in a shallow-marine lagoon and could correspond to RMF 20 or SMF 10 of Flügel (2004).

Within the Mabruk Member in the Dor al Abid Trough this microfacies has only been recognised in one interval in the lower part of the upper Mabruk in well no 105. It is about 5 feet thick and consists of almost the same fauna as on the Dahra Platform along with scattered green algae and calcispheres (Fig.3.4).

Within the Zelten and Harash Formations on the Dahra Platform the composition of this microfacies is similar to the other wells except that the matrix is made up of small fragments of various bioclasts. Petrographic investigation revealed that this microfacies is characterized by the development of possibly laminoid fenestra and/or desiccation cracks in the lower part of Zelten Formation in well no. 8 (Fig.3.4).Therefore it may corresponds to SMF 21 of Flügel (2004).

3.2.2.2.2. Planktic foraminiferal wackestone (PMF4)

The planktic foraminiferal wackestone microfacies exists as thin beds at certain intervals of the Dahra Formation on the Dahra Platform**,** i.e**.** it occurs at single interval in wells no. 8, 9 and 10, while it has not been clearly recognized in well no.7 (Table 3.2). It is comprised chiefly of planktic forams, rotaliids, echinoid spines and calcispheres. Red algae, corals, crinoids, ostracods and bryozoans are less common (Fig. 3.4 D & E). These constituents are contained within a dolomitic and rarely burrowed micrite matrix. Pyrite, phosphate and limonite are rare, but occurring particularly in wells no 9 and 10. Porosity is mostly negligible (Table 3.2). According to grain-types, grain frequency, matrix and depositional fabrics this microfacies may represent deposition in a mid to outer- ramp setting and it would correspond to RMF 5 or SMF3 of Flügel (2004).

In the Dor al Abid Trough this microfacies has been recognized at one interval in well no. 105 only. Its matrix is slightly argillaceous and composed mainly of small fragments of different bioclasts, planktics and, less commonly, rotaliids.

Within the Zelten and Harash Formations on the Dahra Platform, the planktic foraminiferal wackestone microfacies occurs only in the Harash Formation in wells no. 7 and 8, and in well no.9 it is developed in both Zelten and Harash Formations; it has not been recognized in well no. 10.Its composition and texture are similar to the above localities with the occurrence of fragments of N*ummulites* in the Harash Formation in

wells no.8 and 9, and rare A*ssillina*, gastropoda and green algae in the Zelten Formation in well no.9 (Fig.3.4). The dolomite crystals, which are associated with pyrite in some cases, are around 80µm in size. Pyrite with some glauconite occurs in both carbonate grains and matrix, and along micro-fractures in the Harash Formation in well no.9 (Fig. 4.10-.next chapter).

3.2.2.2.3. Dolomitic bioturbated wackestone/packstone (PMF5)

Within the Dahra Formation on the Dahra Platform this microfacies occurs mainly in well no.8, and is developed at certain intervals in wells no.9 and 10; it is absent in well no.7 (Table.3.2). It consists predominantly of rotaliids and miliolids. Echinoderm fragments, peloids and planktic forams are less common with scattered bryozoans, coral fragments, red algae and intraclasts (Fig. 3.4). Some grains are frequently coated with one layer of micrite. The micrite matrix has been subjected to fairly extensive burrowing and dolomitization with less common neomorphism. These processes in association with compaction have resulted in the formation of a mottled fabric at 3189 ft in well no.9. Its bioturbartion index is about 4 (Fig.3.5&Appendix.1).

The average size of dolomite crystals is usually 30 – 60µm in well no.8, but they can reach 100 µm in well no.9. A larger size of void-filling saddle dolomite has been noticed in well no.9. A notable feature of this microfacies is the development of internal sediment, fenestral structure, rootlets and/or desiccation cracks along with the brecciated fabric at the upper and middle intervals of the Dahra Formation in well no.8 (Fig.3.4G&Appendix 1). Pyrite, glauconite, phosphate and, locally hematite are scattered locally, particularly in well no.10. Overall porosity is poor to fair (Table 3.2). Based on lithology, faunal assemblage and mud to cement ratio a semi- restricted or open lagoon or bay with moderate to low-water circulation were possibly predominant during the time of deposition of this microfacies. It would correspond to SMF 10 of Flügel (2004).

Within the Mabruk Member in the Dor al Abid Trough the dolomitic bioturbated wackestone/packstone microfacies has only been identified in well no. 105, where it is comprised chiefly of rotaliids, peloids and bryozoans with less common echinoderms and echinoid spines. These bioclasts are floated in bioturbated, dolomitic and slightly argillaceous micritic matrix. An extensive burrowing has developed locally with the

overall bioturbation index around 5 (Fig. 3.5& Appendix.1). Pressure dissolution seams and fractures are locally developed with the occurrence of pyrite.

The dolomitic bioturbated wackestone/packstone microfacies on the Dahra Platfor***m*** has only been recognised in well no.8 in both the Zelten and Harash Formations (Table 3.2). Its total thickness in these Formations is 11 feet and 9 feet, respectively. It composed mainly of rotaliids and bryozoa with less common planktic forams, bivalve shells, nummulites, echinoid spines and intraclasts. Equant crystals of calcite are present as intragranular cement, which are locally Fe-rich. The dolomitized micrite crystals are about 80 μm. In places this microfacies is argillaceous with occurrence of horizontal burrows that are filled by coarser sediments (Fig. 3.5). Almost no porosity has been observed.

3.2.2.3. Dolomitic lime-mudstone (PMF6)

The dolomitic lime-mudstone microfacies is the least common microfacies in the studied interval of the Paleocene succession in the study area. It is recognized within the upper part of the cored interval of the Dahra Formation on the Dahra Platform in well no. 8 only (Table 3.2). It is comprised mainly of fine to very fine dolomite crystals (<20 μm). Its original texture was mud-supported as the amount of carbonate grains is less than 10% and is represented mainly by rotaliids, ghosts of micritic grains (probably peloids) and few gastropods (Table 3.1 & Fig. 3.4 H). Local development of coarse dolomite crystals (< 800 μm) are witnessed in vuggy and moldic porosity. Extensive boring of some bioclasts along with slight burrows are also recognised. Dissolution of some grains and possibly evaporite or even dolomite crystals has also been recorded. Despite the fact that many of these pores have subsequently been plugged partly by coarse dolomite cement, they contribute to the overall fair to good porosity of this microfacies (Fig.3.4).

The presence of benthic forams, peloids and gastropods, and relative absence of typical open-marine fossils, along with the mud-supported texture suggest that this microfacies was deposited in a low-energy environment of probable an inner ramp, lagoonal setting. It may correspond to RMF 19 of Flügel (2004).

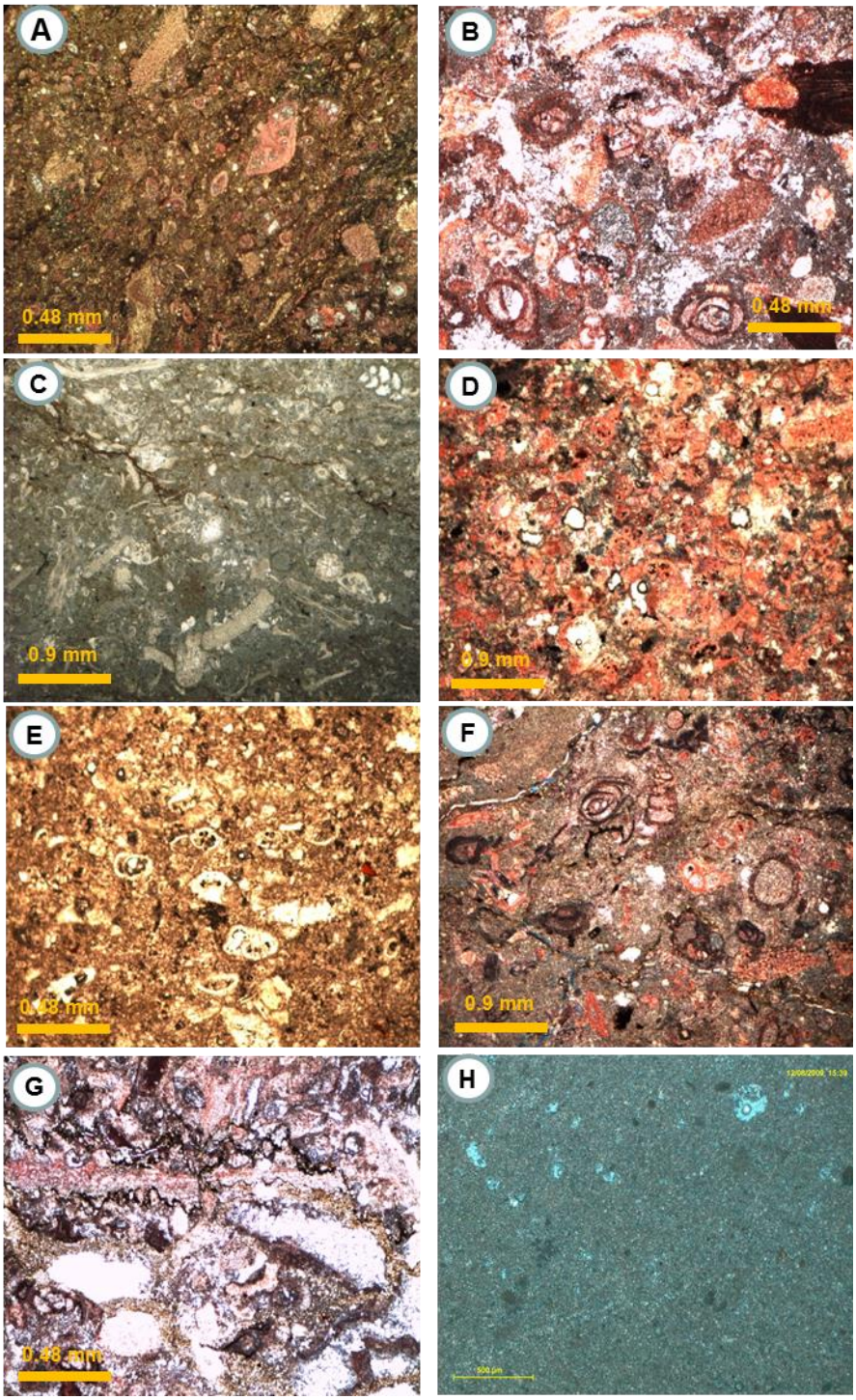

Figure 3.4 A) Bioclastic w/p with rotaliids, echinoderms and small forams, Dahra Fm (3321 ft), Well no.7; B) Miliolids, echinoderms and red algae in bioclastic w/p, Dahra Fm (3181 ft), Well no. 8; C)The same microfacies in Dor al Abid Trough, with rotaliids, bryozoans and echinoderm fragments, Mabruk Mbr (3762 ft), Well no. 105; D) & E) General views of Planktonic foraminiferal wackestone in the Dahra Fm (3296 ft) inWell no. 10, and in the Harash Fm (2687 ft) at well no. 9; F) Dolomitic bioturbated w/p microfacies in the Dahra Fm (3299 ft) in Well no.10; G) Rootlets and/or desiccation cracks in the Dahra Fm (3185 ft) inWell no. 8; H) Dolomitic lime-mudstone microfacies with moldic porosity, Dahra Fm (3079 ft), Well no. 8.

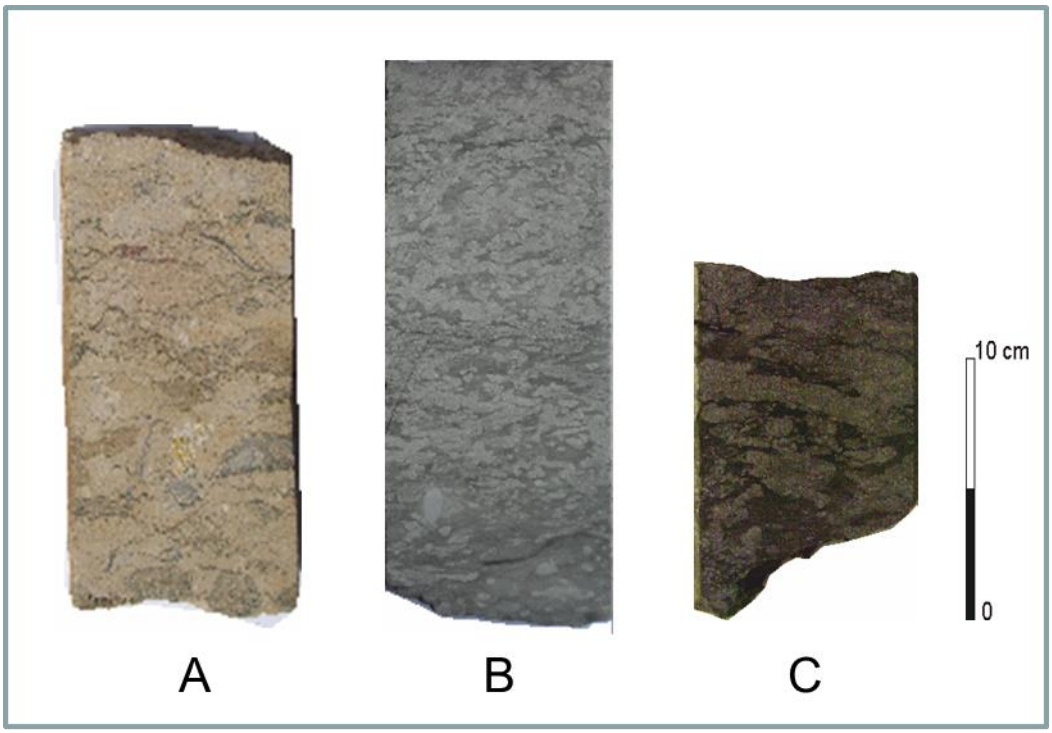

Figure 3.5 Dolomitic bioturbated wackestone/packstone microfacies showing different bioturbation intensity; A) BI= 4, Dahra Formation (3189ft), Well no. 9, Dahra Platform; B) BI=4-5, Mabruk Member (3719 ft), Well no. 105, Dor al Abid Trough; C) BI= 3, Harash Formation (2680 ft),Well no. 8, Dahra Platform.

3.2.2.4. Bioclastic foraminiferal grainstone (PMF7)

This microfacies occurs within the Dahra Formation on the Dahra Platform and its equivalent Mabruk in the Dor al Abid Trough, and has not been identified within the Zelten and Harash Formations (Table 3.2).

Within the Dahra Formation on the Dahra Platform it consists largely of miliolids, rotaliids, superficial ooids, echinoderms, green algae, bivalves, peloids and intraclasts. Other less common bioclasts are gastropods, bryozoans, calcareous algae, ostracods and extraclasts (Fig.3.6 &Table 3.2.). The ooids are coated with thin layers of micrite and there is commonly an isopachous rim of fibrous calcite cement around them. The ooids are commonly dissolved out, deformed and the cement coating in many cases has been fractured and separated away from the grain. This has resulted in the formation of ‘duck’ structures or ‘elephant-parade’ fabric (Folk, 2001) (Fig.3.6B).

The grains are usually cemented by equant sparry calcite cement that is locally iron- rich. Intervals of sub-hedral to eu-hedral crystals of dolomite (60-80 µm) that replaces mainly the matrix, less common bioclasts, are recorded locally. Baroque or

saddle dolomite (180-240 µm) in association with coarse ferroan calcite (350-600 µm) is developed as void and fracture-filling cement. Bored bioclasts, and pyrite, glauconite, phosphate and hematite are all witnessed at 3155ft in wells no. 10. Bioturbation, dissolution of unstable grains (mainly molluscan shells) and development of pyrite along with dolomitic levels are recorded at 3121ft and 3175 ft in wells no. 9 and 10 respectively (Appendix 1). According to grain types, grain frequency and matrix to cement ratio and depositional fabrics this microfacies represents deposition in an inner to mid - ramp situation with good water circulation and relatively high-energy setting. It would correspond to SMF 10 of Flügel (2004).

Within the Mabruk Member in the Dor al Abid Trough the bioclastic foraminiferal grainstone microfacies is quite similar in grain components to the Mabruk elswhere, in addition to the sporadic occurrence of red algae and rhodoliths. Dolomitic intervals are recognised at 3735 ft in well no. 105 along with the occurrence of coarse crystals with curved faces and undulose extinction of saddle dolomite (Fig. 4.6- next chapter). Extensive dissolution has occurred at interval 3068-3075ft in well no. 66 and resulted in the formation of good to very good secondary porosity (Table 3.2 &Appendix.1).

3.2.2.5. Foraminiferal nummulitic packstone (PMF 8)

This microfacies occurs only within the Zelten and Harash Formations on the Dahra Platform, and consists chiefly of N*ummulites* and rotaliids. Miliolids, bryozoa, echinoderms, planktic forams and red algae are also present, with scattered gastropods, echinoid spines, A*lveolina, Operculina* and bivalve shells (Fig. 3.6). The overall texture is poorly sorted and locally is densely packed and highly compacted. The nummulites are commonly intact, although nummulitic debris and fragments are also present. They are ranging in size from 1.5mm to 4 mm long and 1 mm to 2.5 mm wide. Larger nummulites around 6 mm long are also observed at specific intervals within the Harash Formation, particularly in well no.9. In many cases their shells showing microfractures and their internal chambers are commonly filled by sparry calcite, which is usually iron-rich. The micritic substrate has been subjected locally to partial dolomitization and is slightly burrowed. The dolomite crystals chiefly range in size from 20–40 µm, with some larger ones up to 60µm dolomite. Syntaxial overgrowth and intragranular calcite cements and dolomite, commonly ferroan, are sporadically developed. Levels of pyrite

and phosphate were observed in well no.9. Boring, burrowing, dolomitization and chemical compaction are also recorded in this microfacies. Porosity is almost negligible.

On the basis of lithology, faunal assemblage and the overall geological setting of the facies, an inner to mid ramp setting with moderate water circulation was probably predominant during the time of deposition of this facies in the study area. It could correspond to RMF 7 or SMF 10 of Flügel (2004).

3.2.2.6. Algal Packstone (PMF 9)

The algal packstone microfacies has not been developed on the Dahra Platform, nor within the Dahra carbonates and the Zelten and Harash Formations. It occurs at certain intervals inwells no. 66 and 103within the Mabruk Member in the Dor al Abid Trough and has not been recognised in well no.105 (Table 3.2). It is composed largely of red algae, rhodoliths, bryozoans and echinoid spines. Coral fragments, miliolids, rotaliids and echinoderms are less common with scattered molluscan shells, planktic forams and ostracods (Fig.3.6). The depositional texture grades locally to rudstone or even boundstone, particularly in well no. 103. The micritic substrate, which is locally made up of very small bioclastic fragments, is slightly bioturbated and dolomitic. Development of geopetal structure within some rhodolith algae and coral chambers is fairly common at particular intervals (Fig. 3.6).

Sparry calcite and syntaxial rim cements have filled the dissolved bivalves, and vuggy and intergranular pores, respectively. Fractures and veins are usually filled with coarse blocky calcite and large dolomite crystals. up to 160 μm in size. Pressure dissolution seams and stylolites are fairly common. Pyrite and glauconite are scattered throughout.

Based on faunal content and matrix to cement ratio along with stratigraphic position the algal packstone microfacies may represent deposition in back-reef setting of an inner shelf environment, despite the fact that fore reef setting is also inferred at certain intervals. It may correspond to SMF 18 of Flügel (2004).

3.2.2.7. Bioclastic boundstone

3.2.2.7.1. Coral algal boundstone (PMF 10)

The coral algal boundstone microfacies, locally framestone, developed in wells no. 66 and 103 within the Mabruk Member in the Dor al Abid Trough and has not been

recorded on the Dahra Platform (Table 3.2).It comprises mainly of scleractinian corals, coralline algae (rhodoliths), red algae and bryozoans (mainly cheilostome form)(Fig. 3.6). Other less common bioclasts include that of echinoid spines, benthic and planktic forams, and molluscan shells. Red algae and bryozoans commonly encrust different bioclasts such as benthic forams and bivalves.

These components are commonly present in a matrix of micrite that is itself a mixture of small fragments of various bioclasts. There are zones of mottling (bioturbation) and dolomite crystals with an average of 40-80µm.Eequant sparry calcite, void-filling coarse calcite and medium to coarse crystalline dolomite crystals (~ 100µm) are also present. A notable feature of this microfacies is the presence of evaporite crystals (gypsum) at particular intervals in well no. 66, along with fossil sponge, bored bioclasts and geopetal structures (Fig.3.6). Pyrite and glauconite occur locally as well. It seems that scleractinian corals in many places are present in their original growth position (in situ), and thus this faciesis ascribed to a reef setting of shallow inner to middle carbonate shelf. It could correspond to RMF 12 or SMF 7 of Flügel (2004).

3.2.2.7.2. Algal bioclastic boundstone (PMF 11)

This microfacies has also been identified only within the Mabruk Member in the Dor al Abid Trough. It occurs in wells no. 66 and 103 and is interbedded with the algal packstone microfacies and coral algal boundstone microfacies. It consists mostly of rhodolithic algae, corals and branching coralline red algae. Benthic forams, bryozoans, echinoid spine, planktic forams and gastropods are scattered throughout (Fig. 3.6). Although the overall texture is boundstone, the rudstone, floatstone and packstone textures also occur, with local bioturbation. Equant calcite, locally coarse, and dolomite cements that plug most of the previously formed porosity are present. Intervals of bored and/or corroded bioclasts in association with pyrite and glauconite were observed in both wells. Laminoid fenestrae-like structures have been recorded at 3574 ft in well 103. The algal bioclastic boundstone microfacies in this particular location probably represent deposition in a reef to back reef setting, despite the fore reef setting is possibly inferred at certain intervals. It would correspond to SMF 18 of Flügel (2004).

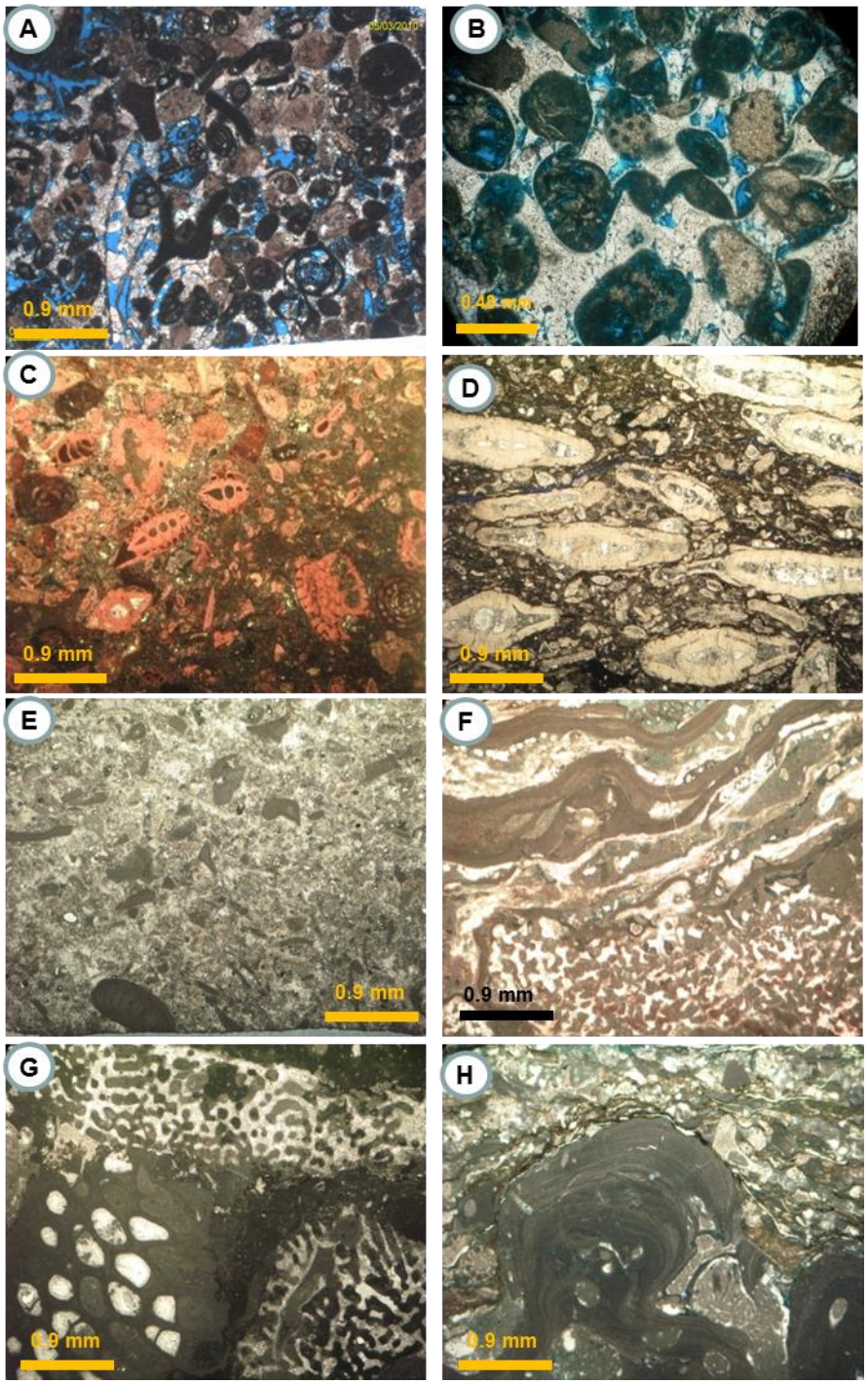

Figure 3.6 A & B) Bioclastic foraminiferal grainstone microfacies with coated grains and superficial ooids. Note the formation of 'duck' structures in B. Dahra Fm (3088 ft and 3181 ft respectively),Well no.9.; C&D) show foraminiferal nummulitic packstone microfacies on the Dahra Platform within the Harash (2731ft) and Zelten (2779 ft) Formations, respectively.E) Algal packstone with abundant red algae and small bioclastic fragments, Mabruk Mbr (3632 ft) in Well no.103; F& G) Coralgal boundstone microfacies with scleractinian corals and coralline algae, Mabruk Mbr (4326 ft) in Well no. 66, and at 3645 ft in Well no.103; H) Algal bioclastic boundstone microfacies shows rhodolithic algae and echinoid spine, Mabruk Mbr (4345ft) in Well no.66.

Table. 3.2. Petrographic investigation summary of the studied wells.

Structural setting	**Dahra Platform**																																				
Well No.	**Well 8**							**Well 9**							**Well 10**					**Well 7**						**Well 66**				**Well 103**		**Well 105**		
Formation	**H & Z**			**D**				**H & Z**				**D**			**H & Z**		**D**			**H & Z**			**D**			**M**				**M**		**M**		
Macrofacies No.	**1**	**2**	**5**	**1**	**2**	**3**	**4**	**1**	**2**	**3**	**5**	**1**	**2**	**4**	**1**	**5**	**1**	**2**	**4**	**1**	**2**	**5**	**1**	**2**	**4**	**1**	**4**	**6**	**7**	**6**	**7**	**1**	**2**	**4**
Texture / Carb. Grains	**P**	**W-W/P**	**P**	**P**	**W-W/P**	**M/W**	**G**	**P**	**W-W/P**	**M/W**	**P**	**P**	**W-W/P**	**G**	**P**	**P**	**P**	**W-W/P**	**G**	**P**	**W–W/P**	**P**	**P**	**W-W/P**	**G**	**P**	**G**	**P**	**B**	**P**	**B**	**P**	**W-W/P**	**G**
Rotaliida	P	C	C	A	C	R	A	C	C	P	R	A	C	A	A	C	A	C	A	A	C	A	A	C	C	P	R	P	-	R	R	A	C	A
Miliolida	P	P	C	C	C	-	C	C	-	-	-	C	C	A	P	P	A	P	A	R	R	-	P	R	A	R	R	R	R	R	R	C	P	C
Nummulites	C	-	A	-	-	-	-	P	P	R	A	-	-	-	R	A	-	-	-	P	-	A	-	-	-	-	-	-	-	-	-	-	-	-
Alveolina	-	-	R	-	-	-	-	-	-	-	P	-	-	-	--	-	-	-	-	-	-	R	-	-	-	-	-	-	-	-	-	-	-	-
Assilina	-	-	-	-	-	-	-	-	R	-	-	-	-	-			-	-	-	-	R	-	-	-	-	-	-	-	-	-	-	-	-
Echinoderms	R	P	P	C	P	-	C	-	R	R	R	P	P	P	R	C	C	P	C	C	C	P	A	C	P	C	C	R	P	-	-	P	P	C
Echinoid spines	-	R	R	-	R	-	-	-	P	-	R	R	R	-	R	-	R	P	R	P	P	R	R	R	-	R	-	P	R	P	R	R	R	R
Crinoids	-	R	R	-	-	-	R	R	R	-	R	-	R	R	-	R	-	-	R	P	R	-	R	-	R	R	R	R	R	-	R	R	R	R
Bivalves	P	-	R	P	R	-	P	R	R	-	R	R	-	P	R	P	P	-	P	P	-	R	P	-	R	R	R	R	R	R	R	R	-	R
Gastropoda	-	-	R	R	-	-	R	-	-	-	-	-	R	R	R	-	R	-	R	R	-	-	R	-	P	R	R	-	R	-	-	R	R	R
Green Algae	-	-	R	R	R	-	P	-	-	-	-	R	R	R	-	-	P	-	C	P	P	-	R	-	P	-	P	-	-	-	-	P	P	R
Calc.. algae	-	-	-	-	-	-	-	-	-	-	-	-	-	R	-	-	-	-	-	-	-	-	-	-	-	P	C	C	C	C	C	-	-	-
Red algae	-	-	R	P	R	P	R	R	-	-	R	R	R	-	R	-	R	-	R	-	-	-	-	-	-	P	C	A	P	A	P	-	-	-
Bryozoa	C	P	P	R	R	R	R	R	R	-	R	R	R	P	P	-	P	R	P	P	R	R	P	R	-	R	R	R	P	P	R	P	P	R
Planktics	R	P	R	R	R	P	R	R	R	R	R	R	R	-	R	-	R	C	R	P	P	R	-	R	-	R	-	R	P	-	-	-	R	-
Ostracoda	-	-	R	R	R	-	-	-	-	R	-	-	R	-	-	-	R	R	-	R	-	-	-	-	-	-	-	R	R	-	-	R	-	R
Coral	-	-	-	-	-	R	-	-	-	-	-	-	-	-	-	-	-	-	-	-	-	-	-	-	-	R	-	P	A	P	A	-	-	-
Ooids	-	-	-	R	R	-	-	-	-	-	-	-	-	R	-	-	R	-	R	-	-	-	P	-	-	-	-	-	-	-	-	-	-	-
Peloids	-	-	-	P	-	-	R	-	-	R	-	R	R	R	-	-	-	-	R	-	-	-	R	R	-	-	-	-	R	-	-	R	-	R

Intraclasts	-	-	-	R	R	-	P	-	-	-	-	-	-	-	-	-	R	-	P	-	-	-	R	-	-	R	-	-	-	R	-	R	-	R
Extraclasts	-	-	-	R	-	-	-	-	-	-	-	-	R	R	-	-	-	-	R	-	-	-	R	-	-	R	-	-	-	-	-	-	-	R
Mineralogical composition																																		
Calcite	A	A	A	A	A	A	A	A	A	A	A	A	A	A	A	A	A	A	A	A	A	A	A	A	A	A	A	A	A	A	A	A	A	A
Dolomite	R	R	R	C	A	A	P	P	P	C	C	C	A	P	P	-	C	C	P	P	R	-	P	R	P	R	R	R	P	P	P	R	-	P
Clays	-	-	-	R	P	P	-	R	-	P	P	P	R	R	-	-	-	-	-	R	R	R	-	R	-	-	P	-	R	-	-	-	P	-
Pyrite	R	R	R	R	P	R	R	P	P	P	R	R	R	R	R	R	R	R	R	P	R	R	R	R	R	P	-	P	P	P	P	P	P	R
Evaporite	-	-	-	-	-	-	-	-	-	-	-	-	-	-	-	-	-	-	-	-	-	-	-	-	-	R	-	-	P	R	-	R	-	-
Glauconite	-	-	-	R	-	-	-	P	-	-	R	-	-	-	R	-	R	-	R	R	R	R	-	-	-	R	-	-	R	R	R	-	-	-
Phosphate	-	R	R	R	R	-	-	R	-	-	R	-	-	-	R	-	R	-	-	R	R	-	-	-	-	R	-	R	R	-	R	-	R	-
Fe- minerals	-	-	P	R	R	-	-	R	-	-	R	-	-	R	R	R	R	-	R	R	R	-	P	-	-	R	-	-	-	-	R	R	R	-
Main diagenetic processes																																		
Bioturbation	-	-	√	√	√	√	√	√	√	√	√	√	√	√	√	-	√	√	√	√	√	√	√	√	-	√	-	√	√	√	√	√	√	√
Dissolution	√	-	√	√	√	√	√	√	√	√	√	√	√	√	√	√	√	-	√	√	-	-	√	-	√	√	√	√	-	-	-	√	-	√
Cementation	√	√	√	√	√	-	√	√	√	√	√	√	√	√	√	√	√	√	√	√	√	√	√	√	√	√	√	√	√	√	√	√	-	√
Dolomitizatio	√	√	√	√	√	√	√	√	√	√	√	√	√	-	√	√	√	√	√	√	√	-	√	√	√	√	√	-	√	√	√	√	-	√
Compaction	√	√	√	√	√	-	√	√	√	√	√	√	√	√	√	-	√	√	√	√	√	√	√	√	√	√	√	√	√	√	√	√	√	√
Fracturing	√	√	√	√	√	-	√	√	-	-	√	√	√	√	√	-	√	√	√	√	√	√	√	√	-	√	√	-	√	√	√	√	√	√
Porosity type																																		
Intergranular	√	-	-	√	√	√	√	√	-	-	√	√	√	√	√	√	√	√	√	√	-	-	√	-	√	√	√	√	-	-	-	-	-	-
Intragranular	√	-	-	√	√	√	√	√	√	-	√	√	√	√	√	√	√	√	√	√	√	√	√	-	√	√	√	√	√	-	√	√	-	√
Intercrystalli	-	-	-	√	√	√	√	-	-	-	-	-	-	-	-	-	√	-	√	-	-	-	-	-	-	-	-	-	-	-	-	-	-	-
Moldic	-	-	-	√	√	√	√	√	-	-	√	√	√	√	√	√	√	√	√	√	-	-	-	-	-	√	√	√	-	-	-	√	-	√
Vuggy	-	-	-	√	√	√	√	√	-	-	√	√	-	√	√	√	√	-	√	-	-	-	-	-	-	√	√	√	-	-	-	√	-	√
Fenestrae	-	-	-	√	-	-	-	-	-	-	-	-	-	-	-	-	-	-	-	-	-	-	-	-	-	√?	-	-	-	-	-	-	-	-
Framework	-	-	-	-	-	-	-	-	-	-	-	-	-	-	-	-	-	-	-	-	-	-	-	-	-	√	-	√	√	√	√	-	-	-
Fracture	√	√	√	√	√	-	√	√	-	-	-	√	√	√	√	-	√	√	√	√	√	√	√	√	-	√	√	-	√	√	√	√	√	√
Porosity category	**N**	**N**	**N**	**F**	**P**	**F**	**G**	**N**	**N**	**N**	**P**	**F**	**N**	**F**	**F**	**G**	**F**	**N**	**G**	**N**	**N**	**N**	**F**	**N**	**F**	**F**	**VG**	**P**	**P**	**N**	**N**	**F**	**N**	**F**

3.3. Facies sequence and environmental interpretation

The depositional setting of the studied interval of the Paleocene succession is investigated based on the general vertical facies succession of the microfacies discussed above. The palaeobathymetry of each facies, and thus its depositional environment,depends on faunal associations and sedimentological features, and is relative with respect to the other facies, despite the fact that there might be small and subtle changes in the water depth and consequently in the associated microfacies, which are beyond the resolution and the number of samples available in this study.

3.3.1. Dahra Formation on the Dahra Platform

According to the literatures and based on the available data for this study, the Dahra Formation on the Dahra Platform was deposited on a homoclinal carbonate ramp with inner, mid and probably outer parts, each with distinctive sub-facies and microfacies (Read 1982, 1985; Tucker and Wright, 1990; Flügel, 2004). In addition to the mid- ramp, most of the subenvironments of the back ramp-inner ramp, tidal flats, lagoon and shoal have also been recognised.

The Dahra Formation is composed of argillaceous limestone with subordinate dolomite interbedded with thin shale (Barr and Weegar, 1972). In the eastern part of the study area the formation consists of 300 feet of shallow-water carbonate with thin interbeds of dark shale (Roohi, 1996). The same author suggested that high-energy conditions prevailed in the south eastern part of the study area during deposition of the Dahra Formation. Apart from minor difference in the thickness of the Dahra subdivisions (A, B and C) in the studied wells and a slight increase of argillaceous content in the upper part of the formation (Dahra A & B) in well no. 7, the core description, petrographic examination and geophysical logs indicate that there are no drastic changes in the facies and associated microfacies throughout the Dahra Formation. It seems that the Dahra was probably deposited under similar conditions across the east and west Dahra Fields on the Dahra Platform.

The cored section of the Dahra Formation begins, from the bottom, with foraminiferal bioclastic wackestone/packstone facies (~21feet thick) that is locally dolomitic and bioturbated. Its middle level is interrupted by a very thin bed (2 feet thick) of bioclastic packstone, light yellowish grey with common bivalve shells, gastropods, green algae and rotaliids. Almost all bivalve shells have been dissolved out

and filled later mainly by iron-rich calcite and, less commonly, Fe-dolomite. Pyrite is also common and occurs both in the substrate and within grains. This unit may represent either a storm bed or short phase of shallowing during the deposition of overall wackestone-wackestone/packstone facies (Appendix. 1). This is followed by about 17 feet thick of alternations of marl, very argillaceous limestone and shale, which represents the second flooding event within the Dahra Formation in the area. The succession passes up to coarser and relatively shallower-water deposits, which are characterized by 20 feet thick of bioclastic foraminiferal packstone facies with local concentrations of dasycladacean green algae and scattered occurrence of pyrite and de-dolomitization features. The later 37 feet are arranged into several shallowing and coarsening-upward cycles (Chapter 5 and Appendix 1).

Another flooding event, and thus development of a new cycle, is represented by the development of 6 feet of alternations of light grey marl and calcareous shale, which in turn are followed by 30 feet of foraminiferal bioclastic wackestone-wackestone/packstone with benthic forams, echinoderm fragments, peloids and rare planktic forams.Upwards an overall regressive trend is evident, with the occurrence of bioclastic foraminiferal grainstone facies with miliolids, rotaliids, ooids and echinoderms.The common small benthic forams, ooids and echinoderms, with scattered green algae, peloids and bivalves, in addition to the high content of lime mud (apart from the uppermost facies, a bioclastic grainstone) suggest that an inner ramp lagoonal setting with semi-restricted circulation, and bioclastic carbonate shoal were probably dominant during the deposition of the lower part of the Dahra Formation in this particular locality (Fig. 3.8).

The middle part of the Dahra Formation is dominated largely by bioclastic shoal deposits as indicated by wide occurrence of grain-supported carbonates with local development of wackestone and wackestone/packstone textures of a lagoonal environment. A noteworthy feature at the top of the middle part is the occurrence of bioclastic wackestone facies with an open-marine fauna (corals, red algae and crinoids) which probably represents a mid-outer ramp setting (Appendix.1). This middle portion of the Dahra, however, started with dolomitic bioturbated packstone with common small benthic forams and is stained reddish brown due to the presence of hematit. This facies passes up into shallower-water deposits of bioclastic foraminiferal grainstone (~ 30 feet thick), slightly dolomitic, with common rotaliids, miliolids, ooids and

echinoderm fragments. Just above that, an interval of dolomitic bioturbated wackestone/packstone microfacies with intraclasts and/or breccia. Compaction has resulted in the formation of a stylo-nodular structure and stylo-breccia fabric. Besides, desiccation cracks, rootlets and internal sediment have been developed at the top interval, along with the occurrences of hematite (Fig. 3.4G).

The stable isotope analysis of this interval shows light positive value of $\delta^{13}C$ (1.82‰) and negative $\delta^{18}O$ (-4.12‰). These overall features strongly indicate pedogenesis, probably in an upper intertidal or supratidal environment. Moreover the absence of evaporite and karstification suggest that the Dahra Formation was subjected to a period of exposure under semi-arid climate.

This significant discontinuity surface was followed by 19 feet thick of wackestone/packstone, locally dolomitic, bioturbated and slightly argillaceous. Its base is highly compacted with the occurrence of iron oxides, in particular hematite. This succession grades upwards into bioclastic foraminiferal packstone/grainstone facies (~32 feet thick) with common rotaliids, miliolids and coated grains. Red algae and calcareous algae are locally present with development of fair to good porosity in its uppermost interval (Appendix. 1). This high-energy facies is overlain sharply by 3 feet of bioclastic wackestone facies with scattered planktic forams, red algae, coral fragments, bryozoans and ostracods. This interval represents the most pronounced flooding event (transgression) in the middle part of the Dahra Formation (might be similar to the drowning unconformity of Schlager, 1981, 1989) (discussed in detail in chapter 5). A well-sorted bioclastic grainstone facies directly overlies the hemi-pelagic wackestone facies, which indicates a sharp shallowing associated with high wave action and current activity. This was probably brought about by falling sea-level, differential subsidence or both.

The upper part of the Dahra succession (about 70 feet thick) is composed mainly of mud-supported carbonates with local development of packstones, particularly in the uppermost part.The inner ramp is indicated by the occurrence of lagoonal facies, whereas the mid-outer ramp setting is recognised close to the top of the formation (Appendix. 1, Fig. 3.8). The topmost part, however, starts at its base with dolomitic lime-mudstone microfacies, passes up into planktic foraminiferal wackestone and ends with bioclastic foraminiferal packstone/grainstone microfacies. Intraclasts and breccia-like features are observed within the later microfacies at a depth of 3132 ft in well no.

10; these maybe the product of significant flooding and reworking (lag) (Fig. 3.7B). Then a major transgression occurred and resulted in the deposition of 65-75 feet thick of shale in the Khalifa Formation in the area (Appendix. 1).

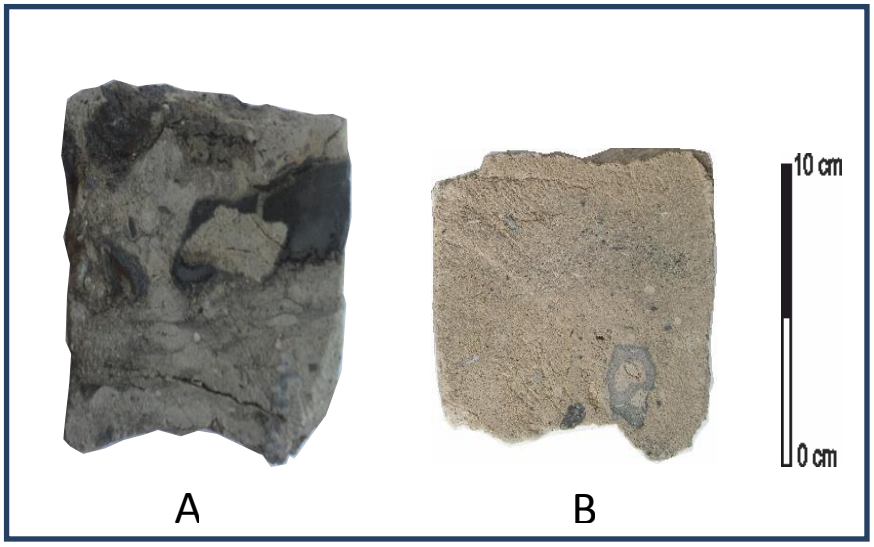

Figure 3.7 Angular intraclasts and/or breccia, with glauconite, in bioclastic foraminiferal packstone-packstone/grainstone facies in A) Dur al Abid Trough, Mabruk Member, Well no. 66 (2249 ft) ; B) Dahra Platform, Dahra Formation, Well no. 10 (3132 ft).

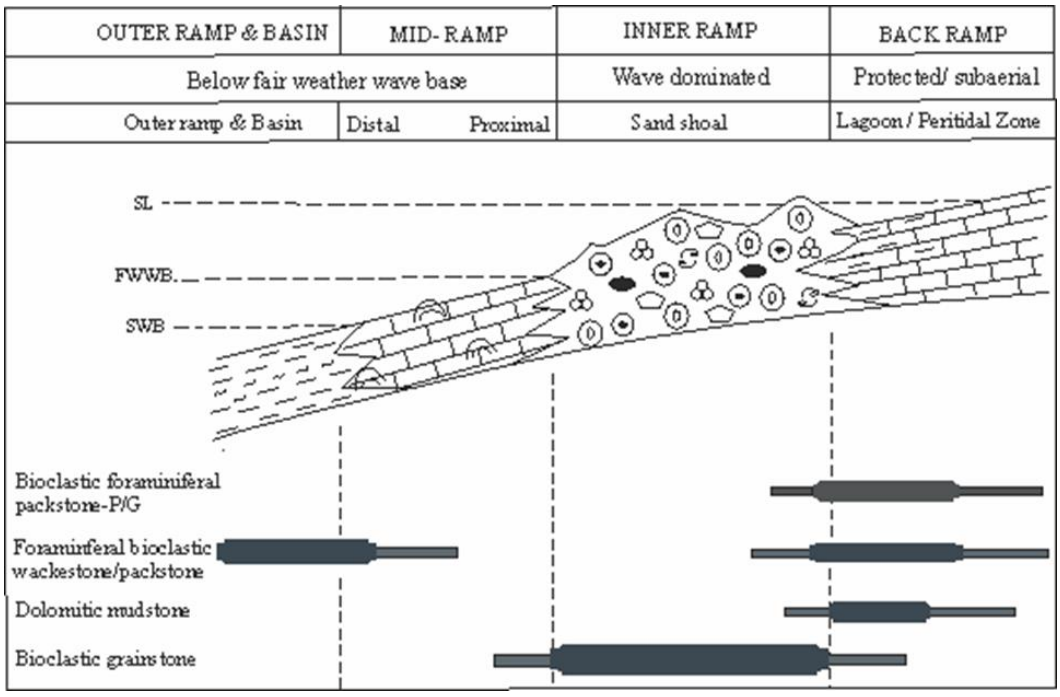

Figure 3.8 Depositional model for the Dahra Formation on the Dahra Platform. The depositional environments and distribution of macrofacies are shown.

3.3.2. Zelten and Harash Formations on the Dahra Platform

In the study area, the Harash Formation conformably overlies the Zelten Limestone and is overlain by the Kheir Formation. In some areas of the basin the Zelten Limestone cannot be differentiated easily from the overlying Harash Formation and thus a Jabal Zelten Group is used instead. Since the studied samples represent the upper part of the Zelten Formation and the lower part of the Harash Formation, both rock units have been dealt with together.

The thickness and gross lithology of the Upper Paleocene rocks (Thanetian) are almost consistent throughout the Sirt basin, and are mainly composed of shelf-margin carbonate at the base and grading upwards to marls and siliceous limestones of a deep-water environment (Bezan, 1996). Wennekers et al (1996) stated that the carbonates and minor shales of the Zelten and Harash Formations were deposited in a semi-restricted shallow- marine environment.

In the study area, the cored interval of the Zelten/Harash succession commences with about 10 feet of light olive grey, sub-fissile and pyritic marl. It grades up to several levels of mainly mud-supported carbonate facies (~58 feet thick) with a mixture of large and small benthic forams, in association with planktics (Appendix. 1). This could represent deposition in a mid–outer ramp setting with fairly restricted circulation and below fair weather wave base (Fig. 3.10). The succession passes upward to around 87 feet thick of chiefly grain-supported facies, in particular bioclastic foraminiferal packstone-packstone/grainstone, locally bioturbated and dolomitic with relatively common rotaliids, nummulites and echinoderm fragments. Pyrite, glauconite, phosphate and rare occurrences of hematite are recognised locally. An inner to back ramp is most likely the depositional environment for this interval of the uppermost part of the Zelten Formation.

The Zelten/Harash boundary is assigned, in this study, to the top of the dolomitic bioturbated bioclastic packstone microfacies and is marked by the presence of slightly deeper-water facies (dolomitic mudstone) over the grain-dominated deposits, that suddenly superimposed the carbonate factory of the Zelten Formation (drowning platform?- Chapter 5). Around 80 feet of Harash Formation, consisting of mixed wackestone and packstone facies, is assigned to a broad ramp setting that ranges from outer ramp to back ramp (Fig. 3.10). In the eastern part of the study area of the Dahra Platform (Dahra East Field) nummulite foraminifera and nummulite fragments occur at

particular intervals through the studied section, whereas the proper foraminiferal nummulitic microfacies occurs mainly at two specific levels (each around 15-20 feet thick); the lower is in the Zelten and the upper is in Harash Formation (Appendix.1). In the Dahra West Field, the nummulitic facies occurs at a single interval in the Zelten Formation, with an average thickness of 3-7 feet, whereas it is developed at two levels in the Harash Formation with a thickness of 10-20 feet (Appendix.1).

A notable feature of this facies is the development of a storm-like-bed at 2693ft depth in the Harash Formation of well no.8. Its base, which is mud-dominated, is characterized by an erosion surface and load structures, with the occurrence of flattened burrows in the form of stylo-nodular fabric. It passes up to grain-supported carbonate with common bioclasts (including nummulites) and pyrite (Fig. 3.9 A). Storm beds show much variation in thickness, grain size and internal structures, depending on the proximity to the area of the storm and the intensity of the storm (Tucker and Wright, 1990). They commonly show marked changes in character with increasing distance from the shoreline and increasing water depth (Aigner, 1982; Aigner and Reineck, 1982). A probable storm bed with common nummulites and concentration of shell fragments, particularly molluscs, occurs in the Harash Formation at a depth of 2675 ft in well no. 9 (Fig. 3.9 B). This bed may represent a lag deposit that possibly formed through storm reworking of the seafloor with no great transport of shells (Kreisa and Bambach, 1982).

A shallow inner ramp or bank with moderate to high energy, above fair weather wave base is proposed for this facies, despite the evidence that throughout the Cenozoic, nummulitids and other large benthic foraminifera were forced to occupy deeper water habitats through time, due to the colonization of the shallowest water environments by novel genera (Chaproniere, 1975; Buxton & Pedley, 1989; Hoheneggar, 1999). Almost the whole succession of the Thanetian and the individual rock units with their facies type and typical thicknesses can be correlated quite well over much of the studied area of the Dahra Platform; this suggests that similar depositional conditions were operating over the region.

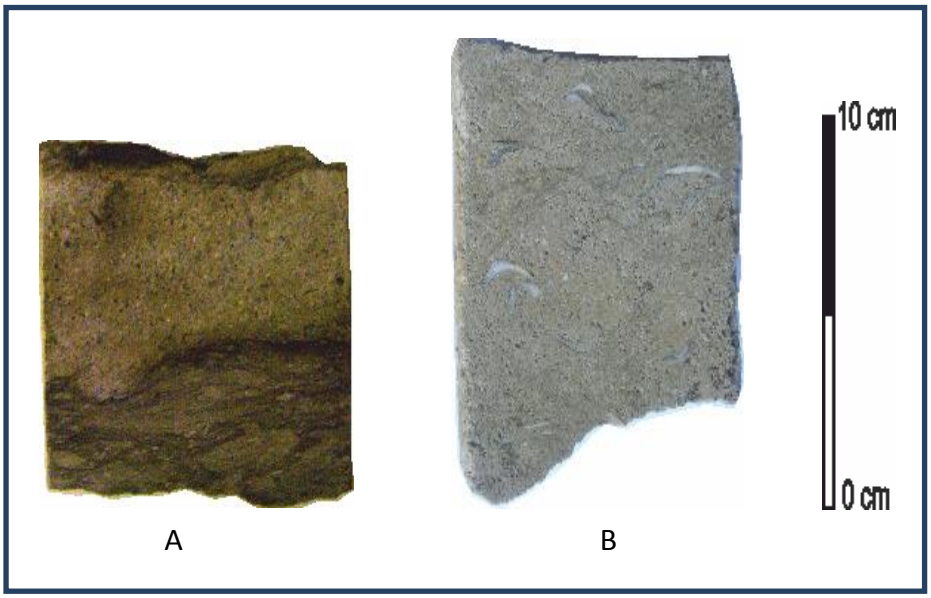

Figure 3.9 Slabbed core samples showing storm beds, A) Grain-supported facies overlying mud-dominated facies with load structure. Dahra Platform, East Dahra Field, Harash Fm, Well no. 8, 2693 ft.; B) Concentration of bioclasts as a basal layer. Dahra Platform, West Dahra Field, Harash Fm, Well no. 9, 2675 ft.

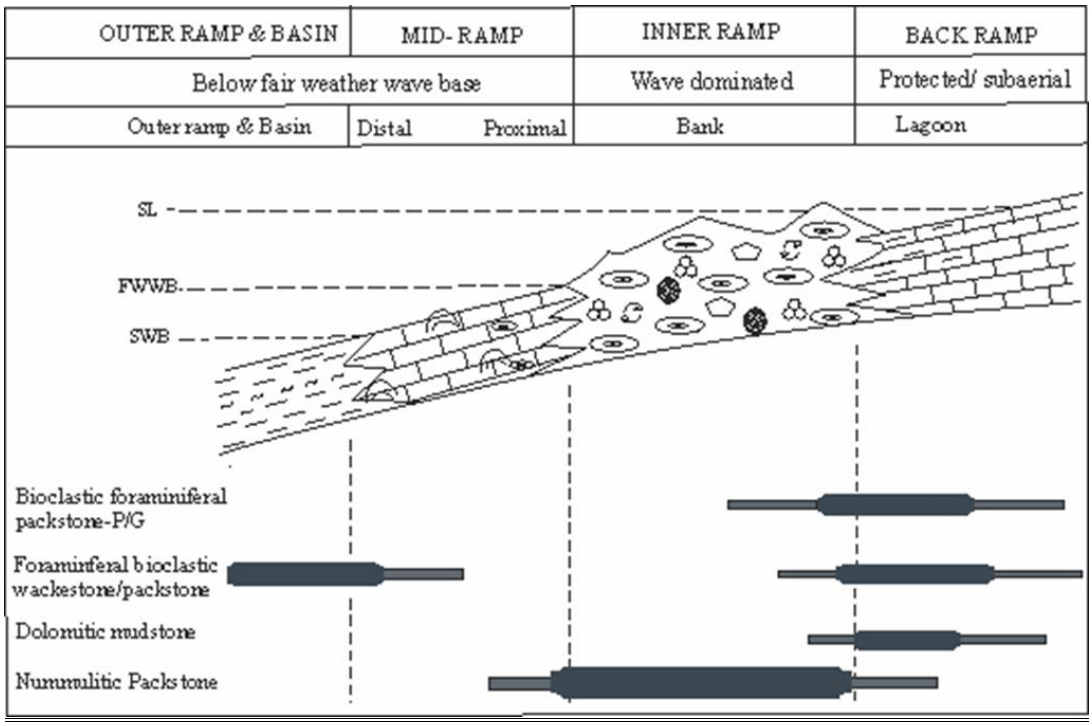

Figure 3.10 Depositional model for the Zelten and Harash Formations on the Dahra Platform. The depositional environments and distribution of macrofacies are shown.

3.3.3. Mabruk Member in Dor al Abid Trough

The carbonate interval of the Heira Formation in Dor al Abid Trough is composed mainly of mud to grain-dominated limestone with the local occurrence of dolomite in the upper part, and marl with intervals of mud-supported limestone in the lower part. Wackestone to grainstone and boundstone are recognised with common grains of small benthic forams, peloids, red algae, corals and rhodoliths.

The Mabruk area has been divided by the operating company into west, central and east segments, although some authors have dealt with the region according to the geographic directions. In their abstract, however, Machhour et.al, (1998) suggested an inner platform for the dolomitized limestone deposits in the southern zone; protected middle shelf for the central zone; and a northern zone where peri-reef deposits prevail. An isolated platform within a deeper basin model has also been proposed (internal report).

The Mabruk rocks show complex lateral and vertical variations from west through central to eastern areas. **The section in the southernmost part of the western area**, which is dominated by mud-supported facies, commences at the bottom, with about 15 feet thick of grey to dark grey, slightly soft marl. This is followed by whitish, soft and argillaceous mudstone, which in turn, grades upward into a thick interval of light grey, locally chalky, mudstone/wackestone facies with negligible to poor vuggy porosity. The whole interval (76 feet thick), which represents the lower Mabruk, is a shallowing-up succession. It is overlain by deeper-marine facies (20 feet of off-white to grey marl) which was probably the result of gradual subsidence of the basin and clastic influx.

The succession passes up to around 53 feet of bioclastic foraminiferal wackestone/packstone with very good vuggy and moldic porosity. The uppermost interval of the Mabruk is represented by 15 feet of white to light grey, moderately hard, argillaceous mudstone that underlies the thick section of marls and shales of the Hiera Formation (Appendix. 1). Overall, this interval of the Mabruk in this location represents deposition of mainly carbonates, bounded above and below by deeper marine marls and shales, and thus this could signify a lagoonal environment of an inner shelf setting (Fig. 3.12).

In the central parts of the East Central Mabruk Area, the section of the Mabruk reservoir starts with an interbedding of algal packstone facies (moderately to well

sorted, slightly bioturbated and dolomitic, with a minor amount of kaolinite (7%) and sporadic quartz and pyrite) and bioclastic foraminiferal packstone/grainstone facies that is characterized by fine to coarse-grains, poor to moderate sorting and common bioclasts of red algae, corals, bivalves and bryozoans. This interval, which has around 5 feet thick of dark greenish grey and slightly bioturbated marl towards the top, could represents deposition in a reefal location between fairweather and storm wave-base, where the energy is moderate to low. The presence of kaolinite in the upper part and below the overlying marl, in association with dolomite, may indicate an influx of riverine clastics through a minor sea-level fluctuation and/or a change to a more humid climate (Chapter. 5).

The middle interval of the Mabruk is occupied by a thick unit of coral algal bioclastic boundstone facies with thickness increases from about 38 feet thick in the northernmost area (well no.66) to around 96 feet in the central area (well no. 103), where it locally interbeds with algal packstone facies. It is light grey to pale orange, fine to coarse-grained, hard, poorly sorted with abundant corals (branching, columnar and massive) and their fragments, coralline (red) algae, small forams, echinoid spines and molluscan shells. At certain intervals, corals are quite large (9cm x 7cm) and they seem to be in their life position (Fig. 3.11). This strongly suggests that the broad middle interval of the Mabruk unit in this location represents a proper reef deposit (Appendix. 1). The shape, type and extension of this reef cannot be investigated with the limited data available.

In the northernmost area, in well no.66, the upper interval of the Mabruk (around 50 feet thick) is categorized mainly by grain-supported facies, with local occurrence of boundstone facies. A notable interval of this part is that of bioclastic foraminiferal grainstone facies (4268-4275 ft) with red algae, echinoderms, miliolids and green algae and rhodolithic algae, bivalves and peloids. Its porosity is mostly very good with intergranular, intragranular, vuggy and moldic types. This particular facies may signify deposition in shallow shoal setting that might have formed just behind the shelf-margin reef, or alternatively in a high-energy setting within the wider reef area (Fig. 3.12).

The uppermost part of the Mabruk is characterised by the presence of a conspicuous facies contrast between bioclastic algal packstone facies below and greenish grey, calcareous shale above (Heira Formation). The transitional bed, 2 feet

thick, is categorized by development of breccias with angular intraclasts, that contain pyrite, glauconite, phosphate, reddish brown stains (hematite?), along with micro-borings (Fig. 3.7A). The intraclasts indicate reworking and could be a lag deposit, associated with a major flooding event. This could be a drowning unconformity (Schlager, 1981, 1989). A number of mechanisms have been proposed in the literature in order to explain the demise of a carbonate platform and the generation of a drowning unconformity; a) rapid sea-level rise or the tectonic collapse of the platform (e.g. Schlager, 1981, 1989); b) lack of reef building organisms, causing a sharp decrease in the rate of carbonate production, thus fostering their drowning when subsidence or sea-level increases (Bice and Stewart, 1990); c) 'Killing' of carbonate platforms by waters polluted with siliciclastics and/or volcaniclastics (Schlager, 1989); d) flooding of platforms by nutrient-rich waters, causing the eutrophication of the carbonate system and a drastic reduction of its growth potential (Hallock, 1988; Follmi, 1989). The proposed Bice and Stewart mechanism is probably the most appropriate cause for the discontinuation of carbonate production in the Mabruk Area.

In the southern part of the East Central Mabruk Area, the entire Mabruk section shows the characteristic features of a lagoonal environment. However, it starts with about 49 feet of alternations of light to medium grey, sub-fissile to sub-blocky marl, and light grey to light greenish grey, argillaceous and locally burrowed, slightly compacted, bioclastic wackestone/packstone-packstone facies. This Lower Mabruk interval could represent a somewhat deeper area in the region of a reefal complex (back reef or fore reef area).

The Upper Mabruk is mostly composed of an intercalation of dolomitic bioturbated bioclastic wackestone/packstone and bioclastic foraminiferal packstone with the local occurrence of marl and greenish grey, calcareous and slightly pyritic shale. Its lower interval (~36 feet thick), which is dominated by wackestone/packstone, is characterized by the presence of small forams, bryozoans, crinoids and echinoid spines with scattered bivalves and green algae. The high content of lime-mud and the presence of an open-marine fauna in association with marl and shale probably suggests deposition in distal area of the inner shelf– to the proximal part of the outer shelf, below fair weather wave base, for the lower part of the Upper Mabruk Member (Fig. 3.12). This interval, which is capped by 8 feet of shale and marl, passes up abruptly into to much shallower deposits, around 20 feet thick, of bioclastic foraminiferal packstone. Its

main components are benthic forams (mainly miliolids and rotaliids), green algae (dasycladacean), echinoderms and molluscan shells. Its overall porosity is good to very good with intragranular, moldic and vuggy pores.

Dasycladacean green algae are common within very shallow-water depths of only a few tens of centimetres down to depths of around10 metres (Flügel 2004; Madi *et al*. 1996). They are most common within the tidal to uppermost sub-tidal zone. Miliolid foraminifera and rotaliids are common in inner shallow shelves. The stable isotope values show low positive carbon (1.63‰) and the negative $\delta^{18}O$ (-5.45 ‰) is the most negative value in this well. Thus the overall depositional environment of this interval was likely a shallow-marine lagoon that was subjected to a periodic exposure, despite the fact that (apart from extensive dissolution) characteristic pedogenic features have not been recognized.

This interval is overlain by 3 feet of medium grey to greenish grey, sub-fissile to sub-blocky marl with a fairly sharp contact that signifies a deepening event, which was probably brought about as a result of rapid basin subsidence and/or sea-level rise (Chapter 5). However, continuous deepening of the basin, which was accompanied by a decrease in oxygen content, resulted in the intercalations of shale, marl and bioclastic wackestone/packstone. This transgressive sediment may represent deposition in a proximal outer shelf and below fair weather wave base, where local reducing conditions prevailed. This is witnessed by the presence of authigenic pyrite all through the interval. The occurrence of dolomite, kaolinite and minor quartz, on the other hand, may reflect proximity to a sediment source and deposition in a relatively nearshore setting (Flugel, 2004) or it could suggest a period of low sea-level.

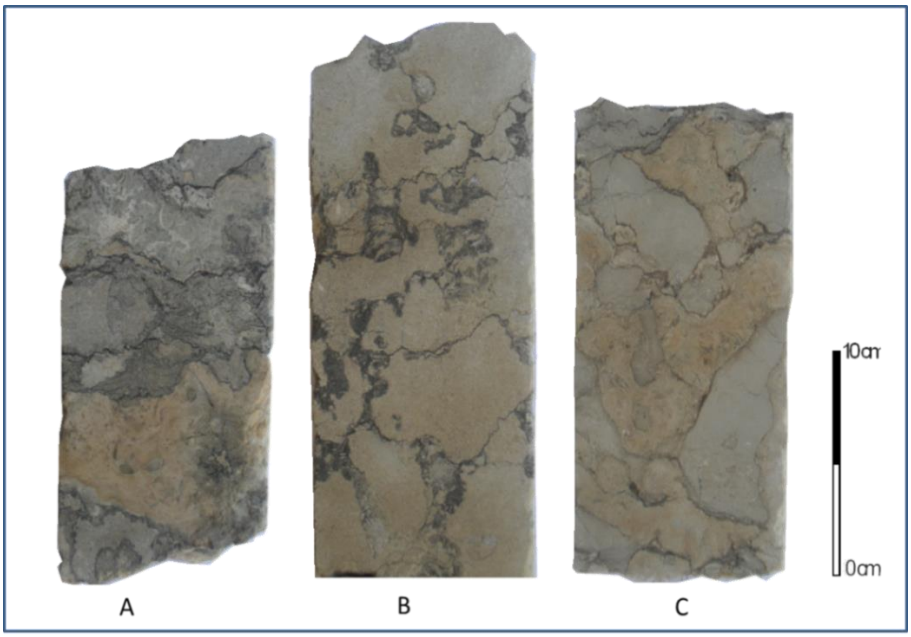

Figure 3.11 Photos of slabbed core showing corals in their growth position in the coral algal boundstone microfacies. Dor al Abid Trough, Mabruk Member, Well no 66, at depth of 4291 ft (A); 4319 ft (B); 4321 ft (C).

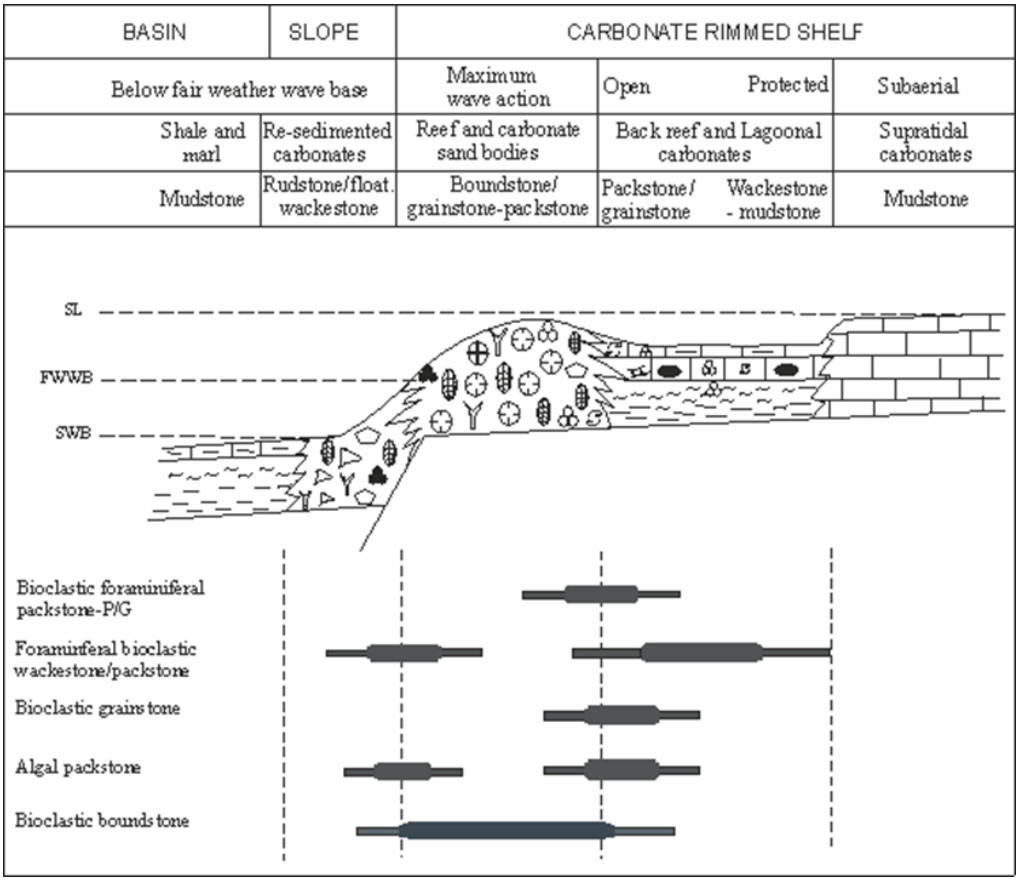

Figure 3.12 Depositional model for the Mabruk Member of the Heira Formation in Dor al Abid Trough. The depositional environments and distribution of macrofacies are shown.

3.5. Summary

Comprehensive investigation of the Selandian/Thanetian carbonates has resulted in the recognition of four major lithofacies; limestone, dolomitic limestone/dolomite, argillaceous limestone/marl, and shale. The marl is widely distributed in the Dor al Abid Trough and covers a large part of the Paleocene succession (Heira Formation), where it locally grades to very calcareous shale. The shale is extensively developed across the Dahra Platform and is usually medium grey to greenish grey, fissile, dolomitic, slightly pyritic with scattered small un-identifiable bioclastic fragments.

Macroscopic and microscopic investigations of the studied samples have resulted in the recognition of seven main macrofacies and eleven associated microfacies within the Selandian/Thanetian carbonate succession. These macrofacies are: Bioclastic foraminiferal packstone-packstone/grainstone; Foraminiferal bioclastic wackestone-wackestone/packstone; Dolomitic lime-mudstone; Bioclastic foraminiferal grainstone; Foraminiferal nummulitic packstone; Algal packstone; and Bioclastic boundstone.

The first four macrofacies have been recognised in the Dahra Field on the Dahra Platform within Dahra, Zelten and Harash Formations, while the fifth one, nummulitic foraminiferal packstone, only occurs within the Zelten and Harash Formations. The main carbonate grains within the Dahra Formation are rotaliids, miliolids, echinoderms, molluscs, ooids and green algae. Desiccation cracks, rootlets and internal sediments in the middle interval of the Dahra Formation are interpreted as pedogenic features that developed under semi-arid conditions.

The Dahra Formation on the Dahra Platform was deposited on a homoclinal carbonate ramp with inner, mid and probably outer ramp facies, each with distinctive sub-facies and microfacies. The core description, petrographic examination and geophysical log indicate that there are no drastic changes in the facies and associated microfacies throughout the Dahra Formation; it seems that the Dahra was probably deposited under similar conditions throughout the east and west Dahra Fields on the Dahra Platform.

The dominant bioclasts within the Zelten and Harash carbonates are benthic forams, molluscan shells, nummulites, bryozoans and echinoderm fragments. The Zelten/Harash boundary is placed at the top of a dolomitic bioturbated bioclastic packstone and is marked by overlying deeper-water facies (mudstone) that suddenly replaced the carbonate factory of the Zelten Formation. The nummulite foraminifera and

nummulite fragments are scattered at particular intervals through the studied section, whereas the foraminiferal nummulitic microfacies itself occurred mainly at two separate levels in the Zelten and Harash Formations.

A similar depositional setting was re-established in Zelten and Harash Formations across the area, with local occurrences of nummulitic packstone instead of bioclastic grainstone in the Dahra Formation and the development of mainly wackestone- packstone.

The central part of the Mabruk Field in Dor al Abid Trough is dominated locally by algal packstone and bioclastic boundstone macrofacies, whereas the eastern and western parts are characterised by the common presence of facies number 1, 2 and 4. The component grains are dominated by benthic forams, peloids, red algae, corals and rhodoliths. The middle interval of the Upper Mabruk Member in the East Central Area is occupied by reef and reef-related facies that increase in thickness towards the south east.

The deposition of a thick succession of shale and marl of the Heira Formation just above the Mabruk Member associated with the presence of angular clasts, glauconite, pyrite and hematite indicates a deeper water environment and the formation of drowning unconformity.The overall interval of the Mabruk Member in the study area represents deposition of mainly shallow-water carbonates that were bounded by deeper-marine marl and shale; these may have accumulated in lagoonal and reefal environments in probably rimmed shelf setting.

CHAPTER FOUR: DIAGENESIS AND RESERVOIR QUALITY

4.1. Introduction

The diagenesis of carbonate rocks includes all of the processes involving dissolution, cementation, lithification and alteration of the sediments during the interval between deposition and metamorphism (Flügel, 1982).

Diagenesis includes obvious processes such as cementation to produce limestones and dissolution to form cave systems but it also includes more subtle processes such as the development of microporosity and changes in trace element and isotopic signature. However, diagenetic changes can begin on the seafloor, as the grains are still being washed around, or it may hold off until burial when overburden pressure has increased or pore-fluid chemistry has changed so that reactions are then induced within the sediments (Tucker and Wright, 1990). Major controls on the diagenesis, according to these authors, are the composition and mineralogy of the sediments, the pore-fluid chemistry and flow rates, geological history of the sediment in terms of burial, uplift, sea-level changes, influx of different pore-fluids and prevailing climate.

Most of these diagenetic processes can operate in different environments, although some are diagnostic of a particular diagenetic environment. Marine diagenesis takes place on the seafloor and just below, and on tidal flats and beaches. The marine phreatic zone is characterized by normal-marine pore fluids supersaturated with respect to $CaCO_3$ in shallow, warm seas. The meteoric diagenesis realm is the zone where rain fall-derived groundwater is in contact with sediment or rock. The mixing zone lies between the meteoric phreatic zone and underlying marine waters. It is characterised by a mixture of marine and meteoric waters (brackish water). Burial diagenesis is generally taken to begin below the depth were sediments are affected by near-surface processes of the marine and meteoric environments (Tucker and Wright, 1990). Burial pore fluids generally are supersaturated with respect to the most stable carbonate species (Choquette and James, 1987).

After deposition, the Selandian/Thanetian carbonate rocks in the western Sirt Basin were affected by various diagenetic processes during their burial history. All three diagenetic environments have been documented; each has its own characteristic features and products. Micritization, burrowing, dissolution, cementation, compaction and dolomitization are all recorded, along with some less important and minor diagenetic events.

Carbonate reservoirs are characterised by extremely heterogeneous porosity and permeability. These heterogeneities are dependent on the environments of deposition and on the subsequent diagenetic alteration of the original rock fabric (Allen and Allen, 1990). Most of the above mentioned diagenetic processes have been recognised in the studied Selandian /Thanetian reservoirs in both the Dahra Platform and Dor al Abid Trough. They affected reservoir quality in two ways; positive diagenetic processes which include the dissolving activity of meteoric water, dolomitization, fracturing, and the migration of oil; and negative processes which include compaction, sediment filling (matrix deposition), pressure dissolution, and cementation (Cook, 1983).

The aim of this chapter is to deliver a detailed description and appropriate interpretation of the post-depositional processes that have affected the studied interval of the Paleocene Succession in the Sirt Basin by using routine petrography, scanning electron microscopy, cathodoluminescence, x-ray diffraction, stable isotopes and fluid inclusions. The impact of these diagenetic processes on the reservoir quality of the Dahra (and Mabruk Mbr), Zelten and Harash Formations is also addressed. The latter issue is reported via petrographic investigations and core analysis.

4.2. Diagenetic processes and products of the Selandian/Thanetian carbonates

The carbonates of the Dahra, Mabruk, Zelten and Harash Formations, in the study area, have undergone a series of diagenetic processes which affected, in different ways, their composition, mineralogy, pore throat system, and hence their reservoir potential. These events vary from early diagenetic processes such as micritization, neomorphism, dissolution, dolomitization, and calcite cementation, to late burial diagenetic changes which include dolomite cementation, dissolution, compaction, and fracturing.

4.2.1. Boring and microbial micritization

The destruction of hard substrates by boring organisms is significant and leads to the breakdown of carbonate skeletons and the production of fine-grained to sand-sized sediments, especially in warm-water environments. It is controlled by illumination, nutrients, sedimentation rate, siliciclastic input and water depth (Flügel, 2004).

Microboring (< 1µm-100µm) is a product of microboring organisms including bacteria, cyanobacteria, fungi, foraminifera and bryozoans. They have a wide bathymetric distribution ranging from supratidal and intertidal environments to subtidal and deeper-water environments. This early diagenetic seafloor process has been recorded at several intervals in the studied succession in both Dahra Platform and Dor al Abid Trough sediments, where microborers and macroborers attacked skeletons, carbonate grains and, locally, the micritic substrate within the Dahra, Mabruk and Zelten Formations (Fig. 4.1E, F, G and H). They are fairly rounded in shape, with an average size of 0.2-0.5 mm in diameter and commonly are filled with small forams, fragments of echinoids and intraclasts, peloids and micrite sediment.

These borings were probably made by clionid sponges. When the bores cut both grains and substrate it may form a hardground surface, which is best developed in areas of slow sedimentation and high current activity at just below the seafloor (Tucker and Wright, 1990). This is possibly the case at a single interval within the studied section of the Dahra Formation in well no.10 (Fig. 4.1H). That surface is characterized by encrusted and bored dolomitic packstone with a high concentration of pyrite, glauconite and phosphate minerals (Appendix 1- sedimentological log of well no.10).

The bivalves and calcareous algae that present at the intervals of borings and hardgrounds are commonly encrusted by bryozoans. Although the bores from the algae occur in grains within the photic zone, grains below it are still being bored but mainly by fungi, which produce bores of diameter 1-2 µm (Zeff and Perkins, 1979). Encrusted bryozoans, brachiopods and oysters, however, occur on both surfaces of hardground (upper and lower surfaces). Differences in encrustation indicate the polarization of the fauna according to the light intensity, rate of sedimentation and turbulence level (Flügel, 2004).

Boring algae and fungi are believed to increase the initial intragranular porosity of sediment during and shortly after deposition (Bathurst, 1966; James and Choquette, 1983). On the other hand, borings filled with internal sediment can play a negative role in terms of reservoir quality, as it reduces the intragranular porosity.

Micritization is the process by which bioclasts are altered while on the sea-floor or just below by endolithic algae, fungi and bacteria (Tucker and Wright, 1990). Although this diagenetic process has affected the Dahra, Zelten and Harash Formations in some wells, overall it is a fairly uncommon feature in the studied interval, particularly within the Dor al Abid Trough. Micrite envelopes and boring are usually

suggestive of microbial action in shallow-marine environments; micrite envelopes are indicative of deposition within the photic zone, however, microboring endolithic organisms are also found in deeper water (Flügel, 2004).

The micritization process helps maintain the outlines of grains in slightly neomorphosed rocks through the formation of micrite envelopes (Fig. 4.1A). Repeated boring and filling in different parts of the shell may result in the formation of a micrite envelope of irregular thickness. Continuous boring processes may lead to totally micritized grains (peloids) that are slightly smaller than the associated skeletal grains.

Micritized grains are characterized generally by an irregular shape, structureless nature, and they mostly range in size from 100 to 300μm (Fig. 4.1C). In view of these characteristics, they have been attributed to a process of complete micritization. Pellets, of probably faecal origin, with smoother shapes and smaller size occur throughout the succession (Fig. 4.1 C&D).

Micritic envelopes due to endolithic cynobacteria can be used as a depth criterion, indicating deposition within the photic zone, less than 100-200m (Zeef and Perkins, 1979). The micritization process itself is an early diagenetic event taking place within the marine phreatic environment, generally in more stagnant, low energy areas, near or at the sediment/water interface (Longman, 1980).

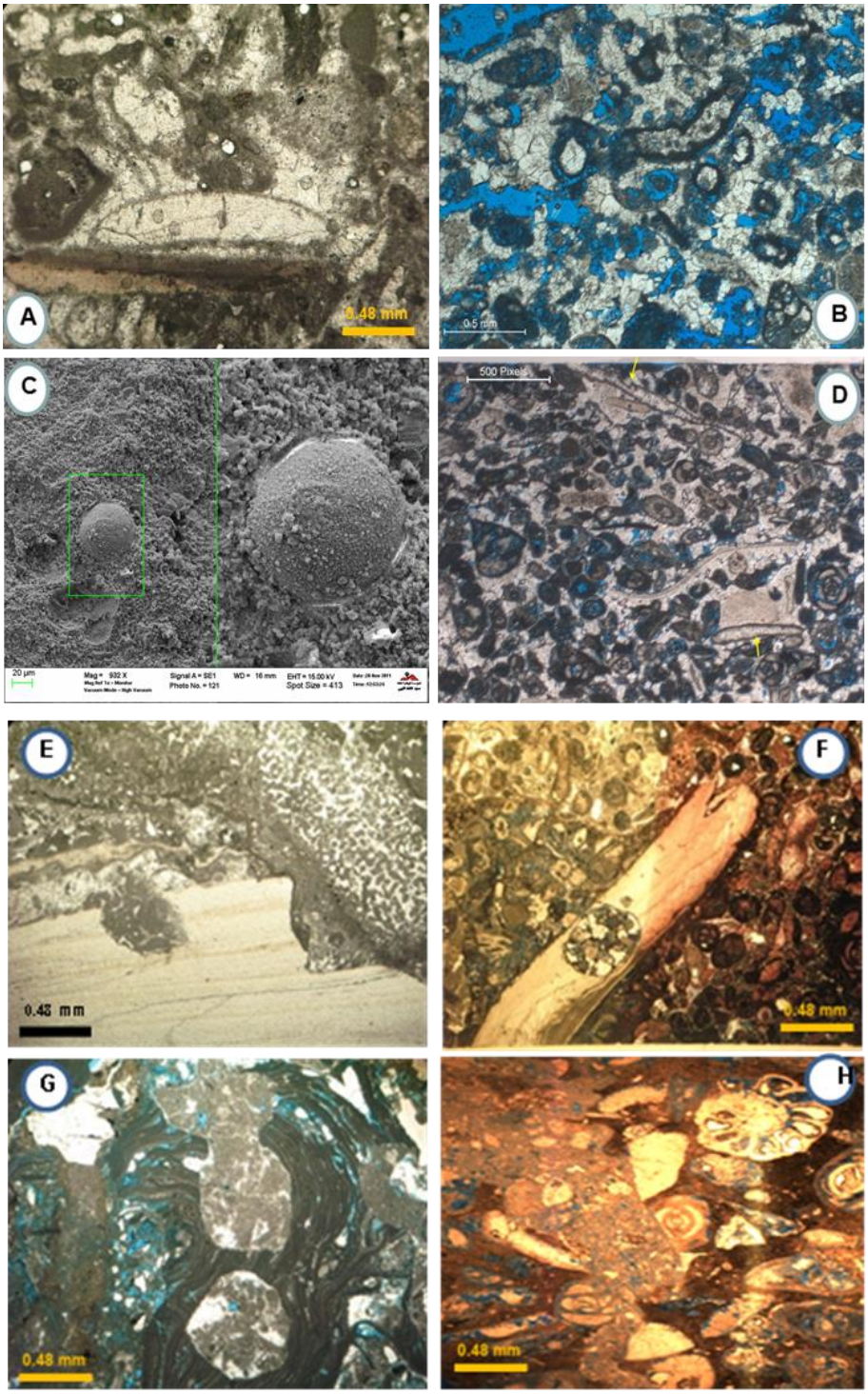

Figure 4.1 Micritization and boring in the Paleocene carbonates.Formation of a micrite envelope around carbonate grains in Mabruk Mbr in well no. 103 (A), and in the Dahra Fm in well no.9 (B).Scanning electron microscopy image of a pellet in the Mabruk Mbr in well no. 66. (C).Peloids and pellets in the DahraFm in well no9. (D). Bored bivalve shells, probably by clionid sponges, in the Mabruk Mbr. in well no. 103 (E), and in the Dahra Fm in well no. 7 (F). Clionid sponge boring of rhodoid algae in the Mabruk Mbr in well no. 66 (G). Possible hardground surface, where boring has cut grains and the matrix in the Dahra Fm in well no.10 (H).

4.2.2. Burrowing

Bioturbation commonly alters or destroys bedding and lamination and contributes to homogenization of the sediment (Reineck, 1963). Burrows, in contrast with borings, are formed within soft unconsolidated sediments by the activity of animals during feeding, resting or migration (Flügel, 2004). Pedley (1992) has proposed the term b*io-retexturing*-the process by which burrowing biota may modify or transform original textures by relocating significant volumes of unlithified sediment into or out of the sedimentary layers.

Burrowing is present throughout the studied section of the Paleocene, particularly in the Dahra Formation, where it is locally extensive. The Zelten carbonates, however, represent the least burrowed interval of the late Paleocene carbonates in the study area. Most of the burrows are flattened and oriented horizontally with some sub-horizontally or sub-vertically. Swirly structures and irregular and lined borders to burrows have locally been recorded (Figs. 4.2; 3.3 and 3.5). A U-shaped burrow with concave-down laminae (*Diplocraterion*) has been developed only at a single interval within the Dahra Formation in Well no.10. It is about 20 cm long and thought to have been made by sessile or semi-sessile endobenthic animals, particularly suspension feeders, predators and scavengers (Tucker, 2011). They believed to have been formed through upward or downward movement of the animal in response to sedimentation or erosion, respectively (Fig.4.2D).

A feature noteworthy is that the burrowed intervals have commonly been dolomitized and subjected to a different intensity of compaction, which in several cases has resulted in the formation a vaugely bedded fabric, making identification of the original depositional texture (wackestone versus packstone) not easy. Differential dolomitization of the burrowed intervals seem to be controlled by the grain type (composition) and grain size of the burrow fill, i.e. many burrows are completely dolomitized whereas others are less dolomitic. The finer crystal size of burrow fills as compared with the micritic matrix may be one factor controlling the often observed selective dolomitization of burrow fills (Zenger, 1992). Bio-retexuring profoundly controls diagenetic processes because it can selectively increase individual bed permeability where coarse burrow back-filling is dominant. On the other hand, locally it can inhibit early sea floor cementation by admixing micritic sediment into grain support fabrics. Feeding, burrowing and irrigation increase solute transport and solid-phase reaction rates, thus leading to rapid carbonate dissolution (Green et al., 1992).

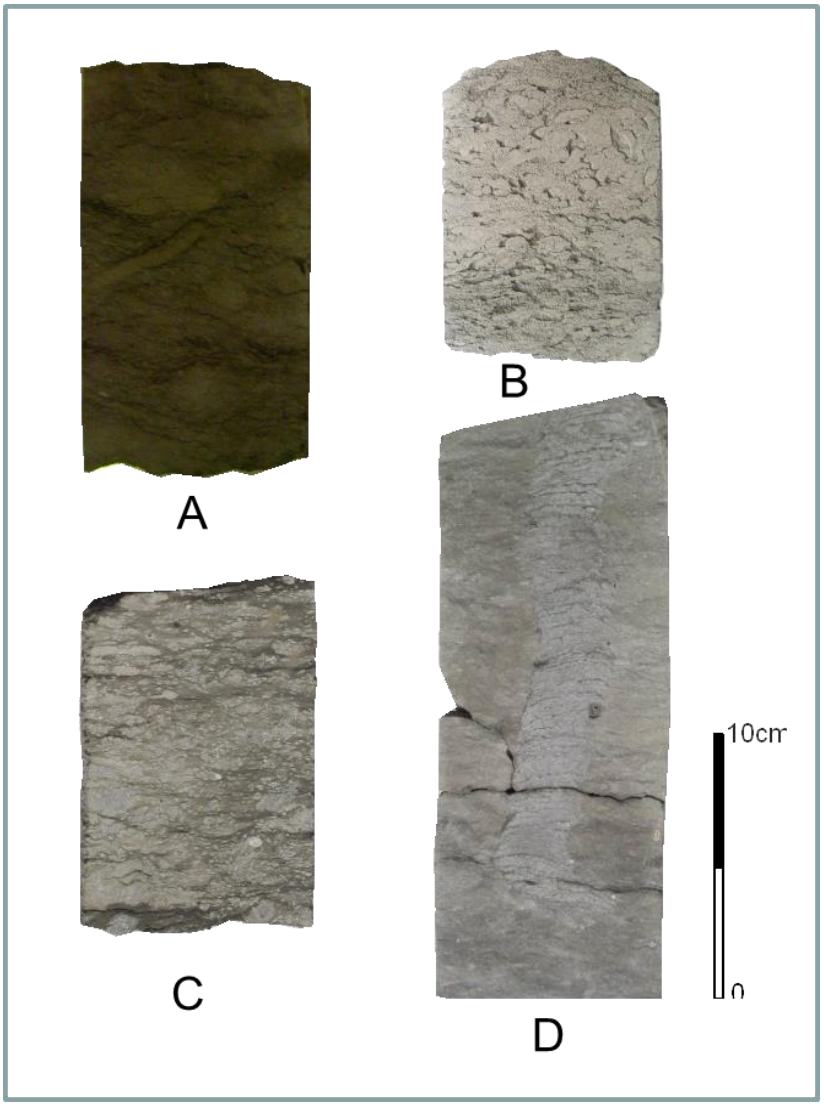

Figure 4.2 Burrows within the Selandian/Thanetian section. A) Horizontal and sub-horizontal burrows in dolomitic bioturbated bioclastic w/p in the uppermost part of Zelten Fm. Well no. 8, 2731 ft.; B) Extensivly burrowed and highly compacted feature in dolomitic bioturbated bioclastic packstone in the middle part of the Dahra Fm. Well no. 7, 3331 ft.; C) Horizontal burrows (grain-dominated) within a mud-supported matrix of the wackestone packestone facies in the lower part of the Harash Fm. Well no. 9. 2655 ft.; D) U-shaped burrow (*Diplocraterion*) inmud-supported interval in the middle part of the Dahra Fm., Well no. 10, 3213 ft.

4.2.3. Neomorphism

The term neomorphism was introduced by Folk (1965) to cover processes of replacement (transformation between one mineral and another) and recrystallization (change in crystal size without any change of mineralogy). Most neomorphism in limestones is of the aggrading type that is leading to a general increase in crystal size, resulting in microsparitic patches, lenses, lamina and beds (Tucker and Wright, 1990).

The term aggrading neomorphism is commonly used in lime mud diagenesis to describe the enlargement of mosaics to microspar (~5-10 μm) or to a coarser pseudospar (>30 μm). The key point about the neomorphism, recrystallization, and calcitization processes is that dissolution and re-precipitation takes place across a thin film and without large-scale dissolution and porosity formation (Adams and Mackenzie, 1998). The transformation of aragonite and high-Mg calcite grains and mud to low-Mg calcite is one of the most important processes in carbonate diagenesis because it controls the ultimate petrophysical properties of limestones and their geochemical composition (particularly stable isotopes and Sr content: Al-Asam and Veizer 1986a, 1986b; Banner 1995; Maliva 1998).

Neomorphism is not a widespread diagenetic process in the studied interval of the Paleocene succession. The micrite matrix in some of the thin-sections, with crystals/grains usually less than 5μm diameter, has been subjected to fairly extensive neomorphism that resulted in the development of a neomorphic fabric of subhedral to anhedral crystal shape with less than15μm crystal size (Fig. 4.3A&B). This aggrading process of neomorphism is evidenced by the irregularity of the microspar crystal boundaries and the patchy scattered development of micrite. However, Folk (1965) suggested that neomorphism from micrite to microspar is commonly a neomorphic response to increasing stress in a wet medium.

The neomorphism process appears less extensive in the mud-supported intervals of the studied succession, where the limestone becomes gradually argillaceous. This is probably because neomorphic effects are most prominent in pure micrites; where there is significant clay content, and then aggrading neomorphism appears to be inhibited (Tucker and Wright, 1990). It has also been suggested that the presence of Mg^{2+} ions prevents neomorphism by forming a cage around the micrite crystals. If this is removed by meteoric water flushing or adsorption of the Mg^{2+} ions on to clay minerals, then microspar crystal growth takes place (Folk, 1974; Longman, 1977).

Based on the petrographic observations and cross cutting relationships it seems that this process has possibly developed in the meteoric diagenetic environment, despite the fact that neomorphism may take place during burial diagenesis or during weathering (Tucker, 1991).

4.2.4. Dissolution

Many carbonate rocks have suffered dissolution as a result of the passage of pore fluids undersaturated with respect to the carbonate phase present.

At least two major phases of dissolution occurred in the studied interval of the Paleocene succession. The first phase has caused the dissolution of the original aragonitic, and probably high Mg-calcite grains together with some matrix. This has resulted in the formation of mouldic and vuggy secondary porosity at different intervals and is present in most of the defined facies of the Dahra, Mabrouk, Zelten and Harash Formations, but to different degrees (Fig. 4.3C). Much of this porosity has subsequently been occluded, partly or completely, by equant non-ferroan, locally ferroan, calcite or dolomite cements (Fig. 4.3 E&F).

This relatively early phase of dissolution probably occurred in the upper part of the meteoric phreatic environment (zone of active circulation), where the meteoric waters are strongly undersaturated with respect to the metastable carbonate species (Longman, 1980). Meteoric diagenesis starts with the loss of magnesium from high-Mg calcite followed by the gradual disappearance of aragonite and the replacement of aragonite by calcite (Flügel, 2004). Although the dissolution is a major process in near-surface, meteoric, diagenetic environments, it can also take place on the sea floor and during deep burial (Tucker, 1991).

The second phase of dissolution has not only resulted in the total leaching of possible evaporites but also the partial dissolution of medium to coarsely crystalline void-filling dolomites. As a result, moldic porosity or dedolomite porosity has been developed on both the Dahra Platform (Dahra Field) and the Dor al Abid Trough (Mabruk Field) (Fig. 4.3D, E &F). This type of porosity has probably been formed by leaching of the dolomite and evaporite crystals at intermediate to burial depths, probably through the presence of strong acidic formation waters. Despite the fact that open dolo-molds may indicate subaerial exposure and dissolution by karst waters (Braun and Friedman, 1970), the dissolution of carbonates in a deep burial setting is attributed to the development of pore waters with high pco_2 formed during the thermal decarboxylation of organic matter or to sulphate reduction.

Such corrosive fluids are most likely to be formed during compaction and thermal maturation of organic-rich shales (Tucker and Wright, 1990). The same authors stated that burial dissolution of sulphate evaporites may led to Ca^{2+} -rich fluids capable of dissolving dolomite and/or causing dedolomitization.

Scanning electron microscopy examination revealed that intercrystalline microporosity has also been developed in the studied rocks, in particular at wells no. 8 and 9. This probably developed as a result of the re-orientation and/or dissolution of outer parts of micrite and/or microsparite crystals (Fig.4.3G&H).

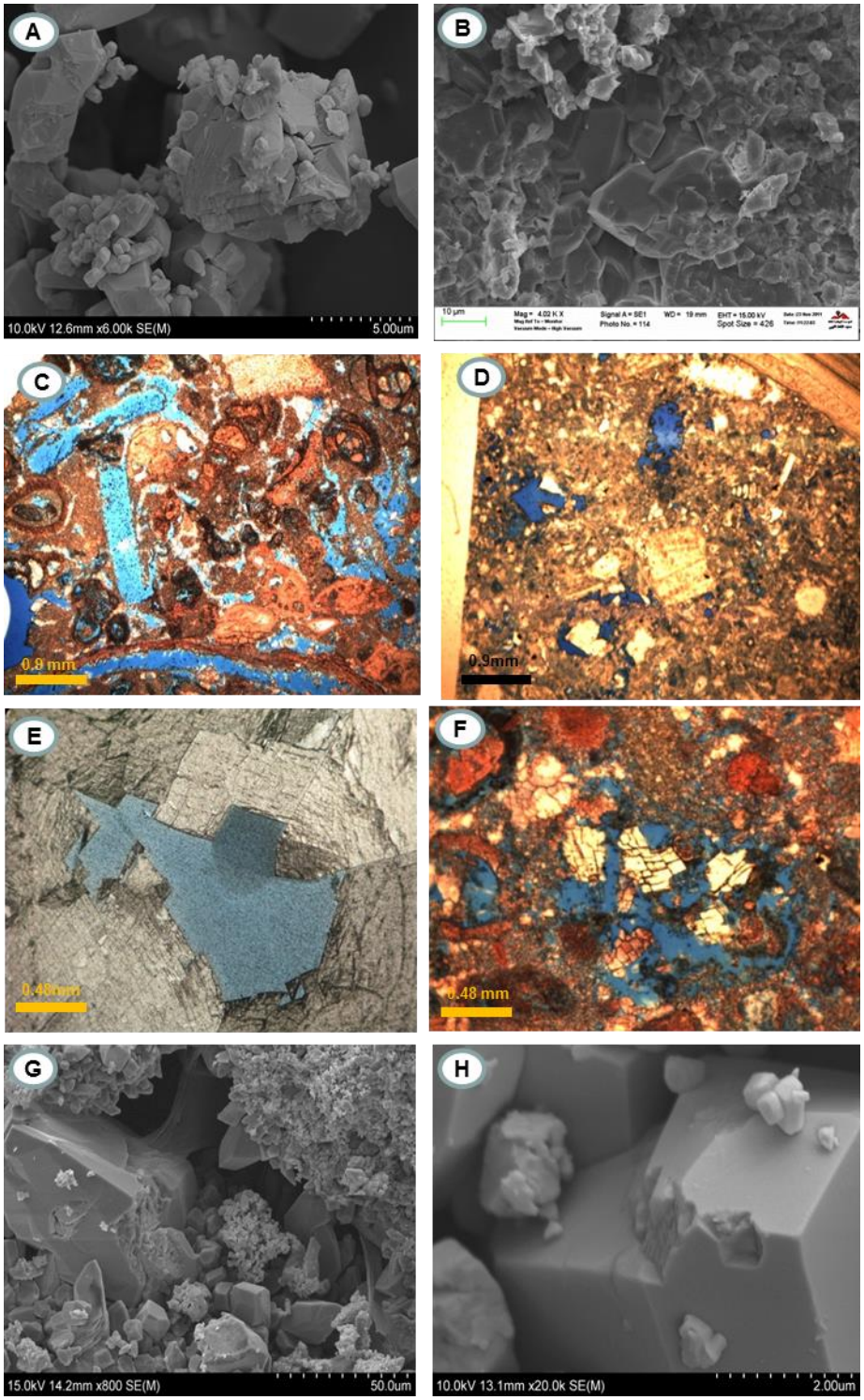

Figure 4.3 A&B: SEM photomicrographs showing neomorphosed micrite to microspar of less than 15 µ in size. Dahra Fm, 3119 ft, Well no. 8 & Mabruk Mbr., 4266 ft, Well no.66, respectively.; C: Dissolution (mainly molds) porosity in the Dahra Fm, 3167 ft, Well no.10.; D: Evaporite molds (left centre) in the Zelten Fm, 2779 ft, Well no.9.; E&F: Partial dissolution of coarse dolomite crystals (late stage) in the Mabruk Mbr, 3736 ft, Well no. 105& in the Dahra Fm, 3167 ft, Well no. 10, respectively.; G&H: SEM photomicrographs showing dissolution of the outer parts of microsparite (G) and micrite (H) crystals which contribute to the overall good porosity in the Dahra Fm at 3076 ft, Well no. 9, and at 3119 ft, Well no.8, respectively.

4.2.5. Cementation

The precipitation of cements in carbonate sediments is a major diagenetic process and takes place when pore-fluids are supersaturated with respect to the cement phase and there are no kinetic factors inhibiting the precipitation (Tucker and Wright, 1990). Most cements in carbonate rocks are themselves carbonates (broadly, calcite and dolomite), although quartz and evaporites occur locally (Adams and Mackenzie, 1998). Apart from dolomite cement, three types of calcite cement have been recognized. These are: isopachous calcite, equant sparry calcite, locally blocky, and syntaxial overgrowth cements.

4.2.5.1. Isopachous calcite cement

The isopachous calcite cement is not abundant and represents the least common cement within the studied rocks. It occurs mainly in the bioclastic foraminiferal packstone-packstone/grainstone and bioclastic foraminiferal grainstone facies, where it consists of elongate crystals oriented perpendicularly with respect to the substrate. The crystals grow mainly on the outer, rarely on the inner, walls of the both non skeletal and skeletal grains, particularly foraminifera (Fig.4.4A). Scanning electron microscope investigation shows that the crystals, which are usually ≤15 μ long, grow towards the pore and increase in size away from the substrate (Fig.4.4B).

The features of this type of cement indicate that it is a low Mg-calcite, although its mode of origin is rather difficult to interpret. It could have been formed from marine water as a direct precipitate or by replacement of unstable minerals. Alternatively, it could also have been precipitated in the meteoric environment.

The shape and distribution of this cement along with its occurrence in a relatively compacted fabric (pre-dating the closer packing of grains) may suggest that it was possibly deposited in marine environment. However, growth of bladed calcite spar, especially in thick isopachous crusts, has mostly been recorded from subsea-floor cemented limestones (Marlowe, 1971; Schroder, 1972; James et al., 1976) and is generally recognised as a fringe of crystals growing normal to the substrate. Thus this isopachous calcite probably pre-dated the dissolution and compaction processes, as suggested by the fact that it is present at the grain contacts, which possibly reduced the effect of mechanical compaction at those intervals.

4.2.5.2. Equant calcite cement and meniscus cement

The term equant refers, in this study, to both equant sparry calcite cement and coarse blocky calcite cement. Together they represent relatively the most common calcite cements within the studied Paleocene carbonates.

The equant sparry calcite cement occurs in most of the defined facies, in particular bioclastic foraminiferal grainstone and bioclastic foraminiferal packstone-packstone/grainstone facies. It virtually occludes the pore spaces as second generation cement, following the early marine cement and is locally ferroan. The calcite crystals of this cement are characterised by clear, equant to slightly elongate, usually subhedral to anhedral, planar to slightly curved boundaries (Fig. 4.4A, E&F).

It commonly shows a drusy mosaic, particularly where it occurs as a mould-filling cement (Fig. 4.4H). The crystals, however, vary in size; they are commonly less than 50µm in diameter, but they can reach 200µm at the pore centre. Under cathodoluminescence, the cement crystals are largely non-luminescent to dull (weak) luminescent, although very thin bright zones towards the outer part of some crystals have been observed (Fig. 4.4 C&D). This could indicate Fe-rich fluids and the incorporation of Fe^{2+} during the early stage of crystal growth. A change in pore-fluid chemistry with the incorporation of manganese into the crystal lattice has probably resulted in the precipitation of the bright outer zone. The zonation of the carbonate crystals is a reflection of fluctuations in the chemistry of the pore-fluids, but also of changes in the rate of crystal growth (Have and Heijnen, 1985).

According to the petrographic observations and cross-cutting relationships among depositional and diagenetic fabrics, this type of cement could have been precipitated in the meteoric phreatic environment. Equant calcite cement, with a drusy mosaic is characteristic of the active zone of the freshwater phreatic environment (Longman, 1980; Flügel, 1982). Drusy sparite is the typical cement of meteoric diagenesis, and this together with its ferroan nature has led to the belief that the main site of limestone cementation is the meteoric phreatic zone (Tucker, 1981).

The coarse blocky calcite cement, which is commonly ferroan, occurs mainly in grain-supported facies of the Dahra, Zelten and Harash Formations on the Dahra Platform and in the boundstone facies of the Mabruk Member in the Dor al Abid Trough. Its crystals range in size from less than 250 µm to more than 650 µm. although 1000 µm and even 1600µm crystal sizes have been also observed in the Dahra Formation in Well no. 10 and in the Mabruk Member in Well no. 103, respectively. It

fills vuggy, moldic, fracture and intergranular porosities and developed as clean, coarse subhedral to euhedral crystals with fairly straight crystal boundaries along with the local occurrence of some inclusions (Fig. 4.5 A-C). Fluid inclusion results showed that the homogenization temperature from petroleum inclusions in the studied section ranges from 48- 67°C, and the homogenization temperature of aqueous inclusions range from 59–90°C. This may indicate two phases of calcite precipitation during the sediment history in the area. See next section (4.3).

The source of iron may have been brought into the sedimentary environment with argillaceous material (Oldershaw, 1971), which is available within the studied Paleocene succession and in the nearby area. The ferroan nature of some calcite cement may be ascribed to subsurface reducing conditions which may be caused by bacterial respiration and/or organic matter oxidation through released oxygen from pore-waters (Claypool and Kaplan, 1974). A high ferrous iron content is common in burial equant spar calcite cements, but can also exist in early cements formed in near-surface anoxic conditions (Scholle and Halley, 1985).

Although meniscus cement is not widely distributed throughout the studied sections, it represents one of the most important petrographic features observed in the studied samples. It is not only a characteristic vadose-diagenetic or pedogenic feature but also a vital factor in the preservation of primary porosity in carbonate rocks. This type of cement has been documented within the bioclastic foraminiferal grainstone microfacies, in the upper part of the Dahra Formation in Well no.7 at a depth of 3277 ft. It is concentrated at grain contacts and formed crescent-shaped cement (Fig. 4.4G), as a result of water held near grain contacts by capillary forces (Tucker and Wright, 1990). Meniscus cements are recorded from some beach rocks and indicate precipitation in the marine vadoze zone (Taylor and Illing, 1969). They mostly originate in the vadose environment but can also be formed microbially in other environments (Hillgaertner et al., 2001). Flügel (2004) pointed out that the meniscus cements characteristically formed in the meteoric-vadose zone but they may also occur in the phreatic-meteoric and the vadose-marine environment.

4.2.5.3. Syntaxial rim cement

This type of cement, in which the cement crystals have grown by the extension of the lattice in depositional grains, is particularly obvious in echinoderm-rich rocks.

This is because echinoderm fragments are large single crystal plates of calcite (Adams and Mackenzie, 1998). Nevertheless, various skeletons besides echinoderms can be seen to have acted as a substrate for syntaxial growth of cement, such as the prismatic layers in gastropods and ostracods (Bathurst, 1975).

The syntaxial overgrowth occurs mainly within the grain-dominated facies in the Dahra, Mabruk, Zelten and, less commonly, Harash Formations. It rarely occurs in wackestone-wackestone/packstone facies, since there is little original pore space (Bathurst, 1975). This cement is commonly a large single crystal developed on echinoid and crinoid fragments in optical continuity with the grain (Fig. 4.5D). Overgrowths on echinoderm fragments grow faster than the polycrystalline cements, since the latter require nucleation, whereas the echinoderm provides an existing calcite lattice (Evamy and Shearman, 1965). Although the echinoderm fragments can be easily distinguished from the overgrowth cement, it may be difficult in a few cases. Locally, in particular in the Dahra Formation, however, the calcite of the inner parts of overgrowth remains unstained whereas the outer parts are stained pink (Fig. 4.5E). Under cathodoluminescence both echinoderm and the inner part of the overgrowth have the same intensity, i.e. light brown to dull luminescence, whereas the outer parts show non luminescence (Fig. 4.5F).This could indicate that the inner unstained parts, which represent the first stage cement, tend to have elevated Mn^{2+} and low Fe^{2+} incorporation in the crystal lattice, whereas the outer parts could indicate changing pore fluid chemistry with less Mn^{2+} incorporation in the crystal lattice.

Based on the petrographic observations, the syntaxial overgrowth cement probably post-dated the isopachous calcite cement and pre-dates grain to grain contact. This indicates that it was probably formed in the freshwater phreatic environment, since one of the characteristic features for recognising freshwater phreatic environments are syntaxial overgrowth on echinoderm fragments (Flügel, 1982). On the other hand, Adams and Mackenzie (1998) pointed that the syntaxial overgrowths are not diagnostic of a particular environment of formation, because they are often chemically zoned and may record precipitation over a long period of time through successive environments.

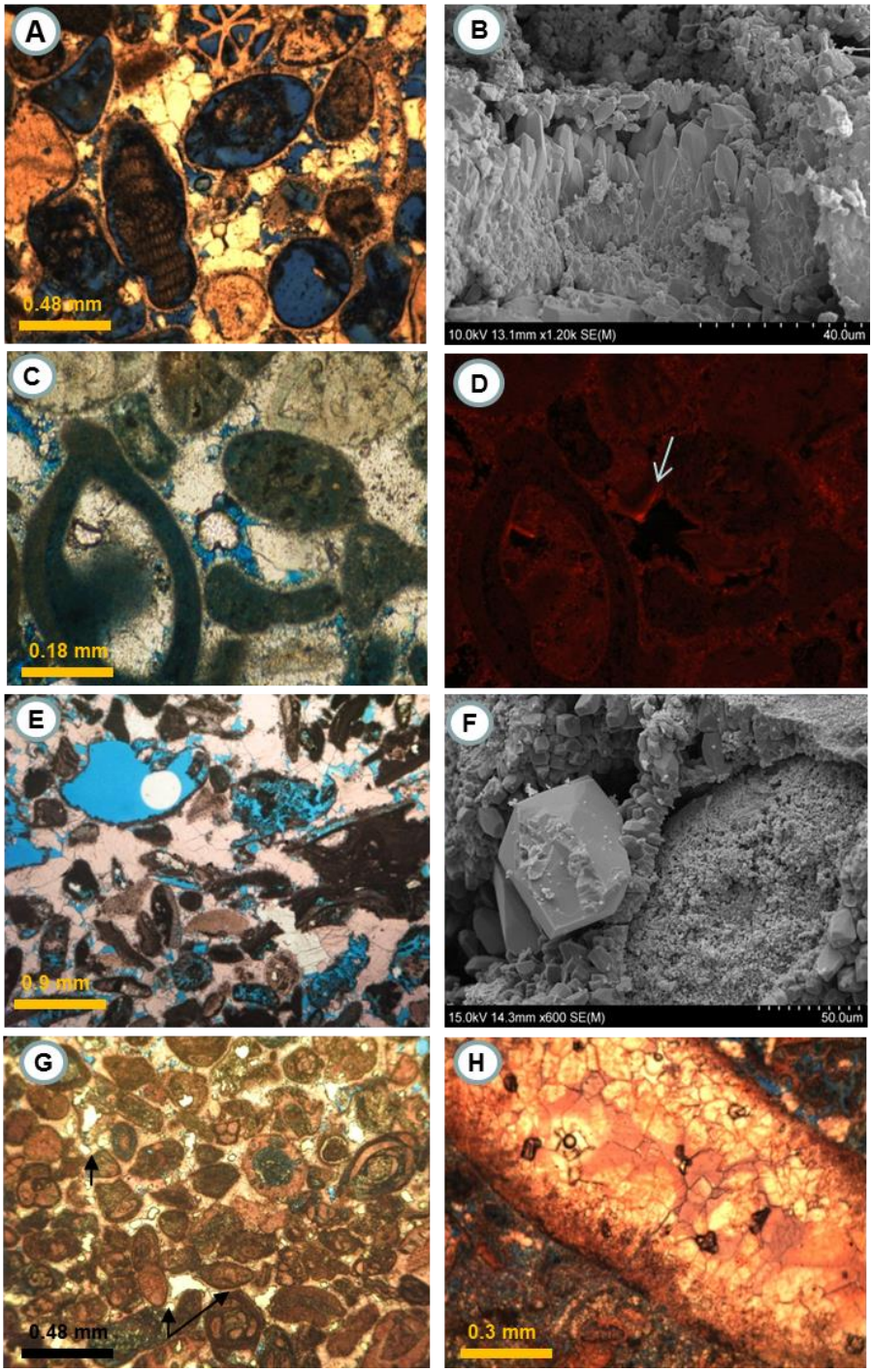

Figure 4.4 A: Isopachous calcite cement, around bioclasts, followed by equant sparry calcite. Dahra Fm, 3158 ft, Well no. 10; B: SEM photomicrograph shows isopachous crystals around a mold. Dahra Fm, 3119 ft, Well no.8; C&D: Plain light and CL of equant calcite, respectively. Note the thin light outer zone of some crystals (arrow). Dahra Fm, 3076 ft, Well no. 9; E: Characteristic colour staining of iron-free sparry calcite cement (pink). Note the development of coarse dolomite crystals. Mabruk Mbr, 4275 ft, Well no. 66; F: SEM photo showing isopachous calcite around a peloid and equant calcite cement plugging the intergranular porosity. Dahra Fm, 3181 ft, Well no.9; G: Meniscus vadose cement (arrows). Dahra Fm, 3277 ft, Well no. 7; H: Drusy mosaic of equant calcite cement, slightly ferroan. Dahra Fm, 3223 ft, Well no. 10.

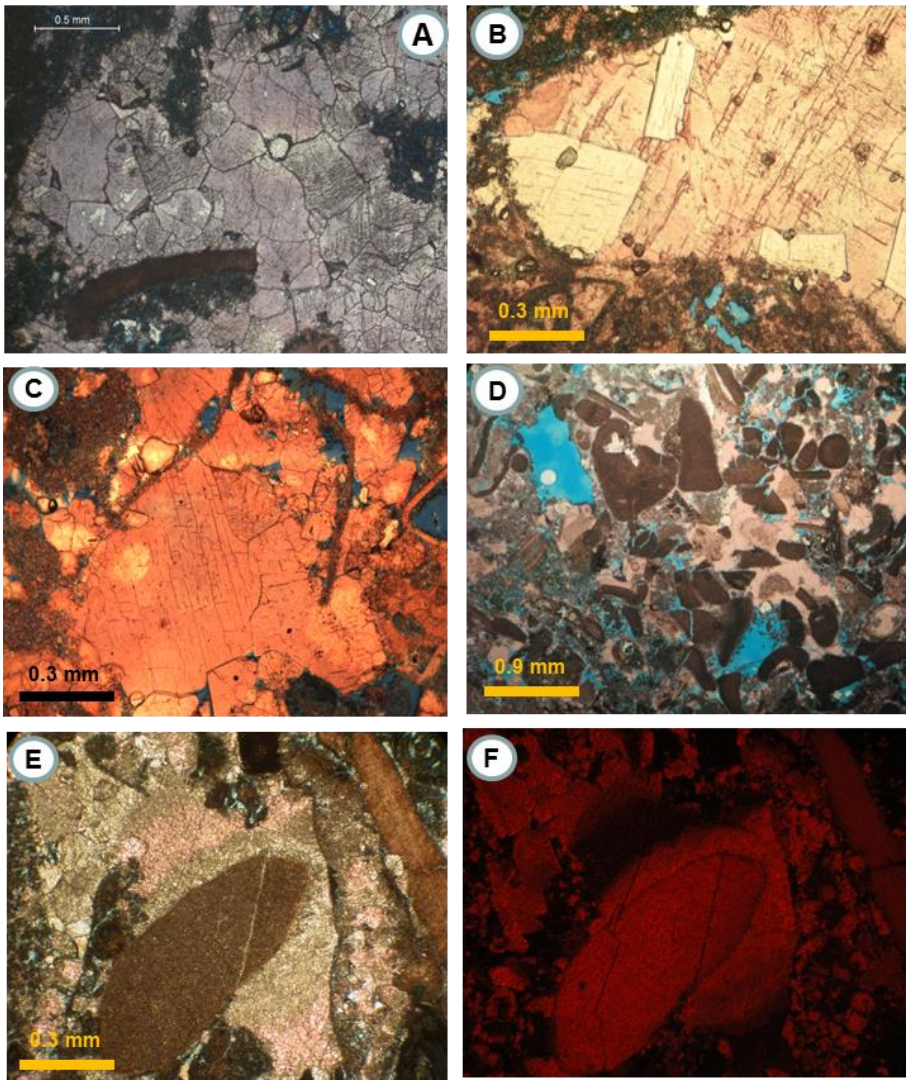

Figure 4.5 A: Coarse ferroan calcite cement in foraminiferal bioclastic W-W/P facies. Dahra Fm, 3098 ft, Well no. 9; B: Very coarse Fe-free calcite cement occludes secondary porosity in bioclastic foraminiferal P-P/G. Note the occurrence of coarse dolomite cement (white). Zelten Fm, 2833 ft, Well no. 7; C: Slightly ferroan coarse calcite cement in bioclastic foraminiferal P-P/G. Dahra Fm, 3167 ft, Well no. 10; D: Syntaxial overgrowth cement around crinoid fragments in algal packstone facies. Note the occurrence of moldic porosity (blue). Mabruk Mbr., 4263 ft, Well no. 66; E&F: Syntaxial rim cement around echinoderm, which is probably dolomitized and followed by equant calcite cement (pinkish).The CL photo (F) shows that both echinoderm and overgrowth have the same intensity, i.e. light brown to dull luminescence, whereas the equant calcite cement shows non luminescence. Dahra Fm, 3134 ft, Well no. 8.

4.2.6. Dolomitization

4.2.6.1. Introduction

Although the dolomite can be primary (direct precipitation) notably when forming in certain lakes and lagoons, most of the dolomite in the geological record is of replacement origin. This replacement process ranges from fabric selective to pervasive and from fabric destructive to retentive depending on the original grain mineralogy and crystal size, timing of dolomitization and nature of dolomitizing fluids (Tucker and Wright, 1990).

Dolomitization can take place whenever the Mg concentration is sufficiently high. This might have been the case in the Upper Paleocene succession, since the dolomite here occurred as a replacive mineral and as a void-filling cement. The replacement origin for much of the dolomite is indicated by the presence of ghosts of precursor grains and biomouldic pores, along with the occurrence of completely micritized grains which resist, to some extent, dolomitization.

Following the terminology of Folk (1962), and based on the crystal size, two types of dolomite have been recognised in the studied succession, these are: very finely to medium crystalline (10-80µm) dolomite and medium to coarsely crystalline (100-600µm) dolomite.

4.2.6.2. Very finely to medium crystalline (10-80 µm) dolomite

The finest crystal size of dolomite observed in the studied section (<20µm) has replaced mainly the matrix in the dolomitic lime-mudstone microfacies in the Dahra Formation at Well no.8. It commonly shows loosely packed subhedral to anhedral dolomite crystals, fairly sucrosic texture with good intercrystalline porosity (Fig.4.6A). The partly dolomitized (and bioturbated) intervals are present all over the studied succession, i.e. in the Dahra, Mabruk, Zelten and Harash Formations. The average crystal size of the dolomitized matrix in the dolomitic bioturbated bioclastic wackestone/packstone- packstone microfacies is about 40-60µm in the Dahra Formation, ~80 µmin the Mabruk Member, and around 30µm in Zelten/Harash Formations. It replaces not only the micite matrix but many carbonate grains have been partially and/or totally attacked in different intensities.

In the Dahra Formation and its equivalent Mabruk, particularly in wells no.9 and 66, the dolomite is almost tightly packed and displays hypidiotopic (planar-s) to xenotopic (non-planar) mosaics. It commonly shows fairly good preservation of the

original texture and poor intercrystalline porosity (Fig. 4.6B). In Wells no. 8 and 10, however, a better preservation of intercystalline porosity has been observed. In Zelten and Harash Formations the very finely to medium crystalline dolomite occurs generally as isolated euhedral to subhedral crystals in the relatively fine- grained matrix of the wackestone/packstone facies.

Since the crystal size can be used to differentiate between early and late diagenetic dolomitization (Lee and Friedman, 1987), the very finely to medium crystalline dolomite that replaced the matrix may represent an early diagenetic process of dolomitization. The local association of this dolomite with peritidal features (fenestrae, desiccation cracks, evaporite moulds, and rootlet structures) suggests an early diagenetic origin (eogenetic dolomite).

4.2.6.3. Medium to coarsely crystalline (100-600µm) dolomite

This coarser size of dolomite crystal occurs mainly in the Dahra Formation on the Dahra Platform and in the Mabruk Member in the Dor al Abid Trough, whereas it is less developed in Zelten and Harash Formations on the Dahra Platform. It usually occurs as pore-lining and/or filling cement and thus contributes in destroying, and more commonly occluding, the intergranular, intragranular, moldic, vuggy and fracture porosity. In the Dahra Formation its average size is 100-300µm and it is characterised by single, usually non-ferroan, euhedral to subhedral crystals, locally with curved crystal faces, and displays some zonation (Fig. 4.6. E&F).

In the Mabruk Member, however, the average size of this type of dolomite is 200-400µm, although a much coarser size (500-900µm) has been observed at specific intervals in well no.105, where it chiefly occurs within fractures and/or veins. Its characteristics are similar to that in the Dahra Formation and they show degree of undulatory extinction giving them an appearance similar to saddle dolomite (Radke and Mathis, 1980) (Fig. 4.6G&H). A similar type of dolomite was named by Beales (1971) as white sparry dolomite and by Zenger (1983) as baroque dolomite. Locally it is associated with scattered medium-sized crystals of evaporite (anhydrite) and shows some dissolution (Fig.4.3E&F).

The average size of this dolomite is 200-300 µm in the Zelten/Harash Formations. It is commonly associated with the coarse, Fe-free calcite cement and together they plug the formerly developed porosity (Fig. 4.7A&C). In a few cases, it has

replaced carbonate grains along with coarse calcite cement with some good preservation of the original structure (Fig. 4.7B).

The cloudy centres in some zoned dolomite crystals, however, suggest that dolomitization took place by waters saturated or slightly under saturated with respect to calcite, whereas the clear rims suggest that the solution was undersaturated with respect to calcite (Sibley, 1979). Carozzi (1993) suggested that the cloudy cores and clear rims indicate that the precursor carbonate was low Mg-calcite or had been converted to it before dolomitization.

The medium to coarsely crystalline dolomite rhombs have two luminescence characters: an inner weakly to non-luminescent and thin outer slightly bright orange zones. These two luminescent zones are the result of the chemical differences between the inner and outer zones which developed as a result of differences in Fe and Mn contents of the dolomitizing fluids (Tucker and Wright, 1990). It has been suggested that the amount of manganese necessary to induce bright luminescence in carbonates ranges from 80 to 100 ppm.

Tucker and Wright (1990) pointed out that the baroque dolomite can occurs in veins and fractures, and is commonly associated with epigenetic sulphide mineralization. It is also commonly associated with hydrocarbons and this has been used to suggest that it forms within the oil window, at temperatures of 60-150°C (Radke and Mathis, 1980).The average crystal size of this dolomite may thus suggest significant depth of formation and relatively slow growth rate. On the other hand, the occurrence of coarse saddle dolomite probably suggests precipitation in the late, deep burial mesogenetic stage. The shales in the older Beda Formation, in the lower part of the Dahra Formation and in the Khalifa Formation are possibly the source of magnesium required for this dolomitization.

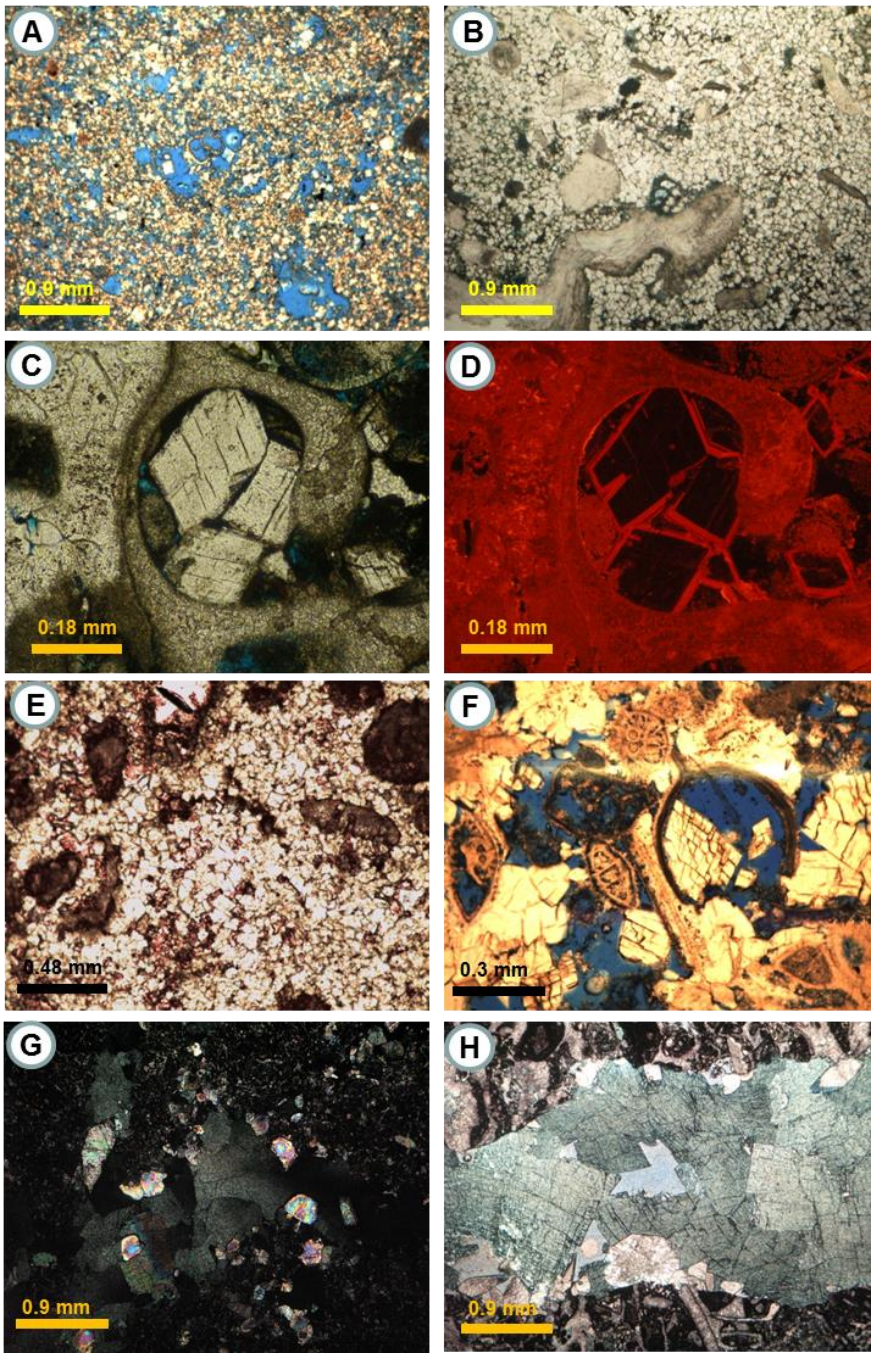

Figure 4.6 Different types of dolomite. A: Very fine-finely crystalline dolomite in dolomitic lime-mudstone facies. Note good intercrystalline and moldic porosity.Dahra Fm, 3079 ft, Well no. 8; B: V. finely-medium crystalline dolomite replaced mainly micrite matrix in dol. biot. bioclastic packstone. Mabruk Mbr, 4285 ft, Well no.66; C & D:Medium crystalline dolomite filling intragranular porosity.Note the two luminescent characters in D. Dahra Fm, 3227 ft, Well no. 9; E: Dolomitized matrix and some grains of fine-medium crystalline dolomite. Dahra Fm, 3205 ft, Well no. 8; F: Coarsely crystalline dolomite filling moldic and vuggy porosity. Note the curved crystal faces and curved cleavage planes of dolomite crystal. Dahra Fm, 3232 ft. Well no. 10. G: XN photo shows undulose extinction of saddle dolomite. Note the presence of anhydrite crystals. Mabruk Mbr, 3731 ft, Well no. 105. H: characteristic features of saddle dolomite filling a vein. Mabruk Mbr, 3736 ft, Well no. 105.

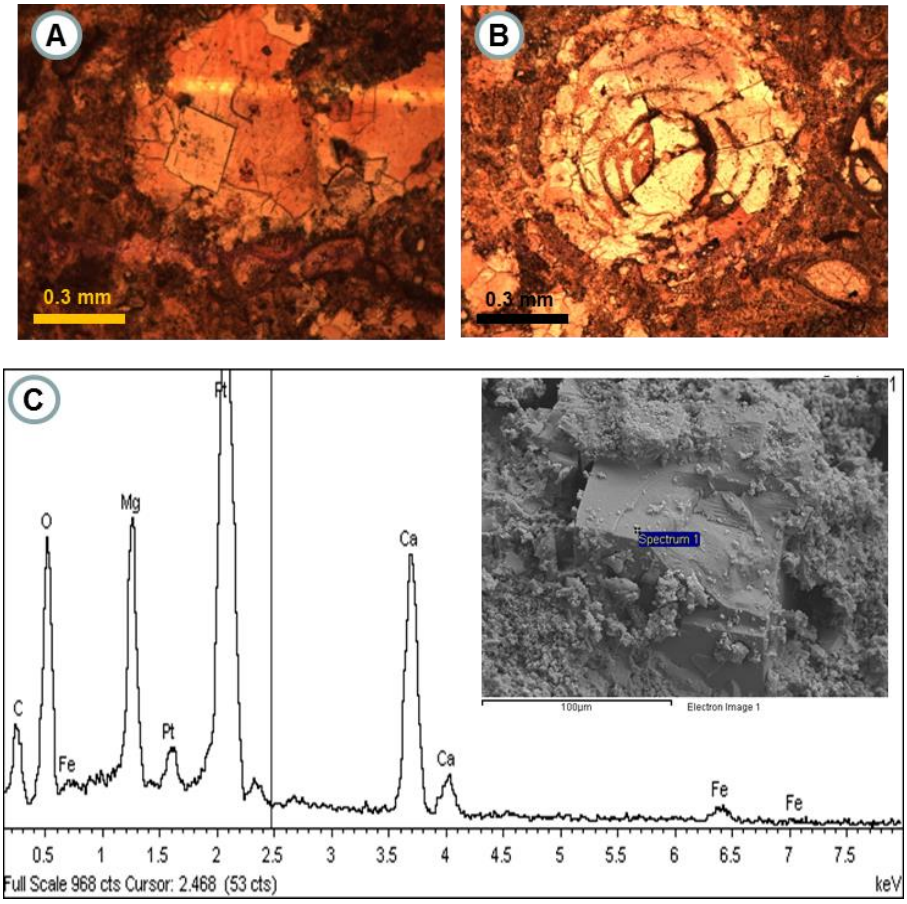

Figure 4.7 Dolomite in Zelten Formation. A: Medium to coarse crystalline dolomite, along with coarse blocky non-ferroan calcite. Note the inclusion-rich core of the dolomite crystals; B: Replacement of *Alveiolina* foraminifera by dolomite and coarse calcite with a retentive fabric. A&B, Zelten Fm, 2731 ft, Well no. 9; C: Energy dispersive spectrometer graph for the medium crystalline dolomitein bioclastic foraminiferal packstone/grainstone microfacies. Zelten Fm, 2779 ft, Well no.9.

4.2.7. Compaction and tectonic features

It has been documented that the degree of compaction is strongly influenced by the presence of early cement, and to some extent by dolomitization. Macroscopic and microscopic examination of the rocks under investigation revealed that they have been subjected locally to considerable compaction (physical and chemical) and to less significante fracturing.

4.2.7.1. Physical compaction

It is well known that physical compaction is common during the first few hundreds of metres of burial in many carbonate rocks that were not completely lithified. The effects of mechanical compaction are found most commonly in grains that were affected by boring, leaching, or other grain-weakening processes during marine or

meteoric diagenesis (Scholle & Scholle, 2003). Local closer packing, deformation and fracturing of carbonate grains have been observed in all the studied formations in both the Dahra Platform and Dor al Abid Trough. Mechanical compaction in which some bioclasts, in particular foraminiferal tests, were crushed and/or flattened were not only observed in the Dahra Formation but also in the Zelten and Harash Formations on the Dahra Platform (Fig. 4.8A & B). While closer packing and deformation features are more common in the mud-supported facies, fracturing of grains (mainly bivalve shells) and substrate is widely developed, especially in the packstone/grainstone facies of the Dahra Formation and Mabruk Member (Fig. 4.8C). The mechanical compaction is locally very substantial, particularly within the Dahra Formation, and resulted in the vaguely bedded fabric and hence, original packstone cannot be distinguished easily from compacted packstone (Fig. 4.2).

Many superficial ooids and coated grains showed breaking and cracking along the lamella and as a result the cortical layer has been spalled off, and intragranular secondary porosity has been produced (Fig. 4.8E). Mechanical compaction, which was probably accompanied with tectonic compression or shearing of the superficial ooids has produced deformed ooids and resulted in the formation of 'elephant-parade' fabric of Folk (2001) in the middle interval of the Dahra Formation (Fig.4.8D). Equant calcite cement was precipitated within the cavities developed in the ooids.

Most of these mechanical compaction features probably occurred at shallow burial depths where the Upper Paleocene carbonates were semi-indurated. On the other hand the development of the sparry calcite within the ooids could strongly suggest that it predated compaction, and hence compaction occurred at a relatively later stage in the history of the sediment. Tucker and Wright (1990) stated that in the early stages of compaction, a preferred orientation of elongate bioclasts may develop parallel to the stratification/seafloor, normal to the principal stress direction. The next stage in the physical compaction involves the fracture of grains and the early cement fringes and the ductile deformation of grains and sediment.

In addition to the above mentioned fractures, networks of microfractures that interconnect different types of porosity have been observed in most of the facies in both structural settings. On the Dahra Platform they have been recorded chiefly in the Dahra and Harash Formations, and fewer are present in Zelten Formation. They are commonly open and in some cases crossed by stylolites (Fig. 4.8H). It is noteworthy to mention that there is a network of open microfractures that were connected to each other and

developed notably within marl/argillaceous limestone intervals in the Dahra Formation at Wells no.7 and 9 (Fig. 4.9A). Coarser (wider) fractures and/ or veins have also been witnessed at several intervals in the studied succession. Although they are not common, they occurred particularly in the Dahra Formation and Mabruk Member. In the former they are partly open, whereas in the Mabruk they are commonly plugged by saddle dolomite, coarse sparry calcite and sulphate minerals (Fig.4.6 G&H).

Faulting, tectonic fractures and/or early diagenetic fractures, on the other hand have been recorded in the Upper Paleocene succession in the study area. A possible strike-slip fault with vague striations has been observed in the lower interval of the Harash Formation at well no.9. Two intervals of 3-5 feet thick of possibly fracture zones have also been observed in the Dahra Formation at wells no. 8 and 10. Tectonic related features are dealt with in Chapter 6.

4.2.7.2. Chemical compaction

With further burial, chemical compaction is one of the most important diagenetic processes. It is a major process in burial diagenesis and can liberate calcium carbonate to the pore fluid for cementation in the immediate vicinity or at same distance if there is an active groundwater system (Tucker and Bathurst, 1990).

Dissolution seams similar to those described by Buxton and Sibley (1981) and Bathurst (1987) occur at many intervals in the studied rocks, particularly in the argillaceous limestone facies. They can be identified in both core samples and thin-section; they display fairly smooth, undulose seams of insoluble residue and usually pass between and around grains (Fig. 4.8G). Dissolution seams tend to be common in more argillaceous limestones, and develop preferentially along the clay layers or at the junctions of clay-rich and clay-poor limestones (Tucker and Wright, 1990). Pressure dissolution occurs through dissolution across a thin film as a result of compressive stress at grain-to-grain boundaries (Weyl 1959; Rutter 1983) or because of dissolution at or just outside the rims of grain contacts resulting in an undercutting (Bathurst 1975; Tada and Siever 1986). Sutured contact between carbonate grains has resulted in the formation of stylonodular structure or stylo-breccia fabric of Logan & Semeniuk (1976) at several intervals in the studied succession, specifically in the Dahra Formation and Mabruk Member (Figs.3.5A & 4.8F). In terms of petroleum reservoir quality, the pressure dissolution processes involve a strong reduction in bulk rock-volume with a

resultant loss in porosity caused by the occlusion of pores by late diagenetic subsurface cements (Wong and Oldershaw, 1981)

Stylolitization is normally absent in limestones with more than 5-10% clay (Tucker and Wright, 1990). It contributes, according to Flügel (2004), to bulk volume reduction, resulting in a marked drop in the original thickness of carbonate units. A variety of stylolite types is developed at various intervals in the studied succession, specifically in the packstone, grainstone and boundstone facies. They include large amplitude, small amplitude and swarms types, and they usually cross grains, matrix and cements, along with fractures in certain cases (Fig. 4.8H). These may have a tectonic origin, since they are developed normal to stress directions. They are commonly filled by insoluble residue (probably clay) which derived from limestone dissolution (Tucker, 1981) and pyrite. Locally, particularly in the Dahra and Mabruk, bitumen and finely crystalline dolomite are also present within them. Most stylolites exhibit very low (small) amplitude (<1cm) with an exception in a few intervals in the Dahra Formation in well no. 8, where their amplitude can reach 3cm (Fig. 4.9B). Overall, the role of chemical compaction in the reservoir history and quality of the studied rocks is locally quite significant.

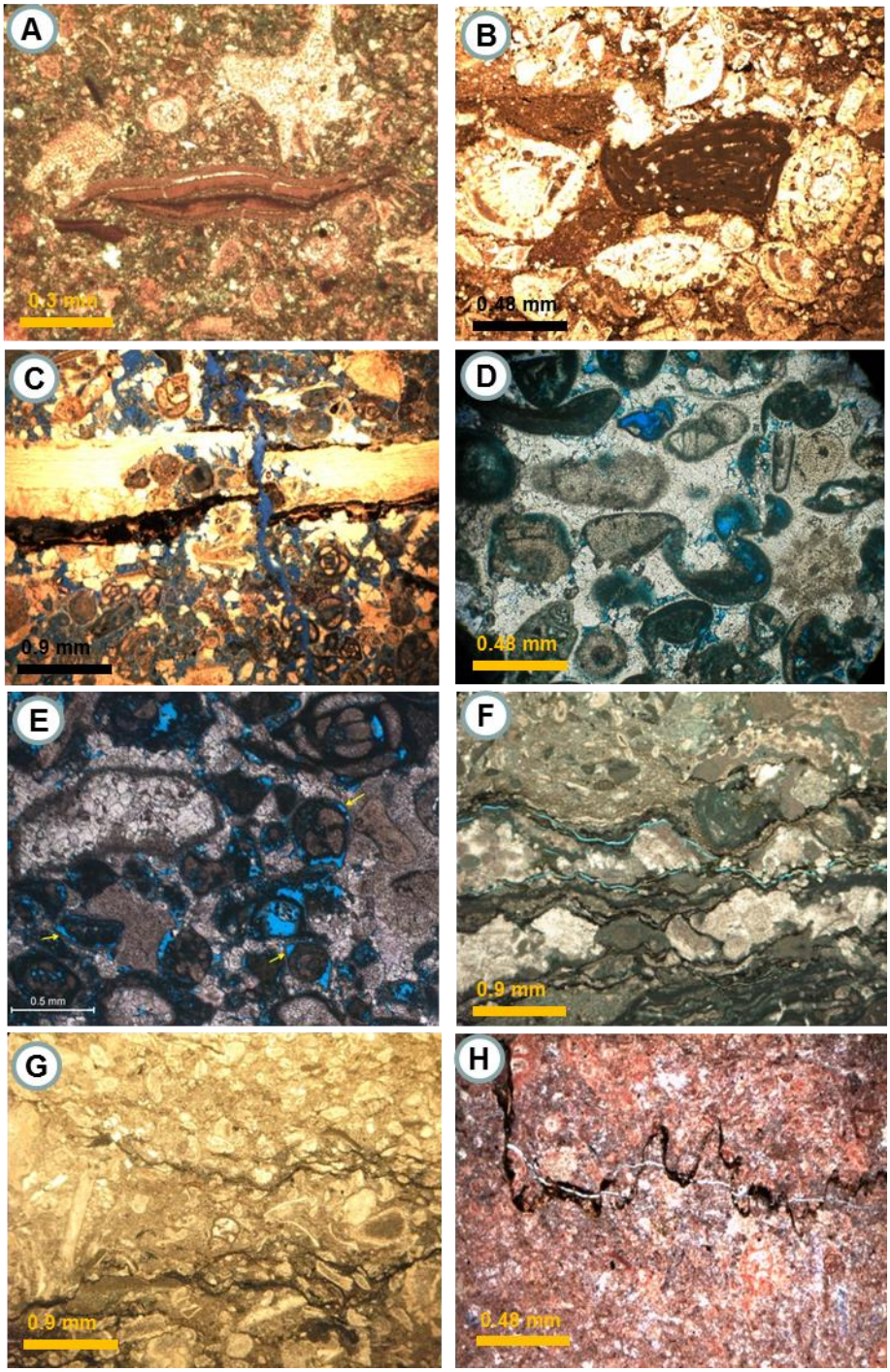

Figure 4.8 Various compaction features in the Upper Paleocene succession. A & B: Broken and flattened foraminifera due to mechanical compaction. Zelten Fm, Well no.7, 2824 ft & Harash Fm, Well no.9, 2669 ft, respectively; C: Bored and then fractured bivalve shell. Note the fracture cuts grains and matrix. Dahra Fm, Well no. 10, 3155 ft; D: Deformation of ooids has resulted in the formation of elephant-parade' fabric of Folk (2001). Dahra Fm, Well no. 9, 3181 ft; E: Physical compaction resulting in collapse and spalling of an early marine cement off micrite-coated grains (arrows). Dahra Fm, Well no. 9, 3213 ft; F: Sutured pressure dissolution seams (stylo-breccia). Mabruk Mbr, Well no. 66, 4314 ft; G: Fairly smooth, undulose dissolution seams. Harash Fm, Well no. 7, 2741 ft; H: Microstylolite cuts across matrix, grains and fracture. Dahra Fm, Well no.8, 3291 ft.

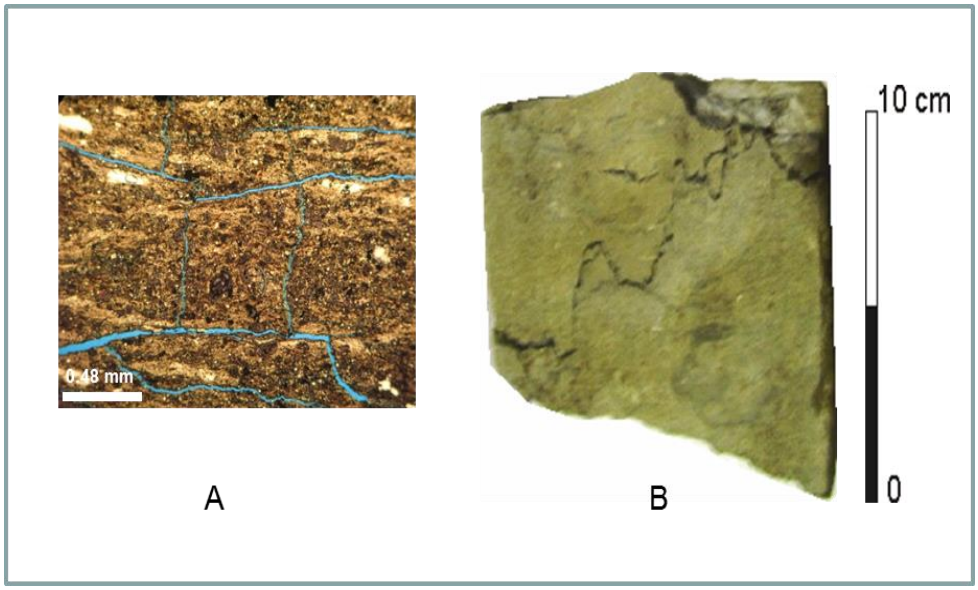

Figure 4.9 A: Open microfracture network developed in marl facies in the lower part of the Dahra Formation. Well no. 7, 3315 ft; B: Relatively large amplitude stylolite developed in bioclastic foraminiferal packstone-packstone/grainstone facies in the upper part of the Dahra Formation. Well no.8, 3115 ft.

4.2.8. Minor diagenetic events

Minor diagenetic events recognized in the Upper Paleocen succession include formation of authigenic pyrite, glauconite, hematite, phosphate, evaporites and clay minerals (Table. 3.2).

Authigenic pyrite is the most common authigenic mineral developed within the studied interval of the Paleocene succession. It occurs in most of facies of the Dahra, Mabruk, Zelten and Harash Formations. An exception is the dolomitic lime-mudstone facies, where pyrite has not been detected. It is normally <5% of the total rock constituents but at certain intervals it can reach upto 10%. Pyrite crystals are locally common replacement of and/ or filling within matrix and various bioclasts including foraminifera, bivalves and echinoderms (Fig. 4.10). They also occur in residual clays of the stylolites and dissolution seams. Under the scanning electron microscope, pyrite crystals appear as spherical aggregates of many tiny euhedral crystals (framboids) that occupied matrix and/or bioclasts. They possibly occurred at shallow burial depths as a result of the decomposition of organic matter under reducing conditions (Lee and Friedman, 1987). Authigenic pyrite commonly forms under reducing conditions replacing organic material or in close proximity to organic material (Flügel, 2004).

Glauconite is usually found in association with pyrite but in very low amounts (< 2%). It occurs mainly within the Dahra and Mabruk, and rarely in Zelten/Harash interval. It is characterised by green colour and very fine texture, and occurs locally as both grains and mud (Fig. 4.10). Glauconite is probably formed in a slightly reducing, anoxic, non-sulphidic, post-oxic diagenetic environment (Berner, 1981). It is usually regarded as an indicator of marine, relatively shallow and slow sedimentation.

In modern oceans glauconite occurs between 50 and 500 m and is abundant in mid-shelf to upper slope settings at depths between 50 and 300m. The glauconite mineral is often concentrated at discontinuity surfaces indicating depositional breaks (Flügel, 2004). Hematite occurs at several intervals in almost all the studied formations; It is characterised by a reddish brown colour and usually occurs at the top (shallowest) of the carbonate cycles. It is accompanied by pyrite and glauconite, and in a few cases with clays (Appendix. 1). At certain intervals within the Dahra Formation, it occurs in association with dessication cracks, fenestrae and rootlets in dolomitic, brecciated and mottled fabric (palaeosoils). Locally meniscus cement has developed just beneath the intervals with hematite.

Within the Zelten Formation on the Dahra Platform the hematite occurs in conjunction with a storm bed that developed just above the most negative oxygen isotope value in well no.9 (-10.49). Hematite normally develops above the water table, and below, if the ground water is alkaline and oxidizing (Tucker, 1981). In view of its importance in both classical and sequence stratigraphy, the hematite will be discussed further in the next chapter.

Replacement of carbonate grains by phosphate occurred sporadically and in trace amounts in the studied succession (Fig. 4.10C). Phosphate can be derived from the decay of disseminated organic matter. Once formed, phosphate nodules, phosphatized limestone fragments and phosphatic fossils are very resistant to weathering and easily reworked in to younger beds. It could deposited during a transgression as a result of current and wave reworking of sediments and winnowing of finer material (lag deposits) (Tucker, 1981). Although no evaporite beds were found in the studied rocks, some samples rarely contain gypsum, anhydrite and halite crystals, particularly within the Mabruk Member in the Dor al Abid Trough and in the Dahra Formation on the Dahra Platform. The gypsum and anhydrite usually occur as isolated, euhedral crystals, commonly in association with finely crystalline dolomite and saddle dolomite (Figs.4.6 G&H and 4.10D). It is well known that sulphate minerals are precipitated from brines

concentrated by extensive or local evaporation of water, but in these cases, probably the sulphate minerals are burial precipitates, not associated with near-surface evaporitic conditions.

A part from the marl/argillaceous limestone facies, clay minerals of kaolinite, chlorite, illite and probably mixed layer illite/smectite have been recorded in the carbonates of the studied cores. They are normally occurring in trace amounts in the wackestone-wackestone/packstone and boundstone intervals in both the Dahra Formation and Mabruk Member (Fig.4.11). Kaolinite, which is the most common clay, can locally reach 10-16% of the total rock volume in the central and eastern Mabruk areas. This may indicate, as previously stated, invasion of riverine clastics through a minor sea-level fluctuation and/or a change to a more humid climate. Clay-mineralogical assemblages of marls at the top of shallowing-upward sequences reflect fluctuating freshwater and marine conditions affecting shallow-water carbonates (Deconinck and Strasser, 1987).

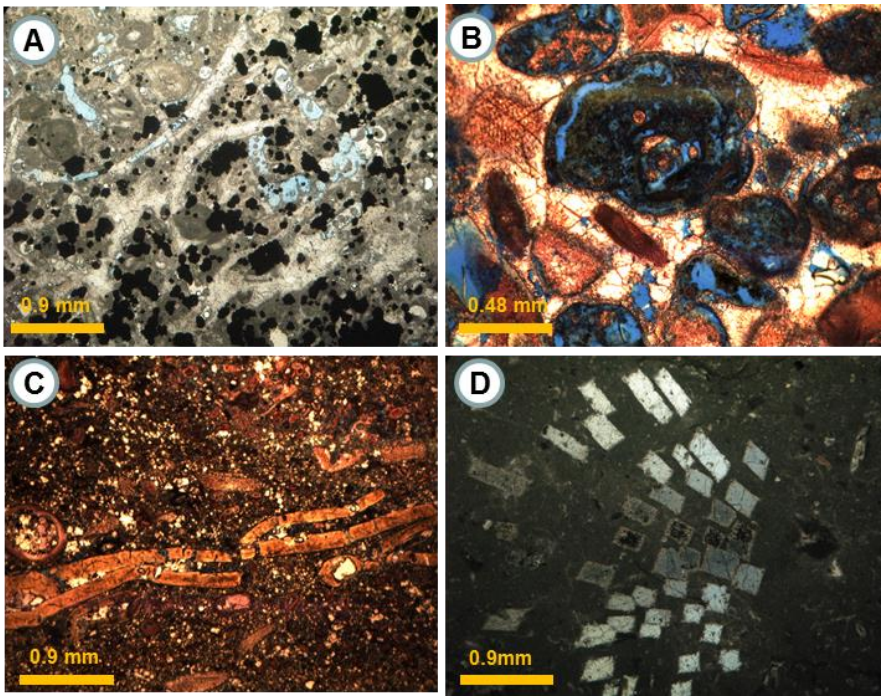

Figure 4.10 Minor diagenetic events in the studied Paleocene section. A: Pyrite mineral occurring in both matrix and grains in foraminiferal bioclastic packstone-packstone/grainstone facies. Mabruk Mbr. Well no. 105, 3737 ft; B: Glauconite precipitated within foraminifera chambersin bioclastic foraminiferal grainstone facies. Dahra Fm., Well no. 10, 3158 ft; C: Compacted, fractured and completely phosphatized skeletal grain in bioclastic wackestone/packstone facies. Dahra Fm, Well no. 9, 3165 ft; D: Aggregates of single euhedral crystals of gypsum in coral algal boundstone facies. Mabruk Mbr., Well no. 66, 4327 ft.,XN.

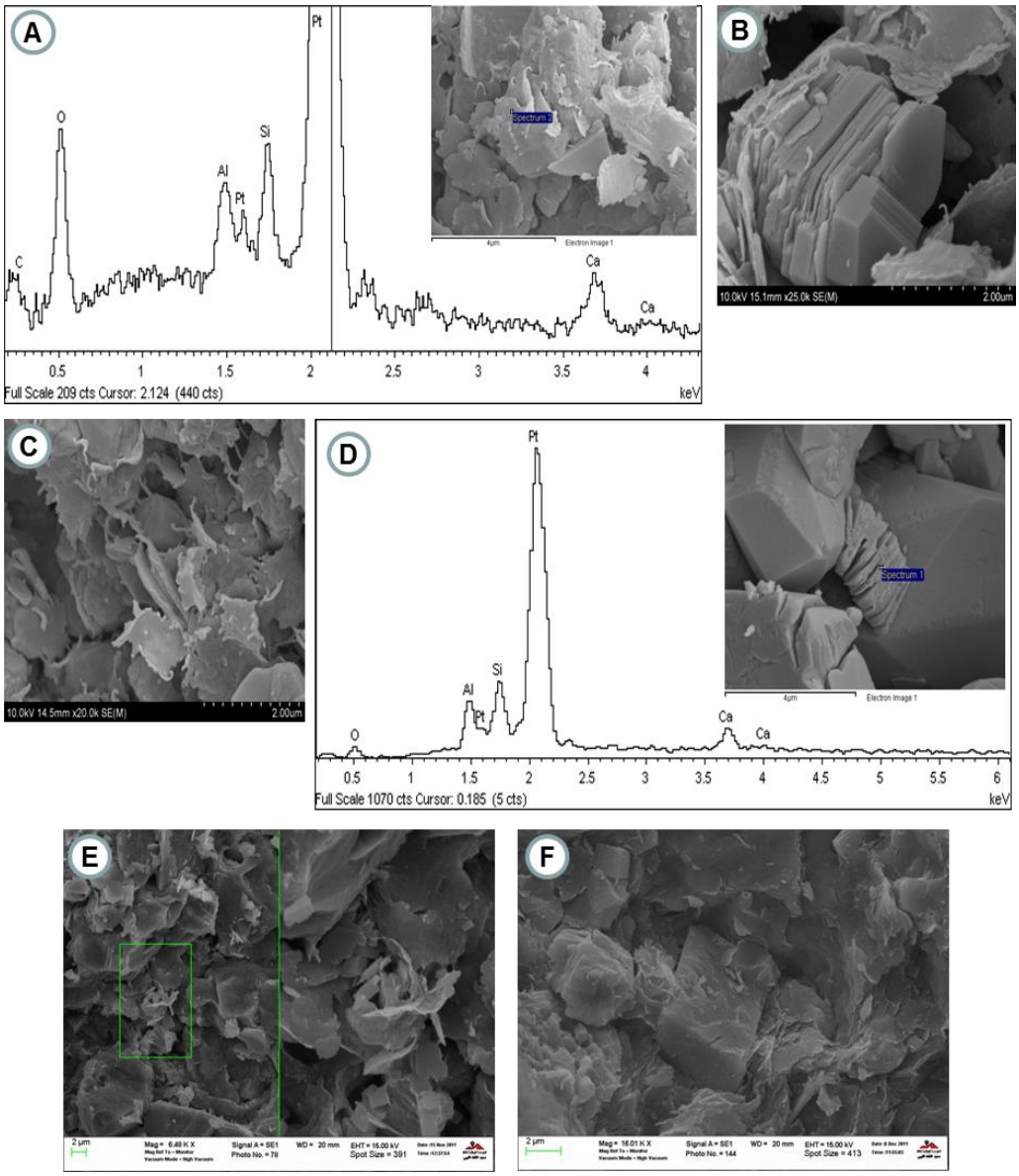

Figure 4.11 Scanning electron microscopy analysis of the studied samples showing clay minerals identified within the Paleocene succession. **A:** SEM photomicrograph showing smectite mineral? between micrite crystals. The chemical composition of this smectite is shown in the EDS spectra; **B:** Kaolinite (book sheets) plugging intercrystalline porosity in bioclastic wackestone/packstone facies. Both photos (A&B) from the Dahra Fm, Well no. 9, 3265 ft; **C & D:** Illite and kaolinite minerals occurred at different intervals in the Dahra Formation in Well no. 8. 3185 ft, and 3119 ft, respectively; **E:** Rose-like chlorite mineral developed within algal bioclastic boundstone facies of the Mabruk Member. Well no. 103, 3577 ft; **F:** Probable illite coating micrite crystals in foraminiferal bioclastic wackestone-wackestone/packstone facies. Mabruk Mbr., Well no. 66, 4335 ft.

4.3. Geochemistry of the Selandian/Thanetian Carbonates

As shown in the previous section, the studied interval of the Paleocene succession has been subjected to a complex series of post-depositional changes from the time of deposition up to the present day. In this section, the results of isotope analyses and fluid inclusion studies are presented, and there is a discussion of paragenesis.

4.3.1. Carbon and oxygen isotopes

The isotopic variation in oxygen and carbon presented here considered in terms of diagenetic evolution; the data are discussed further in terms of stratigraphic trends and sedimentation patterns in the following chapter.

Modern carbonates have carbon and oxygen stable isotope values in the range of 0‰ and +4‰ for carbon and -2‰ and +1‰ for oxygen; the average for ancient limestones is normally between -2‰ and +2‰ $\delta^{13}C$ and -10‰ and -2‰ for $\delta^{18}O$ (Tucker, 1986).

The relative isotopic concentration in a carbonate grain or cement is indicative of the physical conditions of precipitation and the composition of ambient pore water (Marshall and Ashton, 1980). Carbon isotopes are more resistant to diagenetic alteration; in contrast, oxygen isotope values are susceptible to diagenetic alteration due to their variation with the temperature of precipitation and the isotopic composition of the water from which precipitation takes place. The original sediment would have been composed of a combination of aragonite, low and high Mg calcite from lime mud, grains and cements, each with different original isotopic signatures, which could have been altered during diagenesis. Burial cements; either-filling voids or replacing original skeletal material generally have isotopic signals which are more negative for oxygen and also sometimes for carbon too.

The fractionation of oxygen isotopes during calcite precipitation is strongly temperature dependent, such that a 2°C increase in the temperature of precipitation will produce a decrease in $\delta^{18}O$ value of ca. 1% (Friedman and O'Neil, 1977). Diagenetic calcite formed after any substantial amount of burial, then, should be notably depleted in $\delta^{18}O$ relative to soil-formed calcite (Bowen et al., 2001).

The $\delta^{18}O$ values recorded in the studied Paleocene succession range from -10.49 ‰ to +1.15 ‰, whereas the $\delta^{13}C$ measurements fall in the range -4.87‰ to +3.89‰. The Dahra Formation on the Dahra Platform, however, shows more confined $\delta^{13}C$

values that range between -1.78‰ and +3.18‰, whereas the $\delta^{18}O$ values reveal a wider range between -6.83‰ and +1.15‰.

In well no.9, in the Dahra West Field, the base of the cored interval of the Dahra Formation is characterized by a pronounced negative excursion in the $\delta^{18}O$ values from -2.39‰ to -6.14‰ and a slight negative excursion in the $\delta^{13}C$ values from +3.18‰ to +2.56‰ (Fig. 4.12). The negative values of $\delta^{18}O$ could indicate the effects of meteoric diagenesis or burial diagenesis from the more negative isotopic composition of freshwater on the one hand or the higher temperature during burial cementation/alteration on the other. The presence of ferroan calcite cement in this interval, which is a foraminiferal packstone facies could strongly suggest the second interpretation, since the late blocky ferroan calcite filling residual pore spaces has negative $\delta^{18}O$ (Irwin, Curtis & Coleman, 1977; Hudson, 1975). Tucker and Wright (1990) have also pointed out that burial calcite spar is generally more depleted in^{18}O than marine or earlier meteoric cements.

A positive excursion, which is more obvious in the $\delta^{18}O$, is recorded in the upper part of the Dahra Formation in this well (no.9). The $\delta^{18}O$ values change from -4.37‰ to -2.11‰ and the $\delta^{13}C$ values slightly increase from +1.29‰ to +1.58‰ (Fig. 4.12). This pattern in the $\delta^{18}O$ could indicate an upward trend to less meteoric alteration and the preservation of marine values. The low positive carbon values could also be marine signatures, or the reflection of weak meteoric alteration, as it quite usual to find that original $\delta^{13}C$ signatures are retained during diagenesis, while $\delta^{18}O$ values become lighter (Tucker and Wright, 1990). Marshal and Ashton (1980) have also pointed out that precipitates from sea water generally have an equilibrium isotopic composition, with low positive $\delta^{13}C$ and low negative values for $\delta^{18}O$.

In well no.8, in the Dahra East Field, an obvious negative excursion occurs at 3249 feet (Dahra Fm) where the $\delta^{18}O$ value is -5.98‰, and the $\delta^{13}C$ value is +2.65‰ (Fig. 4.13). This could suggest an influence of meteoric diagenesis, or more likely a degree of dolomite precipitation during burial.

A positive excursion occurs in the uppermost part of the Dahra Formation in this well, where the $\delta^{18}O$ and $\delta^{13}C$ values increase from -3.79 ‰ to +1.15‰ and from -1.83 ‰ to +1‰, respectively (Fig. 4.13). This interval is occupied by dolomitic, slightly bioturbated wackestone facies that is characterised by the development of desiccation

cracks and fenestrae. These features indicate subaerial exposure and with the positive $\delta^{18}O$ the dolomite here could be a near-surface precipitate from seawater.

The carbon isotope values of the Zelten and Harash Formations on the Dahra Platform in the east and west fields are quite similar and confined to a narrow range between +2.22‰ to +3.86‰. An exception to this is at a depth of 2742ft in the Zelten Formation (well no. 9) where a value of – 0.9‰ is obtained. The oxygen isotope values range from -10.49‰ to -2.21‰ (Figs. 4.12- 4.14).

At the Zelten /Harash boundary the $\delta^{18}O$ is -2.71‰ and $\delta^{13}C$ is +3.48‰ in well no 9, and -4.28 ‰ and +3.07‰ in well no 8. The carbon isotope values are typical, probably original marine values, whereas the $\delta^{18}O$ values could indicate less diagenetic alteration upwards, possibly as a result of more arid climate, when meteoric diagenesis would have been limited. Marshall and Ashton (1980) pointed out that precipitates from sea water generally have an equilibrium isotopic composition with low positive $\delta^{13}C$ and low negative value for $\delta^{18}O$.

The most negative values recorded in the studied section of Zelten/Harash Formations are at depth of 2742 ft in well no 9, where the $\delta^{18}O$ decreases from -5.00 ‰ to -10.49 ‰, and the $\delta^{13}C$ reduces from +3.8‰ to – 0.90 ‰ (Fig. 4.14). It seems that these values, if they are accurate, are too negative for meteoric water and thus could represent high temperature phase of probably burial diagenesis, which most likely ascribed to the presence of burial calcite. Moreover, the lowering of the sea-level that occurred just few feet below this interval (Appendix. 1) strongly suggests burial diagenesis. The stable oxygen and carbon isotopes for the two analysed wells on the Dahra Platform are shown in figure 4.14.

On the Dahra Platform the overall $\delta^{13}C$ and $\delta^{18}O$ values show fairly similar trends in the Dahra and Zelten/Harash Formations in wells no. 8 and 9, respectively (Figs. 4.12 and 4.13). This coincidence of $\delta^{13}C$ and $\delta^{18}O$ trends are generally considered to reflect late diagenetic over-printing caused either by interaction with meteoric ground waters or by dissolution and recrystallisation at higher temperatures during burial diagenesis (Sakai and Kano, 2001; Keller *et al*., 2004).

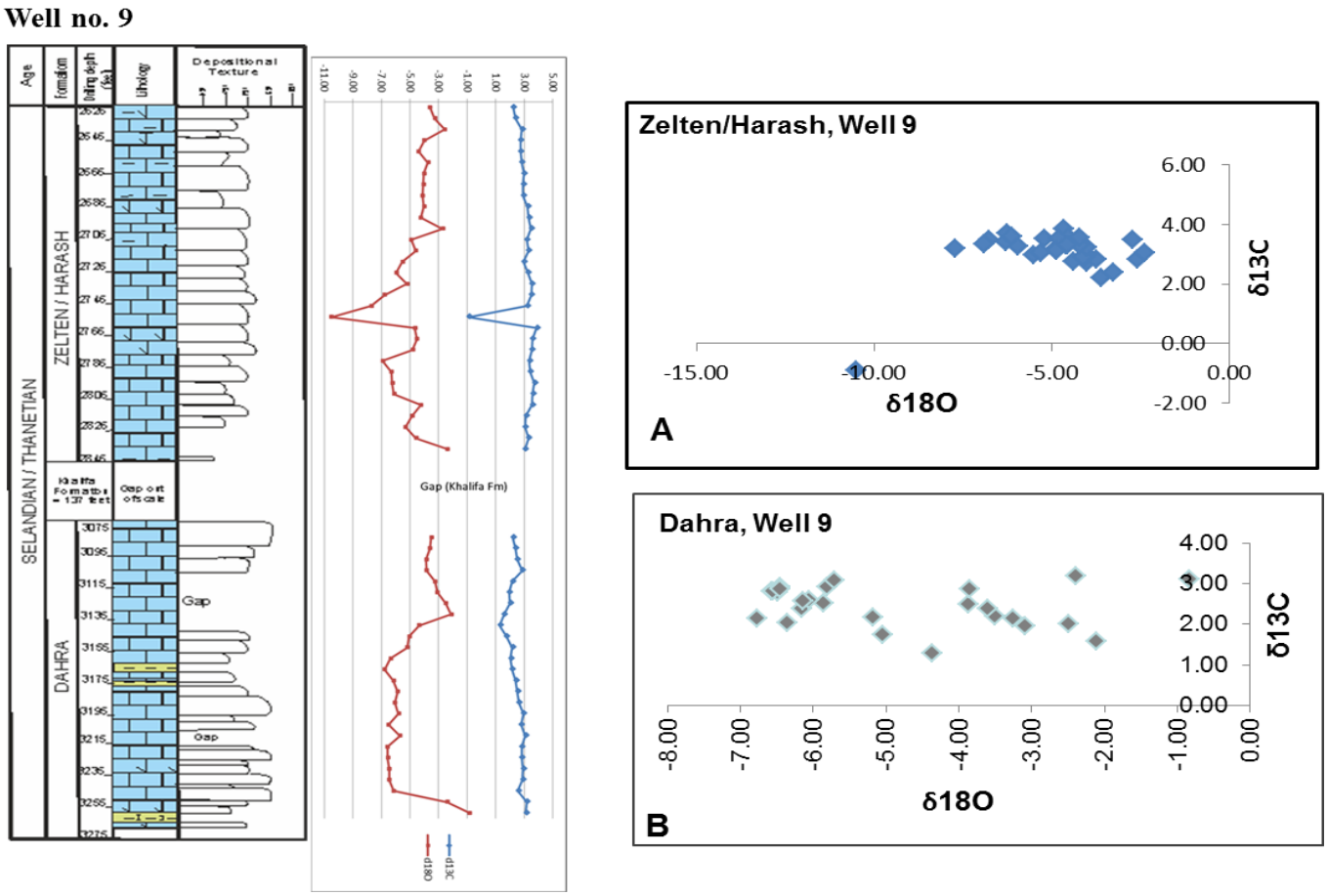

Figure 4.12 Carbon versus oxygen isotopes of the studied Selandian/Thanetian succession in well no. 9 on the Dahra Platform. A: Zelten and Harash Formations; B: Dahra Formation

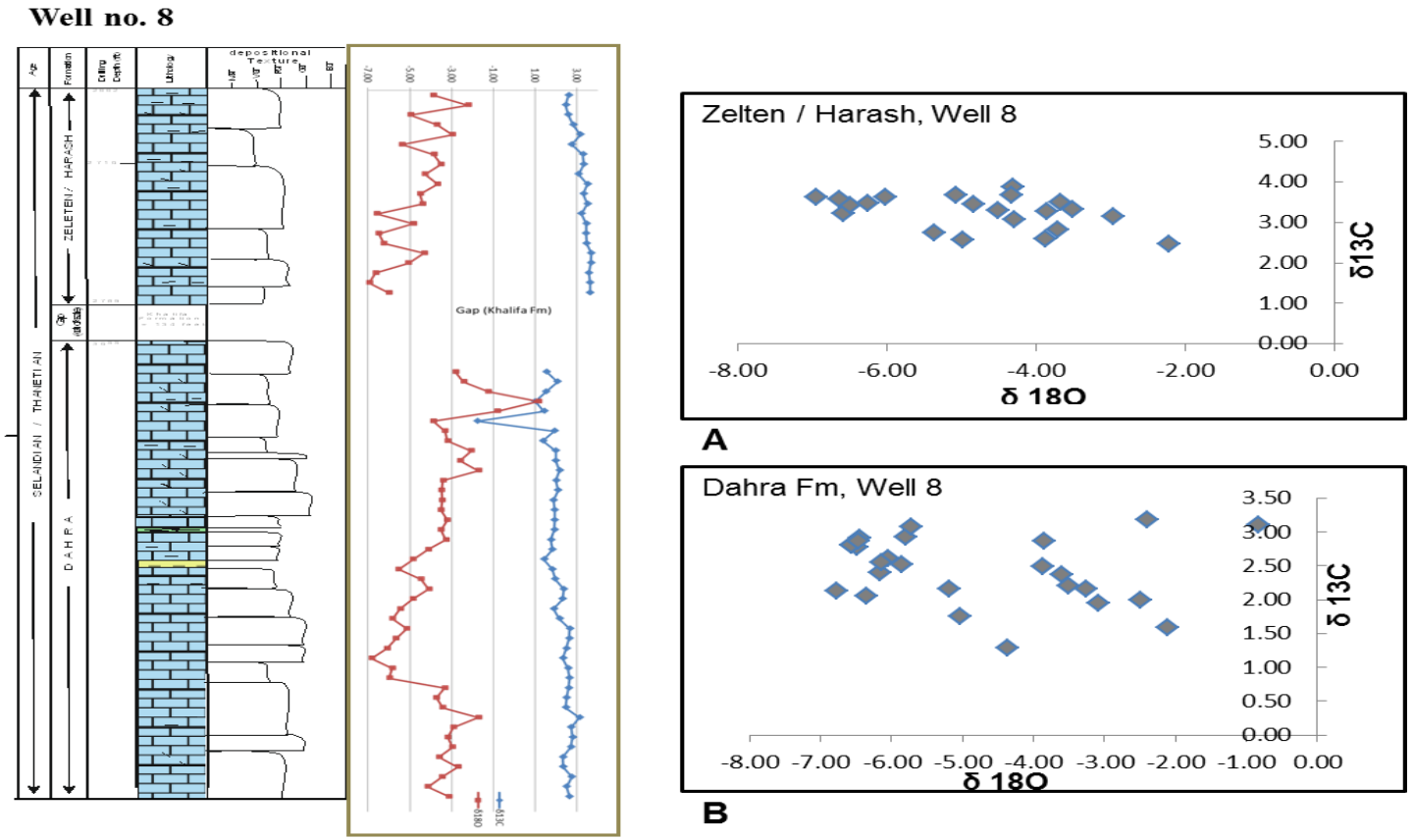

Figure 4.13 Carbon versus oxygen isotopes of the studied Selandian/Thanetian succession in well no. 8 on the Dahra Platform. A: Zelten and Harash Formations; B: Dahra Formation.

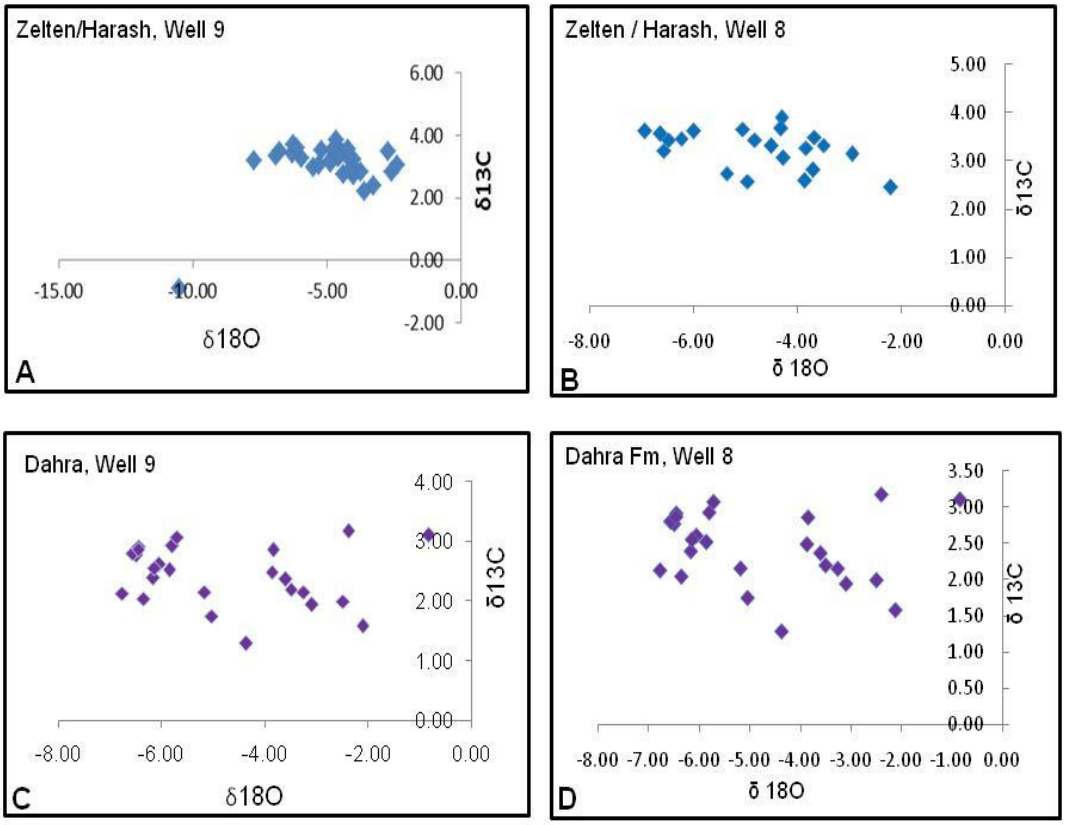

Figure 4.14 Oxygen and carbon isotopes for the Zelten and Harash Formations (A & B) and Dahra Formation (C & D) inWest and East Dahra Fields onthe Dahra Platform.

The overall isotope values of the Mabruk Member in the Dor al Abid Trough range from $\delta^{18}O$ -5.45‰ to -0.77 ‰, and $\delta^{13}C$ 0.00‰ to +3.04‰ (Fig. 4.17). Pronounced negative excursions occur in the lower and upper parts of the cored section of wells no. 66 and 103, respectively, where the isotopic values changed dramatically from $\delta^{13}C$ + 0.87 ‰ to – 6.31‰ and $\delta^{18}O$ from -4.94 ‰ to -7.68 ‰ in the former well, and from -3.87 ‰ to -7.66 ‰ and from +1.15‰ to -4.87‰ in the later (Fig. 4.15). These values in both wells are most likely rogue values (off analyses), as they seem not part of the trend. Alternatively, they may represent deep burial calcite or dolomite.

A clear negative excursion occurs in the middle interval of the Upper Mabruk in well no. 105, where the oxygen isotope values reduced from -2.48‰ to -5.45‰ and the carbon isotope values depleted from +2.23‰ to +1.63‰ (Fig. 4.16). The whole interval (3722 - 3743ft) is characterized by more negative oxygen isotope values and less positive carbon isotope values. This (interval with more negative oxygen values) could

suggest there may have been differences in sea-surface temperatures and/or SMOW at the time of deposition, compared to modern values, or that the values are due to either more intense meteoric diagenesis and/or relatively high temperatures during the precipitation of burial diagenesis cement.

A coincidence trend, similar to that on the Dahra Platform, has occurred in the $\delta^{13}C$ and $\delta^{18}O$ values in the Mabruk Member in the Dor al Abid Trough, particularly in well no.105 (Figs. 4.15 and 4.16). It is probably ascribed to interaction with meteoric ground waters or to dissolution and recrystallisation during burial diagenesis as suggested by Sakai and Kano (2001) and Keller *et al*. (2004).

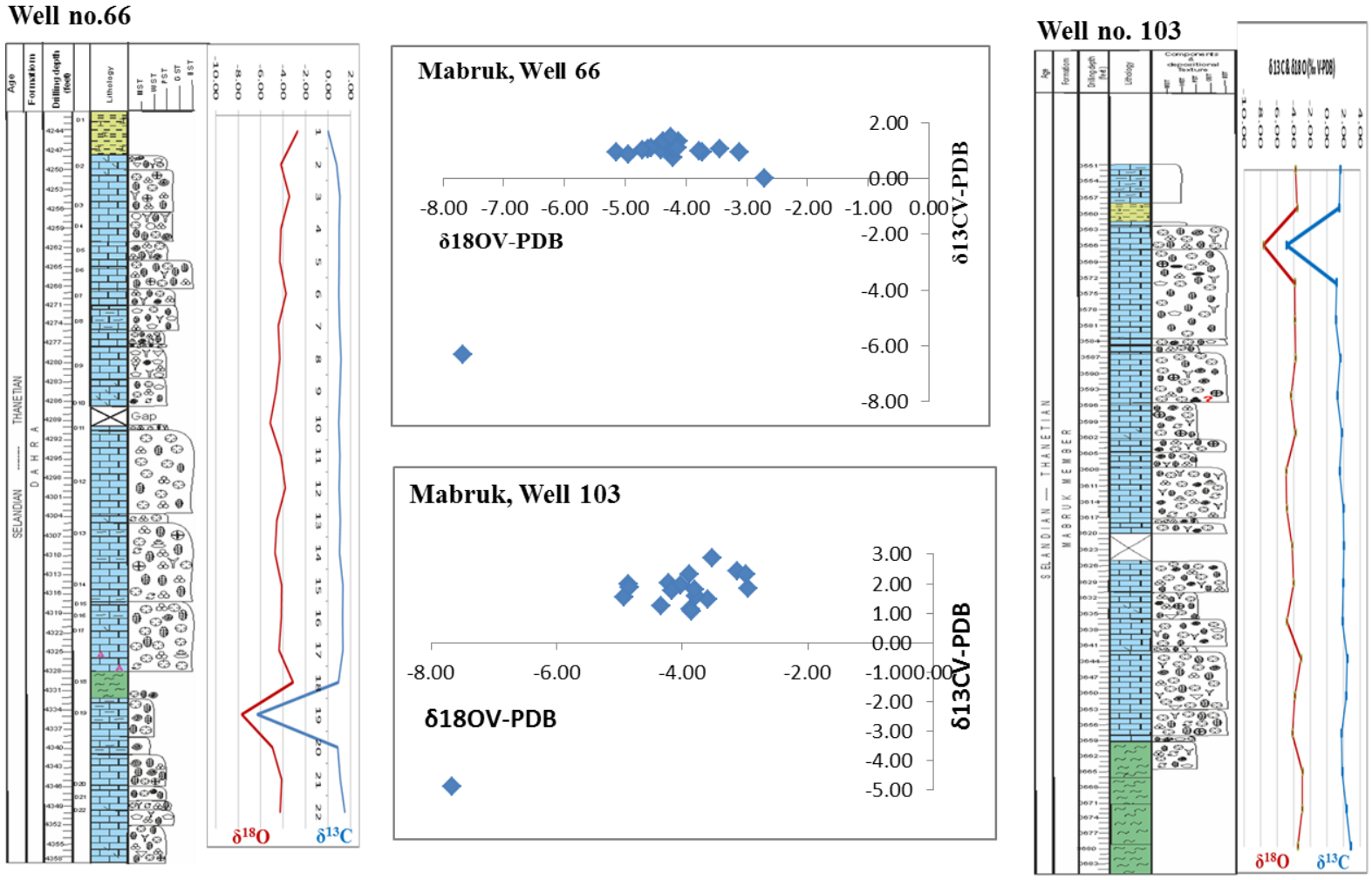

Figure 4.15 Stable oxygen and carbon isotopes for the Mabruk Member in Dor al Abid Trough. Wells no. 66 and 103 (reef area).

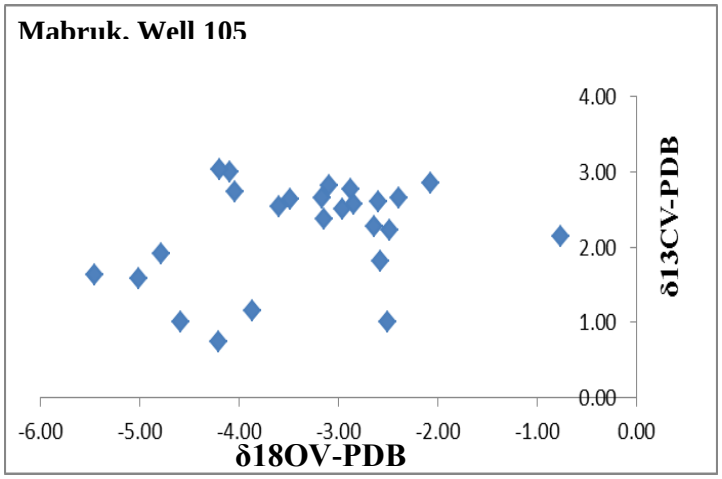

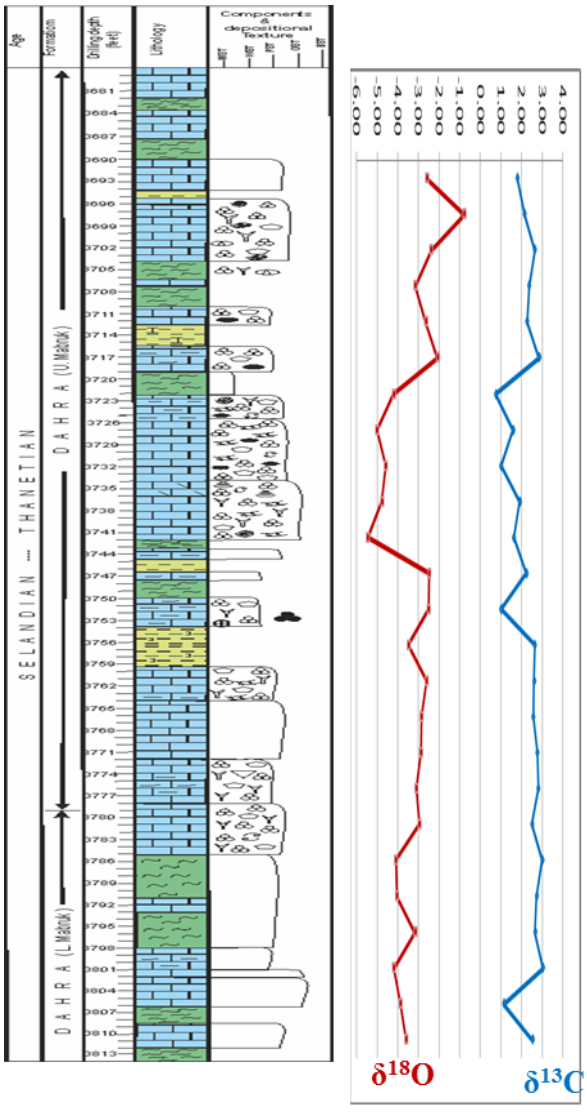

Figure 4.16 Stable oxygen and carbon isotopes for the Mabruk Member in Dor al Abid Trough. Well no. 105, back-reef area (lagoon).

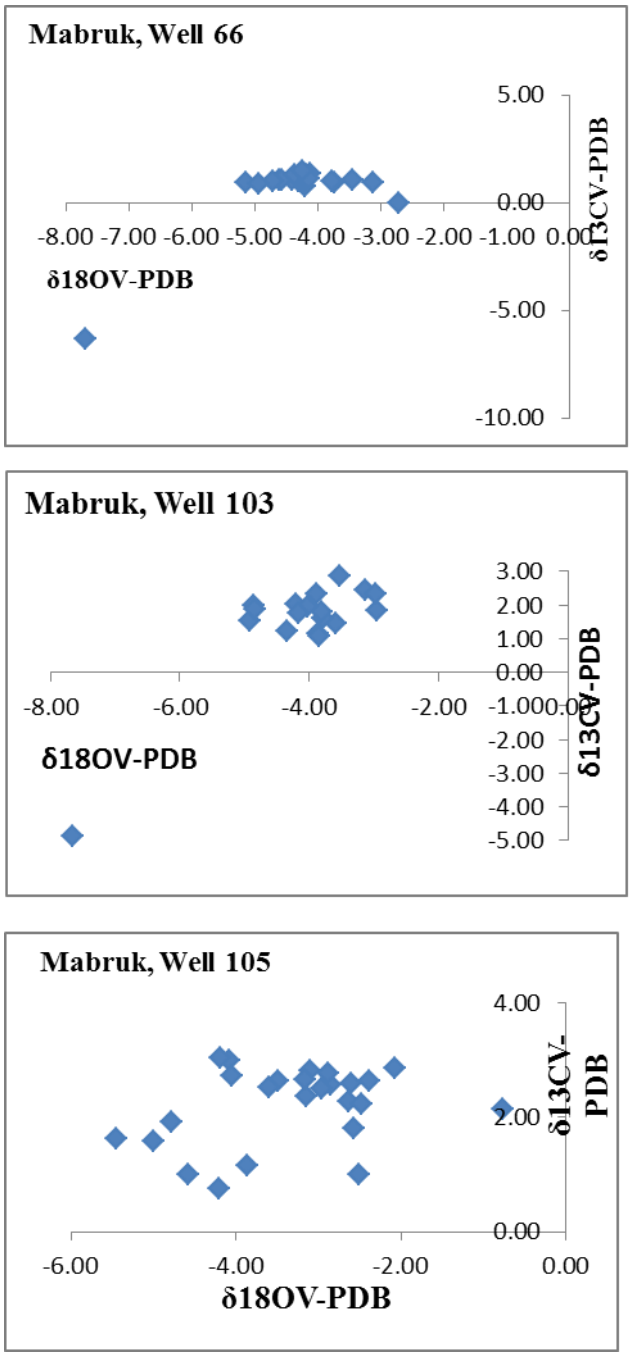

Figure 4.17 Stable oxygen and carbon isotopes for the Mabruk Member in the Dor al Abid Trough. Well no. 66, reef area; well no. 103, reef area, and well no. 105, back-reef area (lagoon).

4.3.2. Fluid Inclusion results

As previously stated the fluid inclusion analysis has been conducted by Fluid Inclusion Technologies, Inc. at its head office in Oklahoma, U.S.A. Ten selected samples from two wells on the Dahra Platform (wells no. 8 and 9) were sectioned and then examined under a petrographic microscope (Tables 4.1 and 4.2). Based on the petrographic examination, 4 samples were further analysed to determine the homogenization temperature of petroleum and aqueous inclusions, melting temperature of aqueous inclusions and salinity (wt %) (Tables 4.3 and 4.4).

The petrographic investigation of these samples revealed that inclusions range from absent through rare to common, with blue, yellow to white fluorescent. Three samples from the Dahra Formation in well no. 8, however, did not show any visible liquid petroleum inclusions in slightly porous dolomitic mudstone (sample no. 25), porous packstone (sample no.29), and marginally porous wackestone/packstone (sample no.58) (Table.4.1). In addition, no visible oil inclusions were identified in porous grainstone (sample no.34), slightly porous and dolomitic packstone (sample no. 39), or fairly porous grainstone (sample no. 52) in the Dahra Formation from well no. 9 (Table 4.2).

Sample no. 49, which was located in the Dahra Formation in well no. 8 at a depth of 3229ft, comprises several occurrences of white fluorescent inclusions within porous and dolomitic grainstone (Fig. 4.18 and Table 4.3), whereas sample no. 46 of the Dahra Fm in well no. 9, at a depth of 3216ft, contains several to common occurrences of blue fluorescent inclusions in porous and bioturbated grainstone (Fig. 4.18 and Table 4.3). Visual abundance is marginally high enough to suggest an oil column or palaeo-column at this depth. In the Zelten Formation, well no. 8 at a depth of 2788ft (sample no. 21), high oil saturation is detected (an oil column or palaeo-column), which contains high visual abundance of yellow fluorescent inclusions in non-porous wackestone/packstone (Fig. 4.19 and Table 4.4). The Harash Formation in well no. 9 (sample no. 13), on the other hand, reveals rare to several, white fluorescent inclusions in non-porous packstone (Fig.4. 19 and Table 4.4).

Detailed analyses of these inclusions show that the homogenization temperature from hydrocarbon inclusions in the succession as a whole ranges between 48 and 67°C and the homogenization temperature from aqueous inclusions is from 59 to 90°C (Fig, 4.20). The homogenization temperature from hydrocarbon inclusions in the Dahra

Formation ranges between 54 and 67°C, in Zelten Formation between 48 and 57°C, and in Harash Formation is 60°C. The homogenization temperature of aqueous inclusions could not be recorded in the Dahra Formation, in the Zelten it is 59°C, and in the Harash it ranges between 67 and 90°C. The melting temperature of aqueous inclusions in Zelten Formation is -10.5°C, and in the Harash Formation range from -21.2 to -4.1°C (Tables. 4.3 and 4.4). It could not be recorded in the Dahra Formation. It is clear that the homogenization temperature of the aqueous inclusions is higher than that of the petroleum inclusions in the Zelten Formation, and is much higher in the Harash Formation; this might also have been the case in the Dahra Formation. This could suggest two phases of calcite precipitation, an earlier, shallow burial one coinciding with some hydrocarbon generation and another later, somewhat deeper phase of calcite precipitation.

Petrographic investigation has resulted in the recognition of mainly two types of equant calcite cement; equant sparry calcite and coarse ferroan calcite. Petrographic relationships also indicate that both types of calcite cement are relatively late diagenetic phases, after compaction and grain fracturing (during mesogenetic phase).

The fluid inclusion data from the studied wells show that the fluids as a whole attained temperatures range between 48 to 90°C, with the homogenization temperature from aqueous inclusions is from 59 to 90°C (Fig, 4.20). The geothermal gradient in the Sirt Basin, according to Hallett (2001), averages 25.5°C/km. The average geothermal gradient in the Sirt Basin is around 2.2°C/100 metres (~6.6°C/1000 feet) and the surface temperature is about 29°C (Gumati and Schamel, 1988) (Fig. 4.21). This suggests that the depth of calcite cementation ranged from ~4500 to ~9300 ft. However, Gumati and Schamel (1988) pointed out that the geothermal gradient in the basin varies between the troughs and the platforms and suggested that this variation is related more to thermal conductivity than to the depth of burial. Bearing in mind that these rocks (Zelten and Harash Fms) now exist at depths ranging from 2600-2900 feet, the features of the calcite cement suggest that precipitation took place at fairly shallow depths, since there is only limited chemical compaction and stylolitization, and the porosity has not been totally destroyed. The cementation is not complete- although it is possible that quite early oil entry prevented full cementation.

Table 4.1 Fluid inclusion petrography from the Dahra and Zelten Formations in well no. 8, the Dahra Platform.

Well No.8																				
Sample depth, code and Formation	Rock Type	Petroleum Fluid Inclusion Populations												Kerogen (possible source rock					Bitumen	
		Population 1				Population 2				Population 3										
	Dominant Subordina	Fluorescence	API	Host mineral &	Abundance	Fluorescence	API	Host mineral &	Abundanc	Fluorescence	API	Host mineral &	Abundanc	Host Rock	Type	OP Fluor	GP Abundanc	OP	Type	Abundance
2788ft (21) Zelten	cb	yl		cc	a			cc	r										ds	r
3079 ft (25) Dahra	cb													cb	op	yl		r	ds	r
3119 ft (29) Dahra	cb																			
3229 ft (49) Dahra	cb	wt		cc	sv														ds	Sv
3287 ft (58) Dahra	cb																		ds	R

ss: sandstone
si: siltstone
sh: shale
cb: carbonate
sa: salt
an: anhydrite
ch: chert
co: coal

mt: metamorphic rock
no: none
br: brown
or: orange
yl: yellow
wt: white
bl: blue

m: moderate
um: upper-moderate
h: high
dq: frac in detrital quartz
dr: quartz dust rim
qc: quartz cement
df: frac detrital feldspar

r: rare
sv: several
c: common
a: abundant
xa: very abundant
go: oil and gas prone
op: oil prone

ds: dead petroleum stain
po: pore-occluding bitmn
pb: pyrobitumen
cc: carbonate cement
ls: live petroleum stain
ul: upper-low

Table 4.2 Fluid inclusion petrography from the Dahra and Harash Formations in well no. 9, the Dahra Platform.

Well No. 9																				
Sample depth, Code and Formation	Rock Type	Petroleum Fluid Inclusion Populations												Kerogen (possible source rock					Bitumen	
		Population 1				Population 2				Population 3										
	Dominant Subordinate	Fluorescence Color	API Gravity	Host mineral & Occurrence	Abundance	Fluorescence Color	API Gravity	Host mineral & Occurrence	Abundance	Fluorescence Color	API Gravity	Host mineral & Occurrence	Abundance	Host Rock	Type	OP Fluor. Color	GP Abundance	OP Abundance	Type	Abundance
2698 ft (13) Harash	cb	wt		cc	sv															
3084 ft (34) Dahra	cb																		ds	sv
3165ft (39) Dahra	cb																		ds	sv
3216 ft (46) Dahra	cb	bl		cc	c														ds	c
5240 ft (52) Dahra	cb	wt		cc	r														ds	r

ss: sandstone
si: siltstone
sh: shale
cb: carbonate
sa: salt
an: anhydrite
cc:carbonate cement

mt: metamorphic rock
no: none
br: brown
or: orange
yl: yellow
wt: white
ls: live petroleum stain

m: moderate
um: upper-moderate
h: high
dq: frac in detrital quartz
dr: quartz dust rim
qc: quartz cement
ul: upper-

r: rare
sv: several
c: common
a: abundant
xa: very abundant
go: oil and gas prone

ds: dead petroleum stain
po: pore-occluding bitmn
pb: pyrobitumen
op: oil prone
l: low
bl: blue carbonate

The degree of thermal maturity of the Upper Cretaceous shale, the regional structure, and the subsidence history of the basin all indicate that over 3,000ft of section was removed from the western flank of the Sirt Basin by uplift and erosion in the mid-Tertiary (Gumati, and Schamel, 1988). Assuming that the highest temperatures of homogenization for aqueous inclusions recorded in the studied samples (90^{o}C) represent conditions at near maximum burial, then palaeogeothermal gradients must have been much higher than at present (22^{o}C/km or 25^{o}C/km), and it supposed to be >70^{o}C/km, and/or that the Paleocene sediments were buried deeper for a time (~9300 feet).i.e. the Mid-Tertiary uplift was actually associated with significant erosion. Supposing that the above temperature is an error measurement, a 59^{o}C has been also recorded in the middle part of the Zelten Formation in well no. 8. Although it is still higher than the temperature expected, taking into account the present day geothermal gradient, a proposed burial diagram of the Thanetian succession in the study area has been constructed (Fig. 4.22).

In the absence of igneous activity in the immediate area, the relatively high temperatures indicated by some fluid inclusions in the studied succession on the Dahra Platform is probably due to low sedimentation rates and the high thermal conductivities of carbonates, and/or fluid flow from deeper parts of the area.

The fluid inclusions in the Zelten/Harash succession have salinities ranging between 6.6 and 23.1 wt% NaCl, which is up to five times more saline than normal sea water. Such fluids may represent sea water and/or more likely evaporated sea water from a lagoonal setting or mixing with subsurface brine. Application of fluid inclusion results and other analytical techniques, along with the wireline logs in the burial history of the studied rocks are dealt with in detail in Chapter 6.

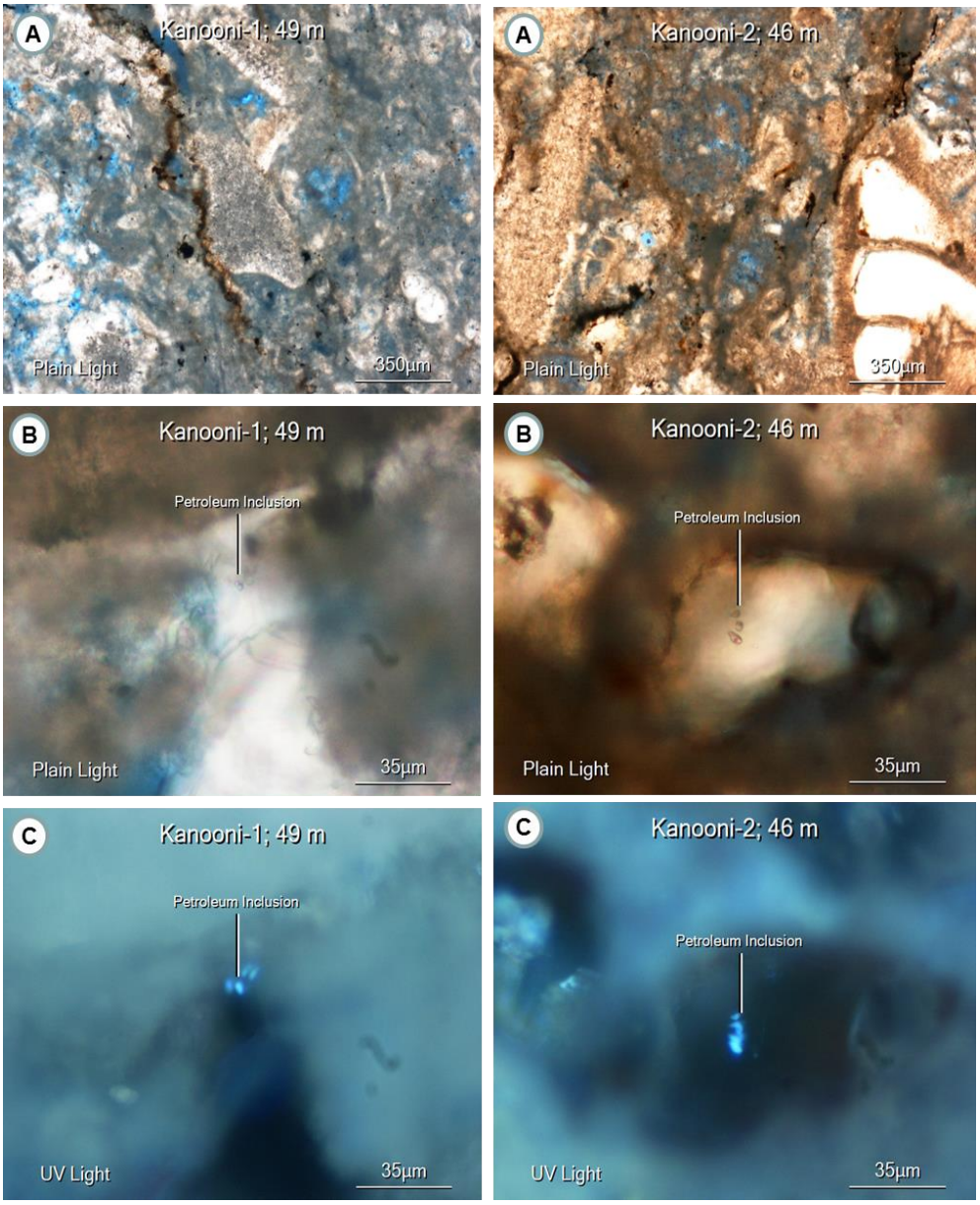

Figure 4.18 A-C (left column) several white fluorescent, unknown gravity oil inclusions in bioclastic foraminiferal grainstone microfacies, Dahra Formation in East Dahra Field, Dahra Platform, Well no. 8 (3229 ft); A-C (right column) several to common occurrences of blue fluorescent, unknown gravity petroleum inclusions in porous bioclastic foraminiferal grainstone microfacies, Dahra Formation in West Dahra Field, Dahra Platform, Well no.9 (3216 ft).

Table 4.3 Fluid inclusion results of sample no. 49, the Dahra Fm, Well no.8 (A), and sample no. 46, the Dahra Fm, Well no. 9 (B).

A

Table 1: Kanooni-1; 49						
Well no.8 – 3229 (D)						
Population	**Fluor Color**	**Th hc (°C)**	**API hc (°)**	**Th aq (°C)**	**Tm aq (°C)**	**Sal (wt%)**
pr/sec; cc	wt	63 (1)				
pr/sec; cc	wt	60 (1)				

B

Table 2: Kanooni-2; 46						
Well no.9 - 3216 (D)						
Population	**Fluor Color**	**Th hc (°C)**	**API hc (°)**	**Th aq (°C)**	**Tm aq (°C)**	**Sal (wt%)**
pr/sec; cc	bl	59 (2)				
pr/sec; cc	bl	54 (1)				
pr/sec; cc	bl	67 (1)				

Legend

Fluorescence Color: based on illumination with Nikon UV-2A filter
Th hc: homogenization temperature of petroleum inclusions
API hc: measured or estimated API gravity of petroleum inclusions

Th aq: homogenization temperature of aqueous inclusions
Tm aq: final melting temperature of aqueous inclusions
mixed: inclusion contains aqueous fluid and petroleum
metastable: final Tm above 0 C precludes accurate salinity

NOTE: data on same line indicate coexisting aq and pet

Sal (wt%): salinity computed from NaCl-H2O system
Capital Letter: population or area

Number in Parentheses: number of inclusions measured
N/A: could not be determined
S?: high Th from deformation of inclusion cavity
pr: primary
sec: secondary
psec: pseudo-secondary

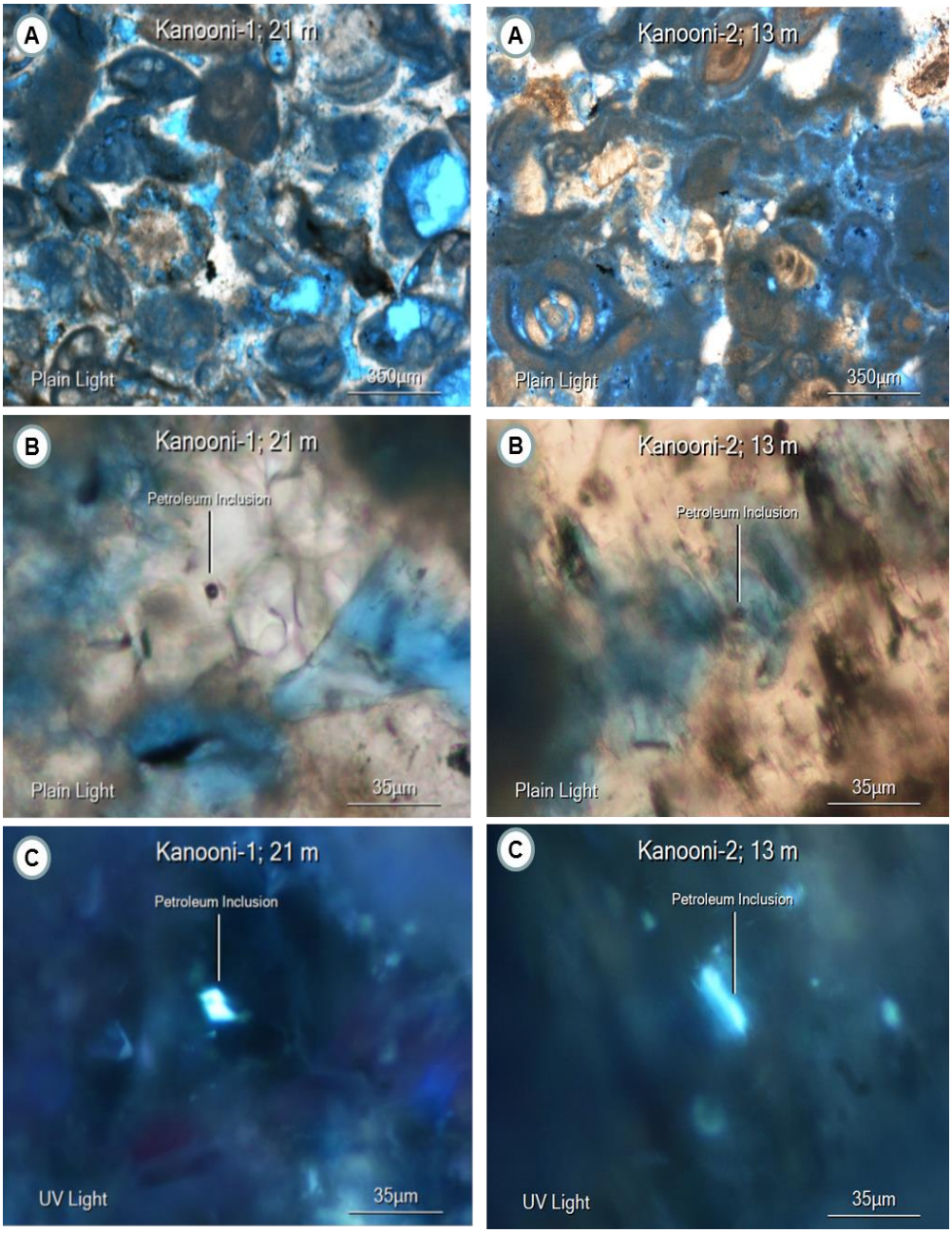

Figure 4.19 A-C (left column) abundance of yellow fluorescent, unknown gravity oil inclusions in porous bioclastic wackestone/ packstone microfacies, Zelten Fm, Well no. 8 (2788 ft); A-C (right column) rare to several white fluorescent, unknown gravity oil inclusions in dolomitic bioturbated bioclastic packstone microfacies, Harash Fm, Well no.9, (2698 ft).

Table 4.4 Fluid inclusion results of sample no. 21, Zelten Fm, Well no.8 (A), and sample no. 13, the Harash Fm, Well no. 9 (B).

A

Table 3: Kanooni-1; 21						
Well no. 8 – 2788 (Z)						
Population	**Fluor Color**	**Th hc (°C)**	**API hc (°)**	**Th aq (°C)**	**Tm aq (°C)**	**Sal (wt%)**
pr/sec; cc	yl	57 (1)				
pr?/sec; cc	yl	48 (1)				
pr?/sec?; cc				59 (1)	-10.5	14.5

B

Table 4: Kanooni-2; 13						
Well no. 9 – 2698 (H)						
Population	**Fluor Color**	**Th hc (°C)**	**API hc (°)**	**Th aq (°C)**	**Tm aq (°C)**	**Sal (wt%)**
pr/sec; cc	wt	60 (1)		90 (1)	-4.1	6.6
pr/sec; cc				67 (1)	N/A	N/A
pr; cc				70 (1)	-21.2	23.1

Legend

Fluorescence Color: based on illumination with Nikon UV-2A filter
Th hc: homogenization temperature of petroleum inclusions
API hc: measured or estimated API gravity of petroleum inclusions

Th aq: homogenization temperature of aqueous inclusions
Tm aq: final melting temperature of aqueous inclusions
mixed: inclusion contains aqueous fluid and petroleum
metastable: final Tm above 0 C precludes accurate salinity

NOTE: data on same line indicate coexisting aq and pet

Sal (wt%): salinity computed from NaCl-H2O system
Capital Letter: population or area

Number in Parentheses: number of inclusions measured
N/A: could not be determined
S?: high Th from deformation of inclusion cavity
pr: primary
sec: secondary
psec: pseudo-secondary

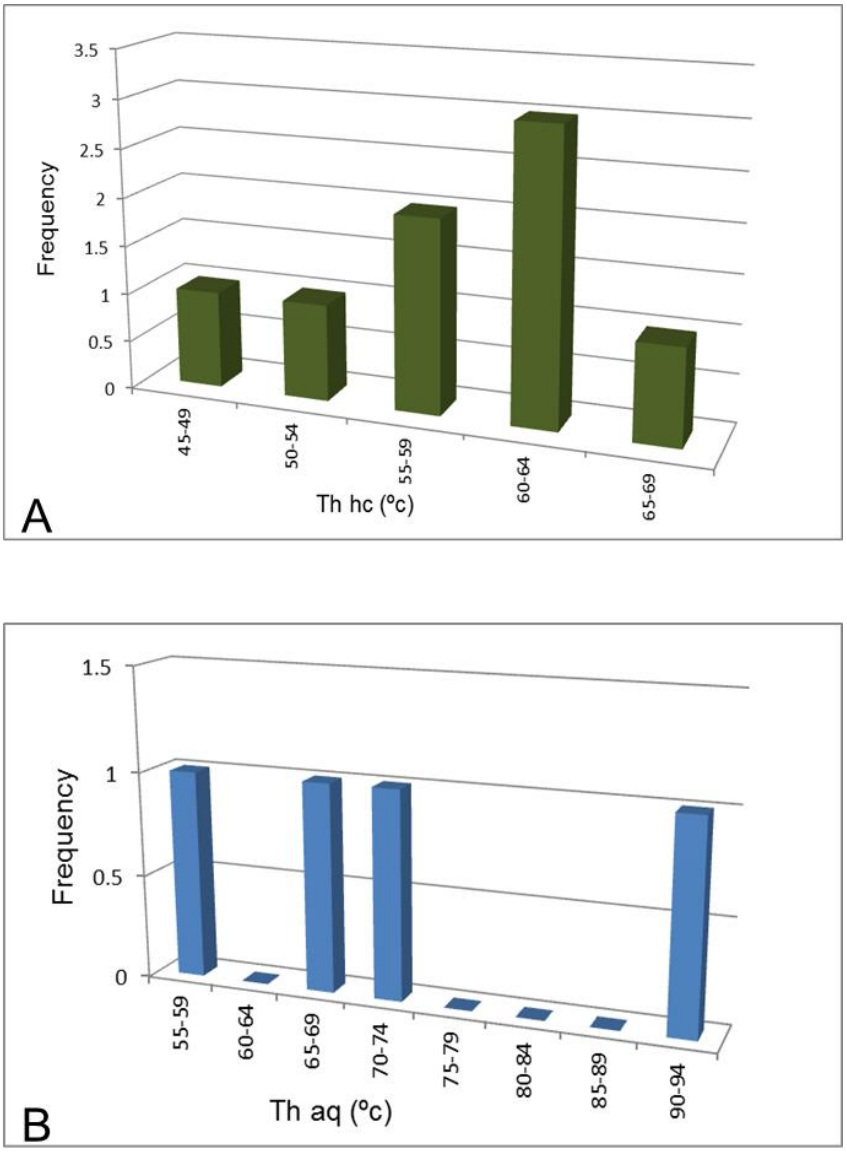

Figure 4.20 Homogenization temperature of petroleum inclusions (A) and aqueous inclusions (B) against frequency in the Selandian /Thanetian succession (Harash, Zelten and Dahra Formations).

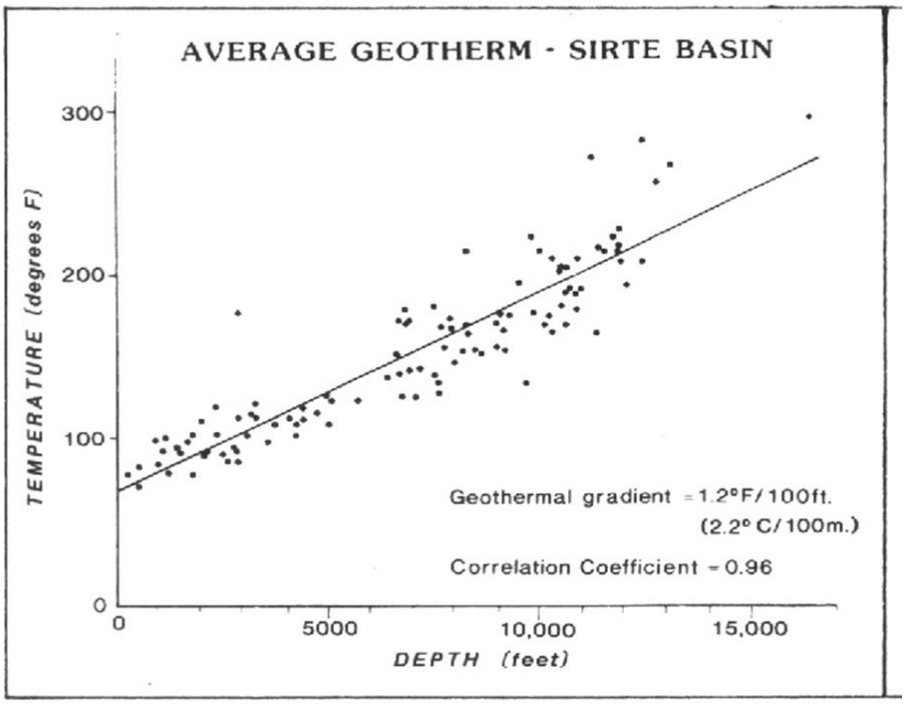

A

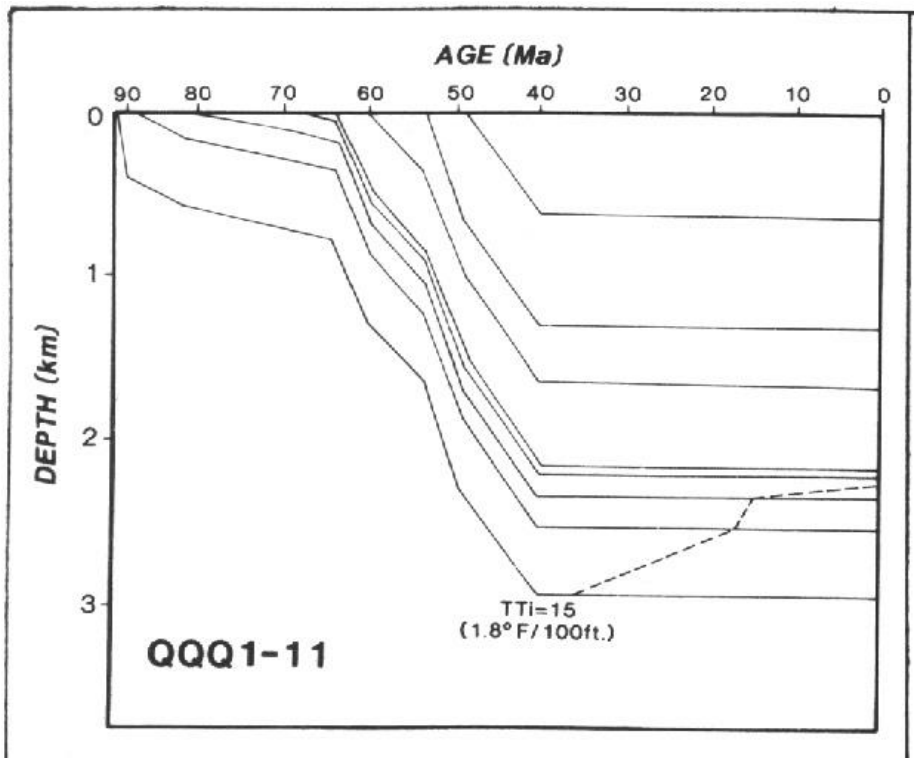

B

Figure 4.21 A) Geothermal gradients posted on well locations for the Sirt Basin; B) Burial history curve of well no.3Q1-11 in the Zella Trough, western Sirte Basin (Gumati and Schamel, 1988).

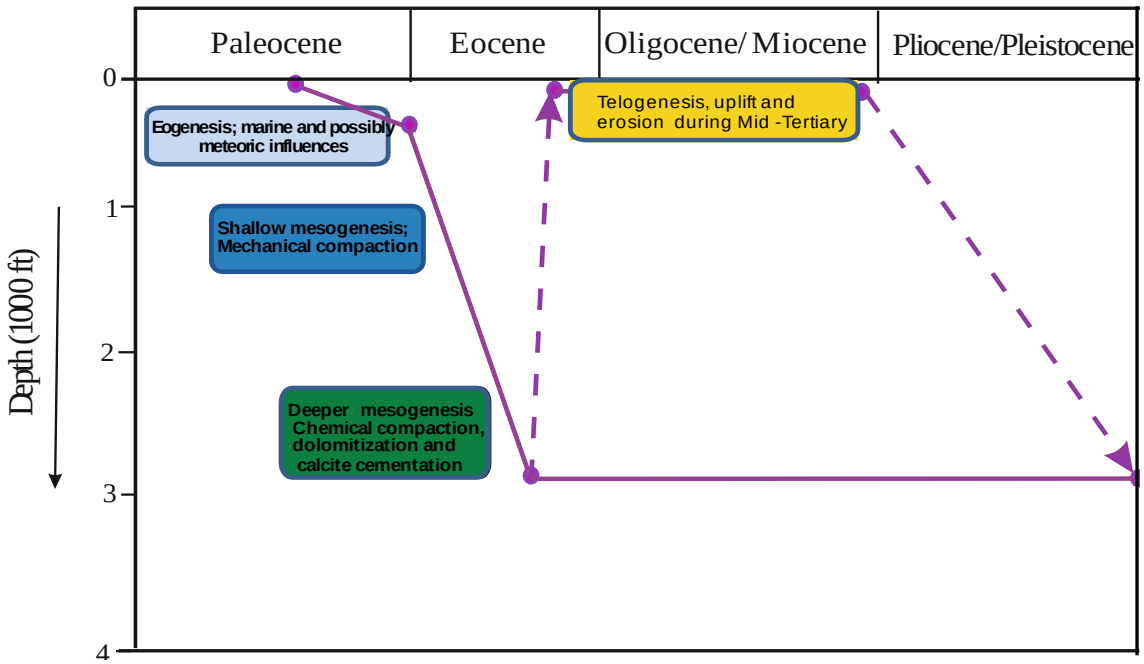

Figure 4.22 Proposed schematic burial diagram of the Thanetian succession in the study area.

4.4. Diagenetic interpretation and paragenesis

As shown in the previous section, the studied interval of the Paleocene succession has been subjected to a complex series of post-depositional changes from the time of deposition up to the present day.

The relative timing of diagenetic features and diagenetic stagesof the Selandian/Thanetian carbonates has been considered on the basis of petrographic observations, cross-cutting relationships among depositional and diagenetic fabrics, and geochemical analyses.

Evidence of the early marine sedimentation and diagenesis is recorded almost throughout the studied sections and is represented by boring of some bioclasts, microbial micritization and formation of micritic envelopes and burrowing. Precipitation of isopachous marine fibrous calcite cement around various carbonate grains has resulted in the preservation of primary intergranular porosity in the Dahra Formation. In addition, positive values of δ^{13}Cand rather low negative δ^{18}O in the

Dahra, Mabruk and Zelten/Harash formations strongly support diagenesis in the marine realm.

The succession has also been affected by meteoric diagenesis on both structures; the Dahra Platform and Dor al Abid Trough. Neomorphism, dissolution, equant sparry calcite and syntaxial rim cement precipitations, along with clay minerals and hematite probably all took place in the meteoric zone. Probably the most characteristic vadose-diagenetic or pedogenic feature in the studied samples is the meniscus cement, which occursin the upper part of the Dahra Formation in well no.7 on the Dahra Platform. Extensive dissolution of unstable grains has been witnessed at several intervals in the Dahra, Mabruk, and Zelten/Harash Formations. The original aragonitic, and probably some high Mg-calcite grains, together with some matrix, have commonly been dissolved and replaced in the upper part of meteoric phreatic environment (zone of active circulation), where the meteoric waters are strongly undersaturated with respect to the metastable carbonate species.

Under cathodoluminescence, the equant calcite and syntaxial rim cement crystals are largely non-luminescent to dull (weak) luminescent. Clay minerals, which are dominated by kaolinite could reflect an influx of riverine clastics through a minor sea-level fluctuation. Hematite, however, occurs in association with desiccation cracks, fenestrae and rootlets in dolomitic, brecciated and mottled fabcies. These features, which occur in the Dahra Formation and in the lower part of the Zelten Formation, provided additional strong evidence of exposure (palaeosoils). The isotopic signature in well no. 8, however, support this interpretation as its $\delta^{13}C$ and $\delta^{18}O$ values increased from -1.83‰ to +1.0‰, and from -3.79‰ to +1.15‰ respectively.

The precipitation of coarse ferroan calcite and coarse, locally saddle, dolomite cements, fracturing, formation of pressure dissolution seams and sylolites are the main evidence that burial diagenesis affected the Selandian/Thanetian carbonates in the study area. Although high ferrous iron content can exist in early cements formed in near-surface anoxic conditions, it is more common in burial equant spar calcite cements (Scholle and Halley, 1985). The medium to coarsely crystalline dolomite has two luminescence characters; inner weakly to non-luminescent and thin outer slightly bright orange zones. The saddle dolomite is commonly associated with hydrocarbons and this has been used to suggest that it forms within the oil window, at temperatures of 60-150°C (Radke and Mathis, 1980).Fluid inclusion results show that the homogenization

temperature from petroleum inclusions in the studied section ranges from 48-67°C, and the homogenization temperature of aqueous inclusions ranges from 59–90°C. This could indicate two phases of burial calcite precipitation during the rock history in the area. The average crystal size of the coarse dolomite (200-400 µm) may thus suggest significant depth of formation and relatively slow growth rate. The occurrence of coarse saddle dolomite probably suggests precipitation in a late deep burial mesogenetic stage, which in turn, has prone to alteration (dissolution) for meteoric waters in the course of telogenesis (during Mid Tertiary).

The above mentioned diagenetic events and their diagenetic environments can be summarised as follow (Fig. 4. 23):

Marine Environment

- Microbial micritization and borings
- Isopachous rim cement
- Glauconite, pyrite and phosphate
- Dolomite?

Meteoric Environment

- Neomorphism
- Dissolution
- Meniscus cement
- Equant calcite cement
- Syntaxial overgrowth cement
- Dolomitization
- Clays and iron minerals

Burial Environment

- Coarse calcite cement
- Dolomite cement
- Dissolution?
- Fracturing
- Solution seams and stylolitization
- Hydrocarbon entry

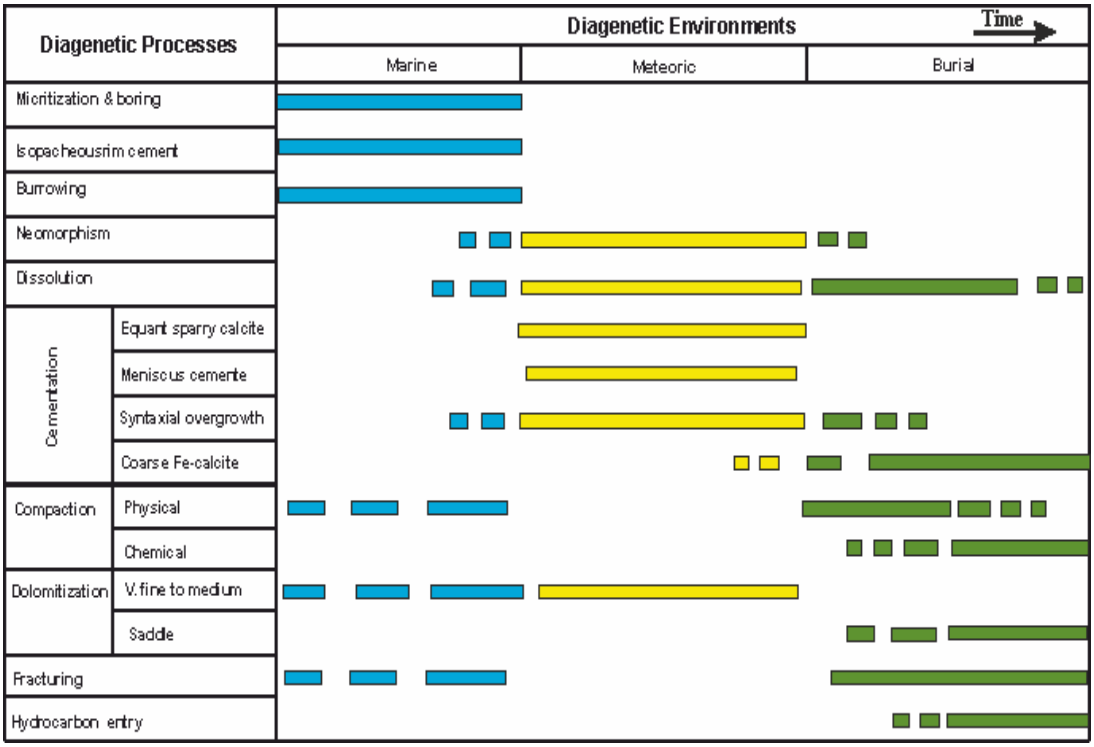

Figure 4.23 Main diagenetic events and environments of the Selandian/Thanetian carbonates in the study area.

4.5. RESERVOIR QUALITY

Carbonate reservoirs are characterised by extremely heterogeneous porosity and permeability on a number of scales - from the km-scale first-order heterogeneities of stratigraphic packages to the microscopic grain scale. These heterogeneities are dependent on the environment of deposition of the carbonate facies and on the subsequent diagenetic alteration of the original rock fabric (Allen and Allen, 1990).

Diagenetic processes affect the reservoir quality in two ways: positive diagenetic processes which include the dissolving activity of meteoric water, dolomitization, decarboxylation, stylolite formation, fracturing, and the migration of oil; and negative processes which include compaction, internal sedimentation, pressure dissolution, and cementation (Cook, 1983). In this section the distribution of porosity and permeability in the studied succession is dealt with through both petrographic examinations and petrophysical analysis.

4.5.1. Porosity and permeability distribution in the Selandian/Thanetian Carbonates

In this section, the two main reservoir parameters (porosity and permeability) of the studied succession will be discussed through core sample (hand specimen) inspection, thin -section observations, core analysis results, and scanning electron microscope examination. In this section the succession is dealt with as two separate intervals on the Dahra Platform; the lower is represented by the Dahra Formation and the upper signifies the Zelten/Harash interval. The Mabruk Member in the Dor al Abid Trough is considered independently.

4.5.1.1. Petrographic observations

The carbonate facies of the Dahra Formation on the Dahra Platform are separated locally by thin beds of shale and marl/argillaceous limestones that act as permeability barriers and these compartmentalize the formation into several major reservoir units. Macroscopic and microscopic investigations revealed that the porosity types developed in the Dahra Formation are dominated by mouldic,vuggy, intergranular and intragranular types, with less common fracture and intercrystalline porosity (Table. 3.2).

The primary intergranular and intragranular porosity have been observed at many intervals within the Dahra Formation in both; the Dahra West and East Fields.

The best primary porosity is developed in bioclastic grainstone and bioclastic foraminiferal packstone-packstone/grainstone facies, where it ranges from negligible to poor (5–10%). The intragranular type of porosity is commonly developed within both the skeletal and non-skeletal carbonate grains, in particular foraminifera and coated grains (Figs. 3.2A, 3.6 A&B, 4.4A). Primary porosity is commonly negligible (<5%) in the rest of facies as a result of precipitation of equant calcite, Fe-rich calcite, dolomite and syntaxial rim cements. The intragranular porosity is developed locally in certain layers and as isolated pores; hence its contribution to Dahra reservoir quality overall seems insignificant. Intergranular porosity, on the other hand, which is negligible as well, appears to have provided pathways for undersaturated fluids to pass through the sediment and thus create secondary dissolution porosity (Figs. 4.1B & 4.3C).

Intercrystalline porosity occurs wherever dolomite is present; in completely dolomitized facies and, less importantly, in partially dolomitic limestone facies. It is the main porosity type, along with moldic, in the dolomitic mudstone facies (Fig. 4.6A). Dolomite-dominated cycles are relatively thin in relation to limestone-dominated cycles; they generally have fair to good porosity even in the mud-supported intervals, reaching to 20 % in some cases (Appendix 1). This is probably related to dolomitization leading to an increase in the particle/crystal size, an increase in pore volume due to a net addition of dolomite, the development of moldic pores and an increasing resistance to compaction (Lucia, 1999).

Selective dissolution of aragonite and possibly high Mg-calcite grains, along with some matrix, has resulted in the formation of moldic and vuggy porosity; this is clearly observed in both hand-specimen and thin-section. This secondary porosity is widespread in the Dahra Formation and occurs in many facies in different proportions, and usually in association with primary inter and intra-granular porosity. Its highest value occurs in grain-supported facies, where it reaches 15% (i.e. fair).

The non-fabric selective type of porosity that cuts across the fabric elements of the rock, namely fracture porosity, has developed locally within the Dahra Formation and is well developed in some wells. A network of open microfractures that were connected to each other developed notably within marl/argillaceous limestone intervals in two wells (Fig. 4.9A). According to the petrographic observations and cross-cutting relationships, this type of porosity developed at different stages of the sediment history; i.e. during the early stages of compaction at shallow burial depths. Fracturing of grains

and substrate has occurred, especially in the packstone/grainstone facies (Fig. 4.8C). Networks of microfractures that interconnect different types of porosity have also been observed in the Dahra Formation. They are commonly open, narrow and short, and locally associated with stylolites (Fig. 4.8 H). Thus it most likely developed at later stages and during relatively deep burial. Partly open and relatively wide fractures and/ or veins have also been observed at a few intervals in the Dahra Formation. The contribution of the fracture porosity as a whole to the reservoir quality of the Dahra Formation seems only locally significant.

Microporosity; refers to that type of porosity which cannot be observed under the light microscope, thus the SEM was the only method by which this type of porosity has been observed and described. Several terms have been used in the literature, such as matrix microporosity, chalky porosity, intramicrite porosity, and pinpoint porosity. It has been developed in the Dahra Formation, particularly in wells no. 8 and 9, and occurs as intercrystalline micro-voids between subhedral to anhedral micrite, microsparite and/or dolomite crystals (Fig. 4.3). It is usually moderately connected through relatively narrow pore throats, but locally it is almost completely isolated. The shape of micrite crystals, however, is generally fairly rounded with a degree of etching. The development of this kind of porosity may be attributed to re-arrangement of the original mud grain in the sediment, which can result in a change in the crystal form or, most likely in this case, to dissolution of the outer parts of micrite crystals (Fig. 4.3). In view of relatively narrow pore throats, which may affect the permeability, the contribution of the microporosity to the reservoir quality of the Dahra Formation seems unimportant.

The best observed porosity in the Dahra Formation is within the bioclastic foraminiferal packstone/grainstone facies in almost all of the studied wells. It is averaging 20-25% in well no. 9, and 15-20% in well no. 8. Most of it is secondary in origin and commonly occurs in the upper parts of shallowing-upward cycles (Fig. 4.33 &Appendix. 1). This is probably related to meteoric influence during minor sea-level fluctuations. Increased porosity near the top of the Dahra Formation may be related to uplift and meteoric exposure during the Mid Tertiary. The latter is evidenced by the dissolution of the late coarse dolomite crystals (Fig. 4.3F). A notable feature in the Dahra Formation is that wherever primary porosity has been preserved, secondary porosity is also better developed. The degree of early cementation in the grain-

supported facies does have a major effect on later compaction; moderate early cement, preserving some useful primary porosity, may render a carbonate less likely to porosity loss during burial (Tucker, 1993). There is no apparent relation between observed porosity and depth (Fig. 4.24). Thus overall, it can be concluded that the porosity evolution in the Dahra Formation was controlled by the original depositional texture, subsequent diagenesis and the pattern of carbonate cycles (Fig. 4.33).

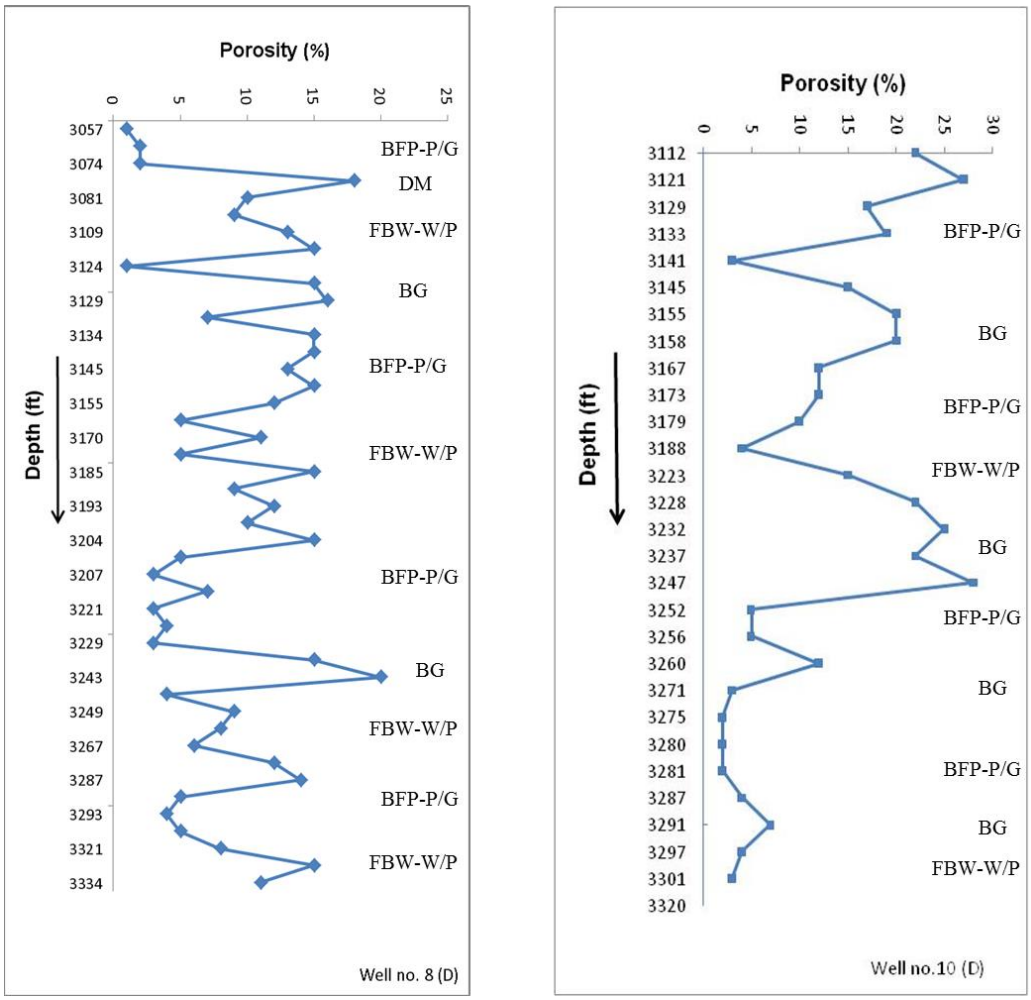

A B

FBW-W/P = Foraminiferal bioclastic wackestone-wackestone/packstone

BFP-P/G = Bioclastic foraminiferal packstone-packstone/grainstone

BFG = Bioclastic foraminiferal grainstone DM = Dolomitic mudstone

Figure 4.24 Depth-porosity (observed) relationship for the cored section of the Dahra Formation in well no. 8 (A) and well no. 10 (B). The facies types are also shown.

The thin-section porosity in the Zelten/Harash interval is generally low, particularly in the Harash Formation (Fig. 4.25). The Zelten Formation, however, has marginally better porosity, especially in the grain-dominated facies. The best porosity in the Zelten Formation isdeveloped in the bioclastic foraminiferal packstone-packstone/grainstone and, less important, foraminiferal nummulitic packstone facies, where it ranges from fair to good and locally reaches very good, especially in well no. 10. The rest of the facies, which are mud-supported commonly have negligible or even zero porosity. A notable feature is that the least estimated porosity in the grain-supported facies is mostly recorded wherever echinoderm fragments are relatively common. This is probably owing to the development of overgrowth cement around echinoderms; this type of cement can grow faster than polycrystalline cements, since the latter require nucleation, whereas the echinoderm itself provides an existing calcite lattice substrate (Evamy and Shearman, 1965).

By way of contrast in the central and eastern parts of the Sirt Basin the Zelten Formation has good porosity and permeability and hence it is the main reservoir in the Zelten Field. It experienced porosity enhancement due to groundwater leaching, and secondary porosity as high as 40% has been reported from bioclastic grain-supported facies (Bebout and Pendexter, 1975). The reservoir quality of the Harash Formation in that area is also fairly good and thus it represents the primary reservoir in the Harash Field.

Although there is also no clear relation between the observed porosity and depth within the Zelten/Harash interval (Fig. 4.25), it is obvious that generally the same carbonate facies within the studied Paleocene succession have the best reservoir properties.

The overall reservoir quality of the Zelten/Harash Formations in the study area is low. This is owing to the presence of mud-supported facies throughout the cored interval, the occurrence of argillaceous materials within the grain-supported facies, fairly extensive compaction, and less important calcite cementation (Table 3.2)

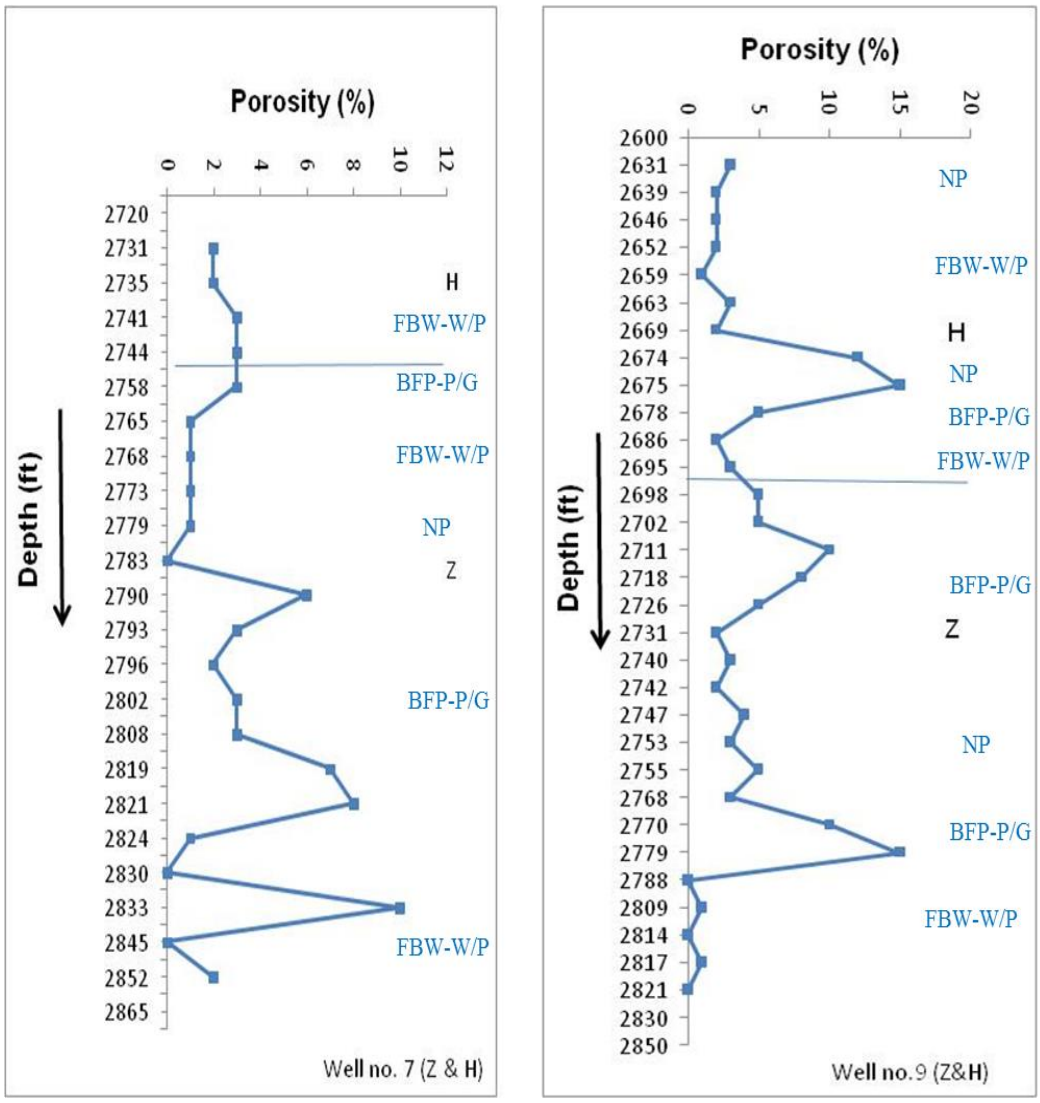

A B

FBW-W/P = Foraminiferal bioclastic wackestone-wackestone/packstone

BFP-P/G = Bioclastic foraminiferal packstone-packstone/grainstone

NP = Nummulitic packstone

Figure 4.25 Depth/porosity (observed) relationship of the cored section of Zelten (Z)/Harash (H) Formations in well no.7 (A) and well no9 (B).

Thin beds of shale and marl/argillaceous limestone separate the Mabruk Member into several reservoir units. The reservoir quality of the Upper Mabruk Member in the Dor al Abid Trough varies from west to east across the area. In the western area, the lower part of the member is characterised by a few tens feet of

bioclastic foraminiferal wackestone/packstone with very good vuggy and moldic porosity.In the Eastern Mabruk Area, particularly in wells no. 66 and 105, the best observed porosity is recorded in the bioclastic foraminiferal packstone-packstone/grainstone facies, where it ranges from fair to good, locally very good, of intergranular, intragranular, moldic, vuggy and channel and/or fracture types (Fig. 4.26).

The bioclastic boundstone facies has commonly negligible porosity, except in two intervals in wells no. 66 and 103 (each is around 4 feet thick), where it ranges from poor to fair with mainly growth framework and microfracture pores. The observed porosity in the algal packstone facies, which developed in wells no. 66 and 103 only, is usually poor and represented mainly by inter, intra-granular (growth framework) and fracture types.

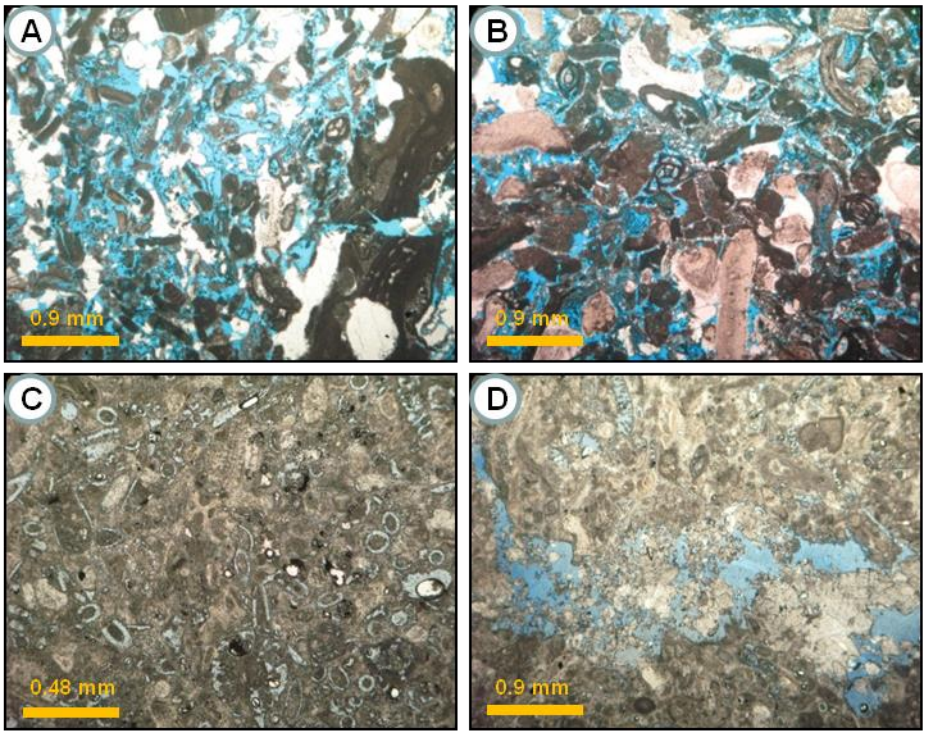

Figure 4.26 Bioclastic foraminiferal packstone-packstone/grainstone facies showing good to very good intergranular, intragranular, moldic, vuggy and fracture porosity (A & B), Mabruk Mbr, Well no. 66 at 4270 and 4275 ft, respectively; Fair to good intragranular, moldic and channel porosity (C & D), Mabruk Mbr, Well no. 105 at 3726 and 3727 ft, respectively.

4.5.1.2. Petrophysical analysis

As noted above, heterogenity in the porosity and permeability of carbonate reservoirs varies from km-scale to microscopic grain scale. It is controlled by the original depositional environment and the subsequent diagenetic alteration of the original rock fabric. Lucia (1999) pointed out that porosity-permeability cross-plots for carbonate reservoirs commonly show a large variability, and there is usually no relationship between them, unless pore-size distribution (volume of interparticle pore space) is included in the analysis. Lucia demonstrated (1983) that three permeability fields can be defined using particle-size boundaries of 100 and 20µm, a relationship that appears to be limited to particle sizes of less than 500 m. The same author (1995) named these three fields as petrophysical class 1 (>100 µm), class 2 (100-20 µm), and class 3 (<20 µm) (Fig. 4.27). The overall relation shows that the interparticle (intergranular) porosity increases as the particle-size decreases. This seems to be the case with the studied samples of the Mabruk wells- since the good porosity interval is associated with the grainstone/packstone facies and it is less well developed in the coarser fabric (boundstones).

No petrophysical measurements of the Dahra, Zelten and Harash Formations in the studied wells were made available in this study and the petrophysical analysis of the studied samples of the Mabruk Member showed that the porosity values and types nearly match the estimated observed porosity.

The measured porosity and permeability of the Mabruk Memberin the studied wells range from 2.4 to 28.4% and 0.02 to 290 mD, respectively. The relation between porosity and permeability in these wells varies somewhat, i.e. it shows a direct relation and noticeable linear trend in wells no. 66 and 105, and a less pronounced trend in well no. 103 (Figs. 4. 28C, 29C, 30C, and 4.31). This may signify that the pore throats in the first two wells are probably wide enough to permit the fluids to pass through them, and hence improved the permeability, whereas in the latter well, these throats are possibly narrow, and thus their contribution to the permeability of the Mabruk rock is insignificant. Also the presence of microporosity in isolated pores is probably an additional reason for that.

The best porosity in the studied wells of the Mabruk Field is recorded in well no. 105, which is located on the southern part of the East Mabruk Area, and represents a back-reef/lagoon setting, whereas the reefal area wells (no. 66 and 103) show lower

porosity values (Fig. 4. 32). The measured porosity in well no. 105, however, ranges from 3.7 to 27.2% and permeability from 0.05 to 95.4mD, with an average porosity of about 15% (fair to good) and the average permeability around 17mD (good). The best measured porosity in this well is developed in the bioclastic foraminiferal packstone-packstone/grainstone facies and bioclastic foraminiferal grainstone facies. The main porosity types in these facies are intragranular and moldic with less important intergranular and microfracture, despite many of it, particularly moldic and fracture, abeing occluded partly or completely by sparry calcite, coarse calcite and saddle dolomite cement, and rarely by anhydrite (Fig. 4. 6 G&H). The lowest porosity values in this well are recorded in the foraminiferal bioclastic wackestone-wackestone/packstone facies (Fig. 4.28 A&B).

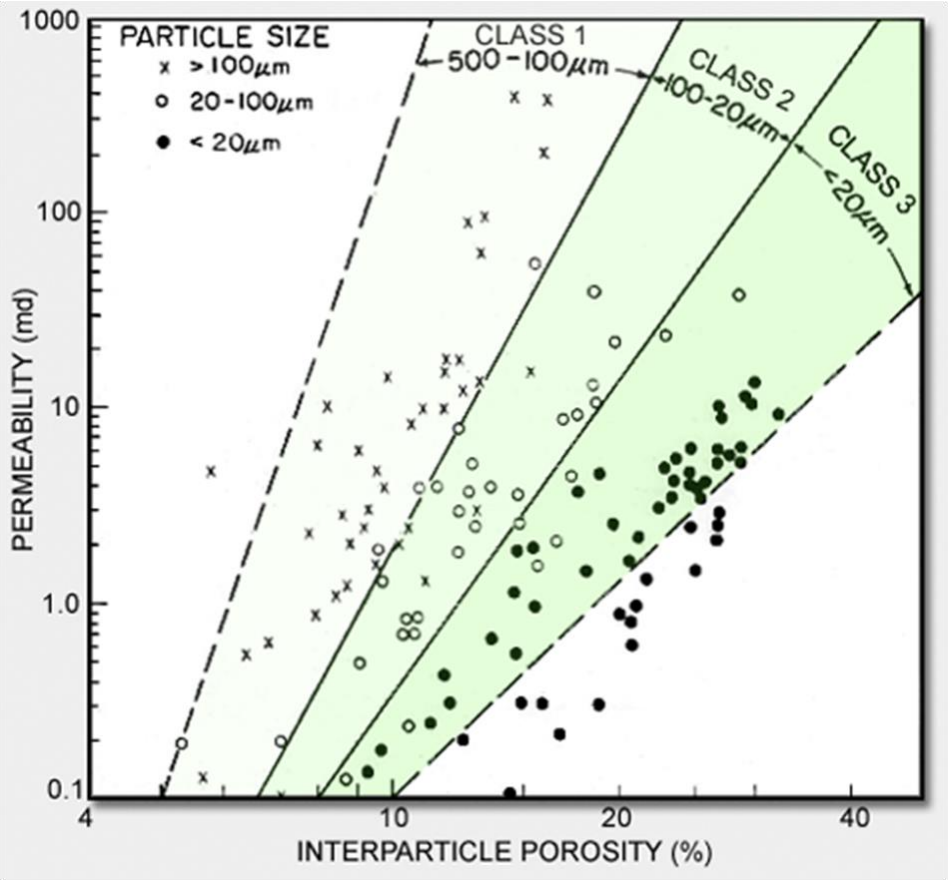

Figure 4.27 Porosity- air permeability relationships for various particle-size groups in non-vuggy carbonate rocks (Lucia, 1983).

In well no. 66, the measured porosity and permeability ranges from 5 to 28% and 0.02 to 290mD, respectively, with the average porosity around 10% (fair) and the average permeability at 10mD (good). The good to very good measured porosity is developed in bioclastic foraminiferal grainstone facies (its average = 20%), whereas the bioclastic foraminiferal packstone-packstone/grainstone, bioclastic boundstone and algal packstone facies have fair (10-15%), poor (5-10%) and poor (8-10%) porosity, respectively (Fig. 4.29 A&B). The primary intergranular and secondary vuggy porosity are the most important contributors to the high porosity value in the bioclastic foraminiferal grainstone facies, despite the fact that they are completely blocked by sparry calcite cement at certain intervals (Fig. 4.4E). Intragranular and moldic porosity also developed but is less significant.

The well no. 103, which is located in the central part of the Eastern Mabruk Area, relatively has the lowest reservoir quality among the studied wells. Its reservoir parameters range from 2 to 14% porosity with an average is about 7% (poor) and 0.04 to 188mD permeability with an average of 6mD (fair). The best measured porosity in this well has been recorded in the algal packstone facies particularly at the depth interval between 3631-3636ft (Fig. 4.30 A&B), where the growth framework and fracture porosity are the most common types. The bioclastic boundstone facies commonly has negligible to poor porosity, especially at the uppermost interval of the cored section, where it is frequently less than 5%.

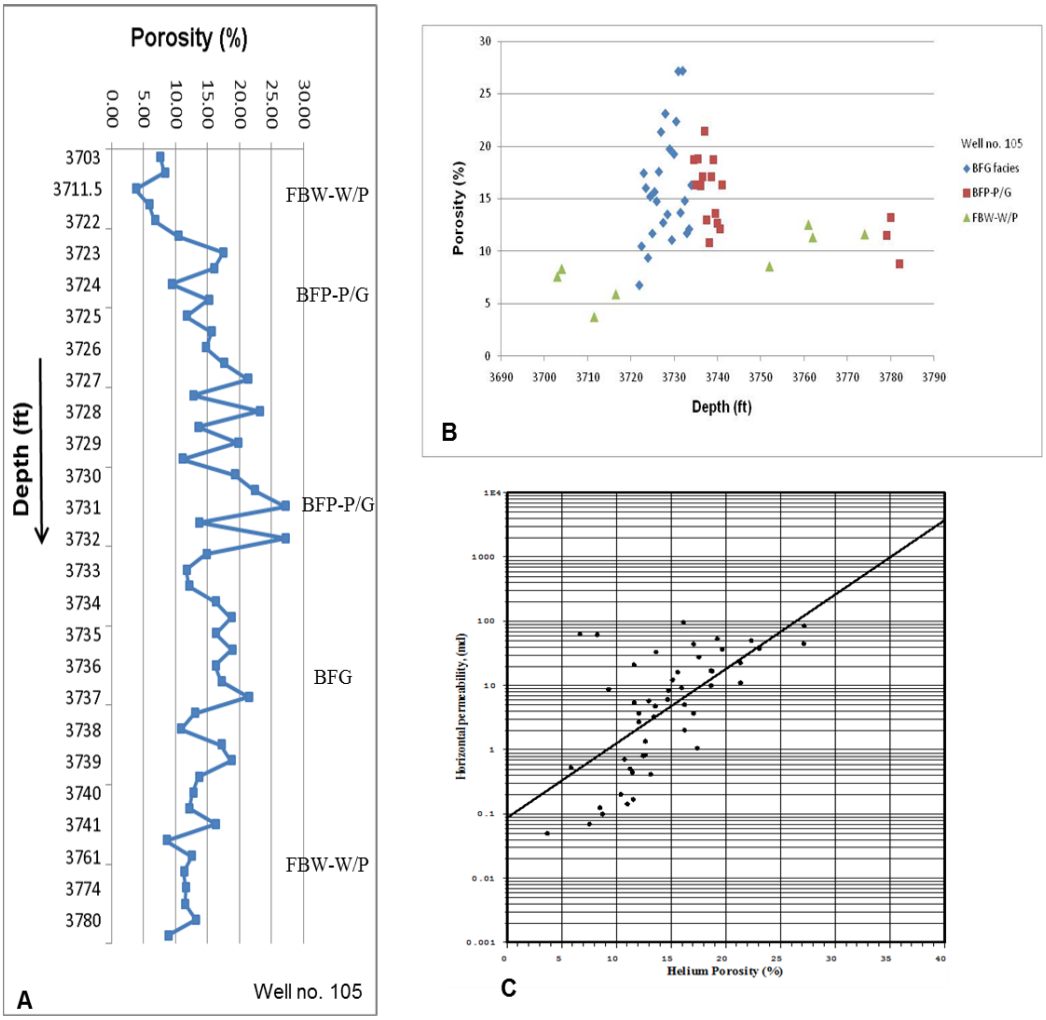

FBW-W/P = Foraminiferal bioclastic wackestone-wackestone/packstone

BFP-P/G = Bioclastic foraminiferal packstone-packstone/grainstone

BFG = Bioclastic foraminiferal grainstone

Figure 4.28 Depth-measured porosity relationship of the cored section of the Mabruk Member in the Dor al Abid Trough in well no. 105 with major facies shown (A); porosity versus depth of the various facies types (B), and a conspicuous linear trend in the relationship between measured porosity and permeability (C).

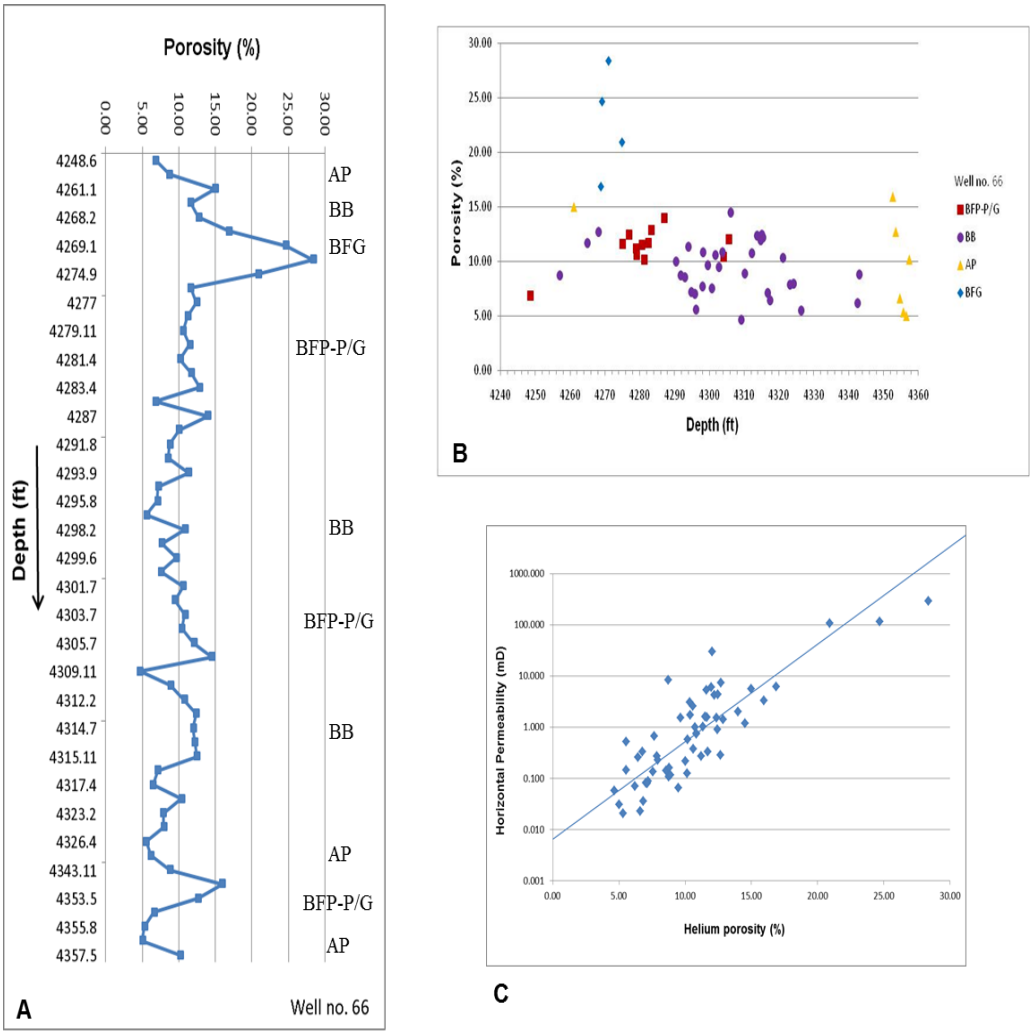

AP = Algal packstone

BB = Bioclastic

BFG = Bioclastic foraminiferal

BFP-P/G = Bioclastic foraminiferal packstone-

Figure 4.29 Depth-measured porosity relationship of the cored section of the Mabruk Member in the Dor al Abid Trough in well no. 66 with major facies shown (A); porosity versus depth of the various facies types (B), and an obvious direct relationship between measured porosity and permeability (C).

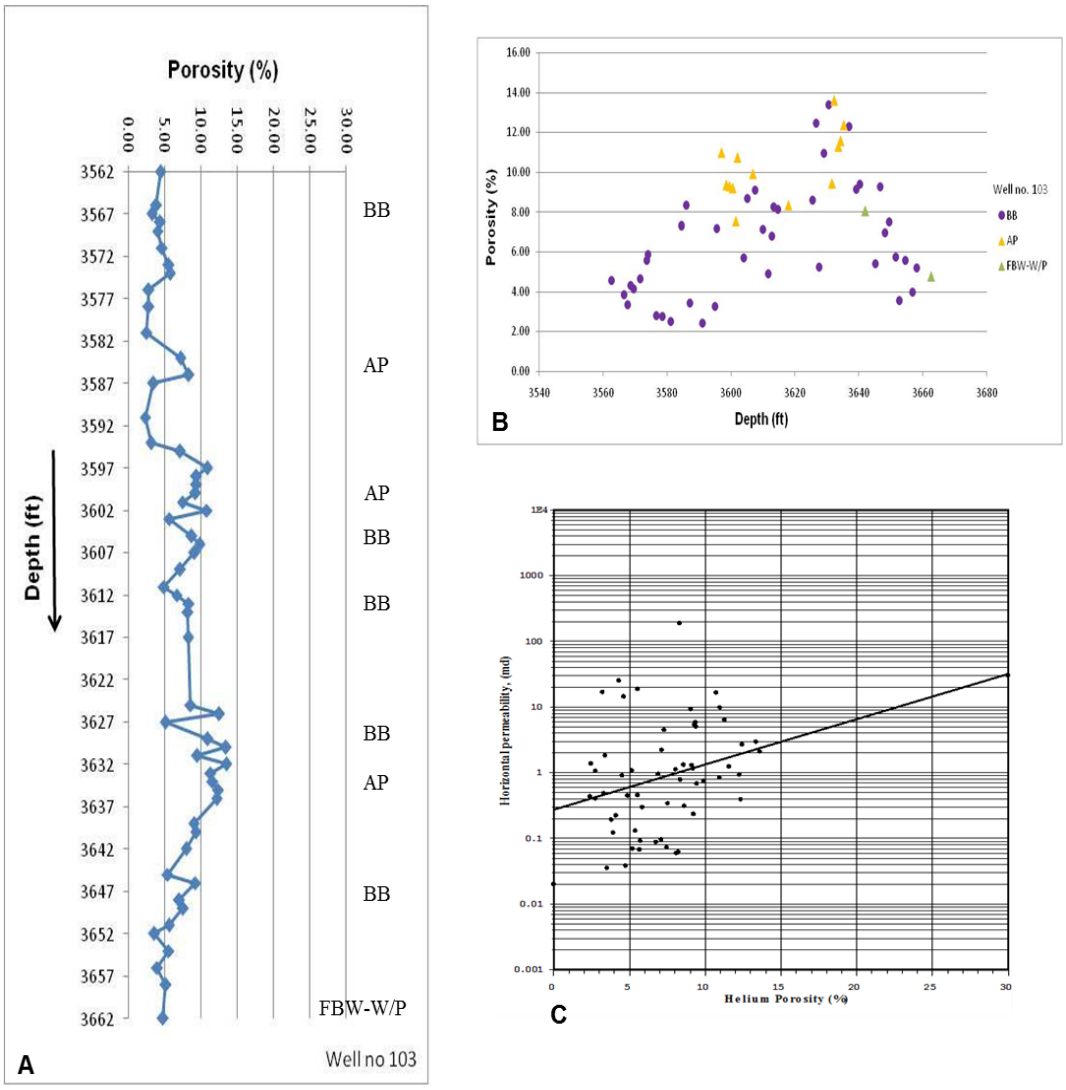

BB = Bioclastic

AP = Algal packstone

FBW-W/P = Foraminiferal bioclastic wackestone-

Figure 4.30 Depth-measured porosity relationship of a cored section of the Mabruk Member in the Dor al Abid Trough in well no. 103 with major facies shown (A); porosity versus depth of the various facies types (B), and the relation between measured porosity and permeability (C).

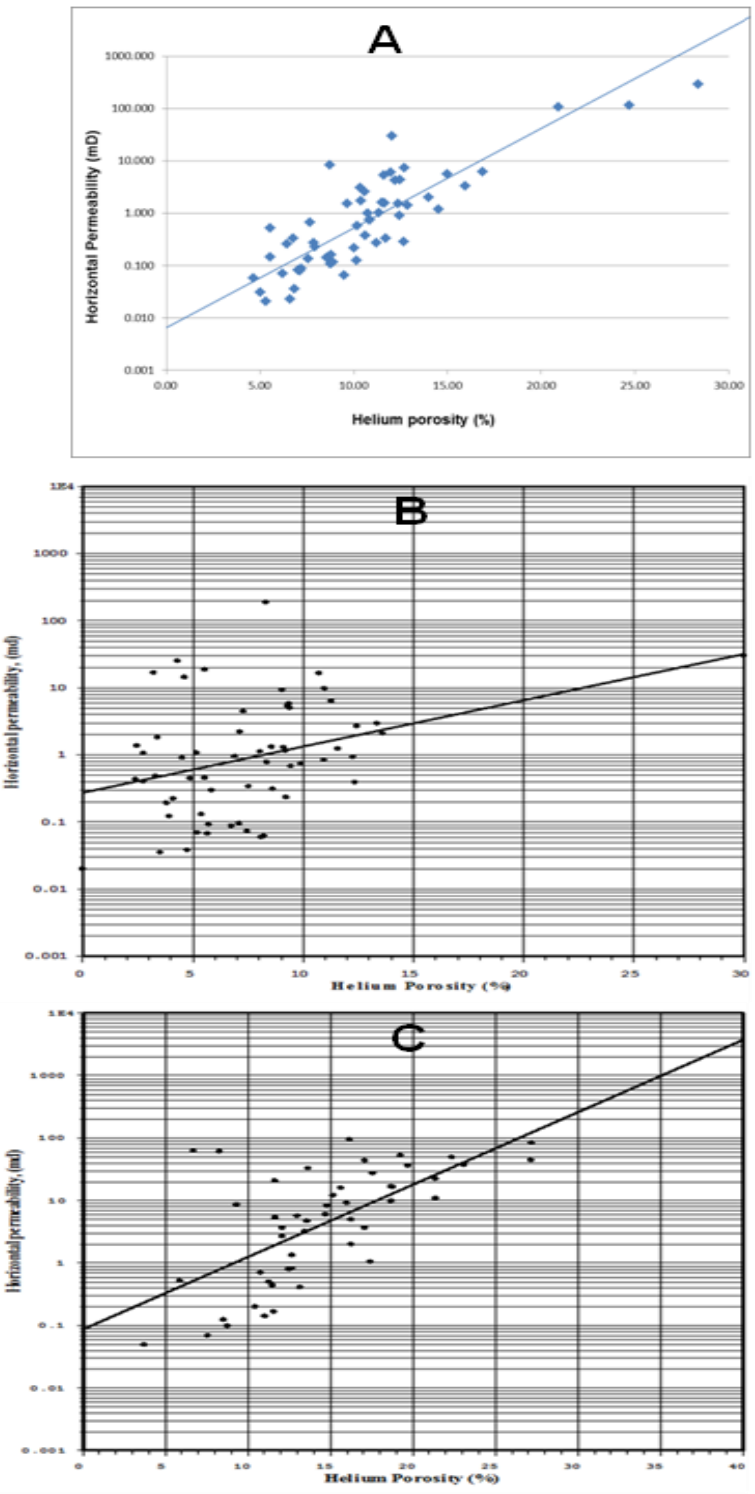

Figure 4.31 Porosity-permeability relationships of the Mabruk Member in wells no. 66 (A), 103 (B), and 105 (C). Note that direct relationships are distinct in A and C, whereas in B is is less well defined.

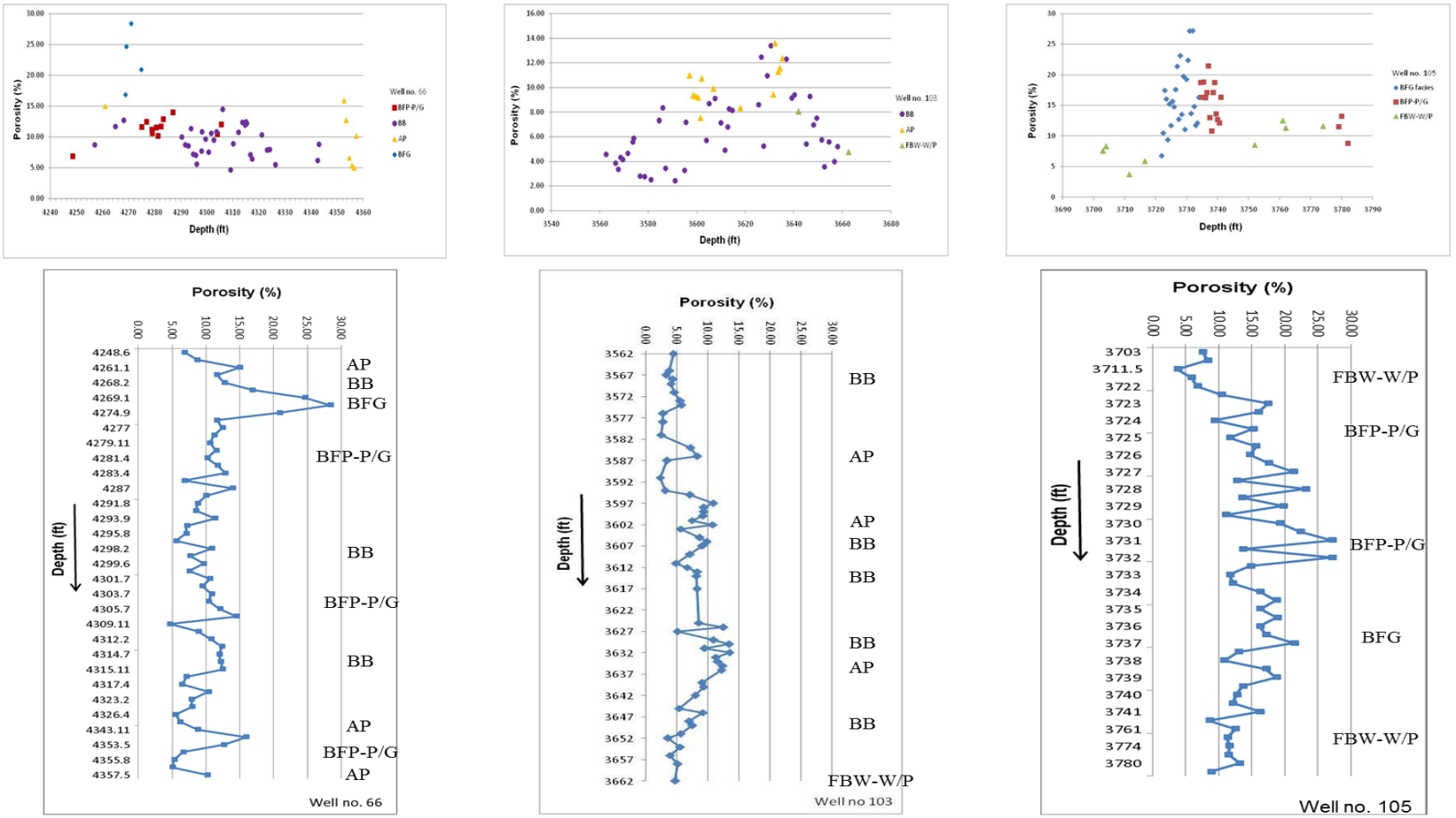

Figure 4. 32 Compiled depth-porosity relationships and the porosity category (value) for each facies as a function of depth in the Mabruk Member in the studied wells.

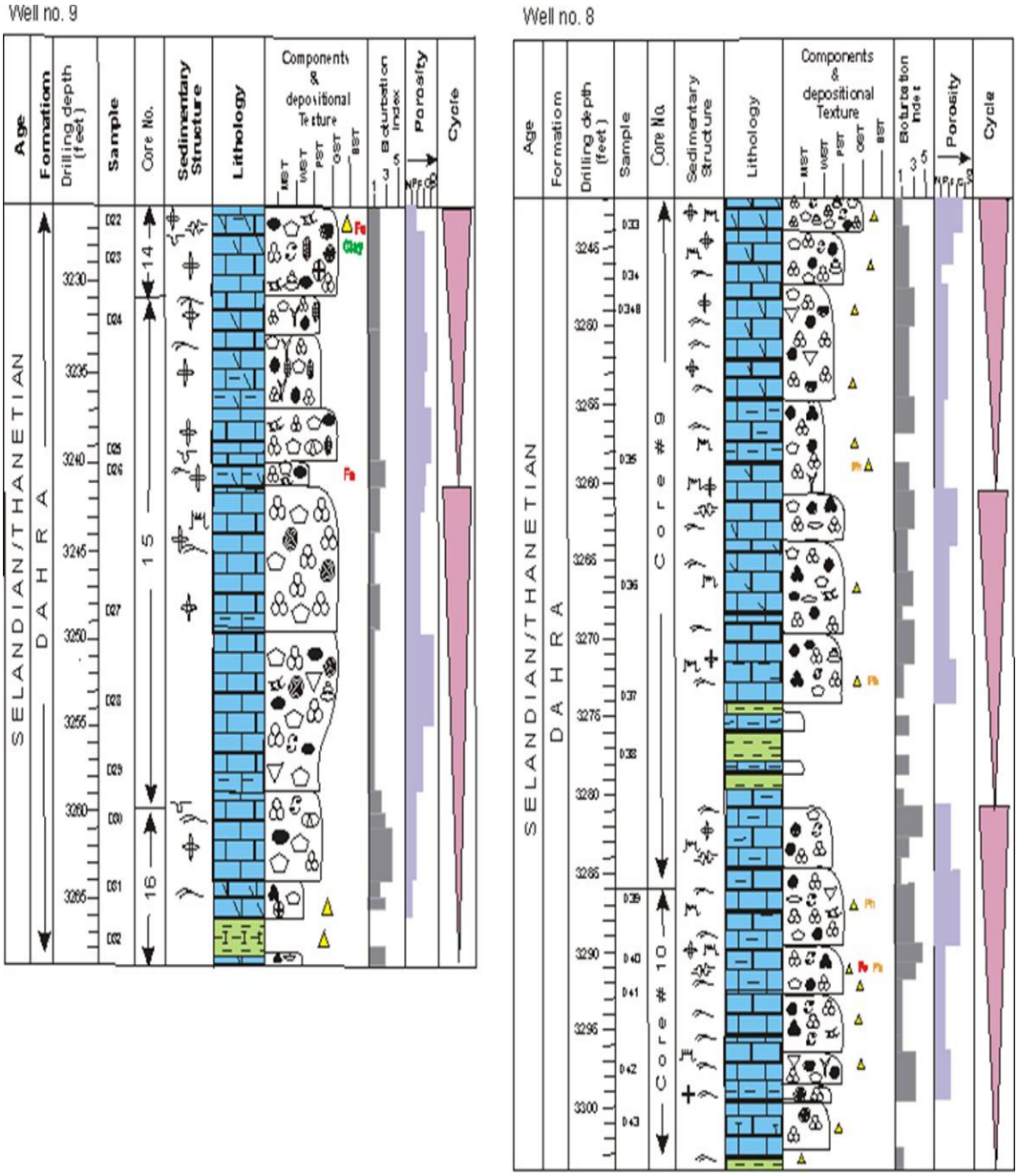

Figure 4.33 Sedimentological core logs showing that depositional texture and the pattern of carbonate cycles, in addition to the diagenesis, all contribute to the porosity evolution in the Dahra Formation on the Dahra Platform. Well no. 8 and Well no. 9.

4.5.2. Summary

The carbonates of the Dahra, Mabruk, Zelten and Harash Formations in the study area, were subject to a ranges of diagenetic processes which affected, in different ways, their composition, mineralogy, pore-throat system, and hence their reservoir potential.

An early diagenetic seafloor process, boring, has been recorded at several intervals inthe studied succession in both Dahra Platform and Dor al Abid Trough sediments, where microborers and macroborers attacked skeletons, carbonate grains and, locally, the micritic substrate within the Dahra, Mabruk and Zelten Formations. Neomorphism is not a widespread diagenetic processes in the studied interval, whereas burrowing is present throughout the studied section, particularly in the Dahra Formation, where it is locally extensive. Most of the burrows are flattened and oriented horizontally with some sub-horizontal or sub-vertical. Swirly structures and irregular to lined burrows have locally been recorded.

Two major phases of dissolution occurred within the Paleocene succession. The first phase, which occurred in the zone of active circulation, caused the dissolution of the original aragonitic and probably high Mg-calcite grains, together with some matrix. The second phase of dissolution, probably a late event, burial and/or telogenetic resulted in the total leaching of probable sulphate minerals (gypsum-anhydrite) and the partial dissolution of medium to coarsely crystalline void-filling dolomite crystals.

Isopachous calcite, equant sparry calcite, locally blocky, and syntaxial overgrowth cements are all documented. The shape and distribution of the isopachous cement along with its occurrence in a relatively less compacted fabric may suggest that it was possibly precipitated in a marine environment. The sparry calcite crystals commonly show a drusy mosaic, particularly where it occurs as a mold-filling cement. The coarse blocky calcite cement is usually ferroan and occurs mainly in the grain-supported facies of the Dahra, Zelten and Harash Formations and in the boundstone facies of the Mabruk Member. Its crystals range in size from less than 250 µm to more than 650 µm and it fills vuggy, moldic, fractures and intergranular porosities. Crescent-shaped cement that concentrated at grain contacts (meniscus cement) has been documented within the bioclastic foraminiferal grainstone microfacies in the upper part of the Dahra Formation. The syntaxial overgrowths occur mainly within the grain-dominated facies in the Dahra, Mabruk, and Zelten, and less commonly, in the Harash Formation.

Two types of dolomite have also been recognised, these are: very finely to medium crystalline (10-80µm) dolomite and medium tocoarsely crystalline (100-600µm) dolomite. The former, which is early diagenetic in origin, replaces the micrite matrix and carbonate grains, and commonly shows loosely packed subhedral to anhedral crystals. The crystal size and its association with peritidal features suggest an early diagenetic origin. The coarser dolomite, which is commonly saddle type, occurs as pore-lining and/or filling cement and shows an inner weakly to non-luminescent and thin outer slightly bright orange zones. Its characteristics suggest precipitation in the late, deep burial mesogenetic stage.

Local closer packing, deformation and fracturing of carbonate grains have been observed in almost all the studied formations in both geological structures. Most of these features probably occurred at shallow burial depths where the Upper Paleocene carbonates were semi-indurated. Dissolution seams that display fairly smooth, undulose seams of insoluble residue and usually pass between and around grains have been observed at many intervals. Large amplitude, small amplitude and swarms of stylolites are also developed at various intervals, especially in the packstone, grainstone and boundstone facies. Minor diagenetic events recognized in the studied succession include formation of authigenic pyrite, glauconite, hematite, phosphate, sulphates and clay minerals.

The $\delta^{18}O$ values recorded in the studied Paleocene succession range from -10.5‰ to +1.15‰, whereas the $\delta^{13}C$ measurements fall in the range -4.87‰ to +3.89‰. In addition to few a negative instances, specific intervals within the Dahra Formation show distinctive positive excursions, particularly in the $\delta^{18}O$, and these suggest a trend to less meteoric alteration and the preservation of marine values in the Dahra West Field, and subaerial exposure in the Dahra East Field.

The general trend of the oxygen isotopic signature of Zelten and Harash Formations is positive, particularly in the Harash Formation. At the Zelten/Harash boundary, the carbon isotope values are probably marine, whereas the oxygen values could indicate the influence of a more arid climate.

The overall isotope values of the Mabruk Member range from $\delta^{18}O$ -5.45‰ to -0.77‰, and $\delta^{13}C$ 0.00‰ to +3.04‰. They commonly followed the sedimentary facies, as the wells with reefal facies have similar isotope values, whereas the wells with lagoonal facies have a completely different trend.

Several occurrences of white, yellow and blue fluorescent fluid inclusions within the Dahra, Zelten and Harash Formations on the Dahra Platform have been documented. The difference in homogenization temperature between the aqueous inclusions and petroleum inclusions is interpreted in terms of two phases of calcite cementation. The highest temperatures of homogenization for aqueous inclusions recorded in the studied samples (90°C) could represent conditions at near maximum burial and thus the palaeogeothermal gradients must have been much higher than at present and/or that the Paleocene sediments were buried to a depth of ~9300 feet for a time. Alternatively, a passage of hydrothermal fluids from deeper parts, low rate of sedimentation and thermal conductivity of the carbonates can also responsible for the high temperature. The fluid inclusions in the Zelten/Harash succession have salinities ranging between 6.6 and 23.1 wt% NaCl; such fluids may represent sea water and/or more likely evaporated sea water in a lagoonal setting or the mixing with subsurface brine.

Macroscopic and microscopic investigations revealed that the porosity types developed in the Selandian/Thanetian succession are dominated by moldic, vuggy, intergranular and intragranular types, with less common fracture and intercrystalline porosity. The best porosity in the studied succession is recorded in the Dahra Formation, whereas the Mabruk Member, Zelten and Harash Formations have relatively lower porosity, particularly the Harash Formation. The best porosity is developed in the bioclastic foraminiferal grainstone, bioclastic foraminiferal packstone-packstone/grainstone facies and, less important, foraminiferal nummulitic packstone,bioclastic boundstone and algal packstone facies. Although there is also no clear relation between the observed porosity and depth within the Selandian/Thanetian succession, it is obvious that almost the same carbonate facies all over the succession have the best reservoir properties.

The relation between porosity and permeability in the Trough wells varies somewhat, i.e. it shows a direct relation and noticeable linear trend in some wells and a less pronounced trend in others. Overall, the porosity evolution in the Selandian/Thanetian succession is controlled by original depositional texture, subsequent diagenesis and the pattern of carbonate cycles.

CHAPTER FIVE: STRATIGRAPHY AND SEQUENCE STRATIGRPHY

5.1. Introduction

Stratigraphy can be considered as the relationship between rocks and time. Stratigraphic analysis of sedimentary basins is critical for stratal correlation and the reconstruction of the geohistory of a basin (Mancini et al., 2005). Stratigraphic analysis based on the transgressive-regressive cycles recorded in a given area can be used to establish a stratigraphic framework for correlation and for interpretation of basin history. These cycles may be related to eustatic sea level changes, but they also are caused by processes of subsidence or uplift, and changes in sediment supply. Cyclicity is a common feature of many limestone successions and occurs in the range of carbonate facies from platform to reef to slope and basin (Flügel, 2004). Up-ward shallowing cycles (parasequences) are the basic building units of thick shallow-water carbonate successions throughout the Phanerozoic and are commonly organized into relatively large-scale depositional sequences (Chen et al., 2001).

As documented in the previous chapters, the Dahra Formation on the Dahra Platform was deposited on a homoclinal carbonate ramp with inner, mid and probably outer ramp facies, each with distinctive sub-facies and microfacies. A similar depositional setting was re-established in Zelten and Harash Formations across the area, with local occurrences of nummulitic packstone instead of bioclastic grainstone in the Dahra Formation and the development of mainly wackestone- packstone. The overall interval of the Mabruk Member in the study area represents deposition of mainly shallow-water carbonates that were bounded by deeper-marine marl and shale, which are accumulated in lagoonal and reefal environments in probably rimmed shelf setting.
Traditionally, the Selandian/Thanetian section in the study area comprises broadly of two thick regressive cycles separated by a relatively thin transgressive cycle. The formers are dominated by carbonate facies, whereas the latter comprises mainly shale and muddy intervals.

The conventional disciplines of process sedimentology and classical stratigraphy are particularly relevant to sequence stratigraphy. Sequence stratigraphy is commonly regarded as only one other type of stratigraphy, which focuses on changes in depositional trends and their correlation across a basin. Owing to the ‘genetic’ nature of the sequence stratigraphic approach, process sedimentology is an important prerequisite

that cannot be separated from, and forms an integral part of sequence stratigraphy (Catuneanu, 2006).

Applying sequence stratigraphic technique in this study has shown that the studied succession composed of several depositional sequences with both transgressive (transgressive systems tracts) and regressive (highstand systems tracts) packages.

This chapter aimed to link the rocks with time through combine sedimentological and stratigrphic features of the studied rocks to get a better understanding of the evolution of the late Paleocene succession through time and places. This is going to be achieved via review and re-examine the stratigraphic evolution of the study area since the base of Tertiary (with an overview of the pre- Teriary section), discuss the transgression-regression cycles, identify cycle types, demonstrate changes in accommodation spac, and distinguish changes in environmental conditions, and hence facies, up through the succession. The overall analysis mainly depends on petrographic investigations and wireline logs, along with core samples and published and un-published reports.

5.2. Stratigraphic evolution of the study area

As stated in Chapter 2 the sedimentary succession in the Sirt Basin ranges in age from Cambro-Ordovician to Recent, and is typical of those developed in a failed rift system. Barr and Weegar (1972) proposed the name Hofra Formation for the silicified quartzose sandstones penetrated in the western Sirt Basin. They assigned it to the Cambro-Ordovician age based on its equivalent to Gargaf Group in western Libya. The Lower Ordovician section has been recorded in north part of the Dahra PLatform, in well A1-10, where it reaches several thousand feet thick, whereas Upper Ordovician strata have been palynologically identifiedin well D1-32 (Wennekers, et al., 1996).

On the other hand, Carboniferous, Permian and Triassic ages have also been assigned to the Hofra Formation in scattered locations in the Sirt Basin, including the Hofra Field, well A1-11. Late Jurassic and Cretaceous strata have also been identified through palynological study conducted by the Sirt Oil Company in 1992. Therefore, the assumption that all the quartzites can be assigned to the Cambro-Ordovician Qarqaf Group is no longer acceptable (Hallett, 2002). The succession in the trough areas, however, commenced with the Hofra Formation, of un-identified age, that overlain by Cretaceous to Tertiary sediments (Fig. 5.1).

A Silurian section has been recognised on the Dahra Platform in well D1-32. Black phyllites have been penetrated in many wells in the western regions of the basin, which are thought to be altered and/or partially silicified Silurian shales (Wennekers, et al., 1996).

According to a CoreLab & LPI report (2008), a Silurian to Devonian succession has been recognised on the northern Dahra Platform, Waddan Platform and in the Zallah Trough, where it overlies Cambro-Ordovician sediments, whereas Permian, Triassic and Early Cretaceous successions are not preserved in these regions. In the Al Hufra Field, on the Dahra Platform, isolated occurrences of rocks dated as Jurassic have been found, presumably as isolated inliers on the Palaeozoic surface (Wennekers, et al., 1996).

Lower Cretaceous siliciclastics (Nubian rocks) have been recorded in the Zallah Trough with around 2000 feet of marine and non-marine strata. The incursion into the deepest rift troughs began in the early Cretaceous, which marks the beginning of the syn-rift phase of basin development. This was followed by a major flooding event in the Cenomanian which extended marine conditions over most of the Sirt Basin, particularly in the trough areas. In the uppermost Cretaceous, subaerial exposure occurred in many parts of the Dahra Platform, which later during the Maastrichtian became submerged.

By the end of the Cretaceous, the structural elements in the study area; namely Zallah and Dor al Abid Troughs and the Dahra Platform, had been almost covered by marine carbonate sediment, with deeper-water facies in low-topographic areas relative to the platforms (distal and proximal facies of the Kalash Limestone Formation).

Upper Cretaceous sediments, which are composed of both siliciclastic and carbonate facies, were extensively deposited across the Sirt Basin and represent a major flooding event and initiation of syn-rift sedimentation. They are well preserved in the western part of the Sirt basin, where they reach up to 400 feet in thickness to the north of the study area and are dominated by limestone and dolomite of an inner-shelf setting. The Upper Cretaceous section has also been recorded by several workers in Zallah Trough.

The start of the Tertiary was associated with a broad sea-level rise and this resulted in the deposition of thick Hagfa Shale in large parts of Zallah and Dor al Abid Troughs, whereas shallower-water carbonates of the Satal Formation, were deposited on the Dahra Platform (Fig. 2.9). During Danian time, a large part of the study area was dominated by the Carbonate Satal Bank, which was locally onlapped by the Hagfa

Shale. The stratigraphic evolution of the entire Paleocene succession, however, is dealt with in the following section below.

Closure of the Tethys Ocean and associated tectonic events affected the pattern of sedimentation during the Eocene in the study area (Hallett, 2002). Eocene rocks conformably overlie Paleocene rocks and are unconformably overlain by Oligocene, Miocene or Holocene sediments. They are relatively thick in topographically lower areas, where it exceeds 5000 feet thick and is composed of a mixture of shales, shallow-water carbonates and evaporites. In the study area, the Eocene rocks started with the Gir Formation, which comprises two members; a lower Facha Dolomite Member and an upper Hon Evaporite Member (Fig. 5.2). The average thickness of the Gir Formation is about 1300 feet over the Paleocene carbonate shelf facies, whereas in the trough areas the thickness exceeds 2900 feet (Abugares, 1996). The same author showed that the members of the Gir Formation represent facies zones; the Facha Member represents a restricted shelf facies, and the Hon Member exhibits an evaporitic facies.

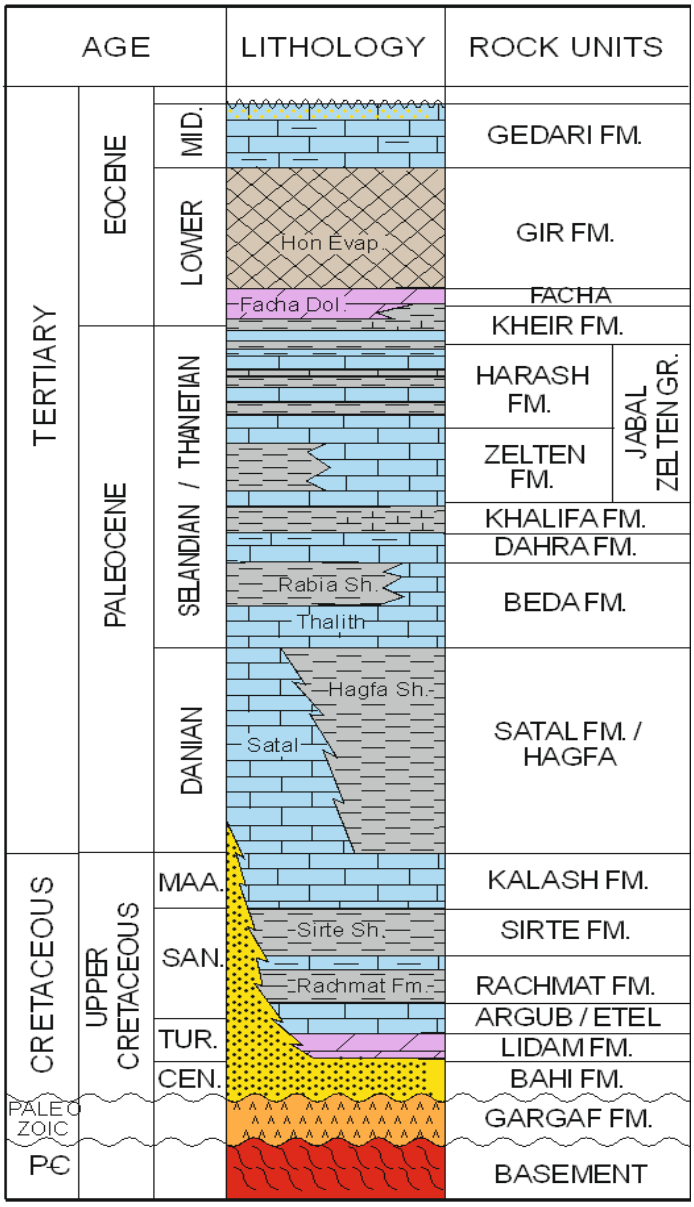

Figure 5.1 Generalized stratigraphic section in the study area of the Sirt Basin (modified from Barr and Weeger, 1972; Montgomery, 1994 and Ahlbrandt, 2001).

5.3. Depositional sequences of the Paleocene Succession

It is well known that variation in eustatic sea-level and subsidence are responsible for the formation of transgressive-regressive sedimentary sequences. Relative sea-level rise commonly leads to a transgression and deepening-upward facies trend (Colombie and Strasser, 2005). However, high sedimentation rate keeping pace with or exceeding the increase in accommodation may result in aggradational or

progradational deposits respectively (Kendall & Schlager, 1981; Handford & Loucks, 1994; Hunt & Tucker, 1995).

For the northeastern Gulf of Mexico, Mancini and Puckett (2002a,b) demonstrated that stratigraphic analysis based on the cyclicity (transgressive-regressive cycles) recorded in succession can be used to establish a stratigraphic framework for correlation and for interpretation of basin history. They used the transgressive-regressive cycles as phases or intervals of a single T-R cycle rather than as a sequence consisting of third-order, or lower, depositional sequences.

In addition to the studied section of the Selandian/Thanetian carbonates, which comprise the Dahra (and Mabruk), Zelten and Harash Formations, the entire Paleocene succession is considered here in terms of transgression/regression episodes, based mainly on sedimentological core description, petrographic investigations, well log characteristics, and available published studies and reports.

5.3.1. Paleocene transgressive-regressive cycles

In the absence of cores, log response may be used to estimate lithology with caveats. Trends in log response therefore may equate with trends in depositional energy, and thus with patterns of sedimentary basin fill. In shallow-marine successions, for example, increasing depositional energy is related directly to decreasing water depth (Milton & Emery, 1996).

The recognition of transgressive-regressive episodes in this study is based on vertical changes of the sedimentary succession and the wireline log responses. In addition to Emery and Myers (1996), the latter have been adapted from Mancini and Puckett (2005) who utilized the following well-log responses to recognize the T-R cycles; a change from higher to lower gamma ray and/or from more to less positive SP log responses identifies the discontinuity in the log records used to separate the transgressive phase from the regressive phase of a T-R cycle. In general, an overall increase in gamma ray or change to more positive SP log response (bell-shaped trend) in a log pattern most probably reflects a transgressive backstepping interval, and an overall decrease in gamma ray or change to more negative SP log response (funnel-shaped trend) in log pattern most likely reflects a regressive prograding interval. A cylindrical gamma ray or SP log pattern is used to recognize a transgressive aggradational interval.

The depositional history of the western part of the Sirt Basin indicates a gradual sea-level rise during the Cenomanian, and overall sedimentation was restricted to the trough areas until the Campanian. The close of the Upper Cretaceous saw the maximum extent of the marine transgression across the Sirt Basin (Wennekers et.al, 1996) and deep-marine conditions resulted in the deposition of the widespread transgressive Sirte Shale of the Campanian Stage.

The overall cycle of shale deposition with intercalation of carbonate reflects alternating transgressive-regressive cycles in the Paleocene succession. Spatially, carbonates are confined to the structurally higher platform areas, while shales occupy the troughs. Several intra-Paleocene unconformities are recognised, which creates a problem in continuous mapping, but played a major role in the trapping of oil and gas (Hallett, 2002).

On the Dahra Platform, the Kalash limestone and Satal Carbonate Formations covered the last remnants of the pre-Sirt relief (Hofra Quartzite or granite highs) (Schröter, 1996). In the trough areas, on the other hand, the Hagfa Shale was predominant. Over large parts of the study area, the shales of the Danian Hagfa Formation change facies laterally to thick shallow-water Danian Upper Satal platform carbonates (Mouzughi, 1991). The Paleocene Epoch, however, commenced with a relatively major phase of subsidence along the marginal areas of the troughs due to movements on basement faults, which resulted in the deposition of a thick carbonate and shale section.

Aboushagur (1991) recognised two transgressive and regressive cycles during the Paleocene and Eocene across much of the Sirt Basin. Two major depositional sequences of the Paleocene succession, consisting of carbonate cycles separated by shale deposits, represent the period between two major transgression events. The lower sequence, which coincides with the Heira Formation in the Dor al Abid Trough extends from the base of Hagfa Shale/ Upper Satal Carbonate to the top of the Khalifa Shale Member. The upper sequence comprises Zelten, Harash and Kheir Formations. It is mainly composed of shelf margin carbonate at the base and grades upwards to planktic foraminifera-bearing marls and siliceous limestones of a deep-water environment (Williams, 1969; Abushagur, 1991 and Bezan 1996) (Fig. 5.2).

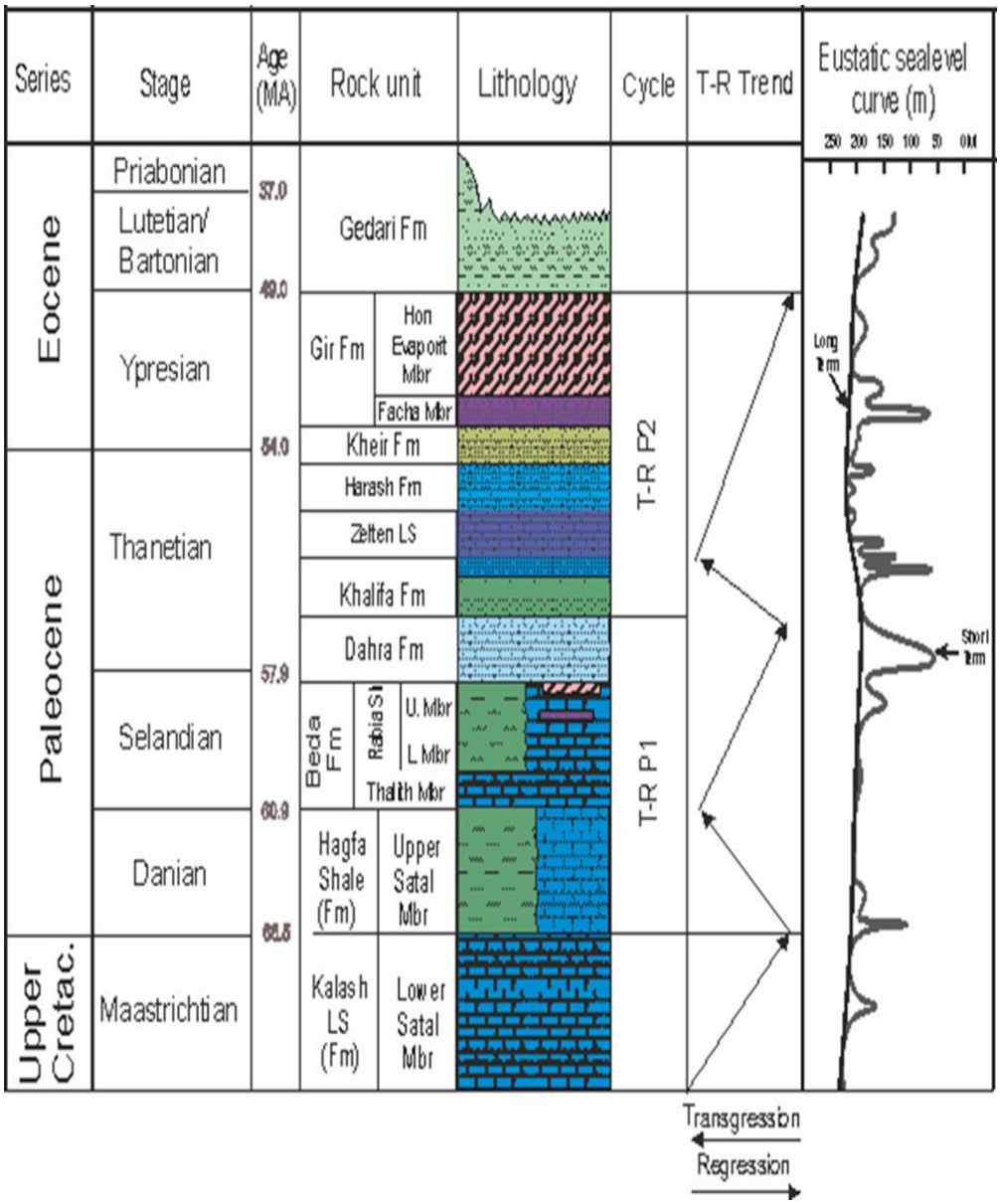

Figure 5.2 Generalized stratigraphic column of the Paleocene succession in the study area, showing possible transgressive-regressive events (After Abushagur, 1991 and Bezan, 1996).

In the eastern part of the Sirt Basin, Mresah (1993) pointed out that the presence of calcareous mudstone facies in the middle and at the top of the Paleocene section helps to define two Paleocene cycles, one in the lower part of the succession and the second in the upper part.

During the Danian time an extensive transgression covered a large part of the Sirt Basin, coming from the north- northwest direction, and resulted in the deposition of thick open marine shale of the Hagfa Formation in the trough areas and carbonate

sediments of the Satal Formation on the stable platforms (Bezan, 1996). The Hagfa Formation is mainly composed of green to greenish grey, sub-fissile to blocky, pyritic and calcareous shale, which grades locally to marl, with thin beds of limestone, particularly in the upper part. A deep-marine environment of deposition is evidenced by common planktic forams. Molluscs, bryozoans and echinoderms are also developed at the top of the formation (Berggren, 1974). In the northern part of the Hagfa (Marada) Trough, to the northeast of the study area, Tmalla (1996) showed that the lower part of the Hagfa Shale is characterised by quite abundant planktic foraminifera (80-90%), indicating water depths in excess of 500 m, on a lower slope or basinal environment (Grimsdale and Van Morkhoven, 1955; Tipsword et al., 1966).

The Upper Satal Limestone Member, of Danian age, consists of massive dolomite with traces of anhydrite and fine-grained limestone, with common benthic forams, algae and molluscs. In the eastern part of the study area it shows a transition from shelf margin to lagoonal and tidal-flat facies. Based on fossil content and sedimentary structures the Satal rocks in the Dahra Field are interpreted to have been deposited in a near-shore, marginal marine environment, within which three shallowing-up sub-environments were recognised: supratidal, intertidal, and subtidal. The latter is subdivided on the bases of faunal content into: shallow marginal, restricted shelf and deep neritic shelf with normal marine fauna (Khoja, 1970). Similar facies and depositional environments were recognised by Kardoes (1991) in the Bahi Field and surrounding areas on the Dahra Platform. According to the well logs used in this study (SP, gamma-ray, resistivity, conductivity, neutron, density and sonic logs), these carbonates were blanketed in many wells by a few metres thick of calcareous shale, which represent the extension of the deep Hagfa shale, i.e. the Satal carbonate bank was onlapped and/or probably drowned by thin interval of deeper marine shale in the study area (Fig. 2.9).

The Beda Formation conformably overlies the Upper Satal Member or the Hagfa Shale Formation. Broadly it consists of skeletal, oolitic and algal packstone/grainstone that passes upward to more restricted shelf facies. In the Dahra Field, on the Dahra Platform, the formation is subdivided into a lower Thalith Limestone Member and an Upper Rabia Shale Member. The Thalith Member, which overlies the Upper Satal Carbonate, is composed of light grey, argillaceous and fossiliferous lime-mudstone with scattered glauconite and pyrite, and subordinate greenish grey, calcareous shale. It

changes locally to a completely shale interval of the Hagfa Formation. The Rabia Shale Member is mainly consisting of dark grey to green calcareous shale with minor light grey, argillaceous limestone beds, i.e. it could represent a later development of the Hagfa Shale Formation.

In the eastern part of the Dahra Platform (Manzila Ridge) the entire Selandian section is represented by carbonates, which comprise part of the thick Paleocene carbonate section (Upper Satal, Beda and Dahra Formations) (Roohi, 1996).

In the northern Zallah and southern Dor al Abid Troughs the Beda Formation is represented by, from older to younger, the Thalith Member, Lower Beda and Upper Beda Members. The lower Beda Member is composed of oolitic and algal limestone passing upward to a lagoonal deposit of the Upper Beda Member. To the south of the study area, the lower Beda Member has been divided by Garea (1996) in to six facies that were deposited in semi-open to restricted shallow lagoon and represented by three shallowing- upward cycles, ranging from 26 to 40 feet in thickness. Abushagur (1991) defined eight shallowing-upward regressive cycles of subtidal, intertidal and supratidal facies, ranging from 7 to 30 feet thick, in the Al Furud Formation (Upper Beda equivalent) in the southern part of the study area (Ghani Field, Zellah Trough).

In the northern part of the Hagfa (Marada) Trough, however, a clear decrease in planktic forams in the uppermost part of the Hagfa Shale and the lower part of the Khalifa Formation (Rabia Shale) is noted by Tmalla (1996), who suggested an apparent decrease in water depth, relative to the proper Hagfa Shale, to a 50-100m deep, middle-shelf environment.

The base of the Thalith Member, which the author believes is part of the Hagfa Shale that onlapped the Satal Carbonate Bank, shows a sharp change from a negative (in Upper Satal Member) to a more positive SP log response, and a sudden decrease in the resistivity curves (Fig. 5.3). This is considered as a transgressive surface, above which the backstepping (deepening-up-trend) was developed. This regional transgression was probably associated with a high rate of carbonate production; it resulted in the deposition of carbonates on the positive areas, whereas in the lower topographic regions a classic transgressive succession (Thalith limestone followed by Rabia shale) was produced. This occupies the lower part of the regressive cycle of Abushagur (1991) and Bezan (1996) (Fig. 5.3).

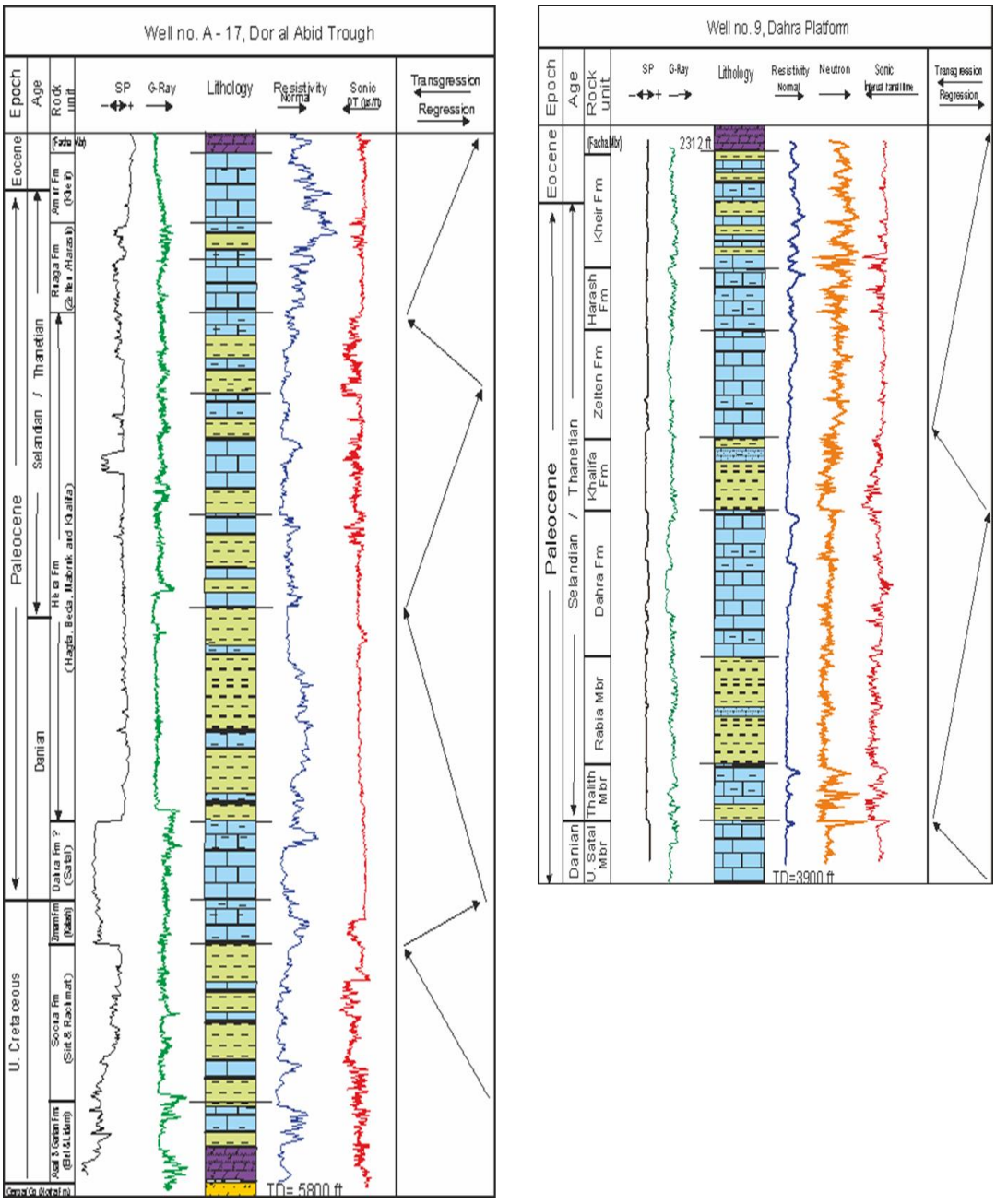

Figure 5.3 Stratigraphy of the Paleocene succession in both Dor al Abid Trough (Mabruk Field) and the Dahra Platform (Dahra Field), showing the log behaviour of the different rock- units and major transgressive/regressive cycles. (The T-R cycles are of Abushagur, 1991 and Bezan, 1996).

In the complex Mabruk area in the Dor al Abid Trough the two above scenarios are present, i.e. Beda carbonate with its two limestone members, and Rabia shale and Thailth limestone Members. A collective name of Hiera Formation, however, is formally used by the operating company in this area for the shales of Hagfa, Beda and Khalifa Formations (Fig. 5.3).

Following the deposition of the Rabia Shale in possibly a deep middle-shelf environment, a sudden change in the sedimentary facies is recorded at the base of the Dahra Formation. It commenced with several feet thick of carbonate that shows a marked change from more to less positive SP log behaviour, distinct increase in resistivity log response and obvious decrease in the sonic log. This could represent a remarkable shallowing which might be associated, at least locally, with subaerial conditions. A gradual shallowing of the sea, however, resulted in the deposition of the Dahra carbonates over large parts of the study area.

On the Dahra Platform the Dahra Formation is mainly composed of light to yellowish grey wackestone to grainstone with local abundance of benthic forams (miliolids and rotaliids), echinoderms, molluscs, ooids and green algae. The interval between the Beda Formation and the lower Dahra Formation is dominated by a regressive cycle (Schröter, 1996).

Major transgression occurred at the end of the Dahra carbonate deposition, and resulted in the deposition of several tens of feet of mainly shale with subordinate limestone of the Khalifa Formation on the platform and in trough areas. The electric logs show a sudden shift to a more positive SP log response, low resistivity behaviour and significant increase in the sonic record (Fig. 5.3). A notable feature is that the log characters of the Rabia shale interval are quite similar to those of the Khalifa Formation, which could support the use of collective name of the Paleocene shales (Hiera Formation).

In the Zallah Trough and in the northernmost part of the study area on the Dahra Platform the Khalifa Formation is represented by grey–green, locally dark grey, chalky, slightly pyritic, and calcareous shale, with a thin limestone unit in the upper part. In the Dahra fields on the Dahra Platform, the formation is characterised by white to light grey argillaceous packstone and lime-mudstone in the upper part, and light to dark grey – green, soft and calcareous shale in the lower part. To the west of the Mabruk field in the Dor al Abid Trough, the Khalifa Formation has similar lithological characteristics; it is composed of wackestone/packstone facies with echinoderm fragments, bryozoans and benthic forams (mainly miliolids and rotaliids) in the upper part, and dark grey, blocky to fissile shale with scattered bioclasts in the lower part. The upper wackestone/packstone interval may represent the onset of the shallowing episode prior to the deposition of the Zelten Formation.

To the north east of the study area (in the Hagfa Trough) the Khalifa Formation is represented almost entirly by shale; a 50-200 m water depth of an outer-middle shelf to deep-marine depositional environment has been suggested for the middle and upper parts of the Khalifa Formation (Tmalla, 1996).

By the end of the Khalifa deposition, however, still-stand conditions probably prevailed allover the Sirt Basin and hence extensive shallow-marine limestone of the Zelten Formation was deposited. Spring and Hansen (1998) demonstrated that the Harash Formation in the Intisar Field, east central Sirt Basin, infills the irregular surface of the Upper Sabil shelf and envelopes the Intisar reefs in the area. They recognised five shallowing-up cycles in the formation.

On the Dahra Platform, the formation consists predominantly of light grey to light yellowish grey packstone, slightly argillaceous and locally dolomitic, with common benthic forams, molluscan shells and echinoderm fragments. Nummulites and bryozoans are locally developed. The base of Zelten Formation on the Dahra Platform is characterized by a remarkable change from positive to more negative SP log response, decrease in gamma ray, slightly higher resistivity, a slight decrease in the sonic log and an important increase in the neutron log behaviour. The fossil contents, characteristic sediments and the electrical log features of the Zelten Limestone suggest an overall regressive interval, with a probable prograding trend upto the top of the Formation (Fig. 5.3).

On the Dahra Platform, these carbonate deposits are overlain by deeper-water facies of mudstone/ wackestone deposits, which probably suggest a major transgression and/or a drowning of the platform. This feature is better defined in well no. 9 in the Dahra West Field, where the basal part of the Harash Formation is characterised by wackestone with planktic forams and the occurrence of pyrite and glauconite. The boundary between the Zelten and Harash Formations shows a sharp change to higher gamma-ray response, slightly lower resistivity, a remarkable increase in the sonic log and a slight decrease in neutron log character (Fig.5.3). These could suggest a transgressive event, above which the deepening up-trend was developed. This is evidenced by the fact that the basal Harash Formation grades upwards to shallower facies of nummulitic wackestone/packstone, which in turn is overlain by grey-dark grey, fissile, calcareous shale intercalated with grey argillaceous calcimicrite and marl of the Kheir Formation.

The Kheir Formation, which marks the end of the Paleocene succession, begins with a slight increase in the gamma-ray log, notable decrease in resistivity behaviour, minor decrease in neutron and significant increase in the sonic record (bell-shaped trend) (Fig. 5.3). The Khier Formation is overlain by the Facha Dolomite Member of the Ypresian Gir Formation (mainly evaporite) all over the basin (Fig. 5.2).

Globally, no scale T–R cycles occurred in the early Danian and the late Selandian. Instead, regional/local tectonic motions, and particularly dynamic topography, overwhelmed any small eustatic fluctuations during these periods of relatively stable global climate and tectonics (Ruban et al. 2012). The same authors pointed out that except for a generally regressive trend occurring in the late Thanetian, no common T–R cycles can be delineated from the study of seven tectonically stable region across the world, which indicates an absence of global-scale T–R cyclicity during the Thanetian (Ruban et al., 2010). They suggest that a warm climate and an absence of major glaciations in the early middle Thanetian, coupled with only slow eustatic change expected from tectonic processes, stabilized Thanetian eustatic sea level. Regional subsidence or uplift possibly generated by mantle flow in the form of dynamic topography, governed transgressions and regressions locally and resulted in an inconsistency between T–R cycles in different parts of the globe.

5.4. Stratal patterns and cycles of Selandian/Thanetian carbonates

In recent decades, there has been much interest in analysing the stacking patterns of high-frequency platform-top carbonate cycles. This analysis has been achieved by the use of accommodation or Fischer plots and supported by various analytical techniques.
The vertical stacking patterns of metre-scale, upward-shallowing cycles, as described by Chen at al., (2001), and others, are mostly controlled by long-term changes in accommodation space; therefore they bridge the gap from individual cycles to the larger-scale depositional sequences, and permit the identification of sequences and their component systems tracts (e.g. Goldhammer et al., 1990, 1993; Osleger and Read, 1991; Elrick, 1995). However, Fischer plots can only give a reliable indication of long-term changes in accommodation if the component metre-scale cycles shallow up to sea-level and in so doing fill all available accommodation space.

5.4.1. Cyclicity in carbonates

Cyclicity is a common feature of many limestone successions and occurs in the range of carbonate facies from platform to reef to slope and basin (Flügel, 2004). In shallow-water carbonates there are small-scale cycles, usually composed of beds, which consist of repetitions of facies. These cycles are on the metre-scale, from 0.5 to 5 metres in thickness, in some cases up to 10 metres. High-frequency cycles also occur in lacustrine and pelagic carbonate successions too; they may all be defined by changes in microfacies, as well as by other features such as grain-size, colour, mineralogy and intensity of bioturbation (Tucker and Garland, 2010). Metre-scale cycles are an important component of sequence stratigraphic analysis and they are commonly referred to as parasequences. Traditionally a typical parasequence exhibits a shallowing-up trend and the parasequence has been defined by Van Wagoner et al., (1988) as a relatively conformable succession of genetically-related beds or bed-sets bounded by marine flooding surfaces and their correlative surfaces.

Spence and Tucker (2007) redefined the parasequence, broadening it out somewhat, to: "A regionally significant metre-scale sedimentary package characterised by a succession of facies that may shallow-up, deepen-up then shallow-up, aggrade, or reflect constant water depth. They stated that in a complete cycle of accommodation change, the nature of the metre-scale cycles may be transgressive and transgressive-regressive, or more typically a simple regressive cycle. Parasequences, therefore, typically shallow-upwards but there may also be a deepening-up and symmetrical (transgressive-regressive) facies arrangement (Tinker, 1998; Spence and Tucker, 2007; Tucker and Garland, 2010).

The bounding surfaces which limit each parasequence are usually a clear, sharp contact. However, this does not mean that it always has to be a flooding surface as described by Wagoner (1988); it can be an exposure horizon or shallower-water facies, but an abrupt change in grain assemblage or facies is typical (Spence and Tucker, 2007). In addition to tectonics, the available accommodation space and sediment supply are the main factors that control the stacking patterns of parasequences (progradational, retrogradational or aggradational). Progradational stacking patterns (regressive cycles) chiefly develop in response to a long-term decrease in accommodation space (third order) and typically are thinning-up cycles. On the other hand, thickening-up cycles

(retrogradational patterns or transgressive) could indicate a long-term increase in accommodation space.

Based on mechanisms that generate cyclic deposits, two types of cycle can be distinguished: Autocycles, which are the result of intrinsic depositional processes (tidal-flat progradation, tidal-island migration, sand-shoal accretion) taking place within the basin itself, and these cycles generally show limited lateral continuity, and random, irregular thicknesses; and Allocycles, that are caused by variation in the external factors affecting sedimentation, such as tectonics, sea-level fluctuations or climatic changes; these cycles typically are laterally extensive and those formed by orbital forcing may show regular thickness stacking patterns (thickening/thinning-up) (Flügel, 2004).

In many instances the interpretation of cyclic carbonates relying on allocyclicity assumes the existence of high-frequency, and low-amplitude, 4^{th} and 5^{th} order sea-level fluctuations that are often explained by changes in the Earth's orbital parameters (Goldhammer et al., 1987; Strasser 1988; Koerschner and Read 1989; Goldhammer et al., 1990; Read et al., 1991). Orbital forcing and resulting sea-level fluctuations are one major control on carbonate platform cycles. Individual shallowing-up cycles are interpreted as the result of 4^{th}-5^{th} order sea-level oscillations. 3^{rd} order cycles (i.e. depositional sequences) in shallow-marine carbonates have been defined by the systematic thickening and thinning of individual cycles over several hundreds of profiles (Flügel, 2004).

In the Sirt Basin, the cyclicity of the Paleocene succession has been studied only briefly in the past and then mainly in terms of larger scale cycles rather than parasequences. Abushagur (1991), as noted earlier, defined eight shallowing-upward regressive cycles of subtidal, intertidal and supratidal facies, ranging from 7 to 30 feet thick, in the Al Furud Formation (Upper Beda equivalent) in the southern part of the study area (Ghani Field, Zellah Trough). To the south of the study area, Garea (1996) divided the lower Beda Member of Selandian age in to six facies that were deposited in semi-open to restricted shallow lagoons, and these defined three shallowing-upward cycles, ranging from 26 to 40 feet in thickness.

Spring and Hansen (1998) studied the Upper Sabil (Zelten Fm equivalent) and Harash Formations in the Intisar Field, east central Sirt Basin, and pointed out that the microfacies analysis of the Upper Sabil Formation shows a generally prograding character. In the Harash Formation they recognised five shallowing-up cycles in core,

with the Harash B cycle comprising a shallowing- and cleaning-up carbonate cycle from outer ramp to mid ramp.

Mresah (1993) recognised two major cycles (without mentioning their thicknesses) in the Paleocene succession in the eastern part of the Sirt Basin; the lower cycle, which he argued, had a clearly defined shallowing-upward trend and a relative increase in energy level, beginning with planktonic foraminiferal mudstone/wackestone grading into dolomitized bioclastic wackestone/packstone through to peloidal bioclastic grainstone, capped with a rotaliid-echinoderm lithofacies. The shallowing-up trend and the relative increase in energy levels seen in the lower cycle are closely repeated and better defined in the upper cycle.

From the above reviews it is clear that the Paleocene succession in the Sirt Basin is dominated by a regressive trend, which is probably the usual rather than the exception as transgressive trends are rare in the geological record and carbonate sedimentation is commonly regressive in nature (Wilson, 1975). The shallowing-up trend of the Late Paleocene succession is likely across the Sirt basin because, with quite similar tectonic subsidence history across the study area (see Chapter 6), platforms would have built up to sea level and above, through progradation of tidal flats and vertical accretion of shallow subtidal sediments (Tucker, 1985).

5.4.2. Cycle types

The studied interval of the Paleocene succession on the Dahra Platform and in the Dor al Abid Trough is mainly composed of shallowing-up cycles, with the possible development of deepening-up cycles particularly in the deeper-water areas. Metre-scale cycle recognition, however, is frequently beyond the resolution of the available data (type and quality of cores, number of thin-sections and quality of wireline logs). On the Dahra Platform, where a ramp model is suggested for the studied formations (the Dahra, Zelten and Harash - see Chapter 3), the inner ramp comprises lagoonal and shallow subtidal cycles (bioclastic shoal), and the mid-outer ramp includes deep subtidal cycles. A carbonate rimmed shelf has been proposed for the Mabruk Member in the Dor al Abid Trough, with reef and back-reef/lagoonal settings.

Since many sedimentological and stratigraphic features (especially the sedimentary structures) are larger than the core diameter, in most cases they could not be recognized with confidence. In fact, apart from bioturbation, most of the sedimentary

structures observed in the cores are compaction-related, such as dissolution seams and stylolites, and almost no depositional structures have been observed. Thus the recognition of cycles and any trends in cycle-type in this study was based mainly on microscopic investigations of facies/microfacies with little information coming from macroscopic observations of core samples and wireline logs.

Trends in cycle-type are somewhat difficult to pick out since the cycle-type depends not only on the ability of carbonate production to pace any change in relative sea-level, but also on the subsidence or consequent uplift of any respective fault blocks (Tucker and Garland, 2010). Although some of the recognized cycles are of the classic type, a shallowing-up facies trend overlain by a flooding event, in many cases it was not easy to recognize the flooding surface, hence the cycle boundary was identified on the basis of a change in faunal type (shallow to open marine) and diversity, along with the lime mud to cement ratio. These limitations make the correlation of an individual cycle between wells difficult, if not impossible; hence correlation has been performed on the basis of cycle packages (parasequence sets).

5.4.2.1. Ramp cycles

5.4.2.1.1. The Dahra Formation

The cored interval of the Dahra Formation is not the same in all the studied wells; in well no. 8 the bottom of the core is at a deeper level than the other wells. Thus, the number of cycles in this particular well is more than the number of cycles in the other wells, although some of the cycles could not be defined precisely and may even be absent in the other wells. Thus the total number of cycles varies from well to well.

The ramp cycles in the Dahra Formation contain the foraminiferal bioclastic wackestone/packstone, bioclastic foraminiferal packstone-packstone/grainstone, dolomitic mudstone, and bioclastic grainstone facies. Back-ramp cycles occur mainly in the lower and upper parts of the Dahra Formation, where they are interrupted at certain levels by mid-outer ramp cycles. The middle part of the Dahra Formation (Dahra C), on the other hand, is mainly occupied by bioclastic shoal cycles of inner- ramp facies. The overall cycle pattern recognized in the Dahra Formation shows predominantly shallowing-up arrangements. In this study the shallowing-up cycles in the Dahra Formation are referred to as type A cycles, whereas the shallowing-up cycles in the Zelten/Harash Formations (next section) are termed type B cycles.

5.4.2.1.1.1. Shallowing-up cycles (type A cycles)

The type A cycles of the Dahra Formation on the Dahra Platform have been subdivided into four sub-types; type A1, type A2, type A3 and type A4 cycles.

The A1type cycles are the most common shallowing-up cycles recognized in the Dahra Formation in the studied wells and are most pronounced in the lower part of the Dahra Formation in well no. 8. In the studied wells, 13 cycles of this type have been recognized with a range in thickness from 7 to 30 feet and an average of 16.8 feet (Table. 5.1 A). The number of individual cycles, types and thickness average and range of cycles in each well can be found in Appendix. 2.

This A1 type of cycle ranges from mid-outer to back-ramp facies, as it shallows from a deep subtidal base to shallow subtidal and lagoonal facies at the top. It commences either with shale and/or marl of deep subtidal facies or with mudstone/wackestone then bioturbated wackestone- with scattered small forams (mainly planktics), echinoid spines, echinoderms and un-identifiable bioclasts which passes upwards into light yellowish grey, bioturbated and slightly dolomitic packstone facies with green algae, bivalve shells, rotaliids and brachiopods (Fig. 5.4). Locally, many of these constituents have been dissolved out and most of the molds are filled with late equant calcite and Fe-rich calcite cements. In a few cases, some dolomite crystals are partly or completely dissolved out (dedolomitization) with the development of desiccation-like cracks.

The type A2 cycles are identified in wells no. 8 and 9 only and their thickness ranges from 6 to 30 feet with an average of 19 feet. Eight cycles of this type have been documented (Table. 5.1A). This type of cycle commonly shallows-up in a normal arrangement from foraminiferal bioclastic wackestone-wackestone/packstone facies, locally bioturbated and argillaceous with a mixture of coral fragments, red algae, planktic forams, echinoderms and benthic forams to very pale orange bioclastic foraminiferal packstone-packstone/grainstone, locally dolomitic with crinoids, molluscan shells, bryozoans and benthic forams (Fig. 5.4). Locally they are capped with light yellowish grey packstone with miliolids, rotaliids, echinoderms, green algae and bivalves, and they show evidence of subaerial exposure (brecciated packstone facies with internal sediment, rootlets and hematite) (Fig. 5. 4).

The type A3 cycles are recognized in the Dahra Formation in wells no. 8, 9 and 10. Nine cycles have been identified in these wells with a thickness range from 14 to 33

feet and an average of 19 feet (Table 5.1A). They seem to be mid-inner ramp facies and normally commence with dolomitic and bioturbated packstone with echinoderm fragments, echinoid spines planktic forams and bivalves through to packstone/grainstone with benthic forams, brachiopods, gastropods and scattered ooids, to grainstone with different types of bioclast including coated grains, ooids, brachiopods, bivalves and green algae (Fig. 5.4). Although they do not show any clear exposure surface, locally but fairly extensive dissolution has occurred in the uppermost part of these cycles, as witnessed by the fair to good porosity.

The type A4 cycles in the Dahra Formation do not show any obvious shallowing-up pattern, despite the fact that they are locally capped either with an important surface or with a flooding surface; they locally display an increase in bioclastic diversity upwards. In view of this they are termed aggradational cycles. They occur in all the studied wells on the Dahra Platform with a total of 9 cycles that range in thickness from 12 to 36 feet and an average of 18.8 feet.

These cycles represent an inner to back ramp setting with deposition mostly in a shallow subtidal realm. In wells no. 7 and 10 they are commonly represented by a package of bioclastic grainstone with a variety of bioclasts, including echinoderms, benthic forams, ooids, coated grains, green algae and bivalve shells (Fig. 5.4). Pyrite and glauconite are locally common. In well no. 8, type A4 cycles exhibit a subtle and minor gradation from packstone/grainstone to grainstone texture with the occurrence of clay in the uppermost part.

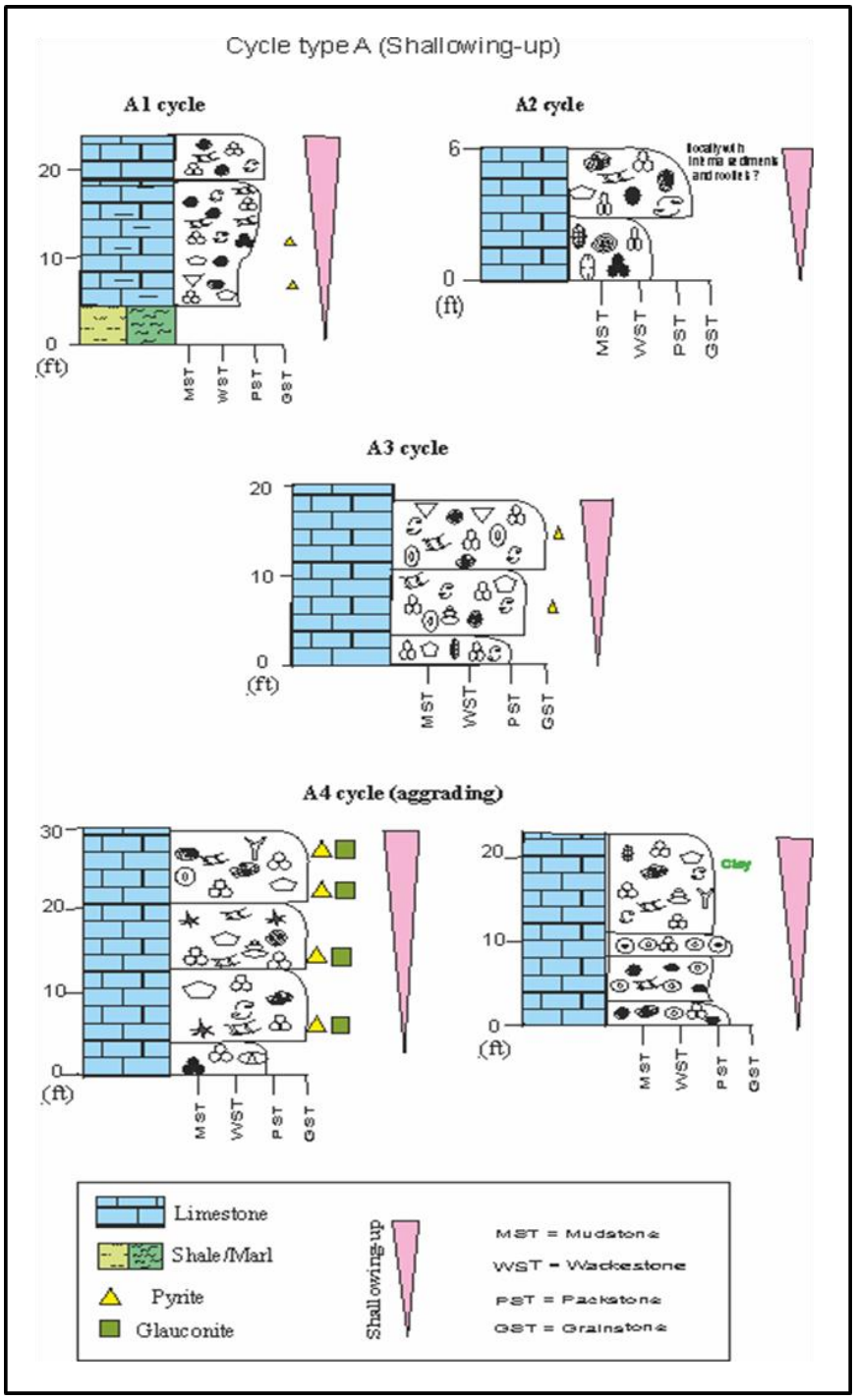

Figure 5.4 Cycle A types recognized in the Dahra Formation on the Dahra Platform

5.4.2.1.2. The Zelten/Harash Formations

The cored section of this interval represents the upper half and lower half of the Zelten and Harash Formations, respectively. As shown in Chapter 3 the lower part of the cored section of the Zelten Formation generally represents middle- to outer- ramp

facies that is characterized mainly by shallowing-up cycles. The upper part of the Zelten Formation includes packages of facies that were deposited in an inner to back ramp setting and mainly comprise shallowing-up cycles. The cored section of the Harash Formation is interpreted as a broad outer to possibly back-ramp setting, also characterized by shallowing-up cycles.

The overall cycle pattern in the Zelten/Harash succession shows chiefly shallowing-up facies arrangements (Fig. 5.5), and its cycles are referred to as type B, which have been subdivided into type B1 and type B2 (Fig. 5.5).

5.4.2.1.2.1. Shallowing-up cycles (type B cycles)

The type B1 cycles are the most common cycles recognized in the Zelten/Harash Formations on the Dahra Platform and they occur in almost all the studied wells. Fifteen cycles of this type have been identified in the studied wells with a thickness range from 7 to 35 feet and an average of 23.3 feet (Table. 5.1B).

They are composed of facies that were deposited in a wide range of depositional settings, from subtidal mid-outer ramp to intertidal lagoonal environments. They exhibit a shallowing-up trend generally with a light grey mudstone or argillaceous mudstone/wackestone at the base passing up through to foraminiferal wackestone/packstone with a pelagic fauna to very pale orange - yellowish grey packstone with more diverse bioclasts. In many cases they are topped with wackestone/packstone with red algae, nummulitic fragments, bryozoans and benthic forams (Fig. 5.5).

Although the type B2 cycles are developed in nearly all the studied wells, they are less common than type B1cycles. They occur in a few intervals in both Zelten and Harash Formations, where they do not exceed 2 cycles in each well.

The type B2 cycles are composed of carbonate facies that signify a shallowing-up pattern from mid-outer ramp to inner-ramp setting. In the studied wells six cycles of this type have been recognized with a range in thickness from 8 to 34 feet and an average of about 23.5 feet (Table 5.1B). They usually commence with light to medium grey planktonic foraminiferal wackestone through to foraminiferal bioclastic wackestone/packstone with brachiopods, echinoderms, echinoid spines and bryozoans; they are then capped with light to yellowish grey, locally bioturbated foraminiferal nummulitic packstone facies (Fig. 5.5).

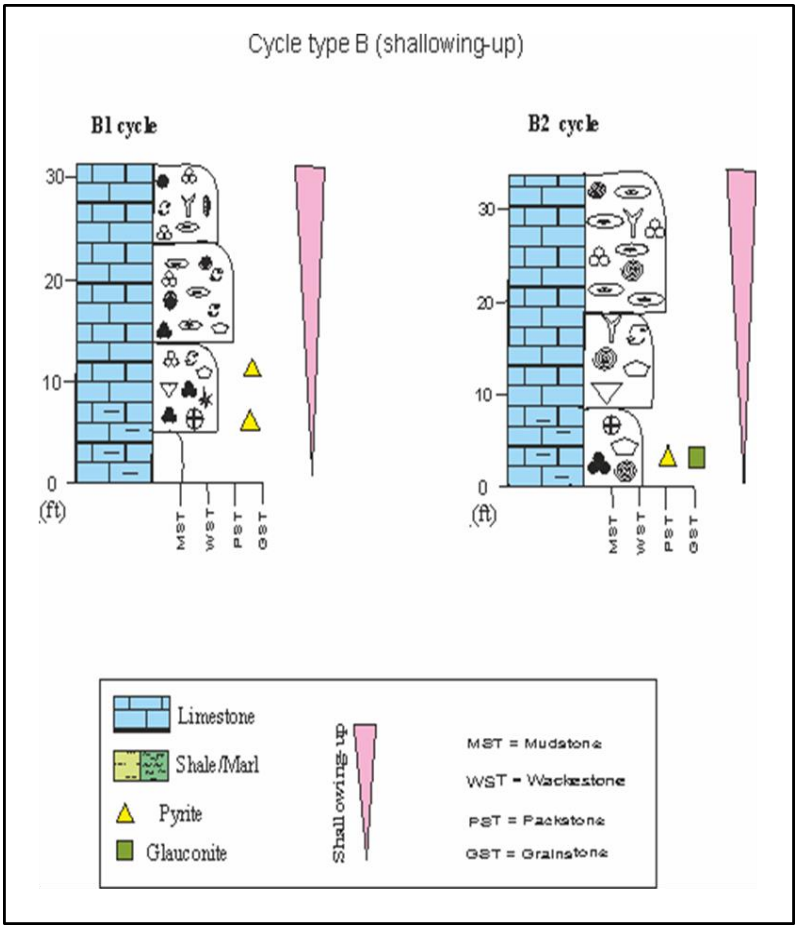

Figure 5.5 Cycle B types defined in the Zelten/Harash interval on the Dahra Platform.

5.4.2.2. Rimmed-shelf cycles

The rimmed carbonate shelf on which the Mabruk Member was deposited comprises lagoonal and reef cycles. The Mabruk Member in western and central parts of the study area is relatively dominated by reef and back-reef facies, whereas the south-eastern area is characterised mainly by the development of lagoonal facies.

5.4.2.2.1. The Mabruk Member

The south-eastern area of the Mabruk Field (well no. 105) is characterised by the common presence of lagoonal facies, where the component grains are dominated by benthic forams, peloids, red algae, echinoderms, green algae and bivalves. The middle interval of the Upper Mabruk Member in the East Central Area is mainly represented by reef and reef-related facies that increase in thickness towards the south east. The central

part of the Mabruk Field in Dor al Abid Trough is dominated locally by algal packstone and bioclastic boundstone facies.

These broad facies constitute several cycles that arranged chiefly in shallowing-upward trends. Six types of shallowing-up cycle have been recognized in the Mabruk Member in the study area; three cycle types are characteristic of a lagoonal environment and three types are diagnostic of reef to back-reef settings. These shallowing-up cycles are referred to as type C cycles.

5.4.2.2.1.1. Shallowing-up cycles (type C cycles)

The C1 type cycles occur at a few intervals in all the studied wells; five cycles of this type have been recognized in the upper and lower Mabruk with a range in thickness from 8 to 23 feet and an average of about 14 feet (Table. 5.1C). They are almost identical to type A1 cycles developed in the Dahra Formation on the Dahra Platform (see Fig. 5.4). This type of cycle shallows from a deep subtidal base to shallow subtidal and lagoonal facies at the top; it commences with shale and/or marl of deep subtidal facies then bioturbated wackestone with scattered planktic and benthic forams which passes upwards into bioturbated packstone/grainstone facies with red algae, benthic forams, echinoderm fragments and bryozoans. Good to very good porosity is recorded in the topmost part of these cycles.

Type C2 cycles are developed in all the studied wells, particularly in well no. 105. Twelve cycles are present in the studied wells with a range of thickness from 5 to 18 feet and an average of 11.5 feet. They are based with shale or lime mudstone-wackestone/ marl with scattered benthic and planktic forams and shell fragments of unidentifiable bioclasts, and pass up to light olive grey, moderately sorted, bioturbated wackestone/packstone with echinoderms, coral fragments, rhodoliths and benthic forams (Fig. 5.6). The C2 cycles are commonly overlain by medium to light grey marl of the overlying cycle.

Type C3 cycles are the most common type of cycle developed in the reef area of the Mabruk Member in the studied wells, in particular well no. 103. Ten cycles are recognized in the studied wells with a range of thickness from 6 to 16 feet and an average of 11.5 feet (Table. 5.1C). They are formed of very light grey to light olive grey, locally mottled, boundstone with corals, rhodolithic algae and scattered bryozoan fragments, which passes up to algal packstone with common red algae, rhodoliths,

bryozoans and echinoid spines. Benthic forams, echinoderms and molluscan shells are scattered throughout (Fig. 5.6). The latter facies is normally dolomitic with the local occurrence of pyrite, hematite, organic material and clay.

Type C4 and C5 are the least common type of cycle in the studied wells; they are represented only by one cycle in wells no. 103 and 66, respectively (Table. 5.1C).
A type C4 cycle is recognized only at the uppermost part of the upper Mabruk Member in well no. 103. Its thickness is around 15 feet and it commences with a thin interval of very pale orange to yellowish grey, poorly sorted coral algal boundstone, and grades upward to a relatively thick interval of highly compacted algal bioclastic boundstone, with common rhodolithic algae, corals and branching coralline red algae. The latter facies is locally dolomitic in its middle interval with the occurrence of hematite and organic matter in its topmost part (Fig. 5.6).

A type C5 cycle is recognised only in well no. 66 with a total thickness of about 16 feet. At the base it is marl, light to medium grey, subfissile to blocky, slightly bioturbated and locally pyritic, with scattered corals fragments, echinoderms and echinoid spines. It passes upward to mottled (very light grey to very pale orange), coarse-grained boundstone with corals and rhodolithic algae (Fig. 5.6). This boundstone facies is locally pyritic with the development of fair to good porosity in its upper part.

A type C6 cycle, which represents the lagoonal setting, occurred at two intervals in well no. 66 and at two intervals in well no. 105. Four cycles have been documented in total with a range in thickness between 8 and 11 feet and an average of 9.7 feet (Table. 5.1C). Although it represents a prograding transition of facies from a probably semi-restricted lagoon to a more restricted lagoonl environment, the subtle transition from packstone/grainstone to packstone facies could suggest an aggradational pattern, similar to that of type A5 cycles in the Dahra Formation. Broadly it shows a mottling, with yellowish brown to very pale orange colour. This type of cycle commences with packstone/grainstone facies with common miliolids, echinoderm fragments, bivalve shells and scattered dasycladacean algae. It passes upward to a well to moderately sorted packstone with abundant green algae and scattered bivalves, rotaliids and echinoderm fragments (Fig. 5.6). On the basis of petrography, the boundary between the packstone/grainstone and packstone facies is characterized commonly by good porosity and the development of pyrite.

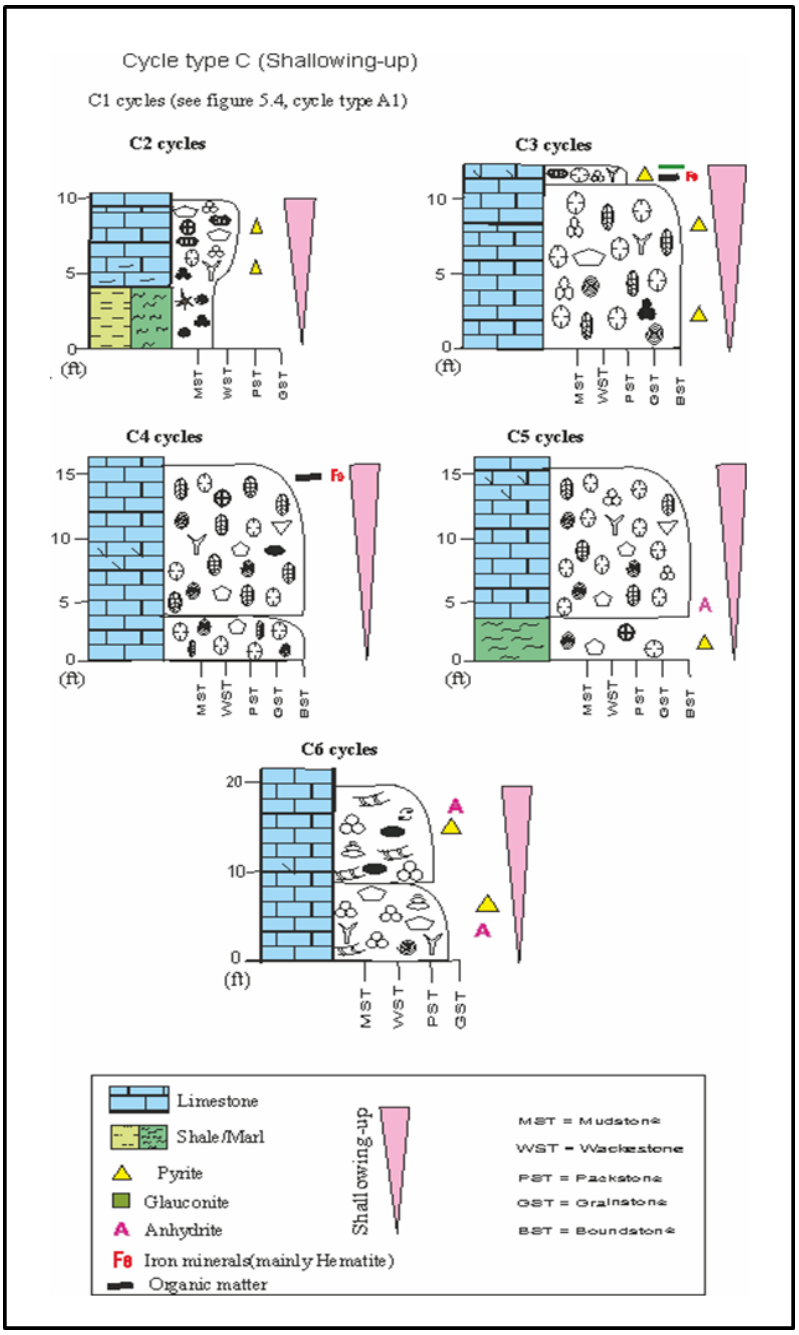

Figure 5.6 Cycle C types defined in the Mabruk Member in the Dor al Abid Trough.

Table 5.1 Summary of cycle types, number, thickness range, and average for the Dahra Formation (A), Zelten and Harash Formations (B), and Mabruk Member (C) in the studied wells.

A

Formation/ Member	Cycle type	Cycle sub-type	No. of cycles	Cycle range (ft)	Average (ft)
Dahra	A	A1	13	7- 30	16.8
″	″	A2	8	6- 30	19
″	″	A3	9	14- 33	19
″	″	A4	9	12- 36	23.6

B

Formation/ Member	Cycle type	Cycle sub-type	No. of cycles	Cycle range (ft)	Average (ft)
Zelten/Harash	B	B1	15	7- 35	23.3
″	″	B2	6	8- 34	23.5

C

Formation/ Member	Cycle type	Cycle sub-type	No. of cycles	Cycle range (ft)	Average (ft)
Mabruk	C	C1	5	8- 23	14
″	″	C2	12	5- 18	11.5
″	″	C3	10	6- 16	11.4
″	″	C4	1	17	17
″	″	C5	1	16	16
″	″	C6	4	8- 11	9.8

5.4.3. Fischer plots

A Fischer diagram shows the thickness of each cycle through a cyclic succession relative to the average cycle thickness (Fig 5.7). Fischer plots are a graphical method to illustrate accommodation changes, and hence depositional sequences, in cyclic platform carbonates, by graphing cumulative departure from mean cycle thickness as a function of time (Fig. 5.7; Goldhammer, 1987; Read and Goldhammer, 1988; Sadler et al., 1993).

Basically the cycle thickness is a reflection of changes in accommodation space, but the relationship is complicated by many factors such as the quasi-periodicity of cycles, variable sedimentation rates, incomplete shallowing to sea-level, and non-linear subsidence rates (Chen et al., 2001).

Fischer Plots are conventionally drawn by cumulative departure from mean cycle thickness against cycle number (Sadler et al., 1993). In this manner, packages of thicker cycles will positively deviate from the mean cycle thickness, and form the rising limbs of the plots, reflecting a long-term increase in accommodation space; whereas packages of thin cycles will be negatively deviated from the average cycle thickness, and form the falling limbs, reflecting a long-term decrease in accommodation space (Fig. 5.7).

Sadler et al., (1993) recommended the use a minimum of 50 cycles in order to separate non-random from random fluctuations. Thus a number of less than 50 cycles may not be sufficiently long for the precise calculation of statistical parameters. Nevertheless, Fischer plots can still be useful in the correlation of platform sections, especially when combined with facies analysis (Tucker and Garland, 2010).

Since the studied Paleocene Formations are not continuous, i.e. separated by gaps of several tens of feet, and the total number of cycles does not reach the number recommended by Sadler et al. (1993), no statistical parameters have been calculated. Furthermore, some recognized cycles are of subtidal facies and do not shallow up to sea-level, and thus their thickness may not reflect accommodation or sea-level changes. Fischer plots are used here to correlate and interpret possible style in cycle thickness patterns in a long term trend. In many cases, it is very difficult to correlate individual cycles from one well to another, but the overall cycle thickness trends are fairly similar.

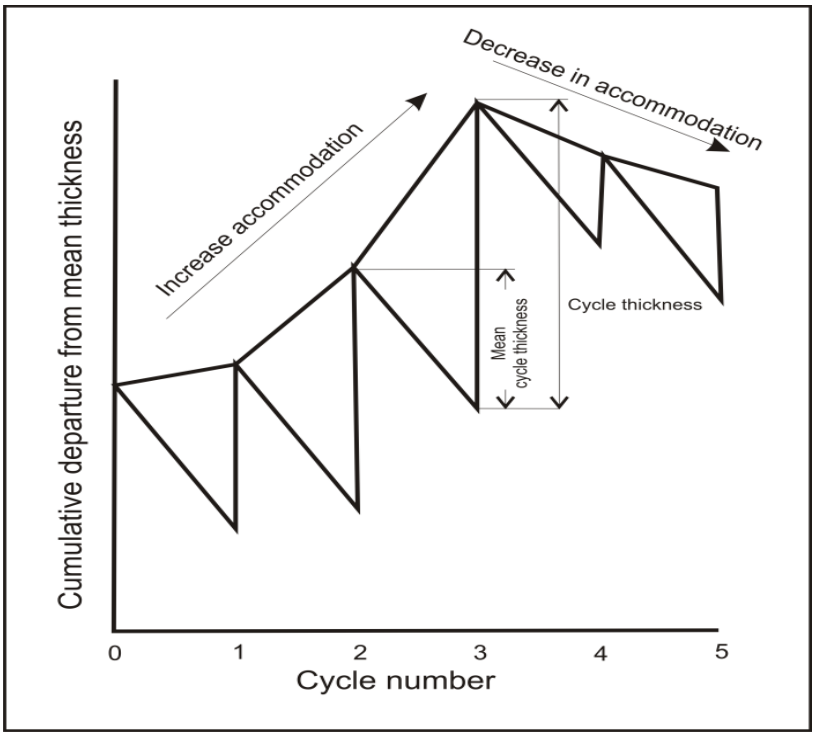

Figure 5.7 Portion of a hypothetical Fischer plot showing changes in accommodation space as a function of cycle number (Husinec et al., 2008).

5.4.3.1. On the Dahra Platform

The Fischer plot for the Dahra Formation in well no. 8 (Dahra East Field) on the Dahra Platform shows 16 cycles with an average thickness of around 18.2ft (Fig. 5.8). In this figure cumulative departure from average cycle thickness of the Dahra Formation in three wells on the Dahra Platform is shown in both cycle number and stratigraphic thickness.

The first half of the plot, which is about 170ft thick, generally shows a positive slope that comprises 7 shallowing-up, coarsening-up and thicker than average cycles. This cound indicate an up-ward increase in accommodation space that was associated with high rate of carbonate production.

The middle part of the plot (cycle no. 8) is characterized by the development of the most conspicuous negative slope of the Fischer plot in this well. Sedimentologically, the interval is composed of dolomitic bioclastic packstone with lithoclasts, peloids, green algae, bryozoans and benthic forams. A breccia-like feature, internal sediments, rootlets and clay minerals are all recorded (Appendix. 1 and Fig. 5. 8). Therefore it is interpreted as exposure surface. This is indicated by, in addition to the above mentioned

features, a sudden landward shift in facies (packstone- packstone/grainstone is overlain by marl and mudstone facies). This negative slope corresponds to the top of the Dahra C and is correlatable to the other wells; it would suggest that the same process was controlling deposition in this part of the Dahra Formation in the study area.

The second half of the plot comprises around 95ft of rather zigzag-like trend with well defined, short negative and positive segments; it is broadly characterized by cycles with lower than average thickness. This could indicate short-term variations in accommodation space and carbonate production that was probably brought about by sea-level fluctuations.

In well no. 9 (Dahra West Field) the Fischer diagram shows 10 cycles with an average thickness of about 19.5ft. A part from significant negative slope that corresponds to top of the Dahra C unit (an exposure surface on top of cycle no. 5), no clear trend can be deduced in the lower part of the plot (Fig. 5.8). The upper part of the diagram shows a pronounced positive slope of two thicker than average cycles, which may suggest an increase in accommodation space during the deposition of this part of the Dahra Formation. Combined Fischer plots of the Dahra Formations in the wells no. 8 and 9 on the Dahra Platform are shown in Figure 5.10.

The Fischer plot for the Dahra Formation in well no. 10 (Dahra West Field) on the Dahra Platform shows 9 cycles with an average thickness of around 21.1ft (Fig. 5.8). The early part of the diagram (~ 50ft) shows negative slope of three shallowing and coarsening-up cycles. This regressive pattern would suggest that accommodation space was decreasing in this part of the Dahra Formation; the overall Dahra Formation is included in the lower Paleocene regressive cycle (Figs. 5.2 and 5.3).

The top of the Dahra C is marked again by a negative slope in the end of the first half of the plot (between cycles 4 and 5). The second part of the plot does not show any clear trend, despite development of remarkable positive slope of thicker than average cycle that fairly correlatable to that of well no. 9.

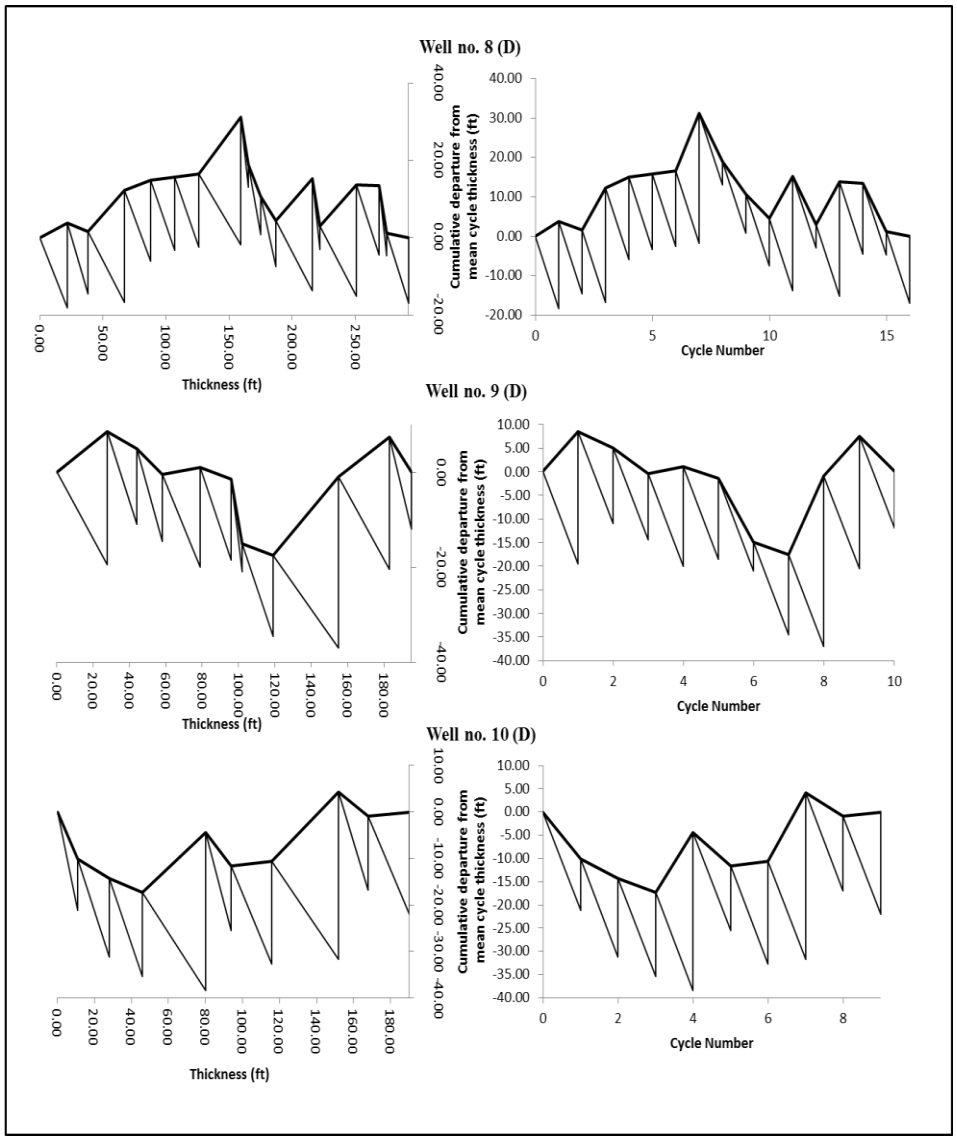

Figure 5.8 Fischer plots of the Dahra Formation in three wells on the Dahra Platform. Cumulative departure from mean cycle thickness (ft) is shown against both cycle number and stratigraphic thickness.

The Fischer diagrams of the Zelten/Harash interval in the Dahra west and east fields show rather similar trends; they broadly exhibit two remarkable positive segments and two short negative slopes. Figure 5.9 below shows the constructed Fischer plots for Zelten and Harash Formations in both fields on the Dahra Platform, in which cumulative departure from mean cycle thickness is shown against cycle number and stratigraphic thickness.

The Fischer diagram of well no. 9 is composed of 9 cycles with an average thickness of about 21.6 ft. The lower half of the plot is dominated by positive slope that

comprises two regressive cycles of rather similar thickness (cycle no. 3&4). This may suggest a remarkable increase in accommodation space was occurred which probably associated with relatively high rate of carbonate production (cycle nos. 3&4). The upper half of the plot displays a similar trend to the lower one. The Harash Formation, however, is represented by only three shallowing-up cycles of mid- inner ramp setting with a total thickness of about 74ft.

In wells no. 7 and 8 (Dahra West and East Fields) the Fischer diagrams show only six shallowing-up cycles with an average thickness of 20.8 and 21ft, respectively. Both plots start, as in well no.9, with a small and steep negative slope of outer – mid ramp cycles (Fig. 5.9). Combined Fischer plots of the Dahra, Zelten and Harash Formations in wells no. 8 and 9 on the Dahra Platform are shown in Figure 5.10.

Apart from the thickness of individual cycles, the overall cycle trend in the studied wells is almost identical, with two prominent positive slopes and two conspicuous negative segments. This strongly indicates a significant variation in accommodation space available during the deposition of the Zelten and Harash Formations, and would suggest that autocyclic processes were involved during the deposition of the upper and lower parts of the Zelten and Harash Formations, respectively.

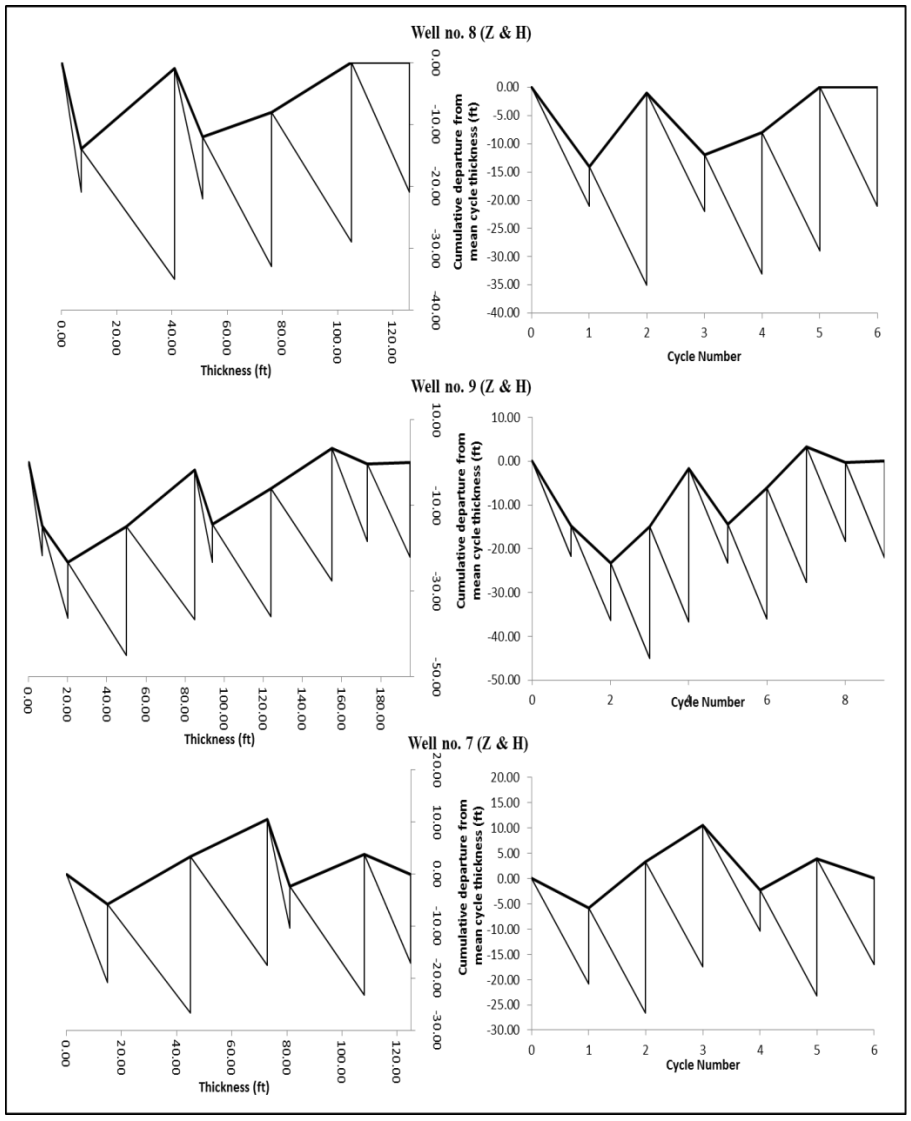

Figure 5.9 Fischer plots of the Zelten and Harash Formations in three wells on the Dahra Platform. Cumulative departure from mean cycle thickness (ft) is shown against both cycle number and stratigraphic thickness.

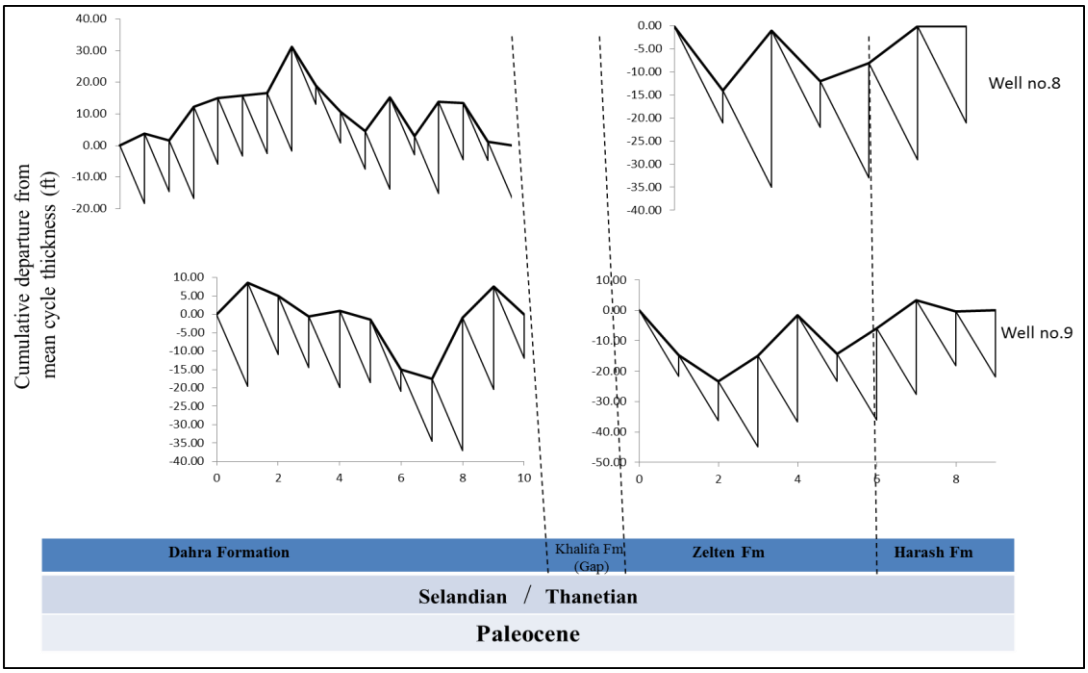

Figure 5.10 Fischer plots of the Dahra, Zelten and Harash Formations in the Dahra east field (well no. 8) and the Dahra west field (well no. 9) on the Dahra Platform.

5.4.3.2. In Dor al Abid Trough

In the Dor al Abid Trough, the overall trend of Fischer plots of the Mabruk Member shows slight consistencies in the reef areas (Fig.5.11). In well no. 66, the cored interval is represented by 10 cycles with an average thickness of 12.8ft. The Fischer plot broadly exhibits two falling limbs and two rising slopes (Fig. 5.11).

The first falling limb consists of three cycles of almost similar thickness. It could suggest that the rate of deposition was possibly low and could not keep pace with the accommodation space available during deposition of this particular interval of the Mabruk Member. This segment is fairly correlatable to the other wells (Fig. 5. 11).

The middle part of the plot, which is about 75ft thick, shows positive trend of four shallowing-up cycles of mainly coral-algal bioclastic boundstone facies, which is interpreted as having been deposited in a proper reef area. Although the lower three cycles in this bundle shallow-up, the overall package displays an aggradational-like pattern (Appendix 1). This may indicate that the rate of carbonate sedimentation was generally equal to the rate of creation of accommodation space. The upper part of the plot is characterized by a prograding transition of facies from a probable semi-restricted

lagoon to a more restricted lagoonal environment. Thus an overall shallowing-up pattern (regressive package) was produced (cycles no. 8 and 9.) just before the advent of major flooding that resulted in the deposition of marl and shale of the Hiera Formation.

The Fischer plot of well no. 103 is composed of 12 shallowing-up cycles with an average thickness of 11.6 ft. The plot shows two major negative slopes; in the early part and close to the end part. The early part of the diagram, which is correlatable to the other wells, is followed by a positive slope of thicker than average cycles that represent the beginning of the proper reef facies. This bundle, which comprises 5 cycles of similar thickness, gives an indication of an aggradational pattern. This bundle is correlatable to the middle part of well no. 66, but with thinner interval.

In well no. 105, the plot represented by 12 shallowing-up cycles with an average thickness of 10.2 ft (Fig. 5.11). The overall diagram, however, shows two positive slopes and four negative slopes. Subsequent to the early negative slope, the diagram shows a fairly steep positive slope of two thicker than average cycles (cycles no. 3 & 4). This could suggest a gradual increase in accommodation space that was probably associated with a relatively high rate of carbonate production. This sudden increase in accommodation space was followed by a gentle negative slope composed of four shallowing-up cycles. This could suggest a low rate of carbonate production during deposition of the lower part of the Upper Mabruk Member.

The second positive slope in the Fischer plot in this well is present close to the top of the diagram (cycle no. 11). This short positive slope is fairly correlatable to the other wells. It could suggest that accommodation space that created during the deposition of cycles no 9 and 10 was possibly filled, before the advent of major flooding that resulted in the deposition of marl and shale of the overlying Hiera Formation.

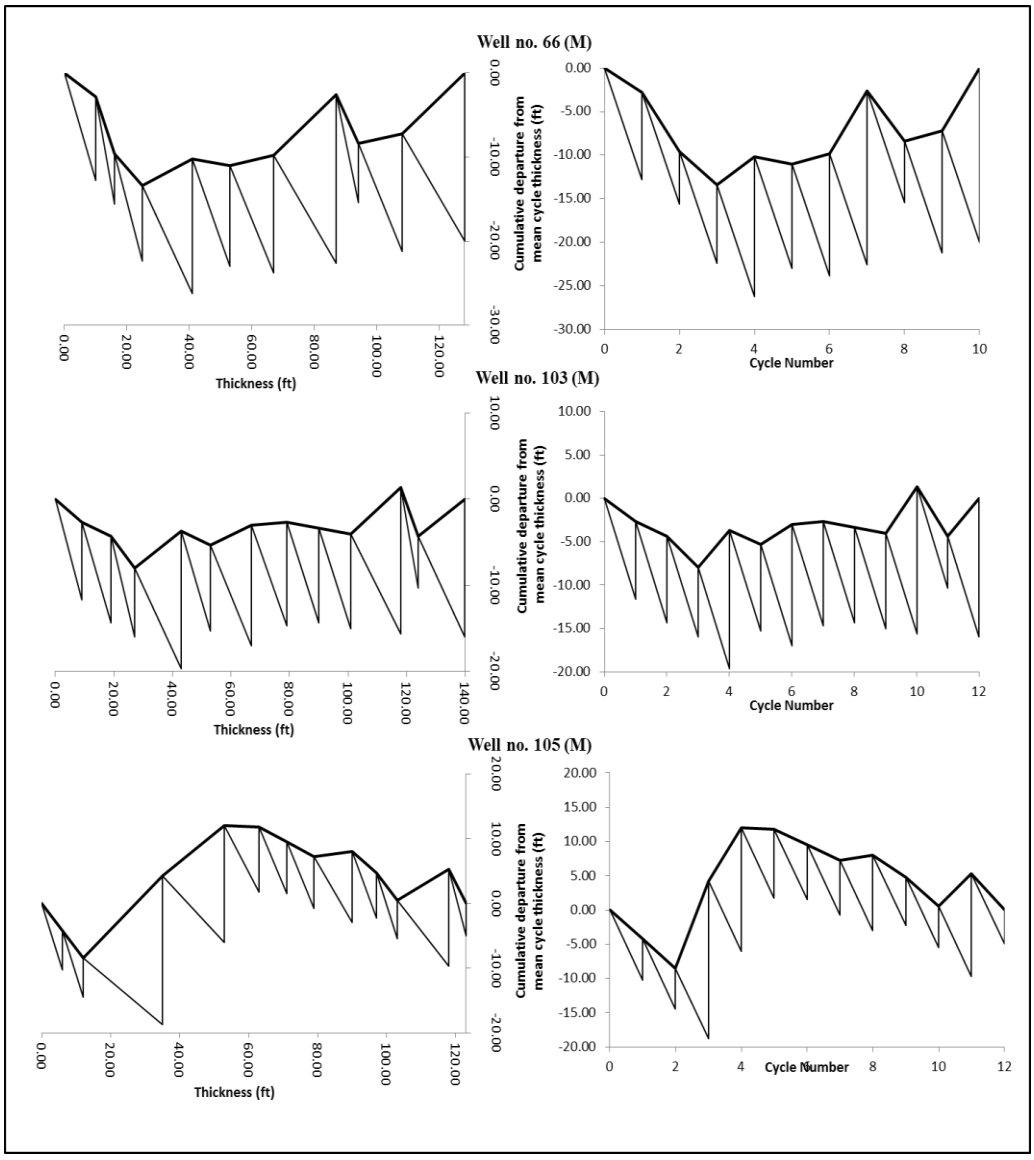

Figure 5.11 Fischer plots of the Mabruk Member of the Heira Formation in three wells in the Dor al Abid Trough. Cumulative departure from mean cycle thickness (ft) is shown against both cycle number and stratigraphic thickness.

5.4.4. Stable Isotope Stratigraphy

In addition to using stable isotopes for the study of the deposition and diagenesis of carbonates, they can also be used in stratigraphic studies, for broad correlations between sections and for detecting changes in environmental conditions up through a succession.

In general, carbon isotope values offer a more reliable approach than oxygen values, since the latter can be strongly affected by diagenesis (Flügel, 2004). When the oxygen isotope data obtained in this study are plotted against carbon (see Figs. 5.12 & 5.13), the oxygen values are seen to extend from quite low negative to high negative values, approaching -10‰. This is most likely a diagenetic trend reflecting the amount of diagenetic alteration, especially the amount of calcite spar cement precipitated and degree of neomorphism / recrystallization during burial (see Tucker & Wright 1990). The carbon data on the other hand are mostly confined to a narrow band (+1 to +4‰), which is typical of marine carbonate, indicating little diagenetic alteration.

The oxygen isotopic signature of carbonate minerals is mainly controlled by temperature of precipitation and the isotopic composition of the fluids; the carbon isotopic signature generally reflects the isotopic composition of the fluid and the source of carbon, which may be derived from bacterial sulphate reduction, fermentation and dissolution of carbonate minerals (Morad et al. 1990; Yoshioka et al. 2003; Ader et al. 2009; Chakraborty et al. 2010).

According to Tucker & Wright (1990), carbon and oxygen stable isotope values for modern carbonate sediments vary between +4‰ and 0‰ and +1‰ to -2‰ respectively, but individual bioclastic grains may vary from this (the so-called 'vital' effect); the average for ancient limestones is normally between 0‰ and +4‰ for $\delta^{13}C$, and -2‰ to -10‰ for $\delta^{18}O$. In this study only whole rock samples were analysed for their isotopic composition, with a preference given to fine-grained facies to avoid too much burial spar cement.

5.4.4.1. On the Dahra Platform (Dahra Fields)

The $\delta^{18}O$ values recorded in the studied Paleocene succession range from +1.15 ‰ to -10.49 ‰, whereas the $\delta^{13}C$ measurements fall in the range +3.89‰ to -4.87‰.
The $\delta^{18}O$ and $\delta^{13}C$ values in the Dahra Formation on the Dahra Platform range between +1.15‰ to -6.83‰ and +3.18‰ and -1.78‰, respectively. In fact the carbon isotope

values of the studied Paleocene succession on the Dahra Platform are all quite similar and do not shows any real significant change up through the section. This suggests that $\delta^{13}C$ seawater did not change significantly through the time of deposition of the Dahra Formation, and that there was little diagenetic alteration of the $\delta^{13}C$ values. The oxygen isotope stratigraphy of the Dahra Formation does show several pronounced shifts.

The basal part of the cored section of the Dahra Formation (3259-3338ft) in the Dahra East Field (well no. 8) shows little change in the isotopic signatures up-section, particularly the carbon values. $\delta^{13}C$ ranges between 2.79‰ to 2.33‰ and $\delta^{18}O$ -2.69‰ to -4.13‰. The interval, which is composed of 4 shallowing-up cycles, is mainly composed of wackestone/packstone facies, slightly dolomitic in the lower part and argillaceous in the upper parts, and is intercalated with shale and marl at two levels. A notable feature is that the upper marly interval shows more positive $\delta^{13}C$ and less negative $\delta^{18}O$ values than the lower shaley interval (2.34‰ to 3.11‰ $\delta^{13}C$ and -2.69‰ to -1.72‰ $\delta^{18}O$). This may indicate that the upper interval was deposited in a slightly lower temperature and/or less warm climate than the upper one.

This is followed by a 19 ft thick interval of pronounced negative excursion of $\delta^{18}O$, from -3.33‰ to -6.83‰ and a minor shift to less positive $\delta^{13}C$, from 2.59‰ to 2.33‰. The most negative shift in the $\delta^{18}O$ in this well occurs at a depth of 3244ft, in a dolomitic bioclastic packstone/grainstone with good intergranular and dissolution porosity. The quite negative $\delta^{18}O$ value and high grade of dissolution could indicate a degree of exposure, and thus the end of a depositional cycle.

Upwards, the interval from 3085-3242ft shows a clear trend with the $\delta^{18}O$ values broadly increasing, apart from slight shifts, to less negative values. The $\delta^{13}C$ values are almost constant with only minor fluctuations (Fig. 5.12). This could indicate a subtle change in sea-water $\delta^{18}O$ or a lower temperature.

The stable isotope trend from 3174-3185ft shows a very slight shift to less positive $\delta^{13}C$ value and to less negative $\delta^{18}O$ value. Sedimentologically the interval is composed of dolomitic bioturbated wackestone/packstone microfacies with intraclasts and/or breccia. Desiccation cracks, rootlets, internal sediment and hematite have been developed in the uppermost part. These features, which correspond with the top of the Dahra C, strongly suggest an important key surface (e.g. sequence boundary and/or ravinement surface), which probably coincides with the global sea-level curve of Haq et al., (1988) that shows a significant sea-level fall during the early Thanetian time.

However, there is no clear event or excursion in the isotope data at this level. Perhaps closer spaced sampling would have revealed an excursion.

The overall trend of the Dahra Formation in well no. 9 is rather similar to that of well no. 8. The lowermost part of the cored section shows a clear shift (upwards) to more negative values of the $\delta^{18}O$, from –0.83‰ to -6.14‰, and a slight change to less positive $\delta^{13}C$ values, 3.11‰ to 2.56‰. Although the isotopic signatures of the lower part of the Dahra Formation in this well do not show any significant changes in $\delta^{18}O$ and $\delta^{13}C$ values, petrographic investigation showed that at least four shallowing-up cycles had developed through it. The quite negative values of the oxygen data (-6.57‰ to -5.04 ‰) could indicate significant diagenetic alteration.

The middle part of the section shows a positive excursion, particularly in $\delta^{18}O$, where the $\delta^{18}O$ values change, upwards, from -4.37‰ to -2.11‰ and the $\delta^{13}C$ values slightly increase from +1.29‰ to +1.58‰. This surface is close to the top of the Dahra C (top of Dahra C to base of Dahra B). The $\delta^{18}O$ pattern could indicate a gradual change in seawater $\delta^{18}O$ or a decrease in temperature; the second could be the result of a climate change or possibly deeper, cooler water.

As noted in Chapter 4, the carbon isotope values of the Zelten and Harash Formations in the Dahra east and west petroleum-fields on the Dahra Platform are fairly similar and confined to a narrow range between +2.22‰ and +3.86‰, which is a bit higher than that of ancient limestones. This may ascribed to an increase in organic carbon, increased organic productivity or fermentation. The overall upward trend of the oxygen isotopic signature is less negative, which is more pronounced in the Harash Formation.

In well no. 8 the Zelten/Harash interval shows a general trend to less negative values for $\delta^{18}O$, and $\delta^{13}C$ values changes little. This may attributed to a change in the oxygen isotope value of seawater.

In well no. 9, the cored section of the Zelten Formation is consisting of six shallowing-up cycles, whereas in the Harash, which is shorter, only three cycles have been recognized. The overall $\delta^{18}O$ shows a slight trend towards more negative values, then to less negative values, and the carbon changes little. The Zelten Formation is more negative than that of the Harash Formation (Fig. 5.12), which possibly could ascribed to the fact that Zelten facies were deposited in warmer shallower water than the Harash facies, or there was a subtle change in $\delta^{18}O$ seawater.

The Zelten/Harash boundary is characterized by an important basin-ward shift in facies (significant deepening) that is more pronounced in well no. 9. Although it is interpreted as a new cycle/parasequence it could indicate a much more important stratigraphic surface or even a drowning unconformity initiating a new sequence. The isotopic signature changes slightly upwards, from 3.16‰ to 3.48‰ and from -4.91‰ to -2.71‰ in well no. 9 (Fig. 5.12). The progressive deepening across the Zelten /Harash Boundary is also indicated by the occurrence of mudstone with planktic forams, echinoid spines, echinoderm fragments and scattered un-differentiated bioclasts. On the basis of sedimentology and isotopic signature this interval may represent one of the deepest portions of the Zelten/Harash section in the area.

Positive $\delta^{13}C$ excursions in a carbonate ramp setting are best explained as intervals dominated by exported carbonate material from shallow areas of the basin (Bádenas et al., 2005). According to the same authors two mechanisms are favoured to explain the shift to more positive $\delta^{13}C$ values: (i) an overall increased rate of sediment supply during long-term sea-level rise, which resulted in an environment that supported the preservation of organic matter in the sediment (Weissert et al., 1998); or (ii) increased sediment supply to the deeper ramp from shallow-ramp regions where surface water productivity is greater.

Eventually, the subtle long-term changes in oxygen recorded in the Zelten/Harash interval could simply be slight changes in sea-water $\delta^{18}O$ or small changes in temperature-climate or depth.

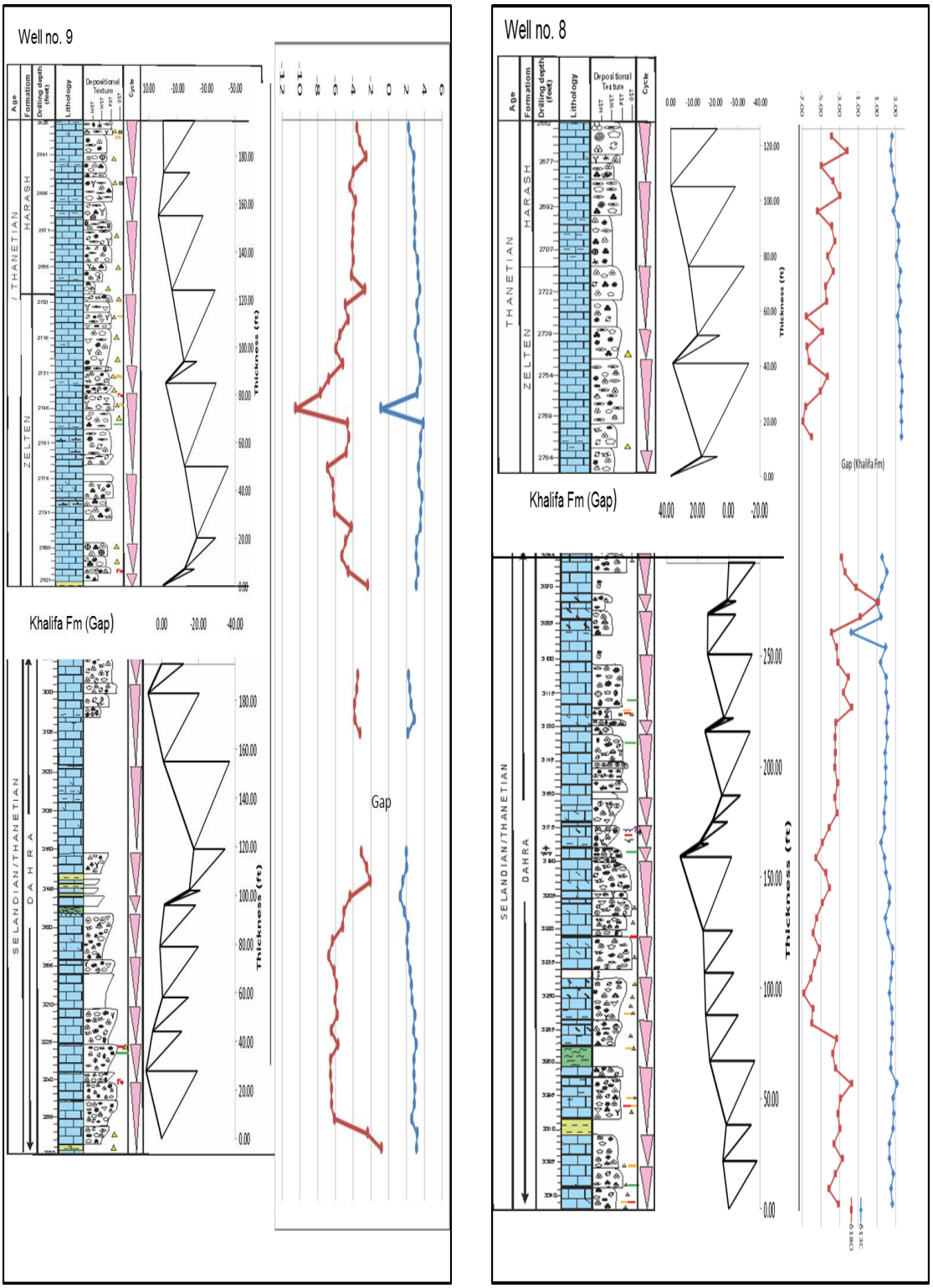

Figure 5.12 Combined stratigraphy, Fischer plots and carbon and oxygen isotope curves of the Dahra, Zelten and Harash Formations in wells no. 9 and 8, Dahra West and East Fields, respectively, the Dahra Platform.

5.4.4.2. In Dor al Abid Trough (Mabruk Field)

As noted earlier, the isotope signatures of the Mabruk Member in the Dor al Abid Trough seem to follow the sedimentary facies, i.e. the wells located in the reef area have very similar isotope values, whereas the well that penetrates lagoonal facies has a completely different trend.

The overall isotope values of the Mabruk Member range from $\delta^{18}O$ - 0.77‰ to -7.68‰ and $\delta^{13}C$ +3.04‰ to -6.31‰. The most obvious real trend in the Mabruk wells is recorded in well no. 105, the east Mabruk area, where oxygen and carbon isotope values are almost identical. The upper part of the lower Mabruk and the lower part of the Upper Mabruk in this well is composed of 5 shallowing-up cycles. There are no significant changes in the isotopic signature, especially in the $\delta^{13}C$ values, which range from 1.01‰ to 3.04 ‰ and oxygen, which range from -4.19‰ to -2.48‰.

A pronounced negative excursion occurs in the middle interval of the Upper Mabruk Member, where the oxygen isotope values become more negative from -2.48‰ to -5.45‰ and the carbon isotope values are depleted from +2.23‰ to +1.63‰ (Fig. 5.13). The whole interval (3722-3743ft) is composed of two shallowing-up cycles and characterized by more negative oxygen isotope values and less positive carbon isotope values. This could reflect a change to higher temperature and/or warmer periods that were possibly brought about by the relative change of sea-level.

Sedimentologically, the interval changes, upwards, from argillaceous limestone/marl through bioclastic grainstone, dolomitic at the top with development of good dissolution porosity and scattered pyrite and anhydrite crystals, to bioclastic foraminiferal packstone/grainstone facies, argillaceous in the uppermost part. This interval therefore represents a progressive shallowing-up succession upto the subsequent flooding (deepening) episode that resulted in the deposition of a thin interval of marl (Fig. 5.13).

The isotope signatures of the Mabruk Member in the reef area (wells no. 66 and 103) do not exhibit any important changes in the $\delta^{18}O$ and $\delta^{13}C$ values; in both wells the values are almost identical, especially the $\delta^{13}C$. The lower interval of the cored sections in this area, however, is dominated by marl and mud-supported facies, whereas the upper interval is characterised by common boundstone and algal packstone facies. The similarity of the isotope signature in both wells may suggest that no significant environmental changes occurred during Mabruk deposition, or, more likely, the changes

were subtle, and consequently the number of samples available in this study could not detect them.

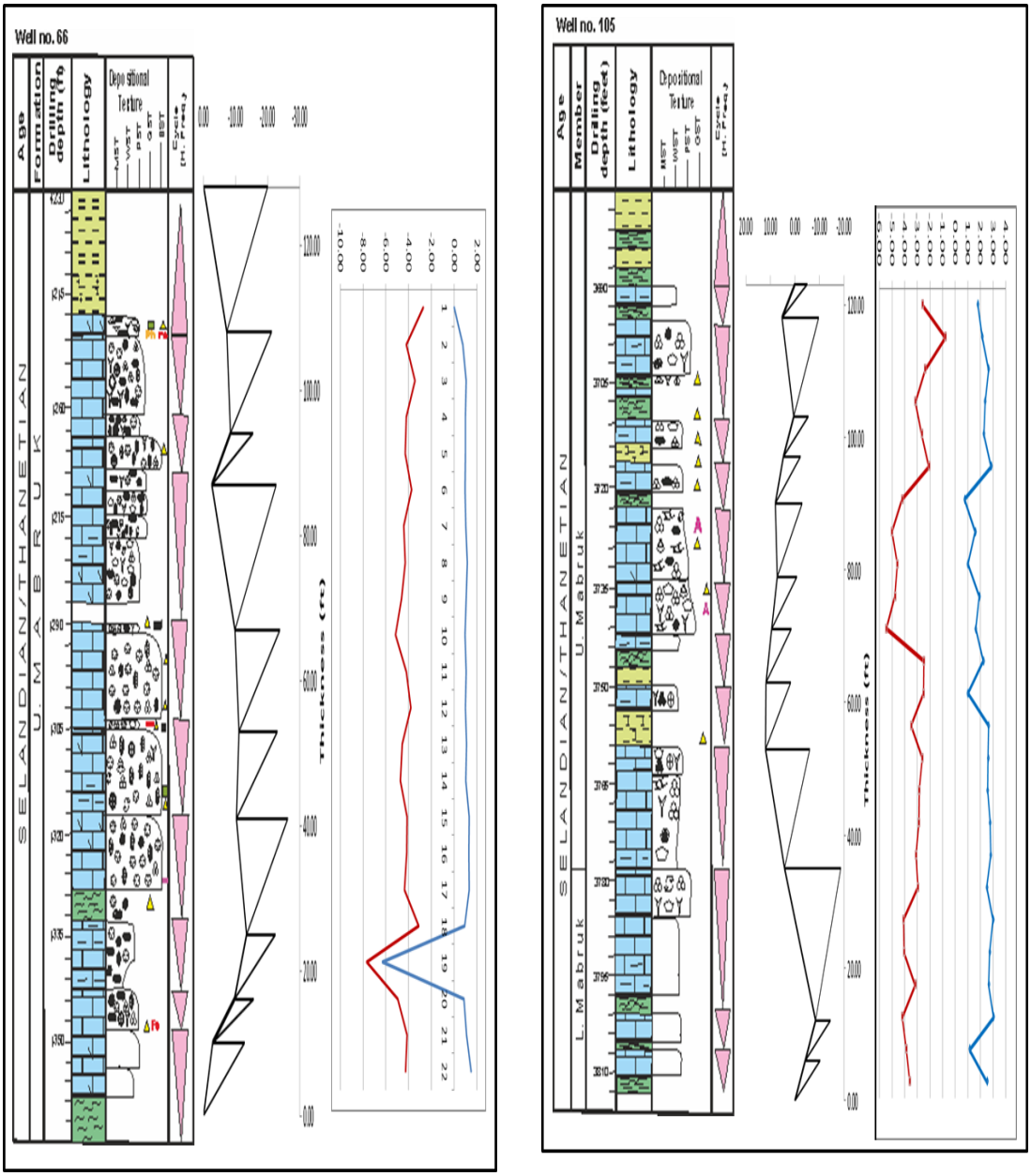

Figure 5.13 Combined stratigraphy, Fischer plots and carbon and oxygen isotope curves of the Mabruk Member (Hiera Formation) in wells no. 66 and 105 in reef area and lagoonal setting, respectively. Mabruk Field, Dor al Abid Trough.

5.4.5. Selandian/Thanetian cycles; duration and mechanism

Estimations of the duration of cycles and cycle-sets are often made to see if there is a relationship with Milankovitch rhythms (Fischer, 1964; Read et al., 1986; Goldhammer et al., 1987, 1990). In his proposal of 50 k.y as an average duration for Triassic peritidal cycles, Fischer divided the total number of cycles in the platform by the approximate age of the platform sequence to derive an average duration for each cycle. Goldhammer et al., (1987) revised the length of Fischer's cycles to 20 k.y. for individual cycles and 100 k.y. for megacycles. Crevello (1991) studied the lower Jurassic carbonates in High Atlas, Morocco, and pointed out that by using an average age for the Liassic stages, individual carbonate cycles ranged in duration from 24 k.y. to 129 k.y. He suggested that the duration of cycles in outer-platform strata are believed to reflect more accurately the lengths of individual sea-level rhythms because a more continuous and complete stratigraphic record is preserved along with better biostratigraphic age control.

Grotzinger (1986) emphasized that the durations of most cycles are of the order of 10^4 years, which is within the range proposed for Milankovitch orbitally-forced perturbations. Later, Goldhammer et al., (1990) assigned metre-scale cycles to 4^{th}–5^{th} order sea-level cycles, which they attributed to Milankovitch orbital rhythms with duration of 20,000 years, 40,000 years and 100,000 years of precession, obliquity and eccentricity, respectively (Tucker and Garland, 2010).

In view of the fact that the studied succession is separated by a number of gaps of several tens of feet, not only between the studied formations but also within them, along with the absence of absolute dating and high-resolution biostratigraphy, no statistical parameters have been calculated, and thus the duration of cycles of the studied section can only be roughly estimated.

The Dahra Formation is considered by some workers to be of Thanetian age and by others as Selandian/Thanetian. The latter is accepted by this author, following the stratigraphic charts that were adapted by CPTL (2001). Using these charts the time span for the Selandian/Thanetian ranges between 60.9 to 54Myr; the Dahra Formation, accordingly is likely to be approximately 2.4Myr in duration, and the Zelten/Harash Formation is about 2.3Myr.

On the Dahra Platform, the most complete section (longest core interval) for the Dahra Formation is in well no. 8, where its cored interval is around 279ft thick. The

total thickness of the Dahra Formation in this well from well logs is 325ft. 16 cycles have been recognized in the core with an average cycle thickness of 18.2ft. A 46ft gap, according to wire-line log interpretation, could represent ~2.5 cycles. Therefore, these give an estimate of cycle duration as 0.129Myr (129kyr), and an average carbonate accumulation rate of 0.141ft (~0.042m) 1000 yr^{-1}. This figure is almost the same as the Upper Cretaceous Bahama platform (0.04m 1000yr^{-1}) (Tucker and Garland, 2010), very close to the value of 0.037m 1000 yr^{-1} for the Devonian succession in Belgium (Tucker and Garland, 2010), and similar to the 0.05 m 1000yr^{-1} for the Barremian-Aptian platform carbonates of France (from Tucker & Wright, 1992).

In the Dor al Abid Trough, and among the studied wells, the thickest cored interval of the Mabruk Member in the Mabruk Field is in well no. 103, which is around 134 ft. Twelve cycles have been identified with an average cycle thickness is 11.6 ft. The total thickness of the Mabruk Member in this particular well is 163ft; A 29ft gap is estimated to comprise around 2.5 cycles, giving a total of 14.5 cycles. Since the Mabruk Member is considered by many authors as a distal equivalent to the Dahra Formation, the cycle duration would be about 0.165Myr (165kyr) and an average sedimentation rate is 0.070ft (~0.021m) 1000 yr^{-1}. This rate of deposition is identical to that of Permian Palmarito Formation in the Venezuelan Andes (Laya-Pereira, 2012) and comparable with the above mentioned ancient carbonate platforms.

It is clear that the rate of deposition of the Dahra Formation on the Dahra Platform is around twice of that of the Mabruk Member in the Dor al Abid Trough, and the cycle duration of the Dahra Formation is much less than that of the Mabruk Member (129kyr and 165kyr). This could support the fact that inner platform area with its various settings (shallow subtidal–peritidal) is normally the site of high carbonate production (carbonate factory) relative to the outer platform areas, and that there was a higher rate of accommodation space development here.

The longest (thickest) cored section of the Zelten/Harash interval on the Dahra Platform has been retrieved in well no. 9, which is 194ft. The time span of this interval, as stated above, is estimated at around 2.3Myr and the total thickness of both formations in this well is about 352ft, i.e. there is around 160ft of the interval is not cored, and the number of identified cycles is 9 with an average cycle thickness is 21.6 ft. Again based on wireline logs and the average cycle thickness, the uncored interval may comprise a further 7.54 cycles, giving a total of 16.5. These give an estimate of cycle duration as

0.140Myr (140kyr) and an average rate of deposition of 0.154ft (~ 0.046m) 1000yr^{-1}, which is again closely comparable with other ancient carbonate platforms. The carbonate accumulation during the deposition of Zelten and Harash Formations on the Dahra Platform is similar to that of the Dahra Formation (0.046 m1000yr^{-1} – as compared to 0.042m1000 yr^{-1}). This indicates a similar rate of creation of accommodation space.

Depositional cyclicity is manifested in carbonate platform sequences throughout the geological record, from Precambrian rocks to Recent sediments (Grotzinger, 1986; Hardie and Shinn, 1986, James, 1989). The origin of metre-scale cyclicity has been discussed by many authors (Lehrmann and Goldhammer, 1999; Schlager, 2005; Bosence et al., 2009), and three mechanisms have been invoked to explain the repetition of shallowing-upward cycles: sedimentary, tectonic and eustatic (Tucker and Garland, 2010). Despite the fact these controlling processes have similar rates of operation, orbital forcing has been the most common explanation for the origin of metre-scale cycles.

The underlying assumption in applying a Milankovitch climate-forcing model to metre-scale cyclicity is that the celestial mechanics of the sun-earth system, which govern the orbital perturbations of the earth, have been in effect since the Precambrian, even though the durations and intensity of these perturbations may have changed through geological time (Crevello, 1991). Thus the Milankovitch model with its three rhythms of precession (~ 20kyr), obliquity (~ 40kyr) and eccentricity (short ~ 100 and long 400kyr) are responsible for variations in the amount of solar irradiance reaching the Earth (Tucker and Garland, 2010).

Interestingly, the extremely approximate cycle durations deduced here for the Paleocene in the Sirt Basin (129, 165, 140kyr) are closest to the short eccentricity rhythm (105kyr), and if missed beats are taken into account (Hardie and Scinn 1986, and Tucker & Garland 2010), one would expect the higher figures obtained.

Since the studied Paleocene succession could not be statistically analysed because of the lack of strong data, and identifying an ordered from disordered, random stacks of cycles, that might have indicated the origin and mechanisms of the Selandian/Thanetian cyclicity, could not be performed. Instead, spatial and temporal variation of the entire Paleocene Epoch in the study area, with emphasis on the

Selandian/Thanetian succession, and the main factors that controlled its facies changes and distribution are dealt with in Chapter 6.

5.5. Sequence stratigraphy of the Late Paleocene succession in the study area

5.5.1. Introduction

Sequence stratigraphy has now developed into a fundamental approach for describing, understanding and predicting the nature of sedimentary units. Over the last three decades, three types of sequence have been defined, with different surfaces chosen for the bounding surfaces: depositional sequences, bounded by subaerial unconformities and their correlative conformities (e.g. Posamentier et al., 1988; Van Wagoner et al., 1988, 1990; Hunt&Tucker, 1992); genetic sequences bounded by unconformable maximum flooding surfaces and their correlative conformities (Galloway, 1989), and transgressive-regressive sequences, bounded by composite surfaces which include the subaerial unconformity and the marine portion of the maximum regressive surface (Embry & Johannessen, 1992).

Following up the early contributions in the application of sequence stratigraphy to carbonate depositional systems, significant progress was made in the early 1990s when the fundamental principles of carbonate sequence stratigraphy, as well as the differences between the clastic and carbonate stratigraphic models, were elucidated (Coniglio and Dix, 1992; James and Kendall, 1992; Jones and Desrochers, 1992; Pratt et al., 1992; Schlager, 1992; Erlich et al., 1993; Hunt and Tucker, 1993; Long, 1993; Loucks and Sarg, 1993; Tucker et al., 1993).

The productivity of pure carbonate systems and their 'carbonate factories,' which dictates the rates of sedimentation (seafloor aggradation and progradation) depends on a number of factors including climate, amount of clastic influx, surface area of the carbonate platform, water depth and illumination, nutrients, salinity and rates of base-level changes (Walker and James, 1992; Schlager, 2005, Catuneanu et al., 2011).

The dominant underlying controls on sedimentary successions are accommodation – the space available for sediment, and sediment supply (Tucker & Garland, 2010). The latter is a key factor to understand sequence stratigraphy, especially in the case of carbonate depositional systems (Catuneanu, 2006). In shelf carbonates sediment production is more often the key, since they are mostly formed and deposited in situ, and this is very much affected by the depositional environment- temperature,

energy levels, nutrients, oxia-anoxia, turbulence, climate, etc.(Tucker and Garland, 2010; Catuneanu et al., 2011).

On carbonate ramps, the most important depositional periods are transgressive and highstand systems tracts. During the former different geometries are produced, depending on the relative rates of sea-level change and carbonate sedimentation; normally backstepping of the shoreline and drowning of the earlier inner-ramp sands take place, or the shoreline retrogrades to produce an onlapping, retrogradational set of parasequences or a transgressive sheet sand. During the HST ramp carbonates aggrade and prograde, downlapping on to the earlier TST sediments (Tucker et al., 1993).

Although the studied core sections are not continuous; separated by several tens of feet gaps, they are discussed and interpreted as a continuous package in terms of a sequence stratigraphic approach, based mainly on the wireline logs in the absence of core samples (thin-sections); an attempt was then made to analyse and interpret the late Paleocene succession on the Dahra Platform as a whole. Because of lack of wirline logs that penetrate the pre Mabruk Member section, only the cored interval of the Mabruk Member in the Dor al Abid Trough is interpreted from sequence stratigraphy perspective.

5.5.2. Sequence stratigraphic analysis

The sequence-stratigraphic analysis of the Late Paleocene succession in the study area depends mainly on petrographic investigations and wireline logs, with less dependence on core samples. Published and un-published reviews and works on structure, stratigraphy, seismic and sedimentology of the study area and surroundings were also used.

In addition to the identified key surfaces, there are probably more subtle surfaces within the Selandian/Thanetian succession that are beyond resolution with the type and volume of data available in this study. In many carbonate successions, particularly the structurally active area with major and minor faulting and folding, it is difficult to use the traditional sequence stratigraphic approach to determine the key surfaces from limited and discontinuous cores, and lack of appropriate seismic sections. In addition, cores and wireline logs can detect only a one-dimensional view of the geology at the well site. All these limitations have played a major role in the sequence stratigraphic analysis, and affected the accuracy of the end results.

On wireline logs, important surfaces, particularly unconformity surfaces are properly correlated to the bottoms and tops of characteristic funnel-shaped and bell-shaped log-stacking patterns. Exposure of the studied succession is indicated locally by the development of rootlets, internal sediments and mineralization phenomena in the Dahra Formation. The depositional sequences in the Late Paleocene succession identified in this study comprise both transgressive systems tracts and highstand systems tracts, whereas lowstand systems tracts were not developed (not recognised) probably due to the low relief ramp setting.

The interval between two successive sequence boundaries recognized in this study, on the Dahra Platform, is regarded as a depositional sequence, and is referred to as Late Paleocene Sequence, regardless of the rock unit it involves or within which it occurs (e.g. LPS1= Late Paleocene Sequence 1, and LPS2 = Late Paleocene Sequence 2). Whereas the depositional sequences recognized in the Mabruk Field in Dor al Abid Trough is referred to as LPSM.

5.5.2.1. Late Paleocene depositional sequences on the Dahra Platform

5.5.2.1.1. Late Paleocene Sequence 1 (LPS1)

As shown in Figures 5.2 and 5.3, the Dahra Formation occupies the upper part of the lower Paleocene regressive cycle defined by Abushagur (1991) and Bezan (1996). A gradual shallowing of the sea resulted in the deposition of the Dahra carbonates over large parts of the study area.

The thickness of this sequence (LPS1) varies from 189ft in well no. 10 to 197ft in well no. 8. It is characterised by a fairly well-defined funnel-shaped wireline-log pattern, especially in its upper part (Sp, gamma-ray, resistivity, sonic and neutron) and thus it is interpreted as upward-shallowing, and locally upward coarsening, a trend which suggest deposition during transgressive and highstand systems tracts (TST&HST).

Following the deposition of the Rabia Shale in possibly a deep middle-shelf environment, a sudden change in the sedimentary facies is recorded at the base of the Dahra Formation. This is interpreted as the lower boundary of the LPS1 that probably corresponds to a global lowering of sea-level during the late Selandian (Fig. 5.2). In the global chart of sea-level of Haq et al., (1988), the eustatic sea-level drops for about 50m (from 201 to 150m) at the late Selandian. A well-defined landward shift in facies from

shale to limestone could support this interpretation. Moreover, the boundary shows a marked change from more to less positive SP log behaviour, a distinct increase in resistivity log response and an obvious decrease in the sonic log (Figs. 5.3 and 5.16).
The upper boundary of this sequence is placed close to the middle part of the Dahra Formation; it coincides with the top of the Dahra C unit (at the boundary between the Dahra B and C), which is correlatable to the other wells. It is characterised in well no. 8 by the development of dolomitic bioturbated wackestone/packstone microfacies with intraclasts and/or breccia. Desiccation cracks, rootlets, internal sediment and hematite have been developed in the uppermost part. The stable isotope trend in this well at this interval shows a very slight shift to less positive $\delta^{13}C$ values and to less negative $\delta^{18}O$ values. It represents the most conspicuous negative slope of the Fischer plot in this well (Figs. 5.8, 5.12 and 5.14).

In well no. 9, however, this upper sequence boundary is marked by significant deepening and consequently a clear shift in depositional environments. The facies below the boundary, bioclastic packstone/grainstone, is characterized by extensive dissolution, and is immediately followed by a significant rise in relative sea-level that resulted in a rapid increase in accommodation space (TST2), and thus two surfaces are possibly amalgamated here (transgressive/ravinement surface and sequence boundary-TS&SB). This is witnessed by the development of a shaly and mud-supported interval of mid-inner ramp facies (Figs. 5.14&5.16).

In well no. 10, this surface exhibits a sudden facies change from bioclastic grainstone below to argillaceous wackestone above, whereas in well no. 7 the cored interval is just few feet below this significant surface. This sequence boundary probably corresponds to a significant fall during the early Thanetian time shown on the global sea-level curve (Fig. 5.2). This eustatic sea-level fall was possibly more than 120m (from about 180 to 55m). Schröter (1996) has probably detected this boundary and used it to separate the Beda Formation from the upper part of the Dahra Formation, when he documented the interval between the Beda Formation and the lower Dahra Formation as being dominated by a regressive cycle. Subsequently, sedimentation took place on a level surface and thickness variations remained uniform into the Eocene.

The transgressive systems tract of the LPS1 (TST1) is only detected in well no. 8, in which this interval is cored, whereas it is not cored in the other wells. In wells no. 9, 10 and 7 the cored interval starts close to the TST/HST boundary (MFS), and

therefore the section represents only the HST. The lowermost part of the LPS1, which is not cored in all the wells, could comprise the lower part of the TST1, including its transgressive surface. In turn, it probably coincides with (according to wireline logs) the lower boundary of LPS1 (Rabia/Dahra contact) (Fig. 5.16).

The TST1 comprises three shallowing-up cycles of A1 type, with a total thickness of 67ft (Fig. 5.14). Although there is no clear deepening-up stacking pattern of these cycles (parasequences/ parasequence set), they do become more argillaceous and thicker-upward. The package shows a very minor change from negative to more positive SP, a small increase in gamma ray, a slightly lower resistivity and a slight decrease in the neutron log (Fig. 5.14). These features might indicate that the rate of carbonate production during deposition of this package could just keep pace with the rising sea-level and hence a retrogradational to fairly aggradational stacking pattern was produced, probably similar to the transgressive aggradational interval of Jurassic and Cretaceous T-R Cycles in Northern Gulf of Mexico (Mancini et al., 2005).

The upper boundary of this TST1 (MFS1) is placed close to the base of the subsequent shallowing–up cycle (lower part of Dahra C), which is composed of about 10 ft of light grey, calcareous and pyritic shale with positive SP, a slight increase in gamma ray, a low resistivity and small decrease in neutron log (Fig.5.14). In fact at this interval the SP for the whole well represents the most positive reading and the resistivity is the lowest.

The subsequent highstand systems tract (HST1) is composed of 3-5 shallowing-up cycles of mainly A3 type together with more restricted facies, which suggest a progradational stacking pattern. Its thickness is generally getting thinner westward as it ranges from 56ft in well no. 7 to 90ft in well no. 8, despite reaching about 96ft in well no. 9. It usually starts with a cycle type A1 followed by an A3 type and capped by an A2 type. Thus, overall shallowing-upward trends are evidenced.

The abundance of grain-supported carbonates in the HST1 with skeletal and non-skeletal grains could indicate a high rate of carbonate production with progradation when sufficient accommodation space was available. A feature worthy of note is that at about mid-way up the HST1 in well no. 7, meniscus calcite cement has been recorded in the upper part of an aggradational parasequence of packstone/grainstone facies (cycle type A4) (Fig. 5.14). This diagenetic feature, which would suggest a degree of exposure, could not be traced in the other wells. This early diagenetic feature alone is not

diagnostic because it may also develop during depositional regression when the system builds into the high supratidal zone, for example on tidal flats (e.g. Halley and Harris, 1979; Gebelein et al., 1980).

As stated earlier, the top of this HST1 (the upper boundary of LPS1) is marked normally by the occurrence of brecciated packstone with indications of meteoric exposure (dissolution and mineralization), but towards the east (well no. 8) it is characterized, along with the brecciated packstone, by the development of rootlets, internal sediments and occurrence of clays (Fig. 5.14). The shallowing-upward trend from shoal/lagoonal to supratidal is indicative of a progradational stacking pattern during the highstand systems tract (Kwon et al., 2006). The above features, particularly those recorded in well no.8, are interpreted to indicate progressive progradation during the late HST1 and a progressive loss in accommodation space up to the sequence boundary.

5.5.2.1.2. Late Paleocene Sequence 2 (LPS2)

The interval between the top of LPS1 and the top of the Dahra Formation is interpreted as occupied by LPS2. Its thickness ranges between 99ft in well no. 9 to 129ft in well no. 8. Although it is not cored in well no. 7, from wireline logs it reaches 118ft. It consists of 5 shallowing-up cycles in wells no. 9 and 10, whereas in well no. 8 it comprises 8 cycles (Fig. 5.14) and almost all types of cycle (A1-A4) are documented in this sequence.

Its lower boundary is the upper boundary of the LPS1, whereas its upper contact is placed at the top of the Dahra Formation. The topmost part of the Dahra Formation (10-15ft thick) is not cored in wells no. 9 and 10.

In fact, apart from its lower and upper boundaries, no important surfaces have been recognized within this sequence (TS or MFS) with confidence. The lowermost part of this sequence is characterized by the development of a shale and mud-supported interval in almost all the studied wells. In wells no. 8 and 10, however, this muddy interval is overalain by bioturbated packstone facies in the top parts of a type A1 cycle with dissolution features, borings, iron stains and development of features similar to desiccation cracks. These phenomena could indicate an important key surface and/or a parasequence boundary. On the other hand, the muddy interval overlying the upper boundary of the LPS1 may represent a transgressive systems tract (TST2), with its

maximum flooding surface (MFS2) placed within the thin shale/mudstone beds that immediately overlie the Dahra B unit (Fig. 5.14).

The Dahra B unit itself, which occupies the lower part of the LPS2, could represent a significant interval as well; it exhibits a very well-defined funnel-shaped trend and shows a notable change from more positive to more negative SP log, a reduction in gamma ray and a substantial increase in resistivity. Furthermore, an aggradational pattern on the scale of a single parasequence has been documented in the upper part of the Dahra B in wells no. 8 and 10. Therefore, the Dahra B could denote the upper part of the transgressive systems tract (late TST2) that was followed by the topmost part of this sequence (HST2), up to the contact with the Khalifa Formation (Figs. 5.14 and 5.16).

5.5.2.1.3. Late Paleocene Sequence 3 (LPS3)

The lower boundary of this sequence coincides with the top of the Dahra Formation, whereas its upper boundary is not clearly identified, although the Zelten/Harash contact is the most probable candidate boundary for it. Its thickness varies from 347ft in well no. 8 to 393ft in well no. 7.

A major transgression occurred at the end of Dahra carbonate deposition, and resulted in the deposition of mainly shale with subordinate limestone of the Khalifa Formation on the platform and in trough areas. The lower boundary of the LPS3 (the contact between the Dahra and overlying Khalifa Formations) is characterized by a sudden shift to a more positive SP log response, low resistivity behaviour and a significant increase in the sonic record (a bell-shaped trend), which confirm the transgressive (major flooding) event. On the other hand, petrographic investigation showed that the uppermost part of the Dahra Formation, across the area, is characterized by the development of bioclastic foraminiferal packstone/grainstone facies, locally dolomitic with fair to good moldic and vuggy porosity and the local occurrence of glauconite and pyrite. Therefore, petrographic features and electric logs characters suggest proximity to an exposure surface associated with (or immediately followed by) major flooding and hence an amalgamated boundary is indicated (SB and TS) (Fig. 5.16).

Only one important surface has been recognized within this sequence; it occurs in the lower part of the Zelten Formation and is charaterised by a positive SP response,

low resistivity curve, high gamma and high sonic log. It is interpreted as MFS3 that separates the TST3 below and HST3 above; the TST3 comprises the entire Khalifa Formation and the lower part of the Zelten, which is argillaceous limestone intercalated with thin shale intervals of mid-outer ramp, whereas the upper part of the Zelten Formation, which comprises six shallowing-up cycles of inner to back-ramp facies, belongs to HST3 (Fig. 5.15).

The upper boundary of the LPS3 is placed roughly at the top of the Zelten Formation. Although no clear evidence of subaerial exposure at the top of the Zelten Formation is detected, the boundary between Zelten and Harash Formations is marked by a facies change from bioclastic foraminiferal packstone/grainstone to mudstone/wackestone deposits with planktic forams and the local ocurrence of pyrite and glauconite. $\delta^{18}O$ shows a slight shift to more negative isotopic signatures, and well-log behaviour exhibits an overall bell-shaped trend, suggesting a major flooding event (Figs. 5.15 and 5.16).

Spring and Hansen (1998) studied the Upper Sabil (Zelten Fm equivalent) and the Harash Formations in the eastern part of the Sirt Basin and demonstrated that the transition between those two formations reflects a sea-level fall followed, after a period of local lowstand deposition, by a marine transgression. They argued that meteoric dissolution and cements observed from core data and reworked materials of Late Cretaceous and Paleocene within the lower part of the Harash, suggest subaerial exposure at the top of Upper Sabil carbonates.

5. 5. 2. 1. 4. Late Paleocene Sequence 4 (LPS4)

The base of this sequence is placed at the Zelten/Harash boundary and its upper boundary is probably located at the base of the Facha Dolomite Member of the Jir Formation. Its total thickness ranges from 380 ft in well no. 8 (Dahra East Field) to 645ft in well no. 9 (Dahra West Field).

The cored section of the Harash Formation comprises two to three shallowing-up cycles of mid- inner ramp setting, that are mainly composed of foraminiferal bioclastic wackestone-wackestone/packstone with less common foraminiferal nummulitic packstone facies. According to the wireline logs the whole interval of the Harash Formation across the studied wells can be subdivided into three major cycles (a parasequence set) that begin with argillaceous limestone and are capped with grain-

supported carbonates (Fig. 5.16). On the basis of their position within the sequence, these parasequence sets are assigned to TST4, despite the fact that an overall deepening-up pattern could not be detected from well-logs. This package is overlain by grey-dark grey, fissile, calcareous shale intercalated with grey argillaceous calcimicrite and marl of the Kheir Formation.

The base of the Kheir Formation is marked by a slight increase in the gamma-ray log, an important decrease in resistivity, a minor decrease in neutron and a major increase in the sonic record (Fig. 5.16), suggesting a maximum flooding surface (MFS4). This could be correlatable to the eustatic sea-level curve of Haq et al. (1988; Fig. 5.2). Consequently the basinal facies of the Kheir Formation could represent the succeeding highstand systems tract (HST4) up to the following sequence boundary at the base of the Eocene Jir Formation.

Most of the defined sequence boundaries on the Dahra Platform match fairly well with the global cycle chart of Haq et al. (1988), which suggest that global eustacy was possibly the main responsible for their development.

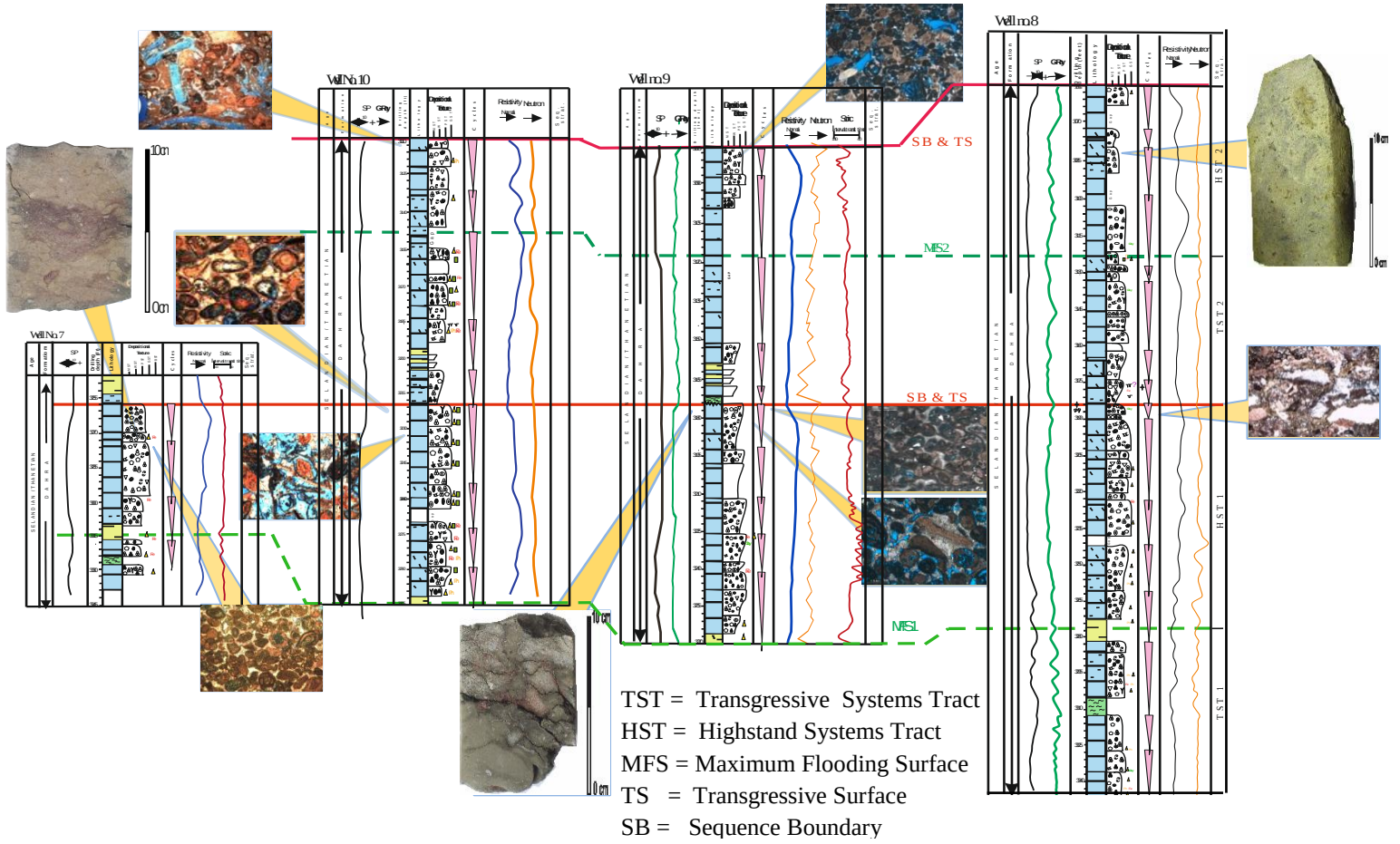

Figure 5.14 Lithological characteristics, cycles, well-log response and sequence stratigraphy of the Dahra Fm on the Dahra Platform.

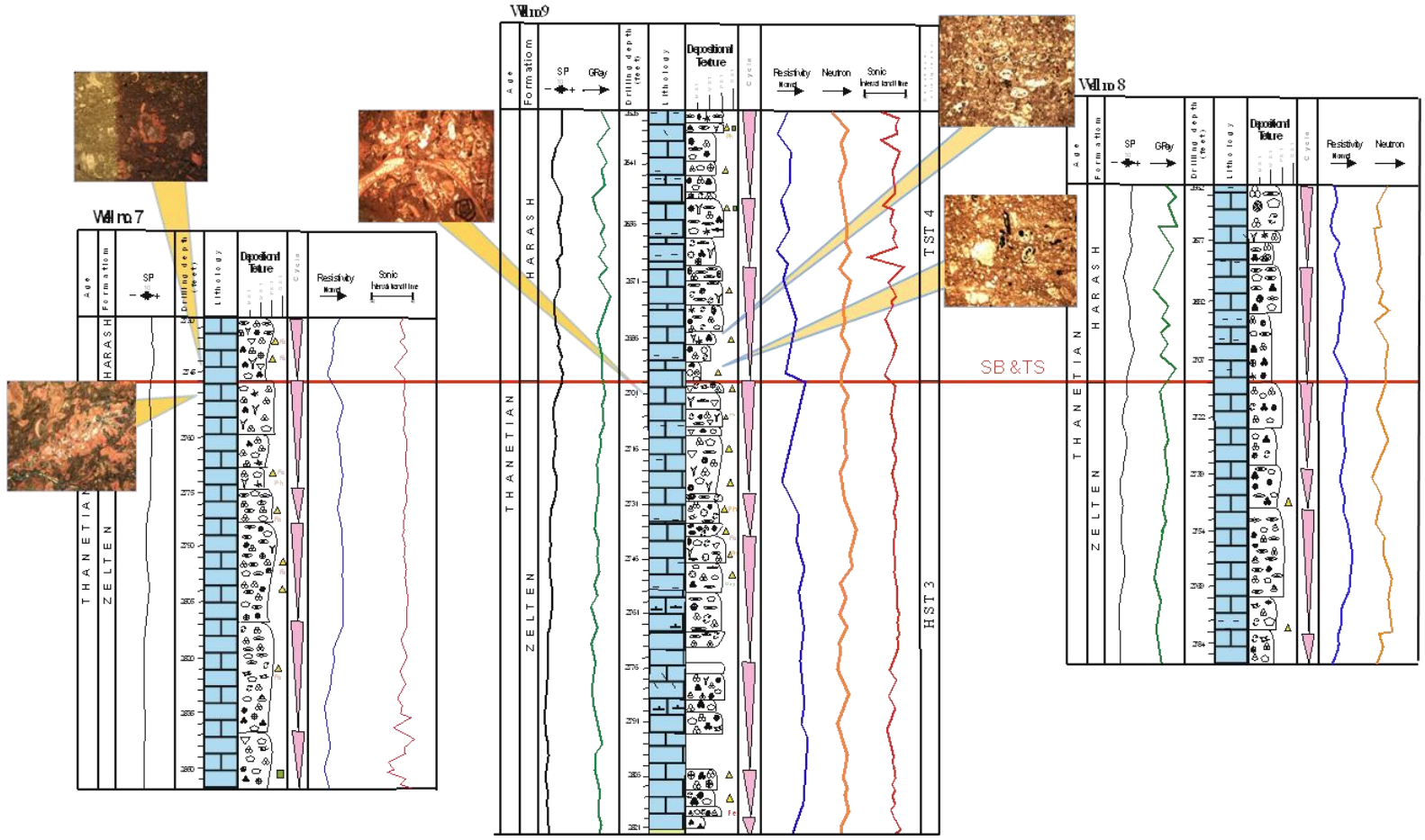

Figure 5.15 Lithological characteristics, cycles, well-log response and sequence stratigraphy of the Zelten/Harash interval on the Dahra Platform.

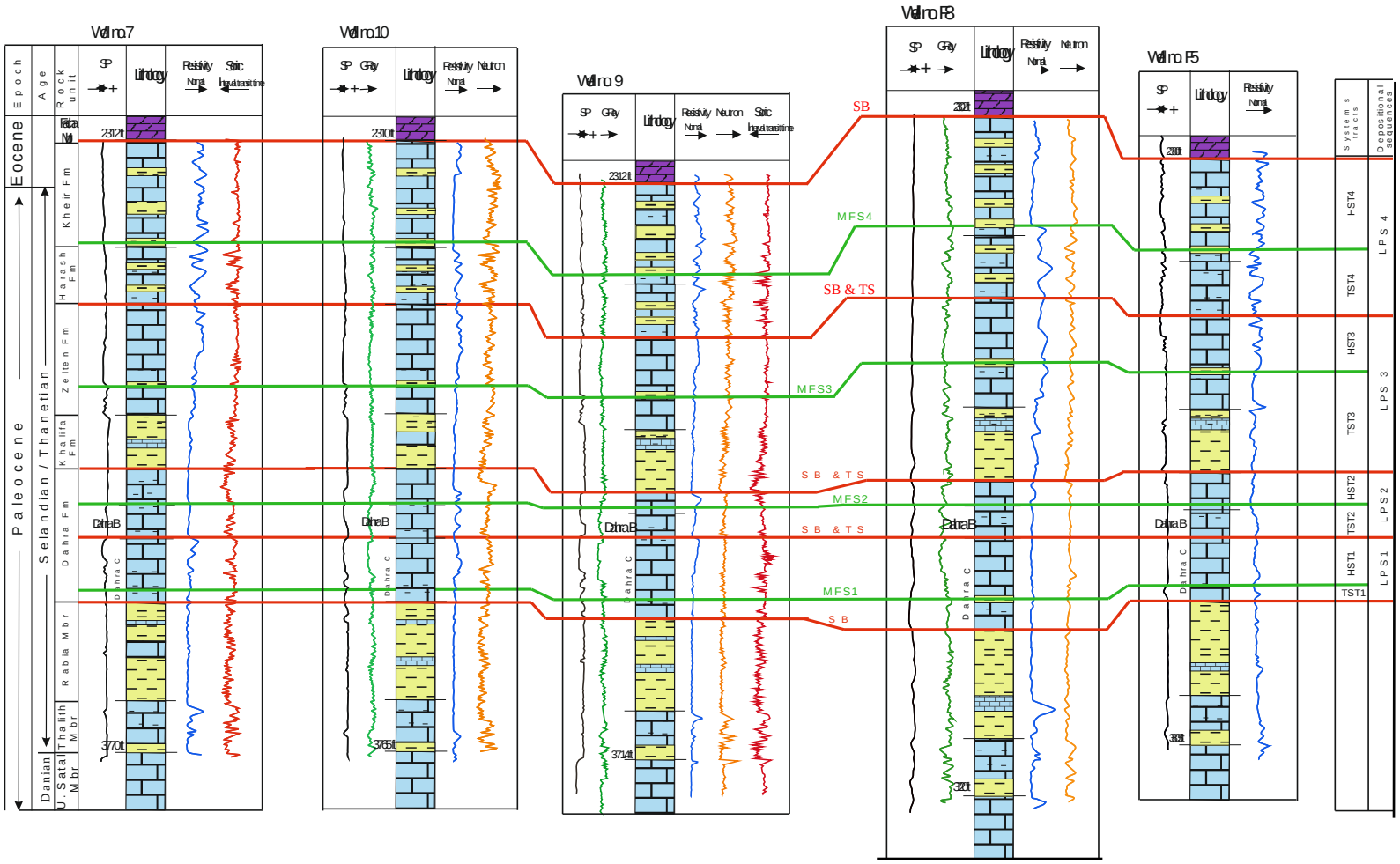

Figure 5.16 Lithological characteristics, well log response and sequence stratigraphy of the studied Selandian/Thanetian succession on the Dahra Platform.

5.5.2.2. Late Paleocene depositional sequences in the Dor al Abid Trough (Mabruk area)

The Mabruk oil-field lies on the west flank of the major axis on which the Bahi and the Dahra oil-fields are situated. As shown in Chapter 3, the Mabruk Member shows complex lateral and vertical variations from the west through central to eastern Mabruk areas. Its overall interval represents deposition of mainly shallow-water carbonates that were bounded by deeper-marine marl and shale; these carbonates accumulated in lagoonal and reefal environments of a probable a rimmed- shelf setting. In view of this the cored interval in the studied wells involves almost the entire Upper Mabruk Member and the upper part of the Lower Mabruk Member, the sequence stratigraphic analysis of this study is focused on the cored interval only.

5.5.2.2.1. Late Paleocene Sequence1 in the Mabruk area (LPSM1)

The thickness of this sequence (LPSM1) varies, in the reef area from 31ft in well no. 66 to 39ft in well no. 103, whereas in the lagoon area (well .no. 105) it is 36ft thick (Fig. 5.17).

Subsequent to the deposition of the Lower Heira Shale Member in probably a deep middle-shelf environment, a rapid to gradational change in the sedimentary facies occurred in the base of the Lower Mabruk member, where the limestone commences and is interbedded with thin beds of shale and marl. The pronounced facies change from a marl-dominated to limestone-dominated interval, started at the base of the Upper Mabruk Member in well no. 105, and at several feet above that base in well no. 103. It is characterized, in the latter well, by a shallowing-upward and locally coarsening-upward trend, which suggests a major change in the depositional facies and their stacking patterns.

In well no. 66, this boundary is characterized by mottling with the development of internal sediments, boring and fracturing. This is interpreted as the lower boundary of the LPSM1 that possibly coincides to the eustatic sea-level fall during the late Selandian/early Thanetian (Fig. 5.2). This boundary shows a marked decrease in the gamma ray log, a distinct increase in resistivity log response and an obvious shift in the neutron/density logs, particularly in the reef area, with an overall fairly well defined funnel-shaped trend (Fig. 5.18).

The upper boundary of this sequence is placed near to the middle interval of the Upper Mabruk Member; in the reef area it is placed at the contact between the coral

algal boundstone facies below and algal bioclastic boundstone (in well no. 66), or algal packstone facies (in well no. 103) above. It is characterised by the development of a thin layer of argillaceous limestone, highly compacted with the occurrence of dolomite, pyrite, glauconite and dark organic materials (possibly bitumen) (Fig. 5.17). The stable isotope trend at this boundary shows a slight shift to more negative $\delta^{18}O$ and very minor change to less positive $\delta^{13}C$ values (Fig. 5.13).

In well no. 105, the boundary is placed at the contact between shale/argillaceous limestone facies and the bioclastic foraminiferal packstone/grainstone, indicating a landward shift in facies (Fig. 5.17). The stable isotope trend in this well at this interval shows a remarkable shift to more negative $\delta^{18}O$ and less positive $\delta^{13}C$ values (Fig. 5.13). The wirline log signatures of this boundary show a very low gamma, a slight high sonic, an obvious shift in neutron/density response and a small increase in resistivity (a funnel-shaped trend) (Fig. 5.18).

The lowermost part of the LPSM1 is characterized by the development of type C2-C4 cycles that include the algal packstone, coral algal boundstone, and foraminiferal bioclastic wackestone- wackestone/packstone facies in wells no. 66, 103 and 105, respectively. In well no. 66 each cycle shallows-up, but the parasequence set shows a deepening-up trend; this is evidenced by the fact that the lower cycle is mainly composed of red algae, benthic forams and scattered rhodoliths, and the upper cycle consists of red algae, rhodoliths and corals with a high argillaceous content (Fig. 5.17). On the basis of these features, along with its stratigraphic position within the succession, it has been assigned to the transgressive systems tract (TST1). Its maximum flooding surface (MFS1) is placed at the marl/shale interval in wells no. 66 and 105, whereas in well no. 103 it is placed at the lowest grain-supported and the highest mud content interval (Fig. 5.17).

The MFS1 is followed by the highstand systems tract of the LPSM1 (HST1). In the reef area, this HST1 is occupied by relatively thick cycles of type C3 and C5 that are characterized mainly by the development of coral algal boundstone facies with the presence of dolomite in their uppermost parts, whereas, in well no. 105 this systems tract is represented mainly by shale, marl and mud-supported facies that, in turn, is followed by a sudden landward shift in facies (SB).

5.5.2.2.2. Late Paleocene Sequence 2 in the Mabruk area (LPSM2)

This sequence is much thicker than the LPSM1, particularly in the north central Mabruk region (towards the reef area). It gets thinner towards the southeast of the Mabruk field (towards the lagoon area), as it varies from 70ft in well no. 66 through to 58ft and 47ft in wells no. 103 and 105, respectively (Fig. 5.17). The lower boundary of this sequence is the upper boundary of the underlying LPSM1, and its upper boundary is placed at the top of the Mabruk Member, where a remarkable basinward shift in facies is recorded (Figs. 5.17 and 5.18).

In the reef area, this upper boundary is characterized by the development of a 2ft thick bed that is characterised by breccia with angular intraclasts showing microborings, and occurrence of pyrite, glauconite, phosphate, kaolinite and hematite (Fig. 5.17). The wireline logs show a pronounced increase in the gamma ray, a marked decrease in resistivity, a sharp shift in neutron/density, and a distinct change in the sonic record (a bell-shaped trend) (Fig. 5.18).

These features are interpreted as an unconformity surface of drowning (drowning unconformity of Schlager, 1981, 1989), despite the presence of the kaolinite (~16%,), reddish brown stains and scattered evaporite crystals, along with fair to good intragranular and moldic porosity in the lagoon area could indicate a short period of exposure just prior to the major flooding (drowning). The percentage of kaolinite and quartz at the top of the LPSM2, according to XRD analysis, increases southeast-ward; both are absent in well no. 66, 10% and 2% in well no. 103, and 16% and 3% in well no. 105, respectively. It is fairly well known that kaolinite-rich sediments would represent a low-sea level. Thus, the occurrence of kaolinite in the topmost part of the Mabruk Member could indicate an influx of riverine clastics through a sea-level fluctuation and/or a change to a more humid climate. In either situation, the upper boundary of the LPSM2 is there, whether it is associated with subaerial exposure or not.

Although the lower part of this sequence (LPSM2) is interpreted as a transgressive systems tract (TST2) that comprises, in the reef area, 2 to 3 relatively thick cycles of type C3, and 4 cycles of type C2 and C6 in the lagoon area, the possibility of development of a lowstand systems tract is not excluded completely (based on the above mentioned features). In well no. 66, however, the deepening-up trend is indicated by the lower cycle consisting of algal bioclastic boundstone and the upper one is coral algal boundstone facies (Fig. 5.17). In well no.105, the lower two cycles are of grain-supported facies, whereas the upper two cycles are composed of shale and mud-

supported carbonates. The stable isotope values of this interval show a remarkable excursion to less negative $\delta^{18}O$ and more positive $\delta^{13}C$, which confirm interpreting it as TST2. Increases and positive maxima in $\delta^{13}C$ correspond to phases of sediment accumulation during sea level high stands and transgressions. A trend towards $\delta^{13}C$ depleted ratios and negative maxima in $\delta^{13}C$ correspond to phases of sediment erosion and reworking during sea level lowstands and regressions (Hilbrecht et al., 1986; Voigt and Hilbrecht, 1997).

The maximum flooding surface of this sequence (MFS2) is placed in well no. 66, at the base of a roughly aggrading pattern that comprises type C6 cycles, and at the top of the bioclastic packstone that comprises coral fragments, bryozoans and scattered un-differentiated bioclasts with the occurrence of pyrite and dark organic matter. In well no. 105 the MFS2 is placed at the upper part of this sequence, in the marl bed, above which a roughly thin shallowing-up pattern that comprises only one cycle is developed (HST2). A notable feature is that this HST2 is getting thinner southeast-ward of the Mabruk area (towards well no. 105); it follows the same trend of thickness variation of the entire LPSM2. This could be the result of the rate of removal of the upper parts of the HST2 in the proximal facies (lagoon area) being more than that of relatively distal facies (reef area).

Following the HST2, a major flooding event took place at the top of the Mabruk Member in the study area. The surface of this event, which could be amalgamated [SB & TS (drowning)] is somewhat similar to the lower boundary of the LPS3 on the Dahra Platform that separates the Dahra and Khalifa Formations. It probably corresponds to the eustatic sea-level rise during the early Thanetian (Fig. 5.2).

From a sequence-stratigraphic point of view, drowning unconformities can be interpreted either as sequence boundaries (SB) or maximum flooding surfaces (MFS), depending on the development (or not) of an intervening exposure phase (e.g. Catuneanu, 2006). As explained in Chapter 3, a number of mechanisms have been proposed in the literature to explain the demise of a carbonate platform and the generation of a drowning unconformity. Shallow-marine carbonate platforms become inactive (drowned) when the platform top is submerged below the depth range of light penetration (photic zone) for effective photosynthetically driven carbonate production (Schlager, 2005), which would prevent platform tops from keeping up and/or catching up to rising sea-level (Kim et al., 2012).

The long-term drowning of carbonate platforms requires that the reduction of growth over long time-scales is largely caused by environmental factors. It has been demonstrated in Jurassic settings that platform drowning is associated with abrupt facies changes (Blomeier and Reijmer, 1999) and, based on fluid inclusion palaeobarometry, that water depth increased at slower rates than normal platform growth (Mallarino et al., 2002). These findings, according to Mutti et al., (2005), require environmental changes for platform drowning. Several processes could have resulted in long-term local environmental changes: increased volcanic activity; changes in circulation that would have resulted in increased local productivity of the surface waters; and changes in sea-level and temperature of the surface waters (Mutti et al., 2005).

In the study area, the possible lack of reef-building organisms, causing a sharp decrease in the rate of carbonate production, thus promoting drowning when subsidence and/or sea-level increased (Bice and Stewart, 1990), is probably the most appropriate cause for the discontinuation of carbonate production in the Mabruk area. In the Sirt Basin, several upper Paleocene coralgal bioherms were drowned at the end of the Paleocene and covered by hemipelagic marls, shales and limestones of the Harash and Kheir Formations (Scheibner et al., 2008).

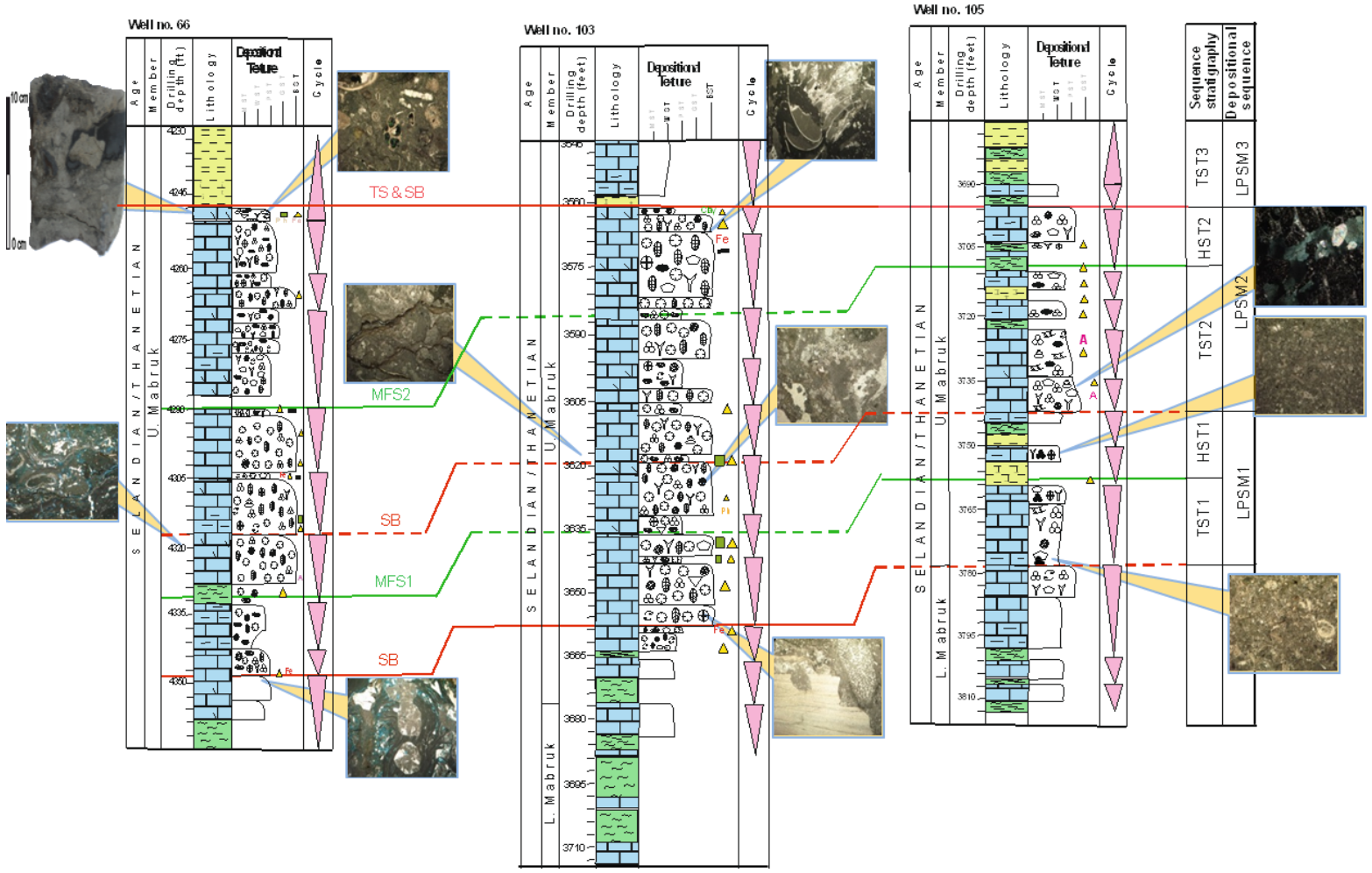

Figure 5.17 Lithological characteristics, cycles and sequence stratigraphy of the Mabruk Member in the Dor al Abid Trough.

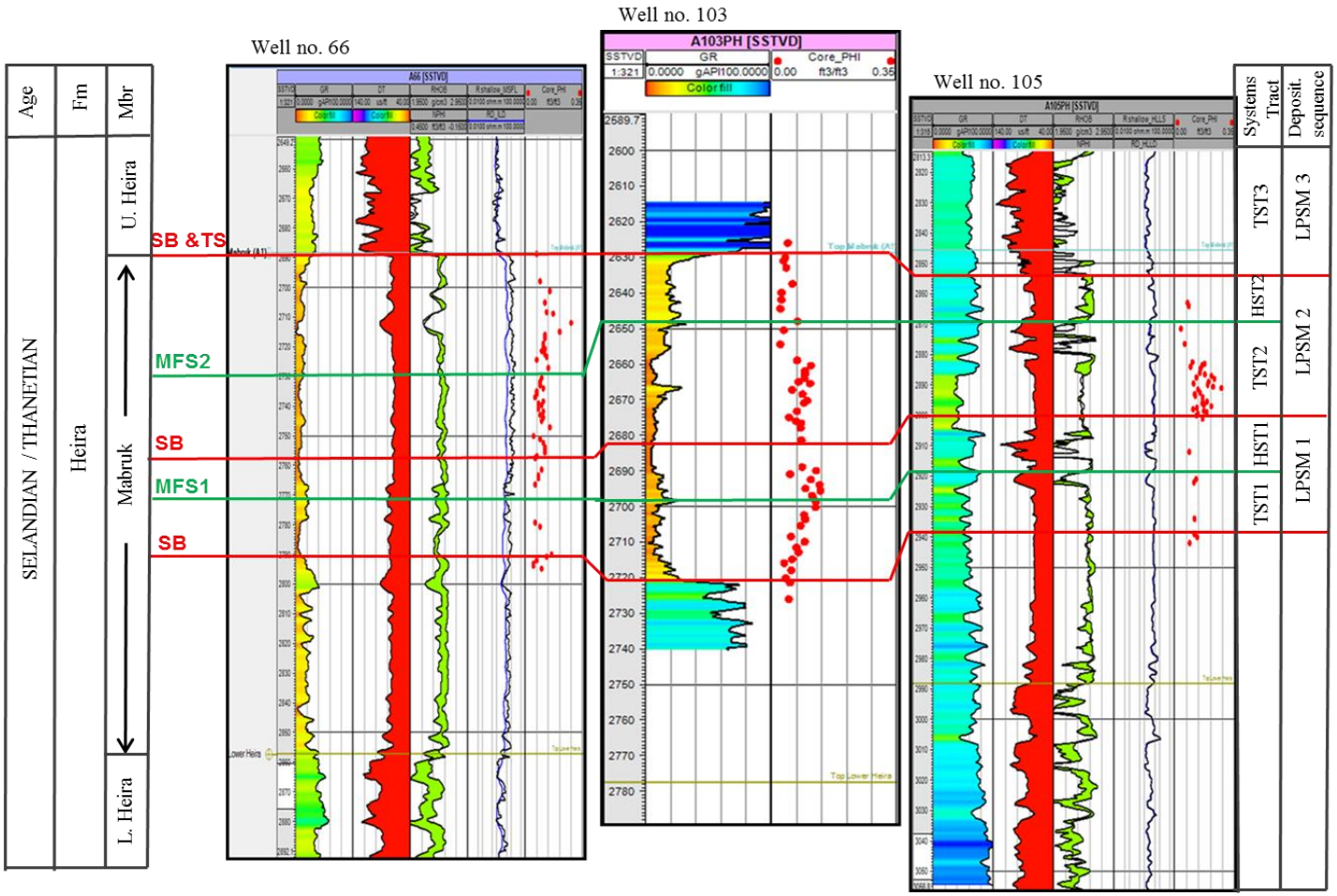

Figure 5.18 Well-log response and sequence stratigraphy of the Mabruk Member in the Dor al Abid Trough.

5.6. Summary

The sedimentary succession in the Sirt Basin as a whole ranges in age from Cambro-Ordovician to recent. In the study area, the Palaeozoic and Mesozoic sections have been recorded in several localities on the Dahra Platform and in Zellah/Dor al Abid Troughs. During the Cenomanian a major flooding event occurred and extended marine conditions over most of the Sirt Basin, particularly in the trough areas. In the uppermost Cretaceous, subaerial exposure occurred in many parts of the Dahra Platform, which later during the Maastrichtian became submerged.

The start of the Tertiary was associated with a broad sea-level rise, which resulted in the deposition of thick Hagfa Shale in large parts of the Zallah and Dor al Abid Troughs, whereas shallower-water carbonates of the Satal Formation, were deposited on the Dahra Platform. The overall cycle of shale deposition with intercalation of carbonate reflects alternating transgressive-regressive cycles in the Paleocene succession.

The Satal carbonates were blanketed by a few metres of calcareous shale, which represent the extension of the deep Hagfa shale, i.e. they were onlapped and/or probably drowned by a thin unit of deeper-marine shale. In the Dahra Field and adjacent areas, the Rabia Shale Member, which consists of dark grey to green calcareous shale with minor light grey, argillaceous limestone beds, could represent a lateral development of the Hagfa Shale Formation. The base of the Thalith Member is considered as a transgressive surface that was probably associated with a high rate of carbonate production, and above which the backstepping (deepening-up-trend) was developed.

A gradual shallowing of the sea resulted in the deposition of the Dahra carbonates over large parts of the study area. A major transgression occurred at the end of Dahra carbonate deposition, and resulted in sedimentation of several tens of feet of mainly shale with subordinate limestone of the Khalifa Formation on the platform and in trough areas.

The log characters of the Rabia shale interval are quite similar to those of the Khalifa Formation, which could support the use of a collective name for these Paleocene shales (Hiera Formation) in the trough areas. The fossil contents, characteristic sediments and the electrical log features of the Zelten Limestone suggest an overall regressive interval, with a probable prograding trend, particularly in the upper part of the Formation. The boundary between the Zelten and Harash Formations shows

a sharp change in facies and log response that strongly suggest an important stratigraphic event.

The studied Paleocene succession is dominated by shallowing-up cycles, with the possible development of deepening-up cycles particularly in the deeper-water areas. On the Dahra Platform, the Dahra, Zelten and Harash Formations comprise lagoonal, shallow subtidal and deep subtidal cycles. In the Dor al Abid Trough, the Mabruk member involved reef and back-reef/lagoonal cycles.

The $\delta^{18}O$ values recorded in the studied Paleocene succession range from +1.15‰ to -10.49‰, whereas the $\delta^{13}C$ measurements fall in the range +3.89‰ to -4.87‰. The carbon isotope values on the Dahra Platform are all quite similar and do not shows any real significant change up through the section, while the oxygen isotope stratigraphy of the Dahra Formation does show several pronounced shifts.

The overall isotope values of the Mabruk Member range from $\delta^{18}O$ -7.7‰ to -0.8‰, and $\delta^{13}C$ -6.3‰ to +3‰. They commonly follow the sedimentary facies, as the wells with reefal facies have similar isotope values, whereas the wells with lagoonal facies have a completely different trend.

The rate of deposition of the Dahra Formation on the Dahra Platform is around twice of that of the Mabruk Member in the Dor al Abid Trough, and the cycle duration of the Dahra Formation is much less than that of the Mabruk Member (129 kyr versus 165 kyr). This probably relates to the fact that an inner platform area is normally the site of higher carbonate production relative to the outer platform area. Carbonate accumulation during the deposition of the Zelten and Harash Formations on the Dahra Platform is similar to that of the Dahra Formation (0.046 m1000 yr^{-1} – as compared to 0.042 m1000 yr^{-1}), which suggest a similar rate of creation of accommodation space.

Sequence stratigraphic analysis of the Selandian/Thanetian section in the study area has resulted in the identification of four depositional sequences on the Dahra Platform, whereas at least two depositional sequences have been recognized in the Mabruk area in the Dor al Abid Trough. These depositional sequences comprise both transgressive systems tract and highstand systems tract, while lowstand systems tract was not developed (or recognised), probably due to the low relief ramp setting or because of the location of the studied wells. A notable feature is that the lower sequences in both structural settings are commonly thinner than those in the upper part of the succession. The sequence boundaries are commonly incorporated with

transgressive surfaces, particularly on the Dahra Platform. The likely development of a drowning unconformity on the top of the Mabruk Member in the Dor al Abid Trough could be ascribed to a possible lack of reef-building organisms in association with tectonic subsidence and/or significant sea-level rise.

CHAPTER SIX: SPATIAL AND TEMPORAL VARIATION OF PALEOCENE STRATA AND SUBSIDENCE PATTERNS IN THE SIRT BASIN STUDY AREA

6.1. Introduction

The Sirt Basin of north-central Libya is a complex rift basin that is considered to have been initiated in the Late Jurassic (Abadi, 2002; Abadi et al. 2008). The many sub-basins of the Sirt evolved as a series of rifted embayments on the northern margin of the North African plate, following the breakup of the supercontinent of Pangaea. However, the duration of rifting in the Sirte Basin is more variable and this in part reflects the complex structural nature of the basin setting. In such structural settings identification of late syn-rift and post-rift thermal subsidence are unclear and this is reflected in the literature with a wide variety of timings across the Sirt Basin (Gumati and Kanes 1985; Gumati and Nairn, 1991; Baird et al 1996; Schroter, 1996; Abadi et al., 2008). Subsidence and extensional fault reactivation are considered here to have continued into the Paleocene and probably early Eocene in response to the plate movements of the African, American and Eurasian plates during the opening of the Atlantic and development of Tethys on the foreland of the African plate (Anketell, 1996). Evidence will be provided to support this late syn-rift timing from burial and subsidence histories of the Dahra platform region of the western Sirte Basin.

Previous studies of Sirte basin subsidence and timing of rifting events have either focused on the regional events with limited datasets (e.g. Gumati and Kanes 1988; Gumati and Nairn, 1991; Baird et al., 1996) or used larger data sets from across the Sirt Basin focusing only on the subsidence histories (e.g. Abadi et al 2008). Here the spatial and temporal variations in the subsidence patterns are investigated using 50 wells, from locations given in Figure 1.1. This is combined with detailed petrography of the key burial diagenetic cements from core of 7 wells, wire-line logs, fluid inclusion analyses and stable isotope data.

The Paleocene was a time of renewed vertical movements, which produced a strong differentiation between the sedimentation patterns on the horsts and in the grabens (Gumati and Kanes, 1985). The Selandian/Thanetian succession on the Dahra Platform is composed mainly of carbonate and shale facies that alternate with each other up to the Eocene. In the trough areas the succession comprises mainly shale and marl, with scattered carbonate facies, particularly in its lower part (Fig. 6.1).

This chapter is aimed at reviewing the spatial and temporal distribution of the Paleocene from the Dahra platform and Dor al Abid/Zallah trough succession. It provides a new appraisal of the Paleocene carbonates and how they are affected by late stage syn-rift tectonics and subsidence. A quantitative subsidence analysis is presented to understand fully the late syn-rift phase and its influence on sedimentation patterns.

6.2. Geological history and rift framework

Rifting commenced in the Late Jurassic, peaked in the Late Cretaceous, and terminated in early Tertiary time, resulting in the triple junction (Sirte, Tibesti, and Sarir arms; see Figure 2.8) within the basin (Harding, 1984; Gras and Thusu, 1998; Ambrose, 2000). According to Anketell (1996), the Early Cretaceous rifting reflected east-west sinistral shear zones (strike-slip) that strongly controlled clastic deposition in the Sarir arm of the triple junction, but Ambrose (2000) alternatively proposed that dextral shear forces dominated this period of deformation in the Sarir arm.

The Sirt Basin is asymmetric, deepening to the east as shown in Figure 2.12. The relative relief on the juxtaposed horst and graben blocks increases to the east coincident with significant thinning of sediments across the province. Erosion and collapse associated with the Sirt Arch resulted in truncation of the Palaeozoic succession during the Early Cretaceous rifting phase (Burke and Dewey, 1974). The drift of the African plate over a fixed mantle hotspot is thought have triggered this event (Van Houten 1983). This early rifting phase coincided with rhyolitic and basaltic volcanism dated at 148-127 Ma (Rossi et al., 1991; Gras and Thrusu 1998; Wilson and Guiraun 1998). A change from northward to westward African plate motion in the Late Cretaceous promoted further thinning of the cratonic lithosphere (Morgan 1980, 1983). This is marked by major basin subsidence, reactivation of faults and crustal extension (Gumati and Nairn 1991). Subsidence and extensional fault reactivation continued into the Paleocene to early Eocene, in response to the relative plate motions of the African, American and Eurasian plates during the opening of the Atlantic and development of Tethys on the foreland of the African plate (Anketell, 1996). Progressive erosion of younger sediments and subsequent episodes of block faulting resulted in placing the Palaeozoic and Mesozoic reservoirs

in a structural high position with respect to thermally mature Cretaceous source rocks that occupied the deeper portion of the Sirt Basin and its sub-basins.

In the western Sirt Basin, Late Cretaceous and lower Tertiary carbonate reservoirs, commonly reefs and platform carbonates on the northwest-southeast-trending horsts, are the dominant reservoirs in the remaining two arms (the Tibesti and Sirte arms) of the triple junction. The western region of the Dahra platform and associated Dor al Abid/Zallah Trough form the focus of this research.

Abadi et al., (2008) identified four tectonic phases in the Sirt Basin, from Late Jurassic to present. They pointed out that the Paleocene rifting phase (65–49 Ma) marked an abrupt deepening of the basin, separated from the Late Cretaceous subsidence by a period of tectonic quiescence in the Maastrichtian. Abdunaser (2012) suggested four graben-fill stages in the western Sirt Basin from the Cretaceous to the end of the Paleocene with the onset of the post-rift stage in the Eocene. He related the rift development in the western Sirt Basin to the break-up of Gondwana represented by the structural evolution of the West-Central African rift system and the South and Central Atlantic, the Tethys and the Indian Oceans.

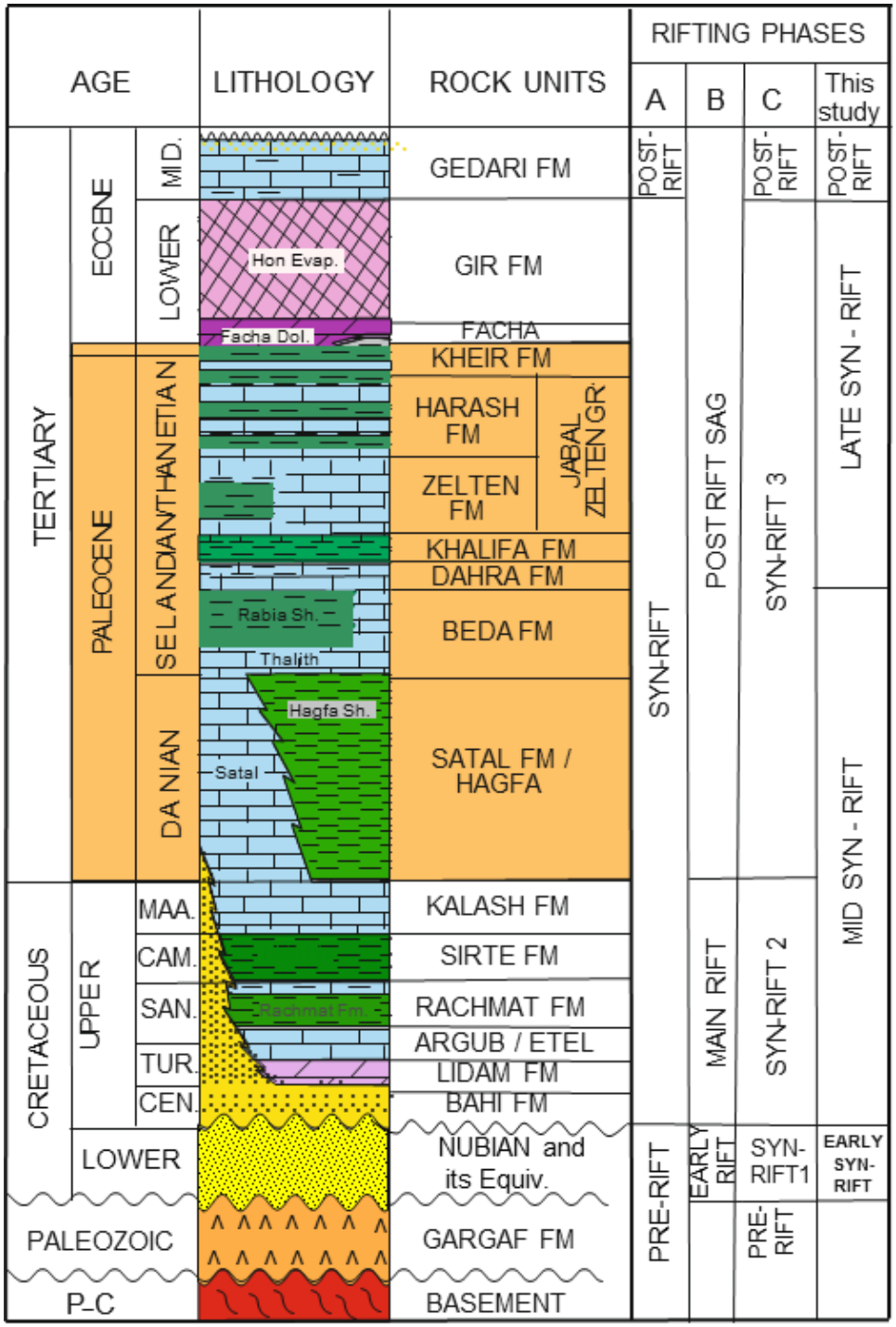

Figure 6.1 Stratigraphic section in the study area showing transgressive-regressive deposits and main rifting phases. A: Montgomery, 1994; Gumati and Kanes, 1985 and Ahlbrandt, 2001; B: Spring and Hansen, 1998; C: Abadi et al, 2008. Nomenclature of Barr and Weeger, 1972.

6.2.1 Criteria for recognition of late syn-rift sedimentation

Active extensional basins are important because their sedimentary fills and associated structures provide i) depocentres with high preservation potential for the sedimentary successions; ii) detailed records of sea–level changes and sediment supply rates, iii) direct information of the fault activity within a rift and; iv) directly attributable spatial and temporal relationships between sedimentation and tectonism. The sedimentary patterns associated with the subsidence and uplift of normal faults has lead to a number of studies focusing on theoretical fault growth models (e.g. Gawthorpe et al., 1997; Gawthorpe & Leeder, 2000) and changes in stratal patterns and thicknesses in hanging-wall depocentres (e.g. Gupta et al., 1998; Sharp et al., 2000). However, most of these studies focus on the main rift tectonic events and their influence on contemporaneous strata.

Prosser (1993) proposed a four-fold division of rift evolution to characterize basin-fill stratigraphy: (1) rift initiation stage, where the rate of displacement is relatively low and sedimentation keeps pace with subsidence; (2) rift climax, where the rate of displacement reaches its maximum value and sedimentation is likely to be outpaced by subsidence; (3) immediate post-rift stage, where active tectonism has ended, only a (decreasing) regional subsidence due to thermal cooling is left and filling of the remnant topography begins; and (4) late post-rift stage, in which a slow peneplanation of the remaining low-relief topography takes place.

Although such a classification that documents the key tectonic events during the life history of a rift is well established and largely used in the references cited above, the late syn-rift phase and its recognition in sedimentation histories has been neglected in the literature (e.g. Schlische and Olsen, 1990; Prosser, 1993, Wilson and Hall, 2010). Furthermore, the tectonic controls on syn-rift successions has largely focused on clastic sedimentary fills (Gawthorpe & Leeder 2000), carbonates provide equally subtle and interesting variations across fault blocks as seen in the Sirt Basin (e.g. Cross et al., 1998; Bosence, 2012). Much of the literature focuses on sedimentation associated with the acme of rifting and subsidence and neglects the late stage syn-rift phases. Several characteristics can be recognized in the Sirt Paleocene stratigraphy of this study to assign it to a late syn-rift phase. These are:

i) Linkage of fault segments to create large (≥10 km-long) faults with discrete influence on sedimentation patterns along their length;

ii) Large-scale regional subsidence of footwall blocks, with uniform sedimentation;
iii) More localized and discrete subsidence along sections of hard-linked fault segments;
iv) Sedimentation ≥ subsidence during the latest phase of syn-rift, leading to sediment bypass;
v) Footwall blocks dominated by steady state platformal carbonates with uniform sedimentation and petrography and;
vi) Hanging-wall blocks dominated by deeper-water facies with mainly shale and less carbonates.

The late syn-rift phase ended by the deposition extensively distributed of early Eocene evaporite and dolomite (Gir Formation) with uniform lithology and thickness variations. These variations in the trough and platform areas have been attributed to the mobility and sensitivity to dissolution of the evaporites, rather than to deposition or tectonic effects (Baird et al., 1996). From the middle Eocene onward, faulting-related differential subsidence decreased (Abadi et al., 2008).

6.2.2. Mid Syn-rift to late syn-rift sedimentation in the Paleocene

Regional structural map, seismic sections and well logs showed that the Kalash Limestone is widespread all over the study area; in the Zallah and Dor al Abid Troughs, and on the Dahra Platform (Figs 6.6 and 6.9). It has revealed that some parts of the Dahra Platform existed as palaeo-highs, probably upto the early Maastrichtian (Fig. 2.9).

The Campanian high subsidence rate in the central Zallah Trough was replaced by intermediate subsidence in the Maastrichtian, the time during which the major faults became inactive (Schröter, 1996). Gumati and Kanes (1985), who considered the rifting phase in the Sirt Basin to include the Cretaceous and Paleocene successions, pointed out that the late Cretaceous and Paleocene rifting phases of the central Zallah Trough are separated by a time of tectonic quiescence. During the Maastrichtian, subsidence patterns in the Sirt Basin appear to become spatially less differentiated and show patterns of less rapid subsidence before reactivation of the NW faulting during the Lower Paleocene (Abadi, 2002).

Therefore, the preceding statements, along with the wide spread occurrence of the Maastrichtian Kalash Limestone in the Sirt Basin, with fairly uniform thickness,

strongly indicate that Maastrichtian time was a significant period within the basin; it probably represents the time of tectonic quietness within the mid syn-rift phase phase of the Sirt Basin, when troughs and platforms were almost discrepancy subsiding. This is witnessed by the fact that the entire Paleocene succession and most of the Eocene are, in contrast with the preceding late Cretaceous, developed in both structural elements (in the Zallah and Dor al Abid Troughs and on the Dahra Platform) with thickness of the individual rock units and overall thickness of the Cretaceous and Tertiary sections on either sides of the Gedari Fault are remarkably different (Fig. 6.3).

The thickness difference between the Dahra Platform strata and the Zallah/Dor al Abid Troughs section, however, is probably due to local differential subsidence on both structural elements that resulted in the difference in accommodation space. Some of the late syn-rift differences can be further ascribed to late stage fault related subsidence.

The Paleocene is widely regarded as a significant renewed phase of rifting in the Sirt Basin (e.g. Gumati and Kanes, 1985; Abadi 2008). The basin is recognised to have deepened again following the Cretaceous rifting episodes with markedly deeper water facies in the basinal troughs (e.g. Hagfa, Rabia and Khalifa shales) and carbonate platforms on the upstanding blocks (e.g. Beda, Dahra and Zelten Formations – this study). Interestingly the Zelten and Harash Formations of the carbonate platform facies demonstrate a pronounced westward extension of the previously formed platforms with more stability and uniform facies distribution. The overlying Kheir Formation is further extensively developed throughout the Sirte Basin. The open marine predominantly muddy facies of the formation can be correlated over several 100's of kilometres and further identifies the stable conditions for sedimentation during the late Paleocene to early Eocene, especially of the footwall blocks (Belazi, 1989).

Abadi et al., (2008) identified the Paleocene as the third phase of four main episodes, with rifting and subsidence most pronounced in the north-east Sirt basin. His tectonic subsidence map of the Paleocene-Early Eocene reveals that the study area has been subjected to a fairly similar rate of subsidence, except in the northern part; the overall subsidence in the Dahra Platform, Zallah and Dor al Abid Troughs is around 100-125m (~300–400ft) (Fig. 6.2). In the central part of the Al Hagfa Trough,

the eastern border of the Dahra Platform, a thickness of over 4000ft (~1220m) of Paleocene is documented (Wennekers et al., 1996). In the offshore area of the Sirt Basin, Bezan (1996) pointed out that the thickness of the Paleocene succession is <100ft of Late Paleocene shale. He ascribed this thinning to the low rate of deposition (starvation), which might be evidence that the coastal area was uplifted during the early Paleocene by the tectonics of the Atlas wrench fault located north of the coastline. The thickness of the Paleocene succession is commonly close to the underlying structure; thicker in the trough areas and thinner over the platforms. Its total thickness, however, in the Zallah Trough and adjacent low areas reaches 3500ft (~1067m), whereas on the Dahra Platform and other high areas less than1500ft (~457m) is recorded (Fig. 6. 4).

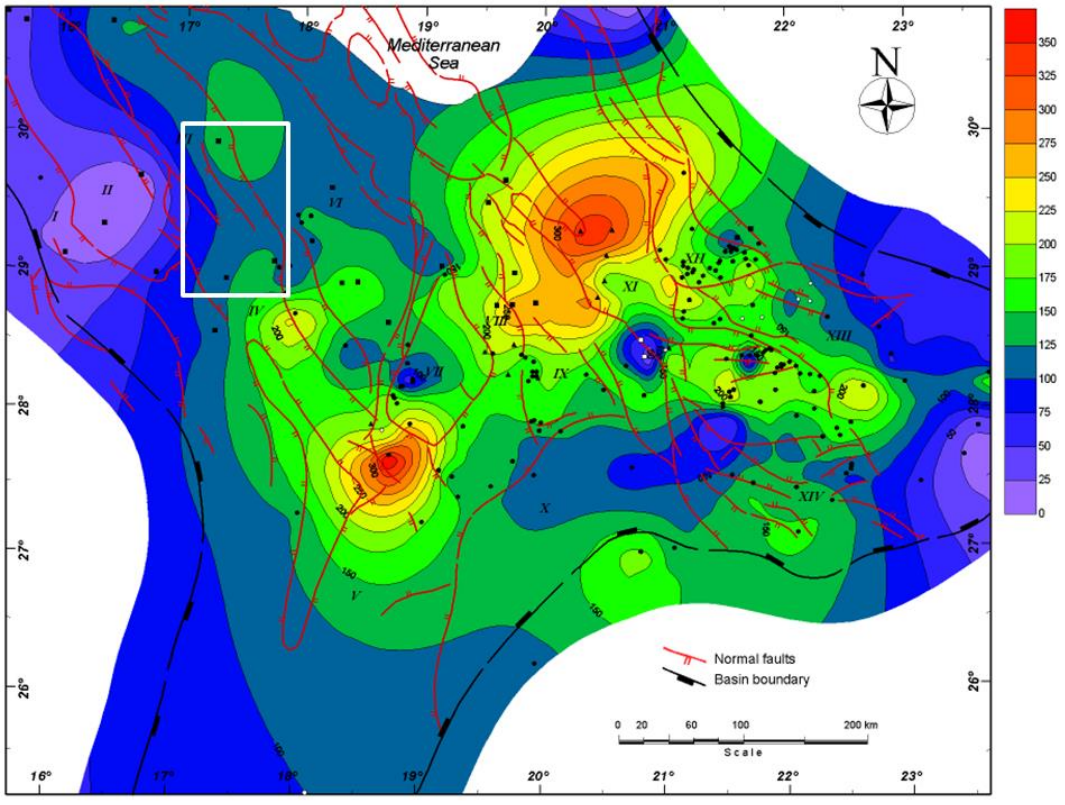

Figure 6.2 Contour map of tectonic subsidence (in metres) of the Sirt Basin (Abadi, 2002). Note that the study area was subjected to a subsidence between 75-150 m (~ 250-500ft) during the Danian-Ypressian time (white rectangle).

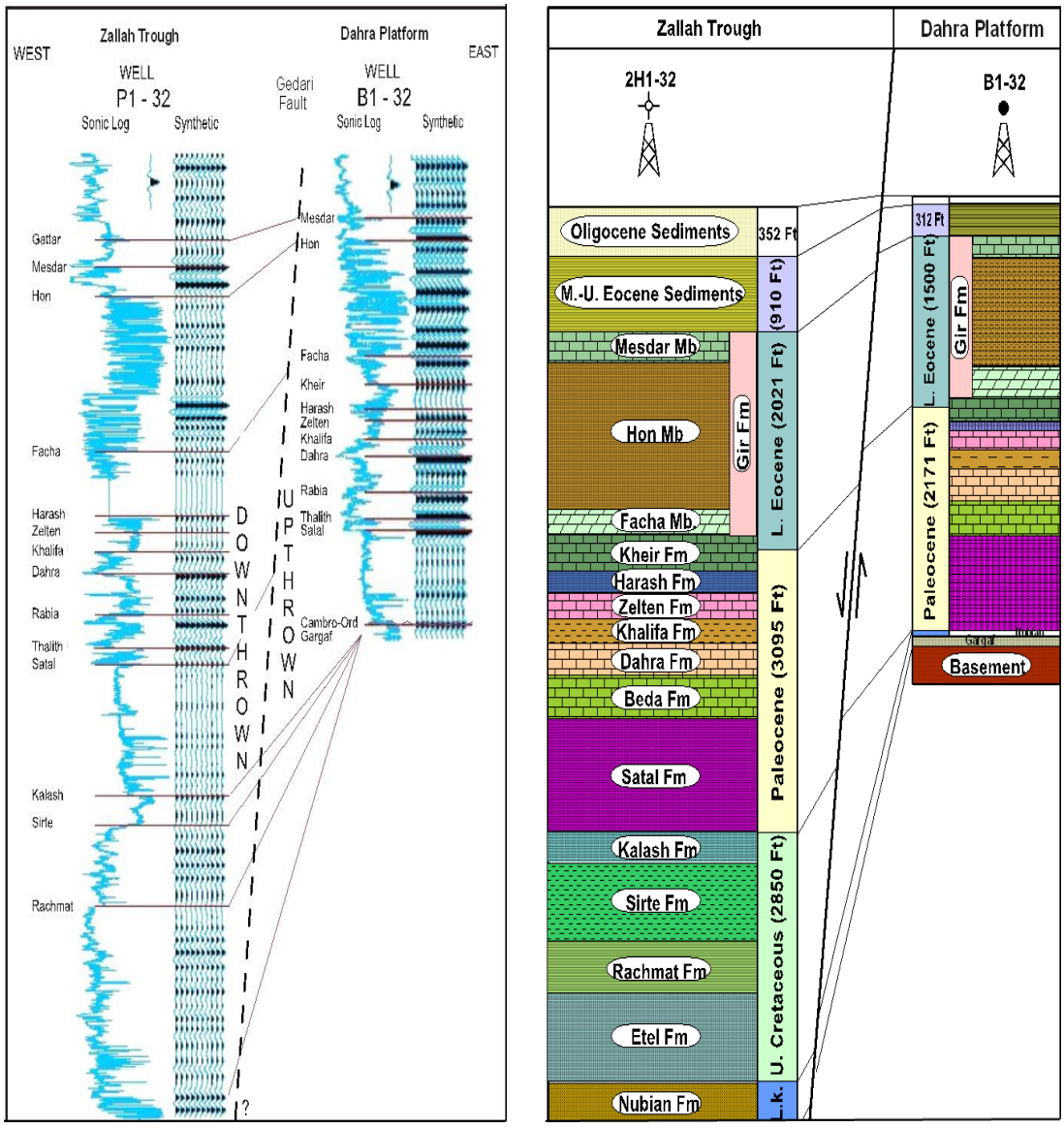

A **B**

Figure 6.3 Variation in stratigraphy and thickness on both sides of the Gedari Fault (the boundary between the Dor al Abid/ Zallah Trough and the Dahra Platform) interpreted from synthetic seismogram and sonic logs (A), and expressed in lithology and thickness (B). Note the thickness variation of the Late Cretaceous-Tertiary succession on both sides of the fault. The thickness discrepancy is less pronounced up-section, suggesting that the Gedari Fault became less active during the late Tertiary. (A: from PRC and TPS, 2003; and B: from Abdunaser, 2012).

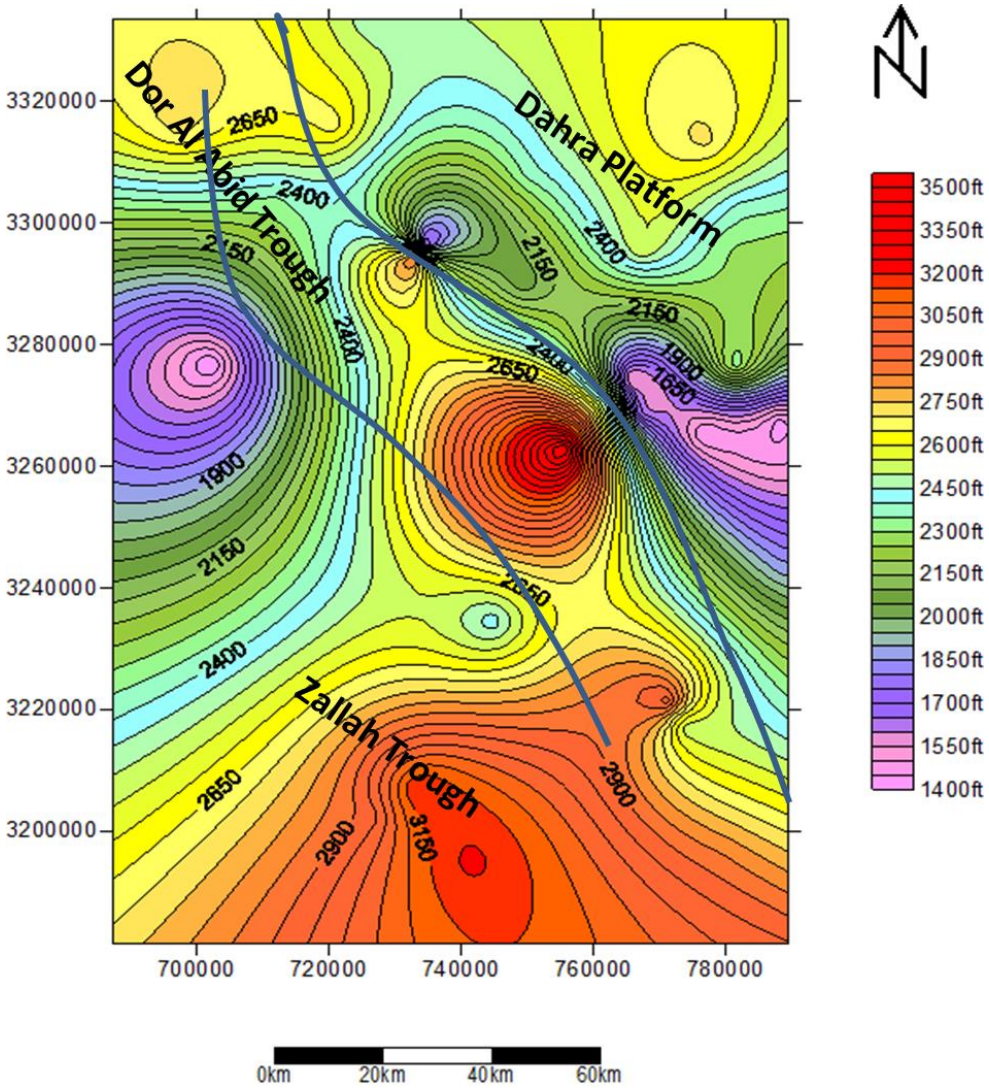

Figure 6.4 Total Paleocene isopach map of the study area. Note that the Paleocene succession is generally thicker in the trough areas and thinner over the platforms.

6.2.2.1. Danian Succession (Hagfa and Satal Formations)

The beginning of the Danian saw a widespread sea-level rise, possibly in response to a regional tectonic event. This resulted in deposition of thick open marine shales in the subsiding areas (Hagfa Shale) in the south and southwestern part of the study area (Zallah Trough), whereas the stable platform (the Dahra Platform) and the high topographic areas within the troughs, on the other hand, were largely dominated by carbonates of the Satal Formation. Thus, a distinctive regional Danian carbonate bank was established (See Figs. 2.9 & 2.13).

The areas with no Satal carbonate, which are smaller than those covered by the Satal Formation, are covered by Hagfa Shale, which onlaps and locally blankets the

Satal carbonate with a few tens feet of shale. Its thickness increases away from the platform area, where it ranges between <50ft on the Dahra Platform and >600 ft in the northern Zallah and Dor al Abid Troughs (Fig. 6.5A). In the south of the Zallah Trough its thickness can reach 1000ft, and in the depocentre of the basin (Ajdabiya Trough) it exceeds 2000ft (Hallett, 2002).

The regional structural map on top of the Hagfa Shale shows strong agreement between the thickness distribution and the pre-existing topography (top of the Kalash Limestone), which persisted until the end of the Hagfa Shale (Fig. 6.7A).

A regional isopach map for the Satal Formation has been constructed, despite the fact that the total depth in many wells does not penetrate the entire section of the Satal Formation. Nevertheless, the map reflects the effect of the underlying palaeotopography. It shows that the thickest section of the Satal mainly occurs at the Dahra Platform/Dor al Abid Trough boundary, which may coincide, towards the southwest, with the Satal Bank edge (Fig. 6.5A). These features could suggest that the rate of deposition was quite high at the bank margins, and probably greater than the available accommodation space, so that prograding clinoforms developed on the northern periphery of the Satal Bank, to the northeast of the Almas Oil Field (Fig. 6.6). It is well known that clastic-free carbonate build-ups are usually characterised by a high rate of carbonate production. Although there is considerable local variability, clean carbonate systems often have faster accumulation rates (up to 3000–6000 gm^{-2} yr^{-1}) than those containing clastics (<3000g m^{-2} yr^{-1}) (Woolfe and Larcombe, 1999; Mallela and Perry, 2007; Lokier et al., 2009). This clastic-free carbonate bank covered the Dahra-Al Bayda platform area, crossed the Dor-al-Abid graben in the northern Zallah Trough and extended to the Manzilah ridge and Al Bayda Platform in the central Sirt Basin (Bezan, 1996).

The structure contour map, 3D surface and wire-frame maps for the top of the Satal Formation reveal that: (i) the western margin of the Dahra Platform (Gedari Fault) dips steeply into the Zallah Trough; (ii) the northeastern side of the Zallah Trough represents the deepest part of the study area; (iii) by the end of Satal deposition two prominent structural highs were established; the eastern high, which is situated on the Dahra Platform and existed since the end of Maastrichtian, was slightly higher than the western one and was running parallel to the Gedari Fault that separates the Dahra Platform from the Dor al Abid Trough in a NW-SE trend (Figs.

6.7A & 6.8). The other high is located in the western part of the study area and seems to separate the Dor al Abid and Zallah Troughs, and is inclined gently towards both of them.

This feature persisted throughout the Paleocene and continued into the Early Eocene. A closer investigation of these highs on top of the Satal Formation showed that the topographic surface of the broad Satal Bank is irregular and uneven, not only on its wider scale but also within its local intra-highs; thus this asymmetrical surface may have played a significant role, particularly on the Dahra Platform, in accommodating (trapping) hydrocarbons in the topmost intervals of the Upper Satal Member.

6.2.2.2. Selandian-Thanetian Succession (Beda and Dahra Formations)

Over a wide part of the study area the Beda Formation of Selandian age becomes more shaley and is subdivided by Barr and Weegar (1972) into two members: a lower carbonate unit (Thalith Member), and an upper shale unit (Rabia Member) (Fig. 2.9). In some localities, the carbonate unit is quite thin and contains shale beds in its lowermost part, making it difficult to be recognised from the broader shale of the Hagfa Formation. (Figs. 6.9 A&B)

The isopach map of the Beda Formation illustrates that the maximum thickness occurs in the central Zallah Trough, where it reaches upto1200ft and gets thinner eastwards, close to the boundary with the Dahra Platform (~500ft). It gets much thinner on the crest of the Dahra Platform where <300ft is recorded (Fig. 6.5A). Thus, thickness distribution and depositional pattern of the Beda Formation show a degree of similarity with those of the Hagfa Shale (thicker in the trough areas and thinner on the platforms), while they differ significantly from those of the Satal Formation. These are witnessed by the fact that the western margin of the Dahra Platform dips gradually into the Zallah Trough and thus the deepest part in the area shifted southwest-ward (Figs. 6.7A & 6.8).

During deposition of the Beda Formation the area was dominated by two local highs; on the Dahra Platform and in the Zallah Trough. The former, which persisted since the Danian, sloped gently towards the south and southwest. The latter, which seems to have developed during deposition of the Beda sediments, runs NNW-SSE, and is sub-parallel to the Gedari Fault (Fig. 6.5A). It is inclined gradually eastward

and steeply westward (towards the depocentre of the Zallah Trough). This is marked by a gradual and rapid increase in thickness of the Beda Formation in those directions, respectively. This could suggest that a significant change in palaeogeographic configuration of the study area occurred during deposition of the Beda Formation, which may be related to local tectonic activity. Bezan and Belhaj (1996) pointed out that the Beda Formation exceeds 1600 feet in the central Zallah Trough and they ascribed this variation in thickness to subsidence along the basement faults and the associated high rate of deposition. Shroter (1996) has documented that high subsidence rates in the trough areas indicate that renewed rifting occurred during the Paleocene, following the deposition of Hagfa/Upper Satal Formations.

The structural map at the top of the Beda Formation shows that the prominent highs, which were created during the Maastrichtian/Danian, were still in existence and kept the same direction. On the Beda level these features are as shallow as -2400ft depth on the Dahra Platform and parts of the Dor al Abid Trough. Low topographic areas at the end of the Beda deposition occurred mainly in the south western part of the study area (Zallah Trough), where the depth to the top Beda Formation is -6400ft (Figs. 6.7A & 6.8).

A notable feature is that at the end of Beda deposition the local depocentre in the east Zallah Trough shifted westwards (towards the central Zallah Trough) (Figs. 6.7A & 6.8). This may indicate that the eastern part of Zallah Trough was probably uplifted by the end of Selandian time. Van Der Meer et al., (1996) demonstrated that the east Zallah Trough experienced significant subsidence during the Late Maastrichtian and Danian, at which time it developed into a local depocentre, trapping large quantities of shale. During the Late Danian and Early Thanetian the east Zallah Trough was uplifted, but subsidence prevailed again toward the end of the Paleocene. During the top Danian/base Selandian a general tend towards uplift has been documented on the Dahra Platform. The same author demonstrated that the subsidence and uplift history for the Zallah and Maradah Troughs, and the Dahra and Zelten Platforms are rather uniform.

A shallowing of the sea, however, has resulted in the deposition of the Dahra carbonates almost all over the study area. On the Dahra Platform the Dahra Formation is mainly composed of light to yellowish grey wackestone to grainstone with thin interbeds of medium to dark grey, calcareous shale. In the Dor al Abid Trough the

Dahra Formation (Mabruk Mbr) is predominantly composed of wackestone/packstone and boundstone with thin intervals of marl, whereas in the Zallah Trough the Dahra Formation is more shaley and the limestone occurs locally in the middle and lower parts.

The isopach map of the Dahra Formation in the study area shows that it ranges from <190 to >500ft (Fig. 6.5A). The maximum thickness occurs again close to the western boundary of the Dahra Platform, where a narrow band of isopach contours trending northwest-southeast is present; corresponding to the direction of the regional Gedari Fault. The thickness of the Dahra Formation decreases away from this location, reaching its minimum thickness of 160ft in the north-eastern corner of the mapped area (Fig. 6.5A).

The regional structural map on top of the Dahra Formation shows that the palaeogeographic configuration developed during the deposition of the Beda Formation persisted (Figs. 6.7A & 6.8). This prominent feature perhaps suggests that the study area has not been affected by differential tectonic activity; it may have been subjected to a similar rate of subsidence in both structural elements. From the middle Paleocene to the early Eocene, rift tectonics had less significant control on sedimentation, and thickness variation from trough to platform was less pronounced (Rusk, 2002). Shroter (1996) also documented that after deposition of the lower Dahra, sedimentation took place on a levelled surface and thickness variations remained uniform into the Eocene. Moreover, petrographic examination and geophysical log correlation show that there are no drastic changes in the facies and associated microfacies throughout the Dahra Formation. It seems that the Dahra was probably deposited under similar conditions across the whole Dahra Platform.

In view of the lack of data, the limestone interval, locally dolomitic, of the Hiera Formation in the Dor al Abid Trough (Mabruk Member) has not been mapped separately; it is incorporated into the Dahra Formation in both isopach and structure maps (Figs.6.5A & 6.7A). The Mabruk rocks show complex lateral and vertical variations from the west through central to eastern Mabruk areas. The broad situation of the area is reflected in the structure maps on top of the Beda and Dahra Formations; they show that a local high developed in the Mabruk area (northwestern part of the mapped area) with an average difference in its elevation (relief) of about 700ft.

6.2.2.3. Thanetian Succession (Khalifa, Zelten, Harash and Kheir Formations)

The transgression that occurred during the early Thanetian (end of the Dahra Formation) resulted in the deposition of the Khalifa Formation across almost all of the Sirt Basin. On the Dahra Platform the Khalifa Formation consists of an upper argillaceous limestone unit and a lower shale interval. The limestone is mainly wackestone/packstone, dark grey, moderately indurated and argillaceous with minor calcareous shale. The lower shale unit is dark grey to black, fissile and slightly pyritic with local thin calcareous intervals.

The thickness of Khalifa Formation gradually increases from the Dahra Platform to the Zallah Trough. On the former it is usually less than 180ft, whereas in the latter it exceeds 450ft (Fig. 6.5B). An average of 220ft is recorded in the Dor al Abid Trough. The structure contour map on top of the Khalifa Formation shows almost the same palaeogeographic configuration as the Dahra Formation (Figs. 6.7B & 6.8).

As noted in Chapter 5, the Zelten Limestone strongly suggests an overall regressive interval, with a probable prograding trend upto the top of the Formation. On the Dahra Platform, the Zelten Formation consists predominantly of light grey to light yellowish grey limestone, slightly argillaceous and locally dolomitic. The limestone is mainly a grain-supported packstone and consists primarily of benthic forams, molluscan shells and echinoderm fragments with less common nummulites and bryozoans. Mud-supported carbonates, which are frequently dolomitized, are sporadically present.

The isopach distribution of the Zelten Formation in the study area shows that the thickest section occurs in the southeastern corner of the mapped area, at the Zallah Trough/Dahra Platform periphery, where it exceeds 400ft (Fig. 6.5B). The thinnest sections of <200ft, on the other hand, are developed in two local areas; on the western edge of the mapped area, and in the northern part of the Zallah Trough. The former coincides with the overall structural elements in the area, but the latter could suggest the development of a new structural high during deposition of the Zelten Limestone in the Zallah Trough. This is indicated by the fact that isopach contours are very close to each other and oriented at right-angles to the main structural elements in the area (northeast-southwest). Alternatively, the lack of enough well data in that particular area could be the main reason for this contour band; bearing in mind that this feature

is not recognized during deposition of the older Khalifa or the younger Harash Formations.

The Zelten Formation in the north central Sirt Basin, where it represents the main reservoir, reaches around 700ft in thickness, of mostly shallow-marine facies. It thins northward and disappears along the coastal area where the Paleocene succession is represented by a thin shale section (Bezan, 1996).

The isopach map of the Harash Formation in the area under investigation illustrates that the Zallah Trough has accommodated the maximum thickness in the study area (>300ft). This thickness decreases away from the Zallah Trough north-northeast ward, reaching its minimum of <100ft on the Dahra Platform (Fig. 6.5B). In the central part of the basin, in the Maradah and Ajdabiya Troughs, it is about 200ft thick (Hallett, 2002). The palaeotopography on top of the Harash Formation is almost identical with that of the Zelten Limestone (Figs. 6.7B and 6.8).

The Paleocene/Eocene Kheir Formation is widely distributed throughout the Sirt Basin. In the study area, however, it comprises shale, marl and less common carbonate. Its thickness ranges from <200ft in the mapped area of the Dor al Abid Trough to >400ft in the Zallah Trough (Fig. 6.5B).

A northeast-southwest trending structural low was developed during deposition of the Kheir Formation in the study area. It has a similar orientation and is in the same area, though larger, to that formed through the deposition of the Khalifa Formation (Figs. 6.5B, 6.7B & 6.8). Subsidence prevailed again towards the end of the Paleocene in East Zallah and the Dahra Platform (Van Der Meer et.al., 1996). The palaeotopography on top of the Kheir Formation is almost identical with that of the Harash Formation (Figs. 6.7B & 6.8).

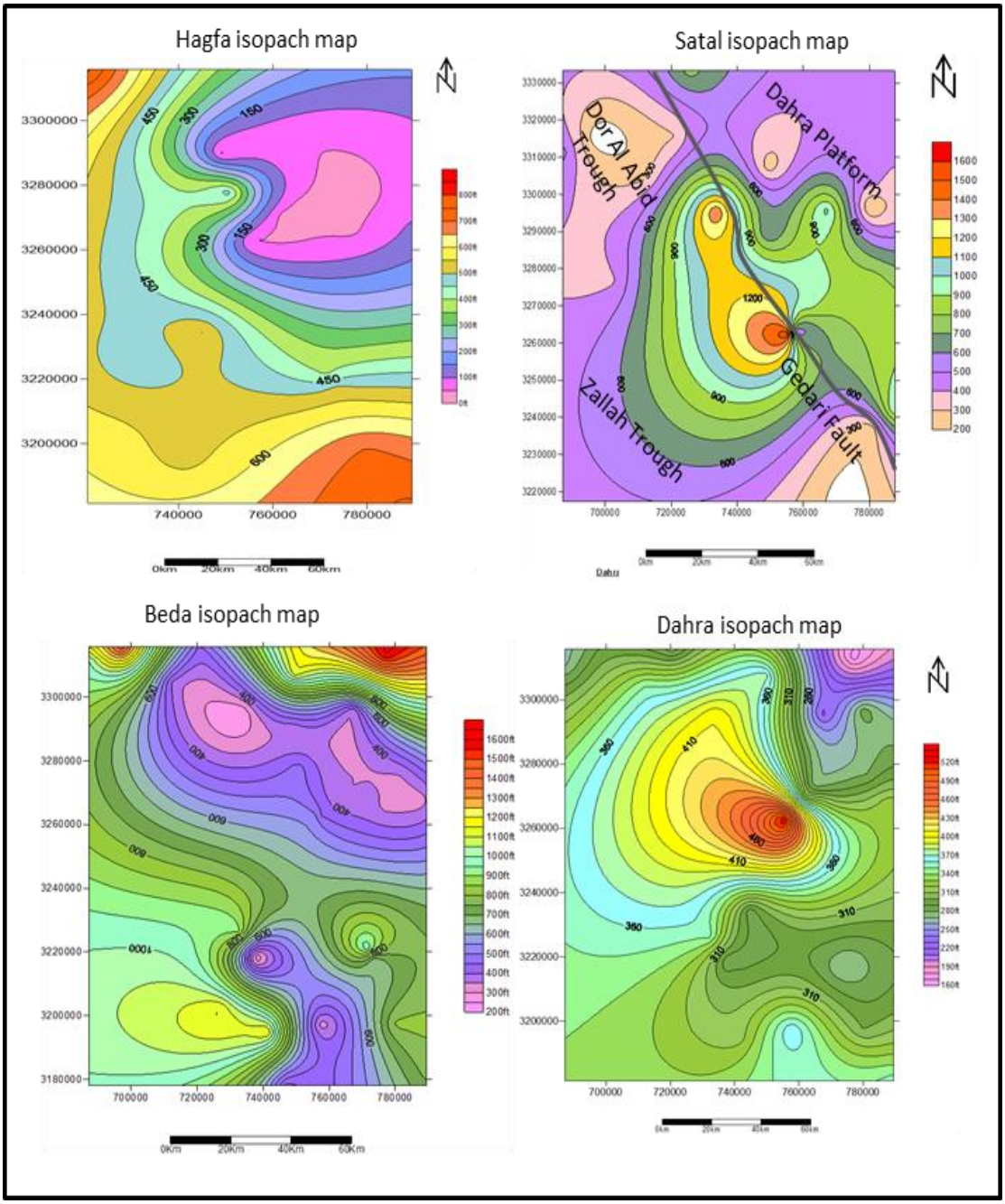

Figure 6.5A Regional isopach maps for the Danian-Selandian/Thanetian section in the study area (Hagfa, Satal, Beda and Dahra Formations).

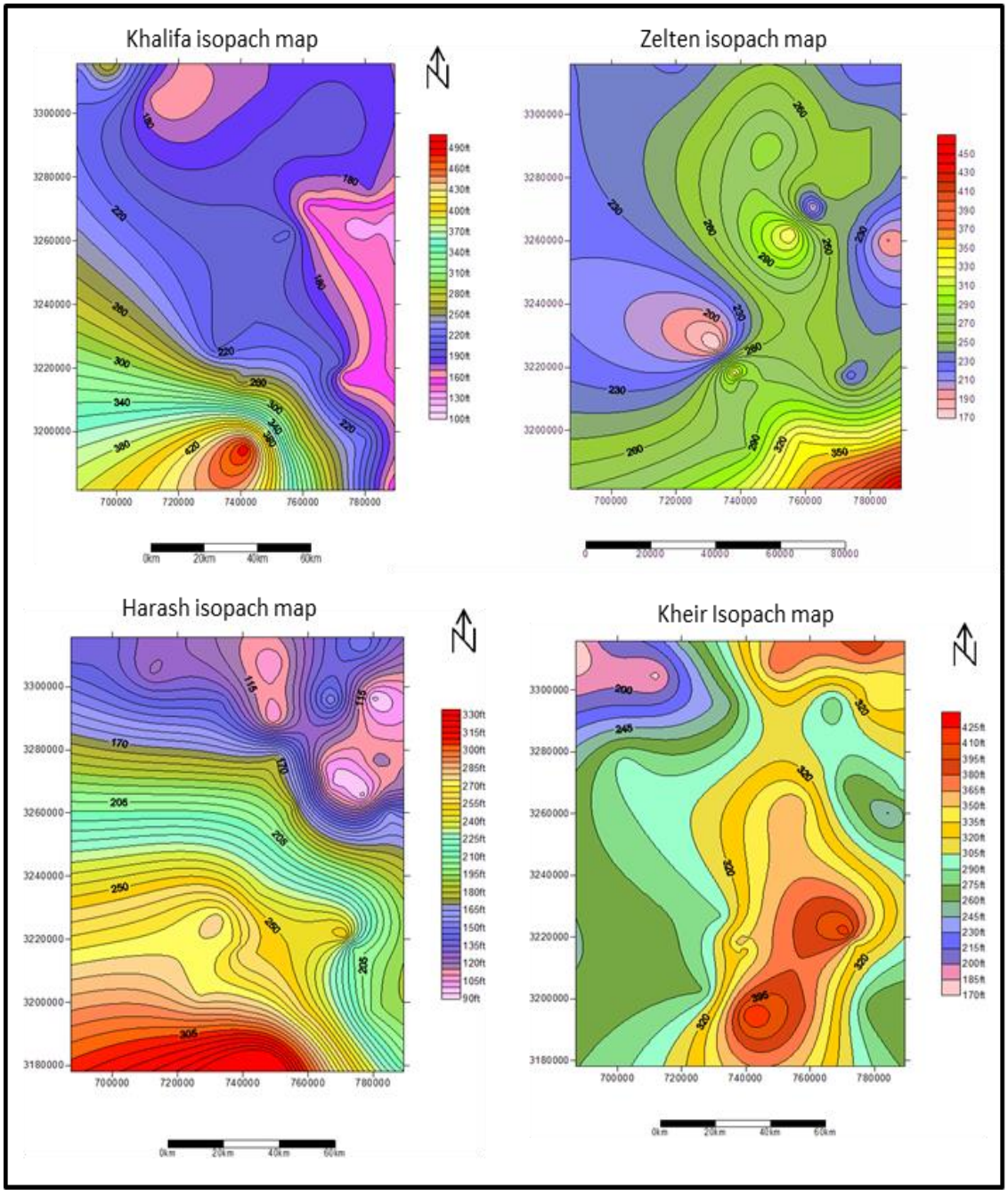

Figure 6.5B Regional isopach maps for the Thanetian succession in the study area (Khalifa, Zelten, Harash and Kheir Formations).

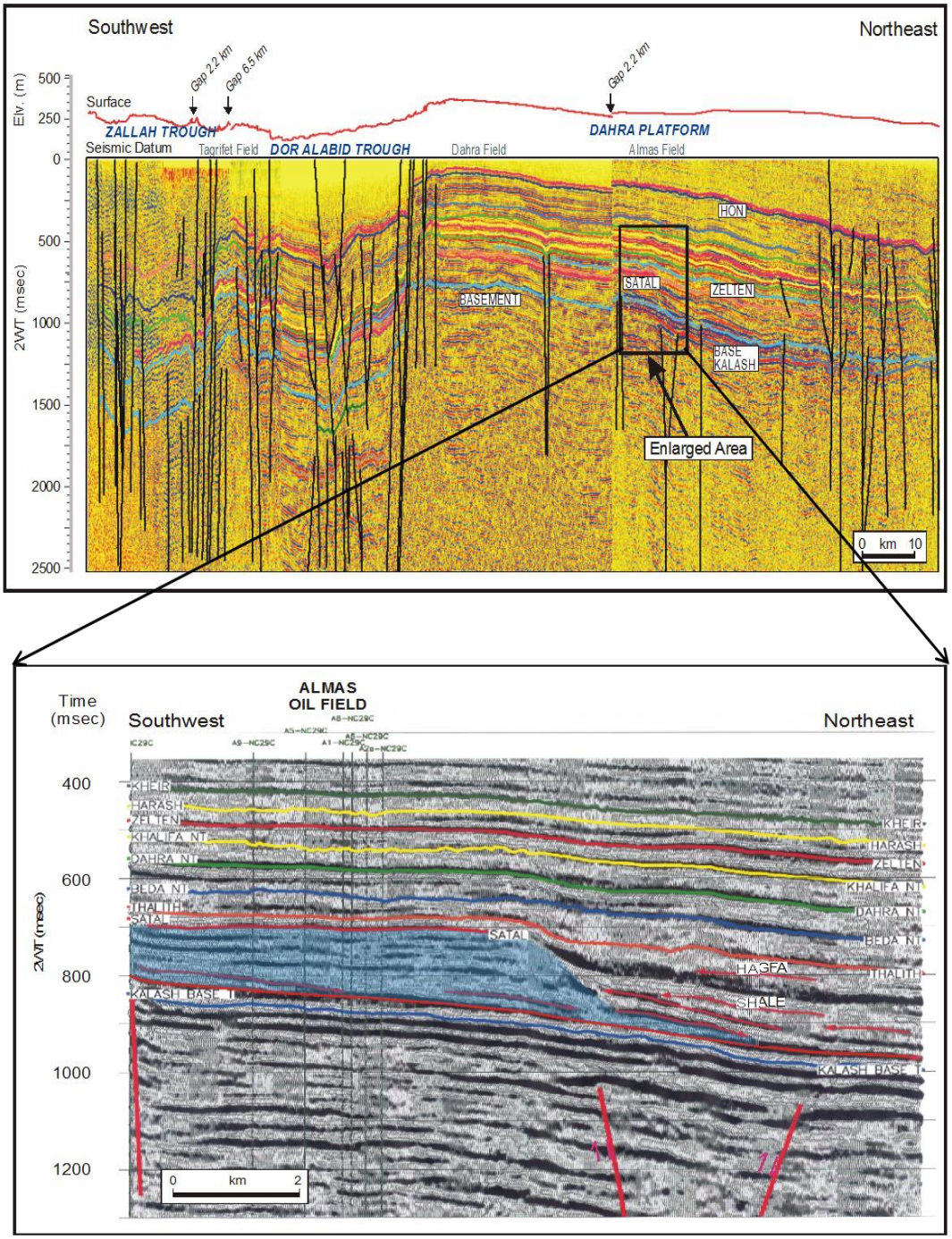

Figure 6.6 Seismic traverse across the Zallah & Dor al Abid Troughs and the Dahra Platform. The enlarged area of the seismic section is showing the details of the onlapping of the Hagfa Shale onto the Satal Carbonate Bank. Note also the uniform thickness of the post-Satal rock units (layer-cake strata) (from PRC and TPS, 2003).

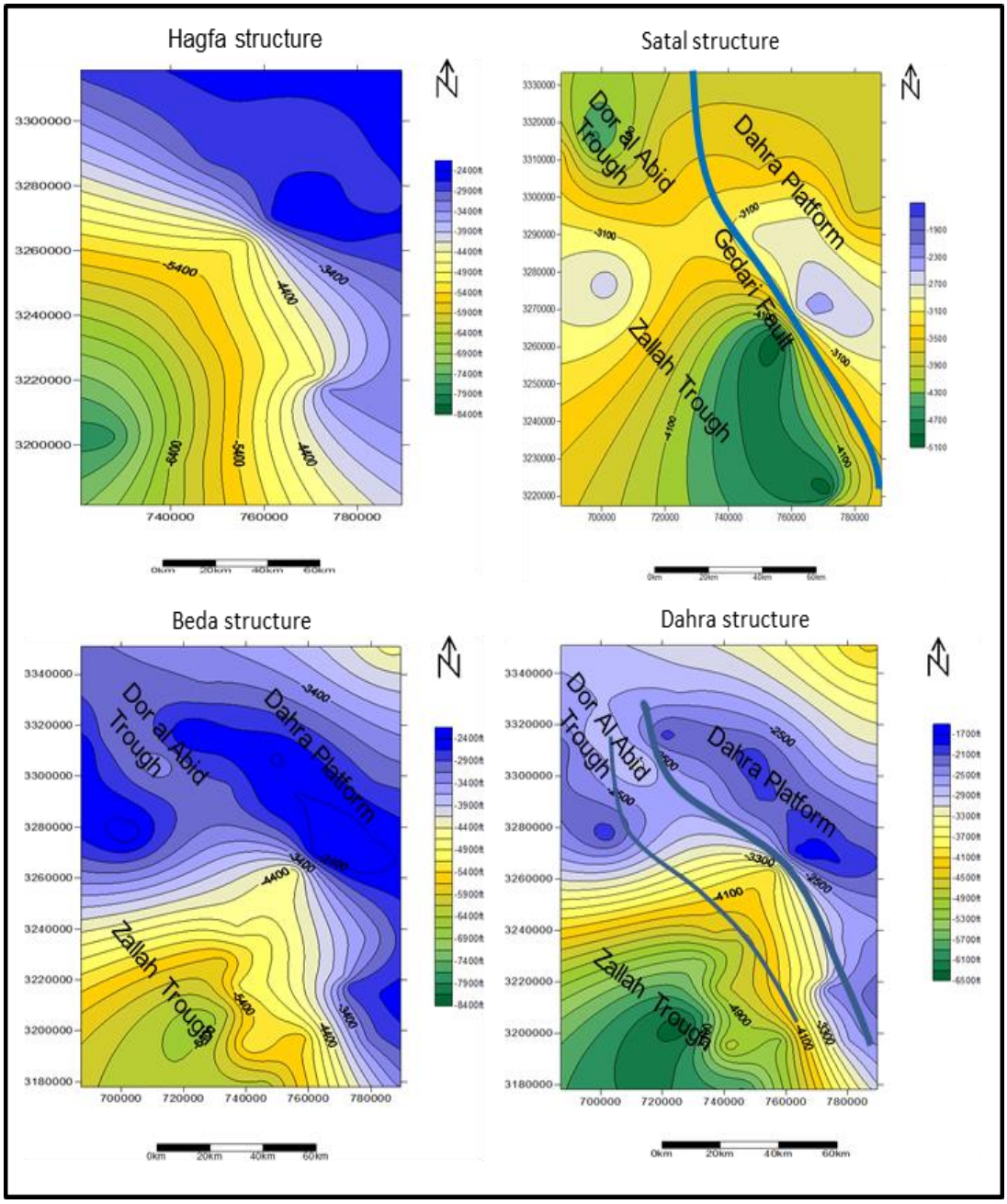

Figure 6.7A Structure contour maps for the Hagfa, Satal, Beda and Dahra Formations in the study area (Danian-Thanetian section).

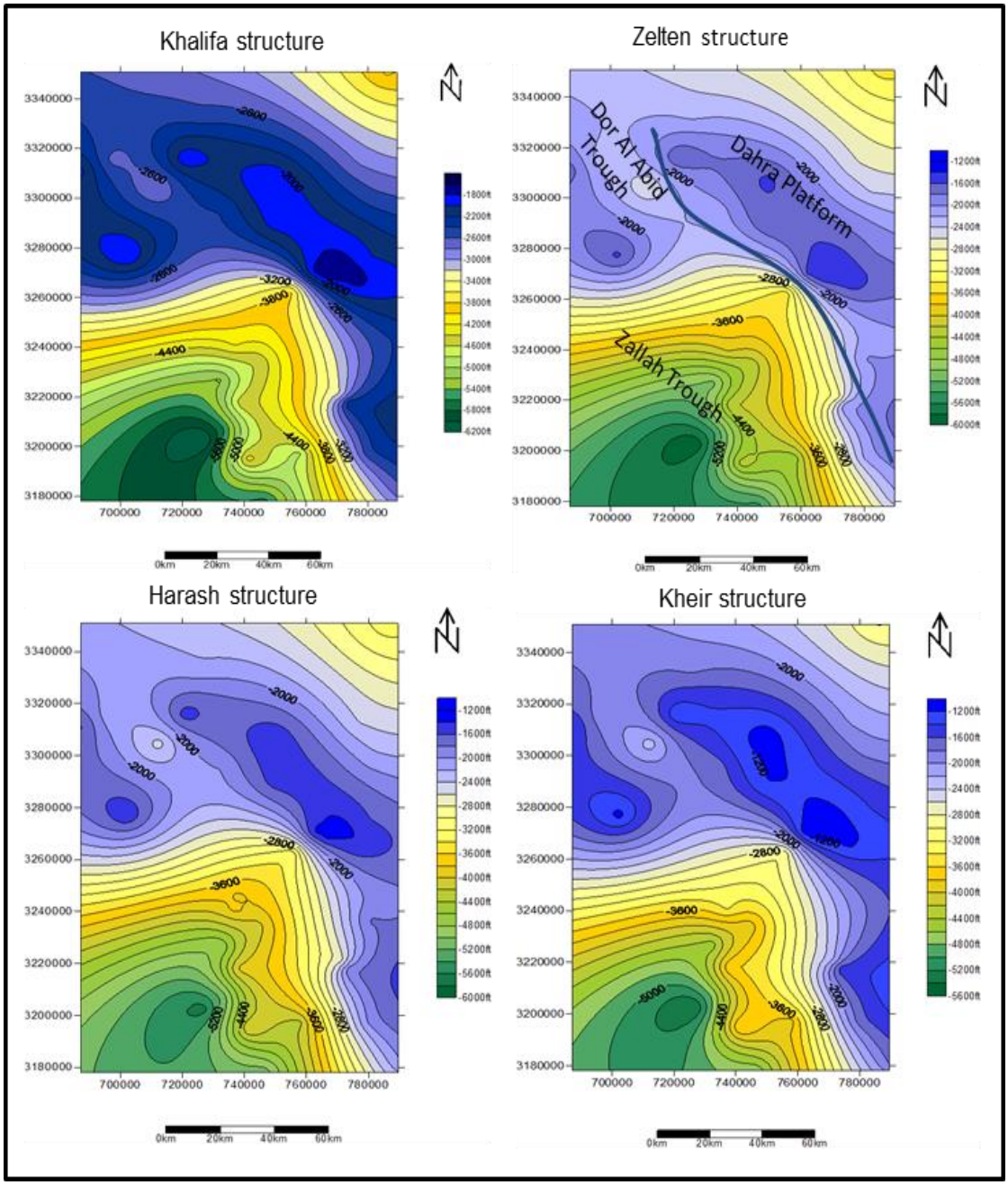

Figure 6.7B Structure contour maps for the Khalifa, Zelten, Harash and Kheir Formations in the study area (Thanetian section).

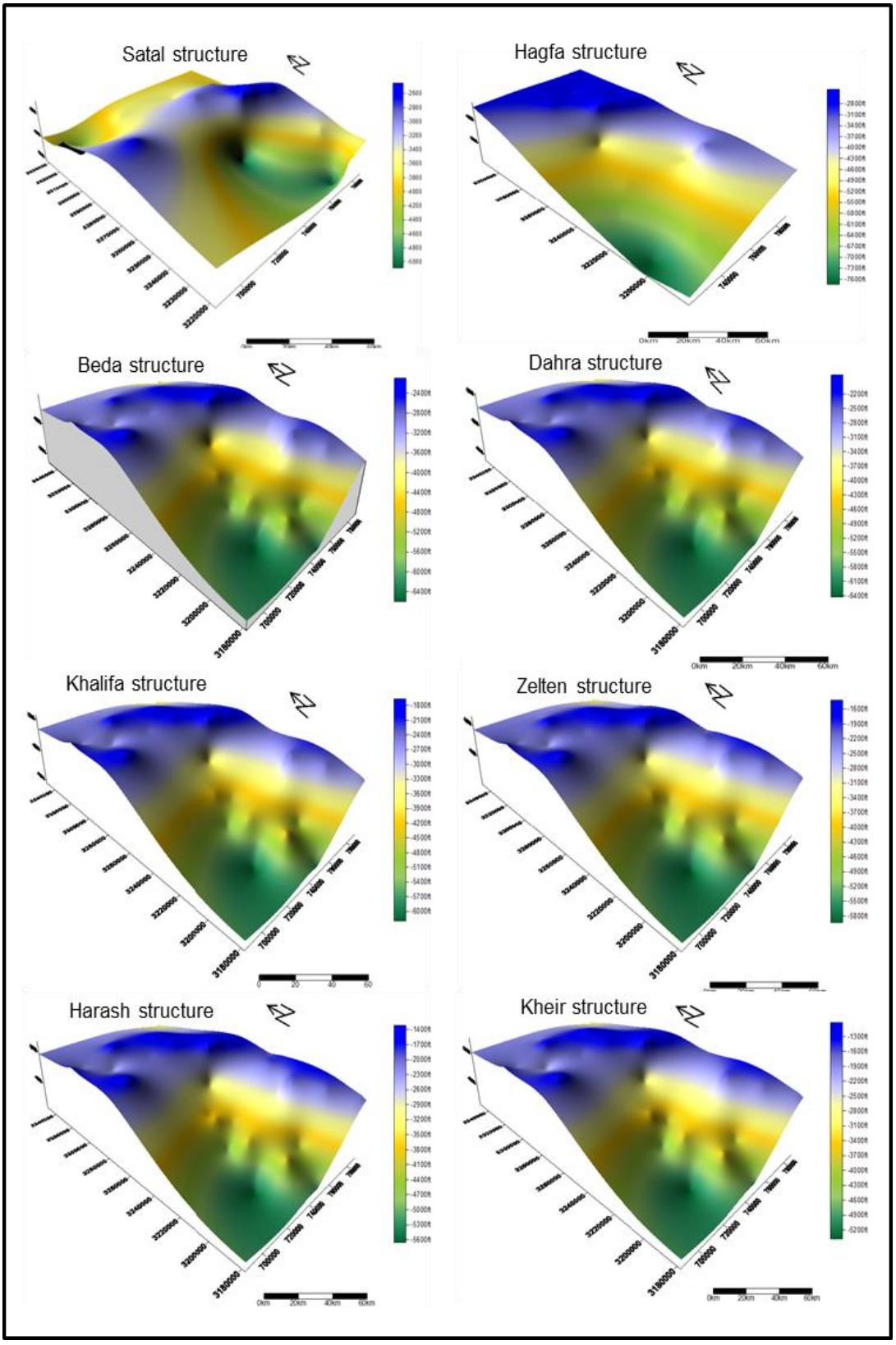

Figure 6.8 3D Structure maps for the entire Paleocene Succession (Hagfa, Satal, Beda, Dahra, Khalifa, Zelten, Harash and Kheir Fms) in the study area.

6.3. Discussion

6.3.1. Sedimentation and facies variability

In the central part of the Al Hagfa Trough, the eastern border of the Dahra Platform, a thickness of over 4000 feet of Paleocene is documented (Wennekers et al., 1996). In the offshore area of the Sirt Basin, the thickness of the Paleocene succession is <100ft (Bezan, 1996). The same author ascribed this thinning to the low rate of deposition (starvation), which might be evidence that the coastal area was uplifted during the early Paleocene by the tectonics of the Atlas wrench fault located north of the modern Libyan coastline.

The Paleocene succession in the study area shows dissimilar thickness in the Dahra Platform and the adjacent Trough when levelled to the top of the Ypresian Facha Member and it shows an almost identical thickness across the Dahra Platform (layer-cake strata) except in the area south of the Bahi Field, where a local depression (probably fault related) has been identified (Fig. 6. 9B). The overall thickness and facies of the Paleocene is commonly close to the underlying structure; thicker in the trough areas and thinner over the platforms. Its total thickness in the Zallah Trough and adjacent areas exceeds 3200ft, whereas on the Dahra Platform and other high areas less than1500ft is recorded (Fig. 6. 4). The thickness difference between the platform and the Trough strata suggest that the trough areas were possibly still subsiding with probably compactional-induced. This gave rise to in a local differential subsidence on both structural elements and hence resulted in the difference in accommodation space.

The thickness distribution of different rock-units in the study area virtually coincides with the isopach arrangement of the Danian, Selandian/Thanetian and the entire Paleocene succession (Fig. 6.10), the carbonate-dominated facies are preferentially located over the major platforms and local highs, whereas the main troughs and low topographic areas are filled mainly with shale and/or marl. The Hagfa Formation has been considered as characteristic of the shallow basins, since it is present throughout the central Sirt Basin as a deeper-water equivalent of the shelfal carbonates. In the study area, however, the Hagfa Shale becomes increasingly calcareous and changes abruptly to the Satal Carbonate.

The regional carbonate Satal Bank, which the author believes was established at the base of the Danian, trends almost at right angles across the Gedari fault zone

with almost similar carbonate facies across the area. This may indicate that the pre-existing substrate during the Maastrichtian played a vital role in the distribution of the Danian Satal carbonates. The widespread distribution of the Maastrichtian Kalash limestone across the Sirt Basin with distal and proximal facies could support this explanation. Besides, Hallet (2002) pointed out that the trough areas in the Sirt Basin had been largely filled by the end of the Maastrichtian, and the topography of the intervening platforms had been levelled to the extent that only very small islands remained.

As shown earlier, the maximum thickness of the Selandian Beda Formation occurs in the central Zallah Trough, where it reaches upto1200ft, and >1600ft has been recorded in the southeast of the study area (Bezan, 1996), whereas on the Dahra Platform it reaches only 300ft. Over large parts of the study area the Beda Formation, regardless of its thickness, is composed mainly of shale (Rabia Mbr) with relatively thin limestone (Thalith Mbr). This discrepancy in thickness and similarity in the facies type could indicate that the rate of deposition was relatively high and outpaced subsidence rates in the trough areas; sedimentation kept pace with subsidence, since high rates of subsidence during the Selandian have been documented (Shroter, 1996). The change in the position of the deepest part of the study area (Zallah Trough) towards the southwest by the end of the Selandian time (Fig. 6.8), in association with uplift of the east Zallah Trough, could be ascribed to the westward shift of Africa relative to Europe during the Paleocene (Anketell, 1996), one consequence was the deposition of thick shale units and relatively deep carbonates in the low topographic areas, and shallow carbonate facies sealed by thin evaporates, on the high areas of the Zallah Trough (Lower Beda and Upper Beda Members). On the platform areas, the classic lithology of the Beda Formation (limestone and shale) resumed.

An abrupt shallowing of the sea resulted in the deposition of the Dahra carbonates across large parts of the study area. It becomes more argillaceous and shaley in the east Zallah Trough, and is replaced by the Khalifa Shale to the east and south east of the Dahra Platform.

The overall facies of the Dahra Formation is quite similar, particularly on the platform areas. In the Dor al Abid and Zallah Troughs it comprises boundstone and marl, and shale and argillaceous limestone, respectively. This facies discrepancy could be attributed to a differential subsidence across the Dahra Platform and Dor al

Abid/ Zallah Troughs, along with the development of local faulting, particularly in the Mabruk area (Dor al Abid Trough). The thickness distribution of the Dahra Formation corresponds with the isopachytes of the entire Paleocene succession. This could suggest that the Gedari fault was active (syn-sedimentary) during deposition of the Dahra Formation, and the rate of tectonic subsidence (differential subsidence) of the platforms and the troughs throughout this interval was nearly similar.

The overall interval of the Mabruk Member in the study area represents deposition of mainly shallow-water carbonates that were bounded by deeper-marine marl and shale; these accumulated in lagoonal and reefal environments in a probable rimmed-shelf setting. The local relief developed in the Mabruk area (~700ft), which probably resulted from local faulting, could explain the development of the various facies in that particular area (lagoon and reef).

The depositional pattern of the Khalifa Formation seems to have been controlled by the pre-existing palaeotopography; as it is thicker in the troughs and thinner on the platform. This thickness discrepancy is probably an additional indication of penecontemporaneous faulting along the trough margins. The regressive and prograding strata of the Thanetian Zelten Limestone on the Dahra Platform are almost identical and composed mainly of wackestone/packstone facies, with local development of large benthic forams, including nummulites. This is almost the case with the overlying Harash Formation with a near uniform thickness and facies across the study area.

In the north central Sirt Basin, the Zelten Formation consists mainly of shallow-marine facies with common corals, algae and hydrozoans, and its thickness in that area is about twice that of the study area (700ft and around 400ft). Both thickness discrepancy and facies variation of the Zelten Limestone across the Sirt Basin is probably attributed to the pre-existing topography that might be coupled with sea-level fluctuations.

The situation during deposition of the Harash Formation a cross the basin was slightly different; its average thickness in the study area and surroundings is about 250ft (~76m) with an almost similar facies. This could suggest that a fairly uniform topography/ or low relief occurred prior to the deposition of the Harash Formation in the study area (at the top of the Zelten Limestone).

Being mainly composed of grey, greenish grey to dark grey shale with some mud-supported limestone, the thickness distribution of the Kheir Formation slightly varies from that of the Harash Formation. This is probably attributed to that the subsequent erosion that the Kheir Formation experienced (Wennekers et al., 1996). The Kheir shale interval represents the time when major changes in the dynamic tectonic regime strongly influenced the distribution and activity of the microcontinents between Eurasia and Afro-Arabia (Smith, 1971; Dewey et al., 1973). This together with the possible increase in igneous activity during the Selandian-Thanetian interval could suggests that tectonic influences may have been dominant over eustasy in controlling the Kheir facies (Baird et al., 1996).

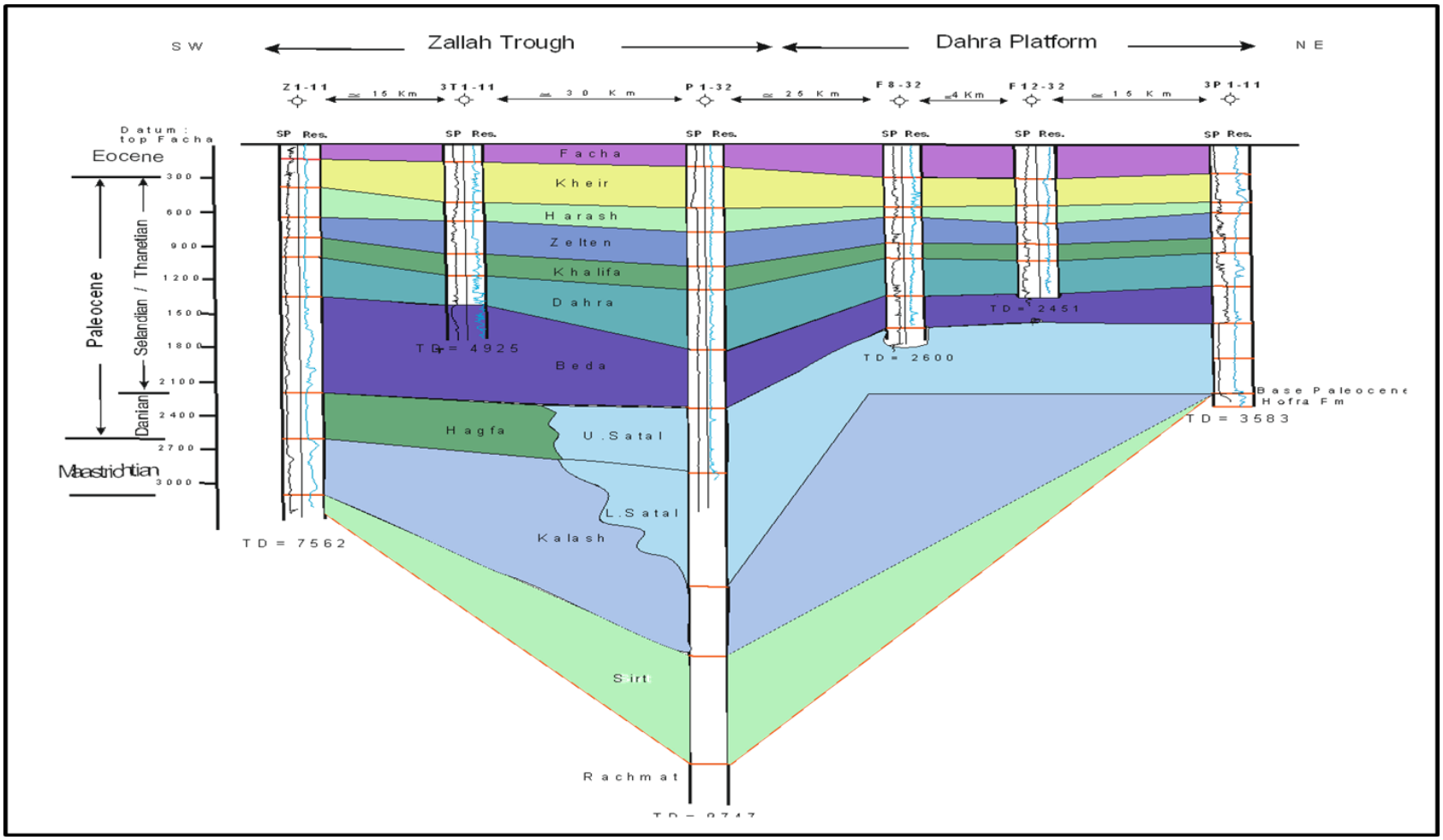

Figure 6.9A Stratigraphic cross-section across the Zallah Trough and the Dahra Platform in the study area.

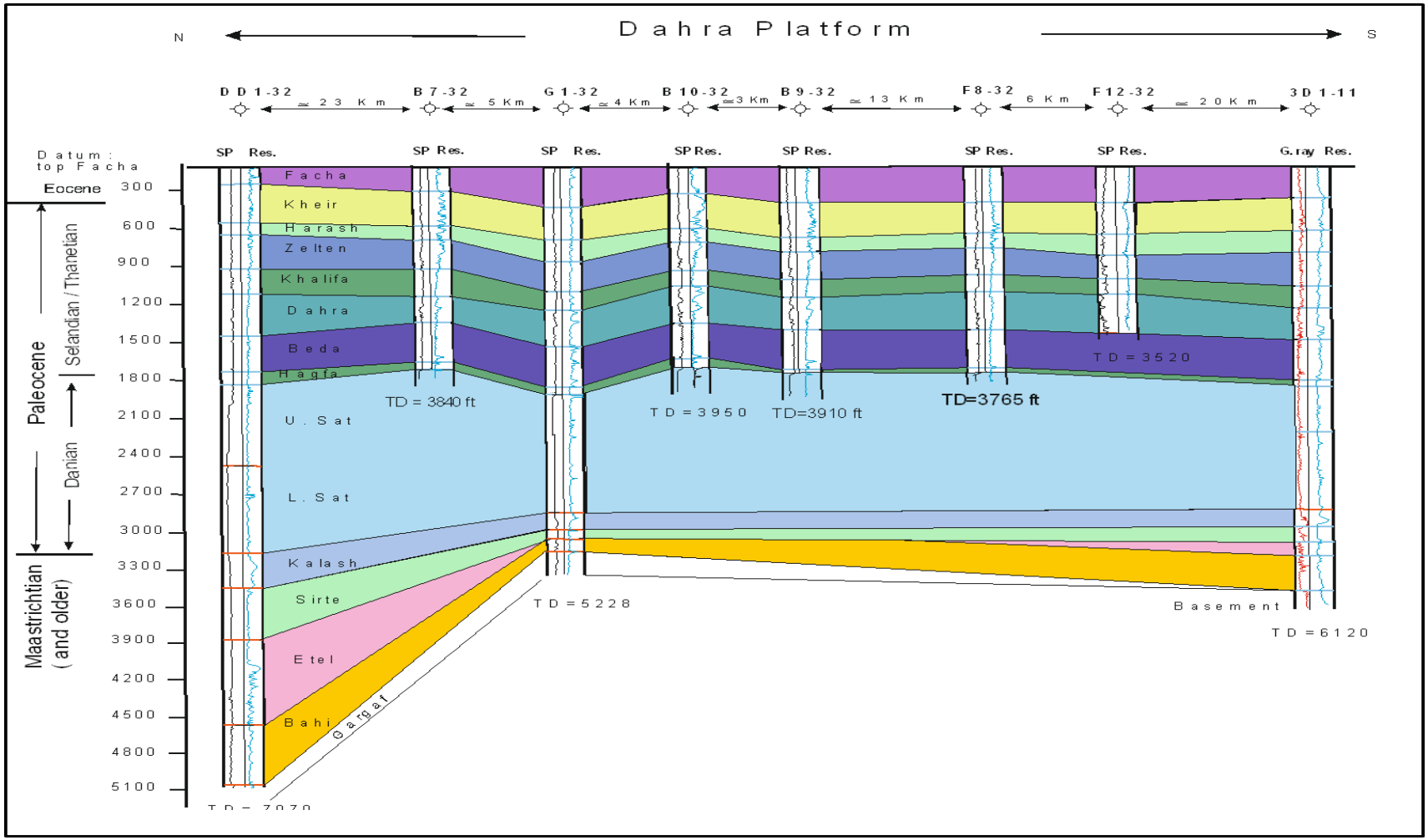

Fig. 6.9 B Stratigraphic cross-section along the western part of the Dahra Platform in the study area.

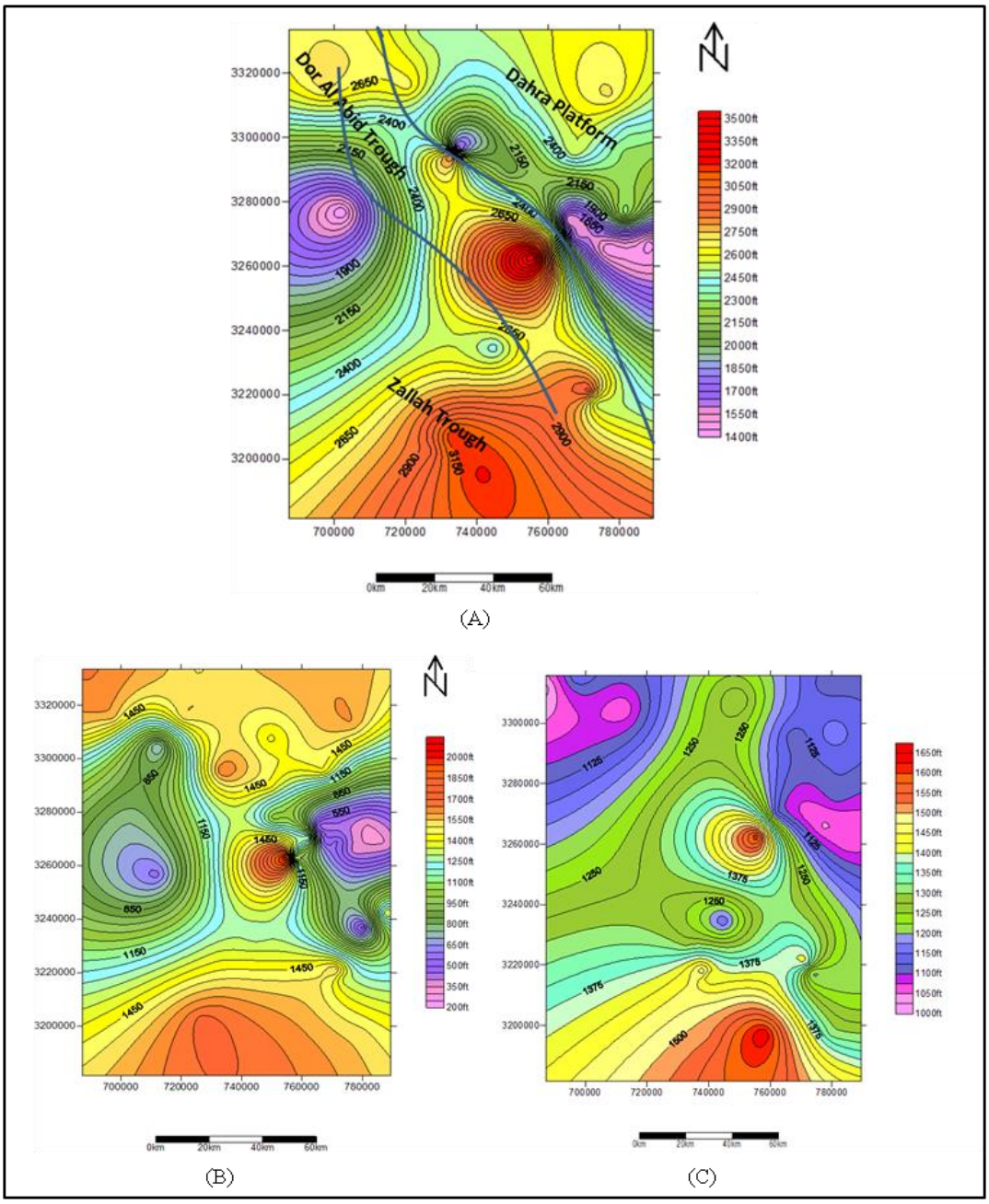

Figure 6.10 Regional isopach maps for the Paleocene Succession; A: total Paleocene, B: Danian/Selandian Section (the Satal, Hagfa and Beda Formations), and C: Selandian/Thanetian Section (the Dahra, Khalifa, Zelten, Harash and Kheir Formations).

6.3.2. Burial history

A new phase of crustal extension beneath the Sirt basin in the Paleocene time was possibly related to the movement of the African Plate towards the northeast. Both Northwestern and Northeastern Africa remained stable in the late Paleocene, but uplift occurred in northern Africa and rifting in central Africa (Guiraud et al., 2005; Swezey, 2009).

Van Der Meer et al., (1996) documented a small uplift at 61 Ma from several wells in the Zallah Trough, which corresponds to the base of the Beda Formation. According to the well-log investigation in the Zallah Trough area, the uppermost part of the Beda Formation is characterized by the occurrence of evaporite beds, which Knytl et al., (1996) attributed to a sabkha environment that existed at the close of shallow-marine shelf deposition. Therefore, this tectonic event (uplift), probably together with sea-level could support the idea that these factors controlled the thickness and facies variations of the lower Paleocene succession across the study area. These facies variations resumed through the whole Danian and most of the Selandian times, but in the latest Selandian-Thanetian/Ypresian the overall facies changes became less pronounced. The Thanetian-Ypresian in the Sirt Basin is characterized by the regional subsidence rates in both grabens and horsts in the basin's history, and hence the middle Paleocene to the early Eocene period rift tectonics had less control on sedimentation (Rusk, 2002).

Wire-line log interpretation and petrographic investigation revealed that the Selandian/Thanetian strata on the Dahra Platform have similar thickness and comparable facies, and were affected by various processes during their deposition and burial. These are summarised in a schematic diagram that shows burial history of the studied succession, fluid inclusion results, stable isotopes and the main burial diagenetic features, along with the previous published subsidence curves in the study area (Fig. 6.11). Van Der Meer et al., (1996) curve, in the Dor al Abid Trough (well P1-32) shows that significant subsidence occurred during the Late Maastrichtian and Early Paleocene, and minor uplift occurred at the top of the Danian (between the Beda and Hagfa Formations), and close to the Kheir Formation/Facha Member boundary. The PRC&TPSL curve on the other hand, exhibits a high subsidence rate during the Middle Paleocene to Early Eocene time, followed by a small uplift in the Middle Eocene (Fig. 6.11).

On the Dahra Platform, although the Van Deer Meer et al., (1996) and Abadi et al., (2008) curves show a fairly similar degree of subsidence during the Late Paleocene/Early Eocene, both diagrams do not exhibit any significant uplift during the Mid-Tertiary. Abadi et al., (2008) concluded that tectonic heat-flow modelling in agreement with the observed uplift in the western Sirt Basin calibrated to observed maturation data, indicates elevated Tertiary palaeo-heat flow in the western Sirt Basin indicative of early and/or late Oligocene and Miocene underplating, preceding erosion.

As discussed in Chapter 4, The carbon isotope values of the Zelten and Harash Formations on the Dahra Platform in the east and west fields are quite similar and confined to a narrow range between +2.22‰ to +3.86‰, whereas the oxygen isotope values are somewhat varies. The fluid inclusion analysis yielded a temperature of 59^0C at depth of 2788ft in well no.8 (Zelten Fm); the depth at which the δ^{18}O and δ^{13}C recorded -6.00‰ and 3.62‰, respectively (Fig. 4.13). Assuming that the isotope values are accurate, the carbon isotope values are typical, probably original marine values, whereas the δ^{18}O value is slightly too negative for meteoric water, suggesting a high temperature phase of burial diagenesis, with the precipitation of calcite that shows dull to non-luminescence characters (Fig. 6.11). Moreover, the location of this interval within the TST3 of the LPS3 strongly suggests burial diagenesis. The overall coincidence and similarity of δ^{13}C and δ^{18}O trends of the studied succession could reflect late diagenetic over-printing caused either by the interaction with meteoric ground-waters or, almost certainly, by dissolution and recrystallisation at higher temperatures during burial diagenesis (Sakai and Kano, 2001; Keller et al., 2004).

According to the geothermal gradient of the Sirt Basin, which ranges between 22-25 ^{0}C/km (Gumati and Schamel, 1988), the temperature at the present depth where the samples are taken (Zelten Fm) should be between 47.7^0C and 50.2^0C. However, the palaeogeothermal gradient could have been much higher than that of today, and could exceeded 35^0 C/km. The first possibility suggests that the recorded fluid inclusion temperature (59^0C) is either due to hydrothermal fluid flow from deeper parts of the area and/or the result of low sedimentation rates and high thermal conductivities of carbonates; the second option could support the idea of uplift and substantial erosion during the Late Tertiary (Fig. 6.11). Additionally, the presence of thick lower Eocene evaporites (~1200ft) on the overlying interval seem have not

contributed. This is indicated by the fact that the temperatures provided by fluid inclusion (both aqueous and petroleum) in the Harash Formation are higher than those of the Zelten Formation (see Table 4.4). Mellow et al., (1995) and Taylor et al., (2010) pointed out that as a result of the high thermal conductivity of salt, a zone of suppressed temperature occurred beneath thick salt sequences; the thermal conductivity of salt is highly temperature dependant and decreases with increasing temperature, thus the contrast is greatest at shallow depths of burial. This is not the case in the study area, as accordingly the temperature of the Zelten Formation supposed to be even lower than 47.7-50^{0}C. Thus, these observations could suggest that the above stated possibilities, accompanied by Mid-Late tertiary uplift and erosion are all contributed.

Abadi et al., (2008) pointed out that maturation depth trends in the western Sirt Basin are slightly higher than in the east, indicative of elevated palaeogeothermal gradients in the Tertiary (up to 30˚C/km). They attributed the high vitrinite reflectance values (R_o) in the area to late Tertiary erosion of about 3280ft, as suggested by Gumati and Schamel (1988). The latter authors pointed out that in the Dor al Abid Trough (well no. 3Q1-11) the organic maturity data of the Tertiary is immature (Ro <0.5%) and the Upper Cretaceous is highly mature (1.2Ro). The elevated maturities at shallow depths in this well suggest an earlier deeper burial of these rocks, i.e. a significant amount of sediment was removed by uplift and erosion. This is evidenced by the fact that the Upper Eocene, Oligocene and Miocene rocks are developed in the subsurface of the central and eastern parts of the basin (see Fig. 2.9). In addition, the total Miocene section has been largely removed by erosion in the Cyrenaica region, in eastern Libya, but thin remnants persist to the east towards Egypt, attesting to their original wide distribution (Wennekers et al., 1996).

The overall palaeotopography throughout the Paleocene seems generally similar; there is no substantial variation between the base and the top of the Paleocene succession, except for the development of a local high that became a prominent feature after deposition of the Beda Formation (Selandian) (Fig. 6.12); this is, despite the fact that it was possibly initiated by the end of Satal Bank time. It probably separates the Zallah and the Dor al Abid Troughs.

The tectonic subsidence map for the Paleocene-Early Eocene (Abadi et al., 2008) reveals that the study area was subjected to a fairly similar rate of subsidence,

except in the northern part; it shows that the overall subsidence in the Dahra Platform, Zallah and Dor al Abid Troughs during this period was around 100-125m (~300–400ft) (Fig. 6.2). These values are greater than those of the Maastrichtian time (75–100m, ~160-300ft, according to Abadi et al., 2008) which could support the idea of transgression at the base of the Paleocene, taking into consideration that these values are general and there might be a local discrepancy within each structural element.

Generally, the thickness of the total Paleocene strata in the trough areas is more than twice that on the platforms. Specifically, the thickest Paleocene section, and its sub divisions, is located in the southern and the central parts of the study area (Zellah Trough) (Fig. 6. 10). The former, which is close to the centre of the Zallah Trough, could refer to the differential subsidence between the platform and trough areas, whereas the latter is close to the Gedari Fault that separates the Dahra Platform and the Dor al Abid/Zellah Trough, i.e. just at the fault escarpment. This area could represent the centre of the fault zone, where subsidence is greater than the rate of eustatic fall (Gawthorpe and Leeder, 2000), and sedimentation can keep pace with the sea-level rise. This evidenced by the fact that apparent vertical displacement of the Gedari Fault at the Dahra Platform/Zallah Trough boundary is >1500 feet, whereas it is much less towards the north, at the Dahra Platform/Dor al Abid Trough boundary and within these structural elements (Figs. 6. 9 and 6.10).

This spatial variation in the Paleocene thickness could indicate that faulting along the edges of the trough areas was penecontemporaneous, with the rate of subsidence in the troughs, and was greater than that of the platforms, and hence resulted in thicker sediment accumulations in the former. The spatial and temporal variations in displacement have a significant impact on relative base level and accommodation around normal fault zones (Gawthorpe and Leeder, 2000).

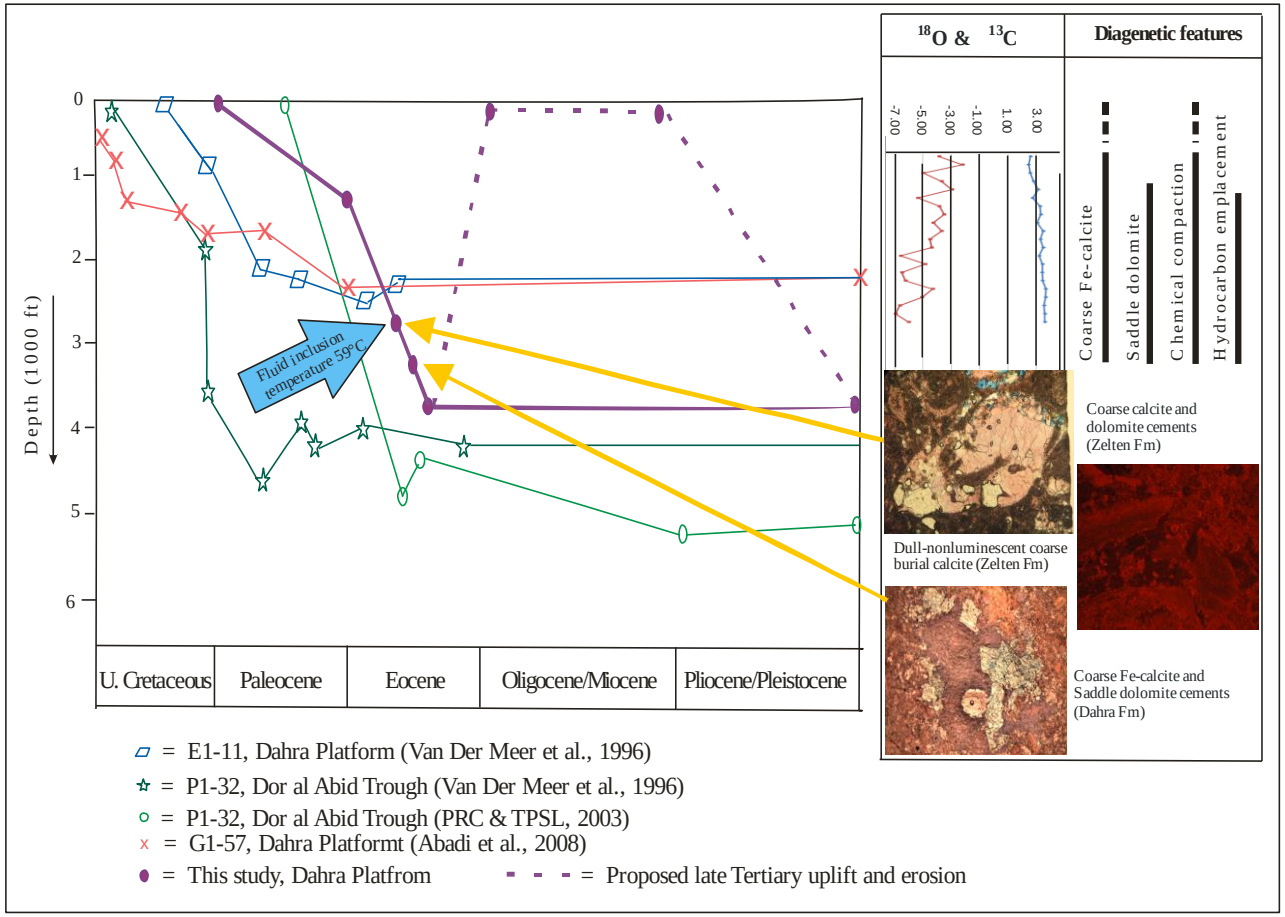

Figure 6.11 Proposed schematic burial diagram of the Paleocene succession in well no. 8 on the Dahra Platform. Two extreme scenarios are shown; proposed Tertiary uplift against continuous burial up to the present day, along with stable carbon and oxygen isotopes and mesogenetic features. The fluid inclusion temperature is recorded in Zelten Fm at current burial depth of 2788ft. Some of the published tectonic subsidence curves for the Dahra Platform and the Dor al Abid/Zallah Trough are also shown.

The Mabruk area experienced extensive faulting with a predominantly NNW-SSE trend of normal faults. This faulting has probably resulted in the different topography, and formation of local highs in the Mabruk area, which could have given rise to the development of different depositional environments on the broad carbonate shelf setting.

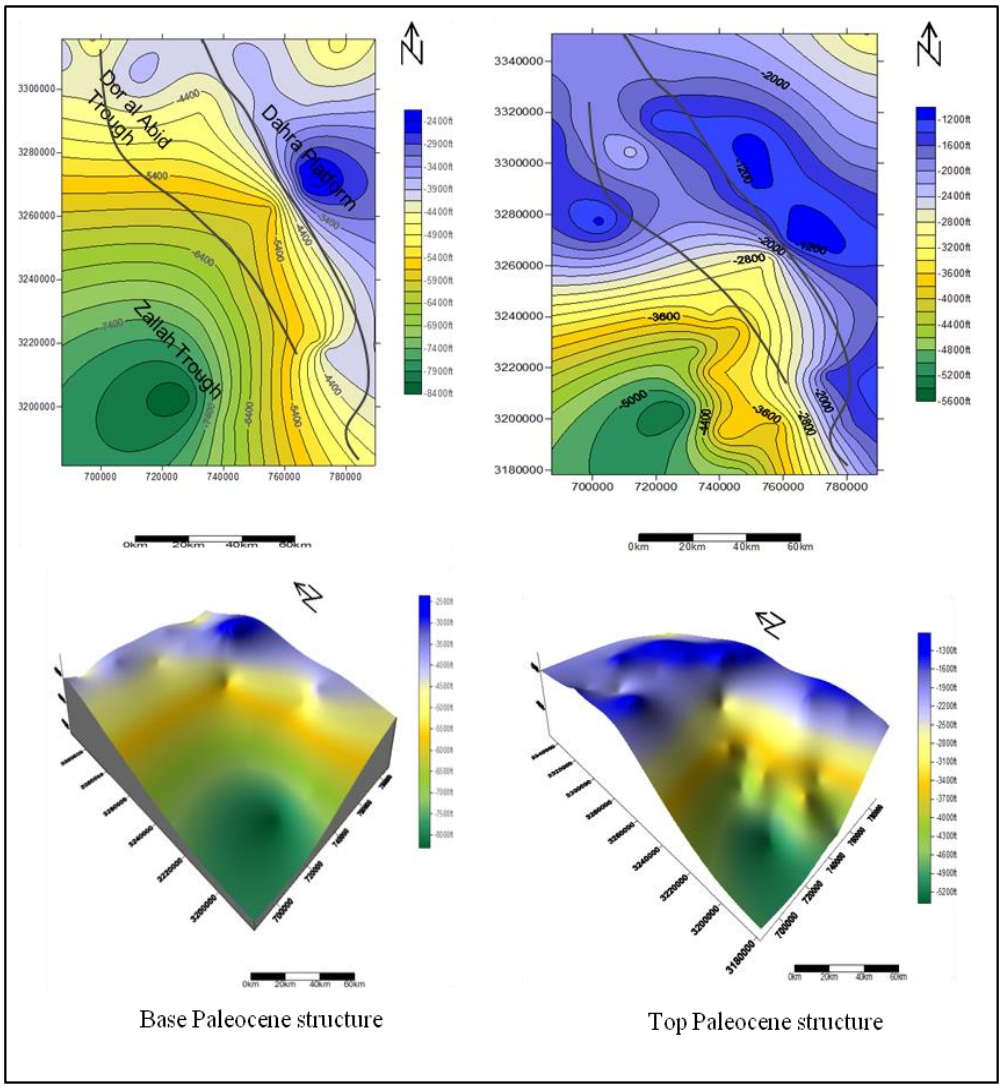

Figure 6.12 Regional structure contour maps on top of the Kalash Limestone (base Paleocene) and on top of the Kheir Formation (close to top of the Paleocene) in the study area.

6.3.3. Processes affecting facies distribution

6.3.3.1. Tectonic-related process

In a broad sense, the Paleocene world was a ‘‘hot house’’ with a rather ‘‘calm’’ tectonic regime. Consequently, sea level was relatively stable, and deviations from this ‘‘stability’’ were not great. Thus, global Paleocene sea- level changes (and consequently transgressions on the continental margins) were not so large as to overwhelm all regional variations (Ruban et al., 2012).

Globally, there were no significant tectonic re-organizations during the Danian–Selandian, although gradual changes in plate motions re-shaped the world (Golonka, 2004; Scotese, 2004; Müller et al., 2008). Therefore, differential subsidence, eustasy and possibly compaction were probably the cause of the variations in depositional environments in this time interval and changes in depositional facies. Limestone, dolomite, and locally anhydrite in the Satal and Beda (U Beda, L Beda and Thalith Members) Formations were deposited on the platforms and on high topographic areas of the Zallah and Dor al Abid Troughs, whereas shale and marl/argillaceous limestone were dominant in the troughs and in low topographic areas of the Dahra Platform.

Rusk (2002) suggested that during the middle Paleocene to early Eocene period rift tectonics had little control on sedimentation. The Thanetian time, which comprises the Dahra, Khalifa, Zelten, Harash and Kheir Formations, is regarded as the period during which a sort of balance between subsidence and the rate of deposition existed, and thus the lithofacies were quite uniform regionally (Raveling, 1970) (Figs. 6.9A & 6.9B). On the Dahra Platform of the study area, tectonic-related features (faulting, tectonic fractures and early diagenetic fractures) have been recognized from the core samples in the Selandian/Thanetian succession. A possible strike-slip fault with fairly well-defined striations has been observed in the lower part of the Harash Formation in well no. 9. Two intervals 3-5 feet thick, of fractured strata were observed in the Dahra Formation in wells no. 8 and 10. Although these tectonic features may have not been developed regionally, they could indicate some local tectonic movements and influence on sedimentation patterns in the Late Paleocene succession on the Dahra Platform.

The thickness variation in the Zallah/Dor al Abid Trough and on the Dahra Platform is apparent in the Cretaceous and Tertiary successions, which suggest pene-contemporaneous movements on both sides of the fault. The early Cretaceous to Miocene is the time period during which the North African continental margin changed

its position as a result of the opening of the Atlantic Ocean. The exact relation between North African plate motions and rifting has been, and still is, a subject of controversy, and the Gedari Fault that separates the Zallah/Dor al Abid Trough and the Dahra Platform is part of this (Jerzykiewicz et al., 2002).

6.3.3.2. Sea-level changes

Globally, Paleocene sea-level was up to 100m above modern sea-level, resulting in widespread marl deposition throughout most of the Paleocene, with superimposed smaller fluctuations (less than 20m) (Haq et al., 1988). Müller et al., (2008) suggested that Paleogene sea level should have been 70–80m higher than present-day, assuming a similar volume for the overall ocean basin, or upward of 120m higher than present-day, if this volume was significantly smaller. The start of the Tertiary in the study area was characterized by the deposition of thick Hagfa Shale in large parts of the Zallah and Dor al Abid Troughs. The lower part of the Hagfa Shale comprises 80-90% planktic foraminifera, indicating water depths of more than 500m (Tmalla, 1996). This high sea-level stand during the early Paleocene in the study area corresponds with the global sea-level curve of Haq et al., (1988) (Fig. 5.2). Broadly, high sea-level persisted throughout the Danian, apart from a minor regression in the middle-late Danian, so that this interval can be regarded as a period of relative eustatic stability; this was also suggested by both Haq and Al-Qahtani (2005) and Kominz et al., (2008).

Selandian time is represented by the Beda Formation that over a large part of the Dahra Platform comprises a lower Thalith Limestone and an upper Rabia Shale members. To the east of the study area, Tmalla (1996) documented an obvious decrease in water depth to around 50-100m relative to that of the Danian Hagfa Shale. This, along with the facies changes across the Danian-Selandian boundary, could suggest a regional lowering of sea-level and/or tectonic uplift. The former is roughly correlated to the eustatic sea-level changes proposed by Haq et al. (1988) although they do not match perfectly. The late Selandian interval was a time of sea-level fall according to Haq et al., (1988) or major eustatic fluctuations according to Kominz et al. (2008). Globally, the late Selandian has been interpreted as a period of relative sea level stability, relatively stable climate and tectonics, which persisted into the early–middle Thanetian (Ruban et al., 2010b & 2012). In either case, however, sea-level change (eustatic and relative) has

probably played a major role in the deposition and distribution of the Selandian facies in the study area.

As documented earlier, the study area has not been affected by any significant tectonic activity during the deposition of the Beda and the Dahra Formations. This, in conjunction with Rusk's (2002) statement of little effect of rift tectonics on sedimentation from middle Paleocene to early Eocene, could signify that eustatic sea-level change was possibly the main factor responsible for the facies change across the Beda/Dahra Formation. The sudden facies change across the Dahra/ Khalifa boundary (the upper boundary of the LPS2) is mainly ascribed to a global transgressive event displayed on the eustatic sea-level chart (Fig. 5.2), with the pre-existing palaeotopography playing an important role in the spatial distribution and thickness variation of the Khalifa facies. This is indicated by the fact that the structure contour map on top of the Khalifa Formation shows almost the same palaeogeographic configuration as the Dahra Formation (Fig. 6.12B).

The entire Khalifa Formation and the lower part of the Zelten Formation are included in the TST3 (Fig. 5.16) and the facies variation from shale to limestone is considered as a gradual and normal shallowing in this systems tract upto the MFS3. The eustatic sea-level curve shows fluctuations during the middle Thanetian time. This may suggest that factors other than eustatic sea-level were responsible for the deposition of the Zelten limestone in the study area; these may have been tectonics, sediment supply (carbonate production) and climate.

Several studies have indicated that sea level was 70–140m higher during the late Paleocene and early Eocene than at present. Third-order sea- level cycles, with durations of hundreds of thousands to a few million years, have also been inferred and argued to represent eustatic variations (e.g., Haq et al., 1987; Speijer and Wagner, 2002; Miller et al., 2005a). In several Tethyan margin sequences, benthic foraminiferal assemblages and lithological evidence also indicate transgression during the PETM (Speijer and Schmitz, 1998; Speijer and Wagner, 2002; Gavrilov et al., 2003).

The latest Paleocene section in the study area, which comprises the Harash and Kheir Formations, is interpreted as LPS4. Despite the evidence for minor fluctuations during the late Thanetian, the long term eustatic sea-level curve shows an overall rise (Fig. 5.2). This may suggest that both eustatic and local tectonics were responsible for the deposition of the Harash and Kheir Formations in the western Sirt Basin.

During the Eocene, evaporitic strata accumulated at many locations across northern Africa, suggesting that the nature of these strata may be related to a fall in eustatic sea level and an interval of relatively arid climate (Swezey, 2009).

6.3.3.3. Climatic processes

During the Cenozoic global climate changed from a Late Cretaceous–Early Eocene ‘‘warm mode” to a Late Eocene–Quaternary ‘‘cool mode” (Frakes et al., 1992). The early Cenozoic is a time interval characterized by repeated changes with respect to global climate. Early Paleocene climate was wet temperate, gradually warming due to global greenhouse conditions, from the latest Cretaceous glaciation of Antarctica (Barrera, 1990). Lower Paleocene sediments from Tunisia, Spain, Israel and Egypt contain abundant kaolinite, considered to indicate warm and perennial humid conditions (Bolle and Adatte, 2001). The climate in the Sahara (North Africa) during the Paleocene is thought to have been generally hot and humid (Bellion, 1989a), although studies of Paleocene strata in southern Tunisia suggest that there was a change from a warm and humid climate during the early Paleocene to a warm and arid climate during the Paleocene–Eocene transition (Keller et al., 1998; Bolle et al., 1999).

The stable isotope analysis on the studied Selandian/Thanetian succession has given quite similar patterns, particularly in the $\delta^{13}C$ values with no real important excursions up through the section. The trends show an overall slight change to less negative $\delta^{18}O$ and to less positive $\delta^{13}C$. This suggests that there was only minor change in $\delta^{13}C$ seawater and climate through the time of deposition of the Dahra, Zelten and Harash Formations.

A long-term rise in eustatic sea-level during the early Thanetian, could have been coincident with a global warming trend that began during the Late Paleocene and ended during the Early Eocene (Miller et al., 1987; Zachos et al., 2001). In addition, a very abrupt and brief episode of global warming (the Late Paleocene Thermal Maximum-LPTM) occurred near the Paleocene–Eocene boundary, superimposed on the general Paleocene–Eocene warming trend (Zachos et al., 1993, 2001). Cycle analysis of the studied succession revealed that cycle duration of the Dahra, Mabruk, Zelten and Harash Formations ranges between 129 and 165kyr, which is very close to the short-eccentricity rhythm (105kyr), and in the range of short-eccentricity to mid-eccentricity (200kyr), as reviewed by Tucker and Garland (2010). This suggests that the studied

carbonates were probably influenced by short eccentricity-driven climate changes that could have been modulated by the long eccentricity rhythm, despite the fact that deciphering the over-riding control of the three controlling processes (eccentricity, obliquity and precision) can be difficult, if not impossible (Tucker and Garland, 2010).

Oxygen isotopic signatures of carbonates are mainly controlled by temperature of precipitation and the isotopic composition of the fluids, where the carbon isotopic signature generally reflects the isotopic composition of the fluid and the source of carbon, which may be derived from bacterial sulphate reduction, fermentation and dissolution of carbonate minerals (e.g. Morad et al. 1990; Yoshioka et al. 2003; Ader et al. 2009; Chakraborty et al. 2010). The high amount of calcite, along with the overall similarity in the $\delta^{18}O$ and $\delta^{13}C$ values throughout the studied Paleocene succession could suggest a warm period that was probably associated with high carbonate productivity.

6.4. Comparison with nearby regions

6.4.1. El Haria Formation (Central Tunisia)

The latest Cretaceous-Paleocene succession in Tunisia (El Haria Fm) mainly consists of shale and marl with thin intercalations of limestone particularly in the Danian part. The palaeogeography was characterized by subsiding troughs in the north and northeast (NW Tunisian Trough and NE Tunisian Basin) and the Gafsa Gulf in the southwest (Aubert and Berggren, 1976; Zaïer et al., 1998; Bensalem, 2002). During the Paleocene, the Kalaat Senan region was situated in the southern proximal part of the subsiding Tunisian Trough and in the vicinity of the emergent Kasserine Island. Prolonged marine sedimentation took place in a neritic setting with high subsidence rates and high sediment input, and with reduced sediment thickness towards Kasserine Island (Bensalem, 2002).

The lower and middle Paleocene part is transgressive (zones P2 and P3), extending over a large part of Tunisia and, in the Tunisian Trough, is followed by a general shallowing trend during the late Paleocene (zones P4 and P5) (Aubert and Berggren, 1976; Kouwenhoven et al., 1997; Guasti et al., 2005). Biostratigraphic studies indicate that the environment at El Kef evolved from an open-marine, outer neritic-upper bathyal setting towards an inner neritic setting during the late Paleocene (Donze et al., 1982; Peypouquet et al., 1986; Kouwenhoven et al., 1997; Guasti et al., 2005).

Lateral facies and thickness variations in the El Haria Fm are thought to be structurally controlled along basement lineaments, resulting in a number of small tectonically controlled basins (Zaïer et al., 1998).

6.4.2. Galala Mountains (Eastern Desert, Egypt)

The Galala Mountains in the Eastern Desert, together with areas in west Sinai represent a southern branch of the Syrian Arc, called the Northern Galala/Wadi Araba High (NGWA High) (Kuss et al., 2000). The Campanian/Eocene sediments of the Galala area has been subdivided into three different environmental regimes of deposition or non-deposition/erosion which remained approximately in the same geographic position (Scheibner et al., 2001a). The most proximal regime is characterized by uplift and erosion or non-deposition resulting mostly from the uplift of the Northern Galala/Wadi Araba High (NGWA), a branch of the Syrian Arc fold-belt. Subsequently, the shallow-water carbonate platform and slope deposits of the upper Campanian/upper Paleocene succession and the upper Paleocene/lower Eocene Southern Galala Formation represent an intermediate system and are found north and south of the NGWA High. The distal regime is represented by basinal chalks, marls and shales of the Campanian/Maastrichtian, and of the Paleocene/Eocene strata.

The distribution and lateral interfingering of these facies reflect different tectonic movements, changing basin morphology, sea-level change and progradation of shallow-water facies (Scheibner et al., 2001a). A combination of a sea-level fall and tectonic uplift in the late Paleocene (59 Ma) resulted in the prominent progradation of the carbonate platform. On the distal platform patch reefs, reef debris and lagoonal to margin/upper slope limestones were deposited (section A1), whereas slumps and debris flows deposits occur on the steeper slope. In the basinal areas mass flow deposits passed into calciturbidites. Farther south only basinal marls were deposited.

Scheibner et al., (2003) assumed that during the early Paleocene the platform/basin configuration remained the same. From Selandian times (59 Ma) onwards the platform/basin configuration changed dramatically with a rapid southward progradation resulting from a combination of tectonic movements and falling sea level. The slope sediments of the late Paleocene platform are characterized by mass transport deposits like slides, slumps and debrites. The proximal basinal sediments are

characterized by calciturbidites that are absent in distal areas farther south (Scheibner et al., 2001a).

Scheibner et al., (2003) concluded that the most important parameters that control the depositional geometries of the late Cretaceous mixed carbonate siliciclastic platform and the Paleogene carbonate platform in the Galala area are changes in relative sea level, sediment flux and initial topography.

6.5. Summary comments

A wide spread occurrence of the Maastrichtian Kalash Limestone in the Sirt Basin with fairly comparable thickness, and the thinning and local absence, of the Upper Cretaceous strata, along with the previous subsidence studies, strongly indicate that the Maastrichtian time is a significant period between Late Cretaceous and Tertiary successions in the Basin; it represents the termination of the main rifting phase and the onset of late stage rifting phase of the Sirt Basin, when troughs and platforms were almost uniformly subsided.

The overall thickness and facies of the Paleocene are closely aligned to the underlying structure; thicker in the trough areas and thinner over the platforms. The thickness distribution of different rock-units in the study area virtually coincides with the isopach arrangement of the Danian, Selandian/Thanetian and the entire Paleocene succession; the carbonate-dominated facies are preferentially located over the major platforms and local highs, whereas the main troughs and low topographic areas are mainly filled with shale and/or marl. The hanging- wall blocks, however, are characterised by subsidence controlled pattern with increased thickness of shale and mudstones. The foot-wall, on the other hand, is dominated by uniform and monotonous strata with remarkably increased thickness of shallow-marine carbonates, suggesting relative stability in tectonic, sea-level and climate.

The thickness distribution of the Dahra Formation suggests that the Gedari fault was slightly active during the Early Thanetian; the thickness difference between the platform and the trough strata suggest that the trough areas were possibly still subsiding with probably compactional-induced. This gave rise to a local differential subsidence on both structural elements and hence resulted in the difference in accommodation space.
The 700ft relief developed in the Mabruk area, which was probably due to local faulting, resulted in the development of the various facies (lagoon and reef). The thickness and facies distribution of the Khalifa, Zelten and Harash Formations in the study area suggest a fairly uniform topography/ or low relief feature prior to the deposition of each, and that the different facies could be ascribed to the pre-existing topography that was coupled with sea-level fluctuations.

The high temperature of the aqueous inclusions recorded by fluid inclusion analysis is possibly the result of the passage of hydrothermal fluids from deeper parts of the area, despite the low sedimentation rate, the high thermal conductivities of carbonate, along with the Mid-Late tertiary uplift and erosion are all involved.

The overall palaeotopography throughout the Paleocene seems to have been broadly similar; there is no substantial variation between the base and the top of the Paleocene succession, except for the development of a local high that became a prominent feature after deposition of the Selandian Beda Formation.

Local biostratigraphic studies, along with the facies changes occurred across the Danian-Selandian boundary suggest a regional lowering of sea-level and/or tectonic uplift had occurred in the study area. The eustatic sea-level curve shows fluctuations during the middle to late Thanetian time, which may suggest that other factors than eustatic sea-level were responsible for the deposition of the Zelten, Harash and Kheir facies in the study area. The high amount of calcite, along with the overall similarity in the $\delta^{18}O$ and $\delta^{13}C$ values throughout the studied Paleocene succession suggest a warm period that was probably associated with high productivity or fermentation. Therefore, various processes have been involved in controlling the vertical and lateral distribution in sedimentation pattern of the studied Paleocene succession in the western part of the Sirt Basin. These mainly include local tectonics, eustatic sea-level fluctuations, basin palaeotopography, and climate.

CHAPTER SEVEN:

CONCLUSIONS AND FUTURE WORK RECOMMENDATIONS

7.1. Conclusions

This chapter brings together all the key findings and main interpretations of the research study. The results of lab work, macroscopic and microscopic investigations presented in this study have been accomplished to define the lithofacies and their associated microfacies, postulate the environments of deposition, address the post-depositional changes and their influence on the reservoir characteristics, investigate major transgressive-regressive cycles, utilize the sequence stratigraphic approach, monitor the spatial and temporal facies variation, and interpret the burial history of the studied Paleocene succession in the western Sirt Basin.

- In the second Chapter the regional geology of Libya including its sedimentary basins was presented, with emphases on the structural setting and stratigraphic evolution of the Sirt Basin and the general geology and lithofacies of its western part. The Sirt Basin is the youngest of the Libyan basins, and was developed through inter- and intra-plate movements resulting from the relative motion of the American, African and Eurasian plates during the opening of the Atlantic Ocean and the development of the Mediterranean on the foreland of the African Plate (Anketell, 1996). The sedimentary succession in the Sirt Basin is typical of those developed in a failed rift system and ranges in age from Cambro-Ordovician to Recent.

The Paleocene succession in the study area consists mainly of alternating shallow-marine carbonates and open-marine calcareous shales, with rapid lateral facies changes, which most likely were controlled by the palaeotopography and the differential subsidence. The Palaeocene succession comprises the following rock units; Hagfa Shale, Satal Limestone, Beda Limestone, Dahra Limestone, Khalifa Shale, Zelten Limestone, Harash Fm and Kheir Fm. The Satal, Beda and Dahra carbonates form reservoirs in many oil- fields in the study area, whereas the shale of Hagfa, Khalifa and Beda (Rabia) represent impermeable top seals for the underlying reservoirs.

- In Chapter 3, the main lithofacies and their associated microfacies, along with the depositional environments of the Dahra (Mabruk), Zelten and Harash Formations have been defined. The Selandian/Thanetian Succession comprises four major lithofacies; limestone, dolomitic limestone/dolomite, argillaceous limestone/marl, and shale. The shale and marl are widely distributed in the Dor al Abid Trough and cover a

large part of the Paleocene succession (Heira Formation). They are also developed across the Dahra Platform, where the shale is usually medium grey to greenish grey, fissile, slightly pyritic with scattered small un-identifiable bioclastic fragments. Detailed microscopic examination has resulted in the identification of seven main macrofacies and eleven associated microfacies. These macrofacies are: Bioclastic foraminiferal packstone-packstone/grainstone; Foraminiferal bioclastic wackestone-wackestone/packstone; Dolomitic lime-mudstone; Bioclastic foraminiferal grainstone; Foraminiferal nummulitic packstone; Algal packstone; and Bioclastic boundstone.

The main carbonate grains within the Dahra Formation are rotaliids, miliolids, echinoderms, molluscs, ooids and green algae, whereas in the Mabruk Member there are benthic forams, peloids, red algae, corals and rhodoliths. The dominant bioclasts within the Zelten and Harash carbonates are benthic forams, molluscan shells, nummulites, bryozoans and echinoderm fragments.

The Dahra Formation on the Dahra Platform was deposited on a homoclinal carbonate ramp with inner, mid and probably outer ramp facies, each with distinctive sub-facies and microfacies. Overall the Dahra Formation was probably deposited under similar conditions throughout the east and west Dahra Fields on the Dahra Platform. A comparable depositional setting was re-established in the Zelten and Harash Formations across the area, with local occurrences of nummulitic packstone instead of bioclastic grainstone in the Dahra Formation and the development of mainly wackestone-packstone facies. The Mabruk Member represents deposition of mainly shallow-water carbonates that were bounded above and below by deeper-marine marl and shale; these may have accumulated in lagoonal and reefal environments in a probable rimmed-shelf setting.

● The major and minor diagenetic processes and their timing, together with their effect on the reservoir quality of the studied carbonates are presented in Chapter 4. Boring, burrowing, neomorphism, dissolution, cementation, dolomitization and compaction are all recognised, in conjunction with the occurrence of minor diagenetic events, such as the formation of authigenic pyrite, glauconite, hematite, phosphate, sulphates and clay minerals.

Two phases of dissolution occurred within the studied rocks; the first phase caused the dissolution of the original aragonitic and probably high Mg-calcite grains, together with some matrix. The second phase of dissolution resulted in the total leaching of probable sulphate minerals (gypsum-anhydrite) and the partial dissolution of

medium to coarsely crystalline void-filling dolomite crystals. Three types of calcite cement have been recognized. These are: isopachous calcite, equant sparry calcite, locally blocky, and syntaxial overgrowth cements. Two types of dolomite have also been recognised, these are: very finely to medium crystalline (10-80 μm) dolomite and medium tocoarsely crystalline (100-600 μm) dolomite. Mechanical and chemical compaction is recorded in almost all the studied formations in both structural settings, particularly in the Dahra Formation and Mabruk Member.

The $\delta^{18}O$ values recorded in the studied Paleocene succession range from -10.5 ‰ to +1.2 ‰, whereas the $\delta^{13}C$ measurements fall in the range -4.87‰ to +3.89‰. In addition to a few negative instances, specific intervals within the Dahra Formation show distinctive positive excursions, particularly in the $\delta^{18}O$, and these suggest a trend to less meteoric alteration and the preservation of marine values in the Dahra West Field, and subaerial exposure in the Dahra East Field. The general trend of the oxygen isotopic signature of the Zelten and Harash Formations is positive, particularly in the Harash Formation. The isotope values of the Mabruk Member range from $\delta^{18}O$ -5.45‰ to -0.77‰, and $\delta^{13}C$ 0.00‰ to +3.04‰. They commonly followed the sedimentary facies, as the wells with reefal facies have similar isotope values, whereas the wells with lagoonal facies have a completely different trend.

Several occurrences of white, yellow and blue fluorescent fluid inclusions within the Dahra, Zelten and Harash Formations on the Dahra Platform have been documented. The difference in homogenization temperature between the aqueous inclusions and petroleum inclusions is interpreted in terms of two phases of calcite cementation.
Macroscopic and microscopic investigations revealed that the porosity types developed in the Selandian/Thanetian succession are dominated by moldic, vuggy, intergranular and intragranular types, with less common fracture and intercrystalline porosity. The best porosity in the studied succession is recorded in the Dahra Formation, whereas the Mabruk Member, Zelten and particularly Harash Formations have relatively lower porosity. The porosity evolution in the Selandian/Thanetian succession is controlled by original depositional texture, subsequent diagenesis and the pattern of carbonate cycles.

- In the fifth Chapter, a classical stratigraphy, sedimentology and sequence stratigraphic approach have all been implemented. The purpose of this chapter is to demonstrate the merits of using sedimentology, petrography, wireline logs and various analytical techniques to assess the regional and local stratigraphy and for establishing a

sequence stratigraphic framework for the Selandian/Thanetian succession in the western Sirt Basin.

The stratigraphic section in the study area extends from the Palaeozoic up to the Recent, with major and minor stratigraphic gaps throughout. The Danian time was associated with an extensive sea-level rise, which resulted in the deposition of thick Hagfa Shale in the trough areas, whereas shallower-water carbonates of the Satal Formation were deposited on the Dahra Platform. The overall cycle of shale deposition with intercalation of carbonate reflects alternating transgressive-regressive cycles in the Paleocene succession. Significant transgression occurred at the end of the Dahra Formation, and resulted in deposition of the Khalifa Formation across the study area. Most of the Zelten Limestone was deposited during a regressive phase with an evident prograding trend up to the top of the formation. The Zelten/Harash boundary shows a sharp change in facies and log response, which suggests an important stratigraphic surface.

The studied succession is dominated by shallowing-up cycles, with the possible development of deepening-up cycles particularly in the deeper-water areas. Lagoon, shallow subtidal and deep subtidal cycles dominated the Dahra Platform, whereas reef and back-reef/lagoonal cycles are abundant in the Dor al Abid Trough. Carbonate accumulation during the deposition of the Zelten and Harash Formations on the Dahra Platform is similar to that of the Dahra Formation, which suggests a similar rate of creation of accommodation space. The high rate of deposition on the Dahra Platform relative to that in the Dor al Abid Trough is probably ascribed to the fact that an inner platform area is normally the site of higher carbonate production relative to the outer platform area.

Four depositional sequences on the Dahra Platform and at least two depositional sequences have been recognized in the Dor al Abid Trough. These depositional sequences comprise both a transgressive systems tract and a highstand systems tract, with no lowstand systems tract recognised, probably due to the low relief ramp setting or because of the location of the studied wells. The sequence boundaries are commonly incorporated with transgressive surfaces, particularly on the Dahra Platform. The possible development of a drowning unconformity at the top of the Mabruk Member in the Dor al Abid Trough could be attributed to a possible lack of reef-building organisms in association with tectonic subsidence and/or significant sea-level rise.

● In Chapter six, the spatial and temporal pattern of the Paleocene facies and the burial history of the studied succession are addressed. The wide-spread occurrence of the Maastrichtian Kalash Limestone in the Sirt Basin with fairly comparable thickness, and the thining and local absence, of Upper Cretaceous strata, along with previous subsidence studies, strongly indicate that the Maastrichtian time was a significant period between Late Cretaceous and Tertiary successions for the basin; it represents the termination of the main rifting phase and the onset of a late-stage rifting phase of the Sirt Basin, when troughs and platforms subsided almost uniformly. In the Paleocene late syn-rift, the hanging-wall blocks, however, are characterised by a subsidence controlled pattern with increased thickness of shale and mudstones. The foot-wall, on the other hand, is dominated by uniform and monotonous strata with a remarkable increased thickness of shallow-marine carbonates, suggesting relative stability in tectonics, sea-level and climate.

The overall thickness and facies of the Paleocene is closely aligned to the underlying structure; thicker in the trough areas and thinner over the platforms. The thickness distribution of different rock-units in the study area virtually coincides with the isopach arrangement of the Danian, Selandian/Thanetian and the entire Paleocene succession, with the carbonate-dominated facies preferentially located over the major platforms and local highs, whereas the main troughs and low topographic areas are mainly filled with shale and/or marl. The high temperature recorded in the aqueous inclusions is possibly due to the passage of hydrothermal fluids from deeper parts of the area.

The overall palaeotopography throughout the Paleocene seems generally similar; there is no substantial variation between the base and the top of the Paleocene succession, except for the development of a local high that became a prominent feature after deposition of the Beda Formation (Selandian); this suggests differential subsidence and sea-level fluctuations, along with climate as the dominant processes that controlled the spatial and temporal variations of the Paleocene facies.

7.2. Future work recommendations

In view of the important amount of the hydrocarbon produced in the Sirt Basin, several studies have been conducted regarding the petroleum geology, reservoir characteristics, structural geology, stratigraphy and biostratigraphy. Nevertheless, the studied succession, and almost the entire stratigraphic section in the basin, is lacking any absolute dating and high-resolution biostratigraphy. Moreover, the time and mechanism of the Sirt Basin creation and evolution are still debatable, which is in part related to the poor age-dating of the deep stratigraphic succession.

During the course of this study, a number of gaps in our knowledge of the sedimentology, stratigraphy and structural geology have been recognised. Many of these gaps can be filled and these would give added value to the overall geology of the Sirt Basin; First, a high resolution biostratigraphy is necessary to improve the vertical resolution in the succession and to enhance the lateral correlation not only within the same structural elements but also between the Dahra Platform and the Dor al Abid/Zallah Trough. Second, continuous core samples of the carbonate formations throughout the succession, along with a complete, up-to-date, set of wire-line logs, are also required to conduct a reliable sequence stratigraphic framework in the area that can be correlated with neighbouring regions and globally. Third, application of state of the art analytical techniques, particularly fluid inclusions on a systematic basis of carefully selected wells, would result in a better understanding of the burial history of the western Sirt Basin. Furthermore, additional closely spaced wells, with a complete set of logs and continuous cores, in the Mabruk Field in the Dor al Abid Trough will allow delineating the shape, type and extent of the reefal deposits in the Mabruk area.

8. REFERENCES

Abadi, A., 2002. Tectonics of the Sirt Basin, inferences from tectonic subsidence analysis, stress inversion and gravity modelling. Ph.D. thesis, Vrije Universiteit, Amsterdam: 187.

Abadi, A.M., van Wees, J.-D., van Dijk, P.M., and Cloetingh, S.A.P.L., 2008. Tectonics and subsidence evolution of the Sirt Basin, Libya. AAPG Bulletin, v. 92: 993-1027.

Abdunaser, K., M., 2012. Structural Style and Tectonic Evolution of the Northwest Sirt Basin–Cretaceous-Tertiary Rift, Libya. Durham theses, Abstract.

Abugares, I. Y., 1996. Sedimentology and hydrocarbon potential of the Gir Formation, Sirt Basin, Libya. in M. J. Salem, M. T. Busrewil, A. A. Misallati, and M. A. Sola, eds., The geology of the Sirt Basin: Amsterdam, Elsevier, v. 2: 31–64.

Abushagur, S.A. 1991. Cyclic transgressive and regressive sequences and their association with hydrocarbons - Ghani field, Sirt Basin, Libya. Third Symposium on the Geology of Libya, v. 5 (eds. M.J. Salem and M.N. Belaid), Elsevier, Amsterdam: 1827-1840.

Adams, A. E., Mackenzie, W. S. and Guilford, C. 1984. Atlas of Sedimentary Rocks Under the Microscope. Longman: 104.

Adams, A. E., Mackenzie, W.S. 1998. A colour Atlas of Carbonate Sedimentary Rocks under the Microscope. Manson publishing Ltd: 180.

Ader, M., Macouin, M., et al., 2009. A multilayered water column in the Ediacaran Yangtze platform? Insights from carbonate and organic matter paired delta C-13. Earth Planet Sci. Lett. 288: 213–227. doi:10.1016/j.epsl.2009.09.024.

Ahlbrandt TS 2001. The Sirte Basin Province of Libya - Sirte-Zelten total petroleum system. US Geol Surv Bull 2202-F: 29.

Ahlbrandt, T. S., 2002. The Sirte Basin province of Libya—Sirte-Zelten total petroleum system. U.S. Geological Survey, http://geology.cr.usgs.gov/pub/bulletins/b2202-f: 1–29

Ahlmann, H. W. 1928. La Libye septentrionale. Geografiska Annaler H: 1-2, Stockholm

Aigner, T. 1982. Calcareous tempestites: storm-dominated stratification in Upper Muschelkalk Limestones)Triassic, SW Germany). In Einsele, G., and Seilacher, A., eds., Cyclic and event Stratification: Berlin, Springer-Verlag: 180-198.

Aigner, T., and reineck, H.-E., 1982. Proximality trends in modern storm sands from Helgoland Bight (North Sea) and their implications for basin analysis: Senck. Marit., v. 14: 183-215.

Aliev, M., Ait Laoussine, N., Avrov, V., Aleksine, G., Barouline, G., lakovlev, B., Korj, M., Kouvykine, J., Makarov, V., Mazanov, v., Medvedev, E., Mkrtchiane, O.,Mostavinov, R., Oriev, L. Oroudjeva, D., Oulmi, M., and Said, A. 1971. Geological stmctures and estimation of oil and gas in the Sahara in Algeria. Sonatrach, Algiers: 265.

Al-Asam, I. & Veizer, J. 1986. Diagenetic stabilization of aragonite and low Mg-calcite II. Stable isotope in rudists. Journalof Sedimentary Petrology. 56:763–770.

Allen, P. A. And Allen, J.R. 1990. Basin Analysis. Blackwell. Oxford: 451.

Ambrose, G. 2000. The geology and hydrocarbon habitat of the Sarir Sandstone, SE Sirt Basin, Libya. Journ. Pet. GeoL v. 23: 165-192.

Anketell, J.M., 1996. Structural history of the Sirt Basin and its relationship to the

Sabratah Basin and Cyrenaican Platform, northern Libya. in M. J. Salem, M. T. Busrewil,A. A.isallati, and M. A. Sola, eds., The geology of the Sirt Basin: Amsterdam, Elsevier, v. 3: 57–87.

Ambrose, G. 2000. The geology and hydrocarbon habitat of the Sarir Sandstone, SE Sirt Basin, Libya. Journ. Pet. GeoL v. 23: 165-192.

Anketell, J.M. and Kumati, S.M. 1991b. Structure of Al Hufrah region - western Sirt Basin, GSPLAJ. Third Symposium on the Geology of Libya, vol. 6 (eds. M.J. Salem, A.M.Sbeta and M.R. Bakbak), Elsevier, Amsterdam: 2353-2370.

Anketell, J.M. and Mriheel, I.Y., 2000. Depositional environment and diagenesis of the Eocene Jdeir Formation, Gabes-Tripoli Basin, Western Offshore Libya. Journal of Petroleum Geology, 23: 425-447.

Aubert, J., Berggren, W.A., 1976. Paleocene benthic foraminiferal biostratigraphy and paleoecology of Tunisia. Bulletin du Centre Recherches Pau-SNPA, 10: 379-469.

Baccelle L., Bosellini A. 1965. Diagrammi per la stima visiva della composizione percentuale nelle rocce sedimentarie. Ann. Univ. Ferrara (N.S.) sez. **9**, 4: 59-62.

Badenas, B., Aurell, M., and **Gröcke, D.R. 2005**. Facies analysis and correlation of High order sequences in middle-outer ramp successions: variations in exported carbonate on basin-wide delta C-13(carb) (Kimmeridgian, NE Spain). Sedimentology, 52**:** 1253-1275.

Badley, M.E., Egeberg, T., and Nipen, O., 1984. Development of rift basins. Illustrated by the structural evolution of the Oseberg feature, Block 30/6, offshore Norway: Geological Society of London Journal, v. 141: 639-649.

Baird, W. D., R. M. Aburawi, and J. N. Bailey, 1996. Geohistory and petroleum in thecentral Sirt Basin. in M. J.Salem, M. T. Busrewil, A. A. Misallati, and M. A. Sola, eds., The geology of the Sirt Basin: Amsterdam, Elsevier, v. 3:3–56.

Baldwin, B. 1971. Ways of deciphering compacted sediments. Journal of. Sedimentary Petrology. **41:** 293-301.

Ball, M. M., 1967. Carbonate sand bodies of Florida and the Bahamas. J. Sediment. Petrol., 37: 556-596.

Banner, J. L., 1995. Application of the isotope and trace element geochemistry of strontium to studies of diagenesis in carbonate systems. Sedimentology 42: 805-824.

Barr, F.T., Berggren, W.A., 1980. Lower Tertiary biostratigraphy and tectonics of northeastern Libya. In: Salem, M.J., Busrewil, M.T. (Eds.), The Geology of Libya 1. Academic Press, London: 163–192.

Barr, F. T, and W. A. Berggren, 1981, Lower Tertiary biostratigraphy and tectonics of northeastern Libya. in M. J. Salem and M. T. Busrewil, eds., Geology of Libya: Tripoli, Libya, Al-Fateh Univ., v. l: 163-191. and A. A. Weegar, 1972, Stratigraphic nomenclature of the Sirte basin, Libya: Petroleum Exploration Society of Libya: 179.

Barr, F. T. and Hammuda, O. S. 1971. Biostratigraphy and planktonic zonation of the upper Cretaceous Atrun Limestone and Hilal Shale, northeastern Libya. In: Proc. 2nd Int. Conf. Plankt. Microfossils (Rome, 1970) (ed. A. Farinacci): 27-38.

Barr, F. T., and A. A. Weegar, 1972, Stratigraphic nomenclature of the Sirt Basin, Libya. Tripoli, Petroleum Exploration Society of Libya: 179.

Barrera, E., 1990, Stable isotope evidence for gradual environmental changes and species survivorship across the Cretaceous/Tertiary Boundary. Paleoceanography, v. 5: 867-890.

Barron, J., Larsen, B., Baldauf, J., 1991. Evidence for Late Eocene to Early

Oligocene Antarctic glaciation and observations on Late Neogene glacial history of Antarctica. results from Leg 119. Proceedings of the Ocean Drilling Program, Scientific Results 119: 869–891.

Bathurst, R.G.C. 1966. Boring algae, micrite envelopes and lithification of molluscan biosparites. Geological Journal, 5: 15-32.

Bathurst, R.G.C. 1975. Carbonate Sediments and Their Diagenesis. Elsevier, Amesterdam, 2nd Edition: 658.

Bathurst, R.G.C. 1987. Diagenetically enhanced bedding in argillaceous platform limestones : stratified cementation and selective compaction. Sedimentology **34:** 749-778.

Beales, F. W. 1971. Cementation by white sparry dolomite. In: Carbonate cements (eds. O.P. Brickers): 339-346. John Hopkins University press, Baltimore, Maryland.

Bebout D.G. and Pendexter, C. 1975. Secondary carbonate porosity as related to early Tertiary depositional facies, Zelten field, Libya. Bull. Amer. Assoc.Pet. Geol. vol. 59: 665-693.

Belazi, H. S., 1989, The geology of the Nafoora oilfields, Sirt Basin, Libya. Journal of Petroleum Geology, v. 12: 353–366.

Bellini, E., Giori, I., Ashuri, O., and Benelli, F. 1991. Geology of the Al Kufrah basin, Libya. Third Symposium on the Geology of Libya, v. 6 (eds. M.J Salem, A.M. Sbeta and M.R. Bakbak), Elsevier, Amsterdam: 2287-2294.

Bellini, E., and Massa, D., 1980, A Stratigraphic contribution to the Paleozoic of the southern basins of Libya. In Salem, M.J., and Busrewil, M.T., eds., The Geology of Libya, 2nd Symposium of the Geology of Libya, v. 1: Amsterdam, Elsevier: 3-56.

Bellion, Y.J.-C., 1989a. Histoire géodynamique post-Paléozoïque de l'Afrique de l'Ouest d'après l'étude de quelques basins sédimentaires (Senegal, Taoudenni, Iullemmeden,Tchad). Centre International pour la Formation et les Échanges Géologiques (CIFEG), Publication Occasionnelle 1989/17: 302.

Bensalem, H., 2002. The Cretaceous-Paleogene transition in Tunisia: general overview. Palaeogeography, Palaeoclimatology, Palaeoecology, 178: 139-143.

Berggren, W.A. 1974. Palaeocene benthonic foraminiferal biostratigraphy and paleoecology of Libya and Mali. Micropaleontology, **20:** 449-465.

Bernasconi, A., Poliani, G. and Dakshe, A. 1991. Sedimentology, petrography and diagenesis of Metlaoui Group in the offshore northwest of Tripoli. Third Symposium on the Geology of Libya, vol. 5 (eds. M.J. Salem and M.N. Belaid), Elsevier, Amsterdam: 1907-1928.

Berner, R. A. 1981. New geochemical classification of sedimentary environments. J. Sedim. Petrol. **51:** 359-365.

Bezan, M. A., 1996, The Paleocene sequence in Sirt Basin. In M. J. Salem, M. T. Busrewil,A. A. Misallati, and M. A. Sola, eds., The geology of the Sirt Basin: Amsterdam, Elsevier, v. 1: 97–118.

Bezan, M. A., F. Belhaj, and K. Hammuda, 1996. The Beda Formation in the Sirt Basin. In M. J. Salem, M. T. Busrewil, A. A. Misallati, and M. A. Sola, eds., The geology of the Sirt Basin: Amsterdam, Elsevier, v. 2: 135–152.

Bice, D. M. and Stewart, K. G., 1990. The formation and drowning of isolated Carbonate seamounts: tectonic and ecologic controls in the Northern Apennines: In, M.E. Tucker, J.L. Wilson, P.D. Crevello, J.R. Sarg, and J.F. Read (eds.), Carbonate platforms: facies, sequences, and evolution: International Association of Sedimentologists Special Publication 9: 145-169.

Biju-Duval, B. 1974. Exemples de depots fluvioglaciaires dans I'Ordovicien superieur et le Precambrian superieur du Sahara central. Bull Cent.Rech, Pau. v. 8: 209-236.

Birkeland, C., 1977. The importance of rate of biomass accumulation in early successional stages of benthic communities to the survival of coral recruits. In: Proc. 3rd Int. Coral Reef Syrup., Miami, 1977, 1: 16-21.

Bishop, W.F. 1988. Petroleum Geology of east-central Tunisia. Bull. Amer. Assoc. Pet. Geol. vol. 72: 1033-1058.

Bolle, M.P., Adatte, T., Keller, G., von Salis, K., Burns, S., 1999. The Paleocene–Eocene transition in the southern Tethys (Tunisia): climatic and environmental fluctuations. Bulletin de la Société Géologique de France 170: 661–680.

Bolle, M.-P., and Adatte, T., 2001. Palaeocene–early Eocene climatic evolution in the Tethyan realm: Clay mineral evidence: Clay Minerals, v. 36, no. 2: 249–261, doi:10.1180/000985501750177979.

Boote, D.R.D., Clark-Lowes, D.D., and Traut, M.W., 1998. Palaeozoic petroleum systemsof North Africa. In MacGregor, D.S., Moody, R.T.J., and Clark-Lowes, D.D., eds.,Petroleum Geology of North Africa: London, The Geological Society of London Special Publications No. 132: 7-68.

Bosellini A 1989. Dynamics of Tethyan carbonate platforms. In: Crevello PD, Wilson JL, Sarg F, Read JF (eds) Controls on carbonate platform and basin development, SEPM Spec Publ 44: 3-13.

Bosence, D., 1998. Stratigraphic and sedimentological models of rift basins. In: Sedimentation and Tectonics of Rift Basins; Red Sea Gulf of Aden. (Eds B.H. Purser and D.W.J. Bosence): 9-25. Champan& Hall, London.

Bosence, D., 2005. A genetic classification of carbonate platforms based on their basinal and tectonic setting in the Cenozoic. Sedimentary Geology, **175:** 49-72.

Bosence, D., 2012. Carbonate-dominated marine rifts. In: Regional Geology and Tectonics: Phanerozoic Rift Systems and Sedimentary Basins.ed. by: David G Robets and A. W. Bally.

Bosence, D.W. J., Cross, N.E., and Hardy, S., 1998. Architecture and depositional sequences of Tertiary fault-block carbonate platforms; an analysis from outcrop (Miocene, Gulf of Suez) and computer modelling. Marine and Petroleum Geology, v. 15: 203–221.

Bosence, D., Procter, E., Aurell, M., Bel Kahla, A., Boudagher-Fadel, M., Casaglia, F.,Cirilli, S., Mehdie, M., Nieto, L., Rey, J., 2009. A dominant tectonic signal in high frequency, peritidal carbonate cycles? A regional analysis of Liassic platforms fromWestern Tethys. Journal of Sedimentary Research, **79:** 389-415.

Bracaccia. V., Carcano, C., and Drera, K. 1991. Sedimentology od the Silurian-Devonian series in the SE part of the Ghadamis Basin. In: M.J. Salem, O.S.Hammuda and B.A.Eliagoubi (Eds.). The geology of Libya 4, Elsevier, Amesterdam: 1727-1754.

Burke, K., and J. Dewey, 1974. Two plates in Africa during the Cretaceous. Nature, v. 249: 313–316.

Burollet, P.F. 1963. Le Trias en Tunisie et Libye. Relations avec le Trias europeen et Saharrien. 86th Congr. Soc. Sav., Colloque Trias, Montpellier 1961: pp. 1-15, 1 czrte.Fr. Bur. Rech. Geol. Minieres, Mem., No. 15: 482-494, Orleans.

Burollet, P.F., Mugniot, J.M. and Sweeny, P. 1978. The geology of the Pelagian Block: the margins and basins off southern Tunisia and Tripolitania. In: The Ocean Basins andMargins,vol. 4B: The Western Mediterranean (eds. A.E.M.Nairn, W.H. Kanes, andF.G. Stehli). Plenum Press, New York: 331-359.

Burton, R., Kendall, C.G.St.C., and Lerche, I., 1987. Out of our depth: On the impossibility of fathoming eustatic sea level from the stratigraphic record. Earth Science Reviews, v. 24: 237-277.

Buxton, M.W.M. and Pedley, M.H., 1989. A standardised model for Tethyan Tertiary carbonate ramps. Journal Geological Society London, 146: 746-748.

Buxton, T. M. & Sibley, D. F. 1981. Pressure solution features in shallow buried limestone. J. Sedim. Petrol. **51:** 19-26.

Carrozi, A. V. 1993. Sedimentary petrology. PTR Prentice Hall, Englewood Cliffs , New Jersey: 263.

Catuneanu, O., 2006. Principles of Sequence Stratigraphy. Elsevier, Amsterdam: 375.

Catuneanu, O., Galloway, W.E., Kendall, C.G.ST.C., Miall, A.D., Posamentier, H.W.,Strasser, A. & Tucker, M.E. 2011. Sequence stratigraphy: methodology and nomenclature. Report for the International Sub-Commission on Stratigraphic Classification.

Cavazza, W. M., F.M. Roure, W. Spakman, G. M. Stampfli, and P. A. Ziegler, 2004. The transmed atlas. Berlin, Springer: 141.

Chakraborty P P, Dey S and Mohanty S 2010. Proterozoic platform sequences of Peninsular India: Implications towards basin evolutions and supercontinent assembly; J. Asian Earth Sci. 39**:** 589–607.

Chen, D., Tucker, M.E., Jiang, M. & Zhu, J., 2001. Long-distance correlation between tectonic-controlled, isolated carbonate platforms by cyclostratigraphy and sequencestratigraphy in the Devonian of South China. Sedimentology, 48: 57-78.

Choquette, P.W., James, N.P., 1987. Diagenesis in Limestones. The deep burial environment. Geoscience Canada 14: 4-35.

Choquette, P.W. and Pray, L.C.(1970). Geologic Nomenclature and Classification of Porosity in Sedimentary Carbonates. Bull. Am. Assoc. Petrol. Geol., **54**: 207 - 250.

Claypool, G. E. And Kaplan, J.R. 1974. The origin and distribution of methane in natural gases in marine sediments. New York, Plenum Press: 99-139.

Clemmensen, A., Thomsen, E., 2005. Palaeoenvironmental changes across the Danian–Selandian boundary in the North Sea Basin. Palaeogeography, Palaeoclimatology, Palaeoecology 219: 351–394.

Cloetingh, S., 1988. Intraplate stresses: A tectonic cause for third-order cycles in ` apparent sea level. In Wilgus, C.K., et al. (eds) Sea-level Changes – An Integrated Approach.Society of Economic Paleontologists and Mineralogists Special Publication, 42:19-29.

Colombié C, Strasser A, 2005. Facies, cycles, and controls on the evolution of a keep-up carbonate platform (Kimmeridgian, Swiss Jura). Sedimentology 52:1207–1227

Conant, L.C. and Goudarzi,G.H. 1967. Stratigraphic and tectonic framework of Libya. Bull. Am. Assoc. Petrol., **51**(5): 719-730.

Cook. 1983. Sedimentology of some allochthonous deep-water carbonate reservoirs, Lower Permian, west Texas: carbonate debris sheets, aprons, or submarine fans? (abs.): American Association of Petroleum Geologists Bulletin, v. 63: 442.

Core Laboratories, 2008. A Regional Geological Evaluation of the Deep Sirt Basin, Libya with emphasis on the Paleozoic.

Crevello, P., Sarg, J. F., Read, J. F. & Wilson, J. L. (eds) 1989. Controls' on

Carbonate Platform to Basin Development. Society of Economic Paleontologists and Mineralogists, Special Publication, 44.

Crevello, P. D., 1991. Termination of carbonate platforms--eustatic fluctuations in base level (abs.): American Association of Petroleum Geologists, Bulletin, v. 74: 635-636

Cross, NE, Purser, BH, Bosence DWJ. 1998. The Tectono-sedimentary evolution of a- rift margin carbonate platform: Abu Shaar, Gulf of Suez, Egypt. In: Sedimentation and Tectonics in Rift Basins, Red Sea, Gulf of Aden.Ed. by: BH Purser and WJ Bosence.

Crouch, E. M., G. R. Dickens, H. Brinkhuis, M.-P. Aubry, C. J. Hollis, K. M. Rogers, And H. Visscher, 2003b. The Apectodinium acme and terrestrial discharge during the Paleocene-Eocene thermal maximum: New palynological, geochemical and calcareous nannoplankton observations at Tawanui, New Zealand, Palaeogeogr.Palaeoclimatol. Palaeoecol., 194, 387 – 403, doi:10.1016/S0031-0182(03) 00334-1.

Davies G, .R. 1977. Former magnesian calcite and aragonite submarine cements in Upper Palaeozoic reefs **of** the Canadian Arctic: a summary. Geology, tology**, 16:** 607-621. **41:** 1018-1025. 5: 11-15.

Davies, G. R., 1977. Turbidites, debris sheets, and truncation structures in Upper Paleozoic deep-water carbonates of the Sverdrup Basin, Arctic Archipelago. In H. E. Cook and P. Enos (eds.), Deepwater carbonate environments: SEPM Spec. Publ. 25: 221-247.

De Boer, P & Smith, D., 1994. Orbital Forcing and Cyclic Sequence. In: Boer, P. D., Smith, D., (eds) Orbital Forcing and Cyclic Sequence. International Association of Sedimentologists, Special Publication, **19:** 1-14.

Deconinck, J.-F. and Strasser, A. 1987. Sedimentology, clay mineralogy and depositional environments of Purbeckian green marls (Swiss and French Jura). Eclogae Geol. Helv., 80: 753-772.

De Heinzelin, J., El-Arnauti, A. and Gaziry, A.W. 1980. A preliminary revision of the Sahabi Formation. In: The Geology of Libya (eds M.J. Salem and M.T. Busrewil). Academic Press, London, **I:** 127-133.

Desio, A. 1928. Resultati scientific delta missione alia Oasi di Giarabub (1926-27). Pt. 2: La Geologia. Pub.R. Soc. Geog. Ital, p. U-164.

Desio, A. 1935. Studi geologic! sulla Cirenaica, sul deserto Libico, sulla Tripolitania e sul Fezzan orientate. Missione scientifica della R. Accad. d'ltalie a Cufra, (1931), Roma., v. 1: 480.

Desio, A. 1936a. Prime notizie sulla presenza del Silurico fossilifero nel Fezzan. Boll. Soc.Geol. Ital. v. 55: 116-120.

Desio, A. 1936b, Riassunto sulla presenza del Silurico fossilifero nel Fezzan. Boll. Soc. Geol.Ital. v. 55: 319-356.

Desio, A. 1943. L'esploratzione mineraria della Libia. Coll. Sci. Doc, Min. Afr. Ital., v. 10. Milan: 333.

Desio, A. (1971). Outline of the geomorphological evolution of Libya from the early Tertiary. Mem. Accad. No. 2 Lincei, Attisr. Sci. Fis. Mat. Nat., Ser. 8a, v. 10, No.2, 19-65. Milan Univ. 1st Geol. Paleontol. Publ. No. 67.

Desio, A., Rossi Ronchetti, C., Pozzi, R., Clerici, F., Invernizzi, G., Pisoni, C. and Vigano, P.L. 1963. Stratigraphic studies in the Tripolitanian Jebel (Libya). Mem. Riv. Ital. Paleontol. , v. 9: 126, 34 fig., 3 pl., 1 geol. Map scale 1:50,000, Milano.

Dewey, J.F., Pitman, W.C., Ryan,W.B.F. & Bonnin, J. 1973. Plate tectonics and the

evolution of the Alpine system. Bull.geol. Soc. Am. 84: 3173-3180.

Dewey, J. F., M. L. Helman, E. Turoc, D. H. W. Hutton, and S. D. Knott. 1989. Kinematics of the western Mediterranean, in M. P. Coward, D. Dietrich, and R. G.Park, eds., Alpine tectonics. Geological Society (London) Special Publication 45: 265–283.

Dickson, J. A. D. 1965. Amodified staining technique for carbonate in thin section. Nature. **205:** 587.

Donze, P., Colin, J.-P., Damotte, R., Oertli, O., Peypouquet, J.-P., Said, R., 1982. Les ostracodes du Campanien terminal à l'Eocène inférieur de la coupe de Kef, Tunisie Nord-Occidentale. Bulletin des Centres de Recherches Exploration-Production Elf-Aquitaine, 6: 273-355.

Drake, F., **2000.** Global warming - The science of climate changes. Oxford University Press **,** London: 1-288.

Dunham, R.J., 1962. Classification of carbonate rocks according to depositional texture. In: Ham, W.E., (eds) Classification of carbonate rocks. Association of Petroleum Geologist Bulletin. Memoir, **1:** 108-171

Elag, M.O. 1996. Sedimentological study of the Facha Member in the southwest Sirt Basin,Libya. First Symposium on the Sedimentary Basins of Libya, Geology of the Sirt Basin, vol. 2. (eds. M.J. Salem,A.S. El-Hawat and A.M. Sbeta), Elsevier, Amsterdam: 99-114.

EL-Ghoul, A. 1991. A modified Farwah Group type section and its application to understanding stratigraphy and sedimentation along an E-W section through NC 35A, Sabratah Basin. Third Symposium on the Geology of Libya, vol. 4 (eds. M.J. Salem, O.S.Hammuda and B.A. Eliagoubi), Elsevier, Amsterdam: 1637-1656.

Eliagoubi, B. A., and J. D. Powell, 1980. Biostratigraphy and paleoenvironment of Upper Cretaceous (Maastrichtian) foraminifera of north-central and northwestern Libya. In M. J. Salem and M. T. Busrewil, eds., The geology of Libya: London, Academic Press, v. 1: 137– 153

Elrick, M. 1995. Cyclostratigraphy of Middle Devonian carbonates of the eastern Great Basin. Journal of Sedimentary Research, B65: 61-79.

Embry, A. F. & Johannessen, E. 1992. T-R sequence stratigraphy, facies analysis and reservoir distribution in the uppermost Triassic-Lower Jurassic succession, western SverdrupBasin, Arctic Canada. In: Vorren, T. et al.. (eds), Arctic Geology and Petroleum Potential, Norwegian Petroleum Society Special Publication, **2:** 121-146.

Embry, A. F. and Klovan, J.E. 1971. A Late Devonian reef tracts on northeastern Banks Island, Northwest Territories. Bull. Can. Petrol. Geol., **19**: 730 - 781.

Emery, D. And Robinson, A. 1993. Inorganic Geochemintry: Applications to Petroleum Geology. Blackwell Scientific Publications, Oxford: 254.

Erlich, R.N., Longo, A.P., and Hyare, S., 1993. Response of carbonate platform margins to drowning: Evidence of environmental collapse. In Loucks R.G., Sarg, J.F., eds., Carbonate Sequence Stratigraphy: American Association of Petroleum Geologists, Memoir 57: 241–266.

Fairhead, J.D., Binks, R.M., 1991. Differential opening of the Central and South Atlantic Oceans and the opening of the West African rift system. Tectonophysics 187: 191–203.

Fairhead, J.D. and C.M. Green, 1989. Controls on rifting in Africa and the regional tectonic model for the Nigeria and East Niger rift basins. Journal of African Earth Sciences. 8: 231-249.

Fisher, A.G., 1964. The Lofer cyclothems of Alpine Triassic. Geological Survey of Kansas Bulletin. **169:** 107-149.

Fischer, A. G., 1988. Cyclostratigraphy; *in*, Global Sedimentary Geology Program-Cretaceous Resources, Events, Rhythms, Beaudoin, B., and Ginsburg, R. N., eds.: NATO International Exchange Program, Digne, France: 286 p.

Flower, B.P., Kennett, J.P., 1994. The middle Miocene climatic transition: East Antarctic ice sheet development, deep ocean circulation and global carbon cycling. Palaeogeography, Palaeoclimatology, Palaeoecology 108: 537–555.

Flügel , E. 1982. Microfacies Analysis of Limestones. Springer-Verlag, Berlin, Heidelburg, New York: 633.

Flügel, E., 2004. Microfacies of Carbonate Rocks, Analysis, Interpretation and Application. Springer and Verlag, Berlin: 1-921.

Folk, R.L. 1965. Some aspects of recrystallization in ancient limestones. In: Dolomitization and Limestone Diagenesis (Ed. By L.C. Pray and R.C. Murray) Spec. Publ. Soc.Econ. Paleont. Miner. 13: 14 –48

Folk, R.L., 1974. The natural history of crystalline calcium carbonate; effect of magnesium content and salinity. Journal of Sedimentary Research, **44:** 40-53.

Frakes, L. A., Francis, J. E., Syktus, J. I. 1992. Climate modes of the Phanerozoic: The history of the Earths climate over the past 600 million years. Cambridge University Press, Cambridge: 274.

Fraser, W.W. 1967. Geolgy of the Zelten Field, Libya, North Africa. Proc. 7th World Petrol. Congr., V. 2: 259-264, Elsevier, Amesterdam

Friedman, I. and O'Neil, J.R., 1977. Compilation of stable isotope factors of geochemical interest. In: M. Fleischer (Ed.), Data of Geochemistry. U. S. Geol. Sum., Profess. Paper 440-KK.

Futyan, A. and H. A. Jawzi, 1996. The hydrocarbon habitat of the oil and gas fields of North Africa with emphasis on the Sirt Basin. In M. J. Salem, M. T. Busrewil, A. A. Misallati, and M. A. Sola, eds., The geology of the Sirt Basin: Amsterdam, Elsevier,v. 2: 287–307.

Galloway, W.E., 1989. Genetic stratigraphic signatures in basin analysis I: architecture and genesis of flooding-surface bounded depositional units. American Association of Petroleum Geologists, Bulletin, v. 73: 125–142.

Garea, B. B., 1996, Environment of deposition and diagenesis of the Bead Reservoir in Block NC74F, southwest Sirt Basin, Libya. In M. J. Salem, M. T. Busrewil, A. A. Misallati, and M. A. Sola, eds., The geology of the Sirt Basin: Amsterdam, Elsevier, v. 2: 115–134.

Gavrilov, Y.O., Shcherbinina, E.A., Oberhänsli, H., 2003. Paleocene–Eocene boundary events in the northeastern Peri-Tethys. In: Wing, S.L., Gingerich, P.D., Schmitz, B., Thomas, E. (Eds.), Causes and Consequences of Globally Warm Climates in the Early Paleogene: Boulder, Colorado. Geological Society of America Special Paper, v. 369: 147–168.

Gawthorpe, R.L. & Leeder, M.R. 2000. Tectono-sedimentary evolution of active extensional basins. Basin Res., 12: 195-218.

Gawthorpe, R. L., Sharp, I.R., Underhill I., J.R. &Gupta, S. 1997. Linked sequence stratigraphic and structural evolution of propagating normal faults. Geology, 25: 795-798.

Gebelein, C. D., Steinen, R. P., Garrett, P., Hoffman, E. J., Queen, J. M. and Plummer, L. N., 1980. Subsurface dolomitization beneath the tidal flats of central west Andros Island, Bahamas. In: D. H. Zenger, J. B. Dunham and R. L.

Ethington (Eds.), Concepts and Models of Dolomitization. SEPM Spec. Pub. No. 28: 31-49

Gohrbandt, K.H.A. 1966b. Upper Cretaceous and Lower Tertiary stratigraphy along The western and southwestern edge of the Sirt Basin, Libya. In: South-central Libya and northern Chad (ed. J.J. Williams). Petrol. Explor. Soc. Libya, 8th Annu. Field Conf.: 33-41.

Goldhammer, R. K. 1997. Compaction and decompaction algorithms for sedimentary carbonates. Journal of Sedimentary Research. **67:** 26-35.

Goldhammer, R.K., Dunn, P.A. and Hardie, L.A. 1987. High frequency glacio-Eustatic sealevel oscillations with Milankovitch characteristics recorded in Middle Triassic platform carbonates in northern Italy. Am. J. Sci., 287: 853–892.

Goldhammer, R., Dunn, P., Hardie, L., 1990. Depositional cycles, composite sea-Level changes, cycle stacking patterns, and the hierarchy of stratigraphic forcing: examples from Alpine Triassic platform carbonates. Geological Society of America Bulletin, **102:** 535-562.

Goldhammer, R.K., Lehmann, P.K., and Dunn, P.A., 1993. The origin of high Frequency platform cycles and third order sequences (Lower Ordovician El Paso Gp, Western Texas): constraints from outcrop data and stratigraphic modelling. Journal of Sedimentary Petrology, v. 63: 318–359.

Golonka J., Krobicki M., Oszczypko N., S³aby E., Popadyuk I. & Netchepurenko A., 2004. Mesozoic volcanism associated with triple-junction zone of the Eastern Carpathians (Ukraine). Mineralogical Society of Poland – Special Papers, 24: 45–50.

Goudarzi, G.H. 1970. Geology and mineral resources of Libya - a reconnaissance. U.S.geol. Surv. Prof. Pap., **660**:104.

Goudarzi, G. H., 1980. Structure-Libya. In M. J. Salem and M. T Busrewil, eds.. Geology of Libya: Tripoli, Libya, Al-Fateh University, v. 3: 879-892.

Goudarzi, G.H. and Smith, LP.1978. Prelimi nary structure-contour map of the Libyan Arab Republic and adjacent areas; 1:2,000,000. U.S. Geol. Surv. Misc. GeoL Invest., Map I-350C.

Gradstein, F., Ogg, J., Smith, A., 2004. A Geologic Time Scale. Cambridge University Press. United Kingdom: 1-589 .

Gras, R., and B. Thusu, 1998. Trap architecture of the Early Cretaceous Sarir andstone in the eastern Sirt Basin, Libya. In S. D. Macgregor, J. T. R., Moody, and D. D. Clark- Lowes, eds., Petroleum geology of north Africa: Geological Society (London) Special Publication 132: 317–334.

Gregory, J.W. 1911. The geology of Cyrenaica. Q. J Geol. Soc. London, **67** (268): 572-615.

Grotzinger, J.P. 1986. Upward shallowing platform cycles: a response to 2.2 billion years of low-amplitude, highfrequency (Milankovitch band) sea level oscillations.Paleoceanography, 1: 403–416.

Guasti, E., Kouwenhoven, T.J., Brinkhuis, H., Speijer, R.P., 2005. Paleocene sea-level and productivity changes at the southern Tethyan margin (El Kef, Tunisia). Marine Micropaleontology: 55, 1-17.

Guiraud, R. 1998. Mesozoic rifting and basin inversion along the northern African Tethyan margin: an overview. In: Petroleum Geology of North Africa,(ed. D.S. Macgregor, R.T.J. Moody, D.D. Clark-Lowes), Geol. Soc. Special Publication No. 132: 217-230.

Guiraud, R, and W. Bosworth, 1997. Senonian basin inversion and rejuvenation of

rifting in Africa and Arabia: Synthesis and implications to plate-scale tectonics. Tectonophysics, v. 282: 39–82.

Guiraud, R., and J. C. Maurin, 1991. Le rifting in Afrique au Cre´tace´ infe´rieur: ynthe`se structurale, mise en e´vidence de deux e´tapes dans la gene`se des bassins, relations avec les ouvertures oce´anique pe´ri-africaines. Bulletin de la Socie´te´ Ge´ologique de France, v. 162: 811–823.

Guiraud,R., R.M. Binks, J.D. Fairhead, andM.Wilson, 1992. Chronology of geodynamic setting of the Cretaceous– Cenozoic rifting in west and central Africa.Tectonophysics, v. 213: 227–234.

Guiraud, R., and Bosworth, W., 1999. Phanerozoic geodynamic evolution of northeastern Africa and the northwestern Arabian platform. Tectonophysics, v. 315: 73-108.

Guiraud, R., Bosworth, W., Thierry, J., and Delplanque, A., 2005. Phanerozoic geological evolution of Northern and Central Africa: An overview. Journal of African Earth Sciences, v. 43: 83-143.

Gumati, Y. D., 1982. Paleocene facies of the Sirte basin and structural evolution of the basin during Paleocene time: Master's thesis. University of South Carolina, Columbia,South Carolina: 55.

Gumati, Y. D., and W. H. Kanes, 1985. Early Tertiary subsidence and sedimentary facies, north Sirt Basin, Libya. AAPG Bulletin, v. 69: 39–52.

Gumati, Y.D., Kanes, W.H. and Schamel, S. 1996. An evaluation of the hydrocarbon potential of the sedimentary basins of Libya. Journ. Pet. Geol.v. 19: 39-52.

Gumati, Y. D., and A. E. Nairn, 1991. Tectonic subsidence of the Sirt Basin, Libya. Journal of Petroleum Geology, v. 14: 93–102.

Gumati, Y. D., and S. Schamel, 1988. Therma maturation history of the Sirte Basin, Libya. Journal of Petroleum Geology, v. 11: 205–218.

Gupta, S., Cowie, P.A., Dawers, N.H. & Underhill, J.R. 1998. A mechanism to explain rift-basin subsidence and stratigraphic patterns through fault array evolution. Geology, 26: 595-598.

Hallett, D., 2002. Petroleum Geology of Libya. Elsevier, Amsterdam. 503p.

Hallet, D., and A. El Ghoul, 1996. Oil and gas potential of the deep troughs areas in the Sirt Basin, Libya. In M. J.Salem, A. S. El-Hawat, and A. M. Sbeta, eds., The geology of Sirt Basin: Amsterdam, Elsevier, v. 7: 455–484.

Halley, R. B. and Harris, P. M., 1979. Fresh-water cementation of a 1,000 year-old oolite. J. Sediment. Petrol., 49: 969-988.

Hallock, P. 1988. The role of nutrient availability in bioerosion: consequences to carbonate buildups. Palaeogeogr., Palaeoclim., Palaeoecol., 63: 275–291.

Hallock, P. and Schlager, W. 1986. Nutrient excess and the demise of coral reefs and carbonate platforms. Palaios, 1: 389–398.

Hammuda, O. S., 1980. Geological factors controlling fluid trapping and anomaolous freshwater occurrence in the Tadrart sandstone, Alhamada Alhamra Area, Ghadamis Basin. In: M.J. Salem and M.T. Busrewil (Eds.). The Geology of Libya2, Academic press, London: 501-508.

Hammuda, O.S. Van Hinte, J.E. and Nederbragt, S. 1991. Geohistory analysis mapping incentral and southern Tarabulus Basin, northwestern offshore of Libya. Third Symposium onthe Geology of Libya, vol. 4 (eds. M.J. Salem, O.S.Hammuda and B.A Eliagoubi), Elsevier, Amsterdam: 1657-1680.

Hamyouni, E. A., Amer, I. A., Riani, M.A., El-Ghull, A. B. And Rhoma, S. A. 1984. Source and Habitat of Oil in Libyan Basins. NOC Tech. Data Library, Rept. Loc. No. 188/3/19: 55.

Handford, C. R., and R. G. Loucks, 1993. Carbonate depositional sequences and systems tracts: Responses of carbonate platforms to relative sea level changes. In R. G. Loucks and J. F. Sarg, eds., Carbonate sequence stratigraphy recent developments and application. AAPG Memoir 57: 3–41.

Haq, B.U. and Al-Qahtani, A.M. 2005. Phanerozoic cycles of sea-level change on the Arabian Platform. GeoArabia (Manama), 10: 127–160.

Haq, B.U., Hardenbol, J., and Vail, P.R., 1988. Mesozoic and Cenozoic Chronostratigraphy and cycles of Sea-level Change. In Wilgus, C.K., Hastings, B.S., Kendall, C.G.S.C., Posamentier, H.W., Ross, C.A., and Van Wagoner, J.C., eds., Sea- level changes: An Integrated approach, v. 42: Tulsa Oklahoma, Society of Economic Paleontologists and Mineralogists.

Hardie, L. A., and Shinn, E. A., 1986. Carbonate Depositional Environments, modern and ancient-pt. 3, tidal flats:Colorado school of Mines Quarterly, v. 81: 1-74

Harding, T. (1984). Graben hydrocarbon occurrences and structural style. Bull. Am. Assoc. Petrol. Geol., **68**(3): 333-362.

Harris, A.D., Miller, K.G., Browning, J.V., Sugarman, P.J., Olsson, R.K., Cramer, B.S., Wright, J.D., 2010. Integrated stratigraphic studies of Paleocene–lowermost Eocene sequences, New Jersey Coastal Plain: evidence for glacioeustatic control. Paleoceanography 25: 3211 doi:10.1029/2009PA001800.

Hilbrecht, H., Arthur, M.A. & Schlanger, S.O. 1986. The Cenomanian-Turonian boundary event: sedimentary, faunal and geochemical criteria developed from stratigraphic studies in NW-Germany. Lecture Notes in Earth Sciences 8: 345–351. DOI 10.1007/BFb0010217

Hillgartner, H., Strasser, A. 2003. Quantification of high-frequency sea-level fluctuations in shallow-water carbonates: an example from the Berriasian–Valanginian (French Jura). Palaeogeography, Palaeoclimatology, Palaeoecology. **200:** 43-63.

Hodell, D.A., Kennett, J.P., 1986. Late Miocene - Early Pliocene stratigraphy and paleoceanography of the South Atlantic and southwest Pacific Oceans. A synthesis. Paleoceanography 1: 285–311.

Hudson, J.D. 1975. Carbon isotopes and limestone cement. Geology, **3:** 19-22.

Hunt, D. & Tucker, M.E., 1992. Stranded parasequences and the forced regressive wedge systems tract: deposition during base-level fall. Sedimentary Geology, 81: 1-9.

Hunt, D. & Tucker, M.E., 1993. Sequence stratigraphy of carbonate shelves with an example from the mid-Cretaceous (Urgonian) of southeast France. In Posamentier, H.W., Summerhayes, C.P., Haq, B.U. & Allen, G.P. (eds) Sequence Stratigraphy and Facies Associations. International Association of Sedimentologists SpecialPublication, 18: 307-341.

Hunt, D. & Tucker, M.E., 1995. Stranded parasequences and the forced regressive wedge systems tract: deposition during base-level fall – reply. Sedimentary Geology, 95: 147- 160.

Husinec, A., Basch, D., Rose, B., Read F.J., 2008. FISCHERPLOTS: An Excel Spread sheet for computing Fischer plots of accommodation change in cyclic carbonate successions in both the time and depth domains. Computers & Geosciences, **34:** 269–277.

Irwin, H ., Curtisc, . & Colemanm, 1977. Isotopic evidence **for** source of diagenetic carbonates formed during burial of organic-rich sediments. Nature, **269:** 209-2 1 3.

Issawi, B. 1972. Review of Upper Cretaceous-Lower Tertiary stratigraphy in central

and southern Egypt. AAPG Bull., 56: 1448–1463.

James, N. P. and Choquette, P. W., 1983. Diagenesis 6. Limestones - The sea floor diagenetic environment. Geosci. Can., 10: 162-179.

James, N. P., Ginsburg, R. N., Marszalek, D. S. & Choquette, P. W. 1976. Facies and fabric specificity of early subsea cements in shallow Belize (British Honduras) reefs. J. sedim. Petrol. **46:** 523-544.

James, N. P. & Kendal, A. C., 1992. Introduction to carbonate and evaporite facies models. In: Walker, R. G. & James, N. P. (eds) Facies models. Response to Sea-level Change: 265- 275.

Janssen, M. E., 1996. Intraplate deformation in Africa as a consequence of plate boundary changes, inferences from subsidence analysis and tectonic modelling of the Early and Middle Cretaceous period: Ph.D. thesis, Vrije Universiteit, Amsterdam: 161.

Janssen, M. E., R. A. Stephenson, and S. Cloetingh, 1995. Temporal and spatial correlation between change in plate motions and evolution of rifted basin in Africa. Geological Society of America Bulletin, v. 107: 1317–1332.

Jerzkiewicz, T., Ghummed, M.A., Tshakreen, S.O. and Abugares, A.A. 2002. Sequence stratigraphic definition of the Ghadamis/Sirt boundary in late Cretaceous time (abstract only). Second Symposium on the Sedimentary Basins of Libya. The Geology of northwest Libya. Book of abstracts: 53.

Jones H. L. 1996. Late Cretaceous-Early Tertiary Stratigraphy of Southern Concession 6, Sirt Basin, Libya. In: The Geology of the Sirt Basin (Eds. Salem, M.J., Mouzughi, A. J., and Hammuda, O. S.), Elsevier, Amesterdam: 169-183.

Jones, B., Desrochers, A., 1992. Shallow Platform Carbonates**.** In: Walker R.G., James N.G. (eds) Facies Models: response to sea level change. Geological Association of Canada: 277-301.

Jordi, H. A. and Lonfat, F. 1963. Stratigraphic subdivision and problems in Upper Cretaceous-Lower Tertiary deposits in northwestern Libya. Rev. Inst. Fr. Petrole, **18**(10-11): 1428-1436.

Keller, G., Adatte, T., Stinnesbeck, W., Stüben, Kramar, U., Berner, Z., Li, L., Salis Perch-Nielson, K., 1998. The Cretaceous–Tertiary transition on the shallow Saharan Platform of southern Tunisia. Geobios 30: 951–975.

Keller, G., Berner, Z., Thierry, A., Stueben, D. 2004. Cenomanian-Turonian and δ13C and δ18O, sea level and salinity variations at Pueblo, Colorado. Palaeoclimatology, Palaeoclimatology, Palaeoecology. **211:** 19-43.

Kendall, C. G. St. C., and Schlager, W., 1981. Carbonates and relative changes in sea level. Marine Geology, v. 44: 181-212.

Khoja, E. R. 1971. Petrography and diagenesis of Lower Paleocene Carbonate Reservoir Rocks, Dahra Field, Sirt Basin, Libya. Ph.D. Thesis, Rice University, Houston, Texas.

Klett, T.R., 2001. Total Petroleum Systems of the Pelagian Province, Tunisia, Libya, Italy and Malta ‐ The Bou Dabbous ‐ Tertiary and Jurassic‐Cretaceous Composite. US Geological Survey Bulletin, 2202-D.

Klitzsch, E., 1971. The structural development of parts of North Africa since Cambrian time. In: Gray, C. (ed), First Symposium on the Geology of Libya, Faculty of Science, University of Libya, Tripoli: 253-262.

Klitzsch, E. and Squyres, C.H. 1990. Paleozoic and Mesozoic geological history of northeastern Africa based upon new interpretation of Nubian strata. Bull.Amer. Assoc. Pet. Geol. v. 74: 1203-1211.

Knytl, J., Brydle, G. and Greenwood, D. 1996. Tectonic history and structural

development of the Kaf-Themar trend of the western Sirt Basin. First Symposium on the Sedimentary Basins of Libya, Geology of the Sirt Basin, vol. 3. (eds. M.J. Salem,M.T Busrewil, A.A. Misallati and M.J. Sola), Elsevier, Amsterdam: 167-200.

Koerschner, W. F., and Read, J. F., 1989. Field and modeling studies of Cambrian carbonate cycles, Virginia Appalachians. Journal of Sedimentary Petrology, v. 59: 654-687.

Kominz, M. A., J. V. Browning, K. G. Miller, P. J. Sugarman, S. Mizintseva, and C. R. Scotese 2008. Late Cretaceous to Miocene sea-level estimates from the New Jersey and Delaware coastal plain coreholes: An error analysis. Basin Res., 20: 211 –226, doi:10.1111/j.1365-2117.2008.00354.x.

Koscec, G. B., and S. S. Gherryo, 1996. Geology of reservoir performance of the Messlah oil field, Libya. In M. J. Salem, M. T. Busrewil, A. A. Misallati, and M. A. Sola, eds., The geology of the Sirt Basin: Amsterdam, Elsevier, v. 2: 365–389.

Kouwenhoven, T.J., Speijer, R.P., van Oosterhout C.W.M., vander Zwaan, G.J., 1997. Benthic foraminiferal assemblages between two major extinction events: the Paleocene El Kef section, Tunisia. Marine Micropaleontology, 29: 105-127.

Kuss, J., Scheibner, C., Gietl, R., 2000. Carbonate Platform to Basin Transition along an Upper Cretaceous to Lower Tertiary Syrian Arc Uplift, Galala Plateaus, Eastern Desert. Egypt. GeoArabia 5: 405-424**.**

Laya-Pereira, Juan, Carlos 2012. Permian Carbonates in the Venezuelan Andes. Doctoral thesis, Durham University. Available at Durham E-Theses Online: http://etheses.dur.ac.uk/3378/

Lear, C.H., Elderfield, H., Wilson, P.A., 2000. Cenozoic deep-sea temperatures and global ice volumes from Mg/Ca in benthic foraminiferal calcite. Science 287: 269–272.

Lee, Y. I. And Friedman, G. M. 1987. Deep burial dolomitizatiopn in the Ordovician Ellenburger Group carbonates, West Texas and Southeastern New Mexico. J. Sediment. Petrolg, **57** (3): 544-557.

Lehrmann, D.J., Goldhammer, R.K., 1999. Secular variation in parasequence and facies stacking patterns of platform carbonates: a guide to application of stacking-patterns analysis in strata of diverse ages and settings. Society of Economic Palaeontologists and Mineralogists Special Publication, **63:** 187-226.

Le Pichon, X., F. Bergerat, and M. J. Roulet, 1988. Plate kinematics and tectonics leading to the Alpine belt formation: A new analysis. In S. Clark, B. C. Barchfiel, and J. Suppe, eds., Processes in continental lithospheric deformation: Geological Society of America Special Paper 218: 111–131.

Littler, M. M. and Littler, D. S., 1984. Models of tropical reef biogenesis: The contribution of algae. Prog. Phycol. Res., 3: 323-364.

Logan, B.W., Semeniuk, V., 1976. Dynamic metamorphism; process and products In Devonian carbonate rocks: Canning Basin, Eastern Australia. Western Australia. Geological Society of Australia special Publication, **6:** 138

Lokier, S.W., Willson, M.E.J., and Burton, L.M., 2009. Marine biota response to clastic sediment influx: a quantitative approach. Palaeogeography, Palaeoclimatology, Palaeoecology, v. 281: 25–42.

Longman, M. W. 1977. Factors controlling the formation of microspar in the Bromide Formation. J. sedim. Petrol. **47:** 347 - 350.

Longman, M. W. 1980. Carbonate diagenetic textures from nearsurface diagenetic environments. Bull. Am. Ass. Petrol. Geol. **64:** 461-487.

Lucia, F. J., 1983. Petrophysical parameters estimated from visual description of carbonate rocks: a field classification of carbonate pore space: Journal of Petroleum Technology, March, v. 35:. 626–637.

Lucia, F J., 1995. Lower Paleozoic cavern development, collapse, and dolomitization, Franklin Mountains, El Paso, Texas, *in* Budd, D. A., Saller, A. H., and Harris, P. M., Eds., Unconformities and porosity in carbonate strata: AAPG Memoir 63: 279-300.

Lucia, F. J. 1999. Carbonate Reservoir Characterization. Springer- Verlag Berlin Heidelberg: 226.

Machhour, L., Masse, J.-P., Oudin, J.L., Lambert, B., Lapointe, P., 1998. Petroleum potential of dysaerobic carbonate source rocks in an intrashelf basin: the Lower Cretaceous of Provence, France. Petroleum Geosciences 4 (2): 139-146.

Macintyre, I. G., Burke, R. G. and Stuckenrath, R., 1977. Thickest recorded Holocene reef section, Osla Perez core hole, Alacran Reef, Mexico. Geology, 5: 749-754.

Madi, A., Bourque, P. A., Mamet, B. L. 1996. Depth-related ecological zonation of a Carboniferous carbonate ramp: Upper Viséan of Béchar Basin, Western Algeria. Facies, **35:** 58-80.

Magara, K. 1980. Comparison of porosity-depth relationships of shale and sandstone. J. Petr. Geol. 3: 175-185

Magnier, P. 1963. Etude stratigraphique dans le Gebel Nefousa et le Gebel Garian (Tripolitaine, Libye). Bull. Soc. Geol. Fr., Ser. 7, V. 5, No. 2: 89-94, 2 fig. Paris.

Maliva, R. G. 1998. Skeletal aragonite neomorphism - quantitative modelling of a two-water diagenetic system. Sedimentary Geology. **121:** 179-190.

Mallarino, G., Goldstein, R.H., Di Stefano, P., 2002. New approach for quantifying water depth applied to the enigma of drowning of carbonate platforms. Geology 30: 783–786.

Mallela, J., and Perry, C.T., 2007. Calcium carbonate budgets for two coral reefs affected by different terrestrial runoff regimes, Rio Bueno, Jamaica: Coral Reefs, v. 26: 129–145.

Mamgain, V. D. 1980. The Pre-Mesozoic (Precambrian to Palaeozoic) Stratigraphy of Libya: A Reappraisal. Ind. Res. Cent., Tripoli, Bull: 104.

Mancini, E.A. and Puckett, T.M. 2002. Transgressiv-eregressive cycles in Lower Cretaceous strata, Mississippi Interior Salt Basin area of the northeastern Gulf of Mexico. Cretaceous Res., 23: 409–438.

Mancini, E.A. and Puckett, T.M. 2002b. Transgressive-regressive cycles: application to petroleum exploration for hydrocarbons associated with Cretaceous shelf carbonates and coastal and fluvial-deltaic siliciclastics, northeastern Gulf of Mexico. In: Armentrout, J.M. and Rosen, N.C., Eds., Sequence Stratigraphic Models for Exploration and Production: Evolving Methodology, Emerging Models and Application Histories. 22nd Annual Gulf Coast Section SEPM Foundation, Bob F. Perkins Research Conference. Houston, Gulf Coast Section, SEPM: 173-199.

Mancini, M.V., Paeza, M.M., Prietob, A.R., Stutza, S., Tonelloa, M., Vilanovab, I., 2005. Mid-Holocene climatic variability reconstruction from pollen records (32–521S, Argentina). Quaternary International 132: 47–59.

Marinelli, O. 1920. Sulla morfologia della Cirenaica. Riv. Georgr. Ital. Firenze. 27: 69- 86.

Marlowe, J. I. 1971. High-magnesium calcite cement in calcarenites from Aves

Swell, Caribbean Sea. In: Carbonate Cements (Ed. By O. P. Bricker): pp. 111-116. The Johns Hopkins University Press, Baltimore, Md.Meister, E.M., Ortiz, E.F., Pierobon, E.S.T., Arruda, A.A.

Masse, J.P., Montaggioni, L.F., 2001. Growth history of shallow-water carbonates: control of accomodation on ecological and depositional processes. Int. J. Earth Sci. 90: 452-469.

Miller, K.G., Fairbanks, R.G., Mountain, G.S., 1987. Tertiary oxygen isotope synthesis, sea level history, and continental margin erosion. Paleoceanography 2: 1–19.

Miller, K.G., Wright, J.D. and Browning, J.V. 2005. Visions of ice sheets in a greenhouse world. Mar. Geol., 217: 15–231.

Miller, K.G., Kominz, M.A., Browning, J.V., Wright, J.D., Mountain, G.S., Katz, M.E., Sugarman, P.J., Cramer, B.S., Christie-Blick, N., Pekar, S.F., 2005. The Phanerozoic record of global sea-level change. Science 310: 1293–1298.

Montgomery, S.L. 1994a. Ghadames Basin and surrounding areas, structure, tectonics, geochemistry and field summaries. Petroleum Frontiers, Pet. Inf. Corp., Littleton, Colorado, v. 10, no. 4: 79.

Montgomery, S.L. 1994b. Sirte Basin, north-cetral Libya: prospects for the future. Petroleum Frontiers, Pet. Inf. Corp., Littleton, Colorado, v. 11, no. 1: 94.

Moore, C. H., 1989. Carbonate Diagenesis and porosity. In Development in Sedimentology No. 46: 338.

Morgan, W. J., 1980. Hotspot tracks and the opening of the Atlantic and Indian Oceans. In C. Emiliani, ed., the sea: Wiley, New York, v. 7: 443–467.

Morgan, W. J., 1983. Hotspot tracks and the early rifting of the Atlantic. Tectonophysics, v. 94: 123–139.

Morgan, M.A., Grocott, J. and Moody, R.T.J. 1998. The structural evolution of the Zaghouan-Ressas structural belt, northern Tunisia. In: Petroleum Geology of North Africa, (ed. D.S Macgregor, R.T.J. Moody, D.D. Clark-Lowes), Geol. Soc. Special Publication No. 132: 405-422.

Mouzughi, A. J. 1991. Petrography and Lithofacies of the Satal Formation in northwestern Sirt Basin, Libya. In: The Geology of Libya (eds M. J. Salem and M. N. Belaid). Elsevier, Amesterdam, v: 1841-1854.

Moyra E. J. and Hall. R. 2010. Tectonic influences on SE Asian carbonate systems and their reservoir development. In: SEPM, Spec. Publ: 13-40.

Müller, R.D., Sdrolias, M., Gaina, C., Steinberger, B., Heine, C., 2008. Long-term sea- level fluctuations driven by ocean basin dynamics. Science 319: 1357–1362.

Osleger, D.A. and Read, J.F. 1991. Relation of eustasy to stacking patterns of meter-scale carbonate cycles, Late Cambrian. USA. J. Sed. Petrol., 61: 1225–1252.

Pallas, P. 1980. Water resources of the Socialist People's Libyan Arab Jamahiriya. Second Symposium on the Geology of Libya., vol. 2 (eds. M.J. Salem and M.T. Busrewil), Academic Press, London: 539-594.

Pedley, M. 1992. Freshwater (phytoherm) reefs: the role of biofilms and their bearing on marine reef cementation.-Sedimentary Geology, 79: 255-274.

Perrier, R. & Quiblier, J. 1974. Thickness changes in sedimentary layers during comapaction history; Methods for Quantitative Evaluation. Bull. Am. Assoc. Petrol. Geol. 58 (3): 507-520.

Petroleum Reasearch Centre and Teknica Petroleum Services Ltd (2001). Geology and Hydrocarbon Evaluation of Tertiary and Mesozoic Rocks, western Sirt Basin, Libya. A Joint Project.

Peypouquet, J.-P., Grousset, F., Mourguiart, P., 1986. Paleooceanography of the Mesogean Sea based on ostracods of the northern Tunisian continental shelf between the Late Cretaceous Cretaceous and Early Paleogene. Geologische Rundschau, 75: 159-174.

Pietersz, C. R. 1968. Proposed nomenclature for rock units in Northern Cyrenaica. Petrol. Explor. Soc. Libya, 10th Ann. Field Conf., 1968. In Geology and Archeology of Northern Cyrenaica (Ed. F. T. Barr): 125-130, Tripoli.

Posamentier, H.W., Jervey, M.T. and Vail, P.R., 1988. Eustatic controls on clastic deposition I—conceptual framework. In Wilgus, C.K. Hastings, B.S. Ross, C.A. Posamentier, H.W.Van Wagoner, J.C. and St.C. Kendall, C.G. Eds., Sea-Level Changes: An Integrated Approach. SEPM (Society for Sedimentary Geology) Special Publication No. 42: 109-124.

Pratt, B. R., James, N.P., Cowan, C.A., 1992. Peritidal carbonates. In: Walker, R.G., James, N.G. (eds) Facies Models: response to sea level change. Geological Association of Canada: 277-301.

Prosser, S. 1993. Rift-related linked depositional systems and their seismic expression. In: Tectonics and Seismic Sequence Stratigraphy (Ed. by G. Williams and A. Dobb), Spec. Publ. Geolo. Soc. Lond., 71: 35-66.

Radke, B. M. and Mathis, R. L. 1980. On the formation and occurrence of Saddle Dolomite. J. Sediment. Petrol., **50**: 1149-1168.

Read, J.F, 1982. Carbonate Platforms of Passive (extensional) Continental Margin: Types, Characteristics and Evolution. Tectonophysics. **81:** 195-212.

Read, J.F., 1985. Carbonate Platforms Facies models. American Association of Petroleum Geologist Bulletin, **69:** 1-21.

Read, J.F. and Goldhammer, R.K. 1988. Use of Fischer plots to define third-order sea-level curves in Ordovician peritidal cyclic carbonates, Appalachians. Geology, 16: 895–899.

Read, J.F., Grotzinger, J.P., Bova, J.A. and Koerschner, W.F. 1986. Models for generation of carbonate cycles. Geology, 14: 107–110.

Read, J.F., Koerschner, W.F., Osleger, D.A., Bollinger, G.A. and Coruh, C. 1991 Field and modeling studies of Cambrian carbonate cycles, Virginia Appalachians – reply. J. Sed. Petrol., 61: 647–652.

Reali S., Ronchi P. and Borromeo O., 2003. Sedimentological model of El Garia Formation (NC-41Offshore Libya). In: Salem, M.J. and Oun, K.M. (Eds) The Geology of Northwest Libya, Sedimentary Basins of Libya, Second Symposium. V. II: 69-97

Reineck, H.E., 1963. Sedimentgefüge im Bereich der südlichen Nordsee: Abhandlungen der Senckenbergischen Naturfoschenden Gesellschaft, **505**: 1-138.

Reyment, R.A., 1980. Biogeography of the Saharan Cretaceous and Paleocene epicontinental transgressions. Cretaceous Research 1: 299–327.

Ricken, W. 1992. Variations of sedimentation rates in rhythmically bedded sediments. Distinction between depositional types. In Einsele, G., Ricken, W., Seilacher, A. eds.Cycles and events in stratigraphy. Berlin: Springer.

Rohlich, P. 1980. Tectonic development of Al Jabal al Akhdar. Second Symposium on The Geology of Libya. vol. 3 (eds. M.J. Salem and M.T. Busrewil), Academic Press, London: 923-932.

Roohi, M., 1996. Geological history and hydrocarbon migrationpattern of the As

Zaahra-Al Hufrah platform. In M. J. Salem, M. T. Busrewil, A. A. Misallati, and M. A. Sola, eds., The geology of the Sirt Basin: Amsterdam, Elsevier, v. 1: 195–232.

Rossi, M. E., M. Tonna, andM. Larbash, 1991. Latest Jurassic–Early Cretaceous deposits in the subsurface of the eastern Sirt Basin (Libya): Facies and relationships with tectonics and sea level changes. In M. J. Salem, A.M. Sbeta, and M. R. Bakbak, eds., The geology of Libya: Amsterdam, Elsevier, v. 6: 2212–2225.

Ruban, D.A., Zorina, S.O., Conrad, C.P., 2010b. No global-scale transgressive–Regressive cycles in the Thanetian (Paleocene): evidence from interregional correlation. Palaeogeography, Palaeoclimatology, Palaeoecology 295: 226–235.

Ruban, D.A., Zorina, S.O., Conrad, C.P., Afanasieva, N.I., 2012. In quest of Paleocene global-scale transgressions and regressions: contraints from a synthesis of regional trends. Proceedings of the Geologists' Associations 123: 7–18.

Rusk, D. C., 2001. Libya: Petroleum potential of the under explored basin centers–A Twenty -first-century challenge. In: Downey, M.W., Threet, J.C. and Morgan, W.A. (Eds), Petroleum Provinces of the Twenty-First Century. AAPG Memoir, 74: 429–452.

Sadler, P.M., Osleger, D.A., Montañez, P. 1993. On the labeling, length, and Objective basis of Fischer plots. Journal of Sedimentary Research, **63:** 360-368.

Saenz de Santa Maria, F. 1993. Tectonic and sedimentary evolution of the Sirt Basin: an overview. Arabian Gulf Oil Company internal report.

Said, R. 1962. The Geology of Egypt. Elsevier, Amsterdam: 337.

Sakai, S., Kano, A. 2001. Original oxygen isotope composition of planktic Foraminifera preserved in diagenetically altered Pleistocene shallow-water carbonates. Marine Geology. **172:** 197-204.

Sandford, R. M., 1970. Sarir oil field—Desert surprise, in M. T. Halbouty, ed., Geology of giant petroleum fields: AAPG Memoir 14: 449–476.

Savostin, L. A., J. C. Sibuet, L. P. Zonenshain, X. Le Pichon, andM. J. Roulet, 1986. Kinematic evolution of the Tethys 1026 Geologic Note belt from the Atlantic Ocean to the Pamirs since the Triassic: Tectonophysics, v. 123: 1–35.

Sbeta, A.M. 1990. Stratigraphy and lithofacies of Farwah Group and its equivalent: Offshore NW Libya. Petrol. Res. Jour. (Tripoli), v. 2: 42-56.

Scheibner, C., J. Kuss, R.P. Speijer 2003. Stratigraphic modelling of carbonate platform-to-basin sediments (Maastrichtian to Paleocene) in the Eastern Desert, Egypt. PALAEO, 200: 163-185.

Scheibner, C., Marzouk, A.M., Kuss, J., 2001a. MaastrichtianEarly Eocene litho-biostratigraphy and Palaeogeography of the northern Gulf of Suez region, Egypt. J. Afr.Earth Sci. 32: 223-255.

Scheibner C, Speijer RP 2008. Late Paleocene–early Eocene Tethyan carbonate Platform evolution - A response to long- and short-term paleoclimatic change. Earth Sci Rev 90: 71-102.

Schlager, W. 1981. The paradox of drowned reefs and carbonate platforms. Geol. Soc. Am. Bull., 92: 197–211.

Schlager, W. 1989. Drowning unconformities on carbonate platforms. In: Controls on Carbonate Platform and Basin Development. Society of Economic Paleontologists and Mineralogists Special Publication, 44: 15-25.

Schlager, W., 1992. Sedimentology and sequence stratigraphy of reefs and carbonate platforms. Tulsa, OK, American Association of Petroleum Geologists

Continuing Education Course Note Series #34: 71.

Schlager, W., 2005. Carbonate sedimentology and sequence stratigraphy. Society of Economic Paleontologists and Mineralogists Concepts of Sedimentology and Paleontology, **8**: 1-198

Schlische, R.W. & Olsen, P.E. 1990. Quantitative ¢lling models for continental extensional basins with applications to earlyMesozoic rifts of North America. J. Geol., 98: 135-155.

Schmitz, B., and V. Pujalte 2007. Abrupt increase in seasonal extreme precipitation at the Paleocene-Eocene boundary. Geology, 35: 215–218, doi:10.1130/G23261A.1.

Scholle, P. A. and Halley, R. B., 1985. Burial diagenesis: out of sight, out of mind. In: N. Schneidermann and P. M. Harris (Eds.), Carbonate Cements. SEPM Spec. Pub. No.36: 309-334.

Scholle, P., Ulmer-Scholle, D., 2003. A color guide to the petrography of carbonate rocks, grains, textures, porosity, diagenesis. American Association of Petroleum Geologist Memoir, **77**: 0-460

Schroder, J. H. 1972. Fabrics and sequences of submarine carbonate cements in Holocene Bermuda cup reefs. Geol. Rundsch., **61**: 708-730.

Schröter, T., 1996. Tectonic and sedimentary developmentof the central Zallah trough (west Sirt Basin, Libya). In M. J. Salem, M. T. Busrewil, A. A. Misallati, and M. A. Sola, eds., The geology of the Sirt Basin: Amsterdam, Elsevier, v. 3: 123–135.

Schwarzacher, W 2000. Repetitions and cycles in stratigraphy. Earth-Science Reviews**, 50:** 51-75.

Scotese, C.R., 2004. A continental drift flipbook. Journal of Geology 112: 729–741.

Selley, R.C. 1968. Facies profiles and other new methods of graphic data presentation: application in a quantitative study of Libyan Tertiary shoreline deposits. J. Sediment.Petrol., **35:** 363-372.

Selley, R.C., 1997. The basins of Northwest Africa; structural evolution. In Selley, R.C., ed., African basins: Sedimentary basins of the world: Amsterdam, Elsevier: 17-26.

Sghair, A. 1996. Late Cretaceous and Palaeocene ostracods from the Waha Limestone and Hagfa Shale Formations of the Sirt Basin, Libya. First Symposium on the Sedimentary Basins of Libya, Geology of the Sirt Basin, v. 1. (eds. M.J. Salem, A.J. Mouzughi and O.S. Hammuda), Elsevier, Amsterdam: 287-382.

Sghair, A.M.A. 1996. Petrography, diagensesis and provenance of the Bahi Formation in the western part of the Sirt Basin, Libya. First Symposium on the Sedimentary Basins of Libya, Geology of the Sirt Basin, v. 2. (eds. M.J. Salem, A.S. El-Haw at and A.M. Sbeta), Elsevier, Amsterdam: 65-82.

Shah, S.H.A., Mansouri, A. and EL Ghoul, M. 1993. Palaeozoic sandstone reservoirs Of the Hamada Basin, NW Libya: effects of synsedimentary processes on porosity. Journ. Pet. Geol. v. 16: 345-352.

Sharp, I.R., Gawthorpe, R.L., Armstrong, B. & Underhill, J.R. 2000b. Propagation history and passive rotation of mesoscale normal faults: implications for syn-rift stratigraphic development. Basin Res., 12: 285-305.

Shoval, S., 2004. Clay sedimentation along the southeastern Neo-Tethys margin during the oceanic convergence stage. Applied Clay Science 24: 287–298.

Sinha, R. N. 1992a. Antiquity of Sirt Basin, Libya - a discussion. Petroleum Research Centre, Tripoli, Unpubl. Rept.

Sinha, R. N., and I. Y. Mriheel, 1996. Evaluation of subsurface Paleocene sequence

and shoal carbonates, southcentral Sirt Basin. In M. J. Salem, M. T. Busrewil, A. A. Misallati, and M. A. Sola, eds., the geology of the Sirt Basin: Amsterdam, Elsevier, v. 2: 153–196.

Smith AG, 1971. Alpine Deformation and the Oceanic Areas of the Tethys, Mediterranean and Atlantic In: Geo. Soc. of America Bull. v. 82 no. 8: 2039-2070

Speijer, R. P. and Schmitz, B., 1998. A benthic foraminiferal record of Paleocene sea-Level changes and trophic conditions at Gebel Aweina, Egypt. Palaeogeography, Palaeoclimatology, Palaeoecology, v. 137: 79-101.

Speijer RP, Wagner R 2002. Sea-level changes and black shales associated with the Late Paleocene thermal maximum; organic-geochemical and micropaleontologic evidence from the southern Tethyan margin (Egypt-Israel). In: Koeberl C, MacLeod KG (eds) Catastrophic Events & Mass Extinctions: Impacts and Beyond, Geol Soc Am Spec Pap, Boulder: 533-549.

Spence, G.H., Tucker, M.E., 2007. A proposed integrated multi-signature model for peritidal cycles in carbonates. Journal of Sedimentary Research, **77**: 797-808**.**

Spring, D. and Hansen, O. P. 1998. The influence of platform morphology and sea level on the development of a carbonate sequence: the Harash Formation, eastern Sirt Basin, Libya. In: Petroleum Geology of North Africa, (ed. D.S. Macgregor, R.T.J. Moody, D.D. Clark-Lowes), Geol. Soc. Special Publication No. 132: 335-354.

Strasser, A. 1988. Shallowing-upward sequences in Purbeckian peritidal carbonates (lowermost Cretaceous, Swiss and French Jura Mountains). Sedimentology, 35: 369– 383.

Sun, Z., et al. , 2010. New paleomagnetic results of Paleocene volcanic rocks from the Lhasa Block: Tectonic implications for the collision of India and Asia, Tectonophysics, doi:10.1016/j.tecto.2010.05.011.

Swezey, C.S., 2009. Cenozoic stratigraphy of the Sahara Northern Africa. J. Afr. Earth Sci.53: 89–121.

Tawadros, E. (Ed.), 2001. Geology of Egypt and Libya. A.A. Balkema, Rotterdam: 468.

Terry, C.E. and Williams, J.J. 1969. The Idris "A" bioherm and oil field, Sirt Basin, Libya: Its commercial development, regionale Palaeocene geologic setting and stratigraphy. In: The exploration for petroleum in Europe and Africa. London, Inst. Petroleum: 31-48.

Taylor, T. R., M. R. Giles, L. A. Hathon, T. N. Diggs, N. R. Braunsdorf,G.V. Birbiglia,M.G.Kittridge,C. I.Macaulay, and I. S. Espejo, 2010. Sandstone diagenesis and reservoir quality prediction:Models,myths, and reality:AAPG Bulletin, v. 94: 1093–1132, doi:10.1306/04211009123.

Taylor, A.M., and Goldring, R., 1993. Description and analysis of bioturbation and ichnofabric. Journal of Geological Society of London, **150**: 141-148.

The Robertson Group, 1991. The Biostratigraphy, Lithostratigraphy, Palaeoenvironments and correlation of 17 wells from the Sirt Basin, Libya. Proprietary report, Sirte Oil Company, Brega, Libya

Thomas, D. 1995a. Geology, Murzuk oil development could boost SW Libya prospects. Oil and Gas Journ.v. 93, no. 10: 41-46.

Thomas, D. 1995b. Exploration limited since '70s in Libya's Sirte Basin. Oil and Gas Journ. v. 93, no. 11: 99-104.

Tinker, S.W., 1998. Shelf-to-basin facies distribution and sequence stratigraphy of a

steep rimmed carbonate margin: Capitan depositional system, McKittrick Canyon, New Mexico and Texas. Journal of Sedimentary Research, **68**: 1146-1174.

Tipsword, H. L., Setzer F. M , and Smith F. L., Jr., 1966. Interpretation of depositional environment in Gulf Coast petroleum exploration from paleoecological and related stratigraphy: Gulf Coast Association of Geological Societies Transactions, v. 16: 119–130.

Tmalla, A. F. A. 1992. Stratigraphic position of the Cretaceous-Tertiary boundary in The northern Sirt Basin, Libya. Mar. Petrol. Geol., **9** (5): 542-552.

Tmalla, A. F. A., 1996. Late Maastrichtian and Paleocene planktonic foraminiferal biostratigraphy of well A1a-NC29A, northern Sirt Basin, Libya, in M. J. Salem, M. T. Busrewil,A.A.Misallati, andM.A. Sola, eds., The geology of the Sirt Basin:

Tripati AK, Delaney ML, Zachos JC, Anderson LD, Kelly DC, Elderfield H 2003. Tropical sea-surface temperature reconstruction for the early Paleogene using Mg/Ca ratios of planktonic foraminifera. Paleoceanography 18:doi:1110.1029/2003PA000937,002003. Amsterdam, Elsevier, v. 1: 195–232.

Tucker, M. 1981. "Sedimentary pathology". An introduction black well scientific publication. Oxford, London Edinburg, Boston, Melbourne: 252.

Tucker, M. E., 1986. Formerly aragonitic limestones associated with tillites in the late Proterozoic of Death Valley, California. Journal of Sedimentary Petrology, **56**: 818- 830.

Tucker, M. E., 1991. Sequence stratigraphy of carbonate-evaporite successions: Models and application to the Upper Permian (Zechstein) of northeast England and adjoining North Sea. Journal of the Geological Society London, **148**: 1019-1036.

Tucker, M. E. 1993. Carbonate diagenesis and sequence stratigraphy. In: Wright, V. P. (Editor.), Sedimentology Review, v. 1. Blackwell Science, Oxford: 51–72.

Tucker, M. E., 2011. Sedimentary rocks in the field. Wiley.

Tucker, M.E., Wright, V.P., 1990. Carbonate sedimentology. Oxford (Blackwell): 0-482

Tucker, M. E. Garland, J., 2010. High-frecuency Ccycles and their sequence Stratigraphic context: Orbital forcing and tectonc controls on Devonian cyclicity, Belgium. Geologica Belgica, **13**: 213-240**.**

Underdown, R., Redfern, J., Lisker, F., 2007. Constraining the burial history of the Ghadames Basin, North Africa: an integrated analysis using sonic velocities, vitrinite reflectance data and apatite fission track ages. Basin Research 19: 557–578.

Van der Meer, F., and S. Cloetingh, 1993a. Late Cretaceous and Tertiary subsidence history of the Sirt Basin (Libya), an example of the use of backstripping analysis. ITC (International Institute for Geo-information Science and Earth Observation) Journal, v. 93, no. 1: 68–76.

Van der Meer, F. D. & Cloetingh, S. A. P. L. 1993. Late Cretaceous and Tertiary subsidence history of the Sirt Basin (Libya): an example of the use of backstripping analysis. ITC Journal, 1993, 68.

Van der Meer, F., and S. Cloetingh, 1993b. Intraplate stresses and subsidence history of the Sirt Basin (Libya): Tectonophysics, v. 226: 37–58.

Van Houten, F. B., 1980. Latest Jurassic–Early Cretaceous regressive facies, northeast African craton. AAPG Bulletin, v. 64: 857–867.

Van Houten, F. B., 1983. Sirt Basin, north-central Libya, Cretaceous rifting over a Fixed mantle hotspot?. Geology, v. 11: 115–118.

Van Wagoner, J.C., Mitchum, R.M., Campion, K.M., and Rahmanian, V.D., 1990, Siliciclastic Sequence Stratigraphy in Well Logs, Cores and Outcrops. AAPG Methods in Exploration, v. 7, AAPG: 55.

Van Wagoner, J., Posamentier, H., Mitchum, R., Vail, P., Sarg, J., Loutit, T., Hardenbol, J., 1988. An overview of the fundamentals of sequence stratigraphy And key definitions. Sea-Level Changes: An Integrated Approach. Society of Economic Palaeontologist and Mineralogist Special Publication **42**: 39–45**.**

Villasante-Marcos, V., Hollis, C.J., Dickens, G.R., Nicolo, M.J., 2009. Rock magnetic properties across the Paleocene–Eocene Thermal Maximum in Marlborough, New Zealand. Geol. Acta 7: 229–242.

Weissert, H., Lini, A., Follmi, K. B., Kuhn, O. 1998. Correlation of early Cretaceous carbon isotope stratigraphy and platform drowning events: a possible link. Palaeogeography, Palaeoclimatology, Palaeoecology. **137**: 189-203.

Wennekers, J. H. N., K. F. Wallace, and I. Y. Abugares, 1996. The geology and hydrocarbons of the Sirt Basin. A synopsis, in M. J. Salem, A. J. Mouzoughi, and O. S.Hammuda, eds., The geology of the Sirt Basin: Amsterdam, Elsevier, v. 1: 3–56.

Williams, J. J., 1968. Augila field, Libya— Depositional environment and diagenesis of sedimentary reservoir and description of igneous reservoir. AAPG Memoir 16, Society of Exploration Geophysicists Special Publication 10: 623–632.

Weyl, P. K., 1959. Pressure-solution and the force of crystallization: phenomenological theory. J. Geophys. Res., 64: 2001-2025.

Wilson, J. L. 1975. Carbonate facies in geologic history. New York. Springer. : 471

Wilson, M., and R. Guiraud, 1998. Late Permian to Recent magmatic activity on the African-Arabian margin of Tethys, in D. S. Macgregor, R. T. J. Moody, and D. D. lark-Lowes, eds., Petroleum geology of north Africa: Geological Society (London) Special Publication 132: 231–263.

Wong P.K. and Oldershaw, A.E. 1981. Causes of cyclicity in reef interior sediments, Kaybob Reef, Alberta. Bull. Can. Petrol. Geol., 28: 411-424.

Wood, B.G.M., 2003. Understanding North African and Middle East Basins: Whole Lithospheric Folding versus Disparate Rifting. Canadian Society of Petroleum Geologists, Technical Luncheon Abstract (23 September 2003).

Woolfe, K.J., and Larcombe, P., 1999. Terrigenous sedimentation and coral reef growth: a conceptual framework. Marine Geology, v. 155: p. 331–345.

Wright, V. P. 1992. Paleosol recognition; a guide to early diagenesis in terrestrial settings. In: Diagenesis, III. Developments in Sedimentology, 47 (K.F. Wolf, G.V. Chilingarian, eds.): 591-619.

Yoshioka, H., Asahara, Y., Tojo, B., Kawakami, S., 2003. Systematic variations in C, O, and Sr isotopes and elemental concentrations in Neoproterozoic carbonates in Namibia: implications for glacial to interglacial transition. Precambrian Res. 124: 69–85.

Zachos JC, Dickens GR, Zeebe RE 2008. An early Cenozoic perspective on Greenhouse Warming and carbon-cycle dynamics. Nature 451:279-28.

Zachos, J.C., Lohmann, K.C., Walker, J.C.G., Wise, S.W., 1993. Abrupt climate change and transient climates during the Paleogene: a marine perspective. The Journal of Geology 101: 191–213.

Zachos, J., Pagani, M., Sloan, L., Thomas, E., Billups, K., 2001. Trends, rhythms,

and abberations in global climate 65 Ma to present. Science 292: 686–693.

Zaïer, A., Beji-Sassi, A., Sassi, S., Moody, R.T.J., 1998. Basin evolution and deposition during the Early Paleogene in Tunisia. In: Macgregor, D.S., Moody, R.T.J., Clark-Lowes, D.D. (Eds.), the King of the Ring. Geological Society (London) Special Publication 132: 375–393.

Zankle, H. 1960. Structural and textural evidence of early lithification in fine-grained carbonate rocks. Sedimentology, v. 12: 241-256.

Zeff, M. L. And Perkins, R.D. 1979. Microbial alteration of Bahamian deep-sea carbonates. Sedimentology **26:** 175-201.

Zenger, D. H. 1983. Burial dolomitization in the Los Burro Formation (Devonian), east-central California, and the significance of late diagenetic dolomitization. Geology, **11**: 519-522.

Ziegler, P. A., 1988. Evolution of the Arctic-North Atlantic and the western Tethys. AAPG Memoir 43: 198 .

Ziegler M, 2001. Late Permian to Holocene Paleofacies Evolution of the Arabian Plate And it's Hydrocarbon Occurrences. GeoArabia, 6:445-505.

Appendix 1. Sedimentological core description logs of the studied wells

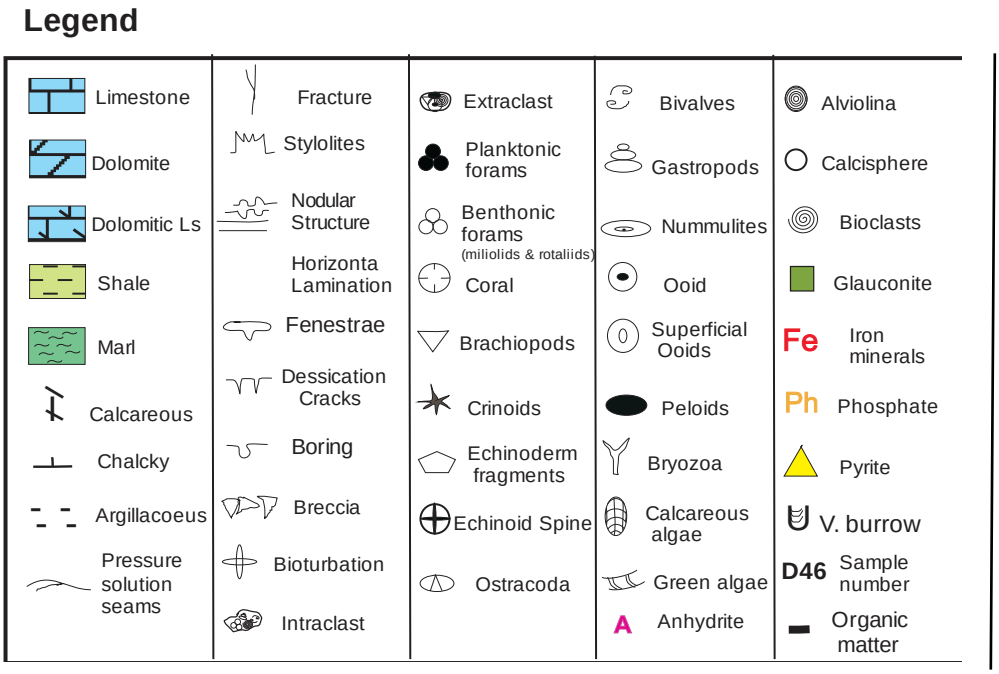

Key to symbols used in the sedimentological logs

Abbreviations used throughout the thesis

* PDS= Pressure disolution seams PMF = Paleocene microfacies W= well

H = Harash Fm Z = Zelten Fm D = Dahra Fm 3275 = Depth in feet

* All photomicrographs in table 3.1are in ppl, unless otherwise stated

H= Harash Fm Z= Zelten Fm D= Dahra Fm M = Mabruk Mbr M = Mudstone W= Wackestone P= Packstone G= Grainstone

B = Boundstone √= exist ft= feet

A = Abundant (> 20 %) C = Common (10 – 20 %) P= Present (5 – 10 %)

R= Rare <5 %

Porosity category:

N = Negligible (< 5%) P = Poor (5-10%) F = Fair (10-15%)

G = Good (15-20%) VG = Very good (20-25%) E = Excellent (>25%)

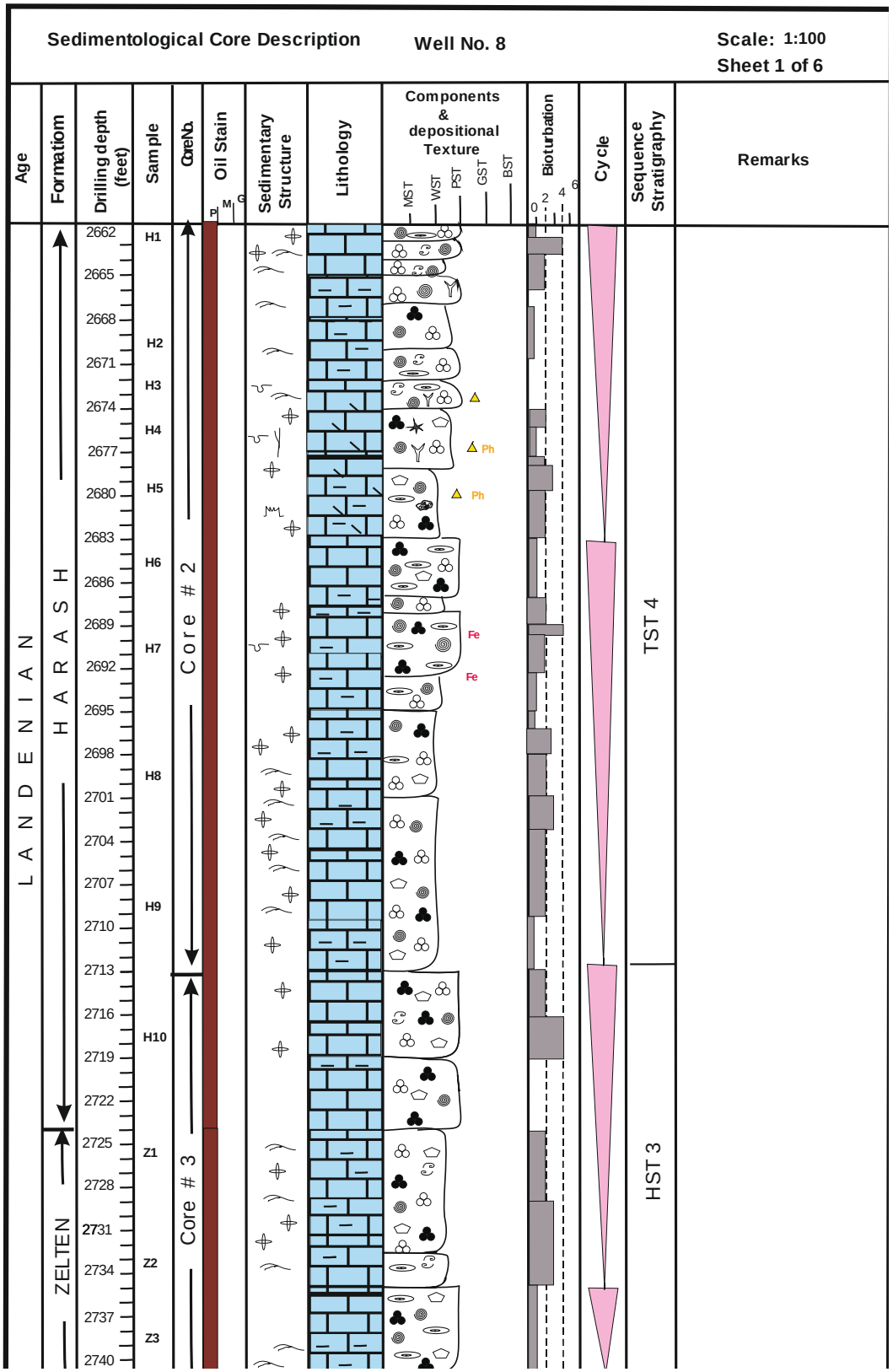
Sedimentological Core Description
Well No. 8
Scale: 1:100
Sheet 1 of 6
Age
Formation
Drilling depth (feet)
Sample
Core No.
Oil Stain
Sedimentary Structure
Lithology
Components & depositional Texture
MST
WST
PST
GST
BST
Bioturbation
Cycle
Sequence Stratigraphy
Remarks
LANDENIAN
HARASH
ZELTEN
Core # 2
Core # 3
TST 4
HST 3
Ph
Fe

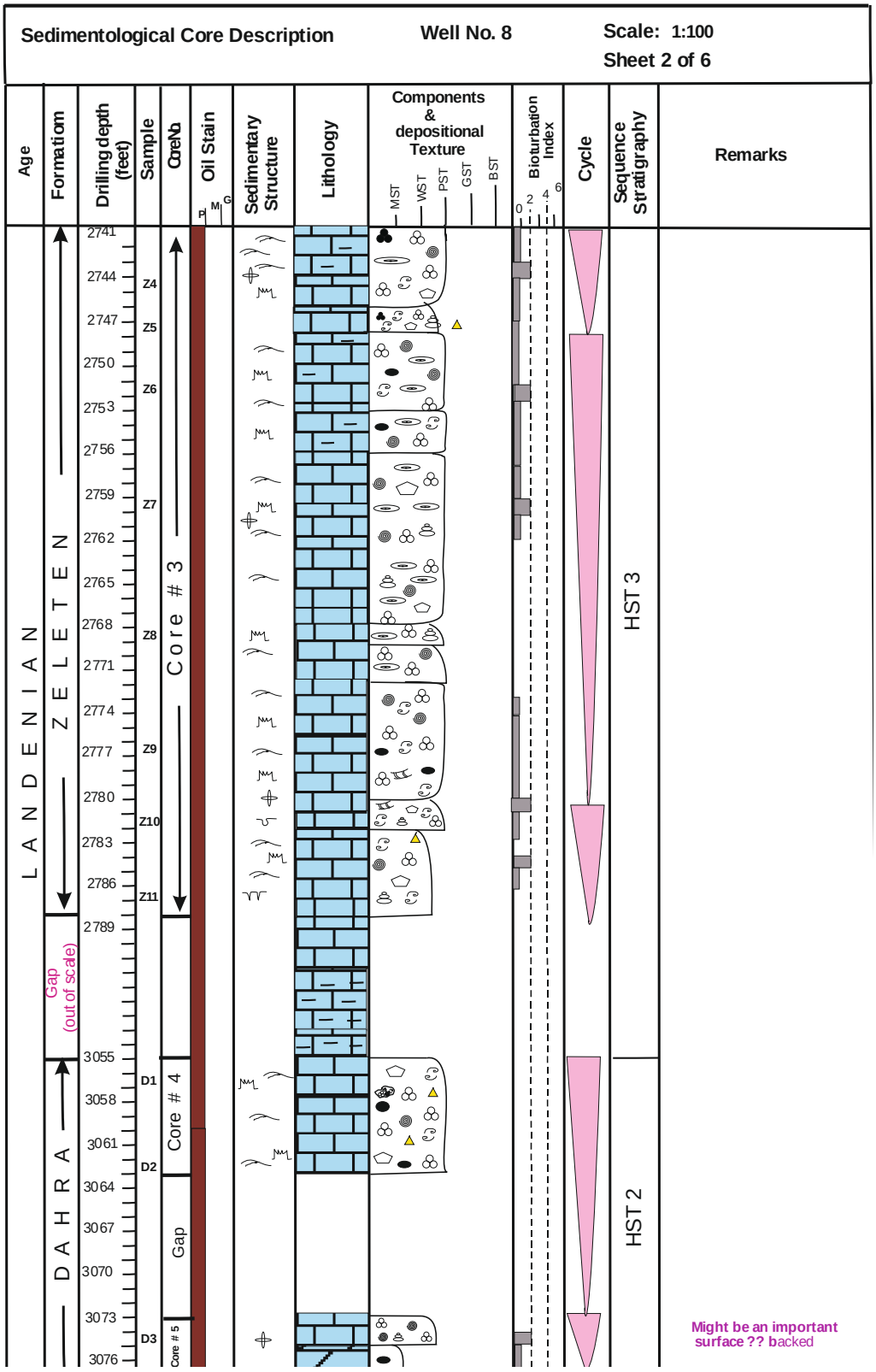
Sedimentological Core Description
Well No. 8
Scale: 1:100
Sheet 2 of 6
Age
Formation
Drilling depth (feet)
Sample
Core No.
Oil Stain
Sedimentary Structure
Lithology
Components & depositional Texture
MST
WST
PST
GST
BST
Bioturbation Index
Cycle
Sequence Stratigraphy
Remarks
LANDENIAN
ZELETEN
DAHRA
Gap (out of scale)
Core # 3
Core # 4
Gap
Core # 5
HST 3
HST 2
Might be an important surface ?? backed

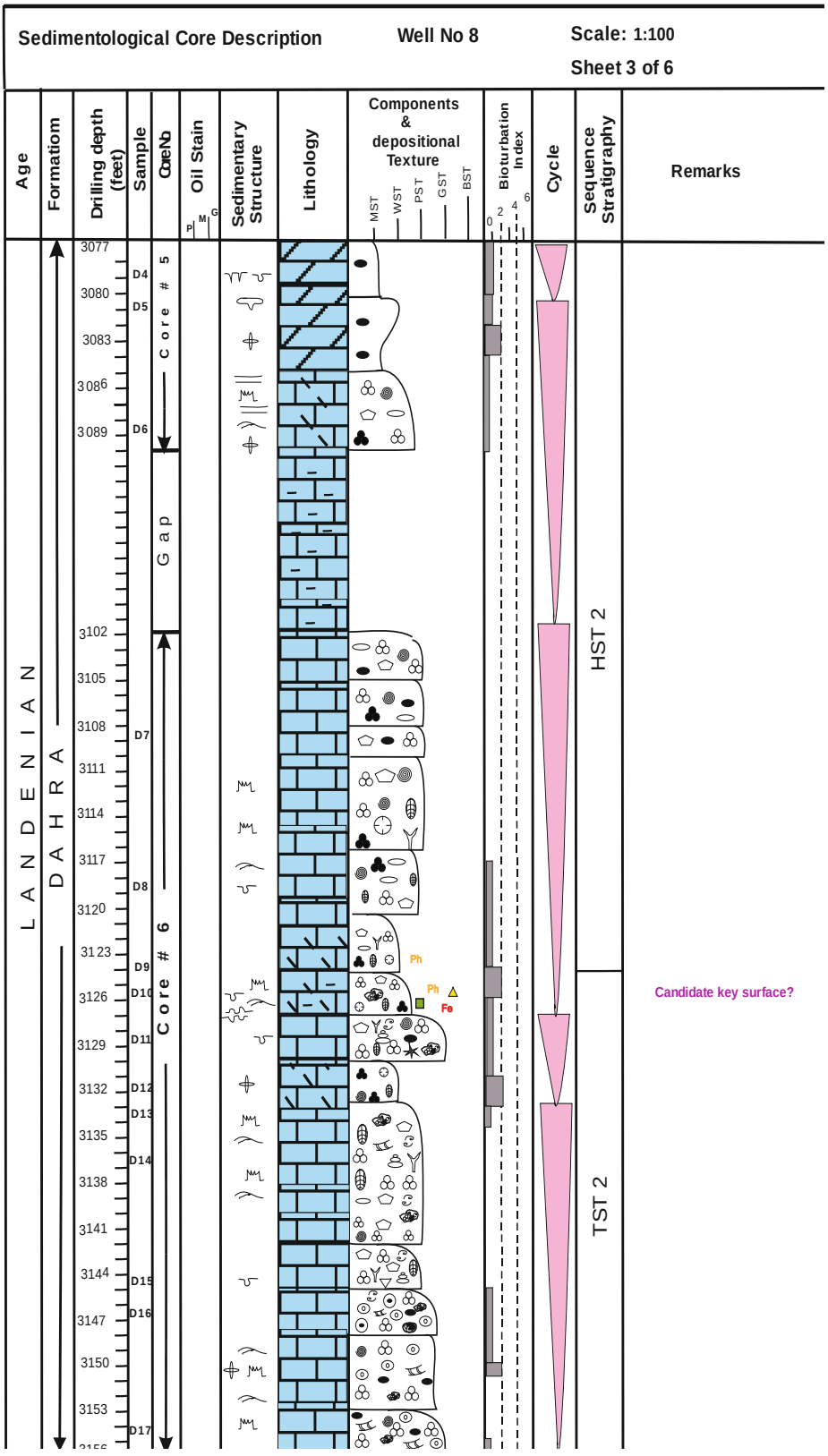
Sedimentological Core Description
Well No 8
Scale: 1:100
Sheet 3 of 6
Age
Formation
Drilling depth (feet)
Sample
Core No
Oil Stain
Sedimentary Structure
Lithology
Components & depositional Texture
MST
WST
PST
GST
BST
Bioturbation Index
Cycle
Sequence Stratigraphy
Remarks
LANDENIAN
DAHRA
Core # 5
Gap
Core # 6
HST 2
TST 2
Candidate key surface?
Ph
Fe

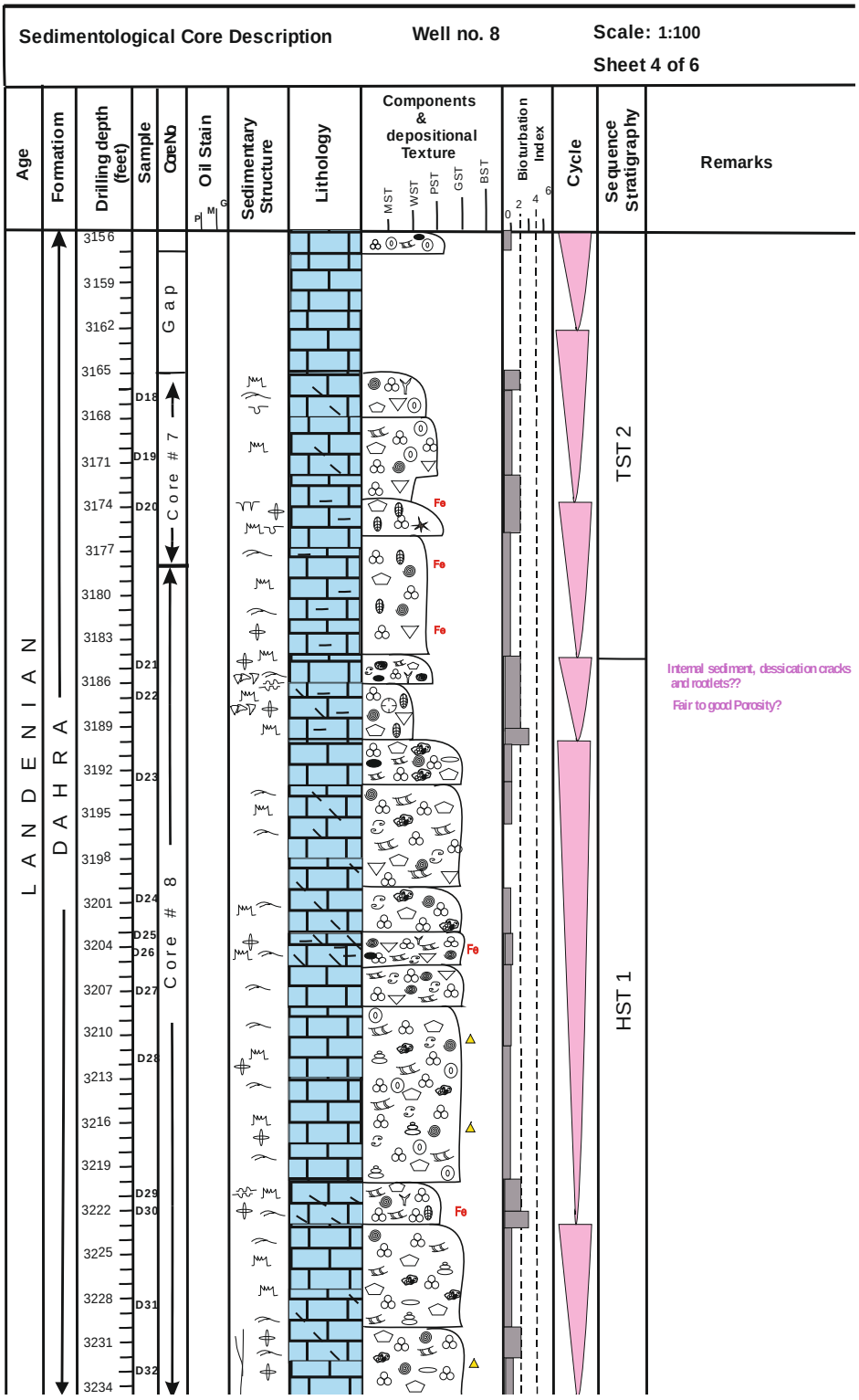
Sedimentological Core Description
Well no. 8
Scale: 1:100
Sheet 4 of 6
Age
Formation
Drilling depth (feet)
Sample
Core No.
Oil Stain
Sedimentary Structure
Lithology
Components & depositional Texture
MST
WST
PST
GST
BST
Bioturbation Index
Cycle
Sequence Stratigraphy
Remarks
LANDENIAN
DAHRA
Gap
Core # 7
Core # 8
D18
D19
D20
D21
D22
D23
D24
D25
D26
D27
D28
D29
D30
D31
D32
Fe
TST 2
HST 1
Internal sediment, dessication cracks and rootlets??
Fair to good Porosity?

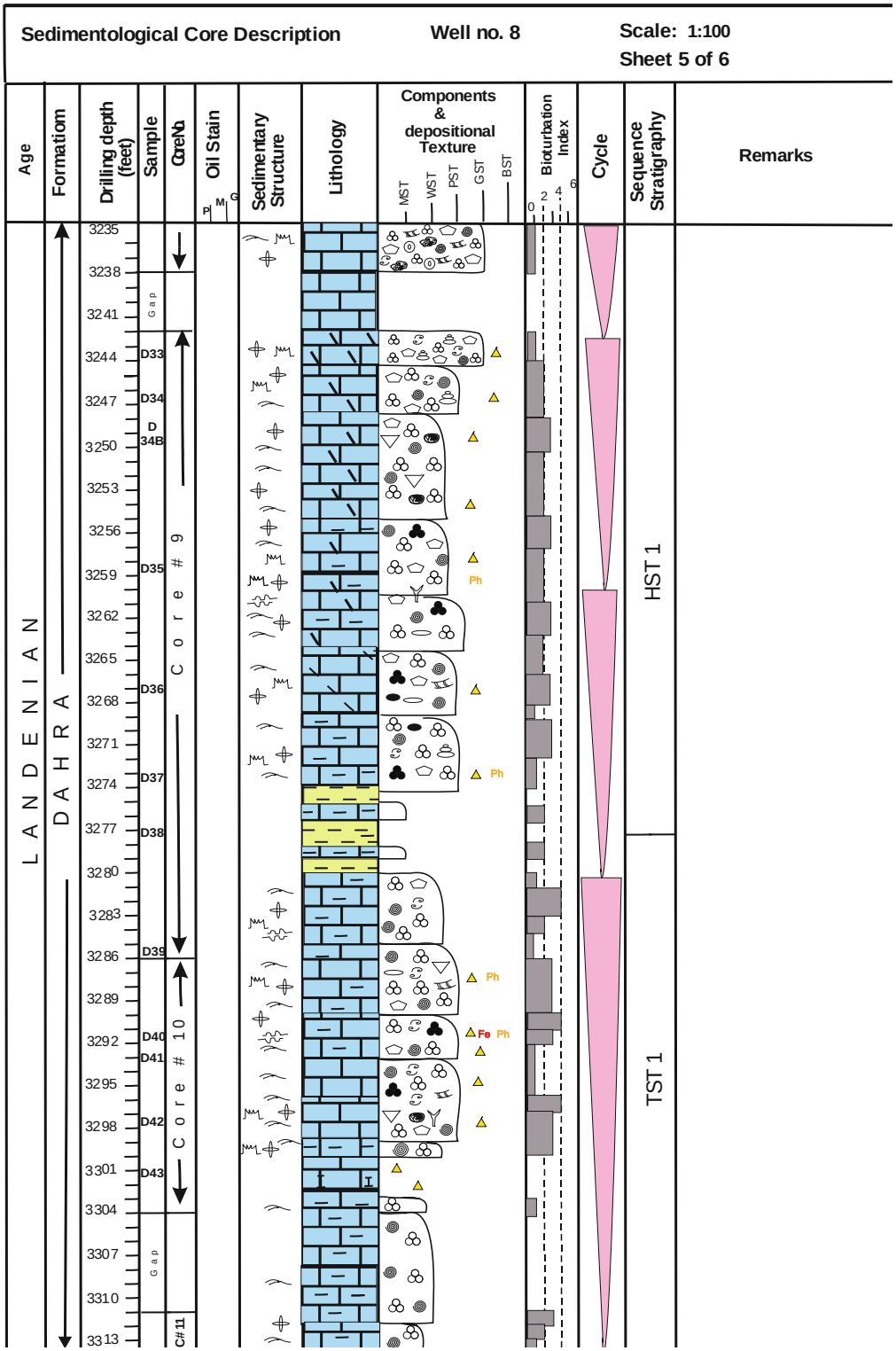
Sedimentological Core Description
Well no. 8
Scale: 1:100
Sheet 5 of 6
Age
Formation
Drilling depth (feet)
Sample
Core No.
Oil Stain
Sedimentary Structure
Lithology
Components & depositional Texture
MST
WST
PST
GST
BST
Bioturbation Index
Cycle
Sequence Stratigraphy
Remarks
LANDENIAN
DAHRA
3235
3238
3241
3244
3247
3250
3253
3256
3259
3262
3265
3268
3271
3274
3277
3280
3283
3286
3289
3292
3295
3298
3301
3304
3307
3310
3313
Gap
D33
D34
D 34B
D35
D36
D37
D38
D39
D40
D41
D42
D43
Gap
C# 11
Core # 9
Core # 10
HST 1
TST 1
Ph
Fe Ph

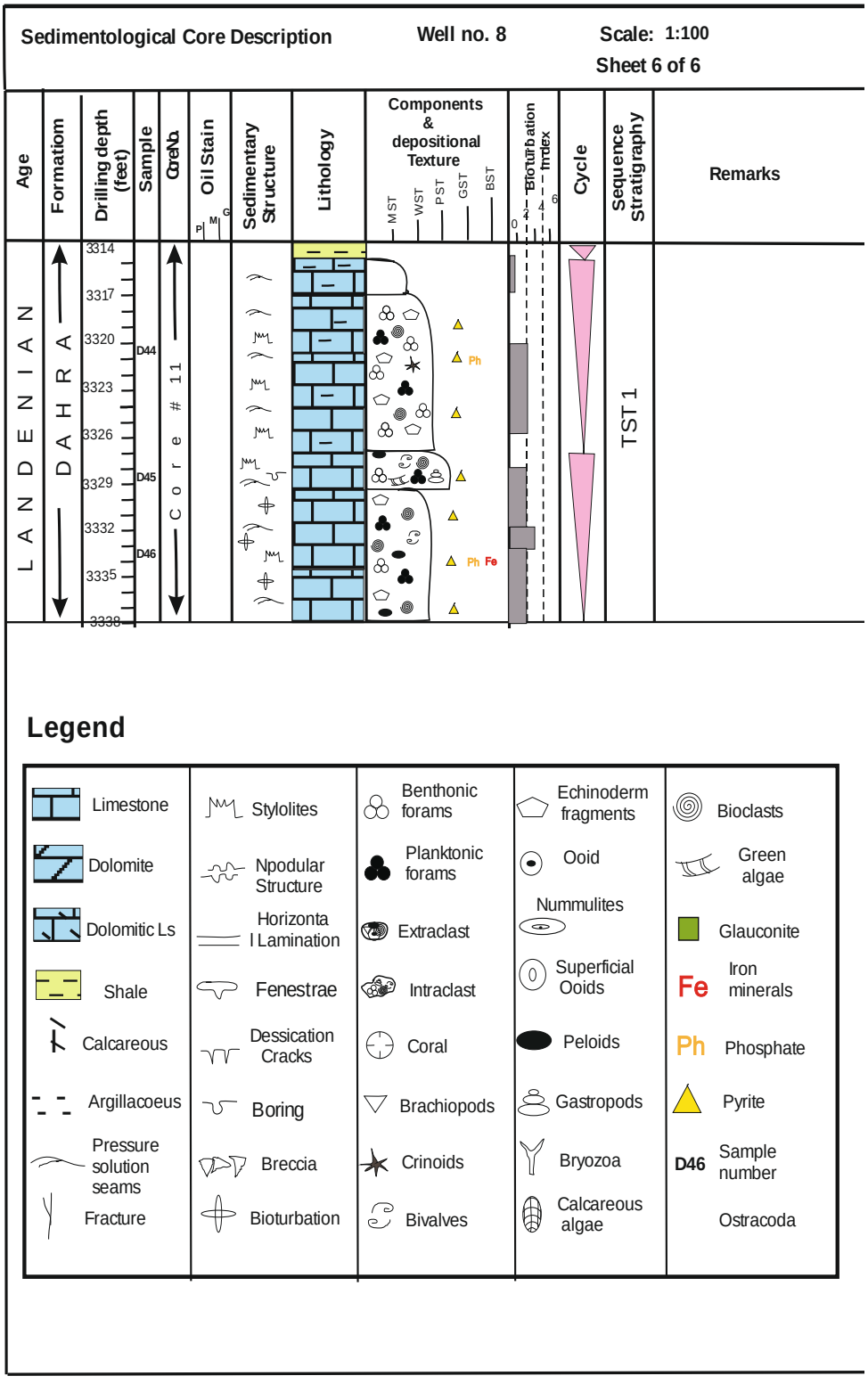
Sedimentological Core Description
Well no. 8
Scale: 1:100
Sheet 6 of 6
Age
Formation
Drilling depth (feet)
Sample
Core No.
Oil Stain
Sedimentary Structure
Lithology
Components & depositional Texture
MST
WST
PST
GST
BST
Bioturbation Index
Cycle
Sequence Stratigraphy
Remarks
LANDENIAN
DAHRA
3314
3317
3320
3323
3326
3329
3332
3335
3338
D44
D45
D46
Core # 11
Ph
Ph Fe
TST 1
Legend
Limestone
Dolomite
Dolomitic Ls
Shale
Calcareous
Argillacoeus
Pressure solution seams
Fracture
Stylolites
Npodular Structure
Horizontal Lamination
Fenestrae
Dessication Cracks
Boring
Breccia
Bioturbation
Benthonic forams
Planktonic forams
Extraclast
Intraclast
Coral
Brachiopods
Crinoids
Bivalves
Echinoderm fragments
Ooid
Nummulites
Superficial Ooids
Peloids
Gastropods
Bryozoa
Calcareous algae
Bioclasts
Green algae
Glauconite
Fe
Iron minerals
Ph
Phosphate
Pyrite
D46
Sample number
Ostracoda

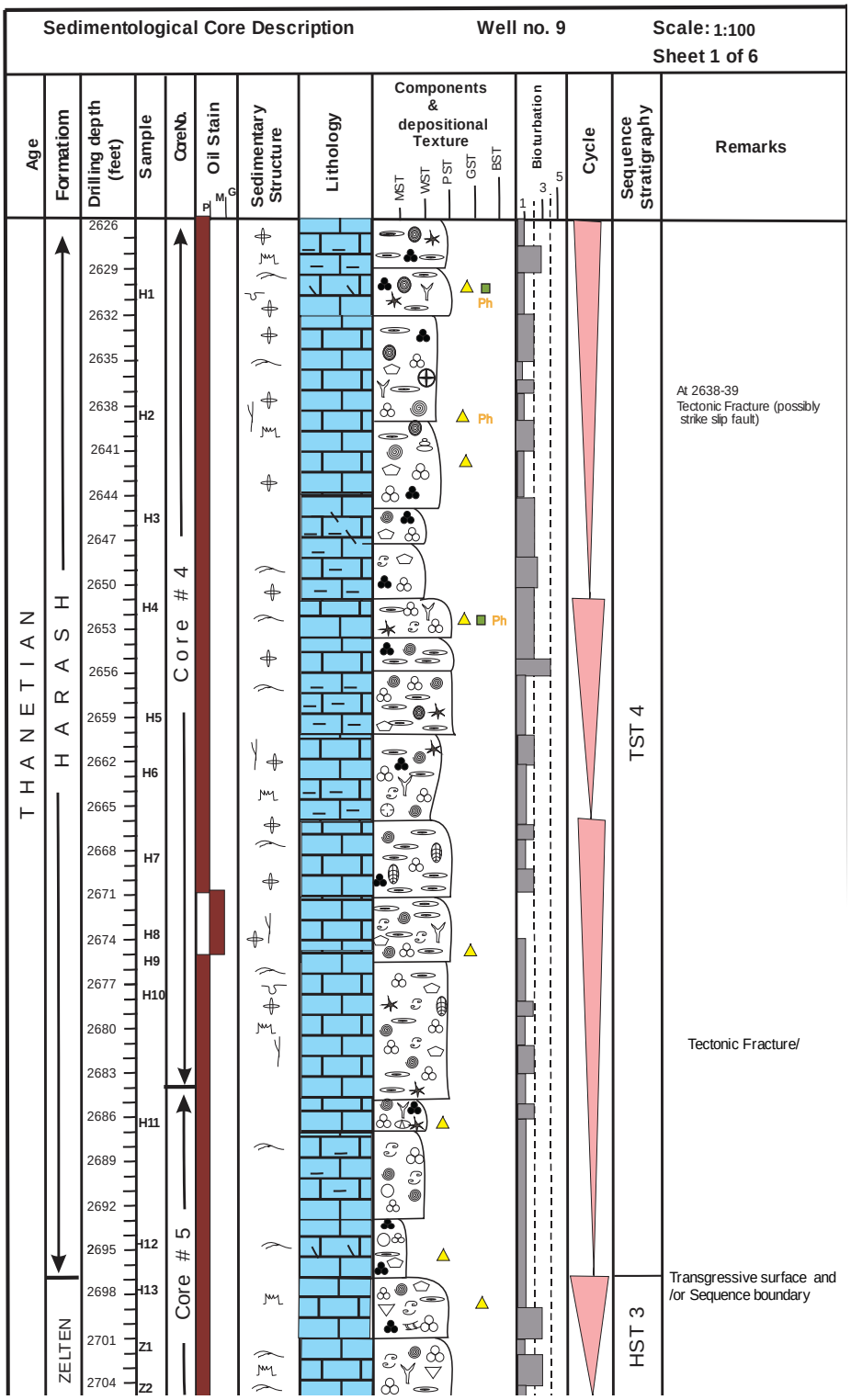
Sedimentological Core Description
Well no. 9
Scale: 1:100
Sheet 1 of 6
Age
Formation
Drilling depth (feet)
Sample
Core No.
Oil Stain
Sedimentary Structure
Lithology
Components & depositional Texture
MST
WST
PST
GST
BST
Bioturbation
Cycle
Sequence Stratigraphy
Remarks
THANETIAN
HARASH
ZELTEN
Core # 4
Core # 5
H1
H2
H3
H4
H5
H6
H7
H8
H9
H10
H11
H12
H13
Z1
Z2
Ph
TST 4
HST 3
At 2638-39
Tectonic Fracture (possibly strike slip fault)
Tectonic Fracture/
Transgressive surface and /or Sequence boundary

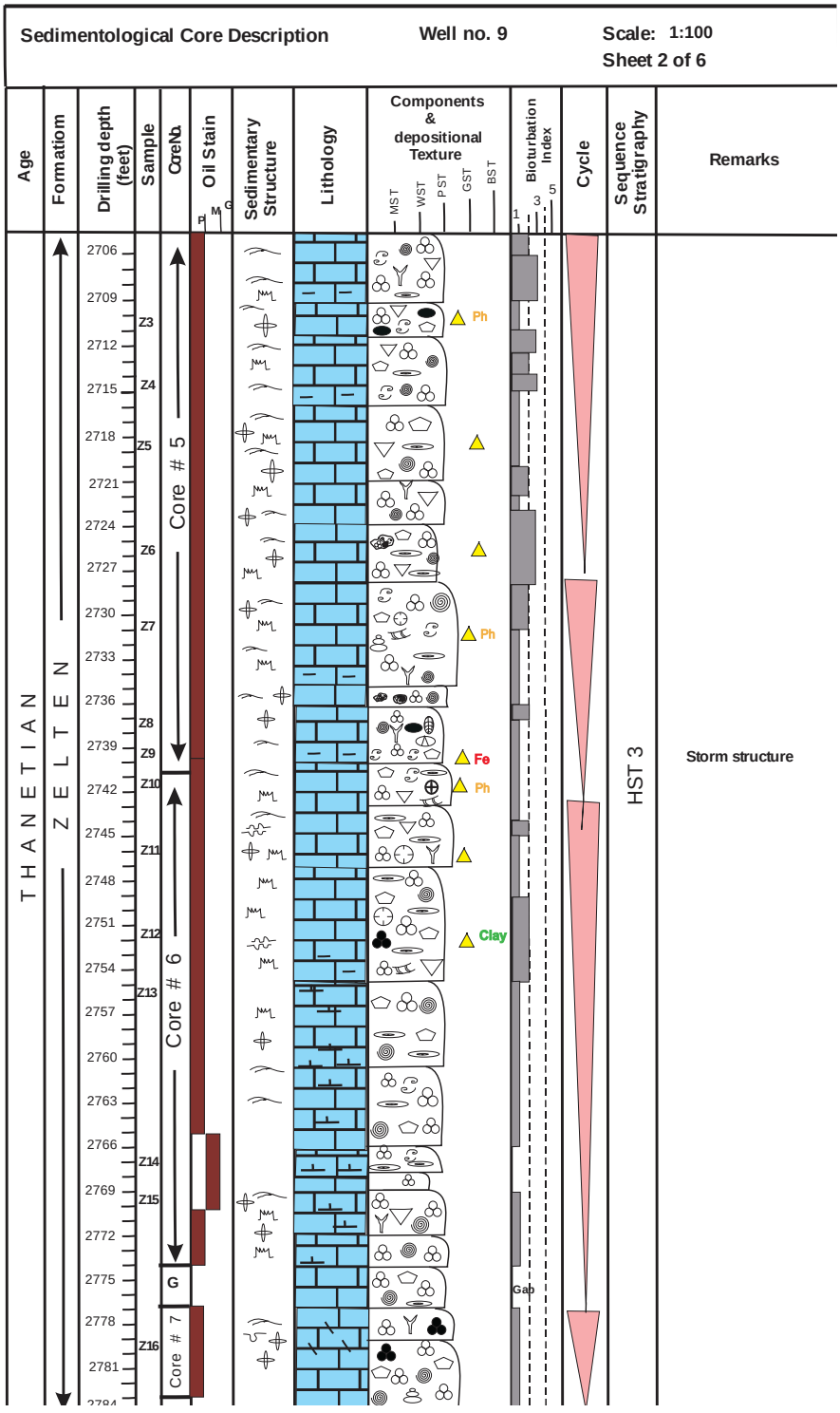
Sedimentological Core Description
Well no. 9
Scale: 1:100
Sheet 2 of 6
Age
Formatiom
Drilling depth (feet)
Sample
Core No.
Oil Stain
P
M
G
Sedimentary Structure
Lithology
Components & depositional Texture
MST
WST
PST
GST
BST
Bioturbation Index
1
3
5
Cycle
Sequence Stratigraphy
Remarks
THANETIAN
ZELTEN
2706
2709
2712
2715
2718
2721
2724
2727
2730
2733
2736
2739
2742
2745
2748
2751
2754
2757
2760
2763
2766
2769
2772
2775
2778
2781
Z3
Z4
Z5
Z6
Z7
Z8
Z9
Z10
Z11
Z12
Z13
Z14
Z15
Z16
Core # 5
Core # 6
G
Core # 7
Ph
Ph
Ph
Fe
Clay
Gab
HST 3
Storm structure

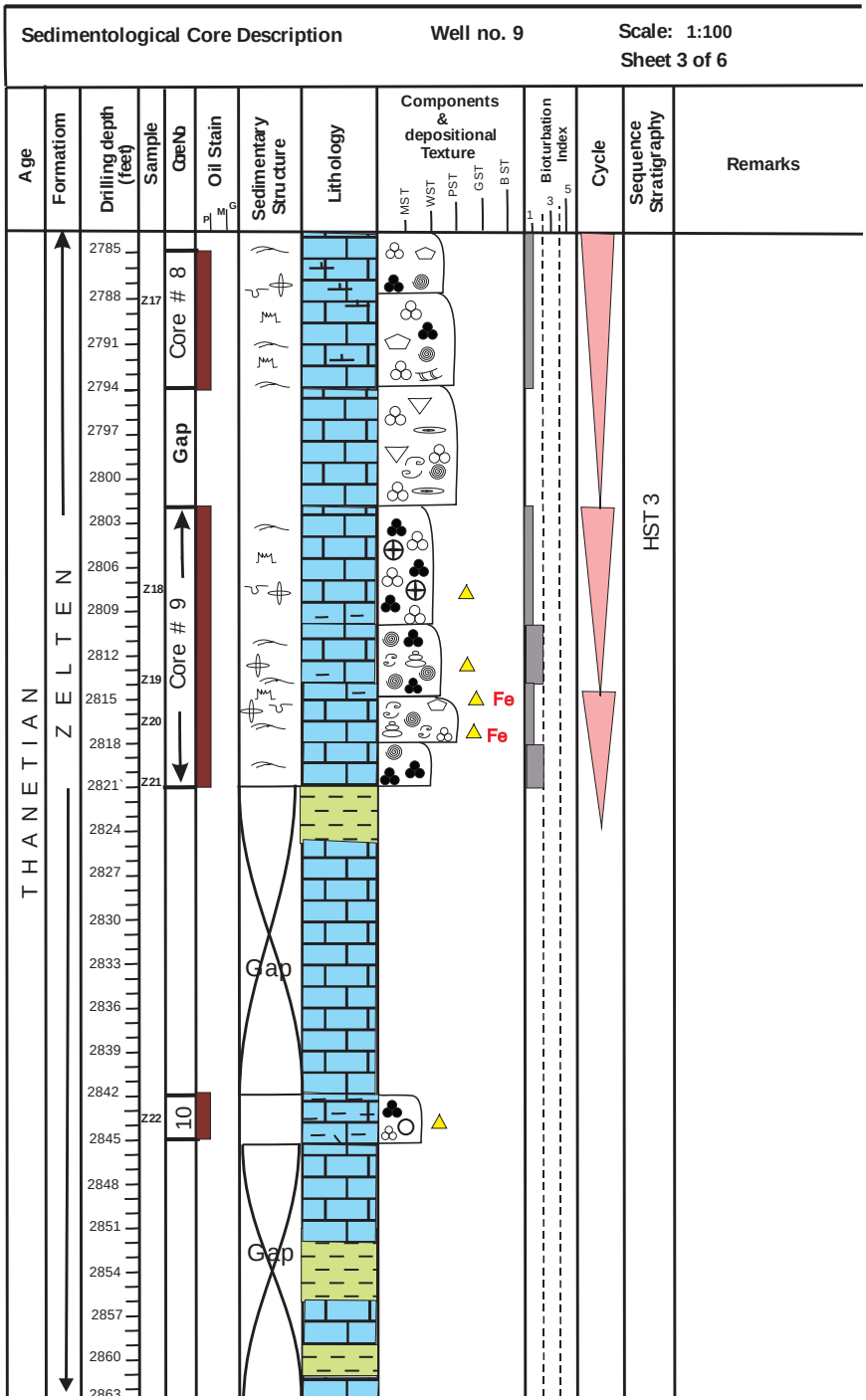
Sedimentological Core Description
Well no. 9
Scale: 1:100
Sheet 3 of 6
Age
Formation
Drilling depth (feet)
Sample
Core No
Oil Stain
Sedimentary Structure
Lithology
Components & depositional Texture
MST
WST
PST
GST
BST
Bioturbation Index
Cycle
Sequence Stratigraphy
Remarks
THANETIAN
ZELTEN
2785
2788
2791
2794
2797
2800
2803
2806
2809
2812
2815
2818
2821
2824
2827
2830
2833
2836
2839
2842
2845
2848
2851
2854
2857
2860
Z17
Z18
Z19
Z20
Z21
Z22
Core # 8
Gap
Core # 9
10
Gap
Gap
Fe
Fe
HST 3

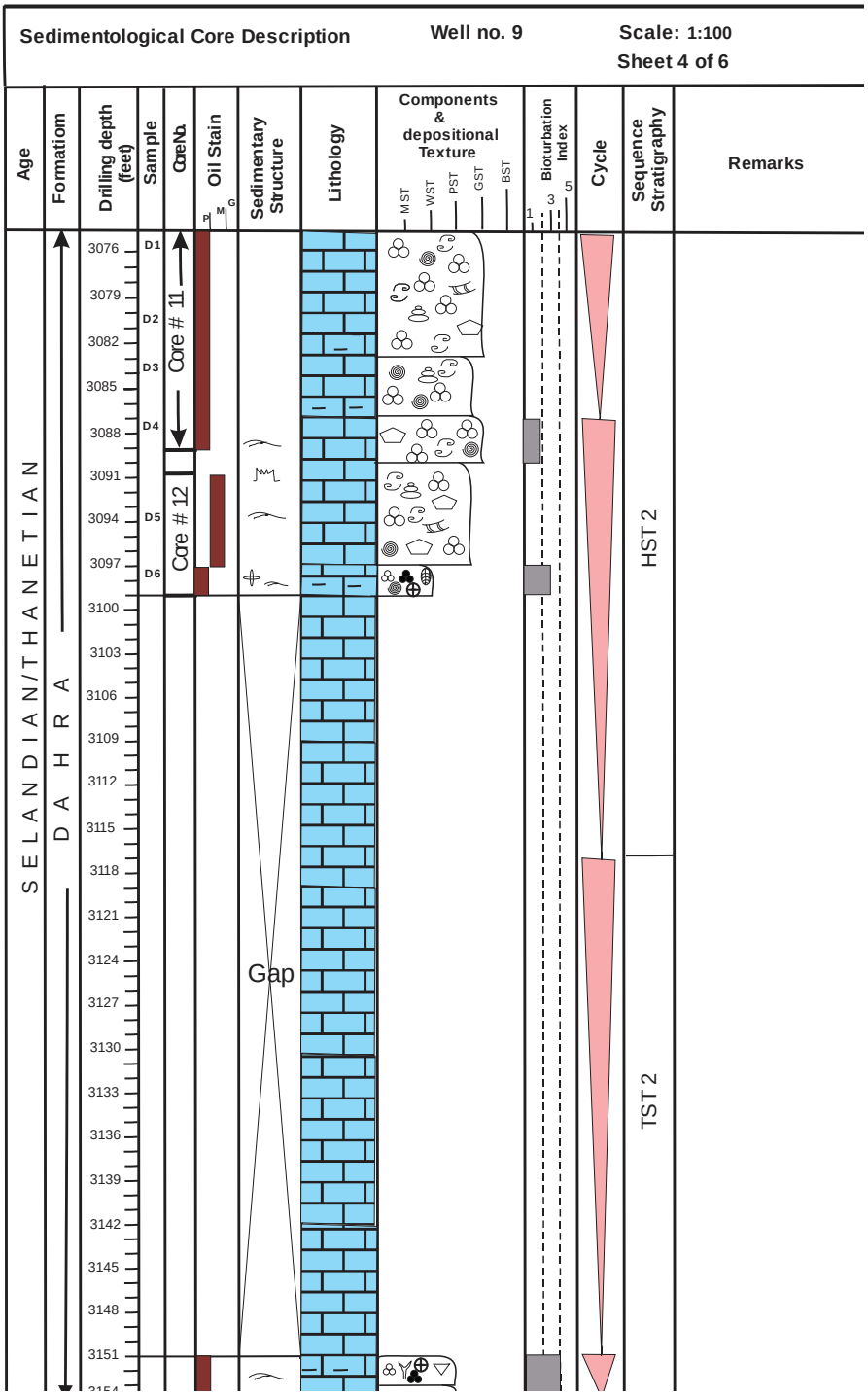
Sedimentological Core Description
Well no. 9
Scale: 1:100
Sheet 4 of 6
Age
Formation
Drilling depth (feet)
Sample
Core No.
Oil Stain
Sedimentary Structure
Lithology
Components & depositional Texture
MST
WST
PST
GST
BST
Bioturbation Index
Cycle
Sequence Stratigraphy
Remarks
SELANDIAN/THANETIAN
DAHRA
Core # 11
Core # 12
Gap
HST 2
TST 2

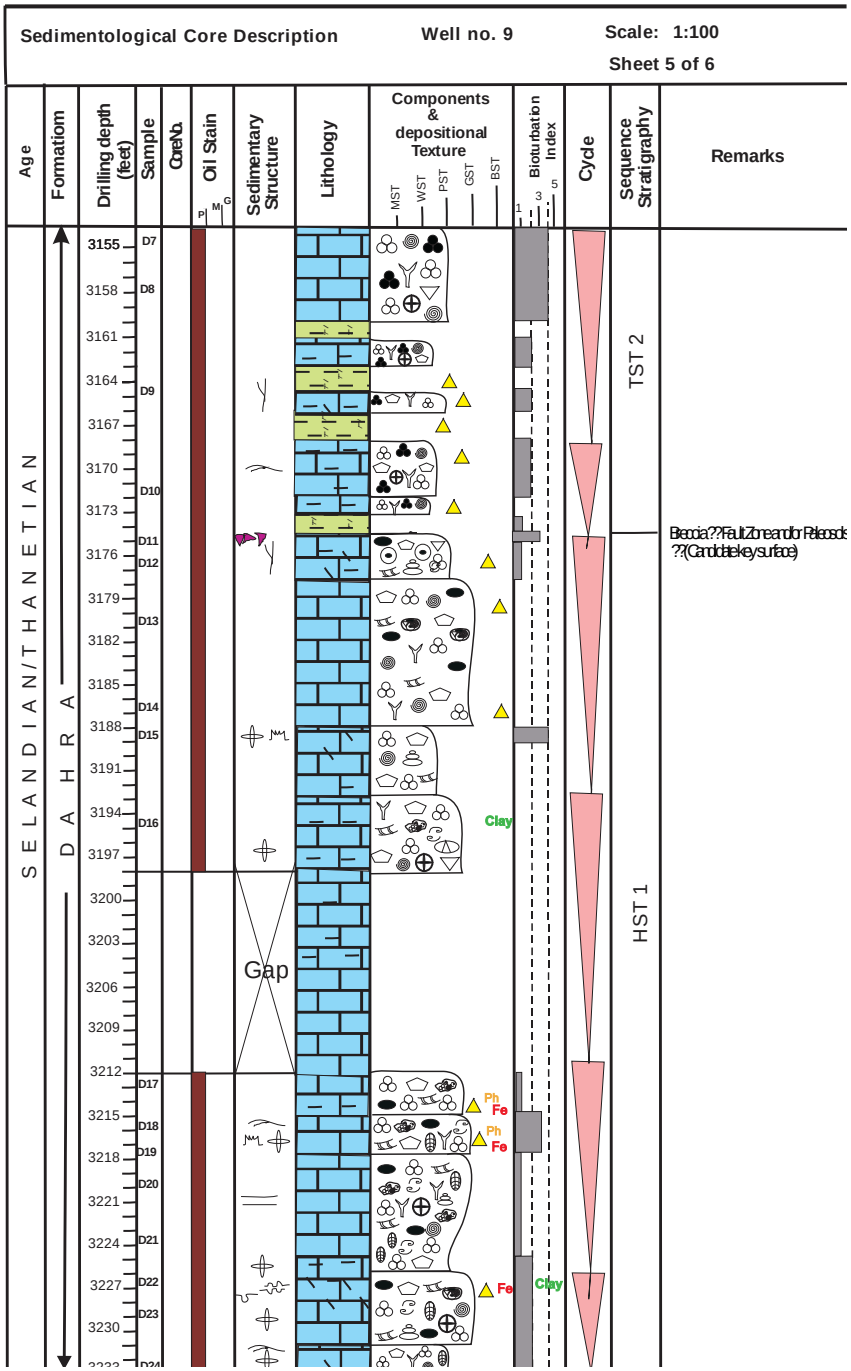
Sedimentological Core Description
Well no. 9
Scale: 1:100
Sheet 5 of 6
Age
Formation
Drilling depth (feet)
Sample
Core No.
Oil Stain
Sedimentary Structure
Lithology
Components & depositional Texture
MST
WST
PST
GST
BST
Bioturbation Index
Cycle
Sequence Stratigraphy
Remarks
SELANDIAN/THANETIAN
DAHRA
TST 2
HST 1
Gap
Clay
Ph
Fe
Clay

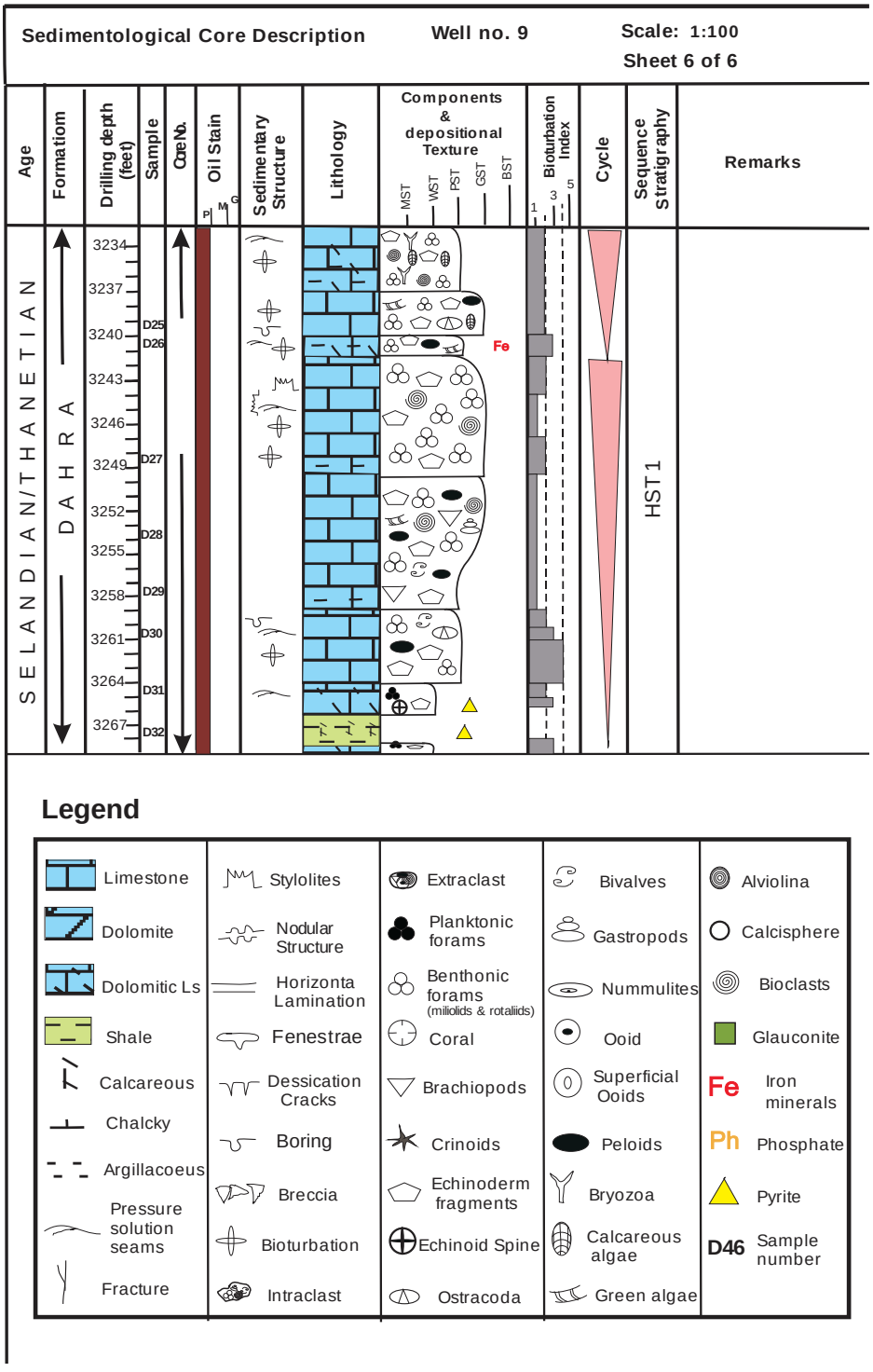
Sedimentological Core Description
Well no. 9
Scale: 1:100
Sheet 6 of 6
Age
Formation
Drilling depth (feet)
Sample
Core No.
Oil Stain
Sedimentary Structure
Lithology
Components & depositional Texture
MST
WST
PST
GST
BST
Bioturbation Index
Cycle
Sequence Stratigraphy
Remarks
SELANDIAN/THANETIAN
DAHRA
3234
3237
3240
3243
3246
3249
3252
3255
3258
3261
3264
3267
D25
D26
D27
D28
D29
D30
D31
D32
Fe
HST 1
Legend
Limestone
Dolomite
Dolomitic Ls
Shale
Calcareous
Chalcky
Argillacoeus
Pressure solution seams
Fracture
Stylolites
Nodular Structure
Horizonta Lamination
Fenestrae
Dessication Cracks
Boring
Breccia
Bioturbation
Intraclast
Extraclast
Planktonic forams
Benthonic forams
(miliolids & rotaliids)
Coral
Brachiopods
Crinoids
Echinoderm fragments
Echinoid Spine
Ostracoda
Bivalves
Gastropods
Nummulites
Ooid
Superficial Ooids
Peloids
Bryozoa
Calcareous algae
Green algae
Alviolina
Calcisphere
Bioclasts
Glauconite
Fe
Iron minerals
Ph
Phosphate
Pyrite
D46
Sample number

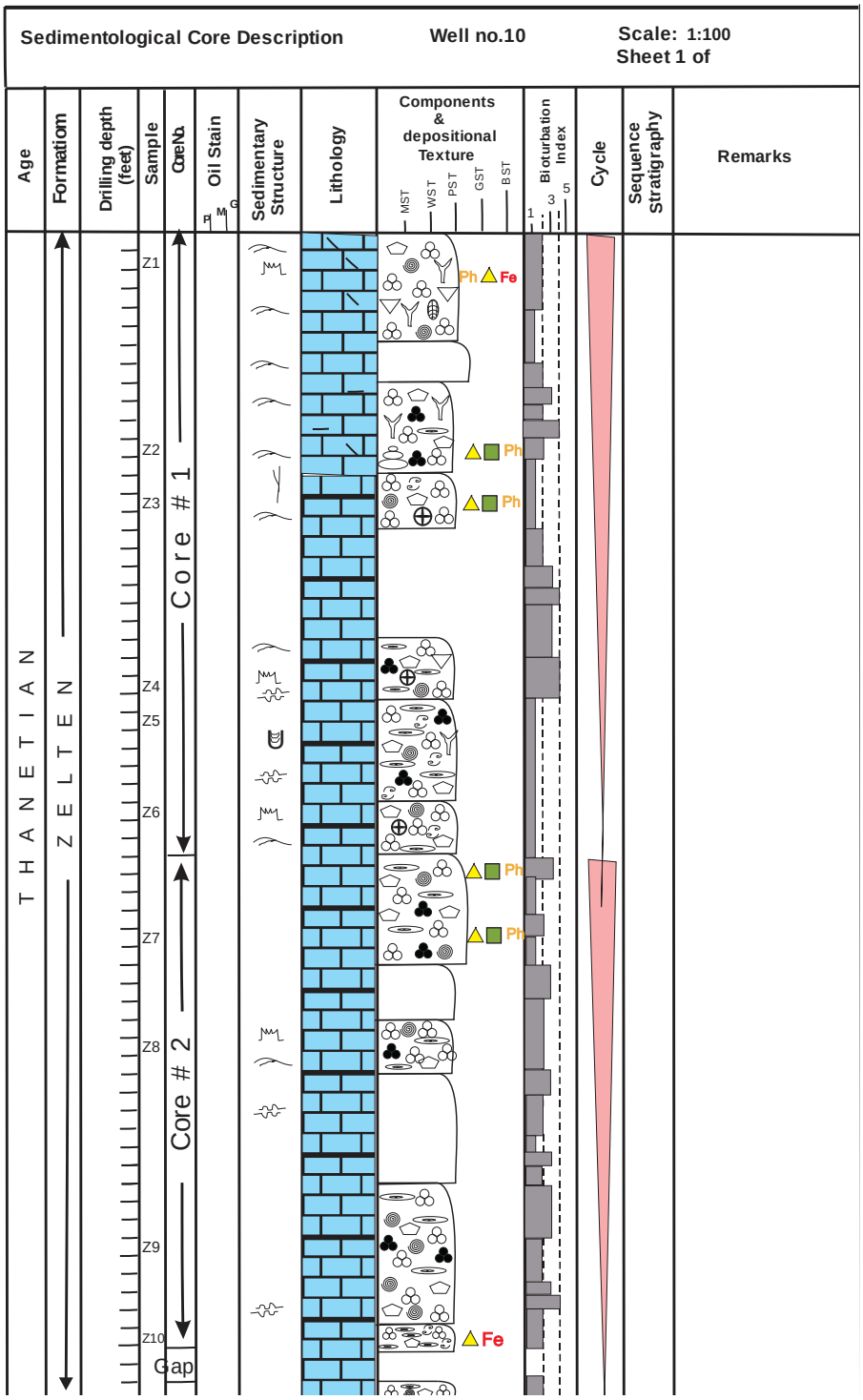
Sedimentological Core Description
Well no.10
Scale: 1:100
Sheet 1 of
Age
Formation
Drilling depth (feet)
Sample
Core No.
Oil Stain
Sedimentary Structure
Lithology
Components & depositional Texture
MST
WST
PST
GST
BST
Bioturbation Index
1
3
5
Cycle
Sequence Stratigraphy
Remarks
THANETIAN
ZELTEN
Z1
Z2
Z3
Z4
Z5
Z6
Z7
Z8
Z9
Z10
Core # 1
Core # 2
Gap
Ph
Fe

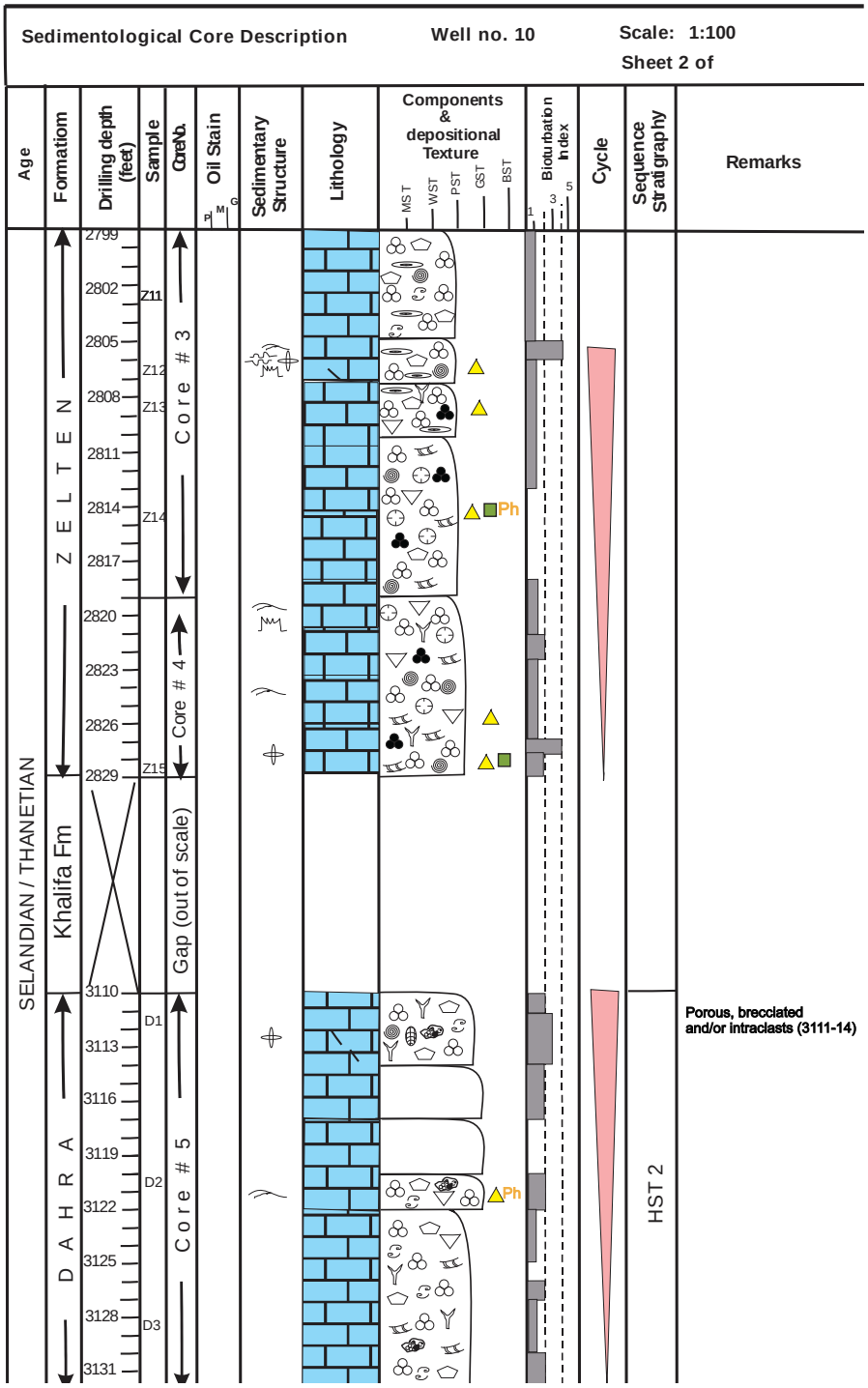
Sedimentological Core Description
Well no. 10
Scale: 1:100
Sheet 2 of
Age
Formation
Drilling depth (feet)
Sample
Core No.
Oil Stain
Sedimentary Structure
Lithology
Components & depositional Texture
MST
WST
PST
GST
BST
Bioturbation Index
Cycle
Sequence Stratigraphy
Remarks
SELANDIAN / THANETIAN
Khalifa Fm
D A H R A
Z E L T E N
Core # 3
Core # 4
Core # 5
Gap (out of scale)
Ph
HST 2
Porous, brecciated and/or intraclasts (3111-14)

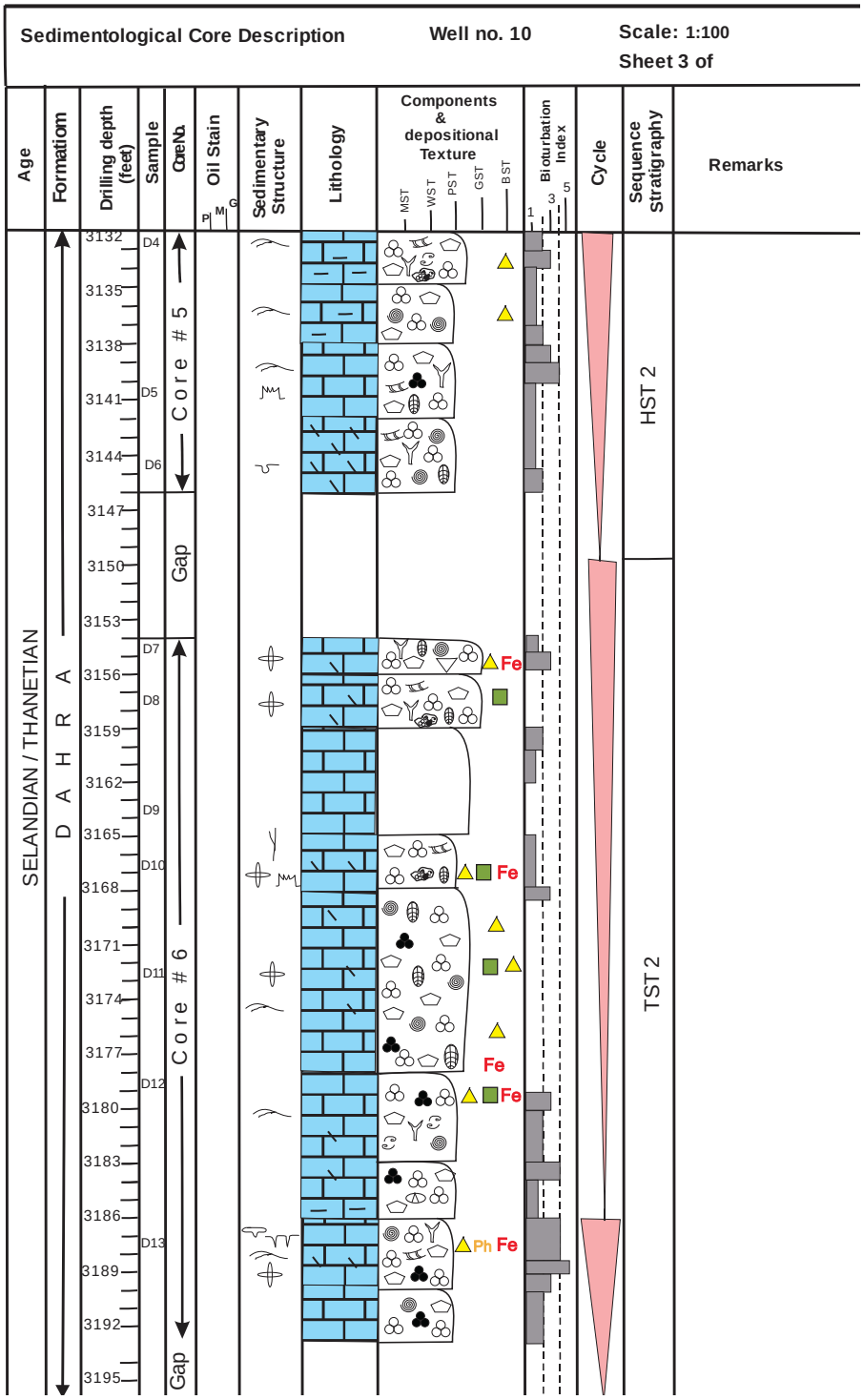
Sedimentological Core Description
Well no. 10
Scale: 1:100
Sheet 3 of
Age
Formation
Drilling depth (feet)
Sample
Core No.
Oil Stain
P M G
Sedimentary Structure
Lithology
Components & depositional Texture
MST WST PST GST BST
Bioturbation Index
1 3 5
Cycle
Sequence Stratigraphy
Remarks
SELANDIAN / THANETIAN
D A H R A
3132
3135
3138
3141
3144
3147
3150
3153
3156
3159
3162
3165
3168
3171
3174
3177
3180
3183
3186
3189
3192
3195
D4
D5
D6
D7
D8
D9
D10
D11
D12
D13
Core # 5
Gap
Core # 6
Gap
Fe
Ph Fe
HST 2
TST 2

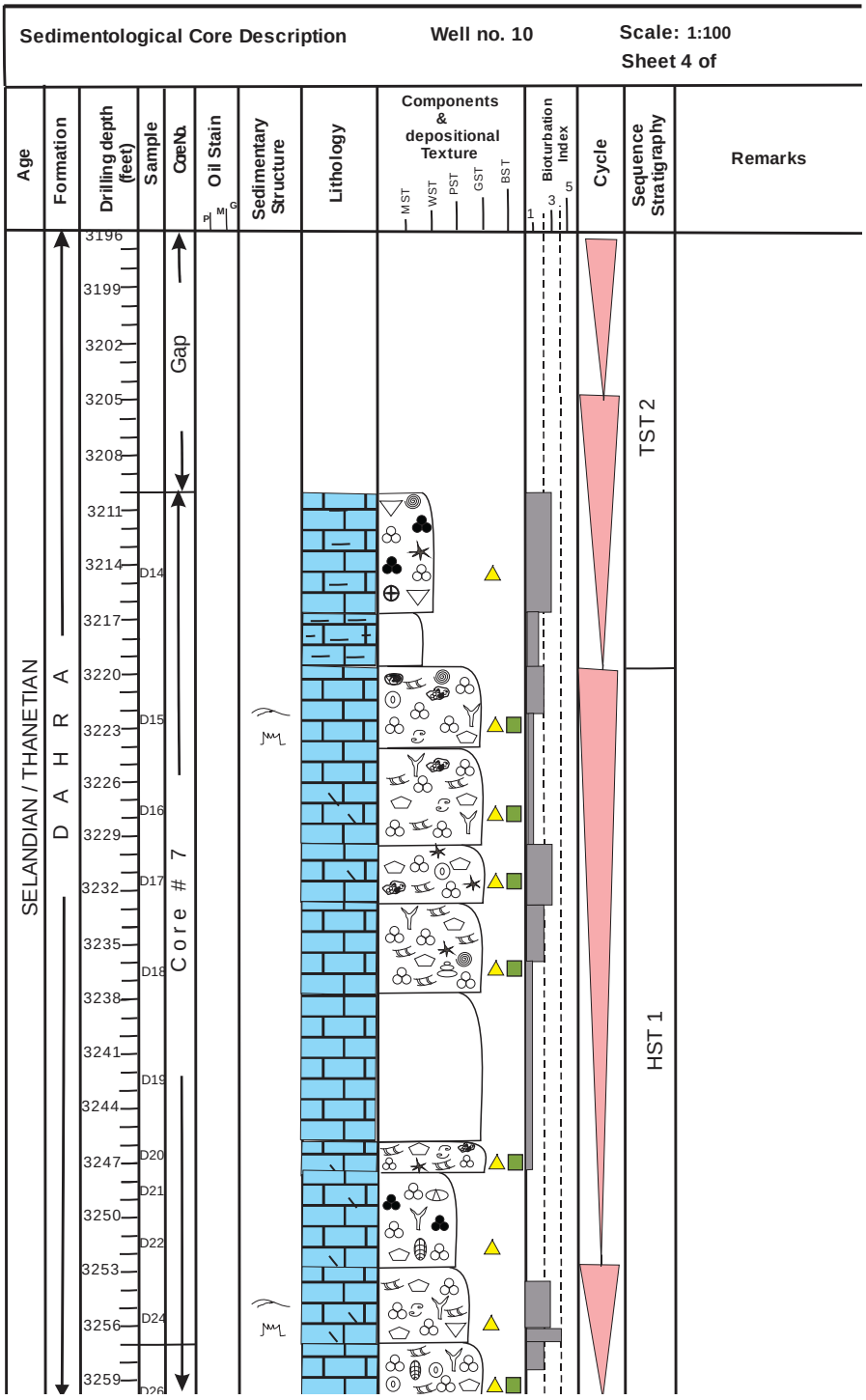
Sedimentological Core Description
Well no. 10
Scale: 1:100
Sheet 4 of
Age
Formation
Drilling depth (feet)
Sample
Core No.
Oil Stain
Sedimentary Structure
Lithology
Components & depositional Texture
MST
WST
PST
GST
BST
Bioturbation Index
Cycle
Sequence Stratigraphy
Remarks
SELANDIAN / THANETIAN
D A H R A
3196
3199
3202
3205
3208
3211
3214
3217
3220
3223
3226
3229
3232
3235
3238
3241
3244
3247
3250
3253
3256
3259
D14
D15
D16
D17
D18
D19
D20
D21
D22
D24
D26
Gap
Core # 7
TST 2
HST 1

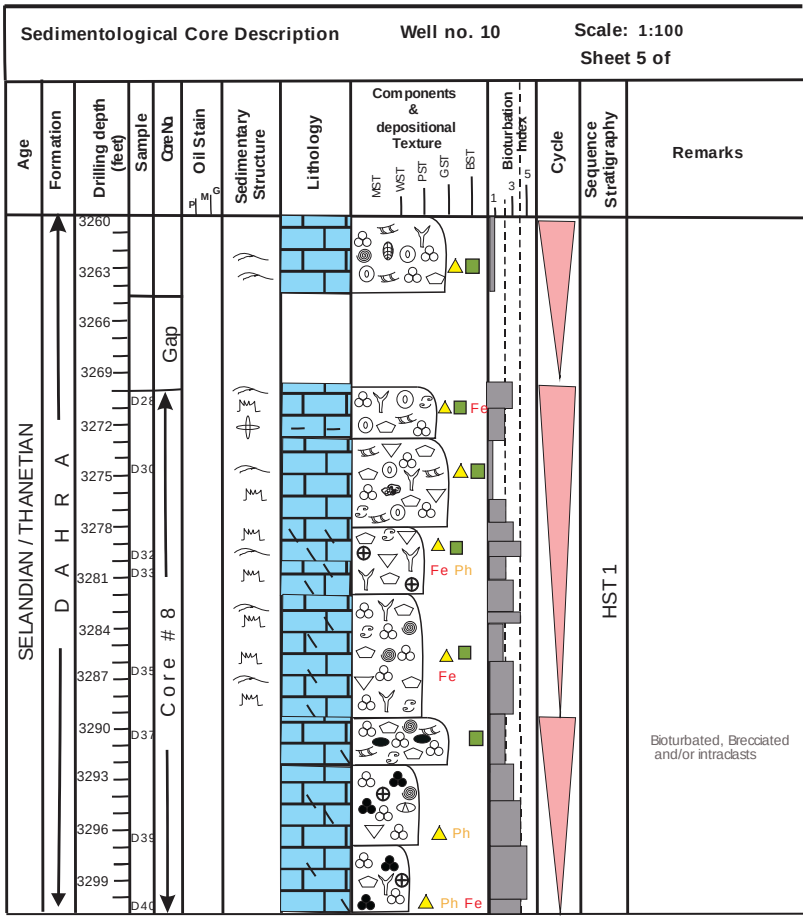
Sedimentological Core Description
Well no. 10
Scale: 1:100
Sheet 5 of
Age
Formation
Drilling depth (feet)
Sample
Core No.
Oil Stain
Sedimentary Structure
Lithology
Components & depositional Texture
MST
WST
PST
GST
BST
Bioturbation Index
Cycle
Sequence Stratigraphy
Remarks
SELANDIAN / THANETIAN
D A H R A
3260
3263
3266
3269
3272
3275
3278
3281
3284
3287
3290
3293
3296
3299
Gap
Core # 8
D28
D30
D32
D33
D35
D37
D39
D40
Fe
Fe Ph
Fe
Ph
Ph Fe
HST 1
Bioturbated, Brecciated and/or intraclasts

Legend

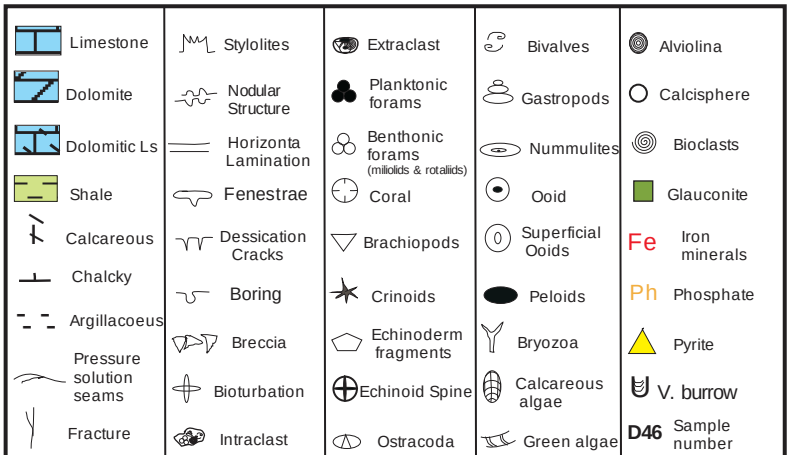
Limestone
Dolomite
Dolomitic Ls
Shale
Calcareous
Chalcky
Argillacoeus
Pressure solution seams
Fracture
Stylolites
Nodular Structure
Horizonta Lamination
Fenestrae
Dessication Cracks
Boring
Breccia
Bioturbation
Intraclast
Extraclast
Planktonic forams
Benthonic forams (miliolids & rotaliids)
Coral
Brachiopods
Crinoids
Echinoderm fragments
Echinoid Spine
Ostracoda
Bivalves
Gastropods
Nummulites
Ooid
Superficial Ooids
Peloids
Bryozoa
Calcareous algae
Green algae
Alviolina
Calcisphere
Bioclasts
Glauconite
Fe Iron minerals
Ph Phosphate
Pyrite
V. burrow
D46 Sample number

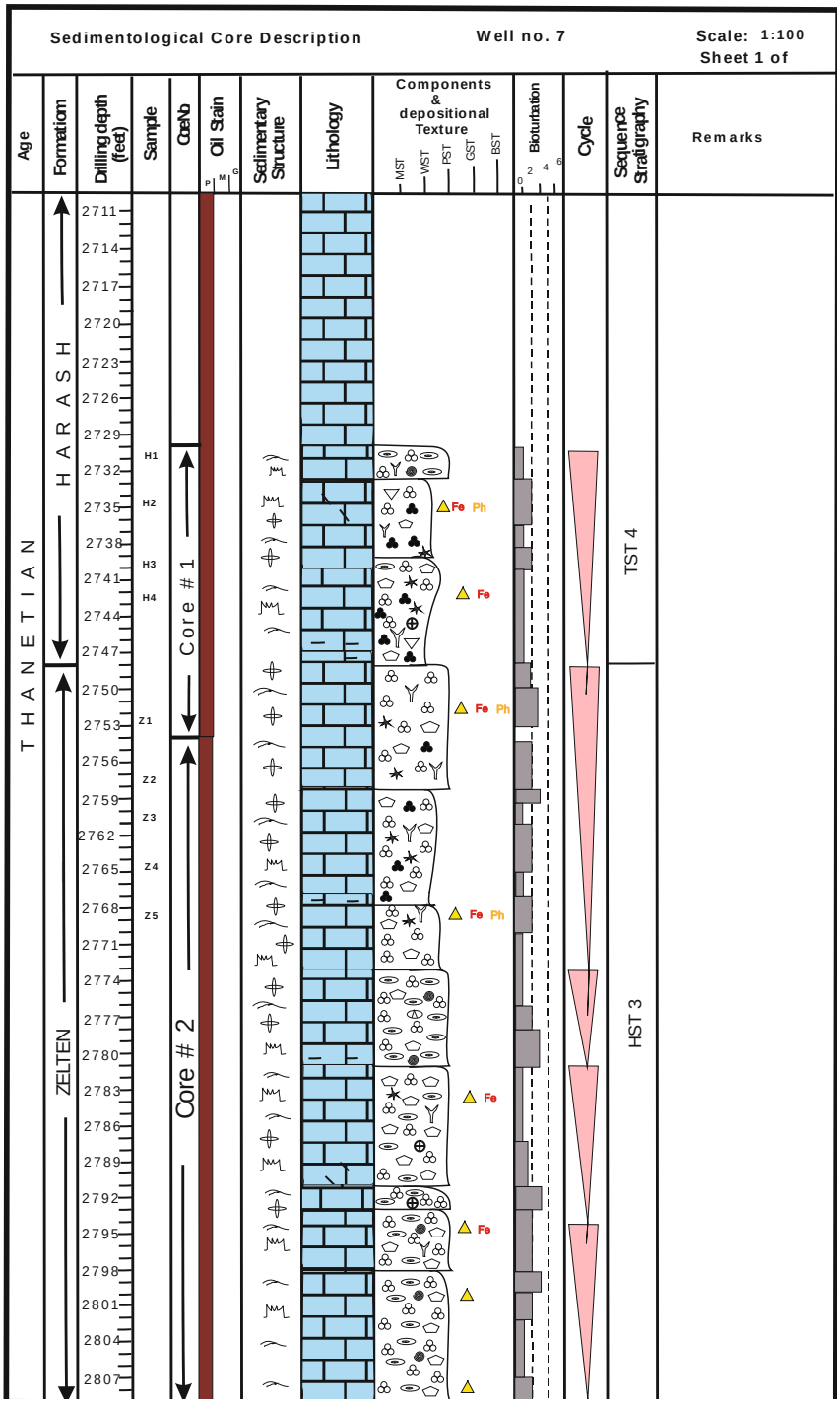
Sedimentological Core Description
Well no. 7
Scale: 1:100
Sheet 1 of
Age
Formation
Drilling depth (feet)
Sample
Core No
Oil Stain
Sedimentary Structure
Lithology
Components & depositional Texture
MST
WST
PST
GST
BST
Bioturbation
Cycle
Sequence Stratigraphy
Remarks
THANETIAN
HARASH
ZELTEN
Core # 1
Core # 2
H1
H2
H3
H4
Z1
Z2
Z3
Z4
Z5
Fe
Ph
TST 4
HST 3

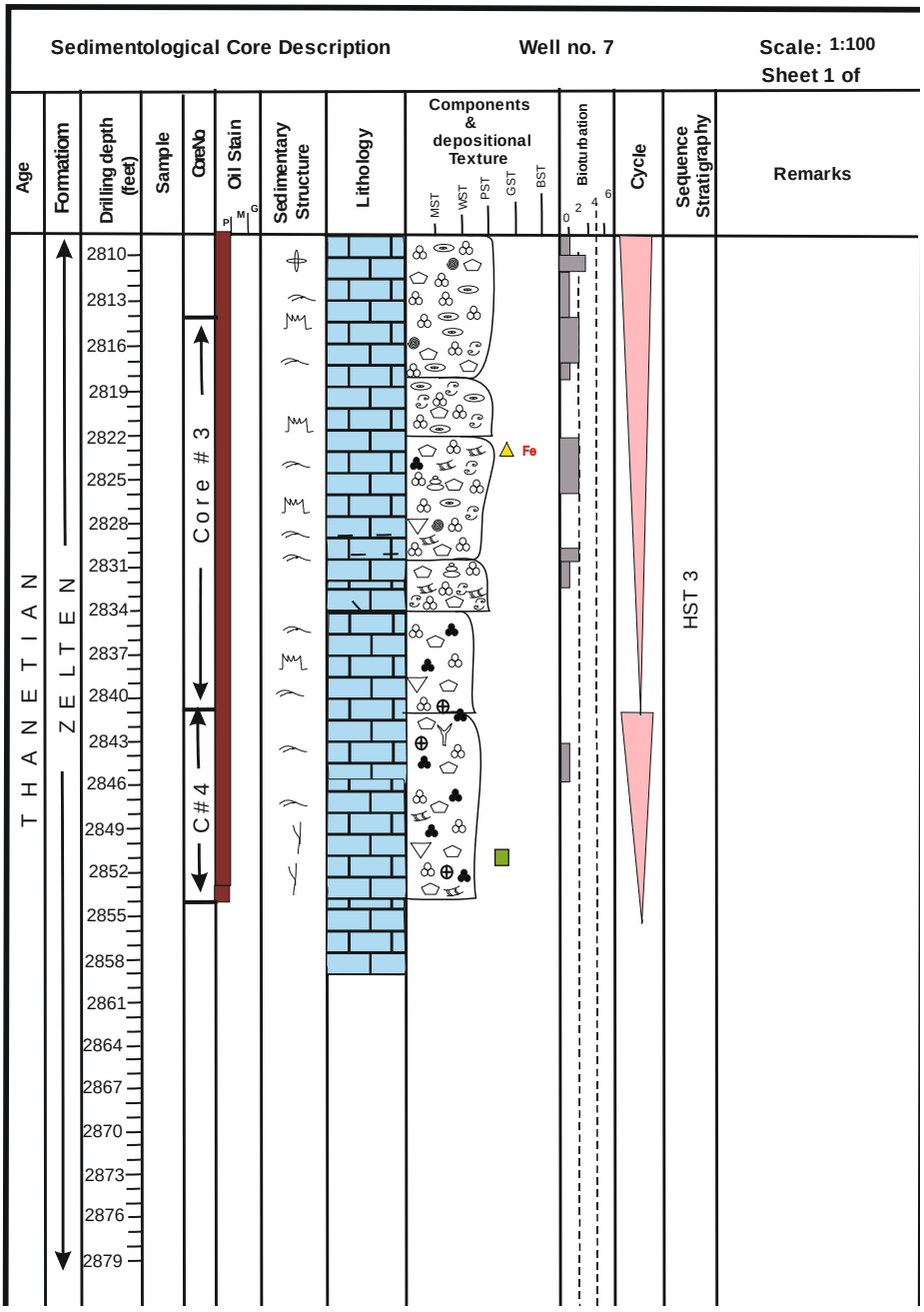
Sedimentological Core Description
Well no. 7
Scale: 1:100
Sheet 1 of
Age
Formation
Drilling depth (feet)
Sample
Core No
Oil Stain
Sedimentary Structure
Lithology
Components & depositional Texture
MST
WST
PST
GST
BST
Bioturbation
Cycle
Sequence Stratigraphy
Remarks
THANETIAN
ZELTEN
2810
2813
2816
2819
2822
2825
2828
2831
2834
2837
2840
2843
2846
2849
2852
2855
2858
2861
2864
2867
2870
2873
2876
2879
Core # 3
C#4
Fe
HST 3

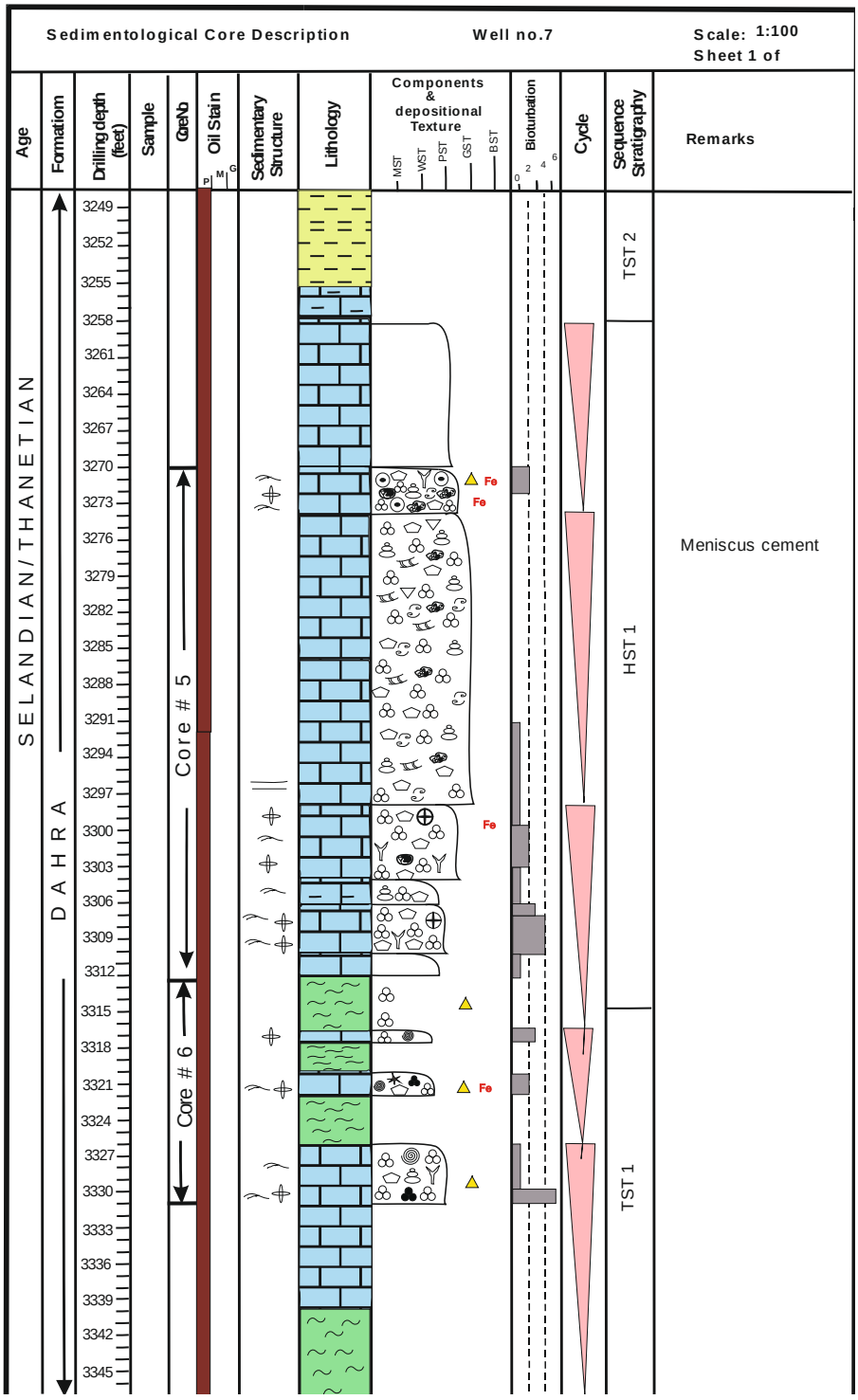
Sedimentological Core Description
Well no.7
Scale: 1:100
Sheet 1 of
Age
Formation
Drilling depth (feet)
Sample
Core No
Oil Stain
Sedimentary Structure
Lithology
Components & depositional Texture
MST
WST
PST
GST
BST
Bioturbation
Cycle
Sequence Stratigraphy
Remarks
SELANDIAN/THANETIAN
DAHRA
Core # 5
Core # 6
Fe
TST 2
HST 1
TST 1
Meniscus cement

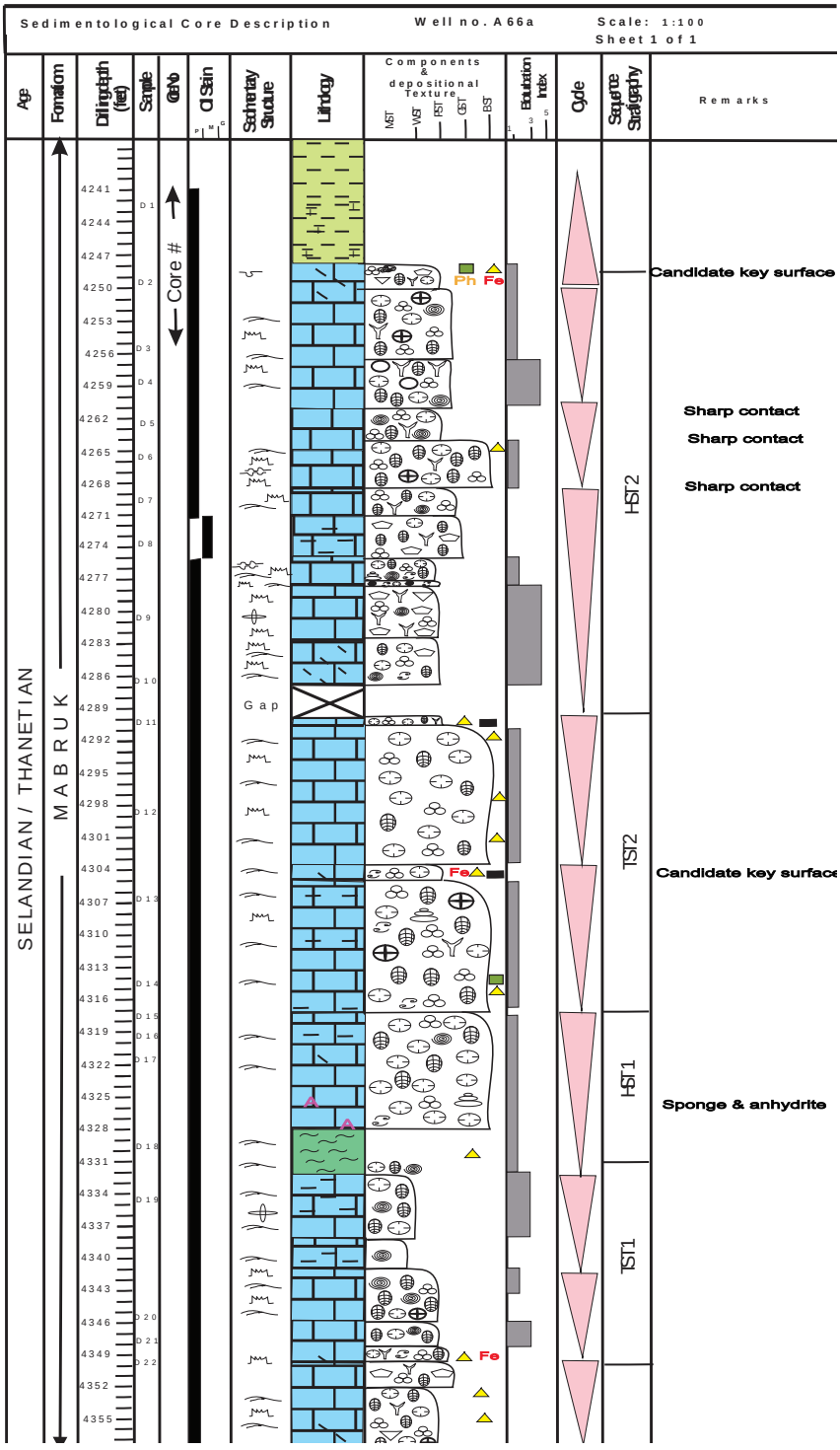
Sedimentological Core Description
Well no. A66a
Scale: 1:100
Sheet 1 of 1
Age
Formation
Lithology
Components & depositional Texture
Remarks
SELANDIAN / THANETIAN
MABRUK
Core #
Gap
Ph
Fe
Candidate key surface
Sharp contact
Sharp contact
Sharp contact
HST2
TST2
Candidate key surface
HST1
Sponge & anhydrite
TST1

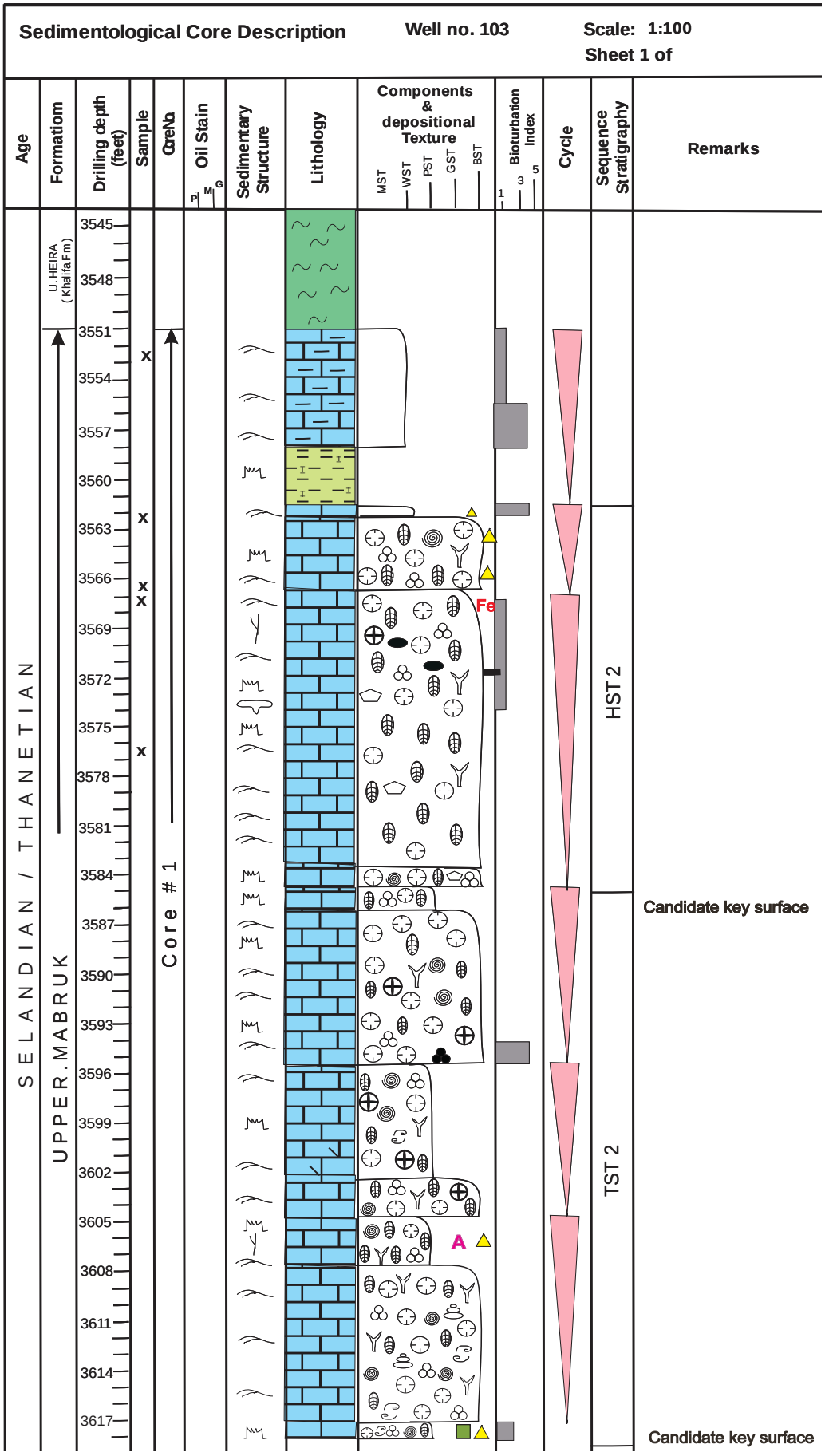
Sedimentological Core Description
Well no. 103
Scale: 1:100
Sheet 1 of
Age
Formation
Drilling depth (feet)
Sample
Core No.
Oil Stain
Sedimentary Structure
Lithology
Components & depositional Texture
MST
WST
PST
GST
BST
Bioturbation Index
Cycle
Sequence Stratigraphy
Remarks
SELANDIAN / THANETIAN
UPPER.MABRUK
U. HEIRA (Khalifa Fm)
Core # 1
3545
3548
3551
3554
3557
3560
3563
3566
3569
3572
3575
3578
3581
3584
3587
3590
3593
3596
3599
3602
3605
3608
3611
3614
3617
Fe
A
HST 2
TST 2
Candidate key surface
Candidate key surface

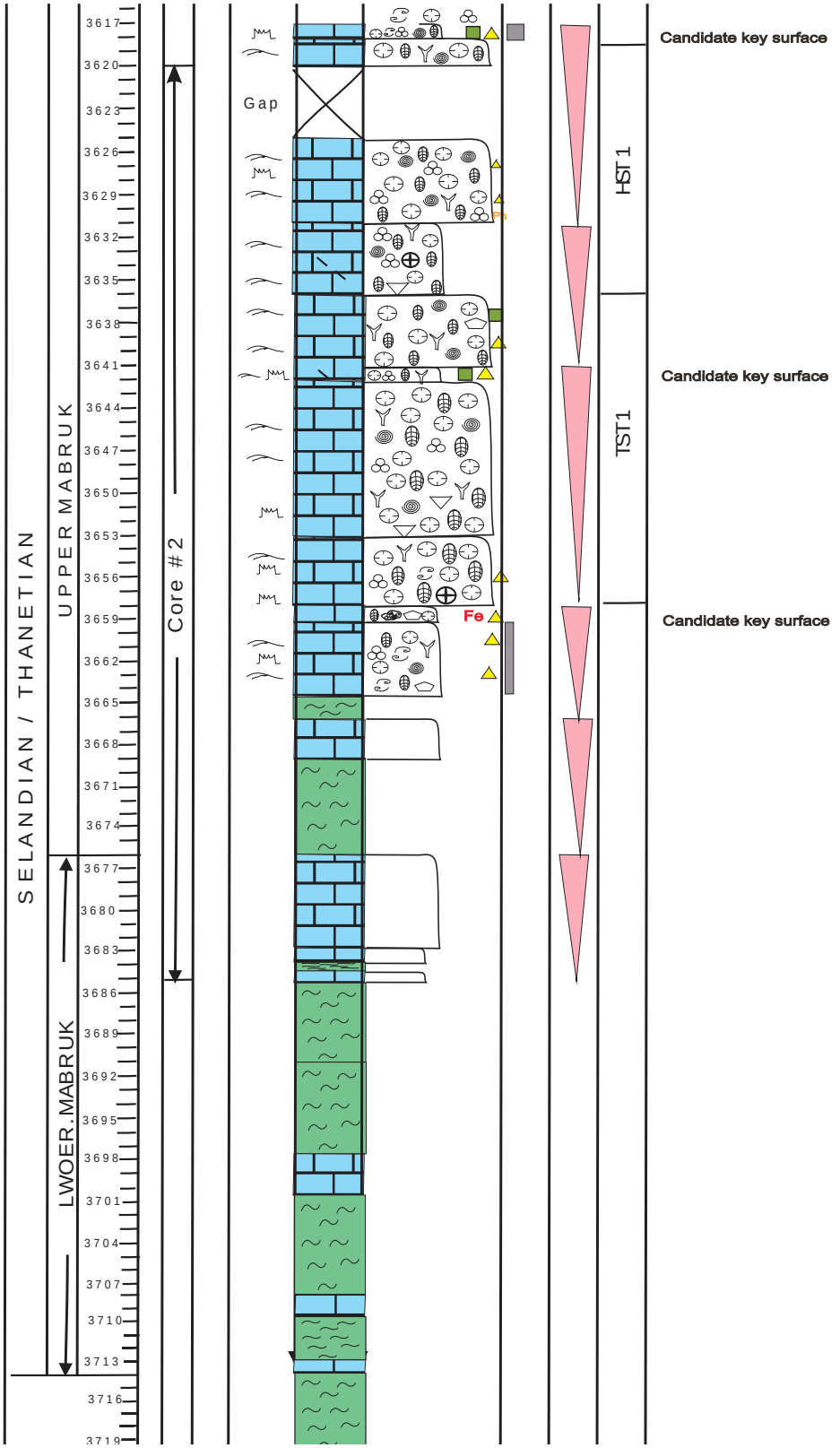
SELANDIAN / THANETIAN
UPPER MABRUK
LWOER.MABRUK
Core #2
Gap
Fe
HST 1
TST 1
Candidate key surface
Candidate key surface
Candidate key surface

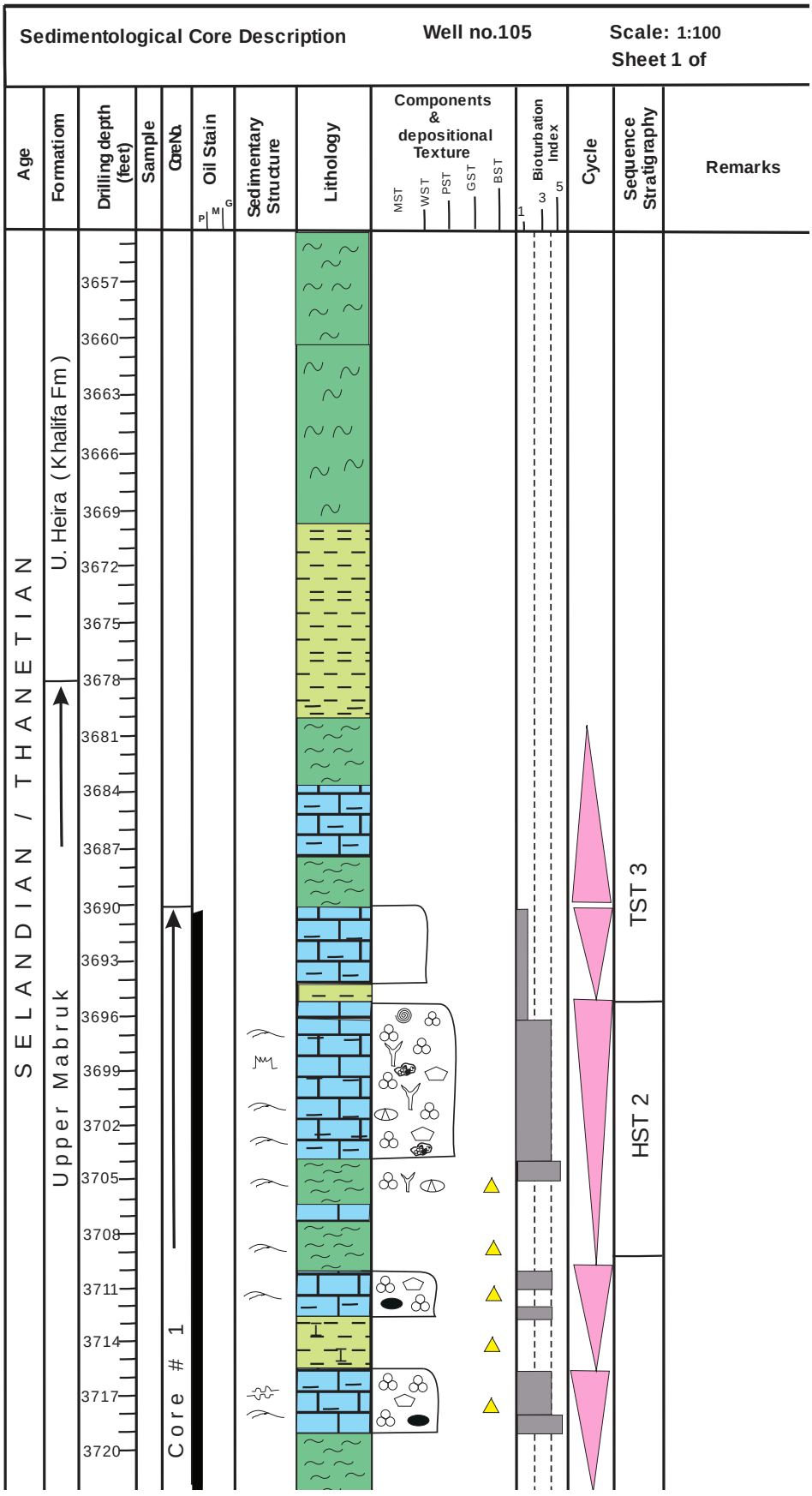
Sedimentological Core Description
Well no.105
Scale: 1:100
Sheet 1 of
Age
Formation
Drilling depth (feet)
Sample
Core No.
Oil Stain
P
M
G
Sedimentary Structure
Lithology
Components & depositional Texture
MST
WST
PST
GST
BST
Bioturbation Index
1
3
5
Cycle
Sequence Stratigraphy
Remarks
SELANDIAN / THANETIAN
U. Heira (Khalifa Fm.)
Upper Mabruk
3657
3660
3663
3666
3669
3672
3675
3678
3681
3684
3687
3690
3693
3696
3699
3702
3705
3708
3711
3714
3717
3720
Core # 1
TST 3
HST 2

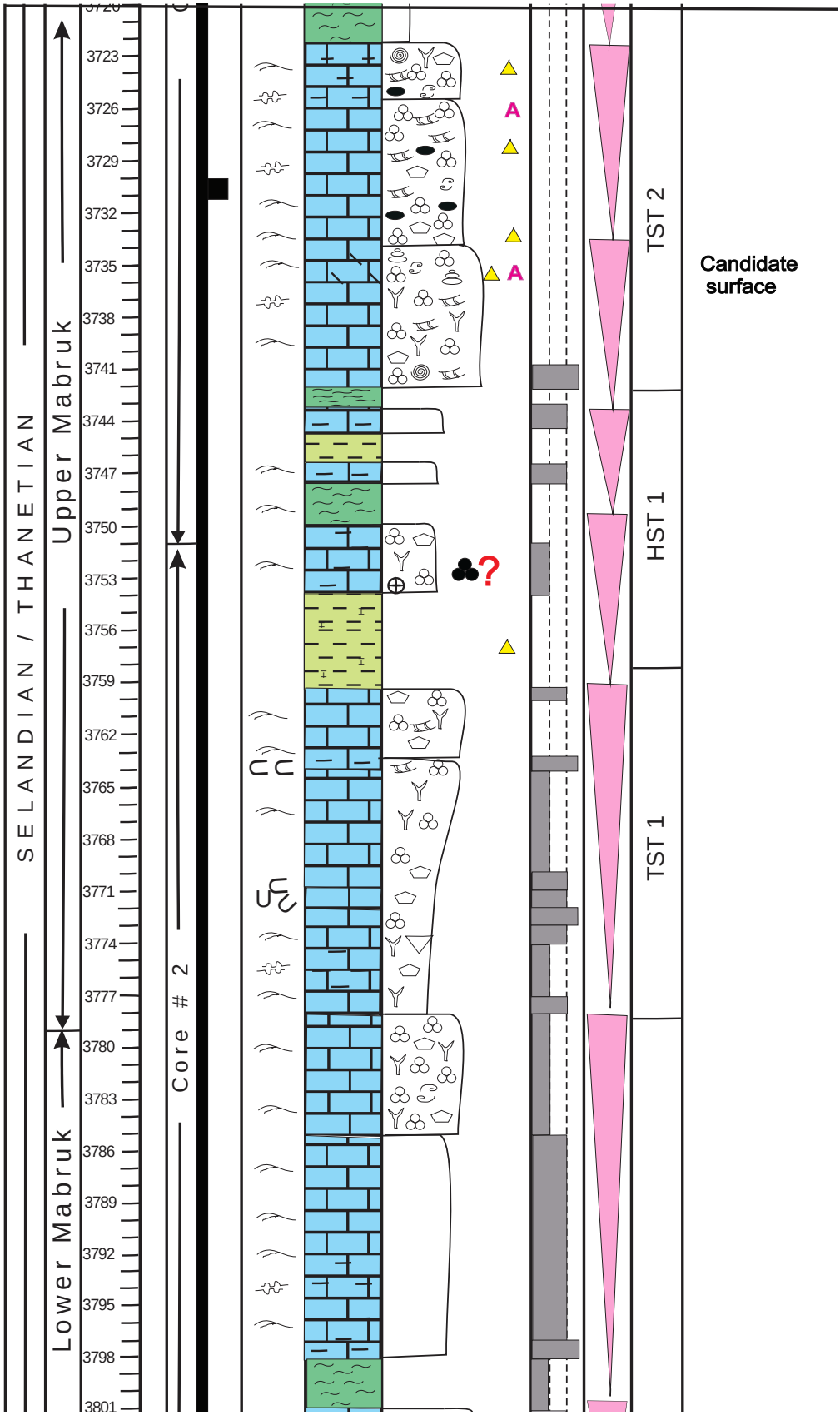
SELANDIAN / THANETIAN
Upper Mabruk
Lower Mabruk
Core # 2
3723
3726
3729
3732
3735
3738
3741
3744
3747
3750
3753
3756
3759
3762
3765
3768
3771
3774
3777
3780
3783
3786
3789
3792
3795
3798
3801
A
A
?
TST 2
HST 1
TST 1
Candidate surface

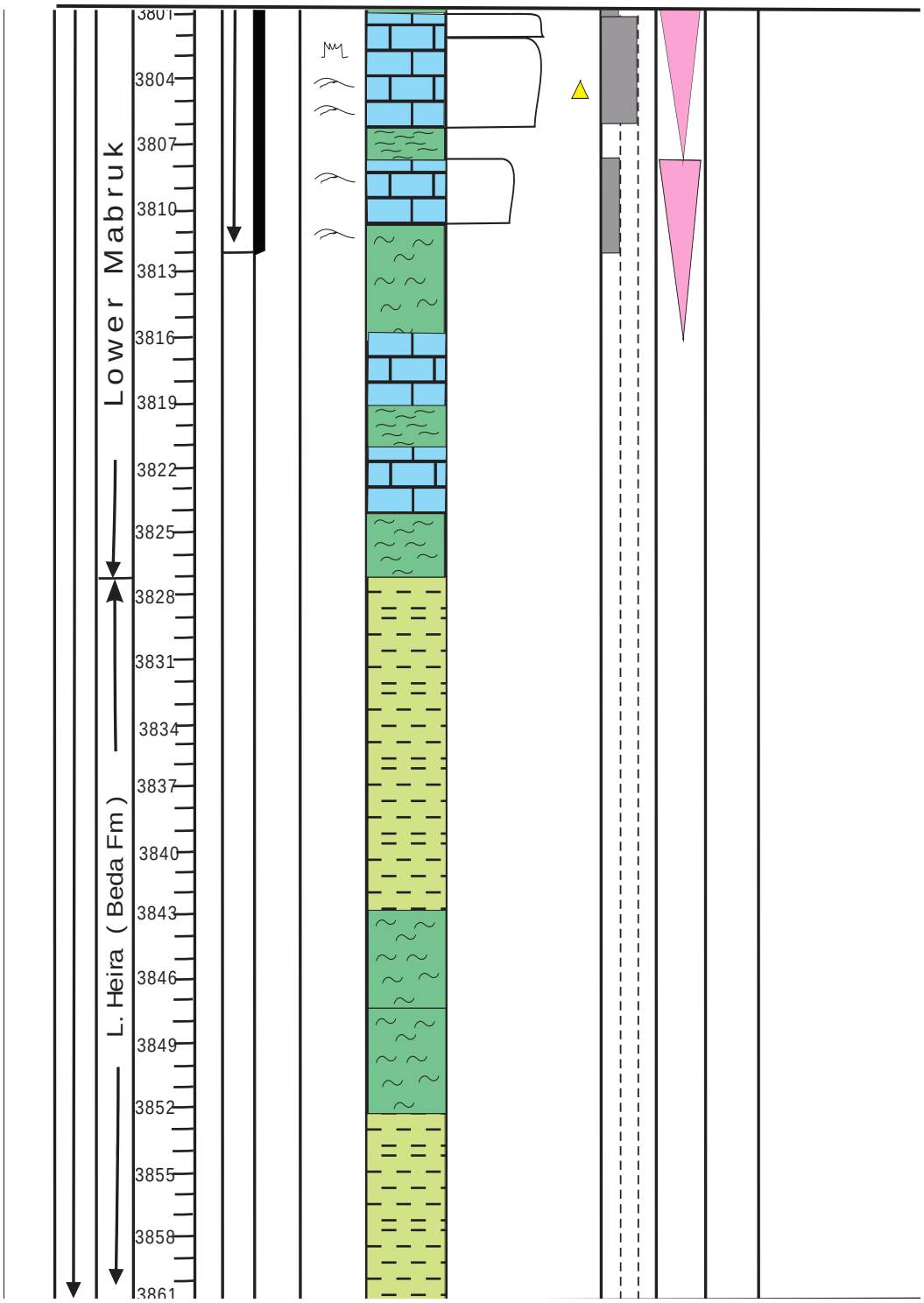
3801
3804
3807
3810
3813
3816
3819
3822
3825
3828
3831
3834
3837
3840
3843
3846
3849
3852
3855
3858
3861
Lower Mabruk
L. Heira (Beda Fm)

Appendix2. Fluid inclusions and Stable (carbon and oxygen) isotopes data

This appendix presents the analytical data that have been collected for this study

1. Fluid Inclusion sample data

Well no. A

No.	Sample No	Depth	Core	Comment
1	F8-H1	2663	Yes	Unwashed
2	F8-H2	2670	″	″
3	F8-H3	2673	″	″
4	F8-H4	2676	″	″
5	F8-H5	2679	″	″
6	F8-H6	2685	″	″
7	F8-H7	2691	″	″
8	F8-H8	2700	″	″
9	F8-H9	2709	″	″
10	F8-H10	2718	″	″
11	F8-Z1	2726	″	″
12	F8-Z2	2734	″	″
13	F8-Z3	2739	″	″
14	F8-Z4	2745	″	″
15	F8-Z5	2748	″	″
16	F8-Z6	2752	″	″
17	F8-Z7	2760	″	″
18	F8-Z8	2769	″	″
19	F8-Z9	2777	″	″
20	F8-Z10	2782	″	″
21	F8-Z11	2788	″	″
22	F8-D1	3057	″	″
23	F8-D2	3063	″	″
24	F8-D3	3075	″	″
25	F8-D4	3079	″	″
26	F8-D5	3081	″	″
27	F8-D6	3089	″	″
28	F8-D7	3109	″	″
29	F8-D8	3119	″	″
30	F8-D9	3124	″	″
31	F8-D10	3126	″	″
32	F8-D12	3132	″	″
33	F8-D13	3134	″	″
34	F8-D14	3137	″	″
35	F8-D16	3146	″	″
36	F8-D17	3155	″	″
37	F8-D18	3166	″	″
38	F8-D19	3170	″	″
39	F8-D20	3174	″	″
40	F8-D21	3185	″	″

41	F8-D22	3187	″	″
42	F8-D23	3193	″	″
43	F8-D24	3201	″	″
44	F8-D25	3204	″	″
45	F8-D26	3205	″	″
46	F8-D27	3207	″	″
47	F8-D28	3212	″	″
48	F8-D29	3221	″	″
49	F8-D31	3229	″	″
50	F8-D32	3233	″	″
51	F8-D33	3244	″	″
52	F8-D34	3247	″	″
53	F8-D34B	3249	″	″
54	F8-D35	3259	″	″
55	F8-D36	3267	″	″
56	F8-D37	3274	″	″
57	F8-D38	3277	″	″
58	F8-D39	3287	″	″
59	F8-D40	3291	″	″
60	F8-D41	3293	″	″
61	F8-D42	3298	″	″
62	F8-D43	3301	″	″
63	F8-D45	3329	″	″
64	F8-D46	3334	″	″

Well no. B

No.	Sample No	Depth	Core	Comment
1	B9-H1	2631	Yes	Unwashed
2	B9-H2	2639	″	″
3	B9-H3	2646	″	″
4	B9-H4	2652	″	″
5	B9-H5	2659	″	″
6	B9-H6	2663	″	″
7	B9-H7	2669	″	″
8	B9-H8	2674	″	″
9	B9-H9	2675	″	″
10	B9-H10	2678	″	″
11	B9-H11	2686	″	″
12	B9-H12	2694	″	″
13	B9-H13	2698	″	″
14	B9-Z1	2702	″	″
15	B9-Z3	2711	″	″
16	B9-Z5	2718	″	″
17	B9-Z6	2726	″	″
18	B9-Z7	2731	″	″

19	B9-Z9	2740	″	″
20	B9-Z10	2742	″	″
21	B9-Z11	2747	″	″
22	B9-Z12	2752	″	″
23	B9-Z13	2755	″	″
24	B9-Z14	2767	″	″
25	B9-Z15	2770	″	″
26	B9-Z16	2779	″	″
27	B9-Z17	2788	″	″
28	B9-Z18	2808	″	″
29	B9-Z19	2814	″	″
30	B9-Z20	2817	″	″
31	B9-Z21	2821	″	″
32	B9-Z22	2843	″	″
33	B9-D1	3076	″	″
34	B9-D3	3084	″	″
35	B9-D4	3088	″	″
36	B9-D5	3093	″	″
37	B9-D6	3098	″	″
38	B9-D7	3155	″	″
39	B9-D9	3164	″	″
40	B9-D10	3172	″	″
41	B9-D11	3175	″	″
42	B9-D13	3181	″	″

43	B9-D15	3189	″	″
44	B9-D16	3195	″	″
45	B9-D17	3213	″	″
46	B9-D18	3216	″	″
47	B9-D19	3217	″	″
48	B9-D20	3220	″	″
49	B9-D22	3227	″	″
50	B9-D23	3228	″	″
51	B9-D24	3233	″	″
52	B9-D25	3240	″	″
53	B9-D26	3241	″	″
54	B9-D27	3249	″	″
55	B9-D28	3254	″	″
56	B9-D30	3260	″	″
57	B9-D31	3265	″	″
58	B9-D32	3268	″	″

2. Oxygen and carbon isotope data

Wells no. 8 and 9

	d13C	d18O
ELK001	**2.59**	**-3.86**
ELK002	2.46	-2.21
ELK003	2.58	-4.97
ELK004	2.82	-3.70
ELK005	3.15	-2.96
ELK006	2.75	-5.36
ELK007	3.28	-3.84
ELK008	3.33	-3.50
ELK009	3.07	-4.28
ELK010	3.50	-3.67
ELK011	**3.31**	**-4.51**
ELK012	3.89	-4.31
ELK013	3.22	-6.57
ELK014	3.44	-4.83
ELK015	3.44	-6.49
ELK016	3.47	-6.24
ELK017	3.68	-4.32
ELK018	3.66	-5.06
ELK019	3.56	-6.64
ELK020	3.62	-6.94
ELK021	3.62	-6.00
ELK022	**1.54**	**-2.80**
ELK023	2.07	-2.43
ELK024	1.53	-1.24
ELK025	1.00	1.15
ELK026	1.43	-0.81
ELK027	-1.83	-3.79
ELK028	1.92	-3.31
ELK029	1.37	-3.19
ELK030	1.98	-2.06
ELK031	1.98	-2.60
ELK032	2.16	-1.72
ELK033	2.00	-3.40
ELK034	2.09	-3.47
ELK035	1.88	-3.45
ELK036	1.92	-3.51
ELK037	1.92	-3.21
ELK038	1.92	-3.51
ELK039	1.75	-3.27
ELK040	1.82	-4.12
ELK041	3.57	-4.72
ELK042	1.82	-5.53
ELK043	1.96	-4.46
ELK044	2.37	-4.09
ELK045	2.31	-4.85
ELK046	1.89	-5.45
ELK047	2.16	-5.82
ELK048	2.65	-5.14
ELK049	2.63	-5.66
ELK050	2.48	-6.09
ELK051	2.33	-6.83
ELK052	2.57	-5.84
ELK053	2.65	-5.98
ELK054	2.59	-3.33
ELK055	2.50	-3.72
ELK056	2.46	-3.43
ELK057	3.11	-1.72
ELK058	2.72	-2.92
ELK059	2.79	-3.18
ELK060	2.70	-2.95
ELK061	2.33	-3.60
ELK062	2.34	-2.69
ELK063	2.74	-3.45
ELK064	2.50	-4.13
ELK065	2.64	-3.12
ELK066	2.22	-3.61
ELK067	2.38	-3.28
ELK068	2.84	-2.58
ELK069	2.73	-4.00
ELK070	2.74	-4.40
ELK071	2.82	-3.74
ELK072	2.96	-4.02
ELK073	2.91	-4.06
ELK074	2.91	-4.12
ELK075	3.23	-4.02
ELK076	3.31	-4.24
ELK077	3.48	-2.71
ELK078	3.16	-4.91
ELK079	3.29	-4.59
ELK080	2.96	-5.53
ELK081	3.25	-5.97
ELK082	3.53	-5.21
ELK083	3.50	-6.77
ELK084	3.18	-7.71
ELK085	-0.90	-10.49
ELK086	3.86	-4.66
ELK087	3.57	-4.52

ELK088	3.53	-4.81
ELK089	3.34	-6.92
ELK090	3.42	-6.30
ELK091	3.71	-6.25
ELK092	3.58	-6.12
ELK093	3.54	-4.23
ELK094	3.12	-4.85
ELK095	3.06	-5.31
ELK096	3.29	-4.57
ELK097	3.06	-2.38
ELK098	2.20	-3.50
ELK099	2.37	-3.60
ELK100	2.49	-3.87
ELK101	2.86	-3.84
ELK102	2.16	-3.25
ELK103	1.95	-3.09
ELK104	2.00	-2.49
ELK105	1.58	-2.11
ELK106	1.29	-4.37
ELK107	1.75	-5.04
ELK108	2.16	-5.18
ELK109	2.05	-6.35
ELK110	2.13	-6.77
ELK111	2.40	-6.16
ELK112	2.52	-5.86
ELK113	2.61	-6.05
ELK114	2.93	-5.80
ELK115	2.77	-6.49
ELK116	3.08	-5.71
ELK117	2.81	-6.57
ELK118	2.81	-6.56
ELK119	2.92	-6.45
ELK120	2.87	-6.46
ELK121	2.56	-6.14
ELK122	3.18	-2.39
ELK123	3.11	-0.83

Wells no. 66,103 and 105

Well 66		Well 103		Well 105	
$d^{13}C_{V-PDB}$	$d^{18}O_{V-PDB}$	$d^{13}C_{V-PDB}$	$d^{18}O_{V-PDB}$	$d^{13}C_{V-PDB}$	$d^{18}O_{V-PDB}$
0.00	**-2.71**	**1.59**	**-3.78**	**1.81**	**-2.58**
0.75	**-4.21**	**1.47**	**-3.59**	**2.15**	**-0.77**
1.07	**-3.45**	**-4.87**	**-7.66**	**2.65**	**-2.39**
1.00	**-4.20**	**1.15**	**-3.87**	**2.38**	**-3.15**
1.00	**-4.30**	**1.07**	**-3.85**	**2.27**	**-2.64**
0.95	**-3.73**	**1.59**	**-3.78**	**2.86**	**-2.07**
1.02	**-4.41**	**1.24**	**-4.34**	**0.75**	**-4.21**
1.16	**-4.29**	**1.80**	**-3.80**	**1.59**	**-5.01**
1.05	**-4.62**	**1.53**	**-4.92**	**1.01**	**-4.58**
0.94	**-5.14**	**1.98**	**-4.85**	**1.91**	**-4.78**
1.06	**-4.19**	**2.04**	**-4.21**	**1.63**	**-5.45**
0.98	**-3.79**	**1.96**	**-4.03**	**2.23**	**-2.48**
1.08	**-4.57**	**1.88**	**-4.84**	**1.01**	**-2.51**
1.02	**-4.72**	**2.44**	**-3.13**	**2.64**	**-3.49**
1.32	**-4.12**	**2.31**	**-3.88**	**2.60**	**-2.60**
1.29	**-4.18**	**1.75**	**-4.17**	**2.58**	**-2.85**
1.31	**-4.37**	**1.84**	**-2.95**	**2.77**	**-2.88**
0.94	**-3.12**	**2.32**	**-2.98**	**2.82**	**-3.10**
-6.31	**-7.68**	**2.85**	**-3.52**	**2.51**	**-2.96**
0.87	**-4.94**			**3.00**	**-4.09**
1.09	**-4.14**			**2.73**	**-4.04**
1.47	**-4.25**			**2.66**	**-3.16**
				3.04	**-4.19**
				1.15	**-3.87**
				2.53	**-3.60**

Appendix 3. Cycle type, number, and average thickness (ft) for the studied wells in the study area.

A. On the Dahra Platform

Formation/ Well no.	Cycle type	Cycle sub-type	No. of cycles	Cycle range (ft)	Average (ft)	Remarks
Dahra						
Well no.8	A	A1	5	8-30	17.6	
Well no.9	″	″	3	7-30	17	
Well no.10	″	″	3	13-22	17	
Well no.7	″	″	2	11-20	15.5	
Well no.8	″	A2	6	6-24	13.5	
Well no.9	″	″	2	19-30	24.5	
Well no.10	″	″	-	-	-	
Well no.7	″	″	-	-	-	
Well no.8	″	A3	3	18-33	23.3	
Well no.9	″	″	3	14-20	16.3	
Well no.10	″	″	3	17-18	17.6	
Well no.7	″	″	-	-	-	
Well no.8	″	A4	2	15-29	22	
Well no.9	″	″	2	12-33	22.5	
Well no.10	″	″	3	21-36	30.3	
Well no.7	″	″	2	16-23	19.5	

Formation/ Well no.	Cycle type	Cycle sub-type	No. of cycles	Cycle range (ft)	Average (ft)	Remarks
Zelten/Harash						
Well no.8	B	B1	4	7-25	15.7	
Well no.9	″	″	7	7-35	20.2	
Well no.10	″	″	-	-	-	
Well no.7	″	″	4	15-30	25	
Well no.8	″	B2	2	29-34	31.5	
Well no.9	″	″	2	22-31	26.5	
Well no.10	″	″	-	-	-	
Well no.7	″	″	2	8-17	12.5	

B. In the Dor alAbid Trough

Formation/ Well no.	Cycle type	Cycle sub-type	No. of cycles	Cycle range (ft)	Average (ft)	Remarks
Mabruk						
Well no.66	C	C1	2	10-20	15	
Well no.103	″	″	1	8	8	
Well no.105	″	″	2	5-23	19	
Well no.66	″	C2	1	9	9	
Well no.103	″	″	3	9-16	17.5	
Well no.105	″	″	8	5-18	8.1	
Well no.66	″	C3	3	7-14	11.3	
Well no.103	″	″	7	6-16	11.6	
Well no.105	″	″	-	-	-	
Well no.66	″	C4	-	-	-	
Well no.103	″	″	1	17	17	
Well no.105	″	″	-	-	-	
Well no.66	″	C5	1	16	16	
Well no.103	″	″	-	-	-	
Well no.105	″	″	-	-	-	
Well no.66	″	C6	2	10-11	10.5	
Well no.103	″	″	-	-	-	
Well no.105	″	″	2	8-11	9.5	

Appendix 4. Data for topographic and isopach maps and cross sections

The following tables present the formation tops and thickness that collected from well log and have been used in this study

Well	Facha	Kh	H	Z	K	D	B	Hag.	Kal/Sat	K.B.	TD
Z1-11 Tops Thickness **2790**	-4363 126	-4489 289	-4778 278	-5056 167	- 5223 207	- 5430 353	- 5783 918	- 6701 452	- 7153 Kal.	444	-7562
3T1-11 Thickness **1708**	- 3217 155	-3372 357	-3729 173	-3902 290	-4192 197	-4389 257	-4646 279 **TD**	-----	----	681	-4925
P1-32 Thickness **3926**	-2763 199	-2962 365	-3327 183	-3510 334	-3844 212	-4056 531	-4587 474	-5061 49	-5110 U.sat -5695 K/T -6689 Kal. 1579 Sat	723	-9747
F8-32 Thickness **1725**	-997 292	- 1167 262	- 1429 93	- 1522 237	- 1759 134	-1893 322	-2215 296	-2501 44	-2555 U.sat 45 **TD**	1165	-2600
F12-32 Thickness **1354**	-1096 297	-1394 242	-1636 157	-1793 188	-1981 142	-2123 328 **TD**	----	-----	-----	1069	-2451
3P1-11 Thickness **2243**	-1246 257	-1503 254	-1757 97	-1854 223	-2077 139	-2216 298	-2514 318	-2832 23	-2855 U.sat -3489 B. Paleocene 634	946	-3583

Well	Facha	Kh	H	Z	K	D	B	Hag.	Sat / Kal	K.B.	TD
3D1-11 Thickness **2774**	-1429 231	-1660 278	-1938 197	-2135 270	-2405 163	-2568 270	-2838 328	-3166 27	-3193/ -3567?? Or - 4208? 1010 Sat	1027	- 5085
F12-32 Thickness **1354**	-1097 297	-1394 242	-1636 157	-1793 188	-1981 142	-2123 328 TD	------	-----	------	1069	-2451
F8-32 Thickness **1725**	-875 292	-1167 262	-1429 93	-1522 237	-1759 134	-1893 322	-2215 296	-2511 44	-2555 45 TD	1165	-2600
B9-32 Thickness **1894**	-815 294	-1109 266	-1375 99	-1474 245	-1719 148	-1867 270	-2137 332	-2469 44	-2513 196 TD	1201	-2709
B10-32 Thickness **1810**	-861 170	-1031 295	-1326 101	-1427 248	-1675 142	-1817 319	-2136 305	-2441 45	-2486 185 TD	1279	-2671
G1-32 Thickness **2762**	-757 328	-1085 314	-1399 130	-1529 226	-1755 146	-1901 310	-2211 326	-2537 32	-2569/ -3519 950	1211	-4017
B7-32 Thickness **1716**	-909 190	-1099 302	-1401 104	-1505 252	-1757 168	-1925 273	-2198 313	-2511 42	-2553 72 TD	1215	-2625
DD1-32 Thickness	-1028 ? 190	-1210 302	-1524 104	-1638 252	-1926 168	-2120 273	-2464 313	-2748 42	-2838/ -3913 72 TD	1112	-5958

No.	Well	Facha	Kh	H	Z	K	D	B	Hag.	Kal/Sat	K.B.	TD
1	**F8-32**	-997 292	- 1167 262	- 1429 93	- 1522 237	- 1759 134	-1893 322	-2215 296	-2501 44	-2555 U.sat 45 **TD**	1165	-2600
2	**B7-32**	-909 190	-1099 302	-1401 104	-1505 252	-1757 168	-1925 273	-2198 313	-2511 42	-2553 72 TD	1215	-2625
3	**B9-32**	-815 294	-1109 266	-1375 99	-1474 245	-1719 148	-1867 270	-2137 332	-2469 44	-2513 196 TD	1201	-2709

4	**B10-32**	-861 170	-1031 295	-1326 101	-1427 248	-1675 142	-1817 319	-2136 305	-2441 45	-2486 185 TD	1279	-2671
5	**F5-32**	-1087 254	-1341 294	-1635 118	-1753 248	-2001 182	-2183 281	-2464 312	-2776 45	-2821	1029	-4036
6	**F6-32**		-1346 263	-1609 118	-1727 213	-1940 137	-2077 328	-2405 232	-2637 100	-2737 Sat.	985	-2780
7	**F12-32**	-1097 297	-1394 242	-1636 157	-1793 188	-1981 142	-2123 328 TD	------	-----	------	1069	-2451
	C1-32	-871	-1131	-1421	-1548	-1778	-1977	-2213	----	-2584 Sat -2969 kal	1179	-3952
8	**G1-32**	-757 328	-1085 314	-1399 130	-1529 226	-1755 146	-1901 310	-2211 326	-2537 32	-2569/ -3519 950	1211	-4017
9	**DD1-32**	-1028 ? 190	-1210 302	-1524 104	-1638 252	-1926 168	-2120 273	-2464 313	-2748 42	-2838/ -3913	1112	-5958
10	**P1-32**	-2763 199	-2962 365	-3327 183	-3510 334	-3844 212	-4056 531	-4587 474	-5061 49	-5110 U.sat -5695 K/T -6689 Kal. 1579 Sat	723	-9747
No.	**Well**	**Facha**	**Kh**	**H**	**Z**	**K**	**D**	**B**	**Hag.**	**Kal/Sat**	**K.B.**	**TD**
11	**A1-32**	-877	-1070 378	-1448 105	-1553 264	-1817 181	-1998 375	-2373 1135	--- 245 sat	-3508 Sat. -3753 Kal.	957	-4973
12	**H1-32**		255	361	175	283	237	274	?	471			
13	**2H1-32**		140	355	164	251	180	386	450	- 510 Sat		
14	**M1-32**	-2814 790	-2024 390	-2414 150	-2564 223	-2787 187	-2974 165	-3139 1601	---	-4740 Kal.	686	-6514
15	**D1-24**	-1602 249	-1851 293	-2144 137	-2281 244	-2525 217	-2742 352	-3094 747	--- 743Sat	-3841Sat -4584 Kal	706	-5264
16	**C2-16**		-5330	-5648	-5812	-6307	-6490	---	-6670	-8637	430	-10584
17	**M1-16**		-3431	-3661	-3910	-4259	-4321	---	-4709	-5659 Waha Fm	611	-5744
18	**A1-17**		-1242 256	-1498 126	-1624 227	-1851 168	-2019 274	-2373 440	-2813 810	-3623 Sat. -3917 Kal.	807	-4973
19	**A7-17**	-1438	-1726	-1976	-2116	-2375	-2558	-2966	---	-3225 Sat.	924	-7136

		288	250	140	260	182	408	259	1401sat	-4626 Kal.		
20	**F1-17**	-1209 190	-1399 170	-1569 136	-1705 228	-1933 219	-2152 267	-2419 995	--- 535 sat	-3414 Sat. -3949 Kal.	891	-5929
21	**K1-17**	-1663 318	-1981 210	-2191 140	-2331 237	-2568 273	-2841 290	-3131 1445	--- 130 sat	-4576 Sat. -4706 Kal.	919	-6813
22	**L1-17**	-2081 220	-2301 181	-2482 124	-2606 235	-2841 163	-3004 349	-3353 394	 284 sat	-3747 Sat -4031 Kal.	849	-7255
23	**H1-11**	-1315 202	-1517 338	-1855 210	-2065 223	-2289 150	-2438 268	-2706 655	-3361 510	-3871/ -4035	935	-4265
24	**J1-11**	-2032 216	-2248 419	-2667 255	-2922 255	-3177 205	-3382 282	-3664 990	-4654 398	-5052/ -5222	748	-8209
25	**M1-11**		-4201 250	-4451 150	-4601 127	-4728 73	-4821 190	-5011 253	-5264 1042	-6306 Kal.	499	-8353
	Y1-11		-3325	-3843			-4332				632	
26	**Z1-11**	-4363 126	-4489 289	-4778 278	-5056 167	- 5223 207	- 5430 353	- 5783 918	- 6701 452	- 7153 Kal.	444	-7562
27	**2A1-11**	-4619 73	-4692 420	-5112 265	-5377 282	-5659 233	-5892 355	-6247 918	-7165 737	-7902	958	-11595
28	**4A1-11**	-3509 175	-3684 329	-4013 255	-4268 275	-4543 253	-4763 291	-5087 356	---	---	567	-5443
No.	**Well**	**Facha**	**Kh**	**H**	**Z**	**K**	**D**	**B**	**Hag.**	**Kal/Sat**	**K.B.**	**TD**
29	**2P1-11**	-1617 305	-1922 252	-2274 220	-2494 311	-2805 143	-2948 381	-3329 640	-3969 947	-4916	986	-5911
	2V1-11			-1787	-1987		-2587	-3327		-3577 Sat -3777 Kal	1183	
30	**2Q1-11**		-1697 260	-1957 198	-2155 332	-2487 222	-2709 300	-3009 808	-3817 710	-4527	913	-4857
31	**3H1-11**	-3423 148	-3571 427	-3998 291	-4289 279	-4298 490	-4788 315	-5103 1150	-6253 532	-6785	737	-8658
32	**3J1-11**	-3683 188	-3871 383	-4254 258	-4512 339	-4851 300	-5151 370	-5521 323	----	----	341	-5844
33	**3T1-11**	- 3217 155	-3372 357	-3729 173	-3902 290	-4192 197	-4389 257	-4646 279 **TD**	-----	----	681	-4925
34	**3P1-11**	-1246 257	-1503 254	-1757 97	-1854 223	-2077 139	-2216 298	-2514 318	-2832 23	-2855 U.sat -3489 B. Paleocene	946	-3583

										634		
35	**3D1-11**	-1429 231	-1660 278	-1938 197	-2135 270	-2405 163	-2568 270	-2838 328	-3166 27	-3193/ -3567?? Or - 4208? 1010 Sat	1027	- 5085
36	**3V1-11**	-3440 157	-3597 360	-3957 268	-4225 336	-4561 258	-4819 278	-5097 250	---	----	503	-5347
37	**3X1-11**	-3675 220	-3895 170	-4065 240	-4305 245	-4550 210	-4760 285	-5045 710	-5755 555	-6310	625	-9805
38	**A1-57**		-1781 270	-2051 207	-2258 458	-2716 147	-2863 355	-3218 763	-3981 755	-4736	954	-5326
39	**C1-57**	-1676 162	-1838 461	-2299 258	-2557 296	-2853 158	-3010 420	-3430 952	-4382 611	-4993	674	-6484
40	**G1-57**	-1749 248	-1997 378	-2375 256	-2631 306	-2937 138	-3075 453	-3528 1005	-4533 672	-5205	625	-7906
41	**L1-57**		-4735 365	-5108 362	-5470 200	-5670 250	-5920 345	-6265 385	---	----	730	-6650
42	**A1a-NC29A**		-3821 245	-4066 118	-4184 302	-4486 160	-4646 305	-4951 640	-5591	---	454	-8195
43	**C1-NC29A**		-3014 319	-3333 161	-3494 548	-4042 131	-4173 347	-4520	---	---	612	-4779
44	**B1-NC29B**	-1401 289	-1690 348	-2038 93	-2131 250	-2381 190	-2571 286	-2857 878	--- 179 sat	-3735 Sa -3914 Kal	819	-4300
45	**F1-NC29B**		-1409 277	-1686 155	-1841 250	-2091 200	-2291 227	-2518 353	-2871 60 **1035 sat**	-2931 sat -3966 Kal	829	-4741
46	**H1-NC29C**		-1890 335	-2225 188	-2413 168	-2581 240	-2821 201	-3022 371	-3393 471 **409 sat**	-3864 Sat -4273 Kal	788	-4622
47	**B2-NC74A**		-5408 274	-5682 274	-5956 266	-6222 226	-6448 168	-6616 1150	-7766 572	-8338 Kal	1018	-8702
48	**A1-NC74C**		-2918 315	-3233 136	-1372 176	-3584 67	-3615 201	-3816 797	-4613 142	-4755	1202	-7898
49	**G22-NC74F**		-2735 370	-3105 327	-3432 322	-3754 190	-3944 550	-4494 945	-5439 655	-6094 Kal	943	-9139